NASA Contractor Report 166623

Flight and Analytical Investigations of a Structural Mode Excitation System on the YF-12A Airplane

E.A. Goforth, R.C. Murphy, J.A. Beranek, and R.A. Davis

Contract NASA E-69204
April 1987

National Aeronautics and
Space Administration

NASA Contractor Report 166623

Flight and Analytical Investigations of a Structural Mode Excitation System on the YF-12A Airplane

E.A. Goforth, R.C. Murphy, J.A. Beranek, and R.A. Davis

Contract NASA E-69204
April 1987

National Aeronautics and
Space Administration

TABLE OF CONTENTS

LIST OF TABLES

LIST OF FIGURES

LIST OF SYMBOLS AND NOTATIONS

SUMMARY

INTRODUCTION

CANARD EXCITER VANE SYSTEM

- Safety System
- Instrumentation
  - Safety Instrumentation
  - Data Measurement Instrumentation
- Canard Vane Structural Dynamics
  - Canard Vane Flutter
  - Canard Vane Vibration Modes and Frequencies

CANARD EXCITER VANE FLIGHT TEST PROGRAM

- Ground Tests
  - Load Deflection Test
  - Exciter Vane Ground Vibration Test
  - YF-12A Aircraft Ground Vibration Test
- Flight Test Program
  - Test Technique
  - Flight Test Data

AEROELASTIC ANALYSIS

STRUCTURE

INERTIA

AERODYNAMICS

- Doublet Lattice
- Doublet Lattice, Slender Body, Interference Body
- Steady State Doublet Lattice with Uniform Lag
- Steady State Kernel Function with Uniform Lag
- Mach Box
- Piston Theory

TABLE OF CONTENTS (Continued)

STRUCTURE/AERODYNAMIC INTERCONNECTION

FLUTTER ANALYSIS

FREQUENCY RESPONSE

CONCLUSIONS

APPENDIX - YF-12A FREQUENCY RESPONSE PLOTS

REFERENCES

LIST OF TABLES

TABLE	TITLE
1	Canard Vane Operating Characteristics
2	Accelerometer Locations - Airframe Response Measurements
3	Canard Shaker Vane Vibration Frequencies and Mode Shapes
4	Summary - YF-12A Canard Exciter Vane Flight Test Program
5	Vane Ground Test Program
6	YF-12A Symmetric Vibration - Mode and Frequency Comparison
7	Summary of NASTRAN Program Errors
8	YF-12A Substructure Degrees of Freedom
9	Fuel Tank Loadings (Lbs.)
10	YF-12A Aerodynamic Cases
11	YF-12A Reduced Frequencies
12	YF-12A Frequency and Damping Comparison, Test vs. Analysis
13	YF-12A Frequency Response Summary

LIST OF FIGURES

FIGURE	TITLE
1	YF-12A Aircraft with Canard Exciter Vane
2	YF-12A with Canard Exciter Vane
3	YF-12A Shaker Vane Installation
4	Canard Exciter Vane Installation
5	YF-12A Exciter Vane Assembly
6	Exciter Vane Planform
7	YF-12A Shaker Vane System Block Diagram
8	Final Shaker Vane Frequency Response Test, Gain vs. Frequency, Temperature Ambient
9	Final Shaker Vane Frequency Response Test, Phase vs. Frequency, Temperature Ambient
10	Final Shaker Vane Frequency Response Test, Gain vs. Frequency, Temperature 300°F
11	Final Shaker Vane Frequency Response Test, Phase vs. Frequency, Temperature 300°F
12	YF-12A Accelerometer Locations
13	Canard Vane Flutter
14	YF-12A Shaker Vane Ground Vibration Test Shaker Locations
15	YF-12A Shaker Vane Vibration Data - Comparison, First Analytical to Test Mode, Symmetric
16	YF-12A Shaker Vane Vibration Data - Comparison, Third Analytical to Test Mode, Symmetric
17	YF-12A Shaker Vane Vibration Data - First Mode, Test, Antisymmetric
18	YF-12A Shaker Vane Vibration Data - Third Mode, Test, Antisymmetric
19	YF-12A Canard Exciter Vane Program Schedule
20	Exciter Vane - Load vs. Strain Gage Output
21	Exciter Vane Trim Angle vs. Mach No.
22	Frequency Sweep, M = 0.95
23	Dwell and Decay, M = 0.95
24	NASTRAN Model Planform and Substructure Division
25	Actual Structure and NASTRAN Model
26	Flow of the Coupling to Form the Dynamic Model
27	YF-12A NASTRAN Model

LIST OF FIGURES (Continued)

FIGURE	TITLE
28	Fuel Compartment Configuration
29	YF-12A Doublet Lattice Model
30	YF-12A Doublet Lattice Lift Distribution, Mach .70
31	YF-12A Doublet Lattice Lift Distribution, Mach .95
32	YF-12A Doublet Lattice, Slender Body, Interference Body Model
33	YF-12A DLSLIN Lift Distribution, Mach .70
34	YF-12A DLSLIN Lift Distribution, Mach .95
35	YF-12A Kernel Function Optimum Downwash Points
36	YF-12A Kernel Function Load Integration Points
37	YF-12A Kernel Function Lift Distribution, Mach .95
38	YF-12A Mach Box Model
39	YF-12A Mach Box Lift Distribution, Mach 1.25
40	YF-12A Piston Theory Model
41	YF-12A Piston Theory Lift Distribution, Mach 2.0
42	YF-12A Piston Theory Lift Distribution, Mach 2.7
43	YF-12A Velocity - Frequency - Damping (V-f-g) Plot
44	Exciter Vane Force vs. Frequency
45	Cockpit Acceleration Response
46	Outer Wing Acceleration Response

LIST OF SYMBOLS AND NOTATIONS

a	Parameter of lag function C(p)
[ADD]	Mach box aerodynamic influence coefficients for diaphragm boxes
AIC	Aerodynamic Influence Coefficients
[AJJL]	Aerodynamic matrix output from NASTRAN
[A(k)]	Aerodynamic Influence Coefficient matrix as a function of reduced frequency, k
[AWD]	Mach box aerodynamic influence coefficients for cross coupling of wing and diaphragm boxes
[AWW]	Mach box aerodynamic influence coefficients for wing boxes
$[A_o]$	Aerodynamic "stiffness" matrix
$[A_1]$	Aerodynamic "damping" matrix
$[A_2]$	Aerodynamic "inertia" matrix
α	Angle of attack
b	Parameter of lag function C(p)
b_o	Reference length
β	$\sqrt{M^2-1}$
CCV	Control Configured Vehicle
C_{L_α}	Lift curve slope
$C_{L_\alpha}(s)$	Lift curve slope as a function of the non-dimensional time parameter $s(=\frac{Vt}{b_o})$
$C_{L_\alpha(\infty)}$	Lift curve slope as $t \rightarrow \infty$
COSMIC	Computer Software Management and Information Center
C(p)	Lag function $\frac{(a-1)p+b}{p+b}$
[DF]	Matrix to reorder forces for kernel function aerodynamics
DL	Doublet Lattice

LIST OF SYMBOLS
AND NOTATIONS (Continued)

DLSLIN	Doublet Lattice with slender bodies and interference bodies
[DM]	Matrix to reorder moments for kernel function aerodynamics
DOF	Degrees of freedom
[Dθ] } [DZ] }	Matrices used to develop the total differentiation of the aerodynamic deflections to obtain downwash, $[D\theta] - {}^{p}/_{b_o}\ [DZ]$
[D1JK] } [D2JK] }	Matrices used to develop the total differentiation of the aerodynamic deflections to obtain downwash, $[D1JK]^T + ik\ [D2JK]^T$
FAMAS	Flutter and Matrix Algebra System
{F(p)}	Force as a function of differential operator p
{F(ω)}	Force as a function of circular frequency ω
g	Gravitational acceleration
[GZ]	Geometric transformation matrix used in Mach box aerodynamics
g_s	Structural damping
[GTKA]	Geometric transfomration matrix - aerodynamic to structural degrees of freedom
[GT1]	Geometric transformation matrix for load integration points
[GT2]	Geometric transformation matrix for optimum downwash points
[GZθ]	Geometric transformation matrix used in Mach box aerodynamics
i	$\sqrt{-1}$
[K]	Stiffness matrix
k	Reduced frequency, $\frac{b_o \omega}{V}$
KEAS	Knots equivalent airspeed
{L}	Lift
ℓ	Semi-span

LIST OF SYMBOLS
AND NOTATIONS (Continued)

LAMS	Load Alleviation and Mode Stabilization
M	Mach number
[M]	Mass matrix
NASA	National Aeronautics and Space Administration
NASTRAN	NASA Structural Analysis program
ω	Circular frequency
p	Non-dimensional differential operator, $\frac{b_o}{V}\frac{d}{dt}$
P_w	Pressure at C/4 of wing box
q	Dynamic pressure $\frac{1}{2}\rho V^2$
{q}	Modal degrees of freedom
[QL]	Matrix of roll moments
[QM]	Matrix of pitching moments
[QZ]	Matrix of vertical aerodynamic forces
ρ	Atmospheric density
ρ_o	Reference atmospheric density, sea level
s	Non-dimensional time parameter $\frac{Vt}{b_o}$
SCAR	Supersonic Cruise Aircraft Research
[SKJ]	Integration matrix to obtain lifts and moments
σ	Density ratio ρ/ρ_o
t	Time
μ_I	Interference body doublet
μ_S	Slender body doublet
V	Freestream velocity
V_L	Limit velocity
W_S	Downwash for slender bodies

LIST OF SYMBOLS
AND NOTATIONS (Continued)

W_w	Wing box downwash at 3C/4
$\{Z_A\}$	Deflections in structural degrees of freedom
[ ]	Matrix symbol
{ }	Column matrix (vector) symbol

SUMMARY

A structural mode excitation system using an oscillating canard vane to generate the force input was mounted on the forebody of the YF-12A airplane. This shaker vane was used to excite the airframe structural modes during flight in the subsonic, transonic, and supersonic regimes. Structural modal responses due to the shaker vane forces were measured at various flight conditions by accelerometers mounted on the airframe. Aeroelastic analyses of these flight test configurations have been made using the methods of NASTRAN and Lockheed FAMAS programs. Comparison of the experimental and analytical data has been made to determine the validity of the analytical methods as preliminary design tools for future aerospace vehicles.

Analytically, the study involved structural, inertial, and aerodynamic modeling, these results being used in flutter and frequency response analyses. From the flutter analyses, modal dampings and frequencies were obtained and compared with flight test results. The frequency response results consisted of accelerations at various locations on the planform, these being expressed as magnitude and phase angle relative to the oscillating force input of the canard exciter vane. The NASTRAN structural model was found to describe adequately the dynamic behavior of the YF-12A aircraft. Aerodynamic forces were transformed to the structure by use of the surface spline in the NASTRAN program. This transformation gave reasonable lift distributions only when several splines were used to cover the planform. The linear spline transformation in COSMIC NASTRAN was found to give erroneous results. Aerodynamic methods which were found to give acceptable answers were the doublet lattice method, steady state doublet lattice with uniform lag, Mach box method, and piston theory; each method, of course, being applied only to the appropriate speed regime. These methods, carefully applied, were found to predict adequately the dynamic behavior of the YF-12A aircraft; this should also be true for the preliminary design phase of any future aerospace vehicle.

INTRODUCTION

During the past few years, several analytical methods which have general application to aeroelastic problems have come into widespread use. These new capabilities, which include finite element structural and aerodynamic modeling, have been included in NASTRAN and are available throughout the aerospace industry. Using these methods to study a large flexible aircraft over a wide range of Mach numbers and flight conditions and comparing these results to actual flight measurements would prove to be a good test of the methods. Only a few aircraft could be used for this type of test, one of which is the YF-12A. The availability of the airplane at the NASA Dryden Flight Research Center provided a unique opportunity to compare these various analytical aeroelastic methods with experimental data for subsonic, transonic, and supersonic flight.

NASA Dryden Flight Research Center obtained a YF-12A airplane for use in a comprehensive flight research program that covered the period from 1969 to 1980. The YF-12A airplane provided a large flexible vehicle capable of flying in the subsonic, transonic, and supersonic flight regimes. It was an excellent tool for investigations into the fields of structures, materials, propulsion, flight control systems, and aerodynamics, as well as a variety of other disciplines. Many proposals for analytical and experimental aeroelastic investigations were made during the course of the YF-12A program. The success of previous NASA and Air Force programs where the vehicle structural dynamics were controlled by active control systems with high frequency response resulted in several proposals for the application of the Control Configured Vehicle (CCV) technology to the YF-12A aircraft.

One of these programs was prompted by an incident involving an Air Force B-52 aircraft. This plane, while flying along the eastern slopes of the Rockies, encounted gusts that caused the loss of the vertical fin. The Air Force Flight Dynamics Lab set up an analytical and experimental program for application of the CCV concept to the B-52. The concept resulted in the design and the flight test of the Load Alleviation and Mode Stabilization (LAMS) system on the B-52 as reported in Reference 1. The success of this CCV application lead to the refinement of the B-52 LAMS system with additional Fatigue Reduction (FR), Flutter Mode Control (FMC), Maneuver Load Control (MLC), Augmented Stability (AS),

and Ride Control (RC) programs. The B-52 CCV design and flight test results are detailed in Reference 2.

Another program concerning the application of CCV technology was begun during the development phase of the XB-70 aircraft. A joint NASA/Air Force program studied a structural mode control system for use on the airplane. One of the features of the study was the use of a canard shaker vane to excite the modal responses for the evaluation of the structural mode control system. This design study was reported in Reference 3, and resulted in a contract for the installation of the canard vane system on the XB-70 aircraft. The flight investigation results of the Structural Mode Control system featuring the canard shaker vane exciter were reported in Reference 4, and increased the amount of analytical and experimental CCV technology data available to the designer.

NASA Dryden Flight Research Center (DFRC) was presented with the opportunity to continue the study, design, and application of the CCV concepts to large, flexible aircraft with the advent of the YF-12A program. The first step in this direction was a feasibility study in 1970 of a Load Alleviation and Modal Suppression (LAMS) system for use on the YF-12A airplane. The study defined five different LAMS systems and evaluated them for design and performance using analytical techniques. Each of the systems studied had a different combination of force producers. The results of the study set down in 1972 in Reference 5 concluded that a small canard vane mounted on the forebody chines used in conjunction with the outboard elevons would be the best LAMS system for the YF-12A.

The next logical step was the design, installation, and flight test of the proposed LAMS system on the aircraft, just as had been done during the XB-70 program. Budget and schedule constraints of the YF-12A program prevented the implementation of the LAMS program at that time. The availability of the XB-70 canard shaker vanes at NASA in 1974 triggered a feasibility study which found that the design, installation, and flight test program using the canard vane for the excitation and measurement of the structural modal responses could be funded at that time. In 1974, ECP YF-12-75, Reference 6, authorized the YF-12A canard exciter vane program. The exciter vane system was to be designed to the LAMS system requirements if possible to do so without requiring additional

budget. The design and system tests were completed, and the shaker vane kit was available for installation in 1975. Test plans with higher priorities delayed the installation of the shaker vane on the aircraft. In 1978, the decision was made to install and flight test the vane.

The flight test program started in November 1978 and was completed in March 1979. There were six flights in the program that obtained response data at Mach numbers of 0.70, 0.95, 1.25, 2.00, and 2.70. Fourteen accelerometers were placed at locations best suited for measuring the modal responses in the test frequency range.

At the conclusion of the flight test program in 1980, a proposal was submitted (ECP YF-12-123, Reference 7) for using a YF-12A NASTRAN structural model, available from previous programs, with the aeroelastic methods of NASTRAN to analyze the flight test configurations. This report is a response to that ECP. The analytical results are compared with the flight test data for validation of these methods of analysis for use in the preliminary design of future aerospace vehicles.

CANARD EXCITER VANE SYSTEM

The primary purpose of the system was to provide oscillatory excitation of the YF-12A aircraft structure during flight over the frequency range from 1 to 18 Hertz utilizing the XB-70 vanes. A secondary goal of the design effort was to obtain a high frequency response vane system for future use in a LAMS system. The exciter vane was powered by a self-contained hydraulic system controlled by an electronic subsystem. Safety considerations imposed additional constraints on the control system. Strain gages and an accelerometer were used to trigger the emergency shutdown system whenever prespecified limit levels were surpassed. Continuous use of the self-contained hydraulic system could cause overheating resulting in the loss of system pressure, allowing the vane system to be free to rotate. The emergency system was designed to rotate the vane until it engaged a mechanical safety lock. The YF-12A aircraft with the canard exciter vane installed is shown in Figure 1. The canard vane installation is shown in Figures 2 and 3. Figure 4 is a drawing of the vane installation on the YF-12A forebody. The shaker vane components and their locations are shown in Figure 5. The physical dimensions of the vane planform are presented in Figure 6.

The hydraulic power system for the canard vane was an Abex pump/motor with an integral reservoir and pressure compensating system, and a Moog transfer valve/Bertea servo-actuator combination as described in Reference 8. The vane power system was independent of the aircraft hydraulic systems. The servo-actuator was coupled to the vane torque shaft as shown in Figure 5, and was capable of driving the vane through a maximum amplitude of $\pm$ 12 degrees.

Electronic Subsystem

The electronic subsystem, as described in Reference 9, was designed to provide the following:

1) Fixed and variable frequency sinusoidal inputs with variable amplitude to the control system that drives the canard system
2) Control the canard oscillations through servo amplifier/feedback system

3) Detect, indicate, and shutdown the system when strain gage and/or accelerometer levels reach predetermined values.

The electronic system was made up of three main components:

1) Function generator
2) Electronic control box
3) Control panel.

The function generator and electronics box were installed in the rear cockpit, while the control panel was located in the front cockpit. Control of the operating modes, frequency limits, and vane amplitudes were controlled from the rear cockpit.

System on-off, trim, and emergency shutdown were controlled by the pilot in the front cockpit. The interface between the two systems is shown in the block diagram of Figure 7. The operating characteristics are summarized in Table 1.

Safety System

The safety system was designed to provide fail-safe vane positioning for any electrical, mechanical, or hydraulic failure using the mechanical centering and locking system of the torque shaft drive mechanism. The system triggers were:

1) Loss of hydraulic pressure
2) Loss of electrical control power
3) High torsion load on vane torque shaft
4) High bending moment on vane torque shaft
5) High vertical acceleration of forward fuselage near vane shaft
6) Vane shaft strain gage indication of maximum vane lift force limited by forebody loads.

The system design criteria for safety was the centering and locking of the vane system in less than 1/4 of a cycle after a trigger signal.

The frequency responses of the system as determined by bench tests are shown in Figures 8 and 9 for gain and phase for ambient temperature conditions, and gain and phase of the system for a temperature of 300°F are shown in Figures 10 and 11.

Instrumentation

The canard shaker vane instrumentation was a dual purpose system. The primary instrumentation was designed to provide fail-safe operation of the canard vane system within the aircraft design load limits. The second set of instrumentation was installed to measure the structural dynamic responses due to the oscillating vane force inputs.

Safety Instrumentation

The junction of the YF-12A forebody with the wing at Fuselage Station 715 was the critical structural element with the canard shaker vane system operating. Canard vane operating limits set by the structural limits were:

1) 1000 pounds force for each vane
2) ± 0.5 g's vertical acceleration due to modal responses at the location of the shaker vane.

Strain gage bridges on each torque shaft and an accelerometer mounted on the forebody structure at the vane location were calibrated to trigger the safety system when one of the above values were obtained.

Data Measurement Instrumentation

Instrumentation for the measurement of the modal response data used fourteen accelerometers. Locations of those accelerometers are shown in Figure 12, and summarized in Table 2. The YF-12A aircraft free-free symmetric vibration mode shapes were used to locate the accelerometers to insure that the modal response measurements would have large amplitudes over the shaker vane operating frequency range. Flight at the high Mach numbers required by the program necessitated some method of cooling the accelerometers during the test.

The basic method of cooling made use of a stearic acid heat sink. CEC Model 4-205-0001 type accelerometers were used because they met the LAMS system requirements described in Reference 5.

Canard Vane Structural Dynamics

The canard shaker vane system structural dynamic characteristics were determined by the actuation system design. Two criteria that had to be satisfied in the design of the canard vane actuator, backup structure, crank, and torque tubes and supports were:

1) The canard shaker vane system had to have a calculated flutter speed greater than V_D = 575 KEAS, at a Mach number = 0.95

2) The vibration modes of the shaker vane, its support, and actuation system had to have frequencies much higher than the maximum vane excitation frequency of 18 Hertz.

The shaker vane design satisfied both of these criteria.

Canard Vane Flutter

The aerodynamic parameters most important in flutter analysis are the dynamic pressure, q, and the vane lift curve slope, C_{L_α}. The calculations of the vane lift curve slope mounted on the YF-12A forebody chines covered a range of four values from 5.75 per radian to 9.45 per radian. The range was established by using two different aerodynamic theories with and without interference effects due to the chines. The vane planform used for aerodynamic calculations is shown in Figure 6. The canard vane design using the unmodified Bertea actuator, part number 232000-1005, was shown by analysis to have flutter speeds below V_L = 500 KEAS for the two highest values of C_{L_α}, and flutter speeds between V_L and $1.15V_L$ = 575 KEAS for the other two values of C_{L_α}. The hydraulic fluid spring was the most flexible part of the canard vane actuation system. The stiffness of the actuation system was increased by the installation of metal stops in the actuator cylinder bore to reduce the hydraulic fluid volume. The

increase in the actuator system stiffness raised the canard vane flutter speed above $1.15V_L$ for all four C_{L_α} values. The results of this analysis are shown in Figure 13.

Canard Vane Vibration Modes and Frequencies

The second design criteria requiring the canard shaker vane system to have vibration modes and frequencies higher than the maximum vane excitation frequency of 18 Hertz was also satisfied. A summary of the canard vane analytical and experimental vibration frequencies and modes is made in Table 3. The canard vane planform with the shaker locations relative to the elastic axis is shown in Figure 14. A comparison of the canard vane first symmetric analytical mode with the first test mode is made in Figure 15. There is no second analytical mode for comparison with the second test mode noted in Table 3. The comparison of the third symmetric analytical mode with the third test mode is made in Figure 16. Comparison of the shaker vane first antisymmetric analytical mode with the test mode is made in Figure 17. The second antisymmetric test mode has no comparable analytical mode. The third antisymmetric analytical mode is compared with the third test mode in Figure 18. The lowest measured shaker vane mode of 32.26 Hertz is a factor 1.79 times higher than the maximum vane excitation frequency of 18 Hertz.

CANARD EXCITER VANE FLIGHT TEST PROGRAM

Cost and schedule estimates for the installation of the exciter vane system combined with a flight test program reduced in scope from the original plans were submitted as a proposal for a joint NASA/Air Force program in 1978. This proposal was approved in March 1978 and the installation of the exciter vane system completed in November 1978. The flight test phase was started in November 1978 and was completed six flights later in March 1979. The program schedule is shown in Figure 19.

The revised test plan scheduled flight tests at Mach numbers of 0.70, 0.95, and 1.25. At this same time NASA had a major program investigating the feasibility of supersonic cruise (SCAR) vehicles. The Mach number range of interest for the SCAR program covered the three Mach numbers proposed for the YF-12A exciter vane program as well as investigating Mach numbers out to a maximum value of 2.7. As the detailed planning for the YF-12A vane program went forward, it was obvious that additional data points extending the Mach numbers to 2.7 should be included. Thus, the YF-12A shaker vane program would provide a set of aeroelastic response measurements of a large flexible aircraft flying over the Mach number range of interest for the SCAR program. The Mach numbers selected were 0.70, 0.95, 1.25, 2.00, and 2.70. The speeds available for use in the flight envelope constrained the flight test speeds to 330 KEAS, 360 KEAS and 400 KEAS. The data obtained would be available for verification of aeroelastic analytical methods used in the preliminary design of other future aerospace vehicles. The flight test program is summarized in Table 4.

Ground Tests

The YF-12A exciter vane installation ground test program covered the three specific areas shown in Table 5, and is discussed below.

Load-Deflection Test

A structural influence coefficient test of the canard exciter vane was done to calibrate the strain gage bridges that were to measure the flight test vane loads. The loads measurements were used to obtain basic test data as well as a

two flights were checkout flights of the aircraft, the exciter vane system, and the test techniques to be used during the flight test program. These two flights found three areas where changes were needed:

1) Exciter vane trim angle
2) Exciter vane normal accelerometer trigger level for flight safety
3) Method of on-line determination of the airframe resonant frequencies for the dwell test.

The exciter vane trim angles required for zero vane load were calculated prior to the flight test program. The calculated vane angles for zero load for planned test Mach numbers were averaged to provide one trim angle. The vane actuation system had been designed with a mechnical adjustment to provide an angular offset for vane trim purposes. The vane system could then oscillate full travel about this vane trim angle. The first two flights indicated the calculated trim angle was incorrect. The computational aerodynamic methods treated the vane-forebody as a two-dimensional surface. In the early 1970's, the YF-12A airplane during flight test had demonstrated that a vortex was generated by the junction of the chine leading edge with the fuselage on each side of the airplane - these vortices would curl up and aft from that initial location. A visual inspection of Figure 1 shows that these vortices would exert a strong influence on the vane aerodynamics. The results of the first two flights were used to reset the vane trim angle used for the rest of the program. The vane trim angle comparison is made in Figure 21. The calculated values were obtained using a two dimensional analytical structural model so that flexible effects were included in the analysis.

The second change based on flight test results was the threshold setting of the shaker vane flight safety accelerometer. Originally, the accelerometer was set up so that a dynamic value of ± 0.5 g would trigger the vane safety system to drive the exciter vane into the lock. The system was being shut off most of the time with the 0.5 g setting. However, since a value of ± 1.0 g was considered acceptable from a stress viewpoint, the acceleration limits were revised. The 1.0 g setting did not shut down the vane system at all during the rest of the flight test program.

The third change was a switch in methods for identifying the structural resonances uncovered by the exciter vane frequency sweep. Originally these data were to be obtained from the real time strip chart data. However, the elapsed time for obtaining the data in this manner was considered to be unacceptable. The data from the fuselage nose and fuselage tail accelerometers were processed by a dynamic analyzer using Fast Fourier Transform (FFT) techniques to obtain a Power Spectral Density (PSD) analysis with resonant frequency peaks available on the PSD hard copies. The data were analyzed and the test frequencies supplied to the flight crew in less than 40 to 50 seconds of elapsed time.

Test Technique

The YF-12A aircraft with the canard exciter vane was flown in level flight at 1.0 g load factor and at a specified Mach number and KEAS. The exciter vane was set up in the sweep frequency mode. In this mode, the control system drove the vane to oscillate sinusoidally from 1 Hertz to 18 Hertz in slightly over 50 seconds. At the designated end frequency the system automatically shut off. The sweep data were telemetered to the ground and processed by the Dynamic Analyzer to determine the resonant frequency peaks. Each frequency was then set up on the exciter vane control system. When the accelerometer response amplitudes became constant, the shaker vane would be shut off with the accelerometers indicating the decay of the structural mode. This was done for each resonant mode found during the test point.

Flight Test Data

Acquired from each test were time history data for the vane position, the vane force, the fourteen accelerometer responses, and the amount of fuel in each of the six tanks at a given time. Examples of the time histories of the exciter vane sweep frequency inputs along with the airframe response outputs are shown in Figure 22 for a Mach number of 0.95. Examples of the dwell and decay test data for the same test point are shown in Figure 23. The data from each flight were stored on magnetic tape, thus making it available for any processing which was later required.

AEROELASTIC ANALYSIS

As an addition to the YF-12A canard vane flight test program, an aeroelastic analysis of the YF-12A was conducted. This required that various analytical tasks be performed in the following categories:

1) Structural model
2) Inertia models
3) Aerodynamic models
4) Structure/Aerodynamic model interconnection
5) Flutter analysis
6) Frequency response analysis.

At the start of the flight test program, NASTRAN had been updated with the inclusion of an aeroelastic analysis module. Thus NASTRAN was capable of analyzing the data obtained from the YF-12A modal excitation flight test program. The YF-12A analytical structural model had already been constructed using NASTRAN. This computer program could generate steady and unsteady aerodynamic forces for subsonic, transonic, and supersonic flight regimes; in addition, NASTRAN had programs for flutter and forced response calculations. The analytical programs had been well defined by the end of the flight test program. The analysis plan was put together as an ECP, Reference 7, and submitted for approval. Trial runs were made using the various NASTRAN modules to obtain cost data for the ECP. These runs found errors in the NASTRAN programs that COSMIC, the contractor for NASTRAN maintenance, had not uncovered. Since the Lockheed FAMAS computer program system (Reference 29) could do the same analysis, the ECP was formulated to use NASTRAN as the primary analytical tool, with FAMAS to be used when significant problems were encountered with NASTRAN. A summary of the problem areas and the action taken is presented in Table 7. These program errors were encountered in COSMIC NASTRAN, Level 17.5, on an IBM 370 System, Model 3033 computer. Problems of this nature may be peculiar to a given computer system, and may not be encountered with other machines or versions of NASTRAN.

Two types of analyses were done to match the flight test data. First, a flutter analysis was done matching the test Mach number and speed. The structural damping, g_s , was assumed to be zero for the initial analytical calculations. The

flutter program calculated the frequencies and dampings for the structural modes. The structural damping for each mode, which was obtained from ground vibration test results, was then added to the damping value obtained from the flutter program. This final damping, although an approximation, can be compared directly with the measured flight test data. Second, a forced response analysis was done using the measured exciter vane force as the forcing function input. The analytical responses were converted to accelerations and also were compared directly with flight test measured data.

STRUCTURE

The structural model of the YF-12A had previously been constructed using NASTRAN, and it was initially believed that this model could be used with no changes. It was found, however, that the existing model had both nose and main landing gear removed and also did not have certain degrees of freedom retained which were deemed necessary for this study. A description of the old model with a comparison to ground vibration test results (Reference 10) can be found in Reference 11. The problems with the old structural model made it necessary to run all of the substructuring, combining, and reduction operations again.

The YF-12A NASTRAN model consisted of the six substructures shown in Figure 24. The structure was divided as shown in order to minimize substructure boundary degrees of freedom, since these must be retained for later substructure coupling runs. A one-half airplane model was used in the analysis, with only symmetric boundary conditions about the fuselage centerline being considered. As an illustration of the YF-12A modeling, Figure 25 shows a spanwise cross section of the actual aircraft structure and the corresponding NASTRAN finite-element model.

Table 8 gives an indication of the size of the substructures by showing the number of degrees of freedom removed and retained for each. A total of 7689 structural elements, consisting of bars, rods, shear panels, and scalar elastic elements, made up the one-half airplane model. Figure 26 shows how these substructures were coupled and reduced to arrive at the final dynamic model. This was accomplished by using the multistage substructuring capability included in the COSMIC version of NASTRAN Level 17.5.

The locations of the 288 degrees of freedom which were used for the final dynamic model are shown on the structure layout in Figure 27. This model was used to obtain frequencies of natural vibration and eigenvectors, which transform the flutter and response analysis equations to generalized modal degrees of freedom.

INERTIA

Five distinct weight cases were analyzed to correspond to the tested flight conditions. Each case represented a different fuel tank loading; these are presented in Table 9. The location of each fuel tank is shown in Figure 28. A vibration analysis was done for each configuration and the resulting eigenvectors were used to transform to modal degrees of freedom in the flutter and response analysis equations.

The inertia model used in the dynamic analysis was introduced into NASTRAN as a set of direct input matrices, formed externally, and redistributed to the NASTRAN grid points. The same coupling and reduction process which was used for the stiffness matrix in the structural model was then used to transform each mass matrix to the 288 degrees of freedom of the final dynamic model.

AERODYNAMICS

The YF-12A shaker vane flight test program yielded data over a wide range of Mach numbers which allowed a comparison between test and analysis using several different methods of aerodynamic modeling. These are presented in Table 10.

The doublet lattice program used was from NASTRAN, and had the capability of including slender body aerodynamic forces and interference body effects. Piston theory also was generated by the NASTRAN program. The kernel function and the Mach box programs used are part of the Lockheed-California Company's FAMAS system. COSMIC NASTRAN's version of Mach box aerodynamics was found to have programming errors, and was not used.

The method indicated in Table 9 by "steady state with uniform lag" is a means of forming aerodynamic matrices which are explicit functions of p, the differential operator. The unsteady matrices are formed by applying a uniform lag function, representing the growth of lift due to a step input for angle of attack, to the steady state aerodynamic influence coefficient matrix. This results in flutter equations which can be solved in a straightforward manner, and which give true decay-rate solutions for damping. This empirical method, also known as "indicial flutter aerodynamics," has been used extensively at Lockheed and has usually given satisfactory results. In at least one case at Lockheed, involving a low aspect ratio planform, better agreement with test results was obtained with this method than with the complete unsteady kernel function matrices. For this reason, the method was included in the present study.

Doublet Lattice

The doublet lattice aerodynamics used in the analysis of the YF-12A were obtained using the NASTRAN and Lockheed FAMAS program systems. The theoretical basis of the doublet lattice method used in NASTRAN may be found in References 12, 13, and 14.

The aerodynamic influence coefficients (AIC's) are calculated using aerodynamic and geometric matrices created by NASTRAN. The following relationship utilizes these matrices to obtain the doublet lattice AIC's:

$$[A(k)]=[GTKA]\,[SKJ]\left[[AJJL]^{T}\right]^{-1}\left[[D1JK]^{T}+ik[D2JK]^{T}\right]\,[GTKA]^{T}$$

In the above equation, the matrix [AJJL] is an aerodynamic matrix that gives the pressure at the 1/4 chord of each box due to a unit downwash at the 3/4 chord. The code in NASTRAN that is used to obtain [AJJL] was taken directly from the program "N5KA" by Giesing, Kalman and Rodden (Reference 15). The matrix sum, $\left[[D1JK]^{T} + ik\,[D2JK]^{T}\right]$, represents the total (substantial) differentiation of the aerodynamic deflections to obtain downwash. The [SKJ] matrix is an integration matrix that is used to obtain forces and moments. Finally, the matrix [GTKA] is a geometric transformation matrix for transforming the forces and moments of each box in the aerodynamic degrees of freedom (DOF) to forces and moments in the structural DOF. The matrix [GTKA] uses a surface spline interpolation to obtain the desired transformation.

The doublet lattice model of the YF-12A aircraft consists of 25 panels which are divided into a total of 378 aerodynamic boxes. The model is shown in Figure 29. All of the aerodynamic DOF are splined to the structural DOF except those that are located on the fin below Water Line 145. The steady state lift distribution at Mach 0.7 and 0.95 for a unit pitch angle is shown in Figures 30 and 31. Unsteady aerodynamics were calculated at five values of reduced frequency for both Mach 0.7 and 0.95. These reduced frequencies were calculated by using the dwell frequencies determined from flight test data.

Doublet Lattice, Slender Body, Interference Body

The calculation of the doublet lattice aerodynamics with slender bodies and interference bodies (DLSLIN) was performed with the NASTRAN aerodynamic package. The method used in NASTRAN is a modified version of that used in Reference 14. The theoretical basis for the addition of slender and interference body theory to the doublet lattice method is outlined in References 16 and 17.

The output from NASTRAN for DLSLIN is similar to that for DL alone. The relationship to obtain the AIC's is:

$$[A(k)] = [GTKA]\,[SKJ]\left[[AJJL]^T\right]^{-1}\left[[D1JK]^T + ik[D2JK]^T\right][GTKA]^T$$

The aerodynamic matrix [AJJL] is a matrix of pressures at the doublet lattice box 1/4 chord caused by a unit downwash at the 3/4 chord and terms relating interference and slender body singularities to downwashes, i.e.,

$$\begin{Bmatrix} W_W \\ 0 \\ W_S \end{Bmatrix} = \underbrace{\begin{bmatrix} A_{WW} & A_{WI} & A_{WS} \\ A_{IW} & A_{II} & A_{IS} \\ 0 & 0 & A_{SS} \end{bmatrix}}_{[AJJL]} \begin{Bmatrix} P_W \\ \mu_I \\ \mu_S \end{Bmatrix}$$

where W_W = wing box downwash @ 3C/4

W_S = downwash for slender bodies

P_W = pressure @ C/4 of wing box

μ_I, μ_S = interference and slender body doublets

The sum $\left[[D1JK]^T + ik\,[D2JK]^T\right]$ is the total (substantial) differentiation of the deflections to obtain downwash. The [SKJ] matrix transforms the doublet lattice box pressures, interference body doublets and slender body doublets into wing box and slender body forces. The transformation from aerodynamic DOF to structural DOF is performed by [GTKA]. The result is the unsteady AIC matrix in the structural DOF for a specified reduced frequency.

The DLSLIN model of the YF-12A consists of 18 doublet lattice panels, 2 slender bodies, and 2 interference bodies. The model is shown in Figure 32. There are a total of 283 doublet lattice boxes that model the inner and outer wings, the inboard and outboard elevons, and the vertical fin. The slender body simulating the fuselage consists of 30 elements, the corresponding interference body consists of 17 elements. The other slender body represents the engine and spike. This body consists of 11 slender body elements and 14 interference body elements. All of these elements combine to make 648 aerodynamic DOF to be splined to the 288 structural DOF.

The steady state lift distributions for Mach 0.7 and 0.95 are shown in Figures 33 and 34. Aerodynamic matrices were calculated for five reduced frequencies at Mach numbers 0.7 and 0.95.

Steady State Doublet Lattice with Uniform Lag

This method, also called indicial aerodynamics, utilizes the steady state (k=0) aerodynamic influence coefficient (AIC) matrix and an indicial response function for the aerodynamic lag. Together, these items are used to form AIC's which are explicit functions of the differential operator p. The indicial function defines the response of the lift curve slope as a function of time due to a step input for α, the angle of attack. This is based on the one-exponential lag function, $\frac{C_{L_\alpha}(s)}{C_{L_\alpha}(\infty)} = 1 - ae^{-bs}$, where s is the non-dimensional time parameter $\frac{Vt}{b_o}$, and a and b are constants computed by the method outlined in Reference 18. Taking the Laplace Transform results in the lag function $C(p) = \frac{(1-a)\ p+b}{p+b}$, where $p(=\frac{d}{ds})$ is the differential operator. Assuming the lag function to be uniform means that the growth of lift at the quarter chord of each aerodynamic box due to an angle of attack at the three-quarter chord of that box is the same for all boxes on the planform. The lift expressed in the DOF of the final model is then given by the following equation:

$$\{L\} = qC(p)\ [GTKA]\ [SKJ]\ [AJJL^T]^{-1} \left[[D\theta] - {}^{p}/_{b_o}\ [DZ]\right]\ [GTKA]^T\ \{Z_A\}$$

The matrices [AJJL], [SKJ], and [GTKA] come from NASTRAN. The matrix $\left[[D\theta] - {}^{p}/_{b_o}\ [DZ]\right]$ represents the total differentiation of the deflections in order to produce the downwash.

The aerodynamic model used was the same as for the previously defined doublet lattice aerodynamics. Steady state aerodynamic matrices were produced for Mach numbers .7 and .95.

Steady State Kernel Function with Uniform Lag

This method is basically the same as the Steady State Doublet Lattice with Uniform Lag, except that the steady state aerodynamic influence coefficient matrix was obtained from Lockheed's Kernel Function Program (Reference 19). This program was developed from the theoretical work done by Watkins, Runyon, and Woolston in Reference 20. The uniform lag function used was the same as in the doublet lattice case.

The output from the Kernel Function Program consists of three aerodynamic influence coefficient matrices; QZ, QL, and QM. These matrices yield, respectively, the vertical forces, the roll moments, and the pitch moments at the load integration points (Figure 36) due to unit downwash at the optimum downwash points (Figure 35). For the YF-12A model the roll moments were found to be very small and were judged to be insignificant to the flutter analysis. This made it possible to use the NASTRAN surface spline capability to generate transformations from the aerodynamic to the structural model.

The lift is then given by the following:

$$\{L\} = 4\pi\ell^2 q\, C(p)\, [GT1] \left[b_o [DM][QM] - [DF][QZ] \right] \left[[D\theta] - {}^{p}/_{b_o} [DZ] \right] [GT2]^T \{Z_A\}$$

In this equation, [GT1] and [GT2] are the spline matrices from NASTRAN for the load integration points and the optimum downwash points, respectively. [DM] and [DF] are matrices which simply reorder the forces and moments to be compatible with the NASTRAN format. As before, the matrix $\left[[D\theta] - {}^{p}/_{b_o} [DZ] \right]$ represents the total differentiation of the deflections in order to produce the downwash.

The Kernel Function model of the YF-12A consists of 100 downwash points and 90 load integration points as shown in Figures 35 and 36. The planform used for the aerodynamic model is shown in heavy ink. The steady state lift distribution created by the kernel function model is shown in Figure 37.

Mach Box

The aerodynamic influence coefficients (AIC's) for the YF-12A at Mach 1.25 were calculated using the Mach box method. The program used in the calculation of the AIC's was a Lockheed FAMAS system program. It was originally planned that the Mach box section of NASTRAN be used in these calculations, but the available NASTRAN code was found to be defective. For further information on the Mach box method see References 21, 22, and 23. Only part of the diaphragm region was included in the analysis. This method, explained in Reference 24, results in a considerable savings in computer time and has been found to give acceptable results.

The output from the Mach Box Program is a matrix of AIC's for both the wing boxes and the diaphragm boxes.

$$[AIC]_{\text{output}} = \begin{bmatrix} AWW & AWD \\ ADW & ADD \end{bmatrix}$$

This matrix, after applying the factor $\frac{4q}{\beta}$, gives the pressure differential across a box due to unit downwash at the mid-chord of the box. The requirement that the pressure differential across diaphragm boxes be zero results in the following equation, which reduces the AIC's to wing box size:

$$[QZ] = [AWW] - [AWD]\,[ADD]^{-1}\,[ADW]$$

The lift in the final dynamic model DOF is then given by the following equation:

$$\{L\} = \frac{4Aq}{\sqrt{M^2-1}}\,[GZ]^T[QZ]\left[[D\theta] - \frac{ik}{b_o}[DZ]\right][GZ\theta]\,\{Z_A\}$$

Here, A is box area, q is the dynamic pressure, M is Mach number, [GZ] and [GZθ] are transformation matrices, and the matrix $\left[[D\theta] - \frac{ik}{b_o}[DZ]\right]$ represents the total differentiation of the deflections to obtain the downwash. The transformation matrices were obtained from NASTRAN by making a doublet lattice model whose DOF coincided with the Mach box DOF.

The Mach box aerodynamic model of the YF-12A consists of 373 wing boxes and 305 diaphragm boxes (1/2 airplane). The box dimensions are 18 x 24 inches. The model is shown in Figure 38. The steady state lift distribution obtained with the Mach box model is shown in Figure 39.

Piston Theory

The piston theory aerodynamics for the YF-12A were computed with the NASTRAN system. Piston theory, a form of strip theory, was developed by Ashley and Zartarian (Reference 25) for M>>1. The computer program used in NASTRAN is a version of the program developed by Rodden, Farkas, Malcom, and Kliszewski (Reference 26).

The NASTRAN piston theory program directly computes the lift and pitch moment at the mid-chord of a strip due to plunge and pitching motion at that point. This is output as the matrix [AJJL]. The lift in the final DOF is then given by the following:

$$\{L\} = [GTKA]\ [AJJL]\ [GTKA]^T\ \{Z_A\}$$

Here [GTKA] is the spline matrix which transforms from aerodynamic DOF to structural DOF.

The piston theory model consists of 10 strips; this results in 20 aerodynamic DOF - plunge and pitch for each strip. The model is shown in Figure 40. The lift distributions for M = 2.0 and 2.7 are shown in Figures 41 and 42 respectively.

STRUCTURE/AERODYNAMIC INTERCONNECTION

In order to obtain compatible degrees of freedom in the final dynamic model, it was necessary to interpolate between the structural and the aerodynamic models. Because NASTRAN was used to generate the structural model and most of the aerodynamic models, it was decided to use the spline capability contained in this system. The theory of surface splines is discussed by Harder and Desmarais in Reference 27. The low aspect ratio of the YF-12A suggests that this type of spline be used. This was done in all cases except for slender body aerodynamics where the only possibility in NASTRAN is a linear spline.

Because the NASTRAN multistage substructuring capability is not included in the rigid format for aerodynamic generation, the connection between the structural and aerodynamic models could not be done in a straightforward manner. It was necessary to construct a NASTRAN "pseudo-model" to be used in conjunction with the aerodynamic models. This pseudo-model consisted of only the final dynamic model's 288 degrees of freedom, these being linked by bar elements. The stiffness assigned to the bars was not representative of the YF-12A structure. Since the pseudo-model was used only for the aerodynamic transformation, the actual stiffness values were not relevant. Each aerodynamic case was run with this pseudo-model in order to generate the appropriate spline matrix for the structure to aerodynamic transformation. The resulting transformed aerodynamic degrees of freedom directly corresponded to the degrees of freedom of the final dynamic model.

FLUTTER ANALYSIS

A flutter analysis was conducted to determine the decay rate (damping) of oscillatory motion at the flight test frequencies. Two forms of the flutter equation were utilized; the p method, in which the aerodynamic matrices are written as an explicit function of p, the differential operator, and the p-k method, in which the aerodynamic matrices are implicit functions of k, the reduced frequency. Both of these methods yield a solution which represents a true rate of decay damping value, although for the p-k method it is an approximation. This allows a direct comparison between analytical results and in-flight test data. The traditional k method gives a solution which can be interpreted as the amount of structural damping which must be added in order to maintain harmonic motion. This is markedly different from a decay rate solution, and for that reason was not used for this study.

The p-k formulation of the flutter equation is as follows:

$$\left[[M]\frac{V^2}{b_o^2}p^2 + (1+ig_s)[K]-\tfrac{1}{2}\rho V^2[A(k)]\right]\{q\}= 0$$

The p method formulation is shown below:

$$\left[[M]p^2 + \frac{\sigma}{p+b}\left[[A_o] + p[A_1] + p^2[A_2]\right] + \frac{b_o^2}{V^2}[K]\right]\{q\} = 0$$

A thorough discussion by Hassig of the three types of equations along with a comparison of results may be found in Reference 28.

The mass, stiffness, and aerodynamic matrices of both flutter equations were transformed to generalized modal degrees of freedom, {q}, using mode shapes corresponding to the thirty lowest vibration frequencies. The frequency and damping data were calculated with Lockheed FAMAS system programs that utilize determinant iteration. For the p-k flutter solution, unsteady aerodynamic

matrices were calculated for the reduced frequencies shown in Table 11 and input to the flutter program. From the flutter solution, plots of frequencies and dampings versus velocity (V-f-g plots) were created. An example V-f-g plot is shown in Figure 43. The flutter analysis was done with no structural damping included (g_s=0). As an approximation to obtain the true modal damping, structural damping can be added to the solution for the damping which was obtained from the flutter analysis. The structural damping was 0.03 for the two modes lowest in frequency and 0.05 for the next three modes, these values being obtained from ground vibration test data. Table 12 presents a comparison between the damping obtained from the flutter analysis and the damping obtained from the flight test data for the appropriate test point. The analytical results for cases 2 and 5, which used slender/interference body modeling, were clearly incorrect, indicating a problem with the NASTRAN program. These results are not included in the table. Also left out are the results for mode 4, since the analytical model showed several modes in that frequency range but none that agreed with the observed mode shape.

FREQUENCY RESPONSE

To obtain the frequency response data it was required that two types of dynamic equations be used. The first type, "k-method," had aerodynamics as formulated for the p-k method in the flutter analysis. The second type, "p-method," was the same as in the p-method flutter solution. Both equations solved for the resonant response of the structure due to a harmonically oscillating forcing function at a given frequency. Since the test frequencies were arrived at by processing response data which was generated by a frequency sweep forcing function, these points do not correspond exactly to the frequency values at the response peaks. Because the responses were measured with the forcing function holding at each of these frequencies, the test data is directly comparable to the analytical results, although the points will not necessarily fall on the peaks of the response plots.

For the k-method aerodynamics, the frequency response equation is:

$$\left[(1+ig_s)[K] - \omega^2[M] - \tfrac{1}{2}\rho V^2[A(k)]\right]\{q\} = \{F(\omega)\}$$

For the p-method aerodynamics, the equation is:

$$\left[p^2\frac{V^2}{b_o^2}[M] + \frac{V^2}{b_o^2}\left(\frac{\sigma}{p+b}\right)\left[p^2[A_2] + p[A_1] + [A_0]\right] + (1+ig_s)[K]\right]\{q\} = \{F(p)\}$$

Both equations were solved with Lockheed FAMAS system programs. The forcing function was derived from flight test strain gage data - the total shaker vane load being plotted against frequency for each flight test point. From this data it was possible to fit several curves so that the force could be expressed as a function of frequency. A plot of the force level versus frequency for the Mach 2.0 flight test point is shown in Figure 44.

The FAMAS programs resulted in plots of the acceleration response and phase angle for the frequency range of 0.1 to 20 Hertz. As an example, a

graphical comparison of the analytical results and the test data for case 9 (Piston theory, Mach 2.0) is presented in Figures 45 and 46. These show, respectively, the magnitude (g) and phase (degrees) for the cockpit and outer wing accelerations, with respect to shaker vane force, plotted versus frequency (Hertz). The complete set of response plots, for all cases except the doublet lattice with slender and interference body effects (DLSLIN), is included in the Appendix. Due to errors in the NASTRAN program, DLSLIN aerodynamics yielded results which were obviously non-physical. This may be due to the linear spline program in NASTRAN, which contains a known error. Therefore, results from doublet lattice with slender and interference body effects are not included.

A summary of the frequency response results for all cases except the DLSLIN aerodynamics is shown in Table 13. This table is meant to give a qualitative interpretation of the results. Each case has been divided into a low and high frequency range. A comparison of the analysis with test results for both magnitude and phase was then made. For the magnitude, a check (✓) indicates that the analysis matched the experimental results within approximately $\pm$5%. For the phase angle, a check indicates agreement within about $\pm$10 degrees. A negative sign (-) indicates that the analysis value was less than the experimental value; a plus sign (+) indicates the analytical value was greater. An overall impression of the comparison between test and analysis can then be obtained for each of the aerodynamic methods.

CONCLUSIONS

This investigation allowed an evaluation of analytical methods in three different areas - structural modeling, structure/aerodynamic interconnection, and aerodynamic modeling. The rest of the discussion is divided along these lines.

Structural Model (NASTRAN)

The NASTRAN finite-element structural model was previously found to give good correlation with ground vibration test results (Reference 11). Since the structural and inertia modeling for the present study was substantially the same, analytical vibration results for the free-free airplane should correlate well with the actual vehicle, although test data for this condition at zero airspeed is impossible to obtain. There is probably some error due to structural modeling which is observable in the data from Table 12 for the three higher frequency modes. Analytically, mode 3 usually had a lower frequency than the test results, and mode 5 had a higher one. The analytical results for mode 4 did not agree with observed test results, probably due to the presence in the analysis of three other modes which were very close in frequency. When several modes exist within a narrow frequency band, in either the test vehicle or the analytical model, there may be difficulty in correlation. In general, however, the NASTRAN finite-element model appears to describe the dynamic behaviour adequately for a preliminary design effort.

Structure/Aerodynamic Interconnection

The NASTRAN surface spline was used for transforming forces to the structure for all of the aerodynamic methods except slender body theory, which used a linear spline. Caution must be exercised in order to achieve satisfactory results with the surface spline. Experimentation with different configurations showed that the best results were obtained when several splines, each covering a small area of the planform, were used. This assures that an aerodynamic load is not lumped at a distant structural point, and results in a transformation which makes more physical sense. This process requires that some engineering judgement be used in defining the splines. Using a large number of splines is not a problem since it is within the capability of NASTRAN to use many splines for the

aerodynamic/structural interface. A useful check of the spline matrix, [GTKA], can be made by postmultiplying the transpose of the matrix by a column vector which represents a unit pitch motion in the dynamic model degrees of freedom. The resulting column matrix should give the corresponding deflections for unit pitch motion at the aerodynamic degrees of freedom. This is a necessary, but not sufficient, condition in order to obtain acceptable results. Careful application of the surface spline technique to a specific problem will achieve this objective.

The linear spline, however, does not give acceptable results in the COSMIC version of NASTRAN. Load distributions using this method summed to the correct totals, but were clearly incorrect. A small aeroelastic model, much simpler than the YF-12A, was constructed in order to verify that the problem was with the NASTRAN program. This was found to be the case. No attempt was made to correct the NASTRAN program for this problem.

Aerodynamic Models

The same structural model and same type of structure/aerodynamic transformation were used for each of six distinct aerodynamic methods, thus allowing a comparison of theory and experiment based on flutter and frequency response results. For the subsonic cases, since more than one method was used for the same Mach number, the theories may be compared to each other regarding their accuracy.

Subsonically, the results were generally better for Mach .95 than for Mach .70. The results for the DLSLIN method were totally unacceptable, but, as previously stated, the error may have been due solely to the linear spline module in COSMIC NASTRAN. Results using the steady state kernel function with uniform lag for Mach .95 were also poor, although much better than with the DLSLIN method. Steady state doublet lattice with uniform lag actually gave better results than did the complete doublet lattice aerodynamic matrices. This was true for both the modal damping and the frequency response comparison - both of these methods improved at the higher Mach number. This suggests that using the uniform lag function with the steady state doublet lattice aerodynamics may be a cost-effective means of generating the unsteady aerodynamics, especially in a preliminary design environment. For this method, only the aerodynamic matrix for a reduced frequency of zero need be produced; whereas,

for the usual approach with doublet lattice, a matrix for each reduced frequency is required. This could result in considerable savings in computation costs.

Supersonically, both the Mach box and piston theory gave good results, with the exception of the Mach 2.7 piston theory flutter analysis, where the analytical modal dampings and frequencies were only marginally acceptable. The agreement between analysis and flight test was actually better than anticipated considering the lift distributions for pitching motion of the aircraft for these cases (Figures 39, 41, 42). Applying these aerodynamic influence coefficients to the structure did, however, yield satisfactory flutter and frequency response results.

On the basis of the present investigation, either the standard doublet lattice method or the steady state doublet lattice with uniform lag function gives adequate results for a preliminary design study in the subsonic regime. For the supersonic case, either the Mach box or piston theory may be used, the choice depending on Mach number. The accepted range for Mach box aerodynamic theory is Mach 1.2 to 3.0. Piston theory usually is thought to be valid for the Mach 2.5 to 7.0 range. The present YF-12A study indicates that the Mach box method be used for Mach numbers 1.2 to 2.0, with piston theory used for all higher Mach numbers.

TABLE 1. CANARD VANE OPERATING CHARACTERISTICS

PARAMETER	RANGE
OSCILLATING FREQUENCY RANGE	0.1 TO 29.9 Hz
INCREMENTAL ADJUSTMENT	0.1 Hz
CANARD ANGULAR DISPLACEMENT	± 12 DEG. 50% MODULATION 0.1 TO 8.0 Hz
	± 1 DEG. 5% MODULATION 0.1 TO 29.9 Hz
INCREMENTAL ADJUSTMENT	1%
BIAS TRIM ADJUSTMENT	± 12 DEG. (CONTINUOUSLY VARIABLE)

TABLE 2. AIRFRAME RESPONSE MEASUREMENTS

PARAMETER DESIGNATION	DESCRIPTION	LOCATION			
		FUSELAGE STATION	BUTT LINE	WATER LINE	FIN STATION
A4001	CENTER OF GRAVITY VERTICAL	915.0	0.0	—	
A4004	COCKPIT VERTICAL	310.0	0.0	—	
A4019	NOSE VERTICAL	100.0	0.0	85.0	
A4028	LEFT FWD. MISSLE BAY VERTICAL	523.0	21.2L	92.5	
A4029	LEFT AFT MISSLE BAY VERTICAL	682.5	21.2L	94.7	
A4030	TAIL CONE VERTICAL	1258.9	1.6R	93.8	
A4031	LEFT OUTER WING VERTICAL	1135.4	247.5L	97.2	
A4032	LEFT INNER WING VERTICAL	1140.2	106.9L	93.7	
A4033	RIGHT OUTER WING VERTICAL	1135.4	247.5R	97.2	
A4034	RIGHT INNER WING VERTICAL	1140.2	106.9R	93.7	
LCWLACC	LEFT ENGINE NACELLE VERTICAL	818.0	206.0L	95.0	
RCWLACC	RIGHT ENGINE NACELLE VERTICAL	818.0	206.0R	95.0	
LRUDACC	LEFT RUDDER NORMAL	1142.0	—	—	88.9
RRUDACC	RIGHT RUDDER NORMAL	1142.0	—	—	88.9

TABLE 3. CANARD SHAKER VANE VIBRATION FREQUENCIES AND MODE SHAPES

MODE	FREQUENCY - Hz		SHAKER LOCATION	DESCRIPTION	FIGURE NO. OF MODAL PLOT
	ANALYSIS	TEST			
SYMMETRIC					
1	42.89	32.26 RH	1L, 1R	FIRST BENDING	15
2	-	46.74	2L, 2R	MODE SHAPE SIMILAR TO TORSION. MODAL AMPLITUDE APPROX. 1/3 THAT OF REAL TORSION.	-
3	61.17	60.91	2L, 2R	MODAL RESPONSE BARELY ABOVE NOISE LEVEL	-
4	70.93	79.60 LH 80.27 RH	2L, 2R	FIRST TORSION	16
ANTISYMMETRIC					
1	-	38.60	2L, 2R	FIRST BENDING	17
2	-	86.50	2L, 2R	FIRST TORSION	18

TABLE 4. SUMMARY - YF-12A CANARD EXCITER VANE FLIGHT TEST PROGRAM

TEST SUMMARY

FLIGHT NO.	ID	DATE	TEST POINT	MACH NUMBER	KEAS	NOTES
1	935-137	11-22-78	1	0.70	400	SYSTEM CHECKOUT
			2	0.95	400	
2	935-138	12-1-78	1	0.70	400	SYSTEM CHECKOUT. USED
			2	0.95	400	SPECTRUM ANALYZER FOR ON LINE DATA REDUCTION
3	935-139	1-24-79	1	0.70	400	PITCH SAS OFF
			2	0.70	360	
			3	0.70	330	
			4	0.95	400	
			5	0.95	360	
			6	0.95	330	
			7	1.25	400	
			8	1.25	360	
4	935-140	2-16-79	1	2.00	400	PITCH SAS ON
			2	2.00	360	PITCH SAS ON
			3	2.00	330	PITCH SAS ON
			4	1.25	330	PITCH SAS OFF
5	935-141	3-8-79	1	2.00	400	PITCH SAS ON
			2	2.70	400	PITCH SAS OFF
			3	2.70	336	
			4	2.00	-	SYSTEM SHUTDOWN. NO TEST
6	935-142	3-15-79	1	2.00	400	PITCH SAS ON
			2	2.70	400	PITCH SAS OFF
			3	2.70	345 TO 338	DIFFICULTY HOLDING KEAS
			4	2.00	330	

TABLE 5. VANE GROUND TEST PROGRAM

TEST TYPE	TEST ITEM	PURPOSE
LOAD - DEFLECTION	VANE INSTALLATION	CALIBRATION - SAFETY SYSTEM
GROUND VIBRATION	VANE INSTALLATION	VERIFICATION - FLUTTER ANALYSIS
GROUND VIBRATION	AIRPLANE	VERIFICATION - AIRFRAME RESPONSE

TABLE 6. YF-12A SYMMETRIC VIBRATION - MODE AND FREQUENCY COMPARISON

MODE	NASA TM X-2880 TEST (Hz)	18 JAN 1979 CHECK TEST (Hz)	MODE DESCRIPTION
1	3.40	3.50	FIRST WING - FUSELAGE BENDING
2	4.10	4.20	SECOND WING - FUSELAGE BENDING
3	6.70	6.55	THIRD WING - FUSELAGE BENDING
4	8.10	7.80	FOURTH WING - FUSELAGE BENDING
5	8.70	-	RUDDER - FIRST BENDING
6	10.50	10.45	OUTER WING - FIRST BENDING
7	12.20	12.40	OUTER WING - OUTBOARD ELEVON

TABLE 7. SUMMARY OF NASTRAN PROGRAM ERRORS

PROBLEM AREA	SOLUTION
USER TAPES (INPUTI MODULE)	PROGRAM CORRECTION MADE
USER TAPES (OUTPUTI MODULE)	PROGRAM CORRECTION MADE
LINEAR SPLINE	NO ALTERNATIVE PROGRAM
DLSLIN AERODYNAMICS	NO ALTERNATIVE PROGRAM
MACH BOX AERODYNAMICS	USE LOCKHEED FAMAS PROGRAM
PISTON THEORY AERODYNAMICS	PROGRAM CORRECTION MADE
P-K FLUTTER ANALYSIS	USE LOCKHEED FAMAS PROGRAM

TABLE 8. YF-12A SUBSTRUCTURE DEGREES OF FREEDOM

SUBSTRUCTURE	NO. OF GRID AND SCALAR POINTS	NO. DOF REMOVED			NO. DOF RETAINED FOR COUPLING
		SPC	MPC	GUYAN REDUCTION	
1	651	1777	20	1361	748
2	491	1322	35	864	725
3	302	866	126	600	220
4	581	1726	252	1114	389
5	620	1568	142	1667	338
6	307	951	148	604	124
TOTAL	2952	8210	723	6210	2544

TABLE 9. FUEL TANK LOADINGS (LBS.)

INERTIA CASE	TANK 1	TANK 2	TANK 3	TANK 4	TANK 5	TANK 6
W1	2400	2800	9750	8800	14200	12200
W2	3650	0	9500	2380	8000	10620
W3	750	0	2750	650	1250	11350
W4	350	350	9950	5050	12750	12400
W5	300	300	9950	1200	7500	12400

TABLE 10. YF-12A AERODYNAMIC CASES

b = 226.67 IN. FOR ALL K's

CASE	MACH	KEAS	INERTIA	AERODYNAMIC MODEL	FLIGHT #	TEST POINT	REDUCED FREQUENCY
1	0.70	400	W1	DOUBLET LATTICE	935-139	1	0.3738
2	0.70	400	W1	DOUBLET LATTICE, SLENDER BODY, INTERFERENCE BODY	935-139	1	0.5115 0.8149
3	0.70	400	W1	DOUBLET LATTICE, STEADY STATE WITH UNIFORM LAG	935-139	1	1.2114 1.4998
4	0.95	400	W2	DOUBLET LATTICE	935-139	4	
5	0.95	400	W2	DOUBLET LATTICE, SLENDER BODY, INTERFERENCE BODY	935-139	4	0.3110 0.3940
6	0.95	400	W2	DOUBLET LATTICE, STEADY STATE WITH UNIFORM LAG	935-139	4	0.6855 1.016
7	0.95	400	W2	KERNEL FUNCTION, STEADY STATE WITH UNIFORM LAG	935-139	4	1.2573
8	1.25	400	W3	MACH BOX	935-139	7	0.2614 0.5661 0.3261 0.8746 1.1303
9	2.00	400	W4	PISTON THEORY	935-142	1	0.157 0.194 0.342 0.511 0.657
10	2.70	400	W5	PISTON THEORY	935-142	2	0.116 0.167 0.257 0.393 0.409

TABLE 11. YF-12A REDUCED FREQUENCIES

MACH	FREQUENCY	REDUCED FREQUENCY
0.70	0.0 2.42 3.28 5.25 7.97 9.76	0.0 0.3738 0.5115 0.8149 1.2114 1.4998
0.95	0.0 2.55 3.16 5.57 8.33 10.51	0.0 0.3110 0.3940 0.6855 1.016 1.2573
1.25	0.0 2.68 3.38 5.84 8.82 11.60	0.0 0.2614 0.5661 0.3261 0.8746 1.1303
2.00	0.0 2.56 3.18 5.56 8.33 10.71	0.0 0.157 0.194 0.342 0.511 2.0
2.70	0.0 2.56 3.70 5.64 8.61 9.02	0.0 0.116 0.167 0.257 0.393 0.409 2.0

TABLE 12. YF-12A FREQUENCY AND DAMPING COMPARISON, TEST VS. ANALYSIS

MACH 0.70

	MODE 1		MODE 2		MODE 3		MODE 4		MODE 5	
	FREQ	DAMP	FREQ	DAMP	FREQ	DAMP	FREQ	DAMP	FREQ	DAMP
FLIGHT TEST*	2.42	0.14 ± .01	3.28	0.09 ± .03	5.25	0.11 ± .01	7.97	0.08 ± .01	9.76	0.16 ± .05
CASE 1	2.35	0.15	3.05	0.14	5.00	0.09	–	–	10.18	0.09
CASE 2	–	–	–	–	–	–	–	–	–	–
CASE 3	2.38	0.11	3.07	0.14	5.04	0.08	–	–	10.24	0.09

MACH 0.95

	MODE 1		MODE 2		MODE 3		MODE 4		MODE 5	
	FREQ	DAMP	FREQ	DAMP	FREQ	DAMP	FREQ	DAMP	FREQ	DAMP
FLIGHT TEST	2.55	0.18 ± .03	3.16	0.11 ± .03	5.57	0.10 ± .01	8.33	0.11 ± .04	10.51	0.08
CASE 4	2.53	0.17	3.17	0.13	5.23	0.09	–	–	10.85	0.12
CASE 5	–	–	–	–	–	–	–	–	–	–
CASE 6	2.48	0.12	3.18	0.11	5.22	0.08	–	–	10.96	0.08
CASE 7	1.86	0.10	3.16	0.20	5.15	0.13	–	–	10.88	0.07

* CASE NOS. ARE DEFINED IN TABLE 10.

TABLE 12. YF-12A FREQUENCY AND DAMPING COMPARISON, TEST VS. ANALYSIS

MACH 1.25

	MODE 1		MODE 2		MODE 3		MODE 4		MODE 5	
	FREQ	DAMP	FREQ	DAMP	FREQ	DAMP	FREQ	DAMP	FREQ	DAMP
FLIGHT TEST	2.68	0.12 ± .02	3.38	0.08 ± .02	5.84	0.11 ± .02	8.82	0.07 ± .01	11.60	0.11
CASE 8	2.70	0.05	3.28	0.08	5.54	0.06	–	–	11.28	0.07

MACH 2.0

	MODE 1		MODE 2		MODE 3		MODE 4		MODE 5	
	FREQ	DAMP	FREQ	DAMP	FREQ	DAMP	FREQ	DAMP	FREQ	DAMP
FLIGHT TEST	2.56	0.07 ± .01	3.18	0.09 ± .01	5.56	0.06 ± .01	8.33	0.07 ± .02	10.71	0.11 ± .04
CASE 9	2.56	0.05	3.06	0.07	5.38	0.07	–	–	10.68	0.07

MACH 2.7

	MODE 1		MODE 2		MODE 3		MODE 4		MODE 5	
	FREQ	DAMP	FREQ	DAMP	FREQ	DAMP	FREQ	DAMP	FREQ	DAMP
FLIGHT TEST	2.56	0.06 ± .01	3.70	–	5.64	0.07 ± .02	8.61	0.10 ± .02	9.02	0.09 ± .01
CASE 10	2.59	0.03	3.12	0.05	5.4	0.06	–	–	11.08	0.06

TABLE 13. YF-12A FREQUENCY RESPONSE SUMMARY

✓ ANALYSIS vs TEST SATISFACTORY
\+ ANALYSIS vs TEST HIGH
– ANALYSIS vs TEST LOW
L LOW FREQUENCY
H HIGH FREQUENCY

	NOSE	COCKPIT	FWD MIS BAY	AFT MIS BAY	C.G.	TAIL	OUTER WING	INNER WING	NACELLE	RUDDER
CASE 1	DOUBLET LATTICE M = 0.70									
MAG_L	✓	✓	✓	✓	–	–	–	–	–	–
MAG_H	–	–	–	✓	–	–	–	–	–	–
$PHASE_L$	✓	✓	✓	✓		+	✓	✓	✓	✓
$PHASE_H$	+	✓	+	+	✓	+	+	+	✓	+
CASE 2	DOUBLET LATTICE WITH SLENDER AND INTERFERENCE BODIES M = 0.70									
CASE 3	DOUBLET LATTICE, STEADY STATE WITH UNIFORM LAG M = 0.70									
MAG_L	✓	✓	✓	✓	–	–	–	–	✓	–
MAG_H	–	✓	–	✓	–	–	–	–	–	–
$PHASE_L$	✓	✓	✓	✓		✓	✓	✓	✓	✓
$PHASE_H$	+	✓	+	+	✓	+	+	+	✓	+
CASE 4	DOUBLET LATTICE M = 0.95									
MAG_L	✓	✓	✓	✓	–	–	–	–	–	–
MAG_H	–	✓	✓	✓	–	–	✓	–	✓	–
$PHASE_L$	✓	✓	✓	✓	–	✓	✓	✓	✓	✓
$PHASE_H$	+	✓	+	+	✓	+	+	+	✓	+
CASE 5	DOUBLET LATTICE WITH SLENDER AND INTERFERENCE BODIES M = 0.95									
CASE 6	DOUBLET LATTICE, STEADY STATE WITH UNIFORM LAG M = 0.95									
MAG_L	✓	✓	✓	✓	–	✓	–	✓	–	✓
MAG_H	–	✓	✓	✓	✓	✓	✓	–	✓	–
$PHASE_L$	✓	✓	✓	✓	✓	✓	✓	✓	✓	✓
$PHASE_H$	+	✓	+	+	✓	+	✓	+	✓	+

TABLE 13. YF-12A FREQUENCY RESPONSE SUMMARY

✓ ANALYSIS vs TEST SATISFACTORY
\+ ANALYSIS vs TEST HIGH
– ANALYSIS vs TEST LOW
L LOW FREQUENCY
H HIGH FREQUENCY

	NOSE	COCKPIT	FWD MIS BAY	AFT MIS BAY	C.G.	TAIL	OUTER WING	INNER WING	NACELLE	RUDDER
CASE 7	KERNEL FUNCTION, STEADY STATE WITH UNIFORM LAG M = 0.95									
MAG_L	–	✓	+	+	+	–	+	✓	–	+
MAG_H	–	–	–	–	–	✓	✓	–	✓	–
$PHASE_L$	✓	–	✓	+	✓	✓	✓	–	–	✓
$PHASE_H$	+	✓	+	+	✓	+	+	✓	✓	+
CASE 8	MACH BOX, M = 1.25									
MAG_L	✓	✓	✓	✓	✓	✓	✓	✓	✓	✓
MAG_H	–	✓	✓	✓	✓	✓	✓	✓	✓	–
$PHASE_L$	✓	✓	✓	✓	✓	✓	✓	✓	✓	✓
$PHASE_H$	+	✓	+	+	✓	+	+	+	✓	+
CASE 9	PISTON THEORY M = 2.0									
MAG_L	✓	✓	✓	✓	✓	✓	–	✓	✓	✓
MAG_H	✓	✓	–	–	–	–	–	–	✓	–
$PHASE_L$	✓	✓	✓	+	✓	✓	✓	✓	✓	✓
$PHASE_H$	+	✓	+	+	✓	+	+	+	✓	+
CASE 10	PISTON THEORY M = 2.7									
MAG_L	✓	✓	✓	✓	✓	✓	✓	✓	✓	–
MAG_H	✓	✓	✓	–	✓	✓	✓	–	✓	–
$PHASE_L$	✓	✓	+	✓	✓	✓	✓	✓	✓	✓
$PHASE_H$	+	✓	+	+	✓	✓	✓	✓	✓	✓

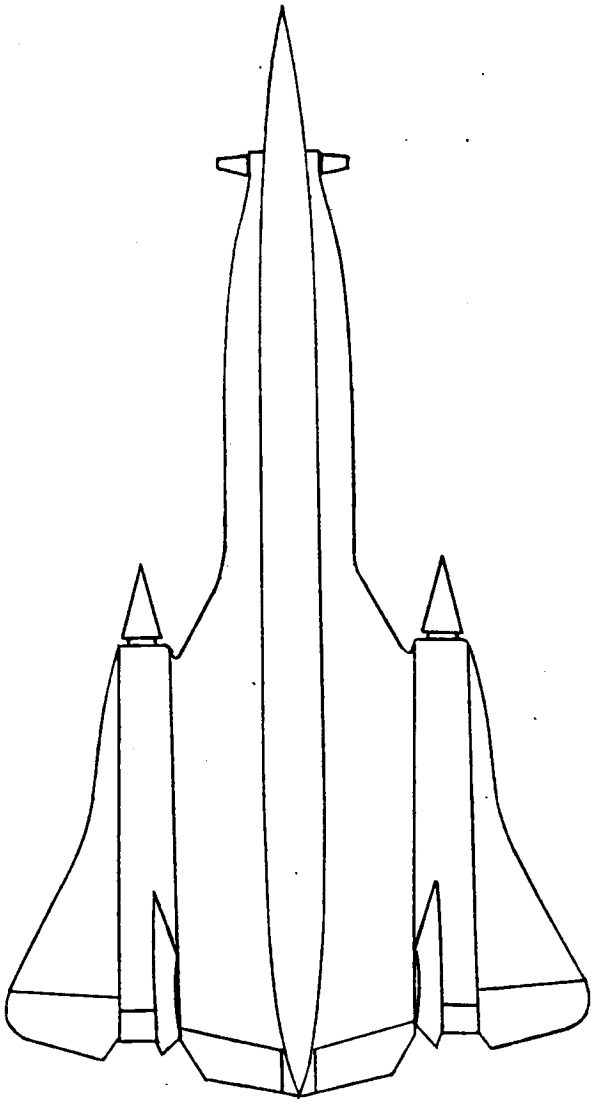

Figure 1. YF-12A Aircraft with Canard Exciter Vane

YF-12 SHAKER VANE INSTALLATION

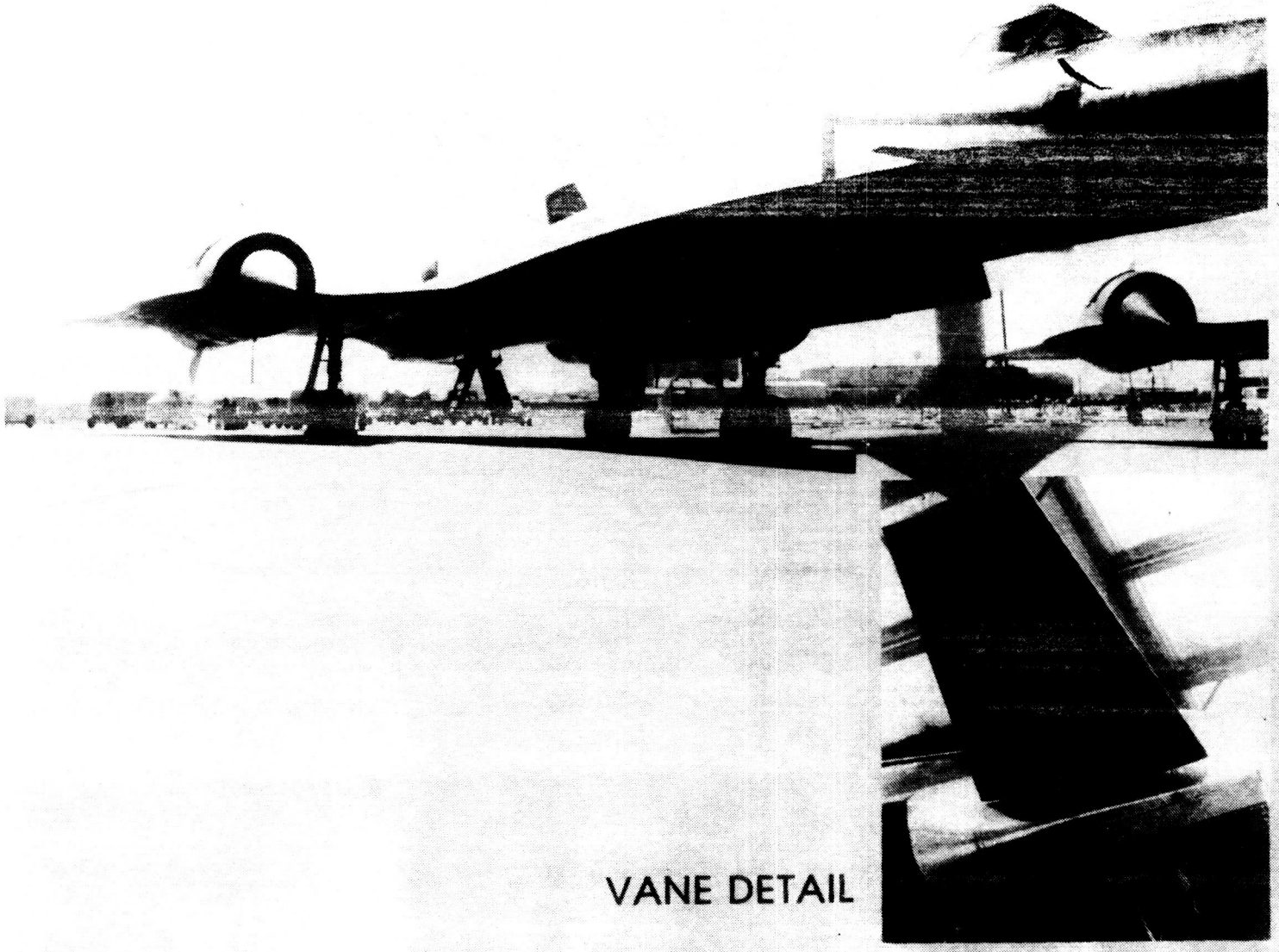

Figure 2. YF-12A with Canard Exciter Vane

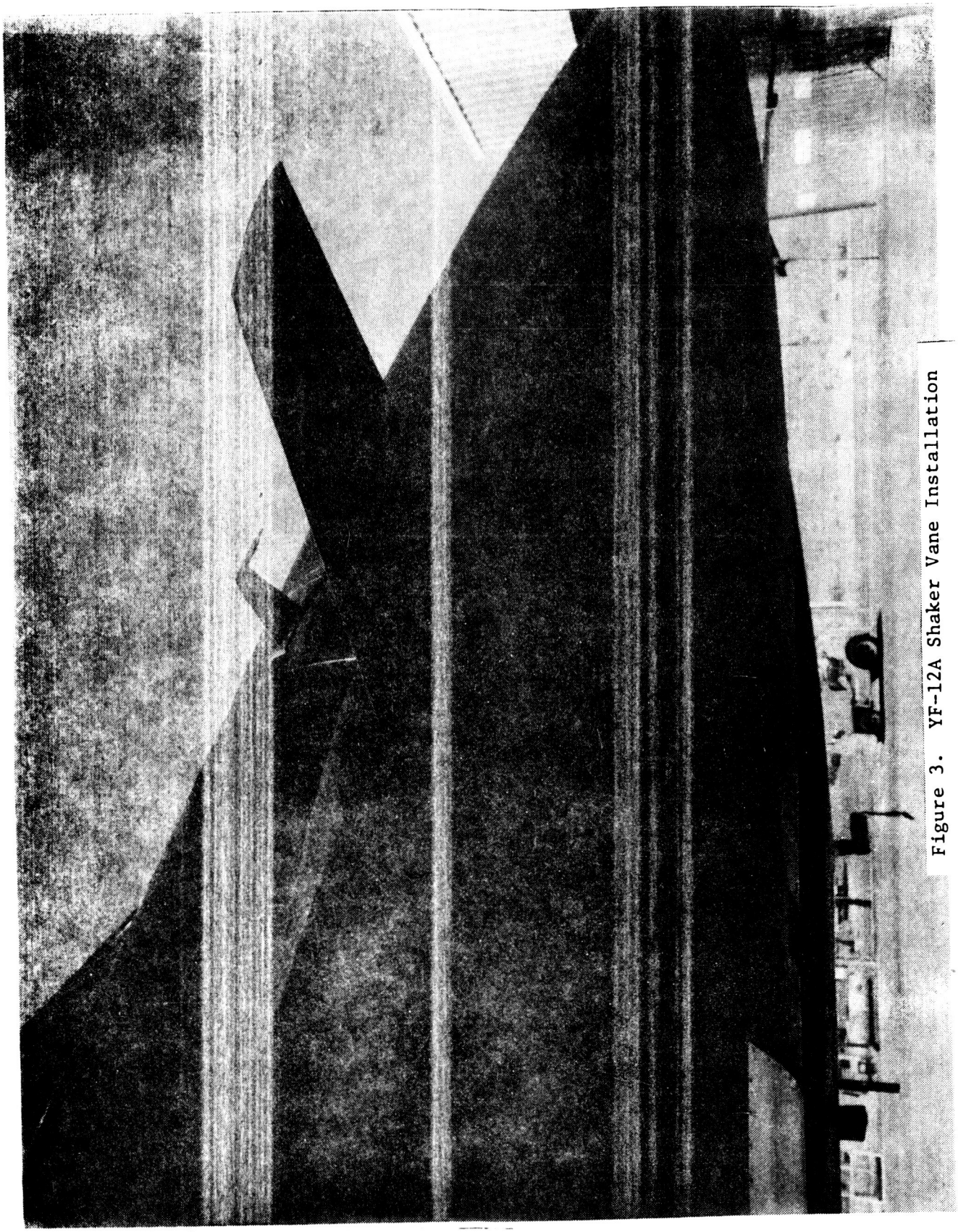

Figure 3. YF-12A Shaker Vane Installation

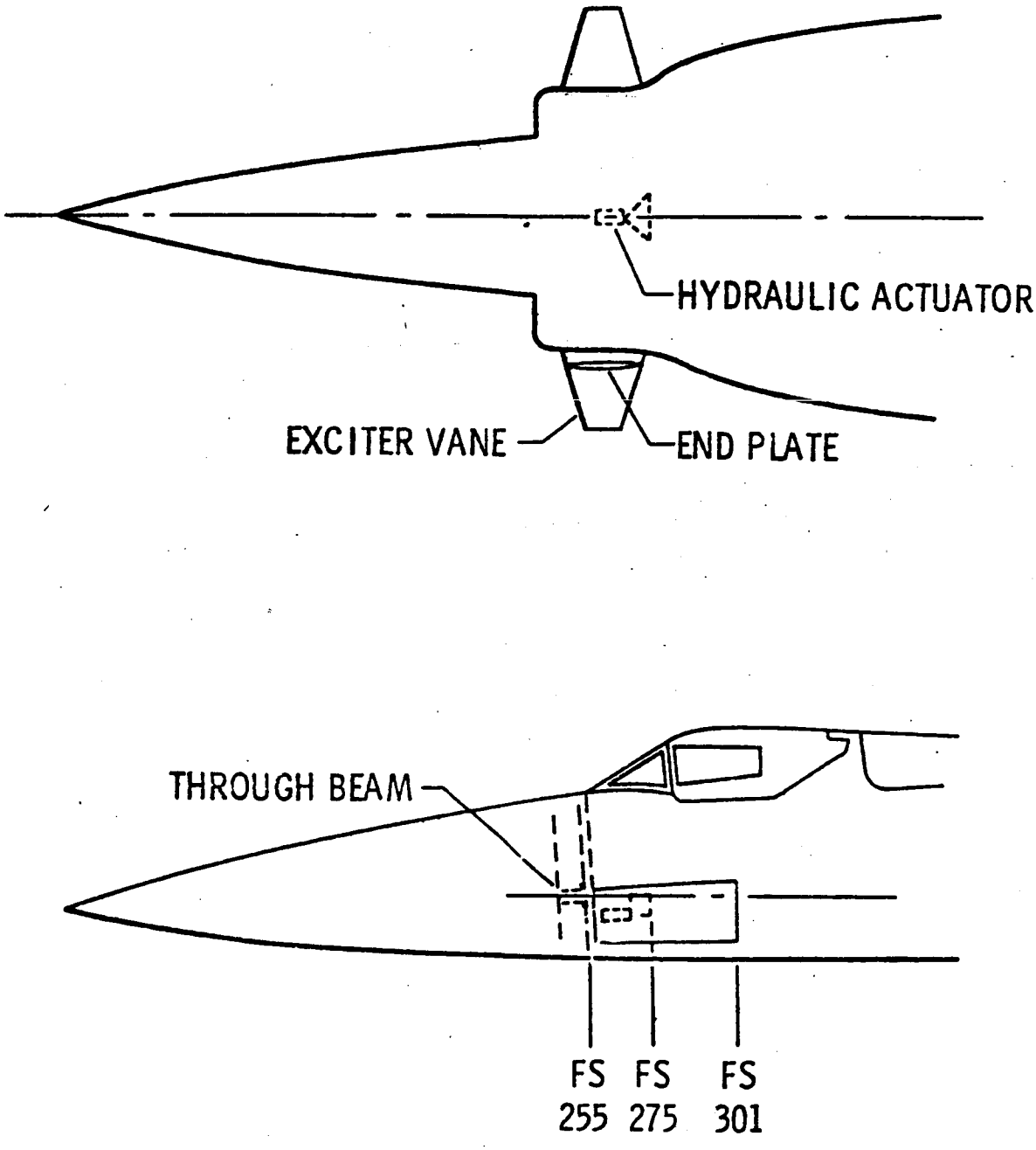

Figure 4. Canard Exciter Vane Installation

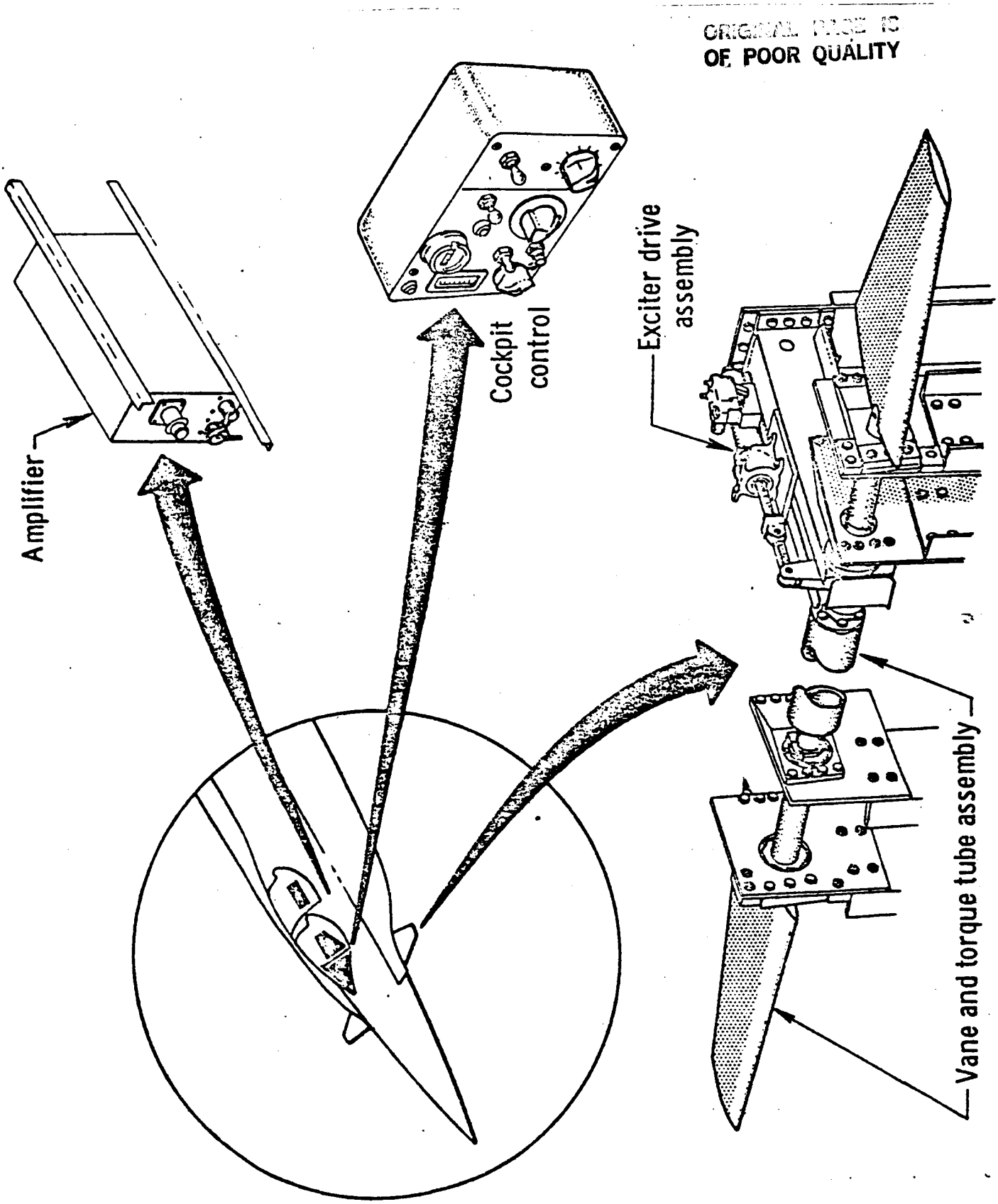

Figure 5. YF-12A Exciter Vane Assembly

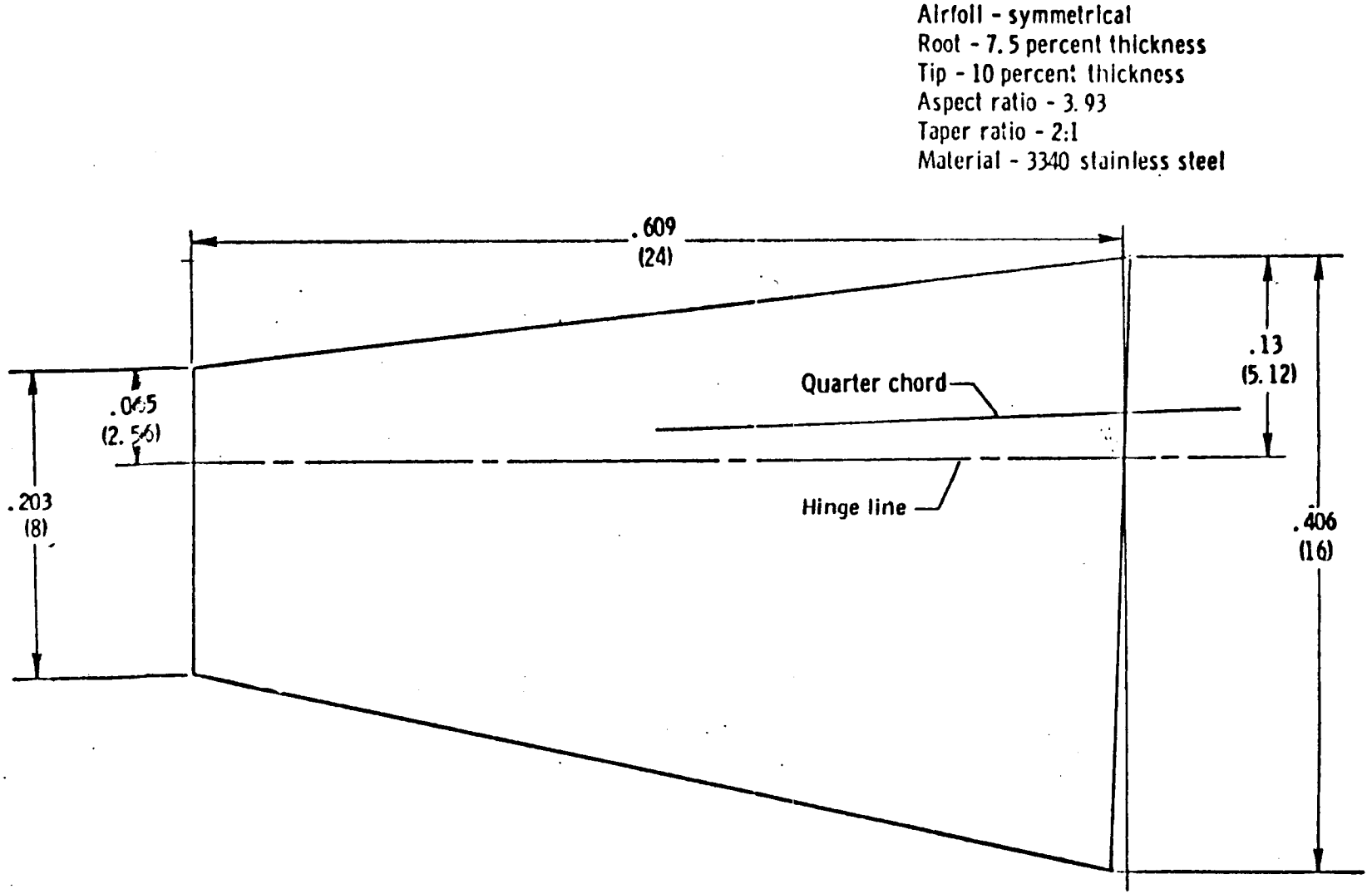

Physical dimensions, meters (inches).

Figure 6. Exciter Vane Planform

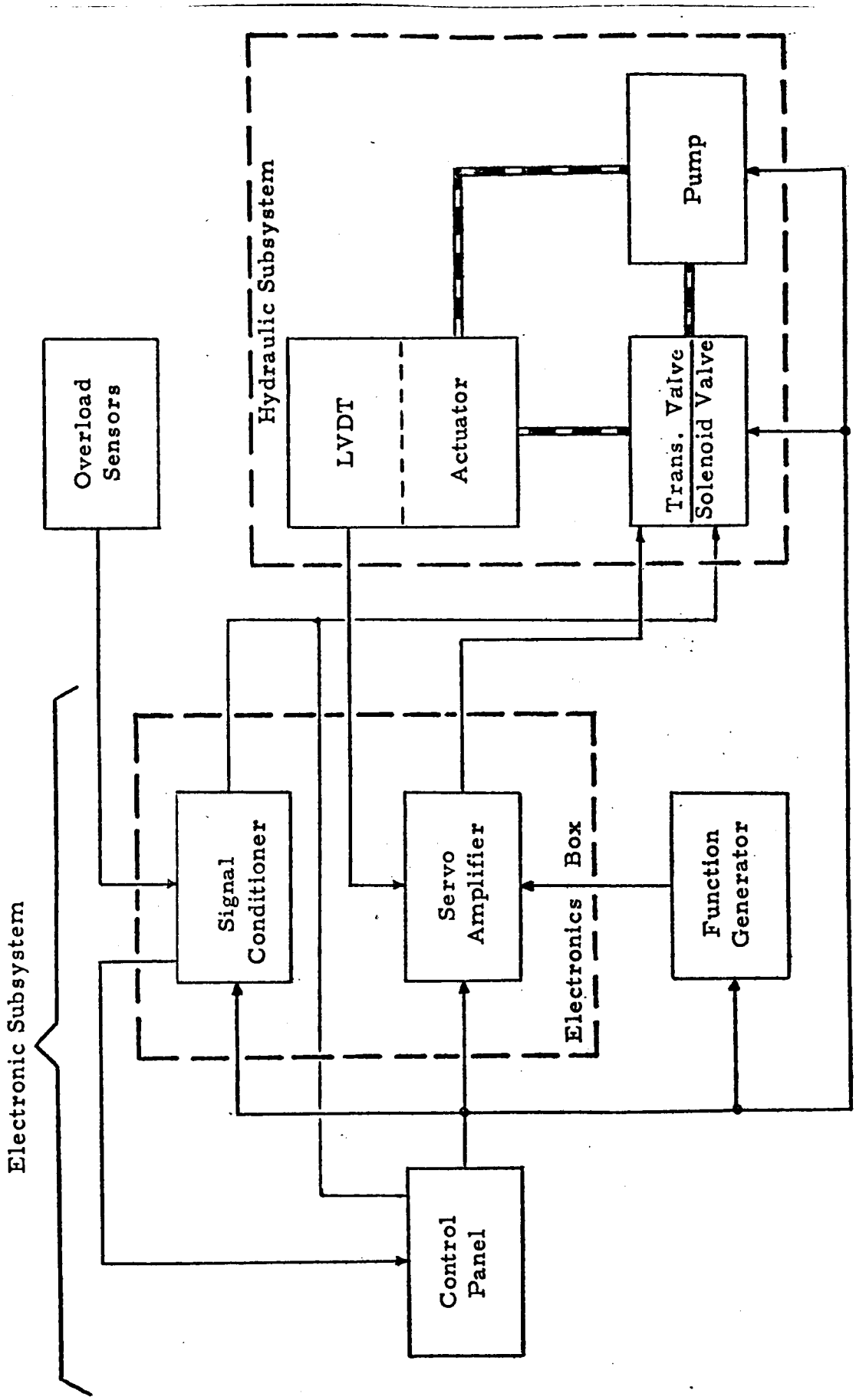

Figure 7. YF-12A Shaker Vane System Block Diagram

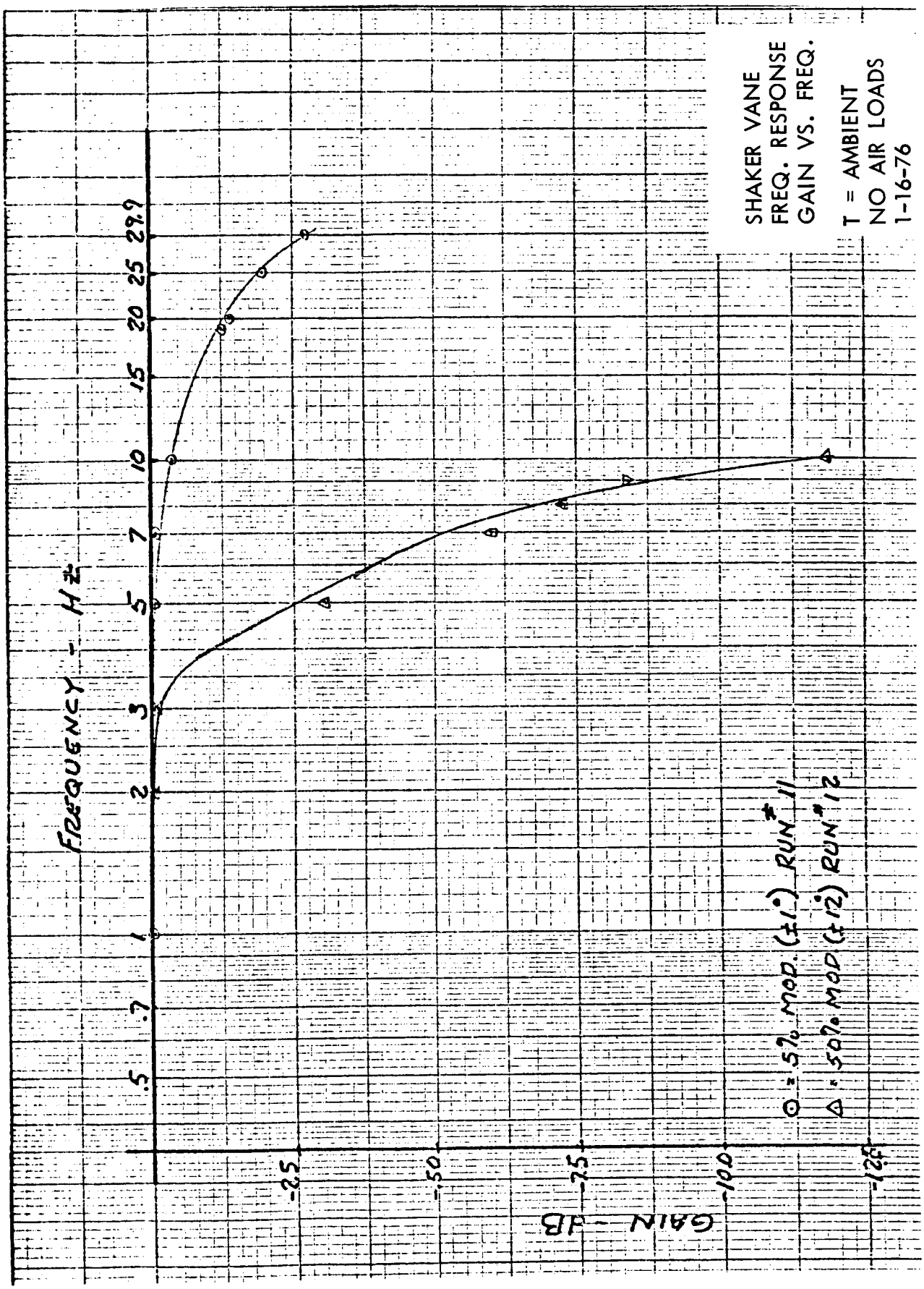

Figure 8. Final Shaker Vane Frequency Response Test, Gain vs. Frequency, Temperature Ambient

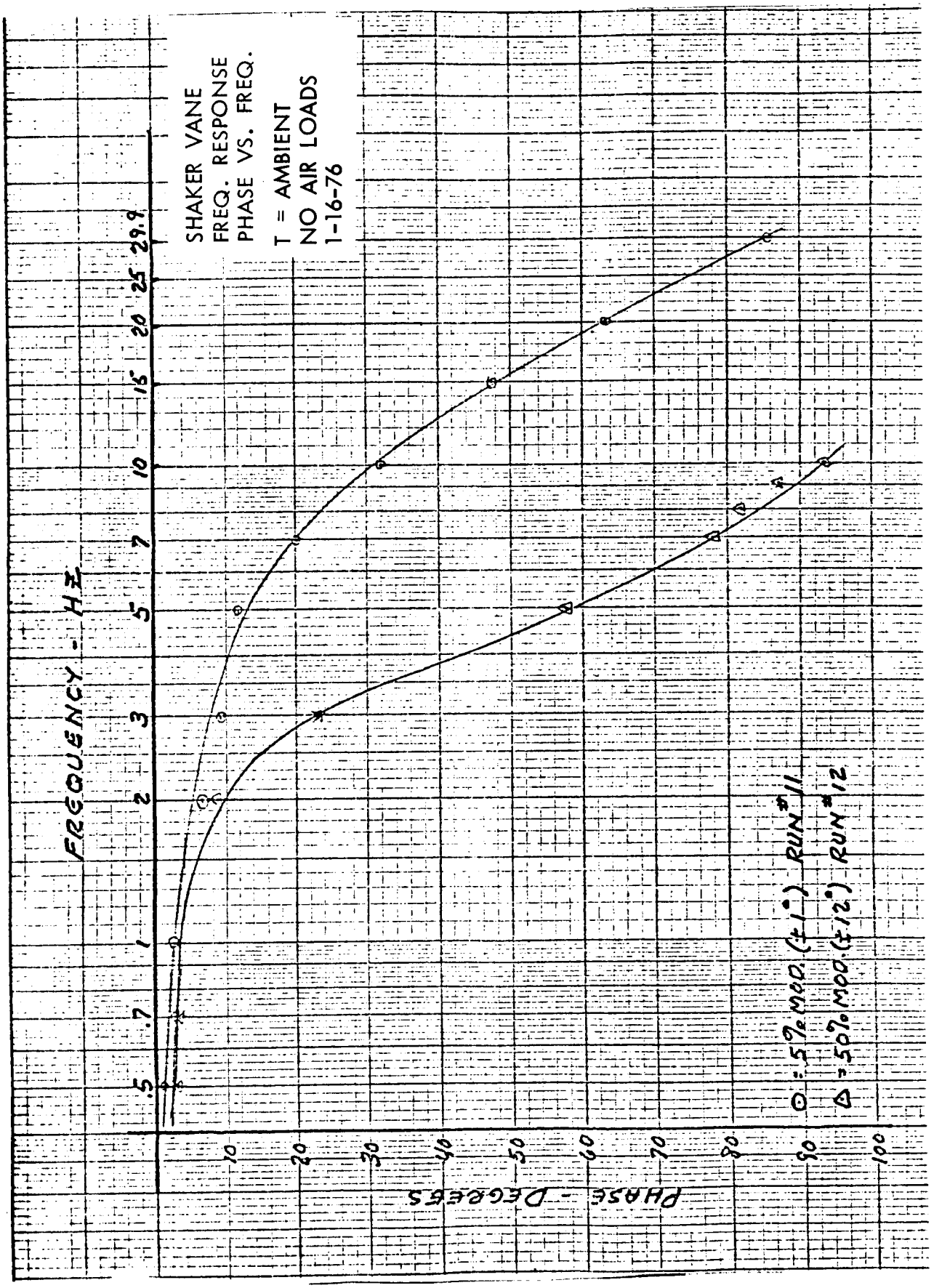

Figure 9. Final Shaker Vane Frequency Response Test, Phase vs. Frequency, Temperature Ambient

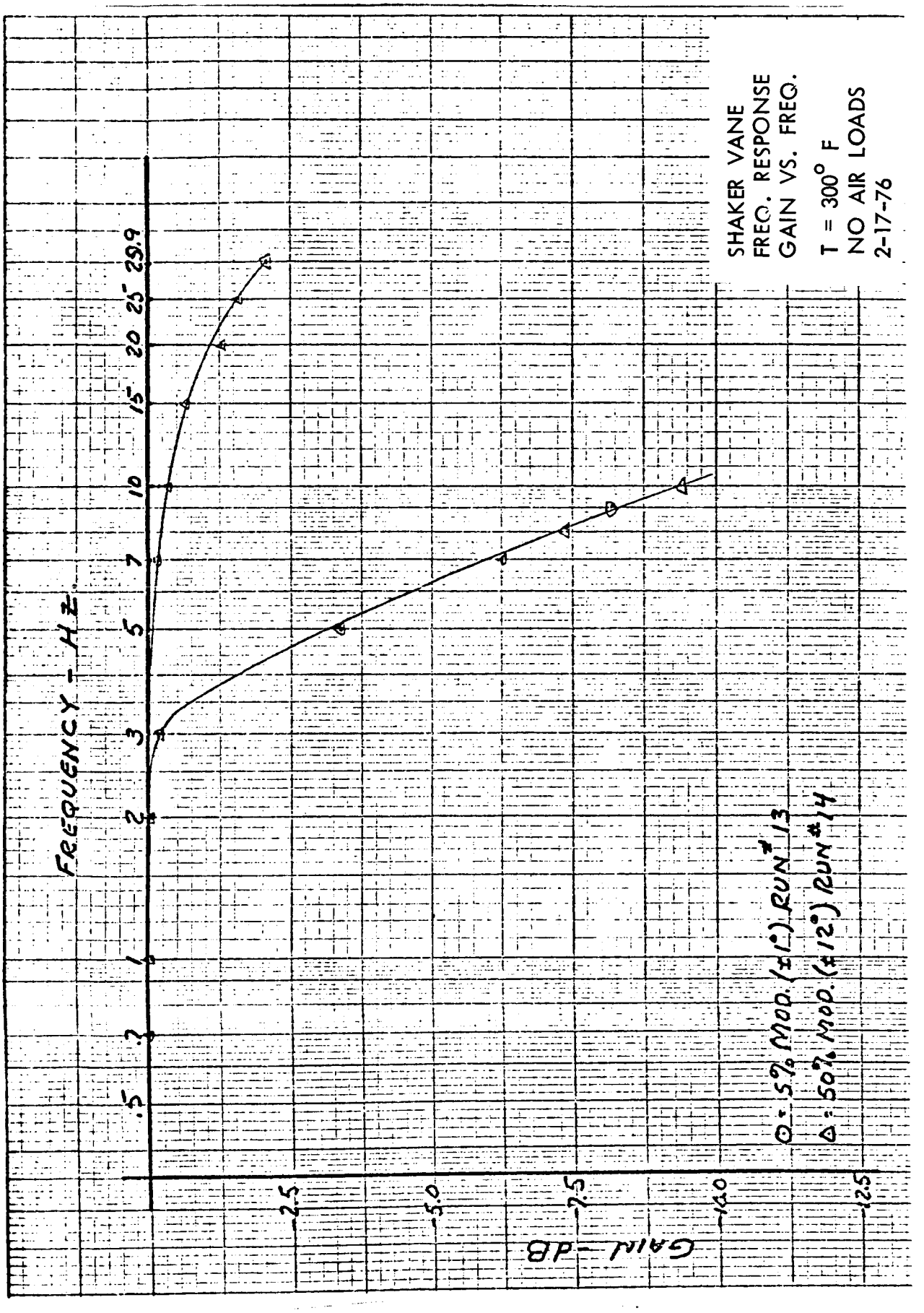

Figure 10. Final Shaker Vane Frequency Response Test, Gain vs. Frequency, Temperature 300°F

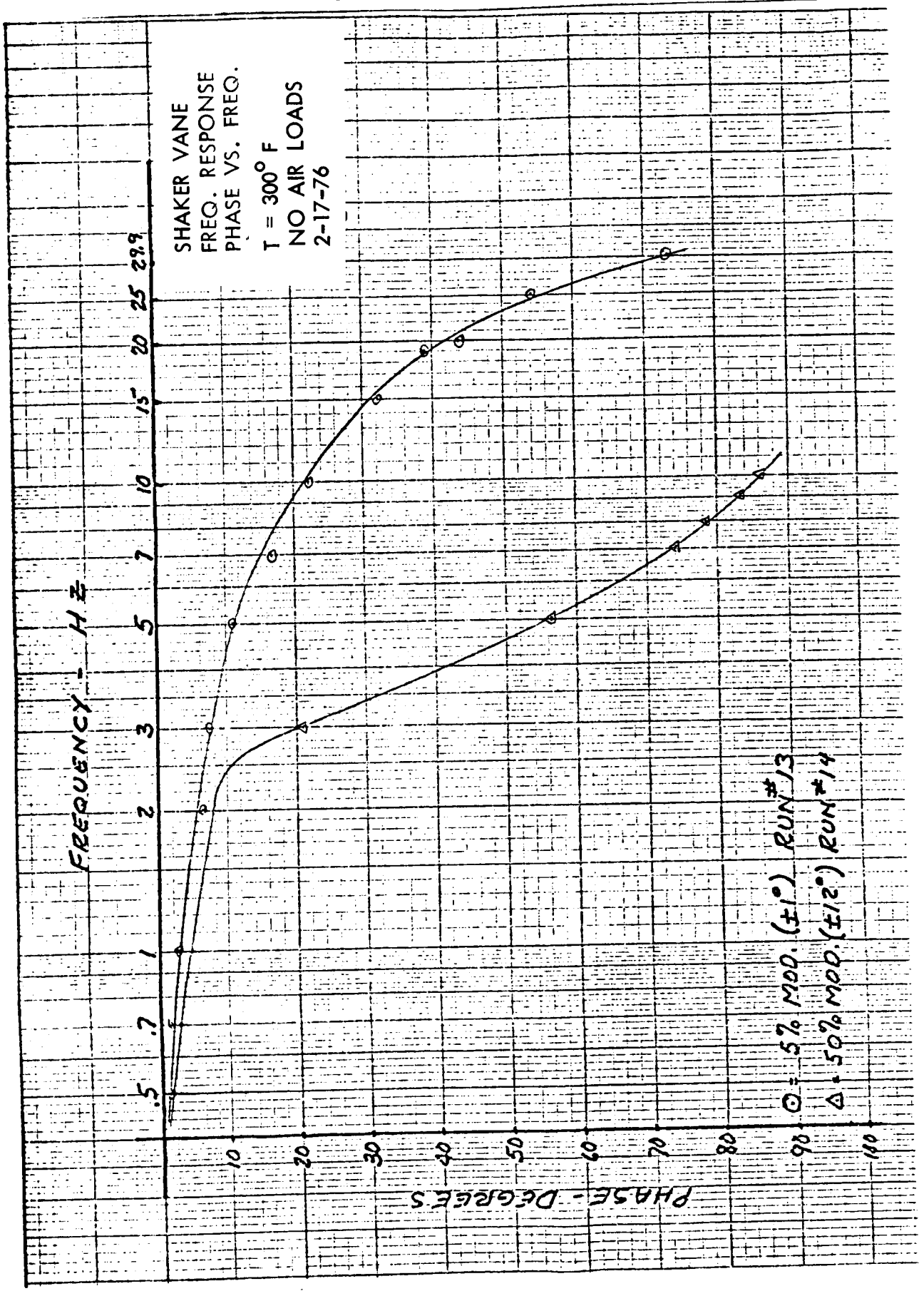

Figure 11. Final Shaker Vane Frequency Response Test, Phase vs. Frequency, Temperature 300°F

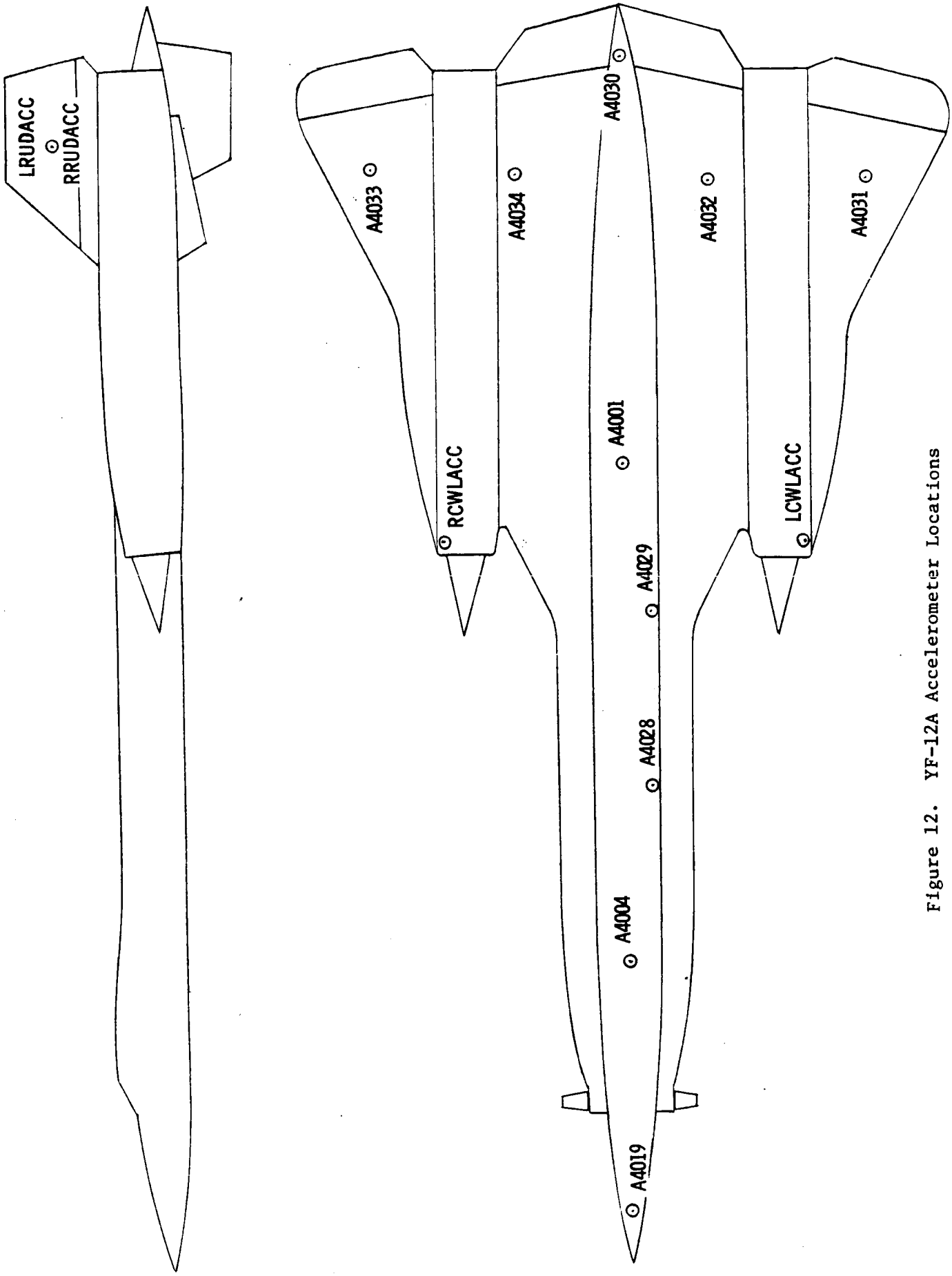

Figure 12. YF-12A Accelerometer Locations

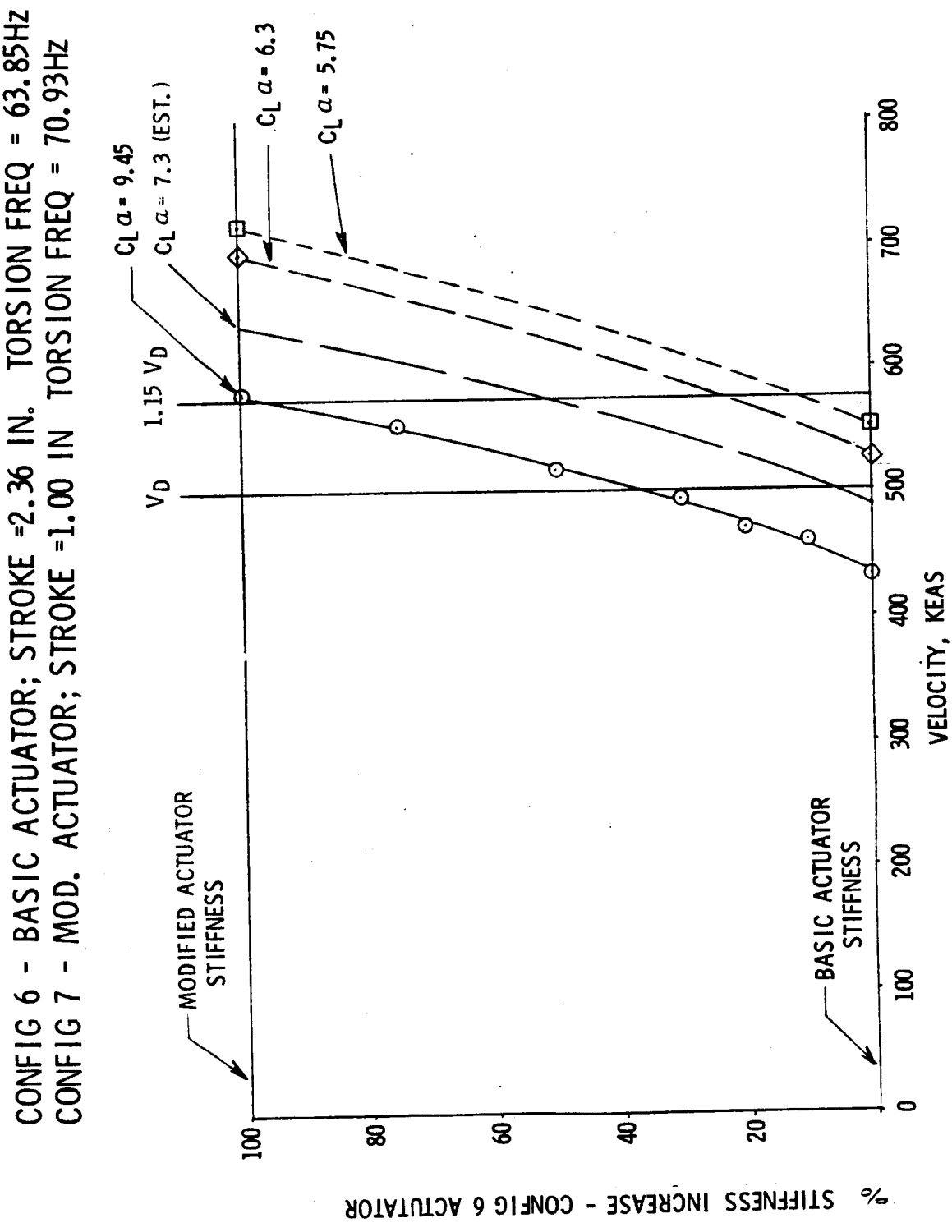

Figure 13. Canard Vane Flutter

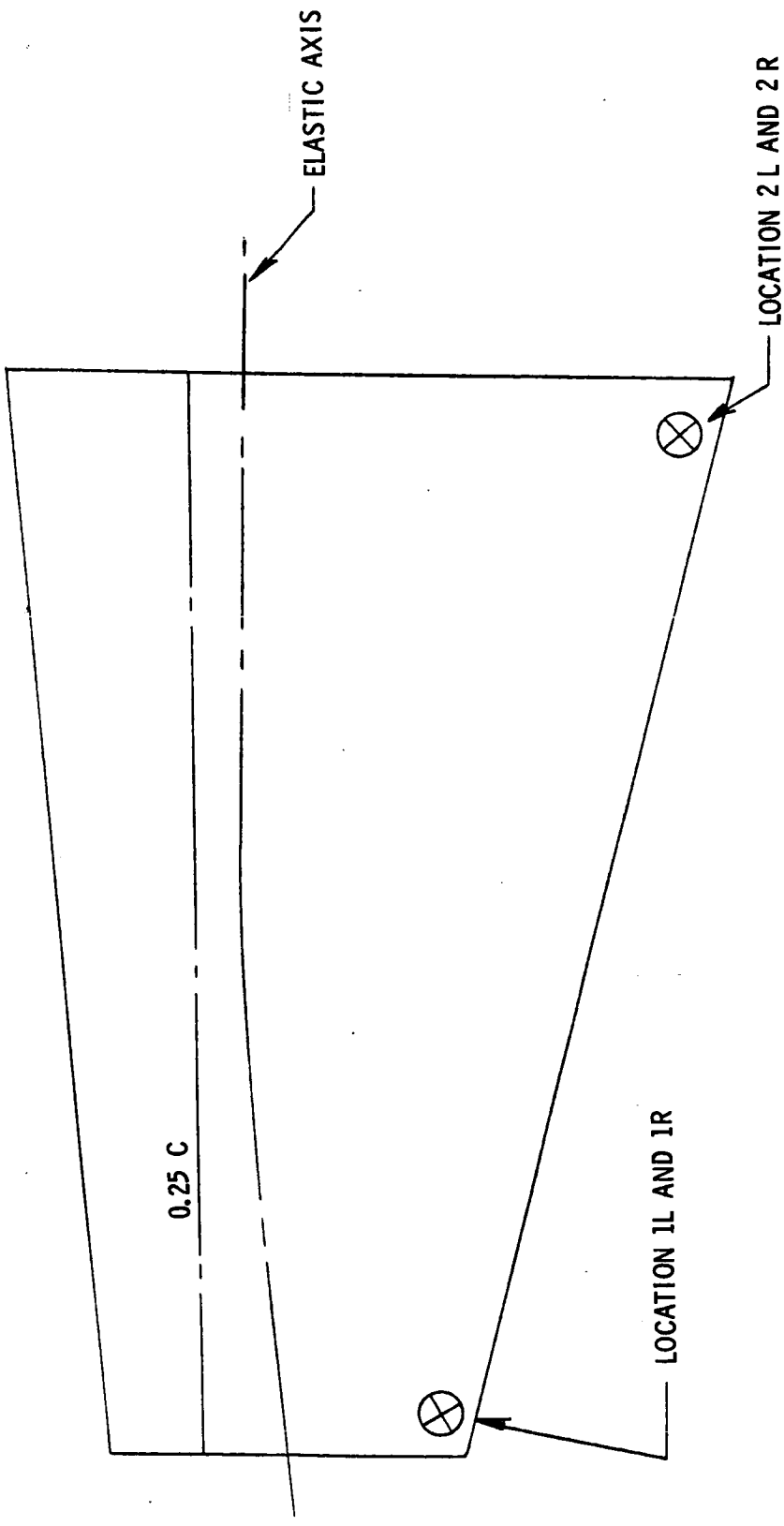

Figure 14. YF-12A Shaker Vane Ground Vibration Test Shaker Locations

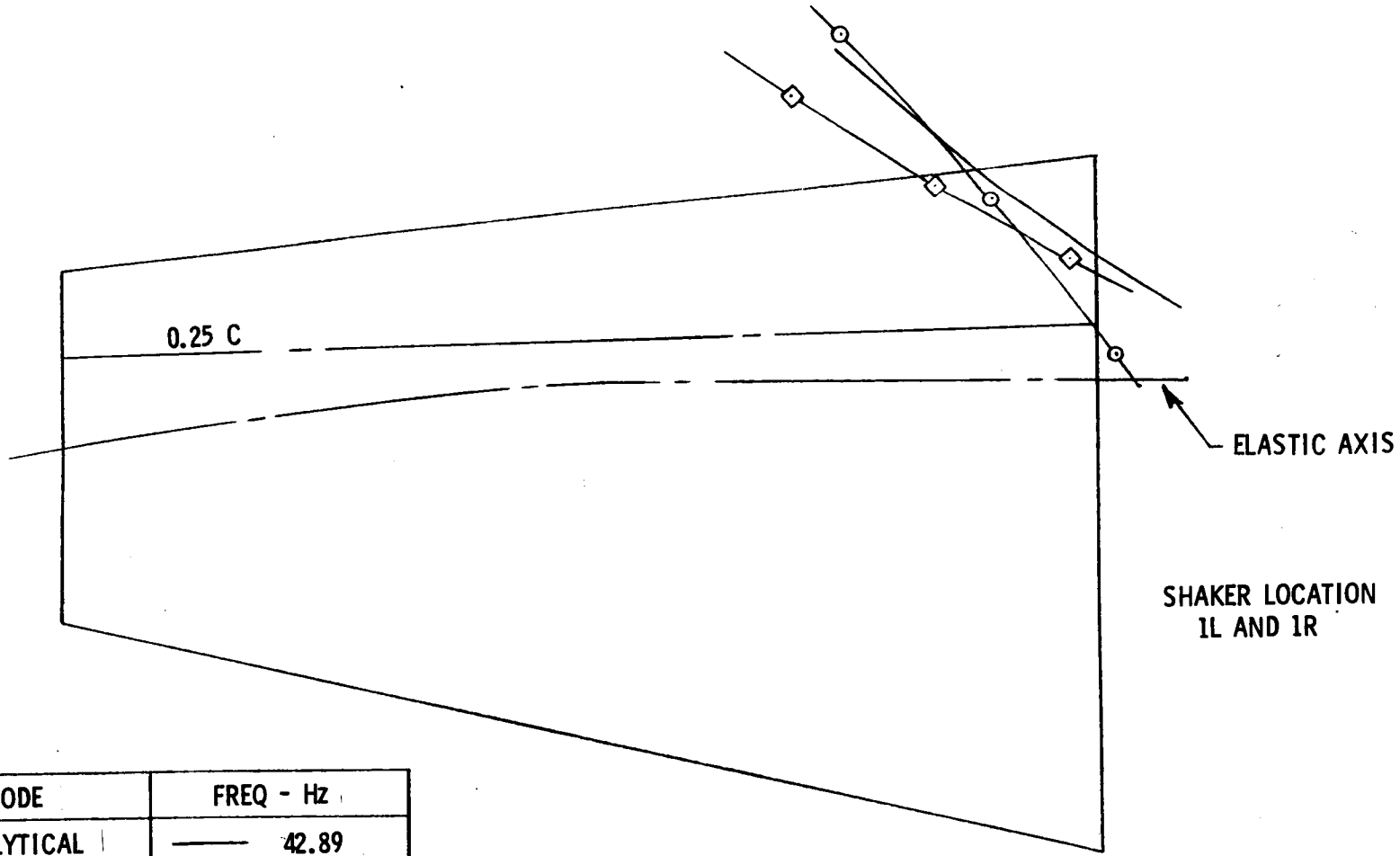

MODE	FREQ - Hz
ANALYTICAL	42.89
TEST	
L.H.	33.20
R.H.	32.26

Figure 15. YF-12A Shaker Vane Vibration Data - Comparison, First Analytical to Test Mode, Symmetric

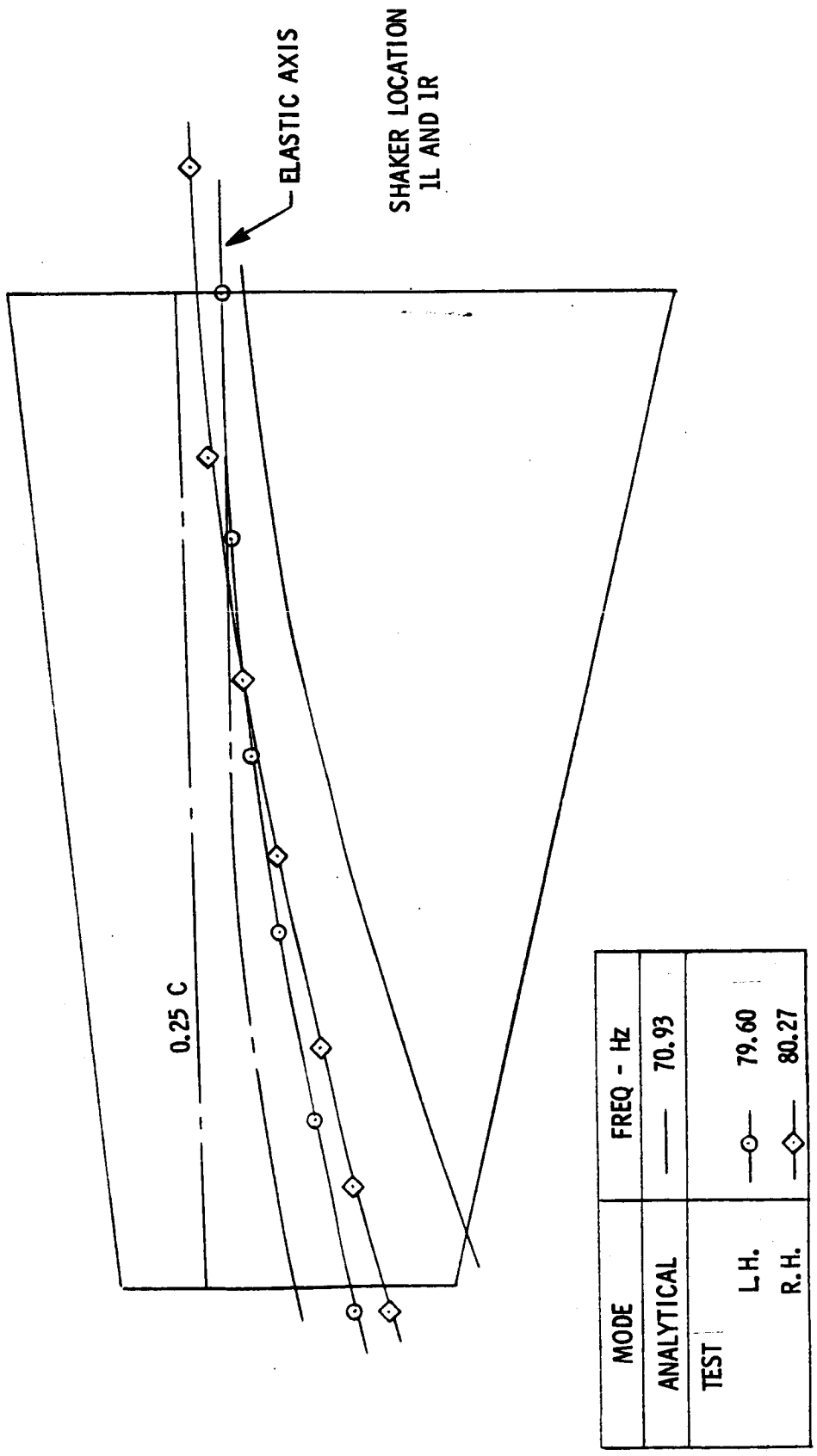

Figure 16. YF-12A Shaker Vane Vibration Data - Comparison, Third Analytical to Test Mode, Symmetric

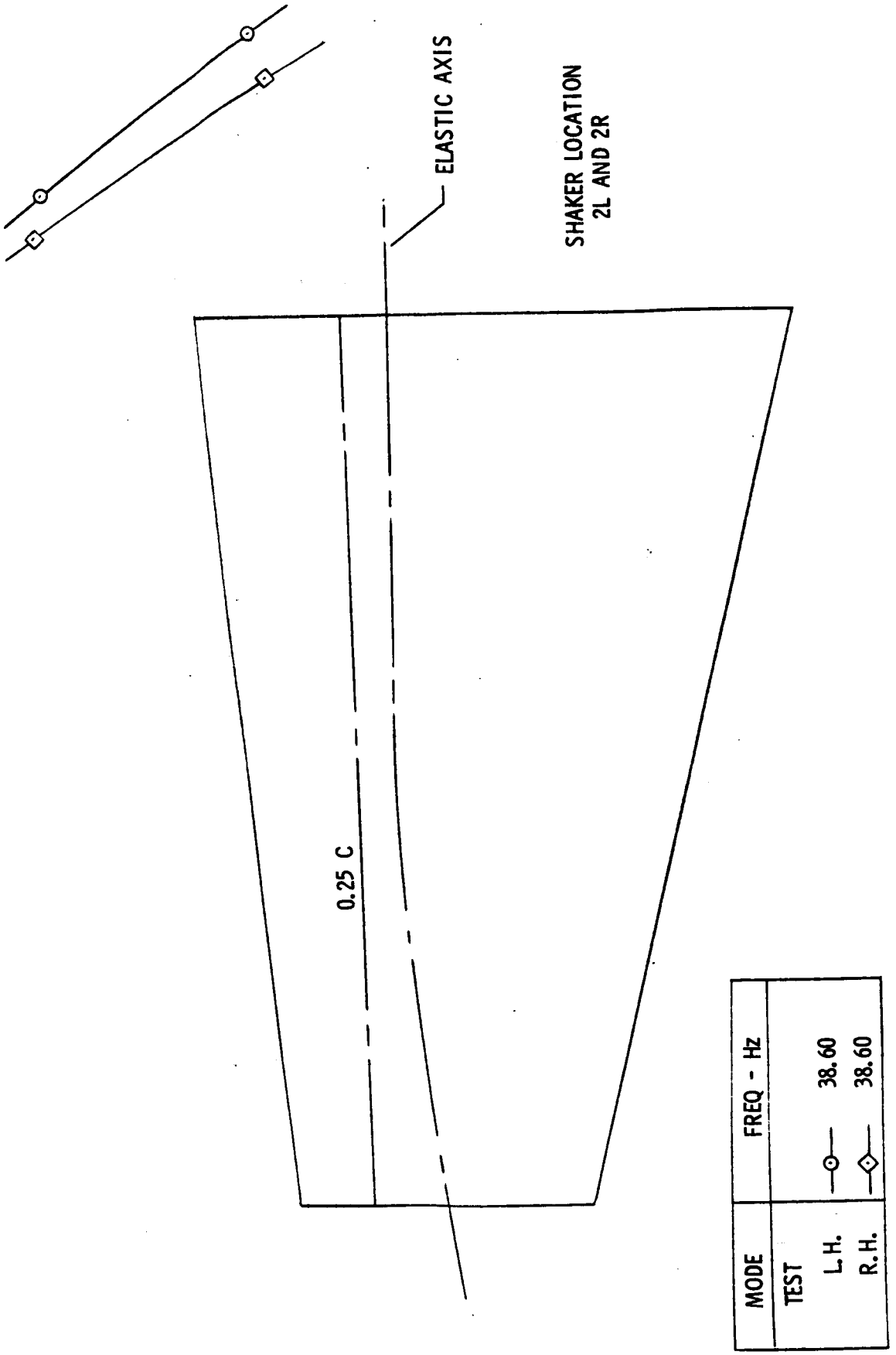

Figure 17. YF-12A Shaker Vane Vibration Data - First Mode, Test, Antisymmetric

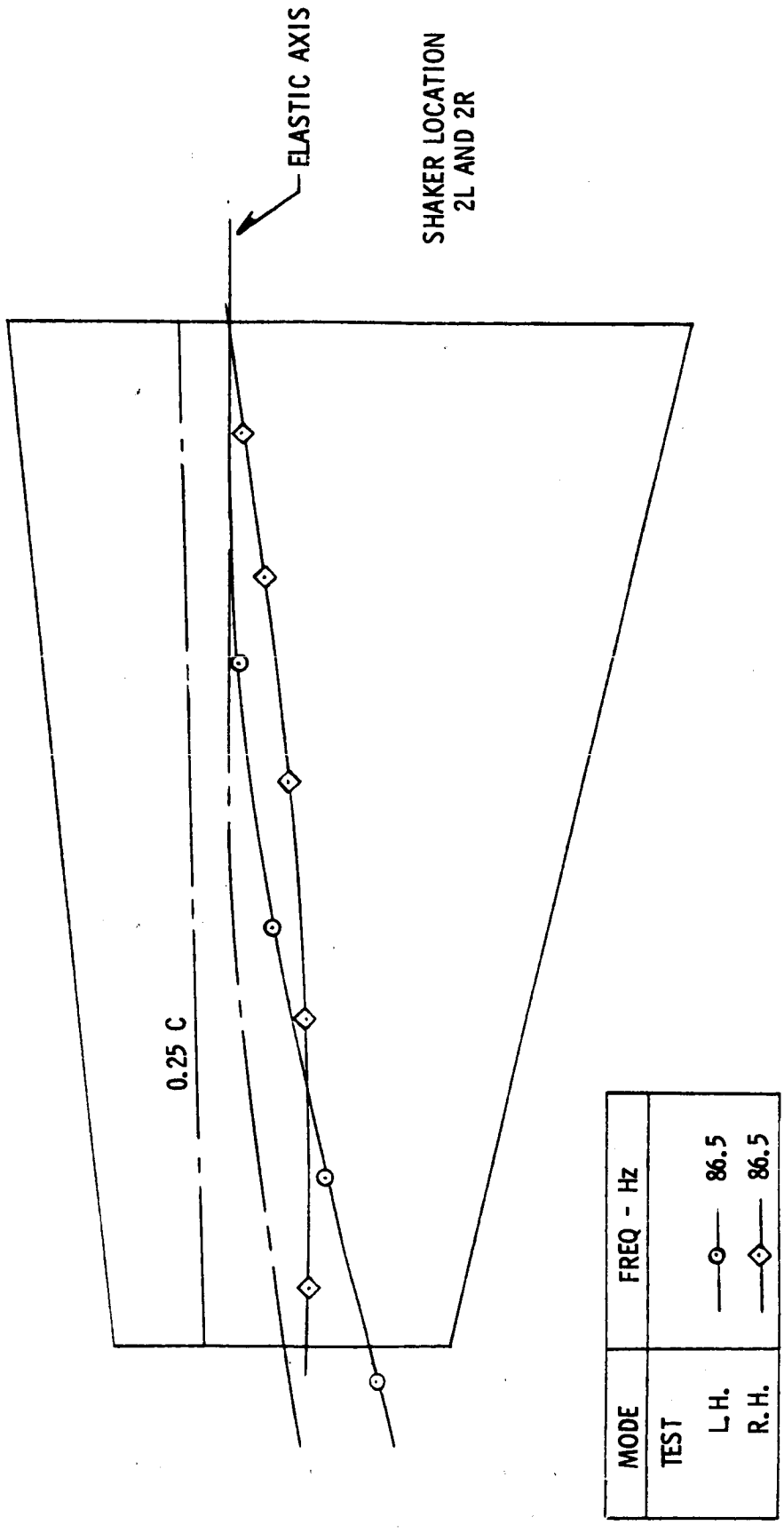

Figure 18. YF-12A Shaker Vane Vibration Data - Third Mode, Test, Antisymmetric

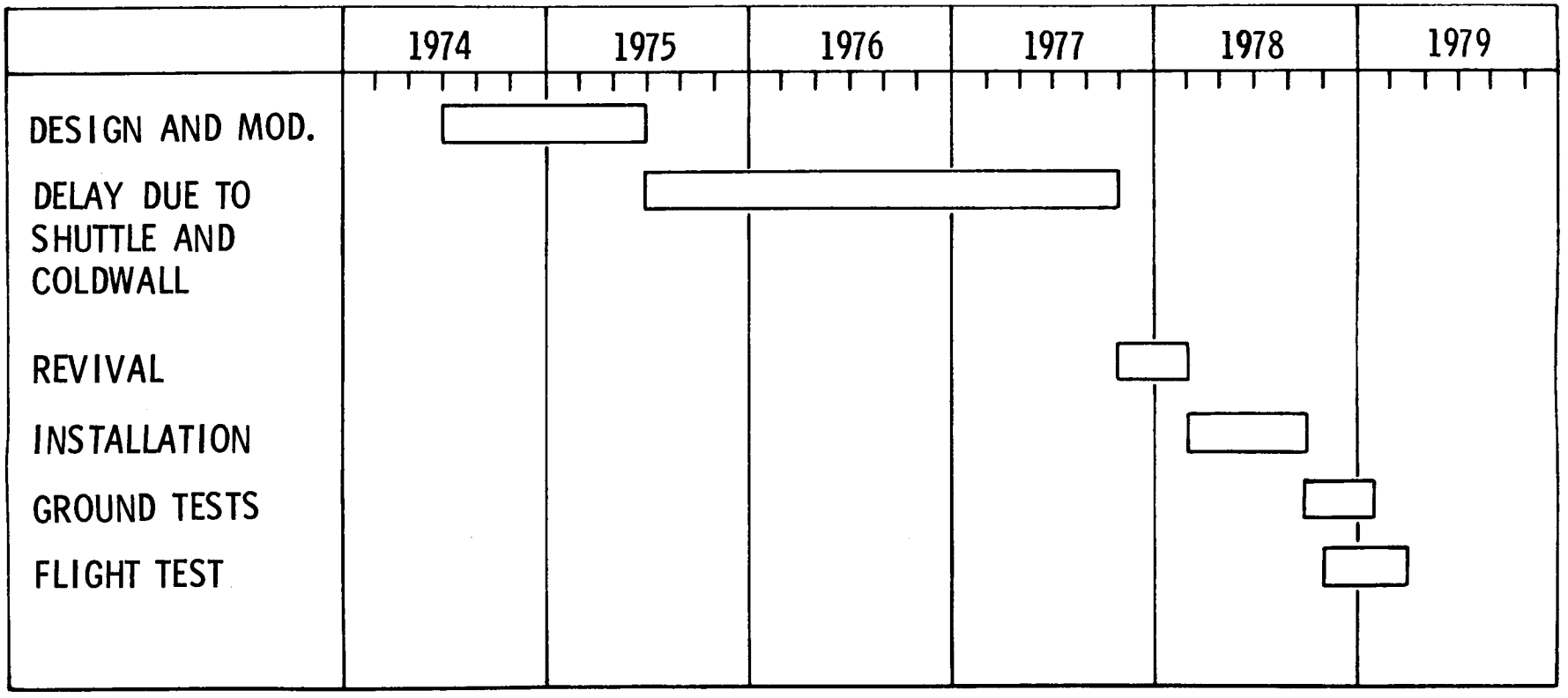

Figure 19. YF-12A Canard Exciter Vane Program Schedule

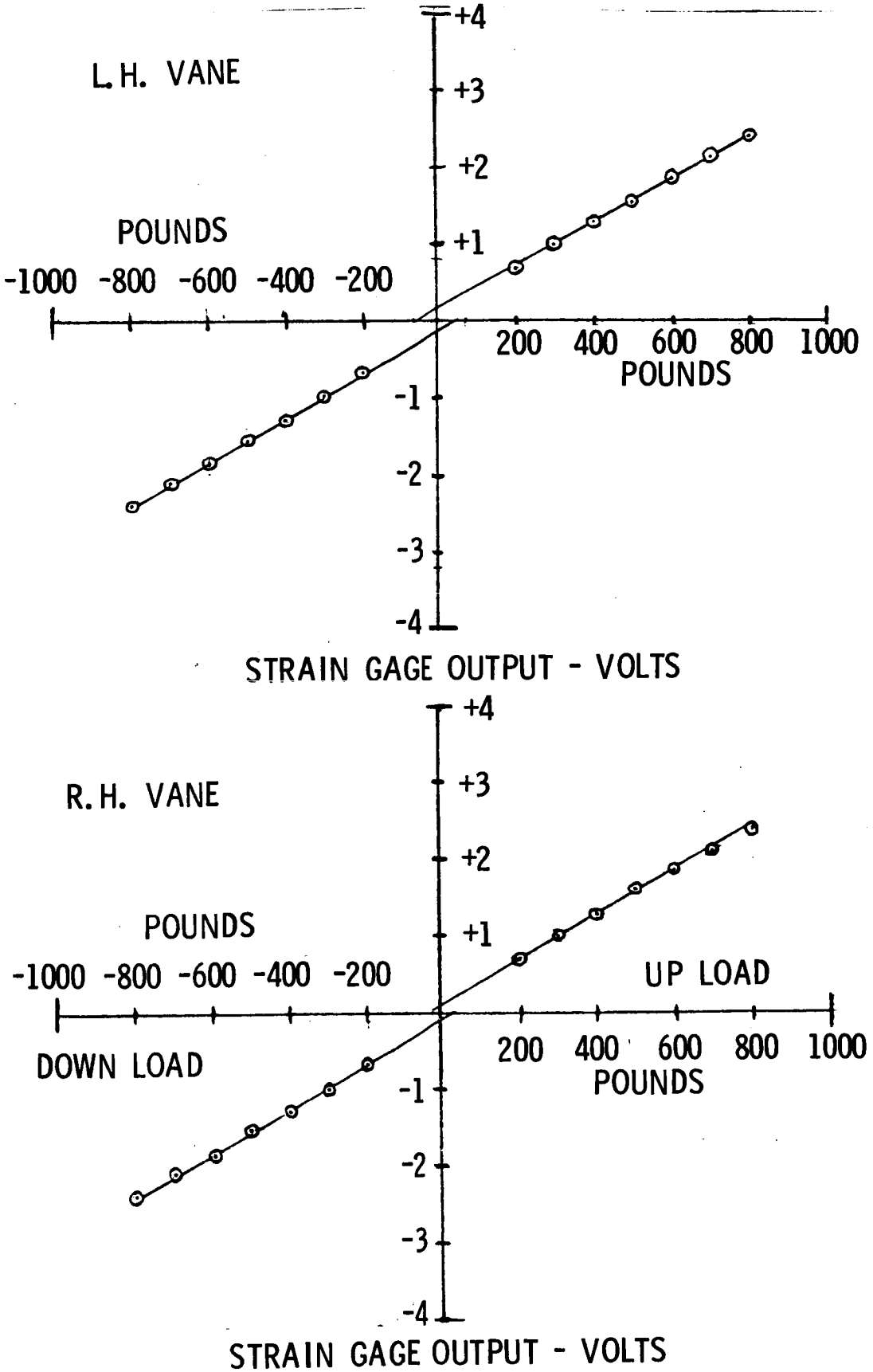

Figure 20. Exciter Vane - Load vs. Strain Gage Output

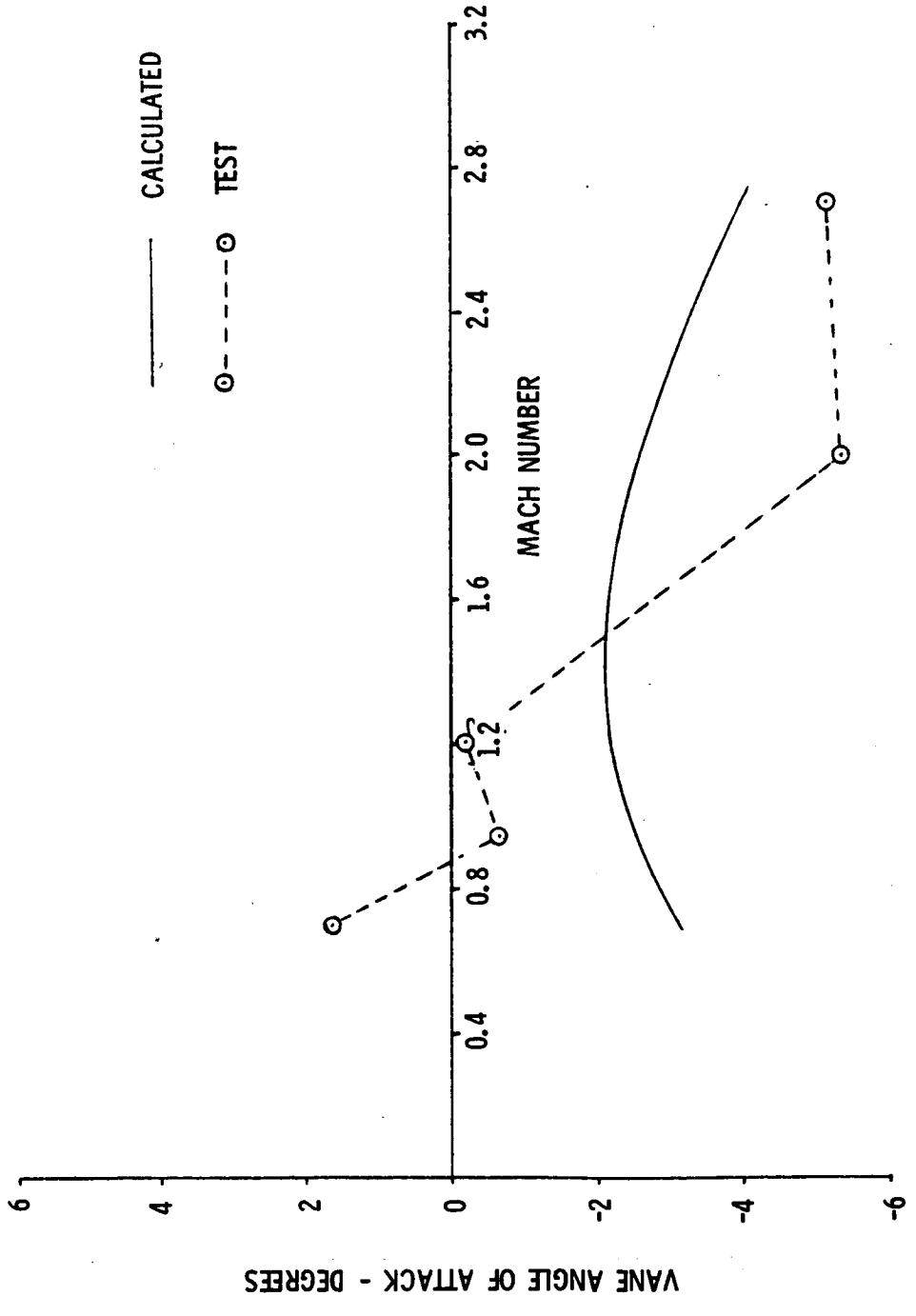

Figure 21. Exciter Vane Trim Angle vs. Mach No.

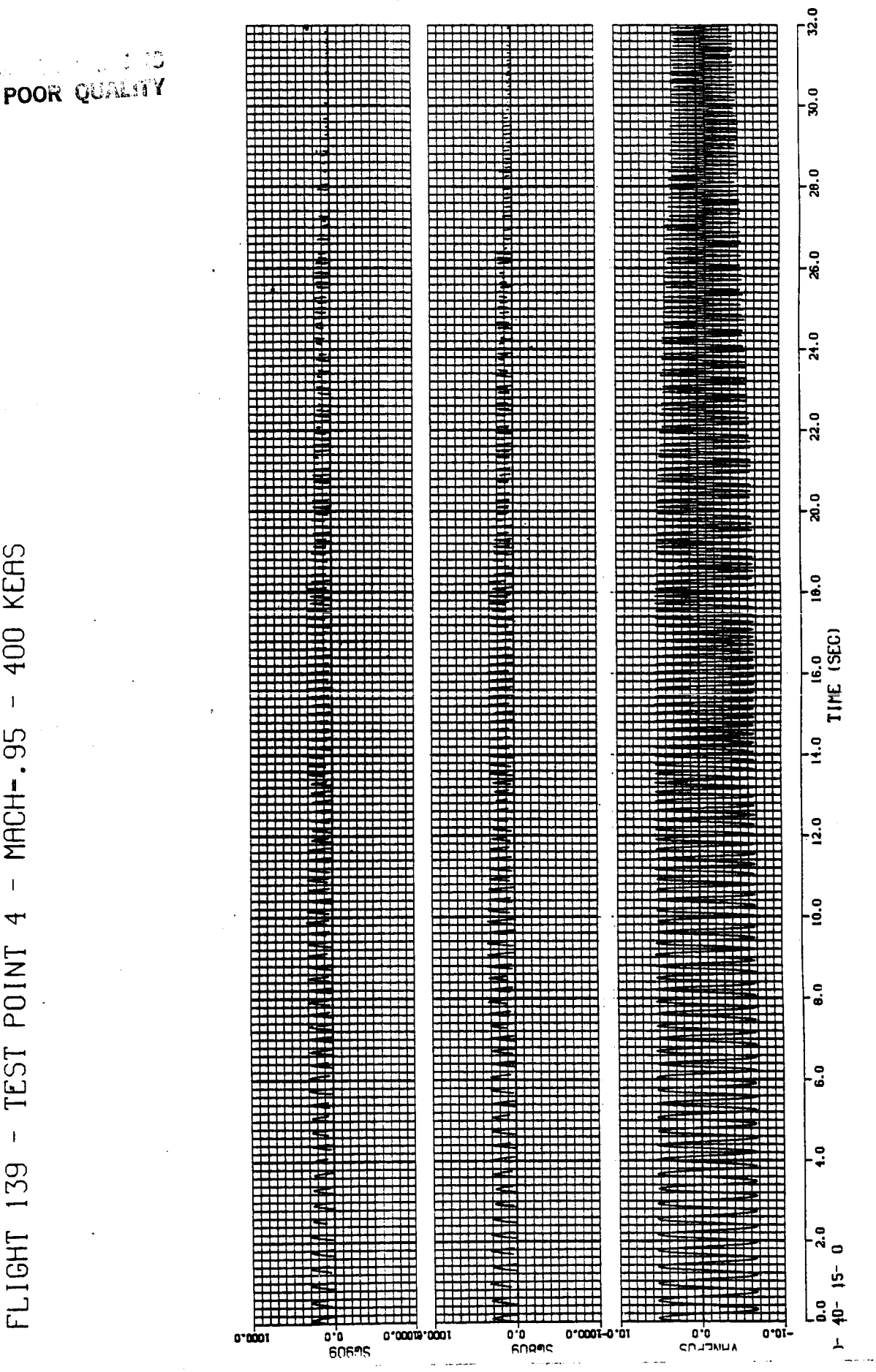

Figure 22. Frequency Sweep, M = 0.95

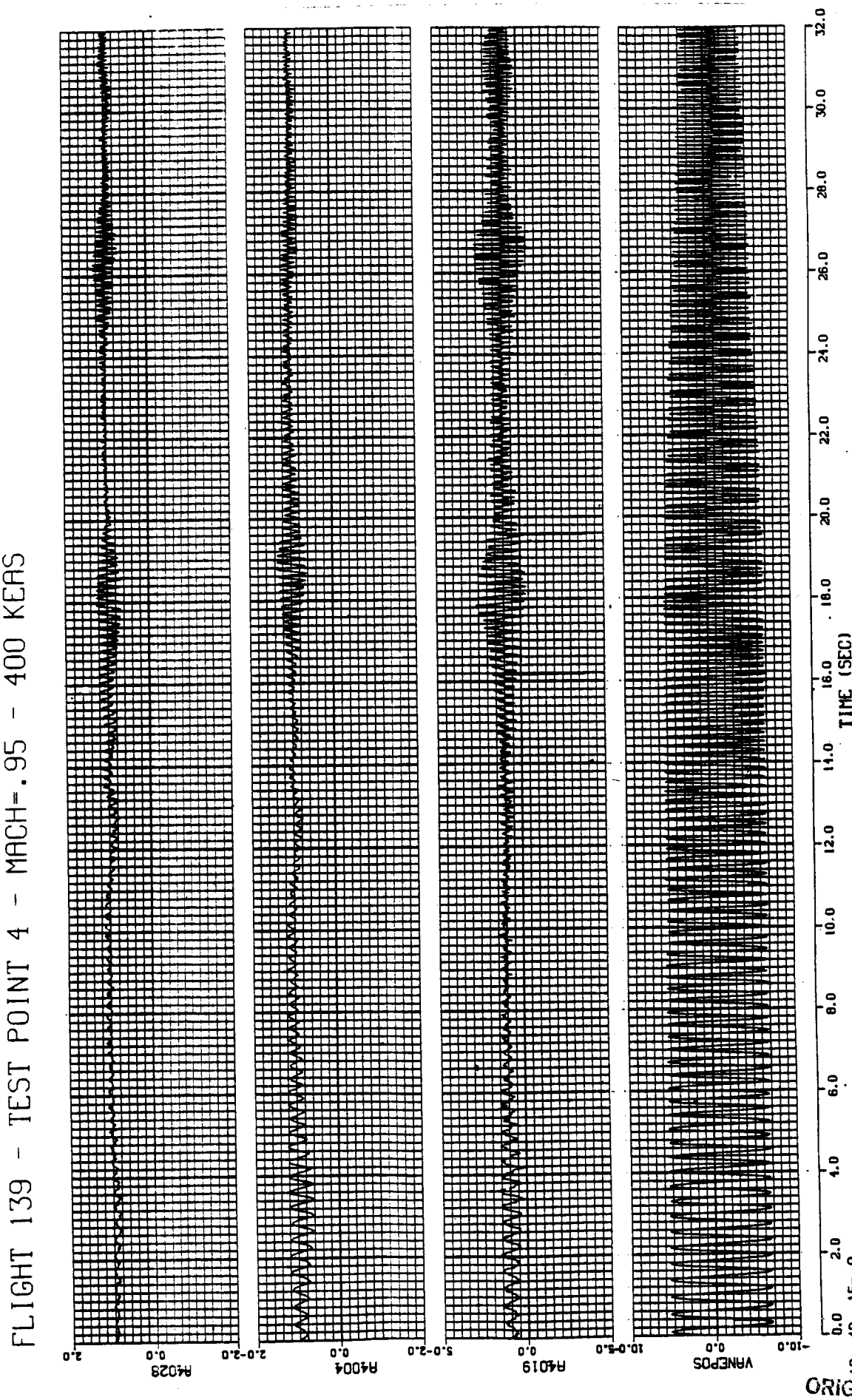

Figure 22. Frequency Sweep, M = 0.95

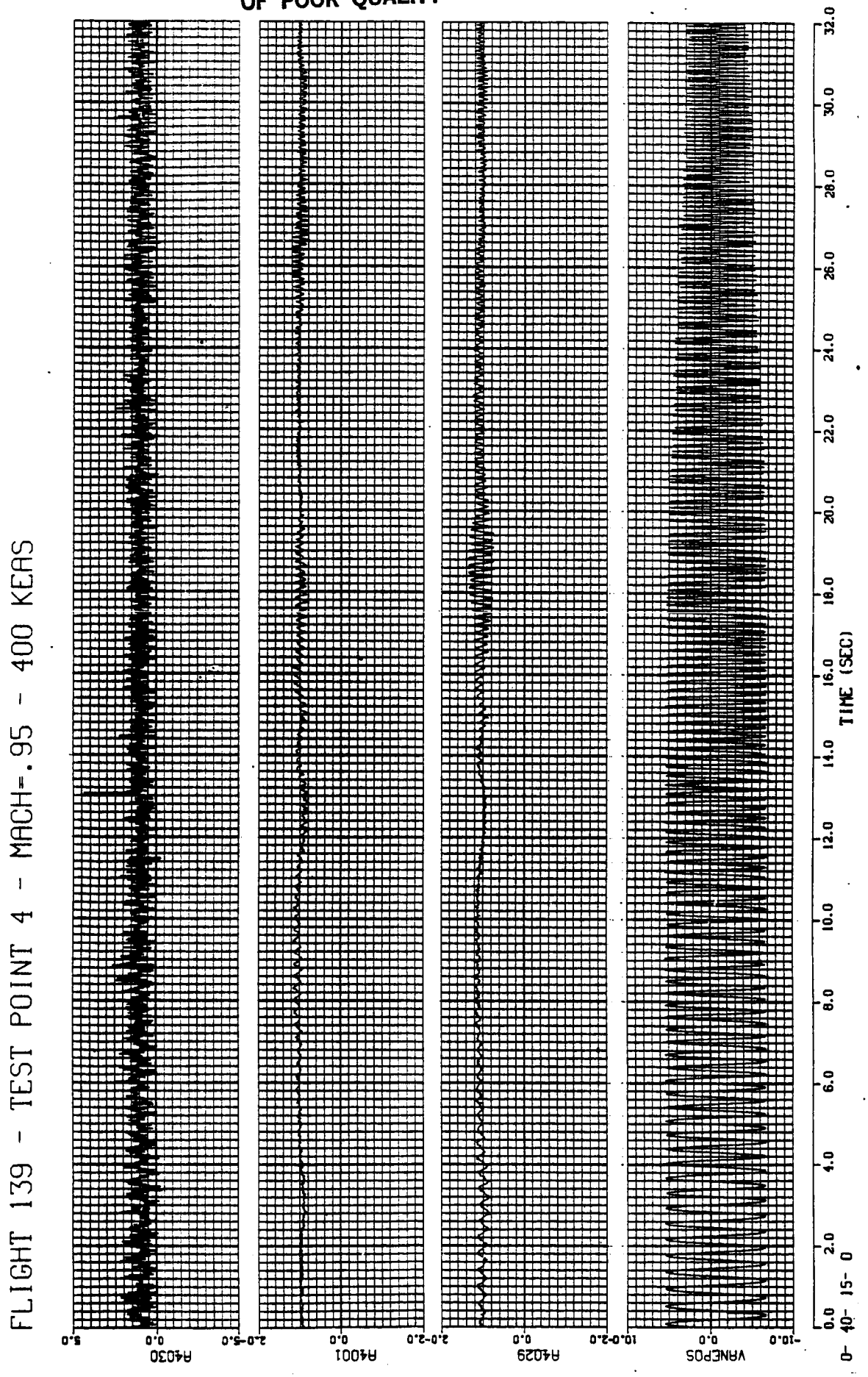

Figure 22. Frequency Sweep, M = 0.95

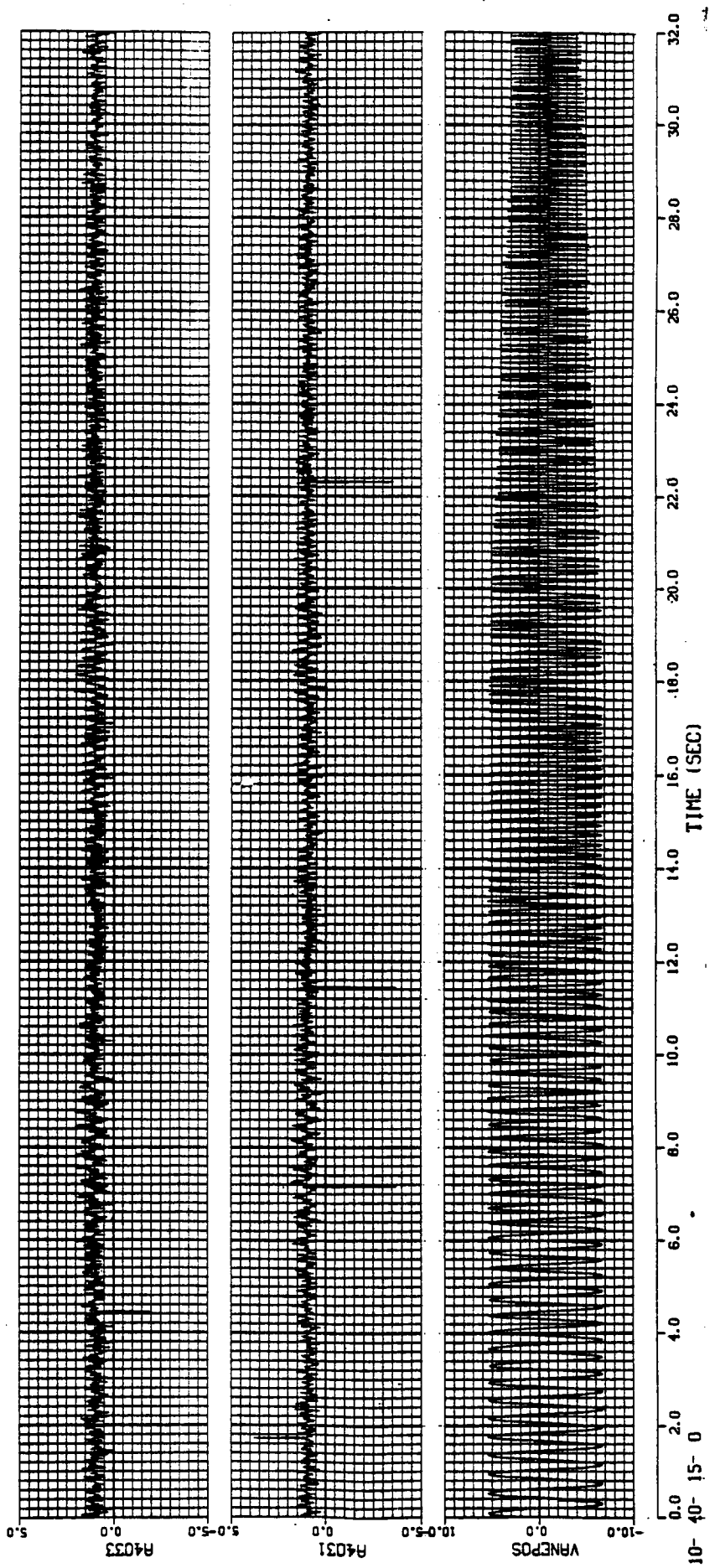

Figure 22. Frequency Sweep, M = 0.95

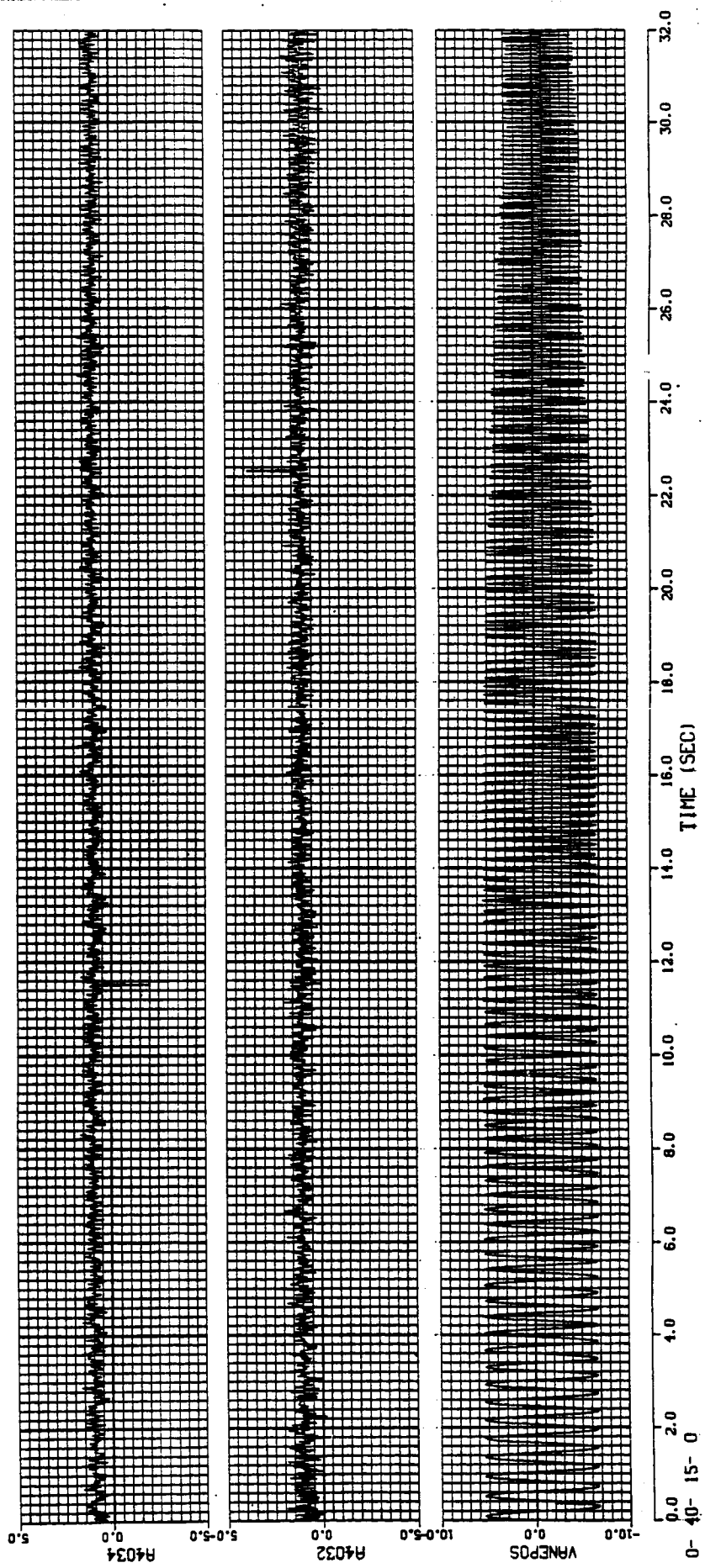

Figure 22. Frequency Sweep, M = 0.95

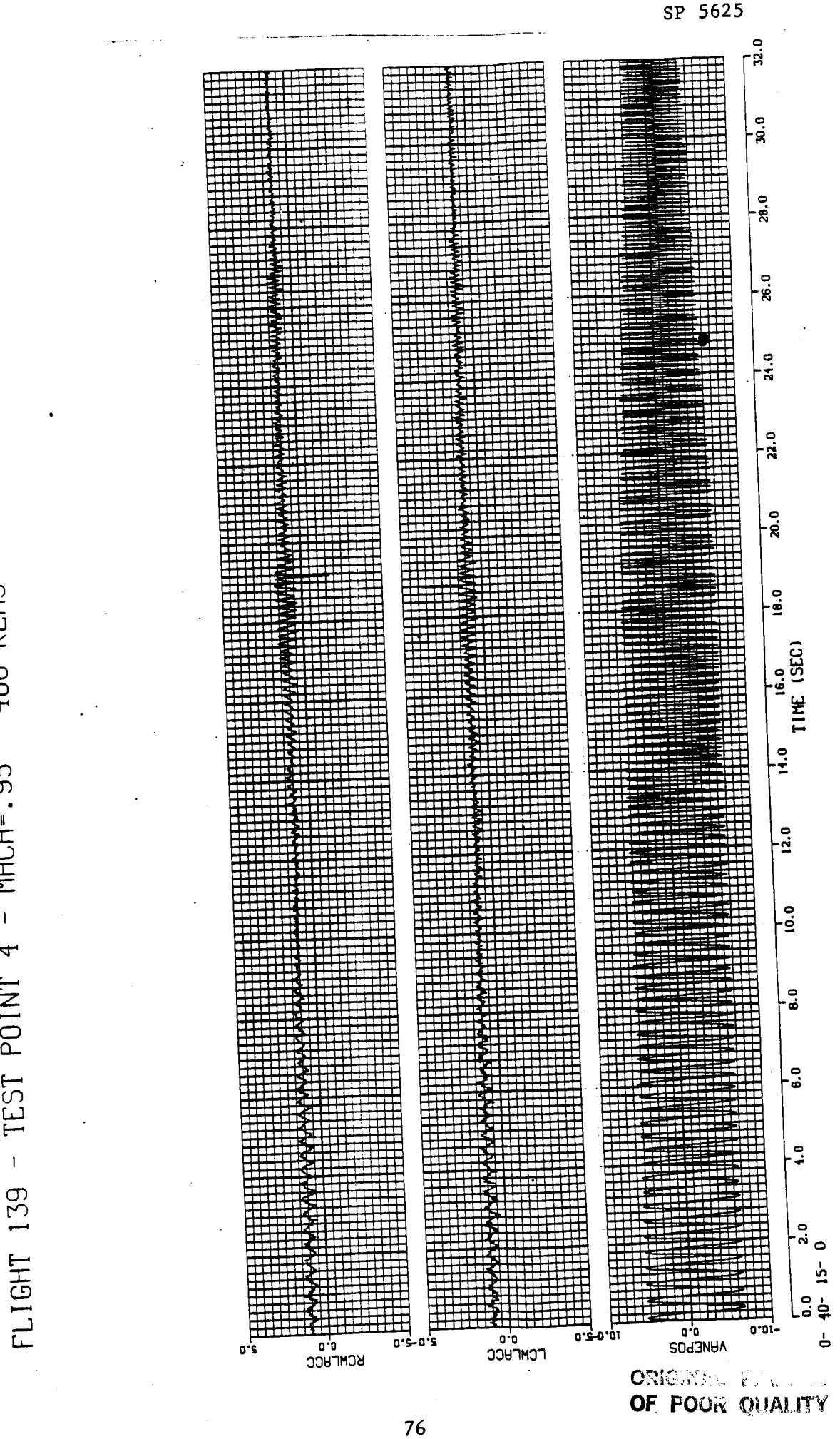

Figure 22. Frequency Sweep, M = 0.95

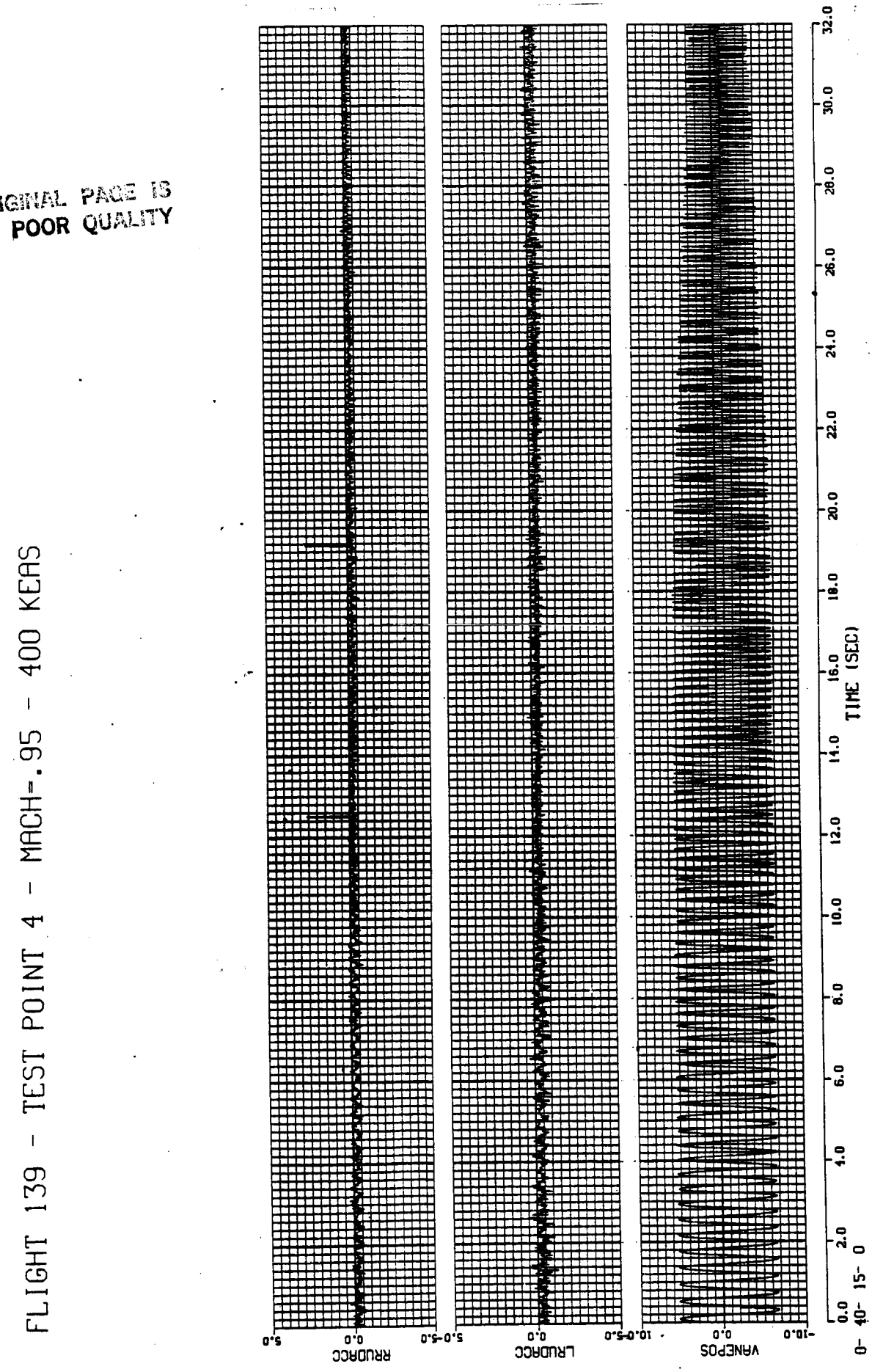

Figure 22. Frequency Sweep, M = 0.95

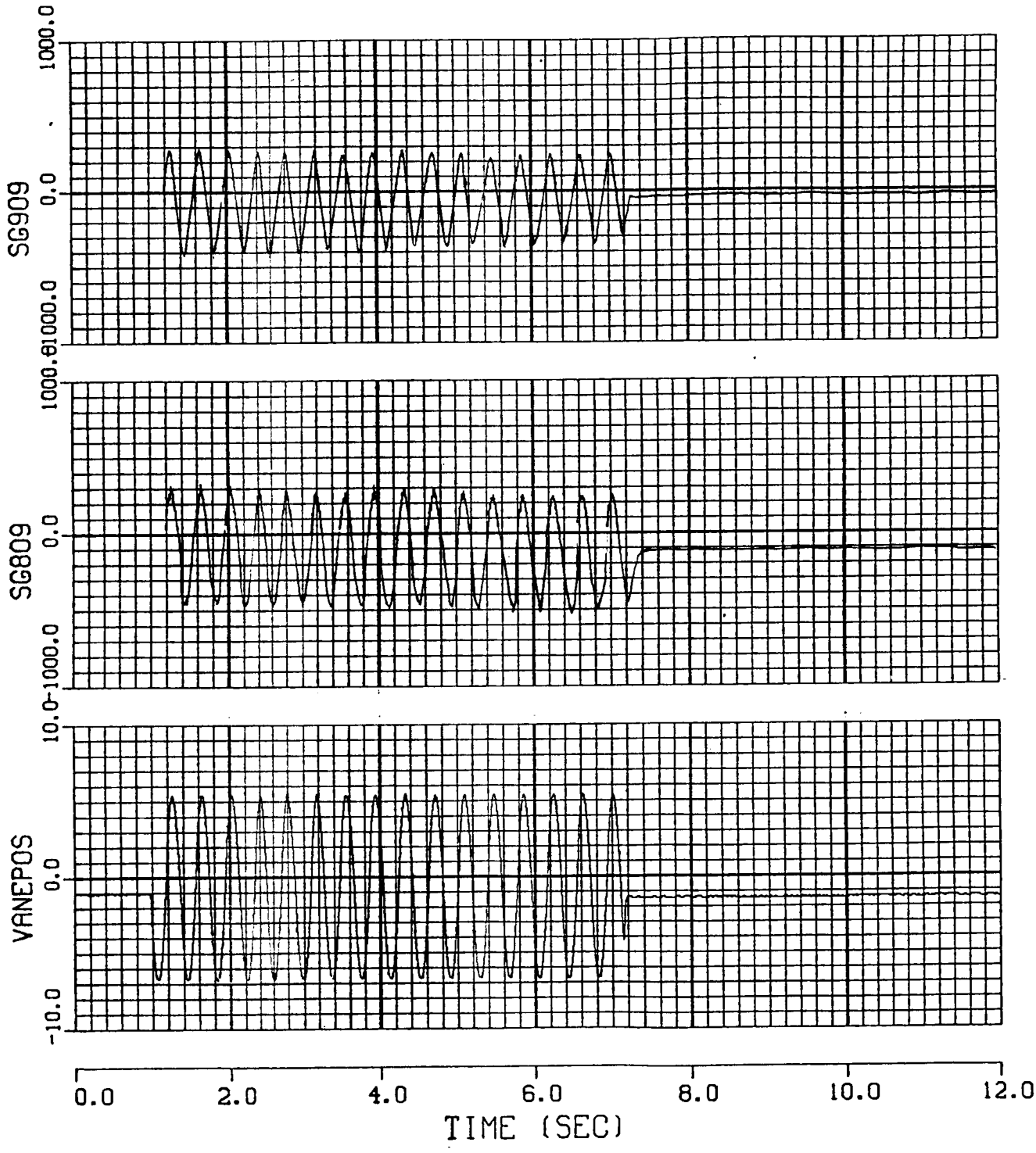

Figure 23. Dwell and Decay, M = 0.95

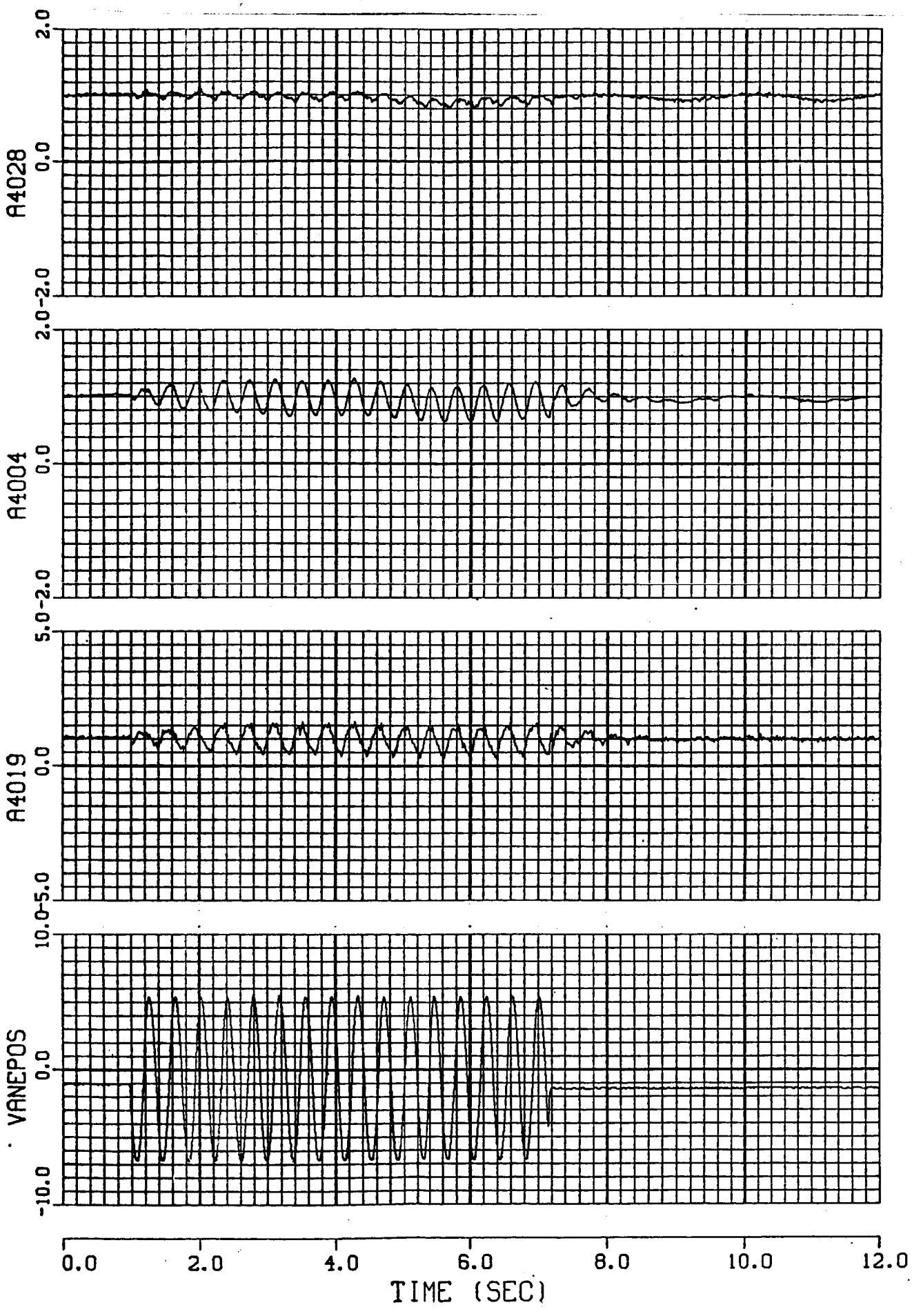

Figure 23. Dwell and Decay, M = 0.95

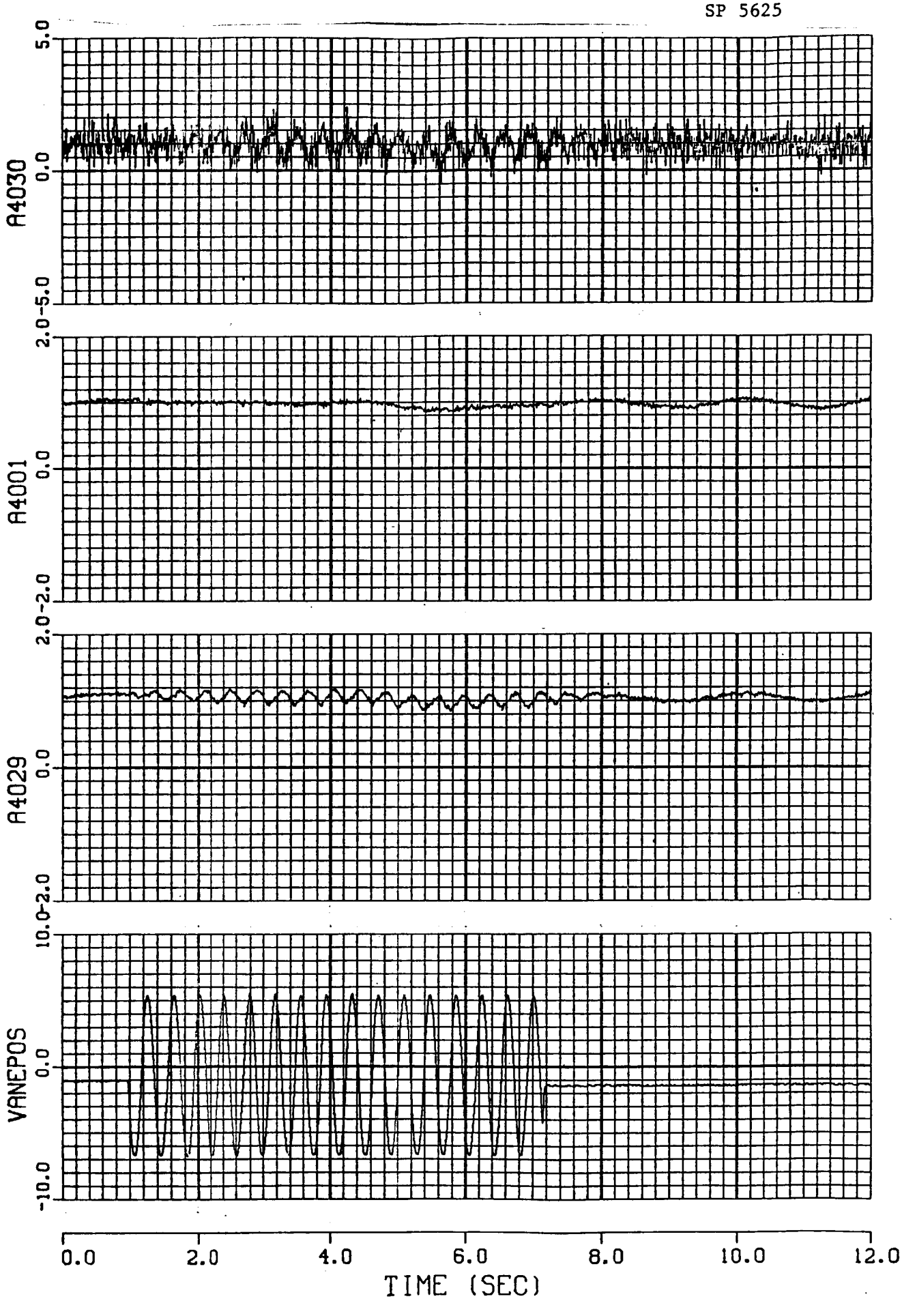

Figure 23. Dwell and Decay, M = 0.95

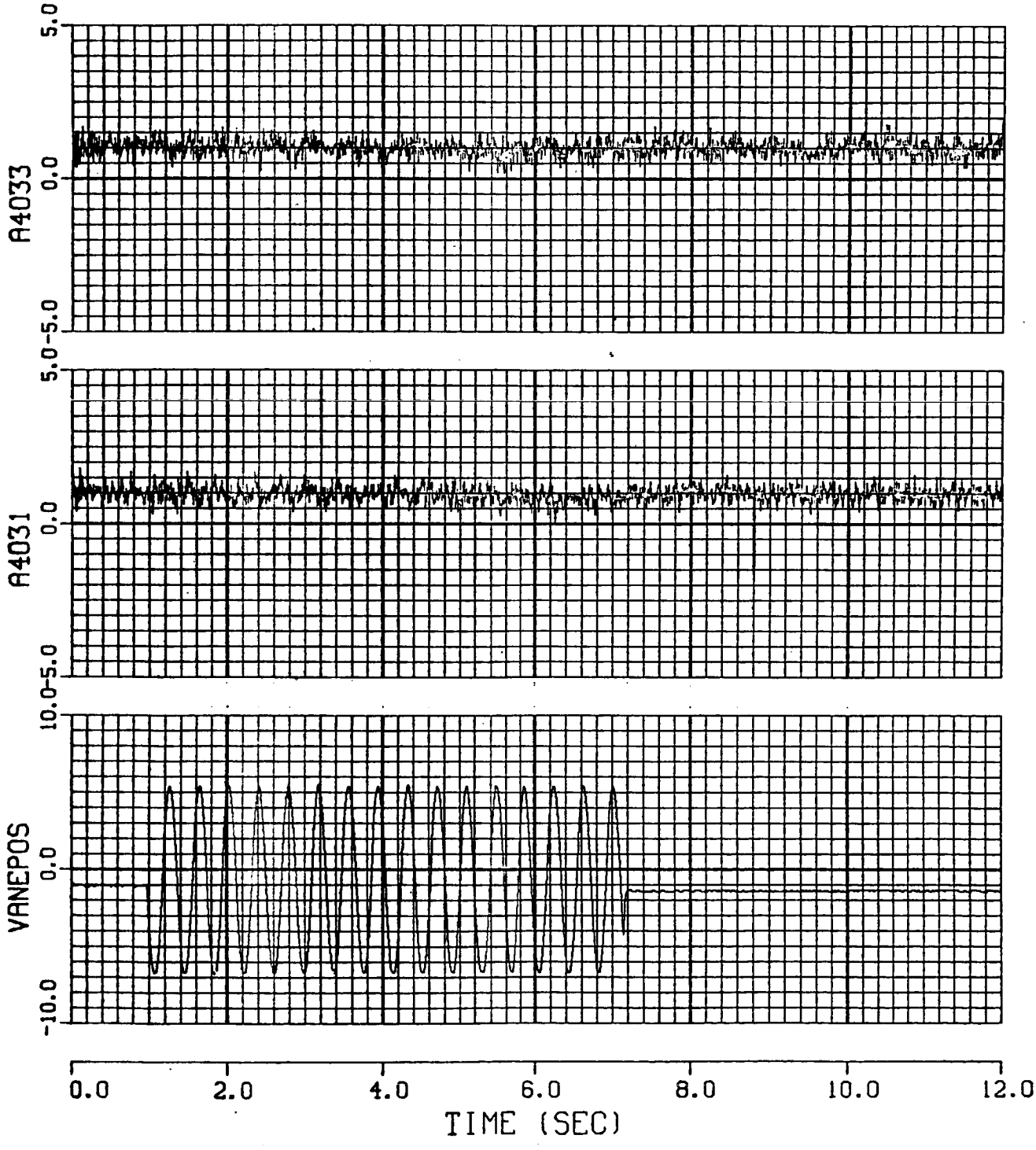

Figure 23. Dwell and Decay, M = 0.95

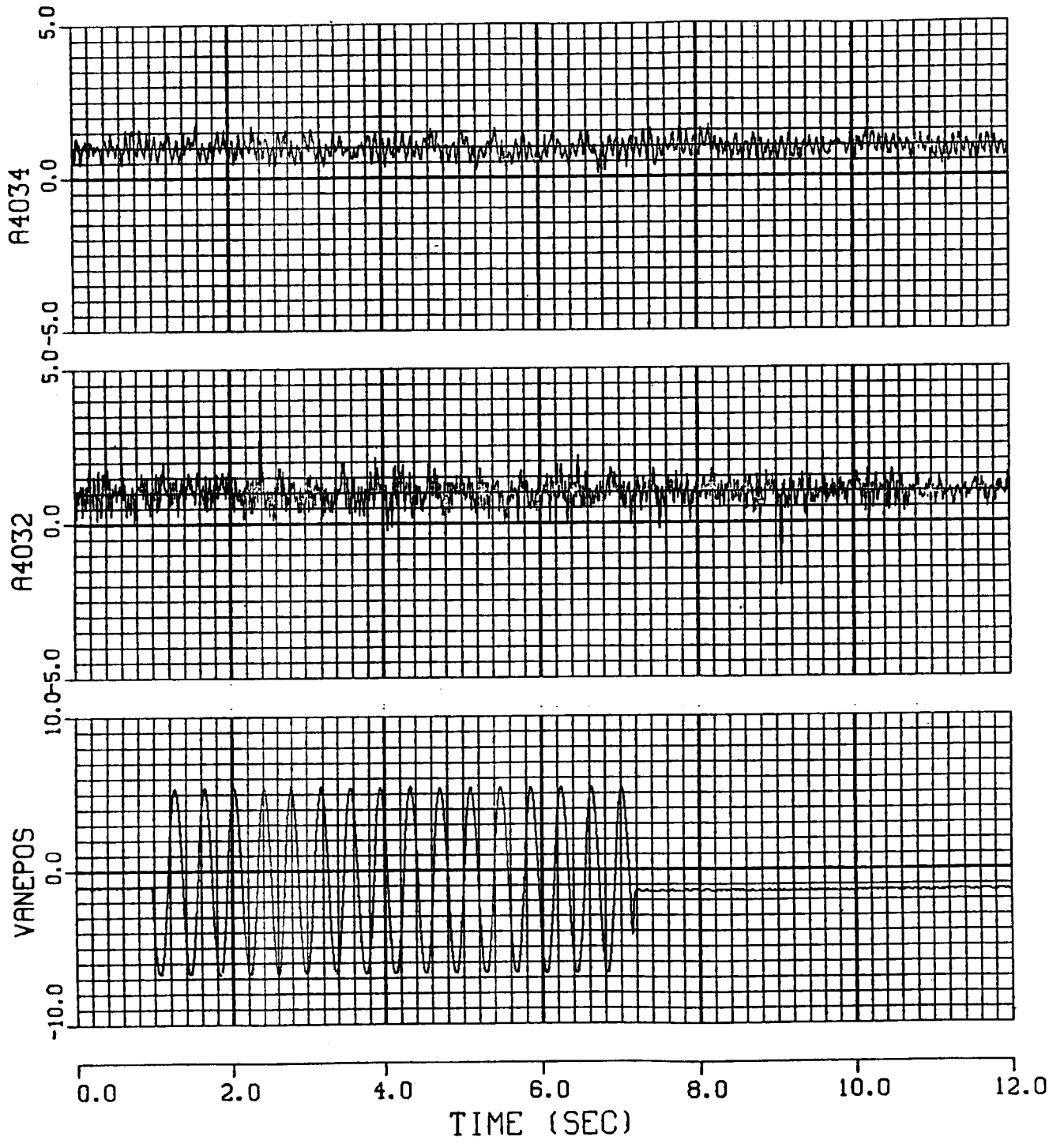

Figure 23. Dwell and Decay, M = 0.95

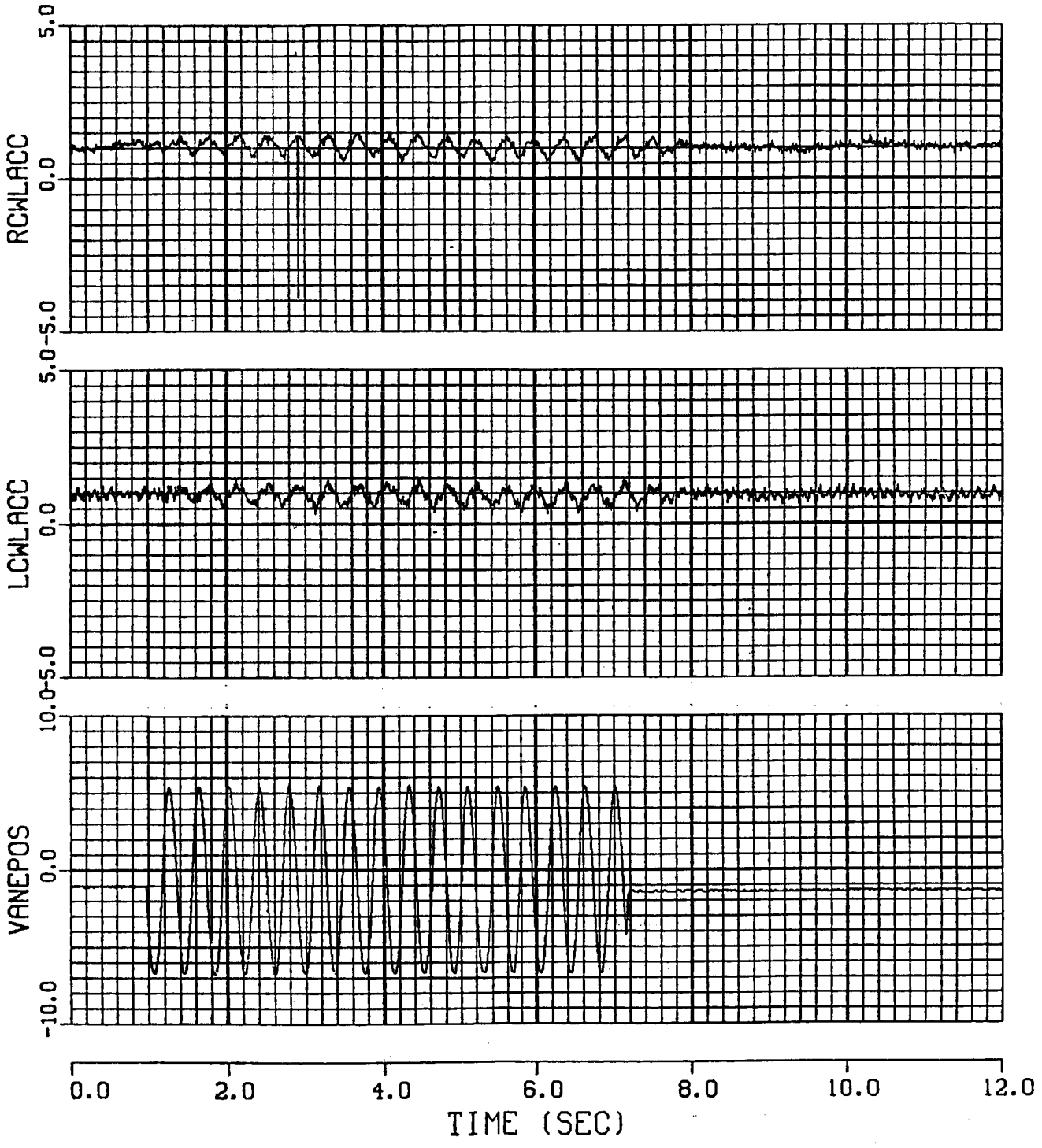

Figure 23. Dwell and Decay, M = 0.95

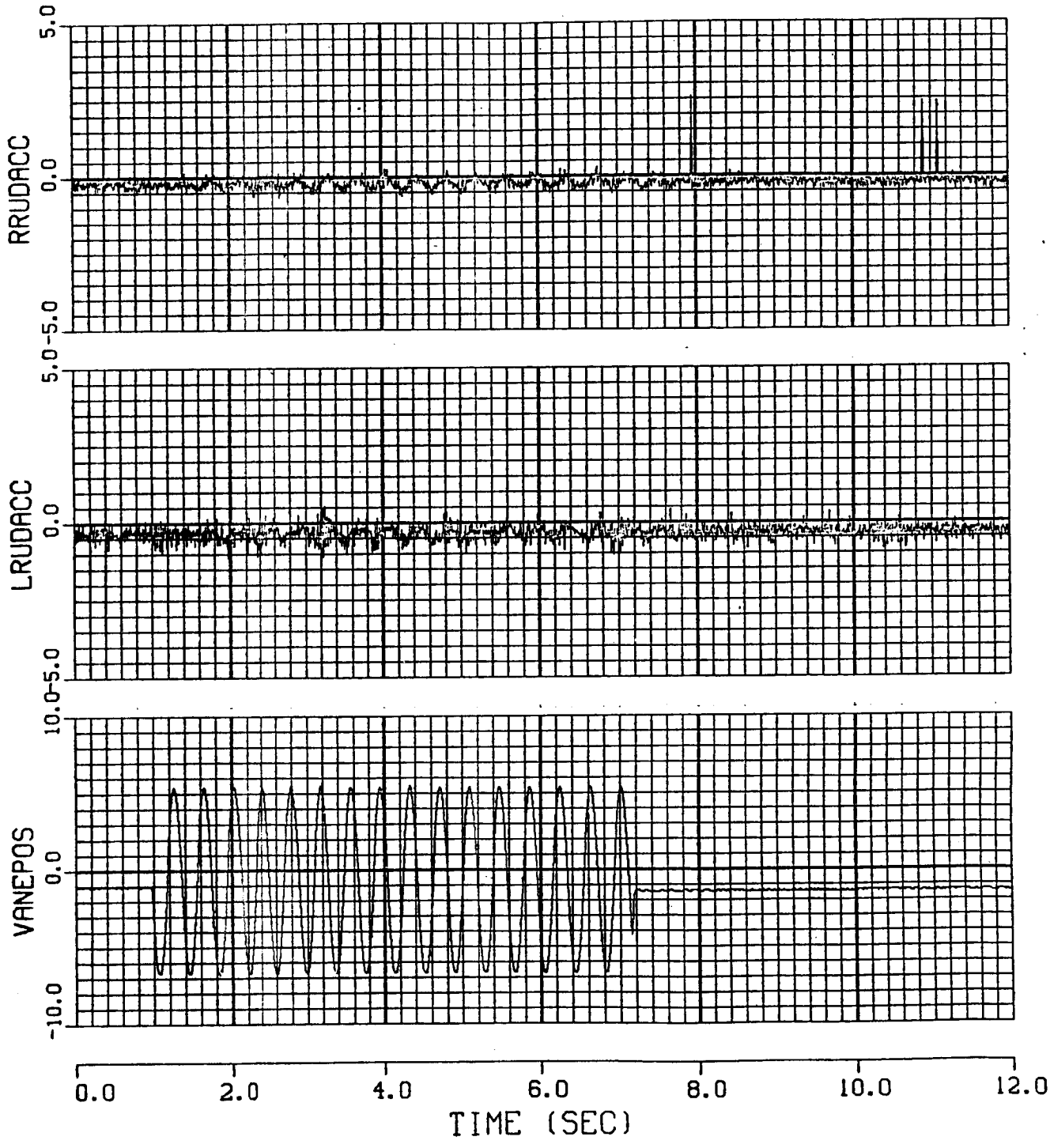

Figure 23. Dwell and Decay, M = 0.95

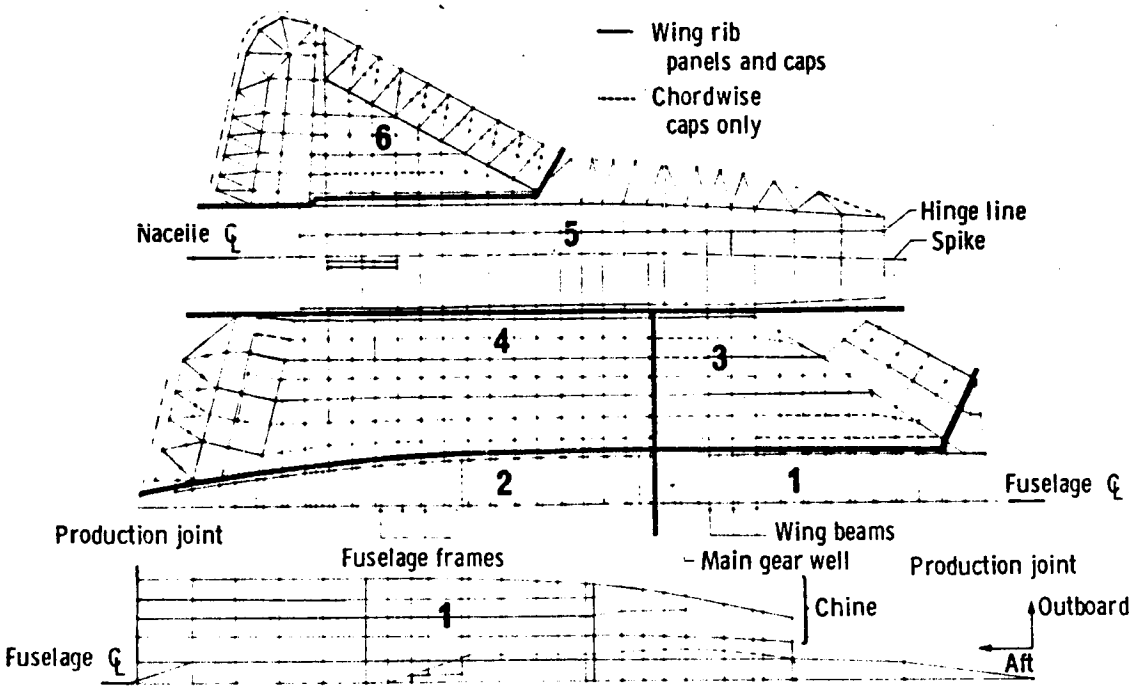

Figure 24. NASTRAN Model Planform and Substructure Division

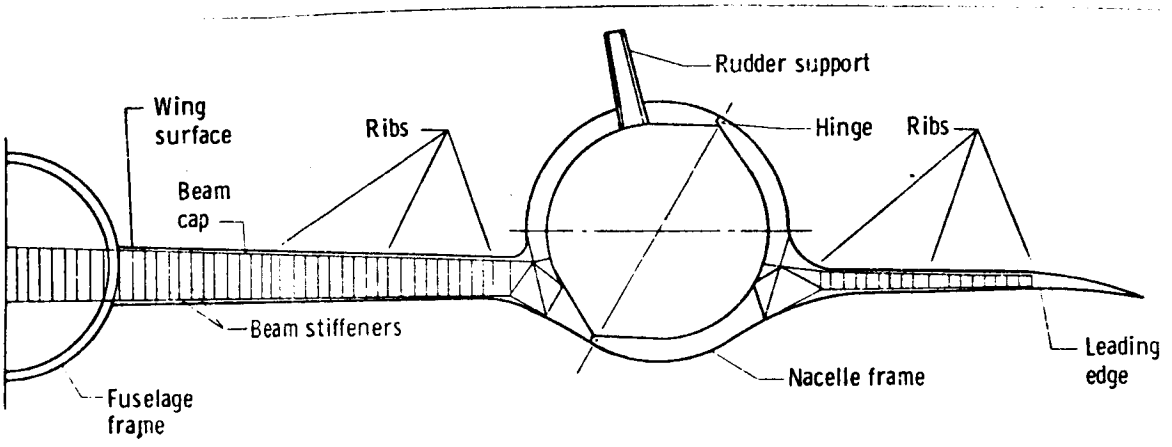

(a) Airplane structure.

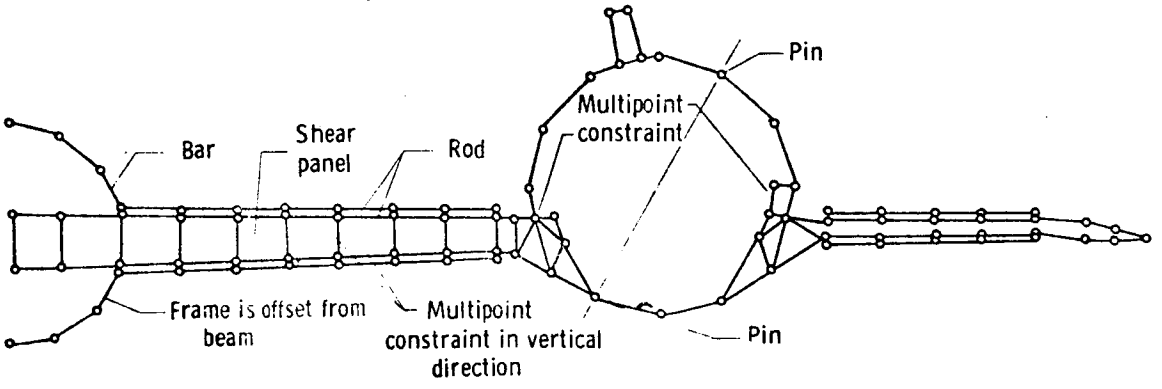

(b) NASTRAN model.

Figure 25. Actual Structure and NASTRAN Model

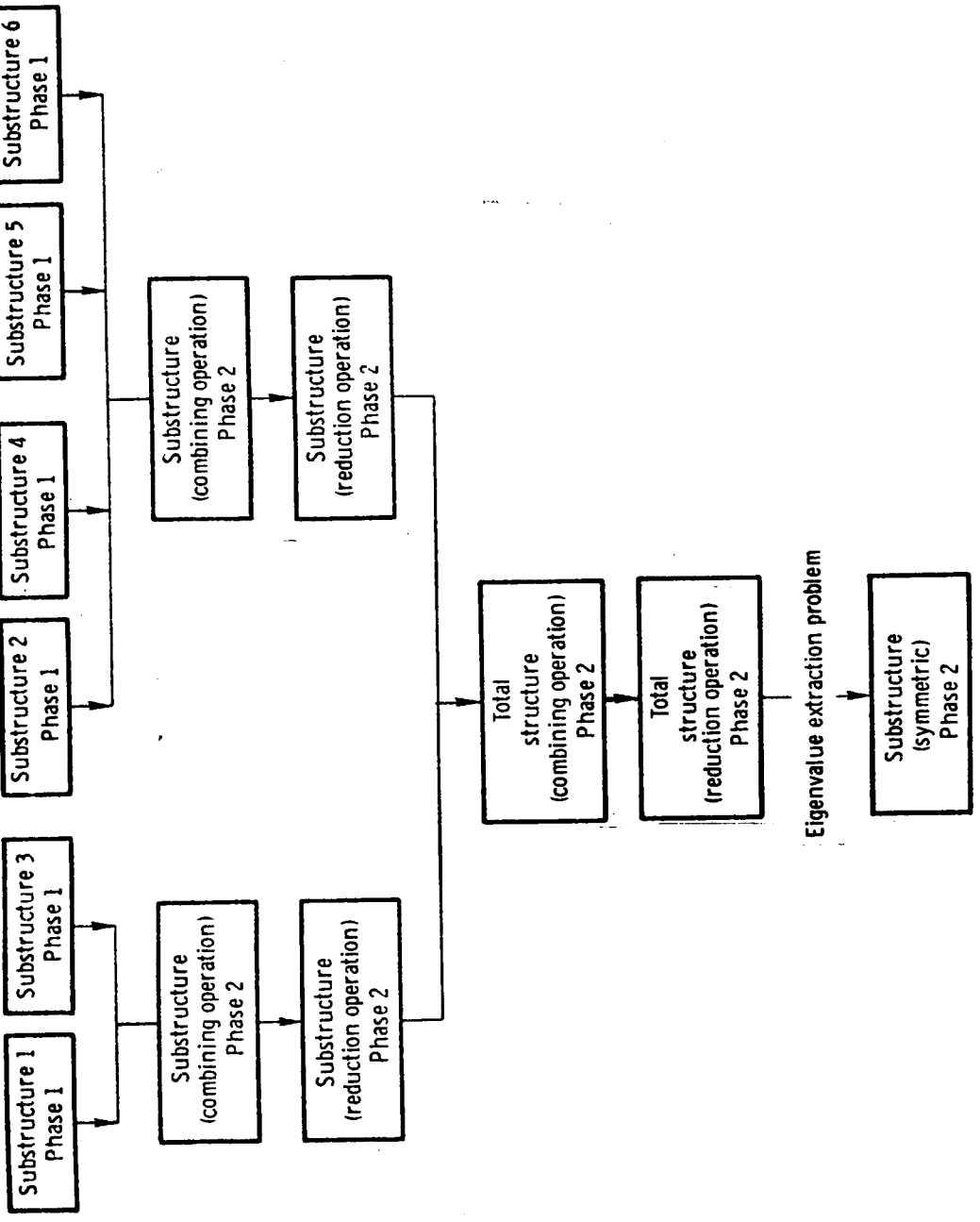

Figure 26. Flow of the Coupling to Form the Dynamic Model

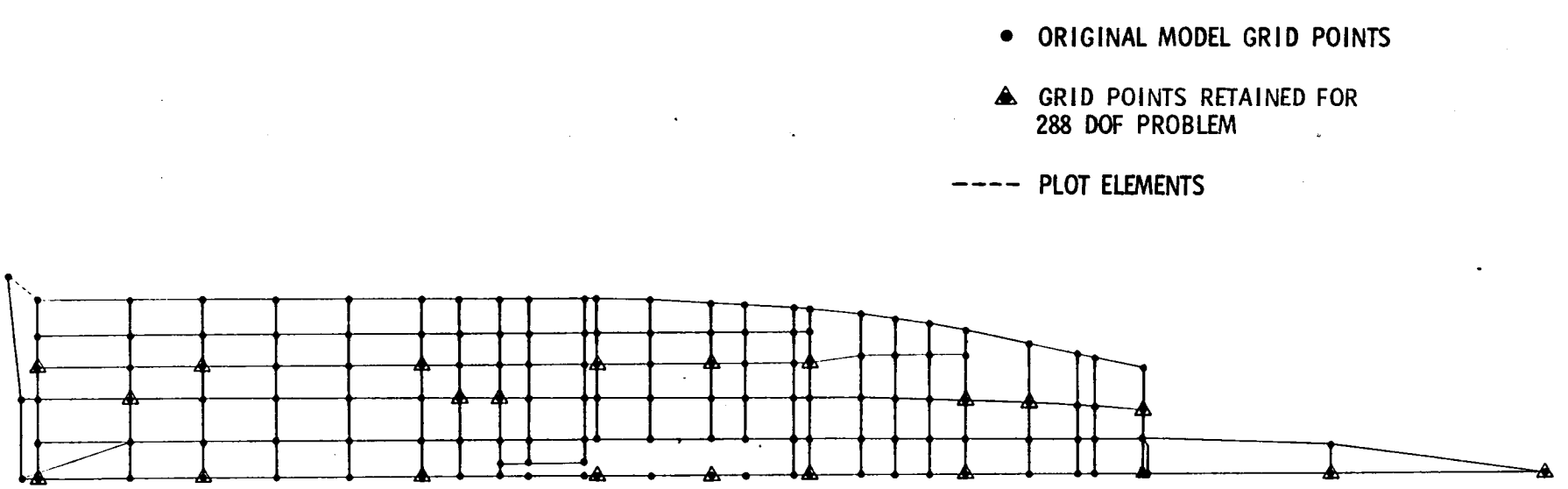

Figure 27. YF-12A NASTRAN Model

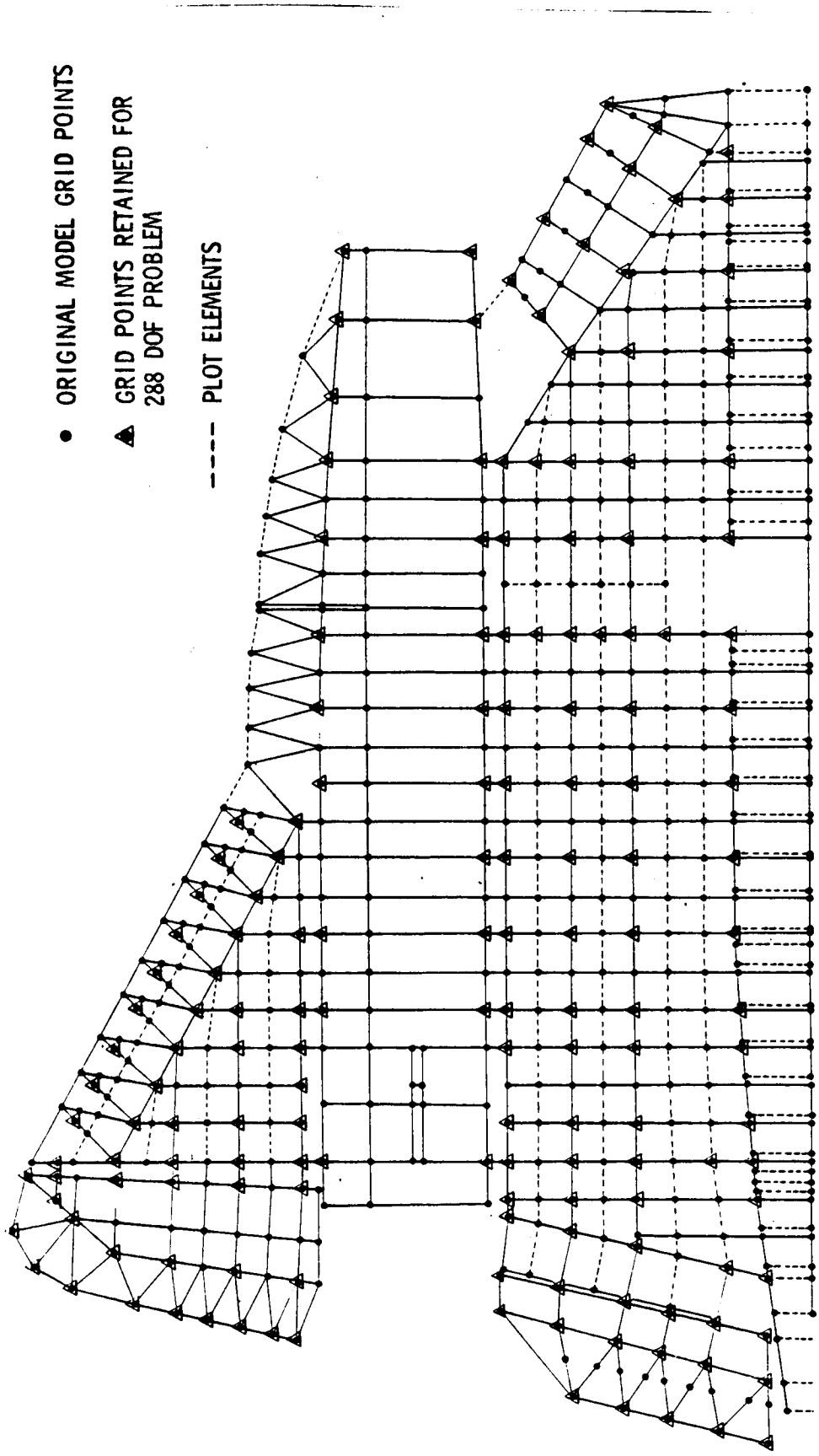

Figure 27. YF-12A NASTRAN Model

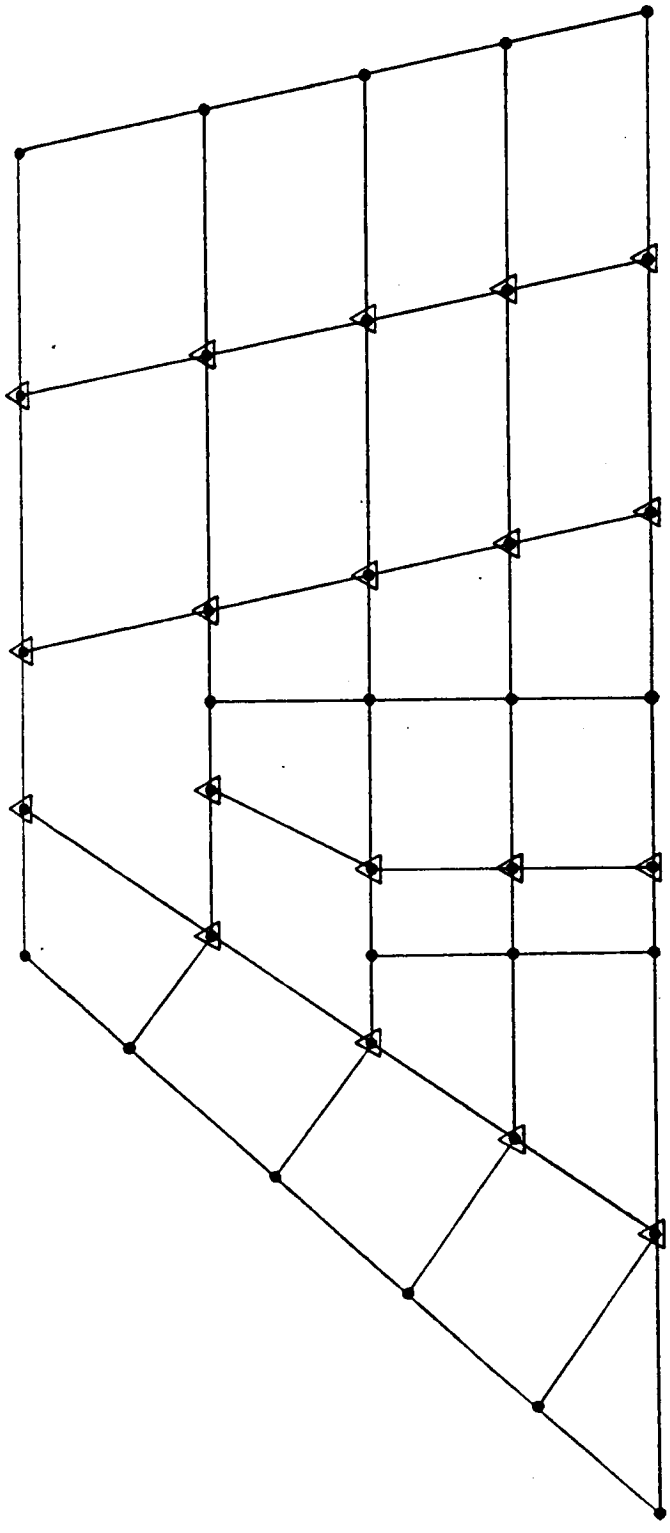

Figure 27. YF-12A NASTRAN Model

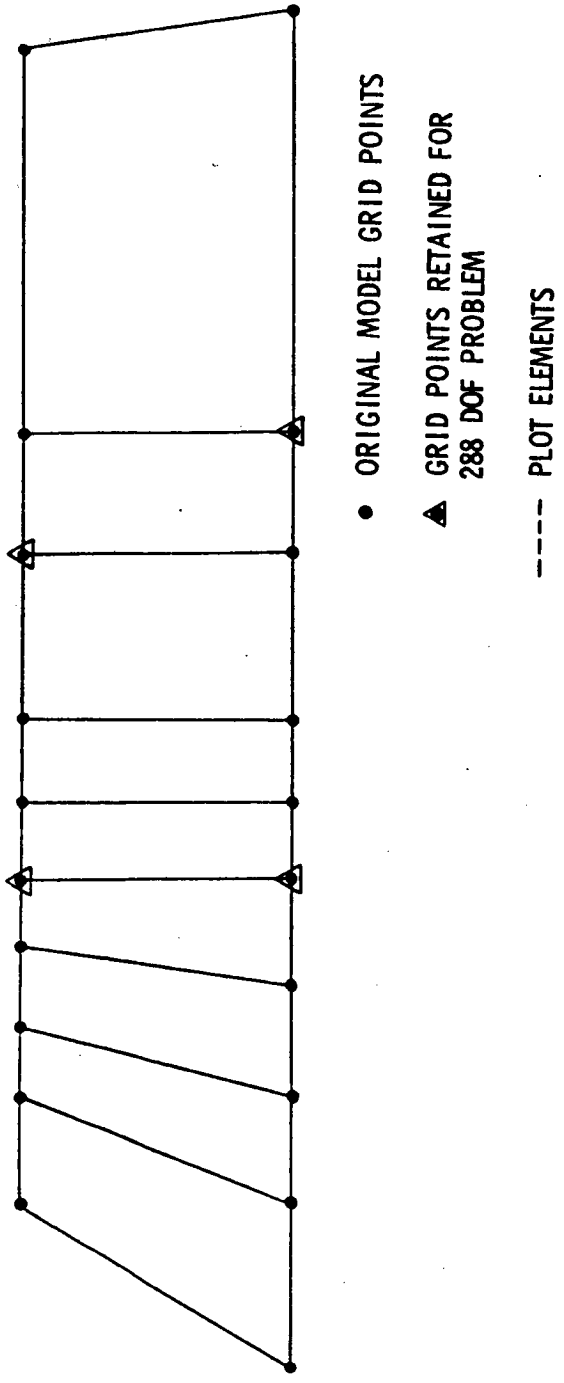

Figure 27. YF-12A NASTRAN Model

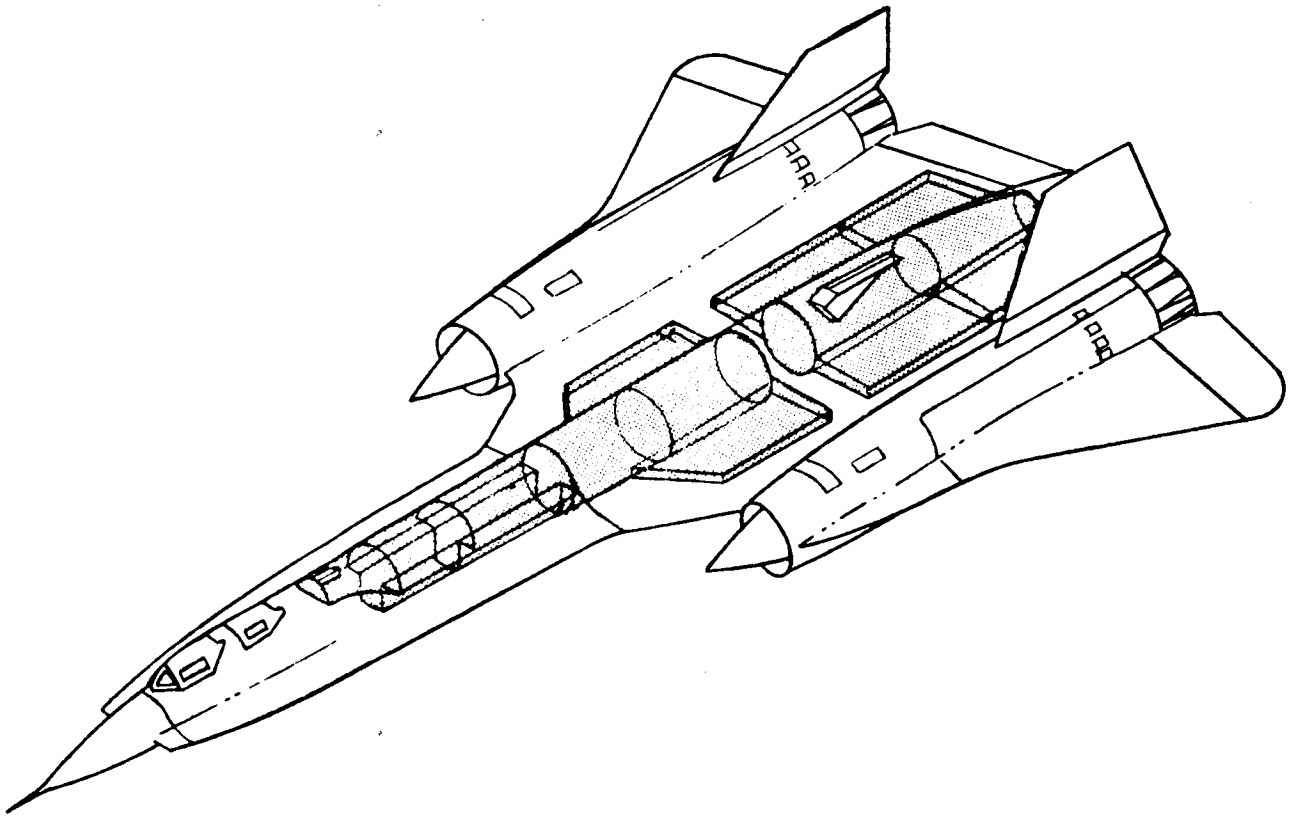

Figure 28. Fuel Compartment Configuration

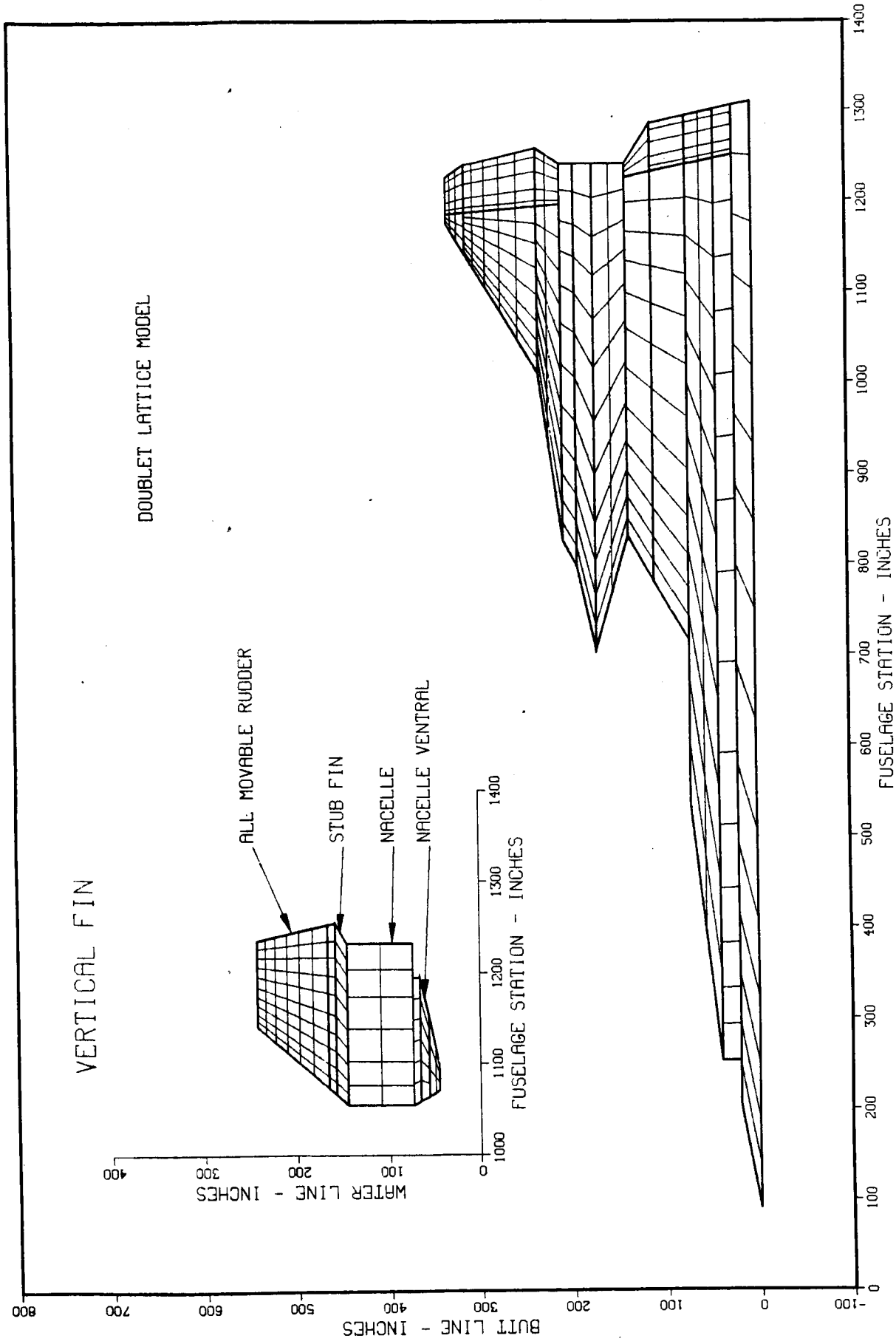

Figure 29. YF-12A Doublet Lattice Model

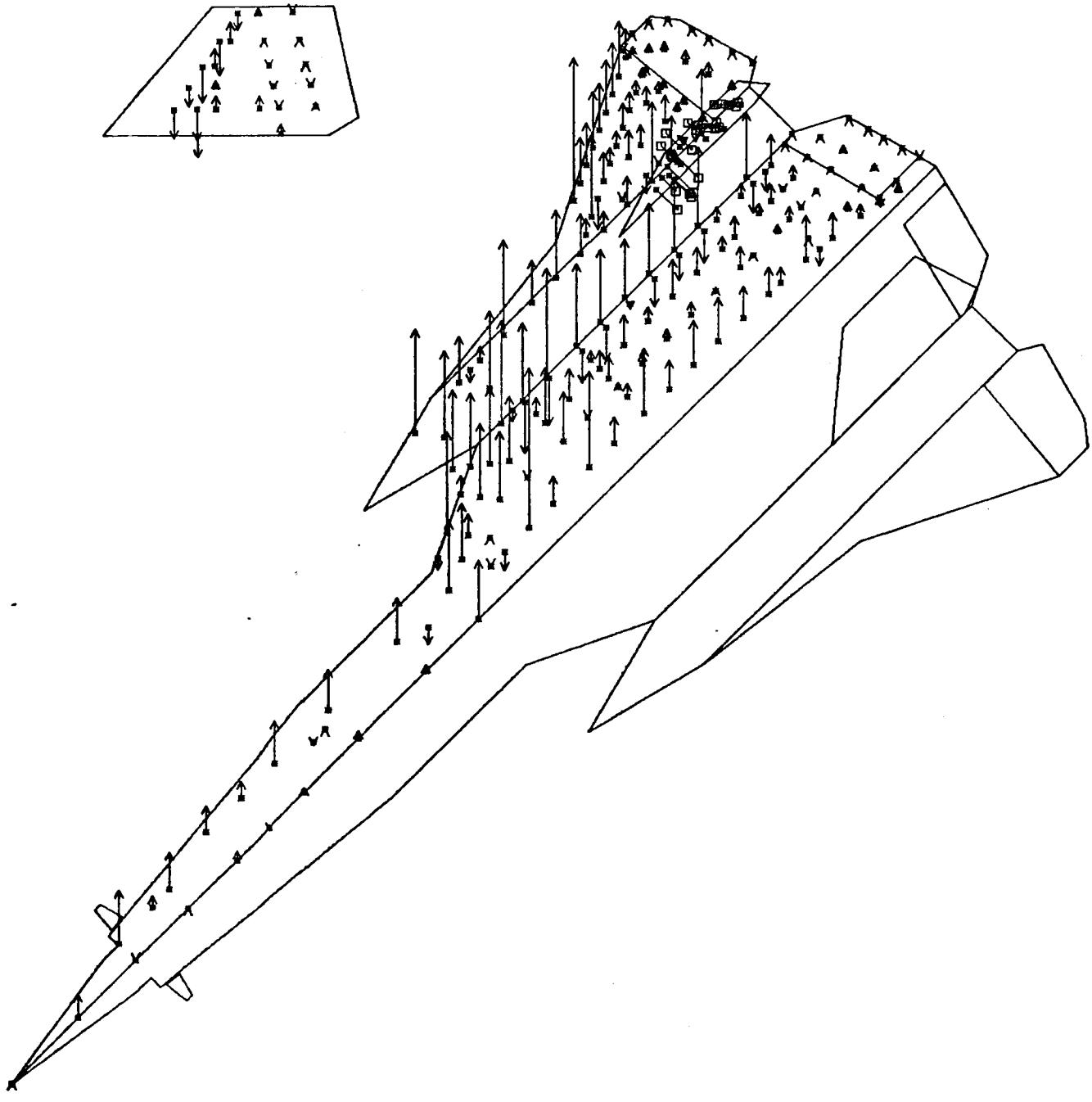

Figure 30. YF-12A Doublet Lattice Lift Distribution, Mach .70

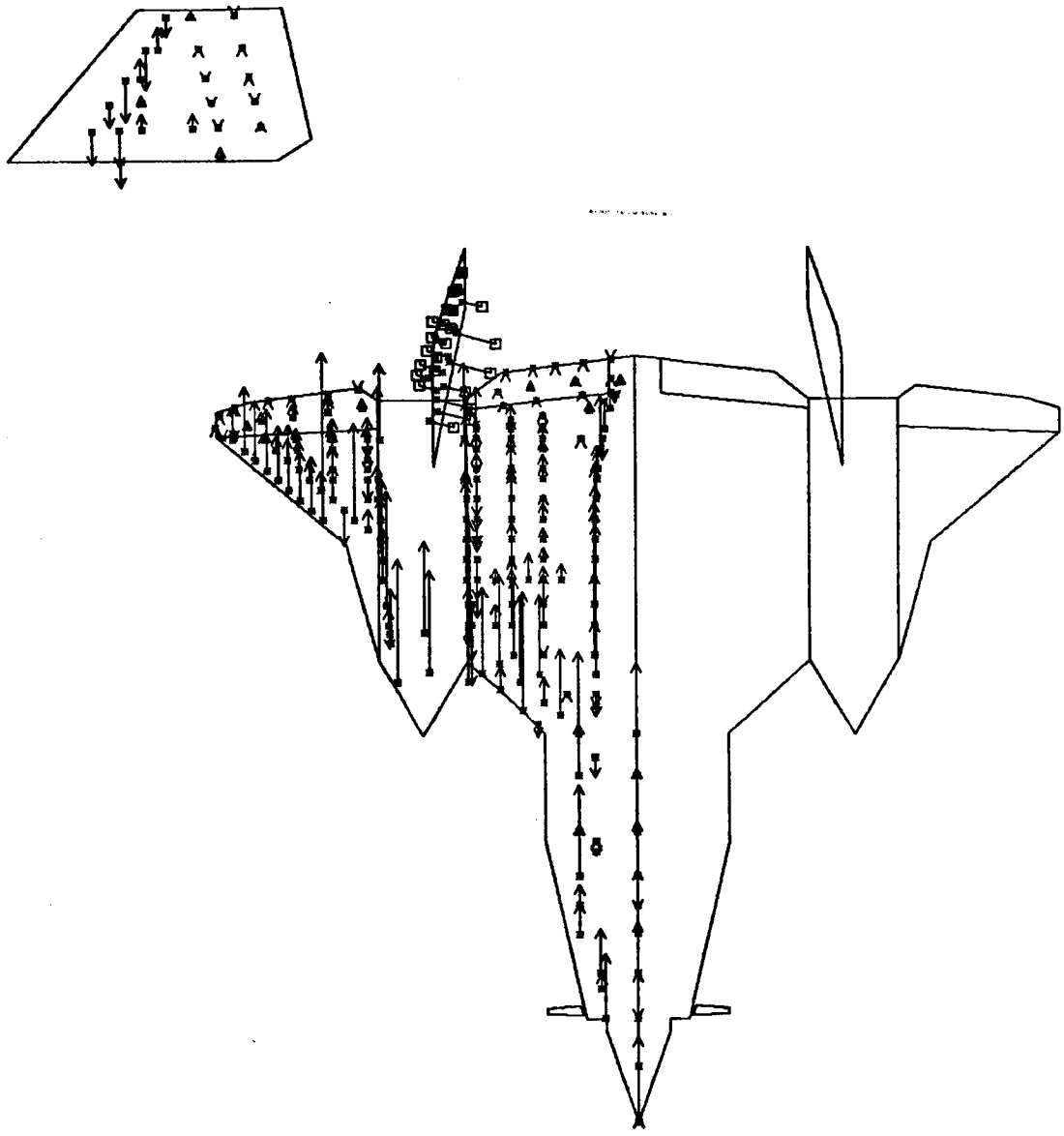

SCALE = 1/ 150

Figure 30. YF-12A Doublet Lattice Lift Distribution, Mach .70

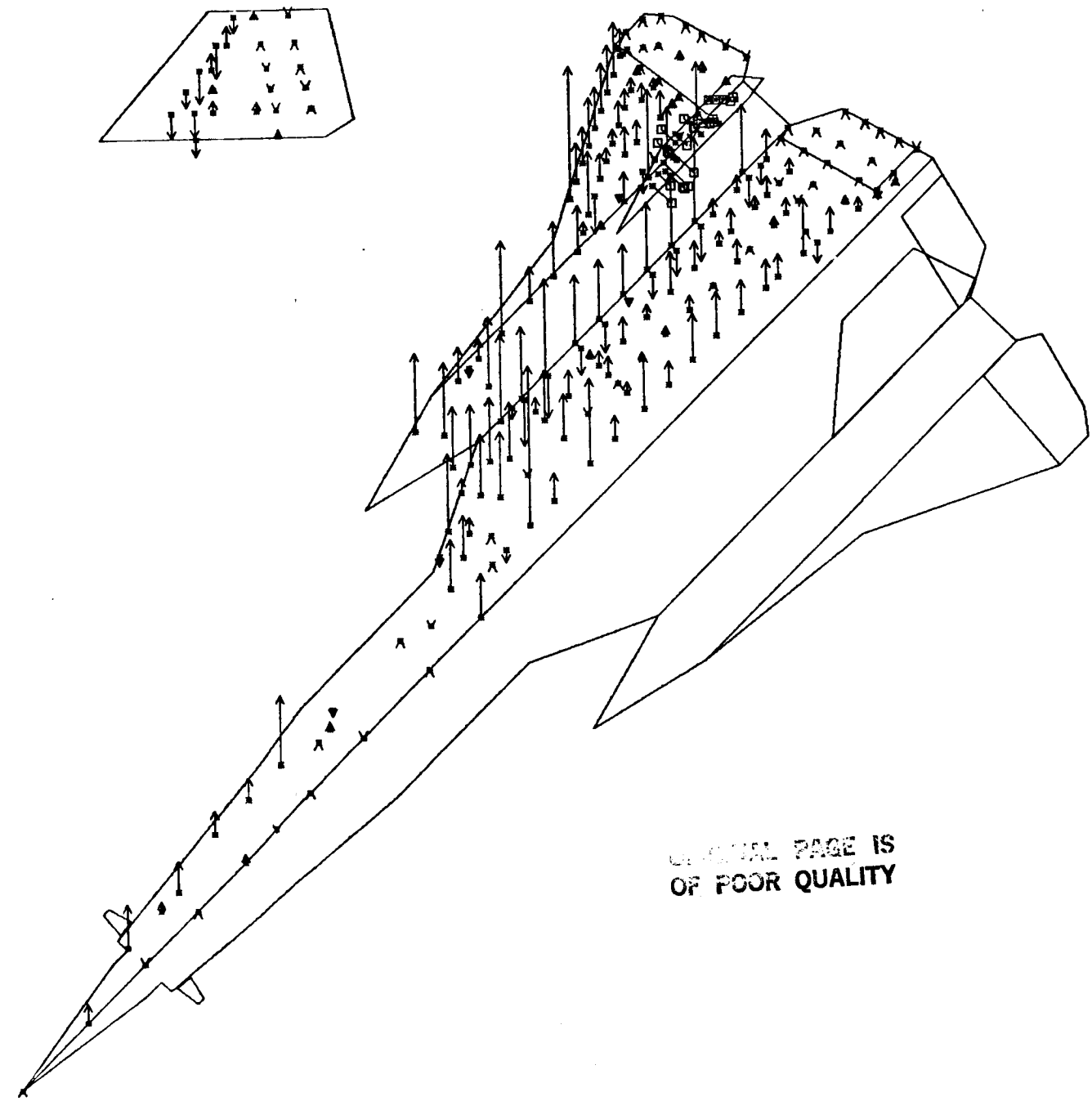

Figure 31. YF-12A Doublet Lattice Lift Distribution, Mach .95

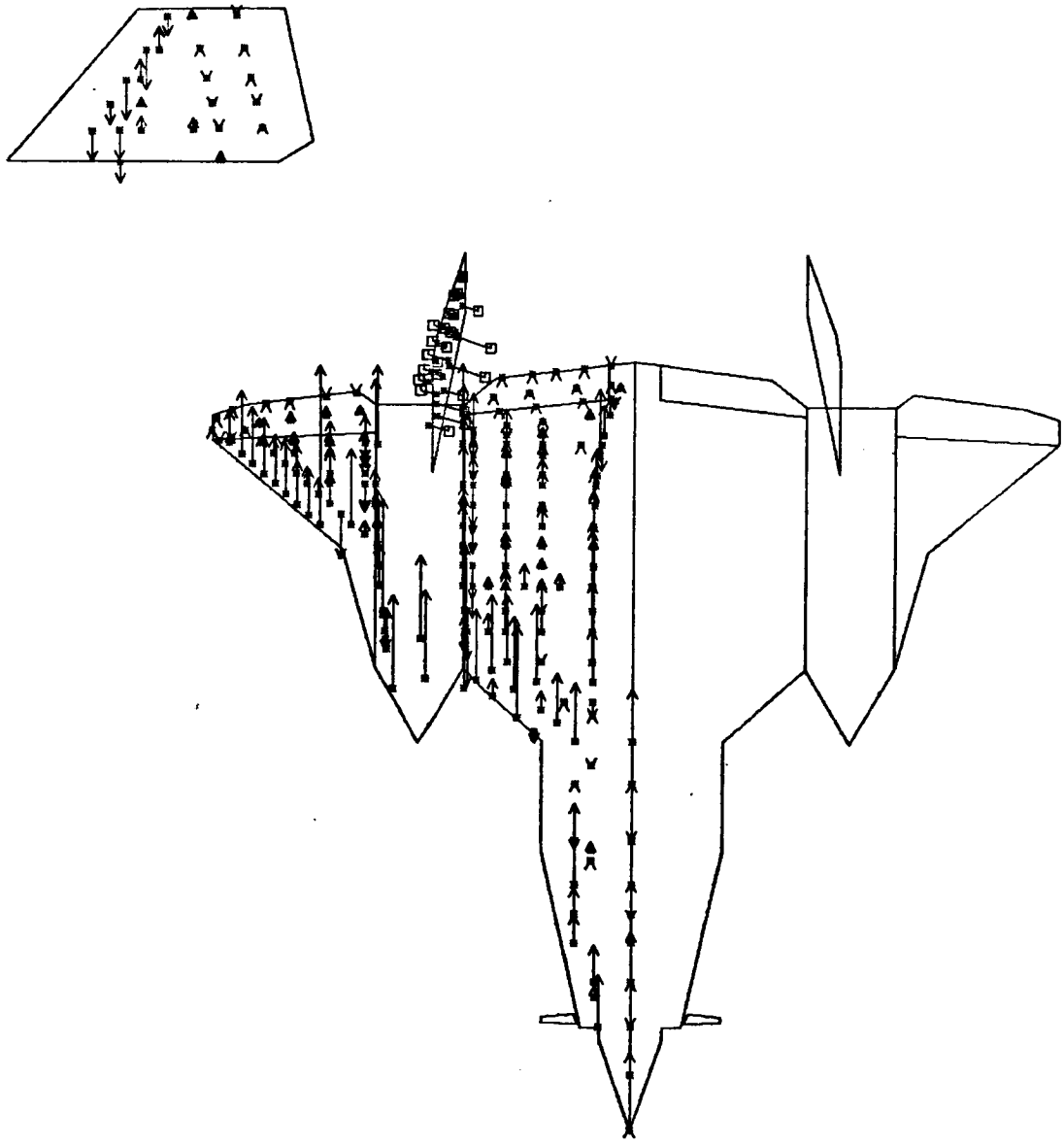

SCALE = 1/150

Figure 31. YF-12A Doublet Lattice Lift Distribution, Mach .95

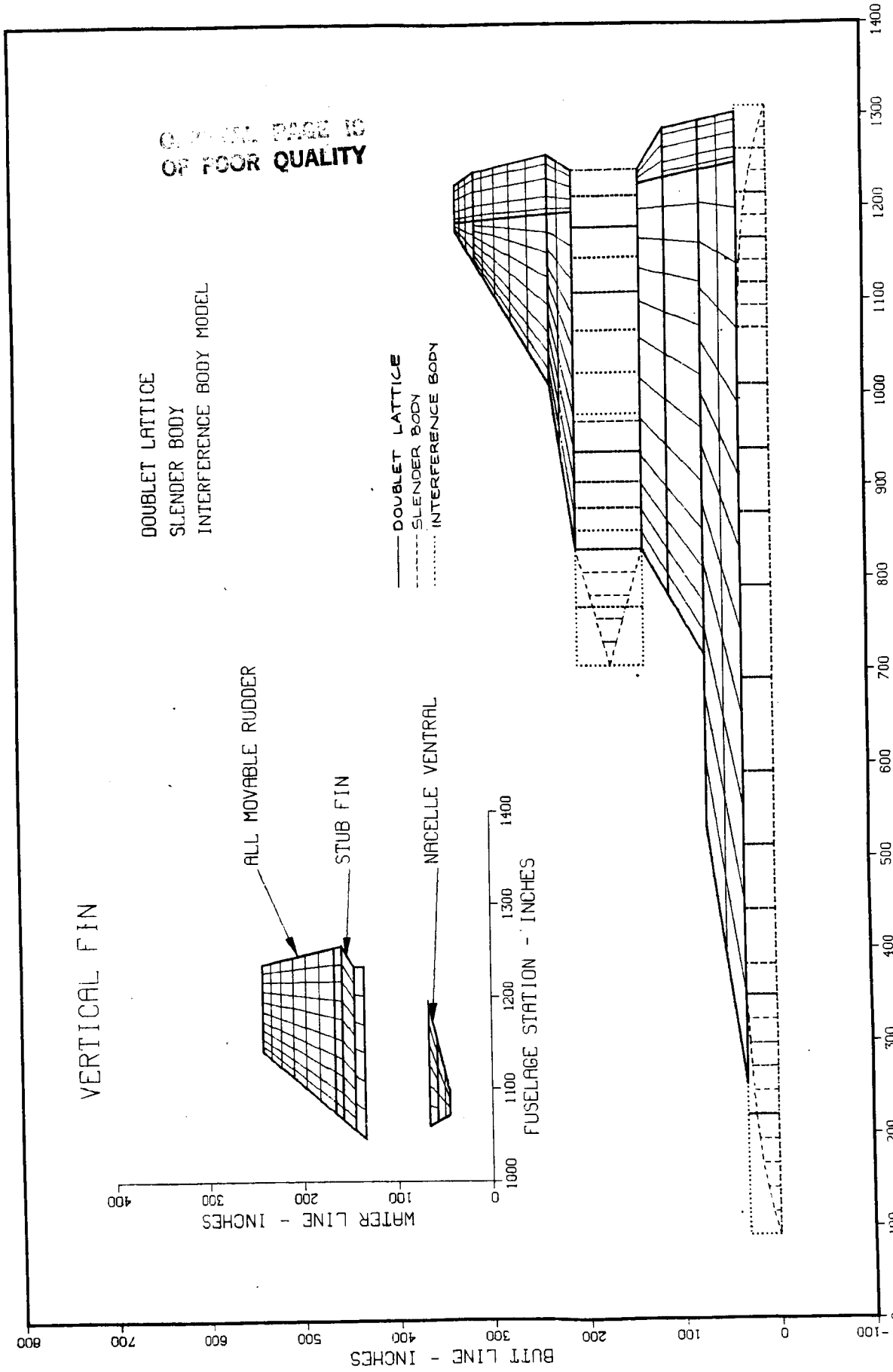

Figure 32. YF-12A Doublet Lattice, Slender Body, Interference Body Model

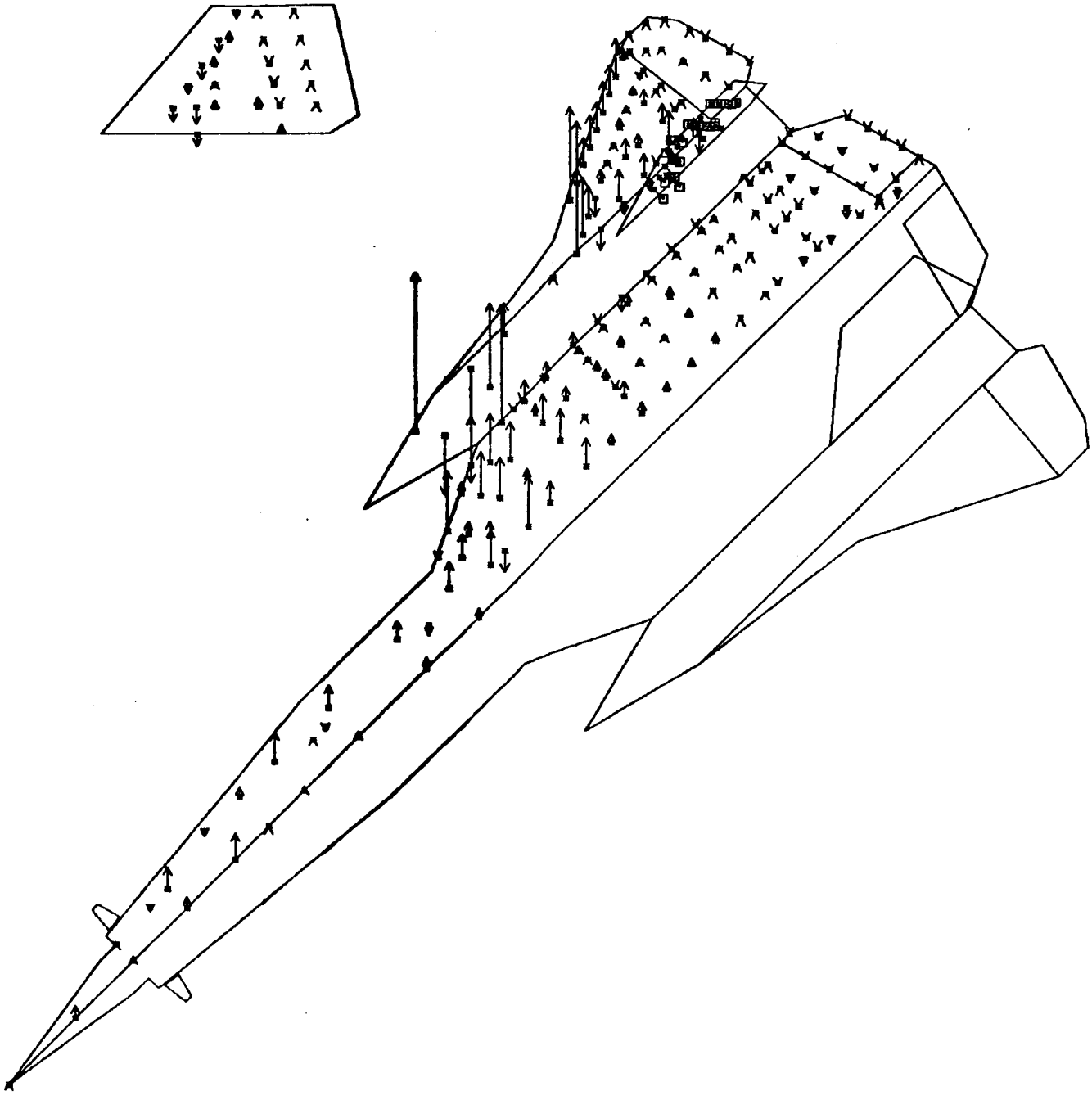

Figure 33. YF-12A DLSLIN Lift Distribution, Mach .70

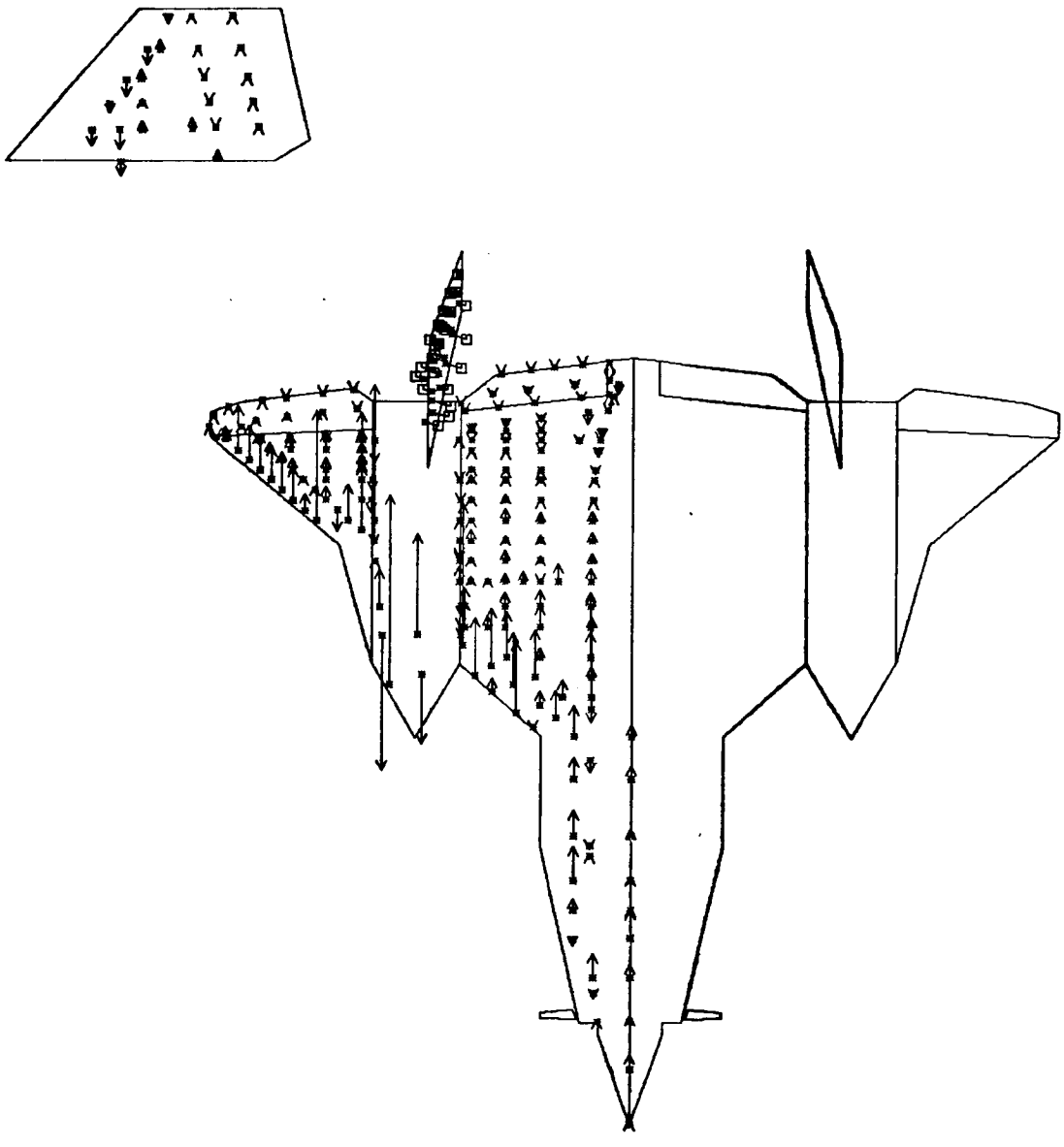

SCALE = 1/ 150

Figure 33. YF-12A DLSLIN Lift Distribution, Mach .70

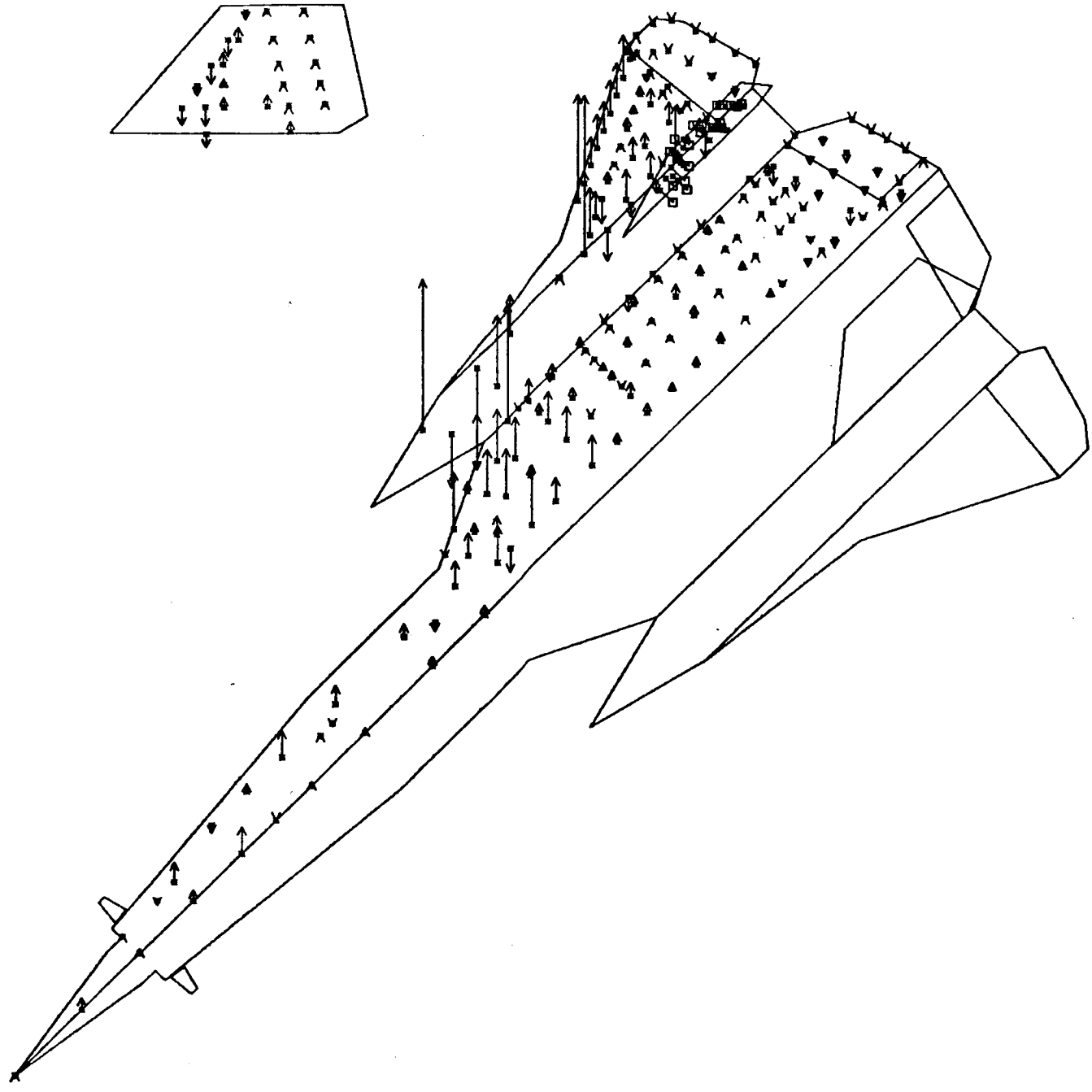

Figure 34. YF-12A DLSLIN Lift Distribution, Mach .95

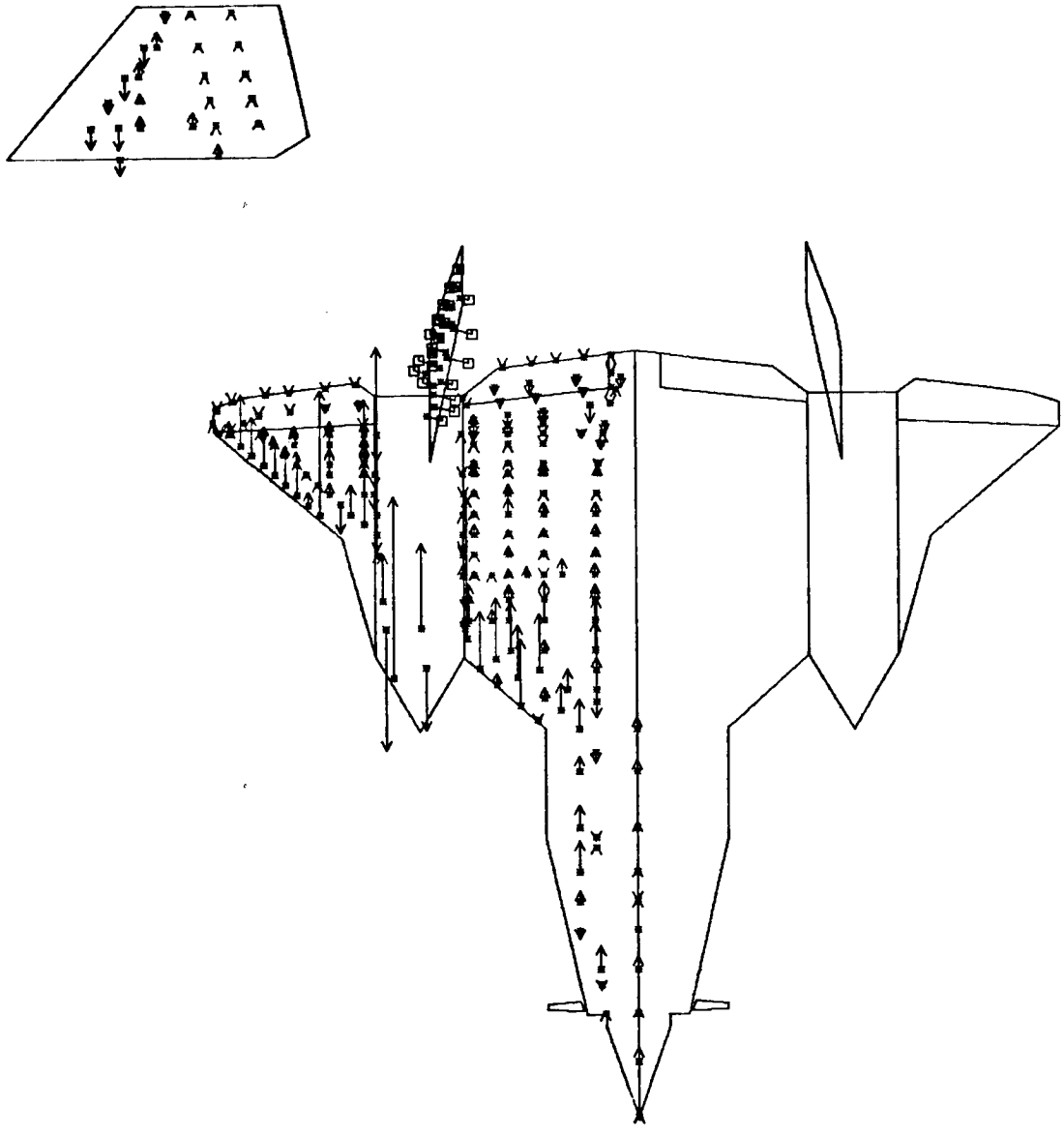

SCALE = 1/ 150

Figure 34. YF-12A DLSLIN Lift Distribution, Mach .95

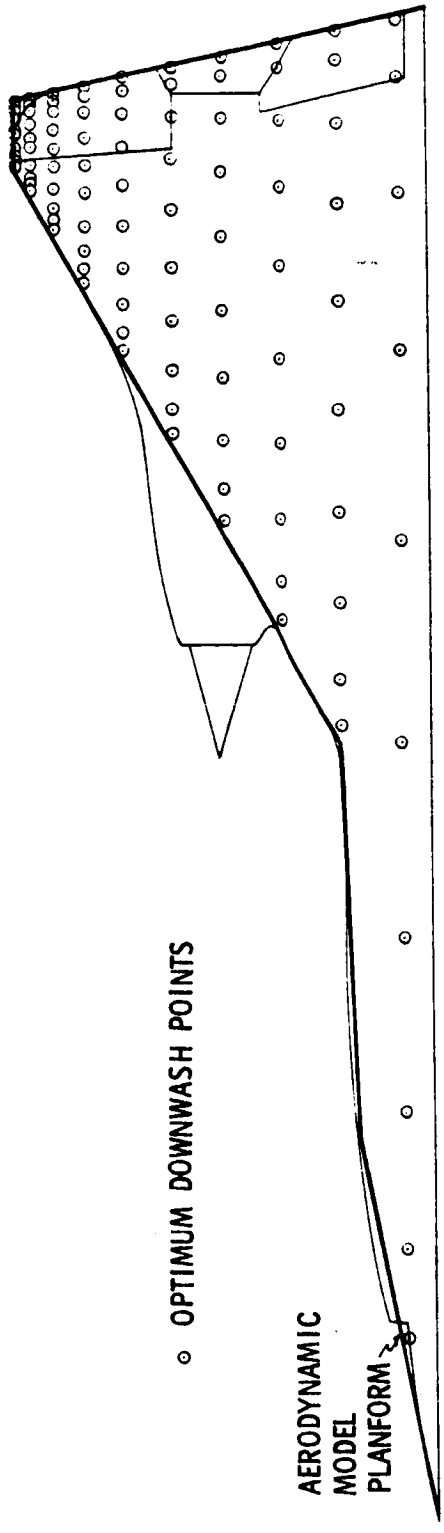

Figure 35. YF-12A Kernel Function Optimum Downwash Points

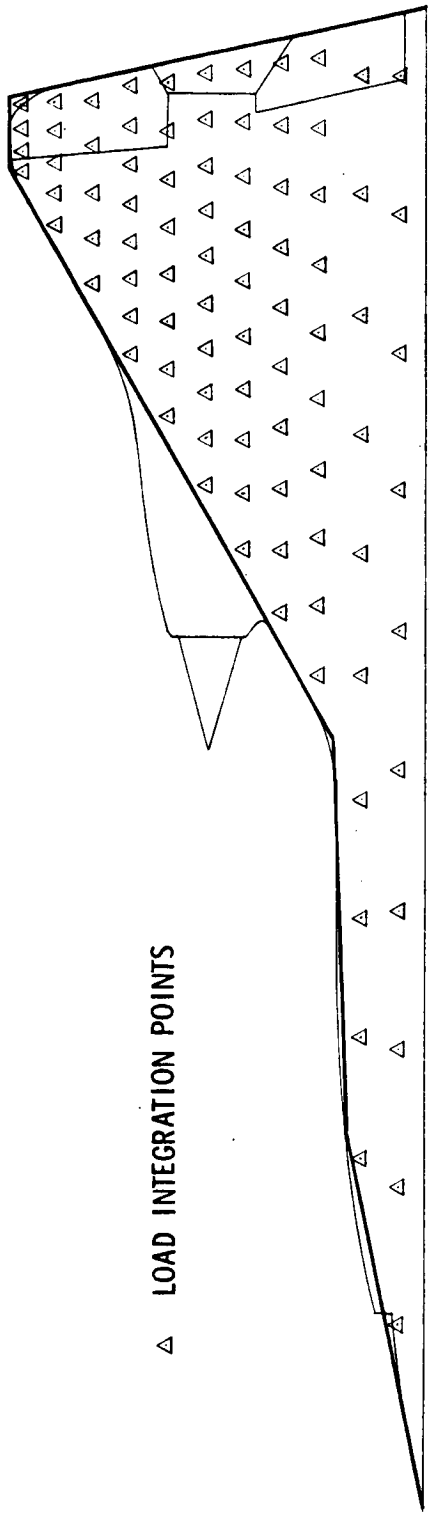

Figure 36. YF-12A Kernel Function Load Integration Points

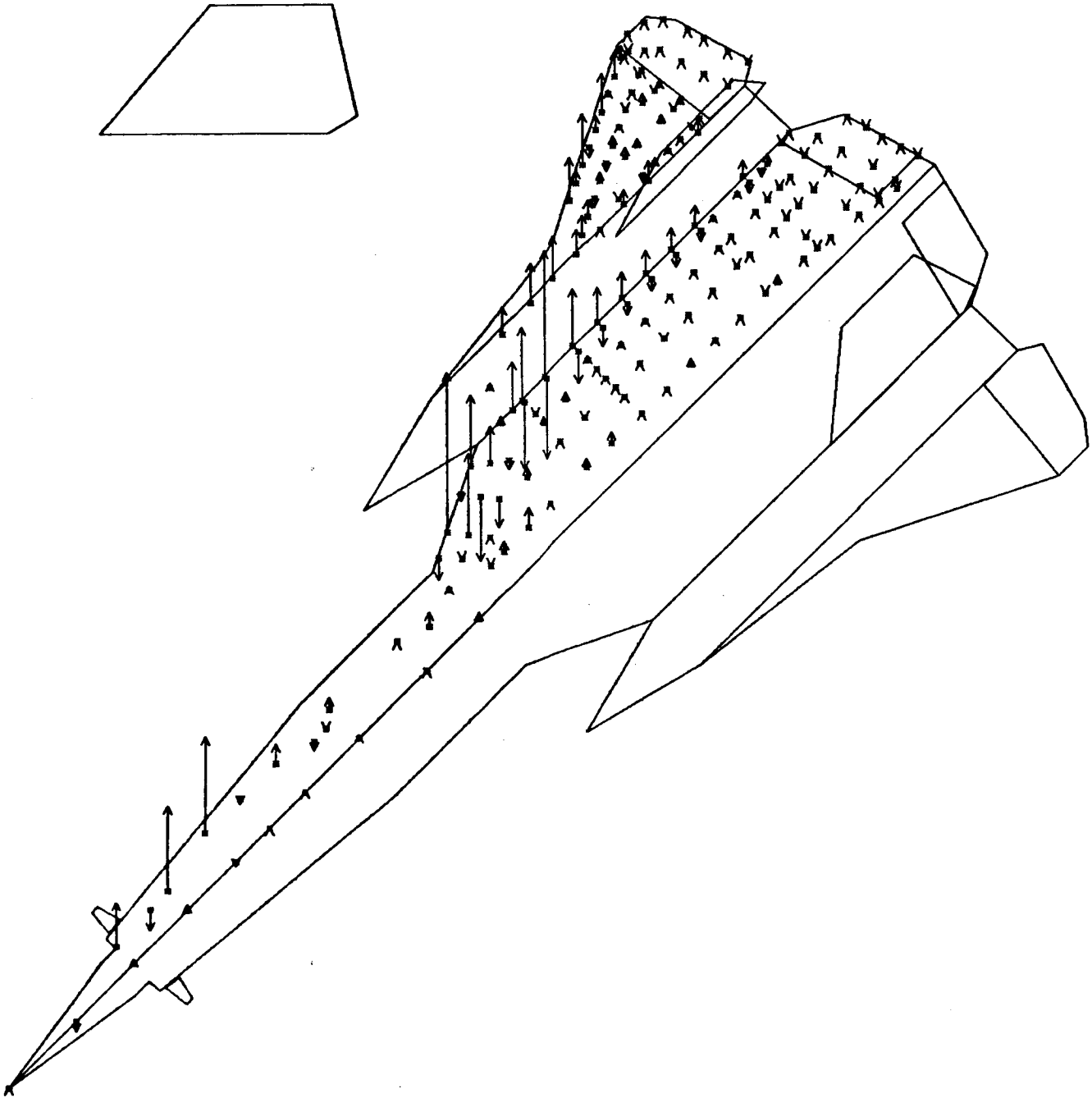

SCALE = 1/ 150

Figure 37. YF-12A Kernel Function Lift Distribution, Mach .95

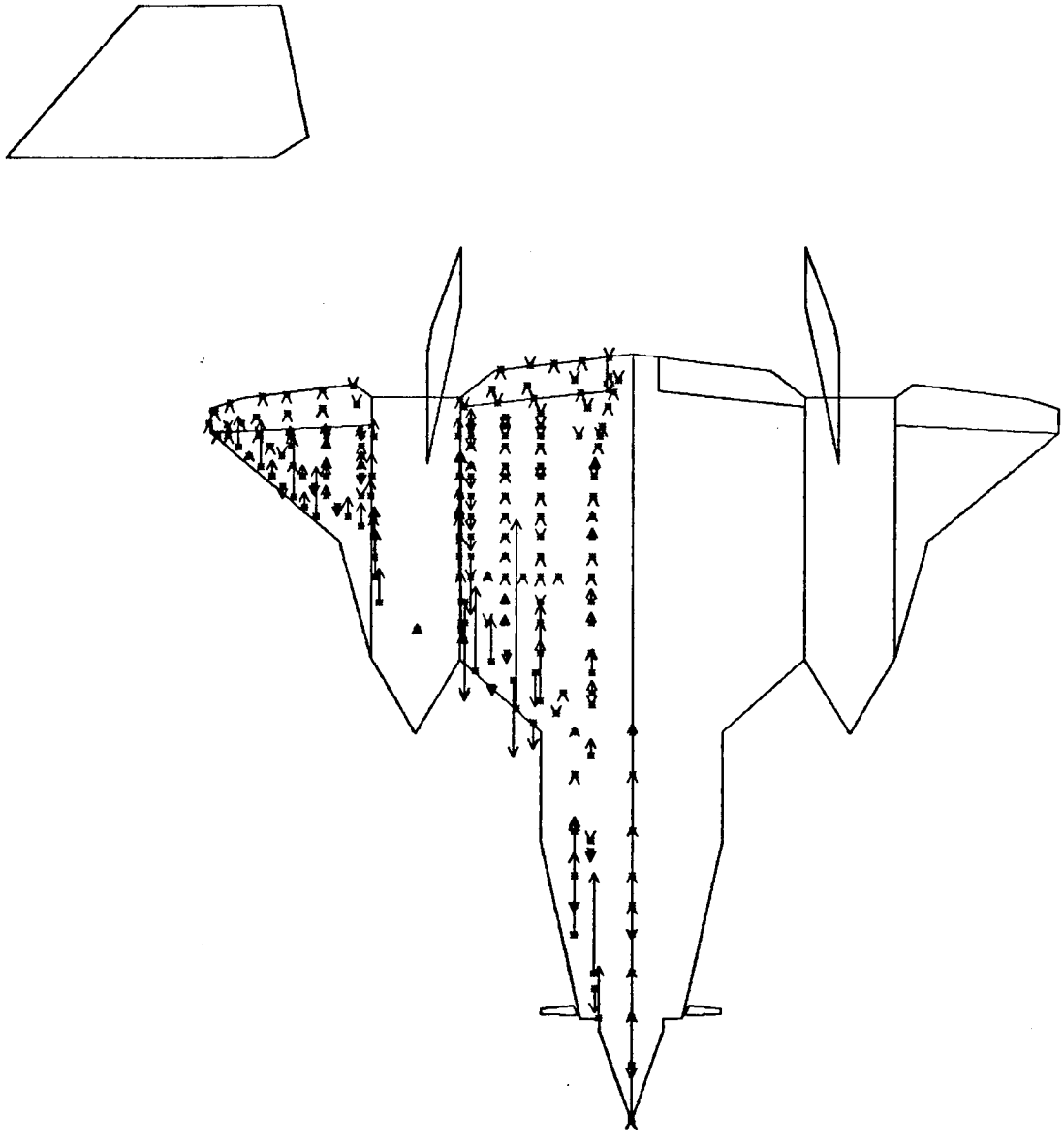

SCALE = 1/ 150

Figure 37. YF-12A Kernel Function Lift Distribution, Mach .95

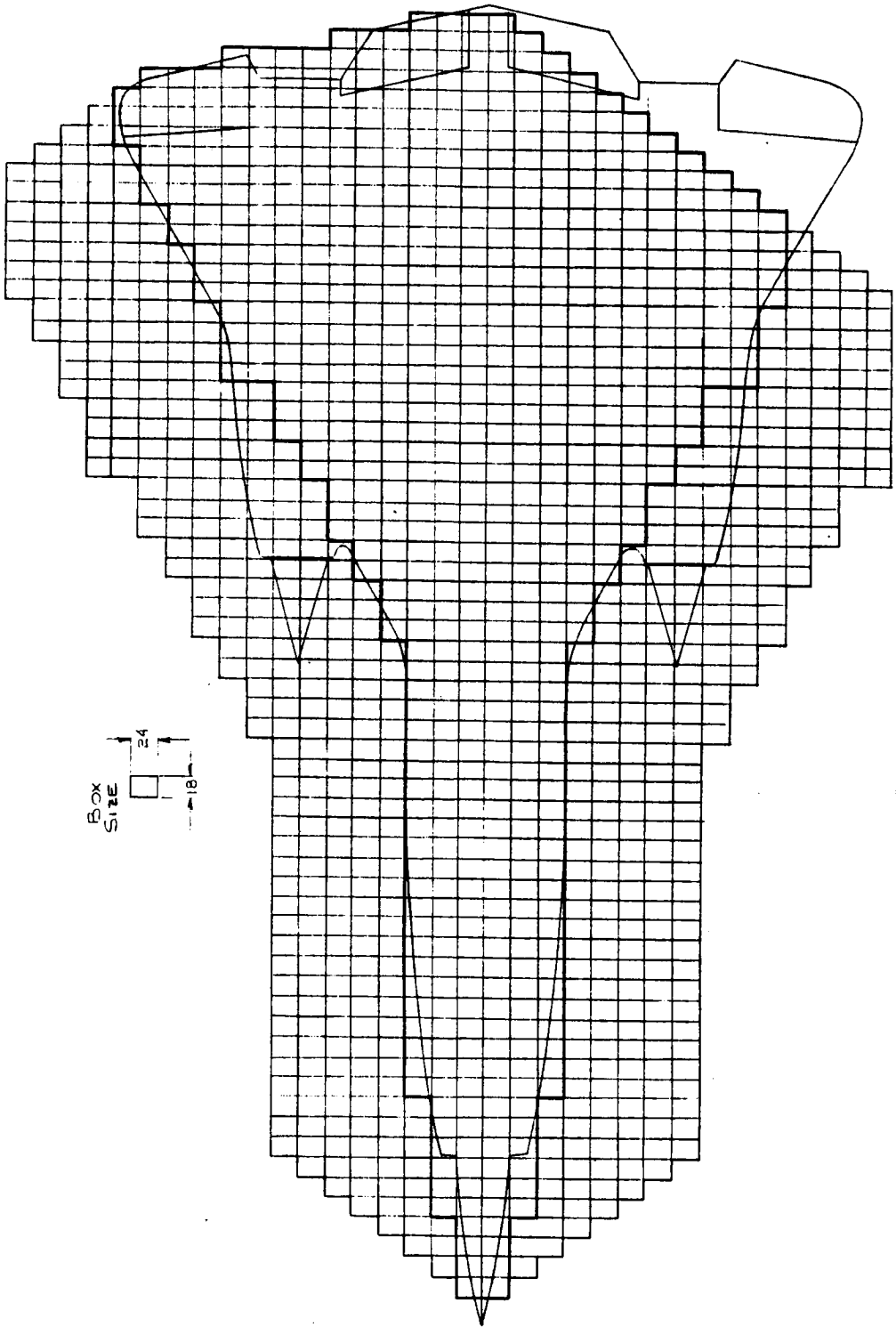

Figure 38. YF-12A Mach Box Model

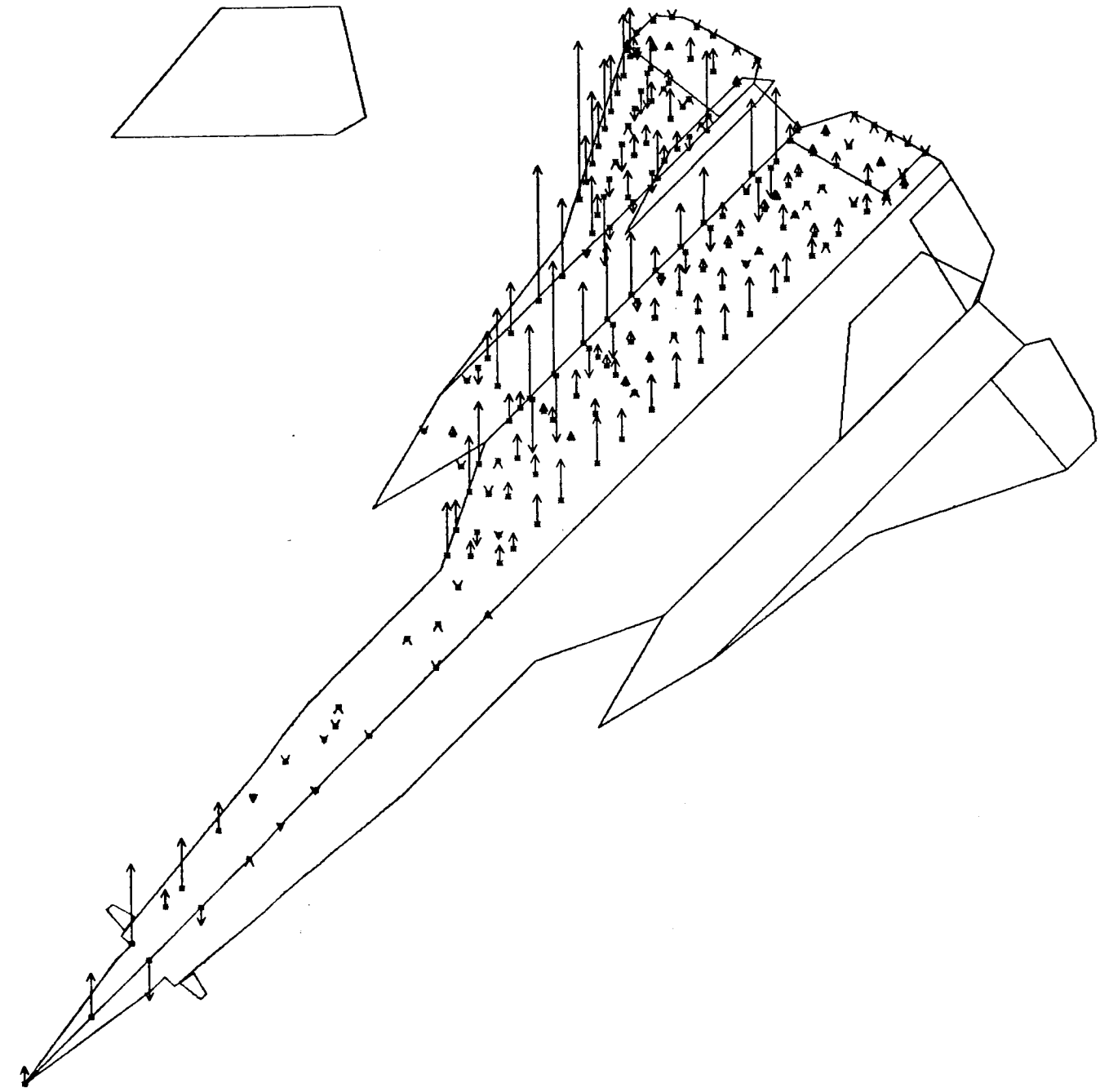

Figure 39. YF-12A Mach Box Lift Distribution Mach 1.25

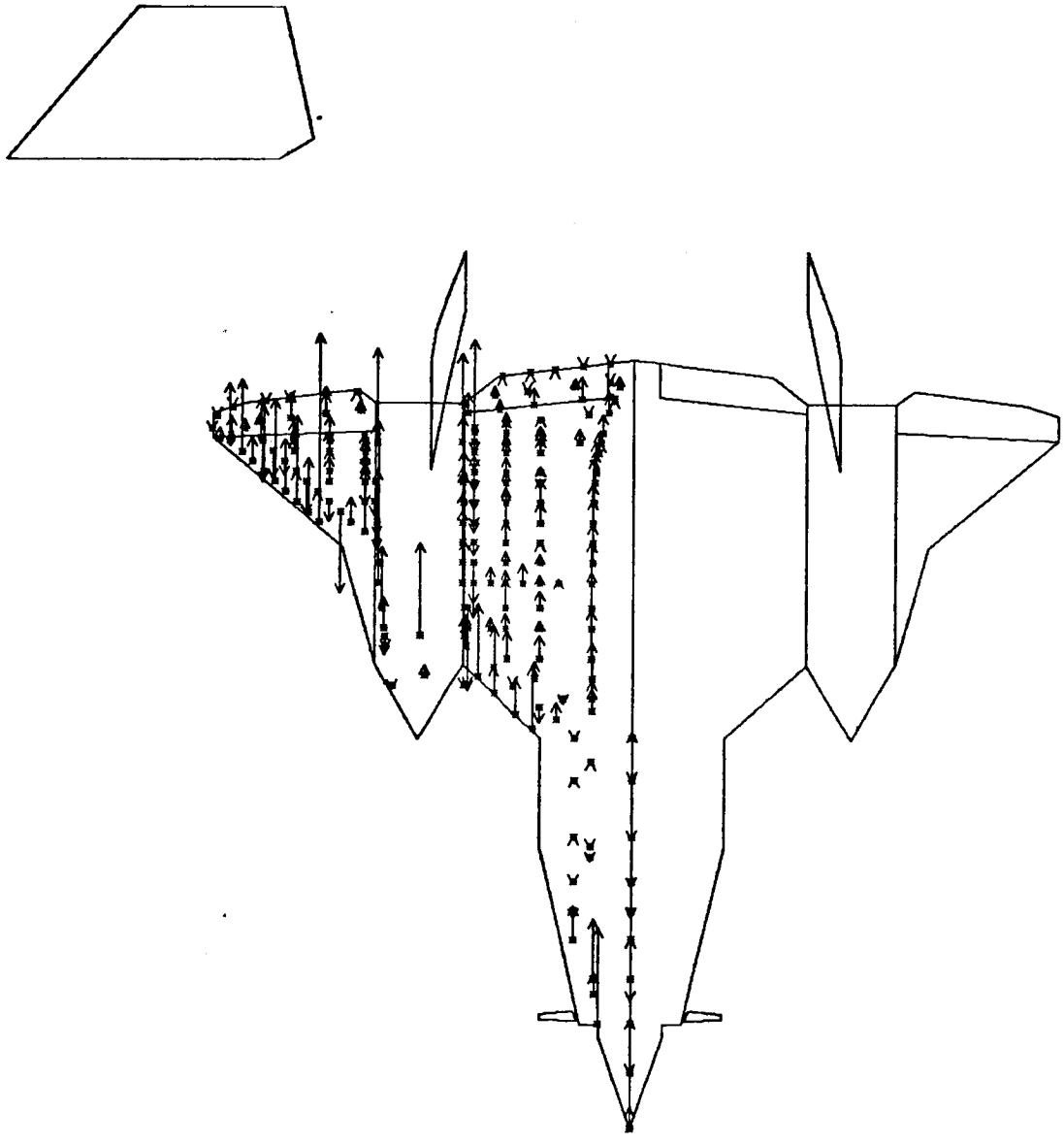

SCALE = 1/ 150

Figure 39. YF-12A Mach Box Lift Distribution Mach 1.25

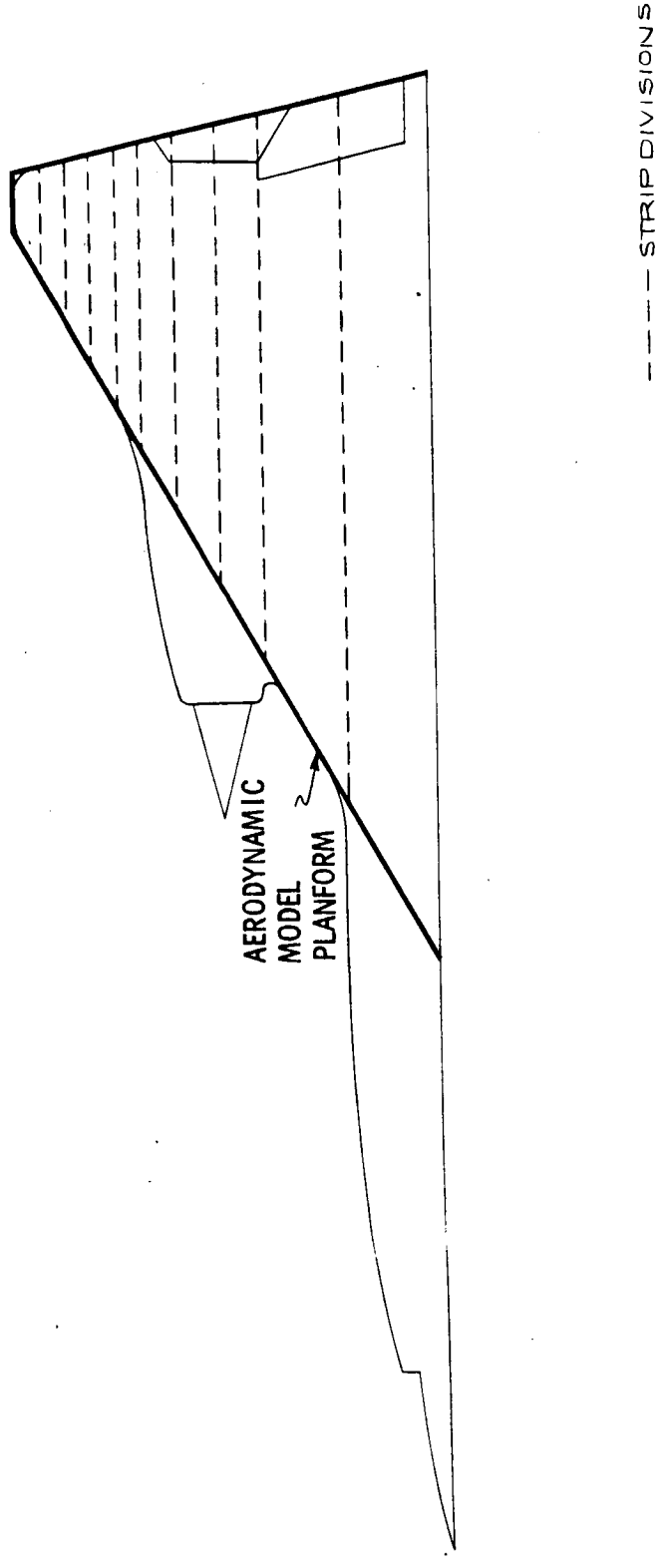

Figure 40. YF-12A Piston Theory Model

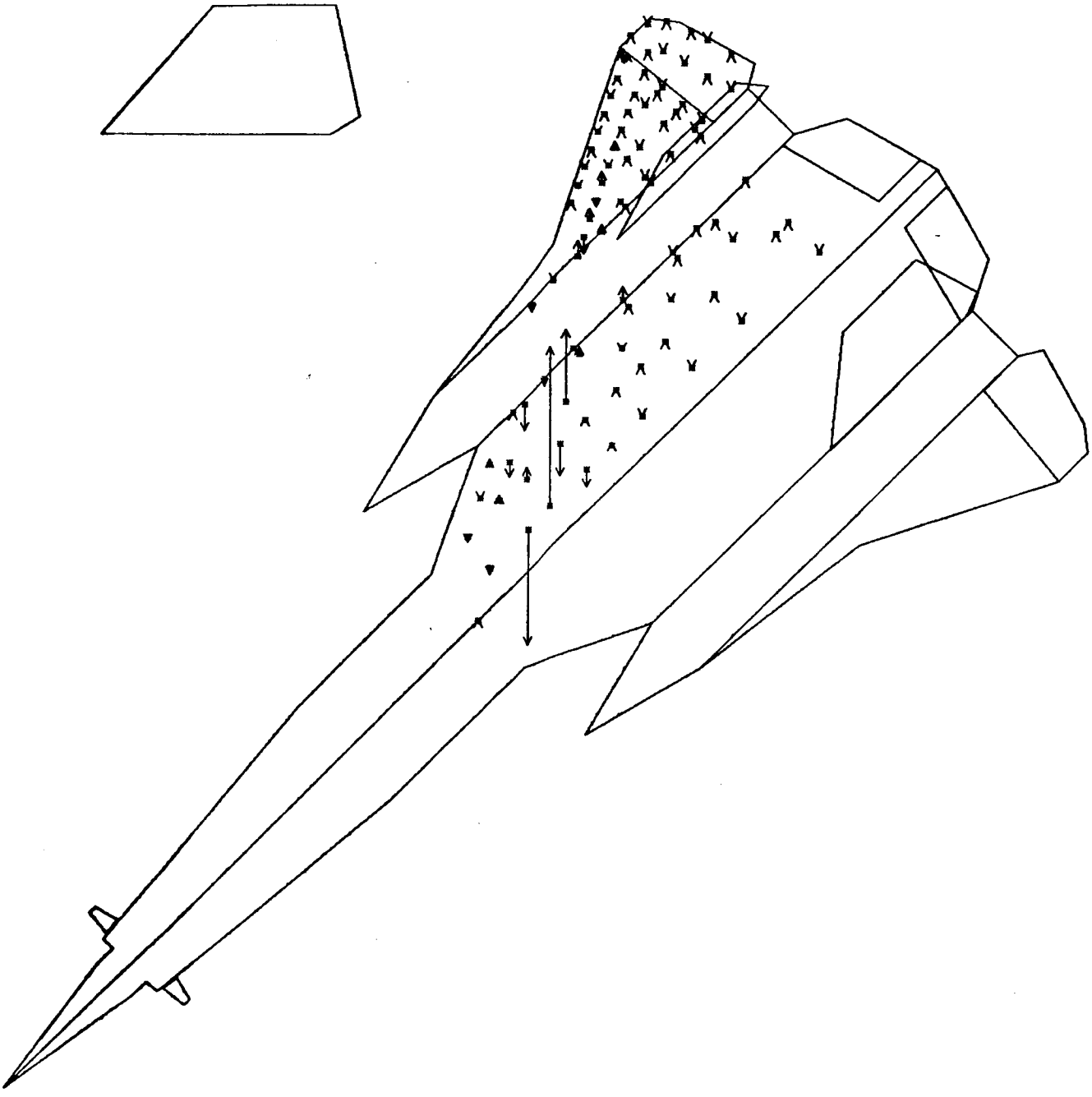

SCALE = 1/ 150

Figure 41. YF-12A Piston Theory Lift Distribution, Mach 2.0

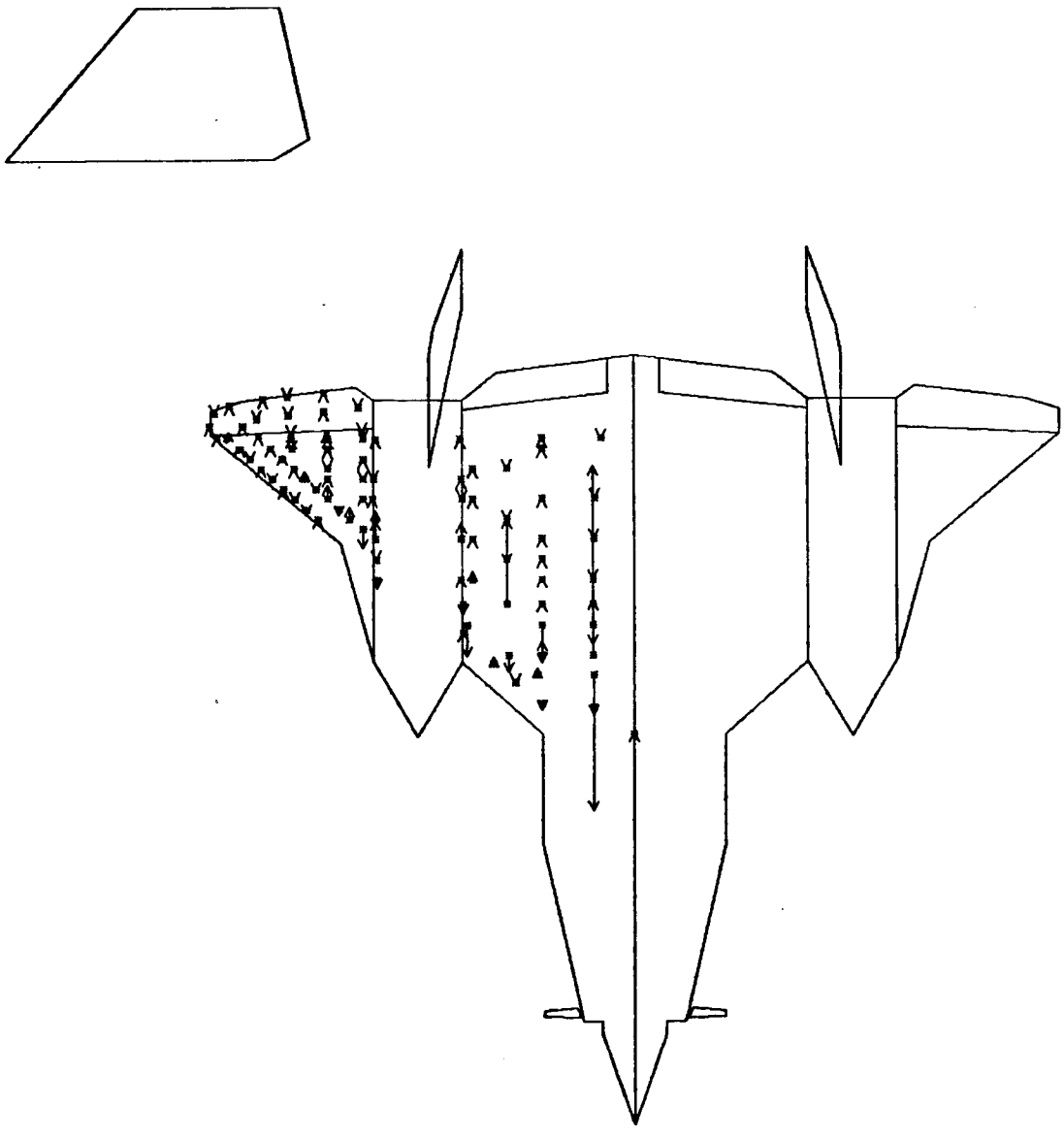

SCALE = 1/ 150

Figure 41. YF-12A Piston Theory Lift Distribution, Mach 2.0

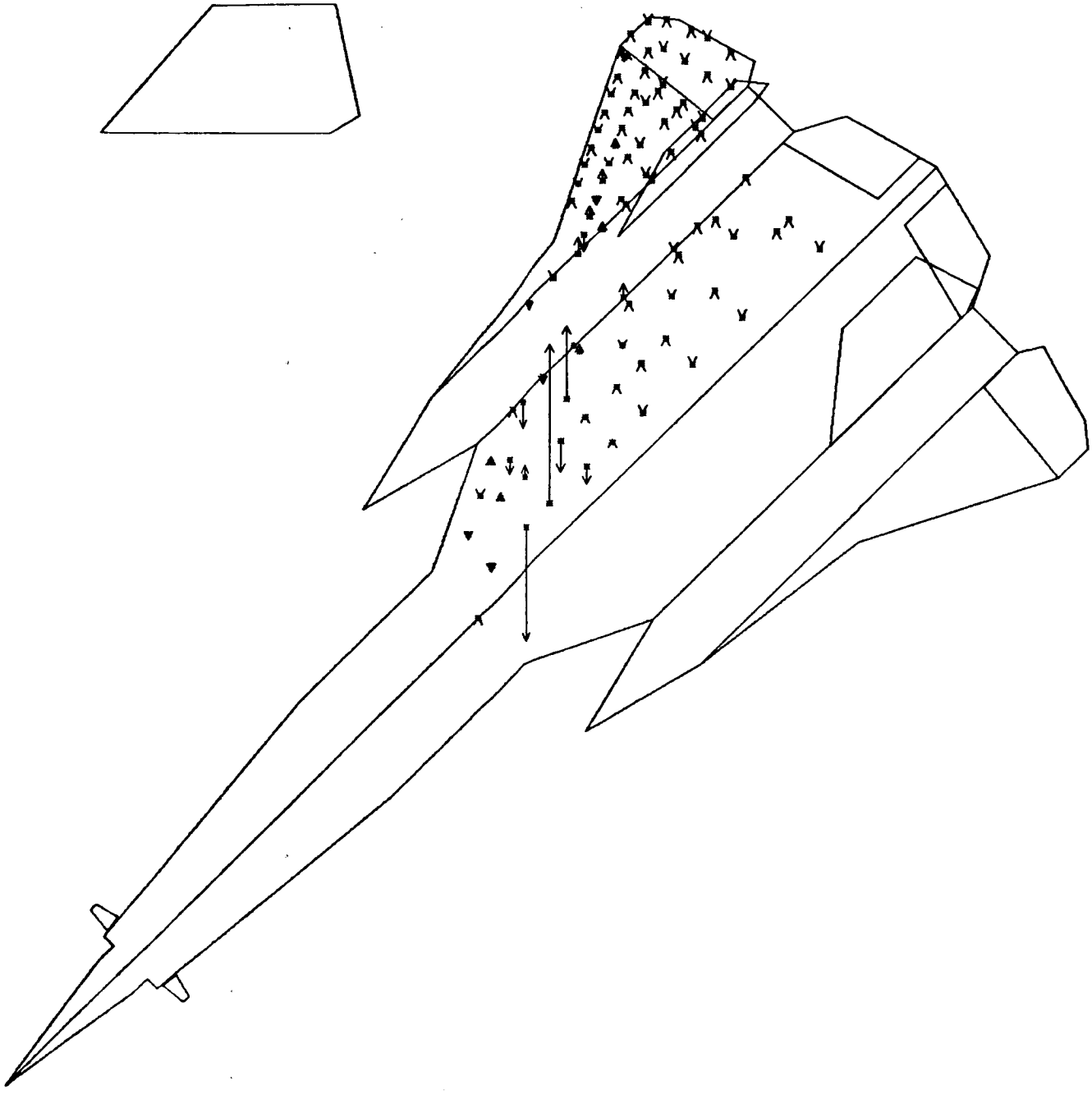

SCALE = 1/ 150

Figure 42. YF-12A Piston Theory Lift Distribution, Mach 2.7

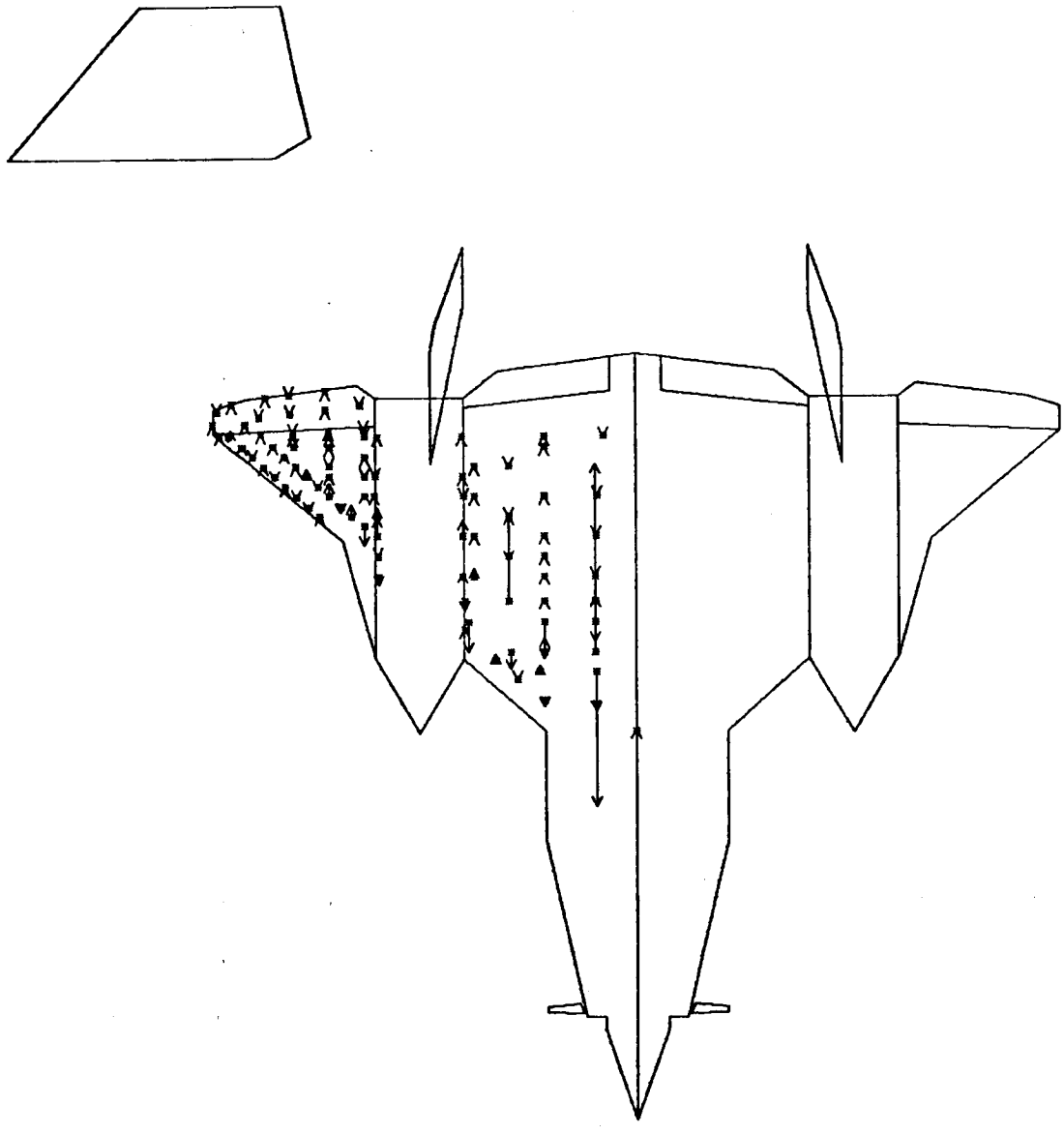

SCALE = 1/ 150

Figure 42. YF-12A Piston Theory Lift Distribution, Mach 2.7

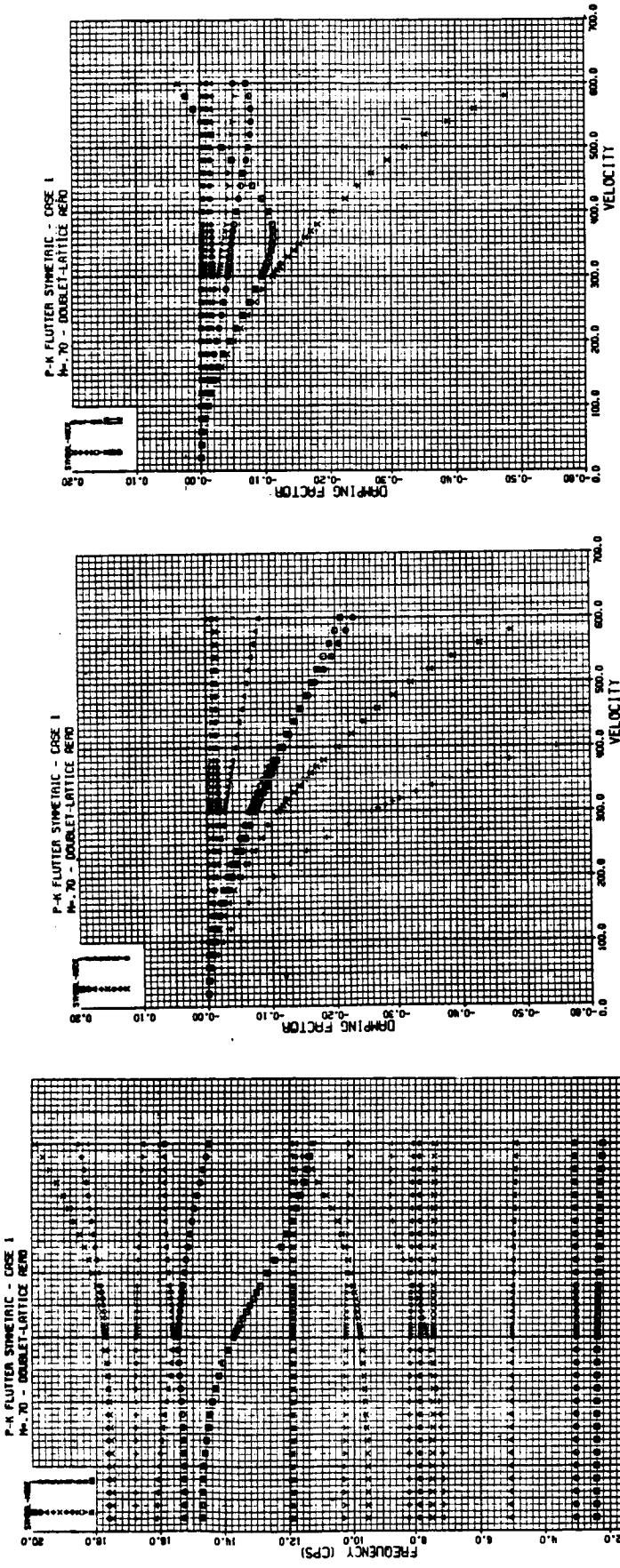

Figure 43. Velocity-Frequency-Damping Plot (VFG)

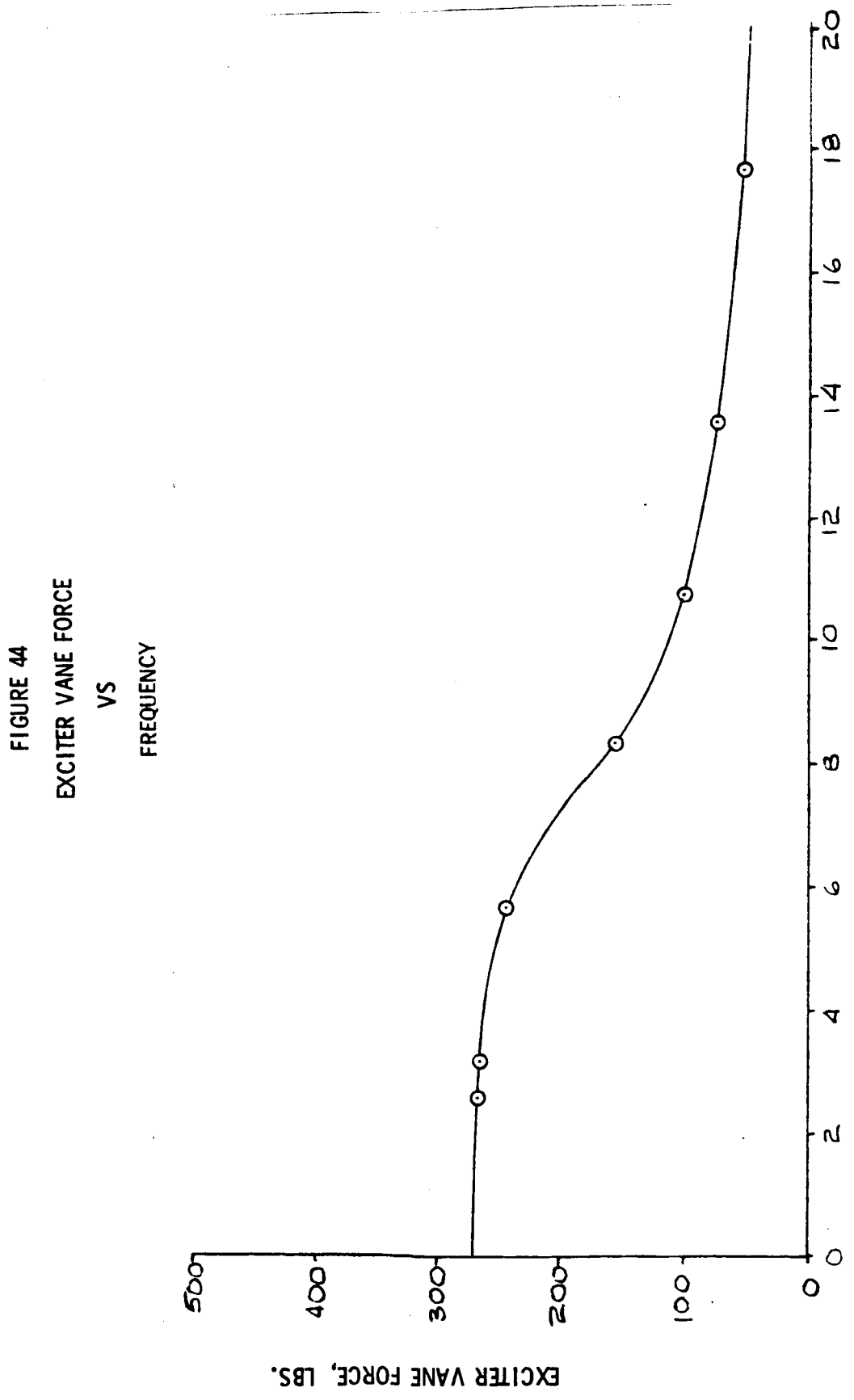

Figure 44. Exciter Vane Force vs. Frequency

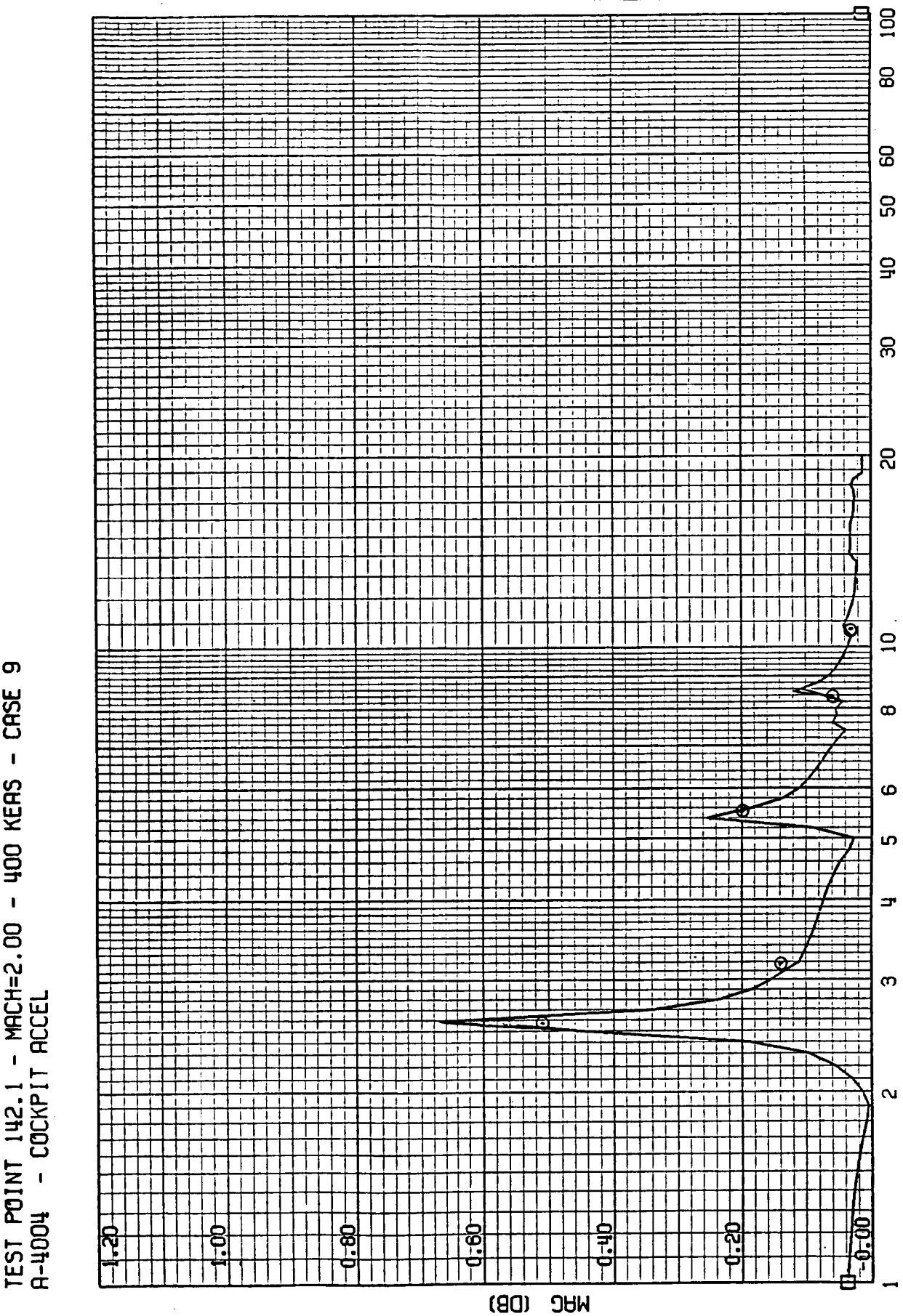

Figure 45. Cockpit Acceleration Response

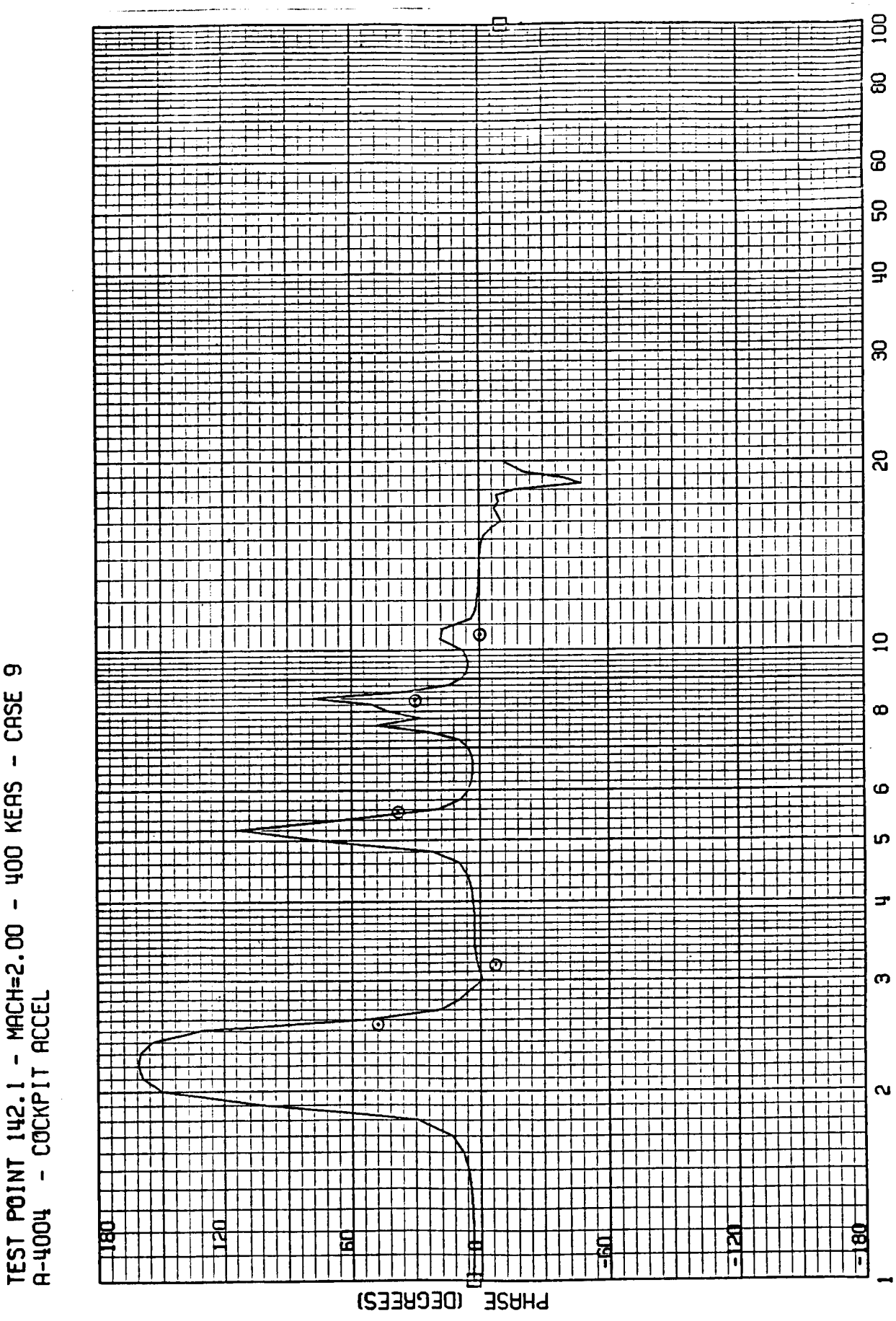

Figure 45. Cockpit Acceleration Response

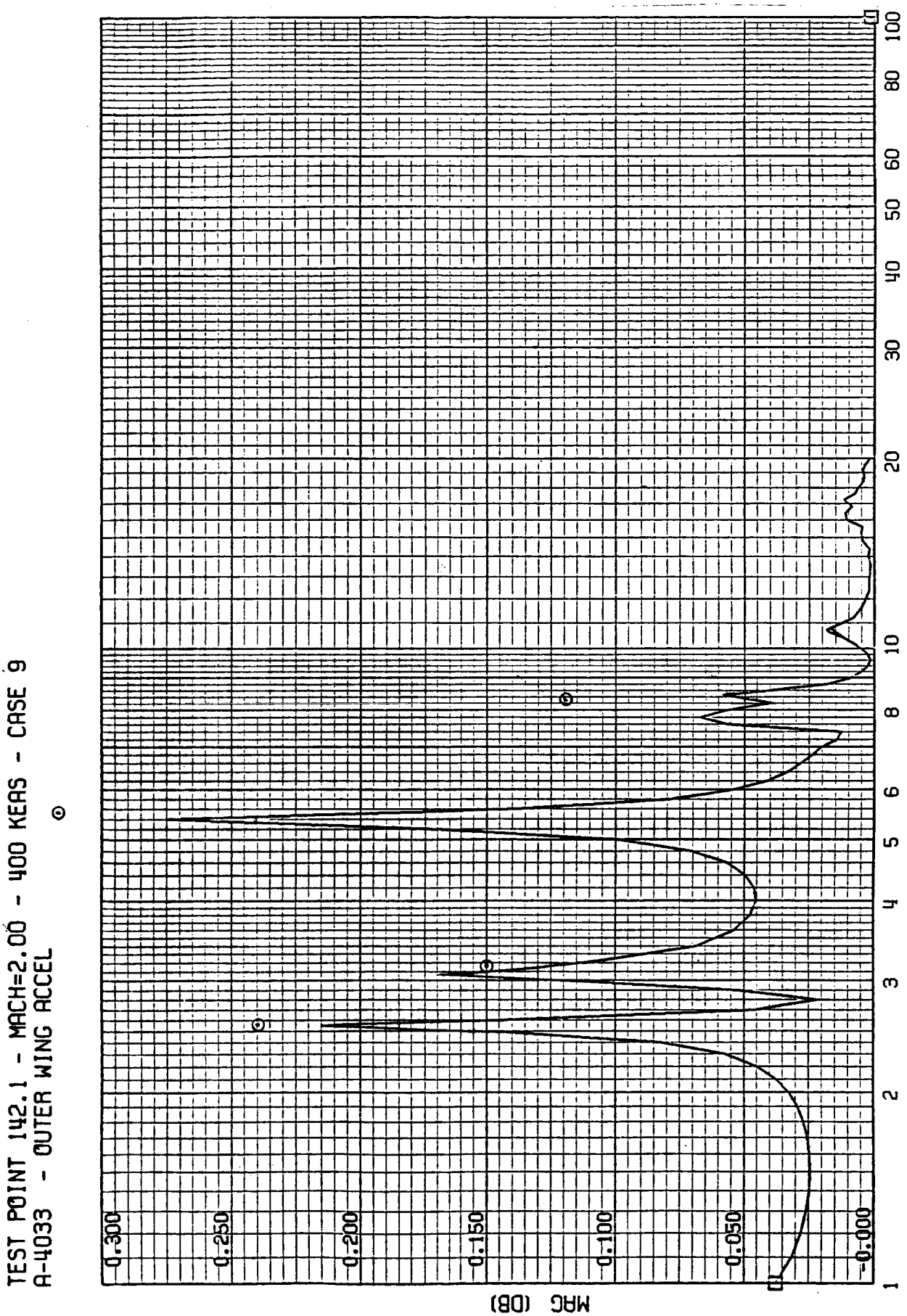

Figure 46. Outer Wing Acceleration Response

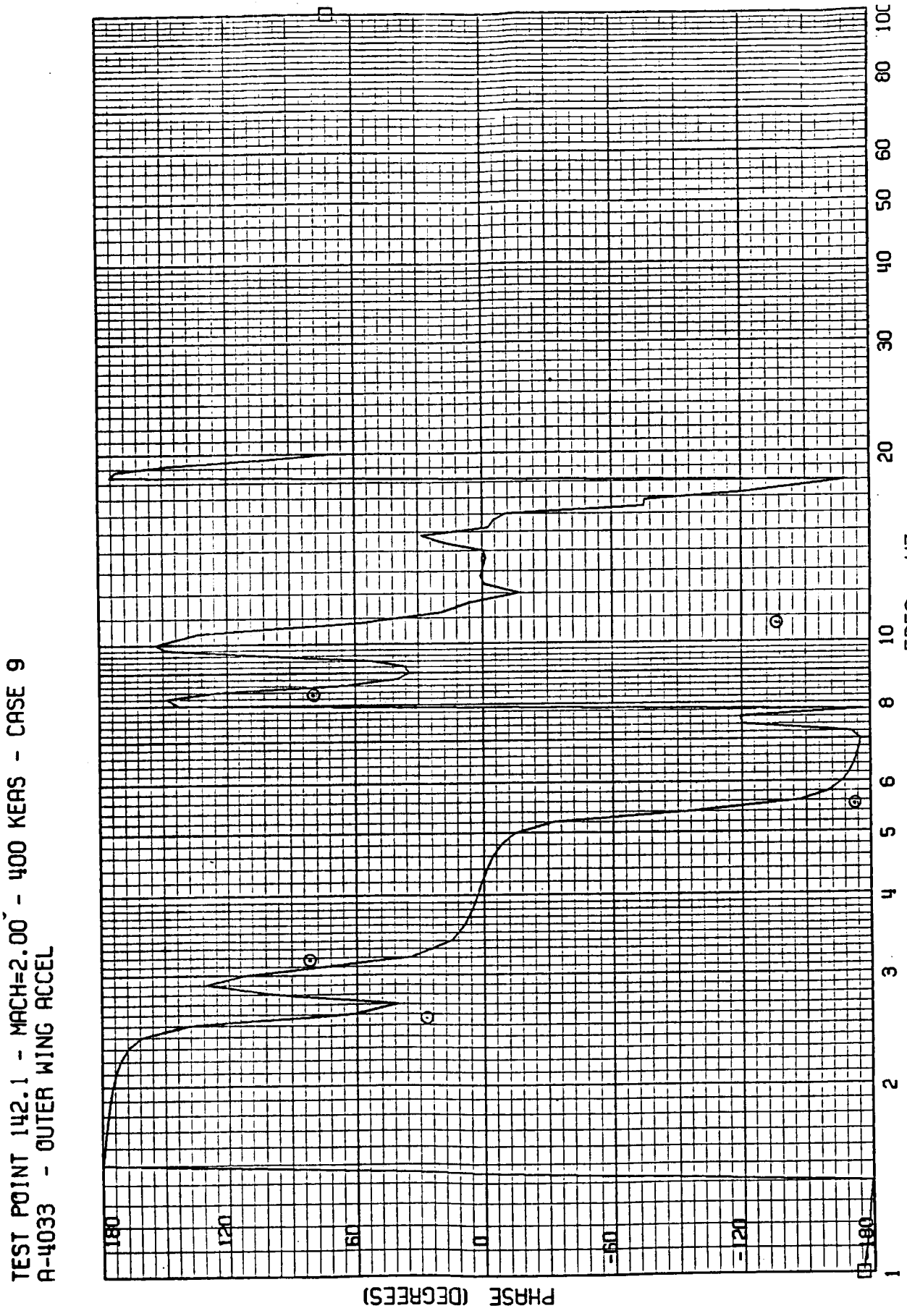

Figure 46. Outer Wing Acceleration Response

APPENDIX

TEST POINT 1 - MACH=.70 - 400 KEAS - CASE 1
A-4019 - NOSE ACCEL

FRAME 1
5 /4 /82

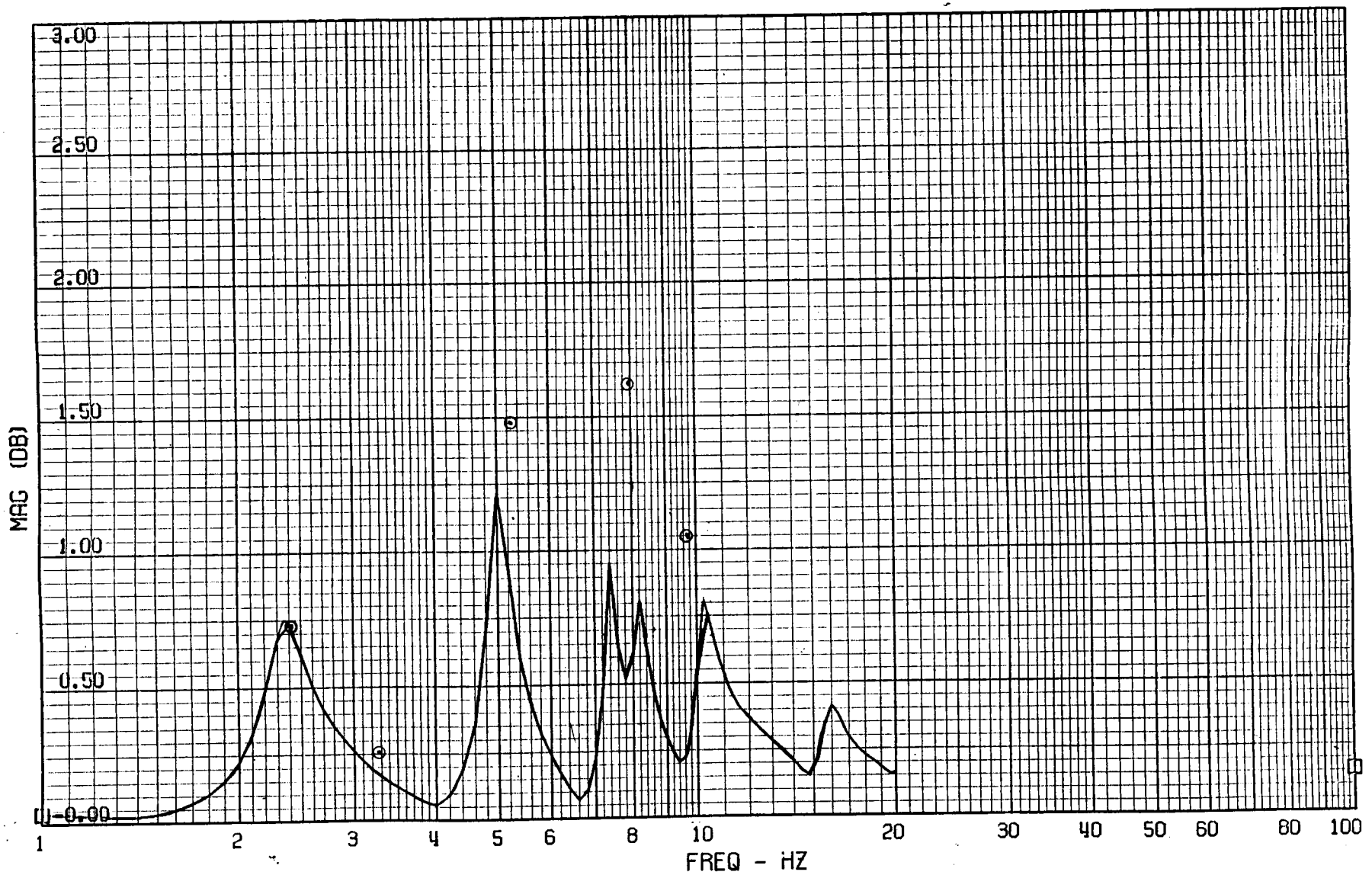

FRAME 1
5 /4 /82

TEST POINT 1 - MACH=.70 - 400 KEAS - CASE 1
A-4019 - NOSE ACCEL

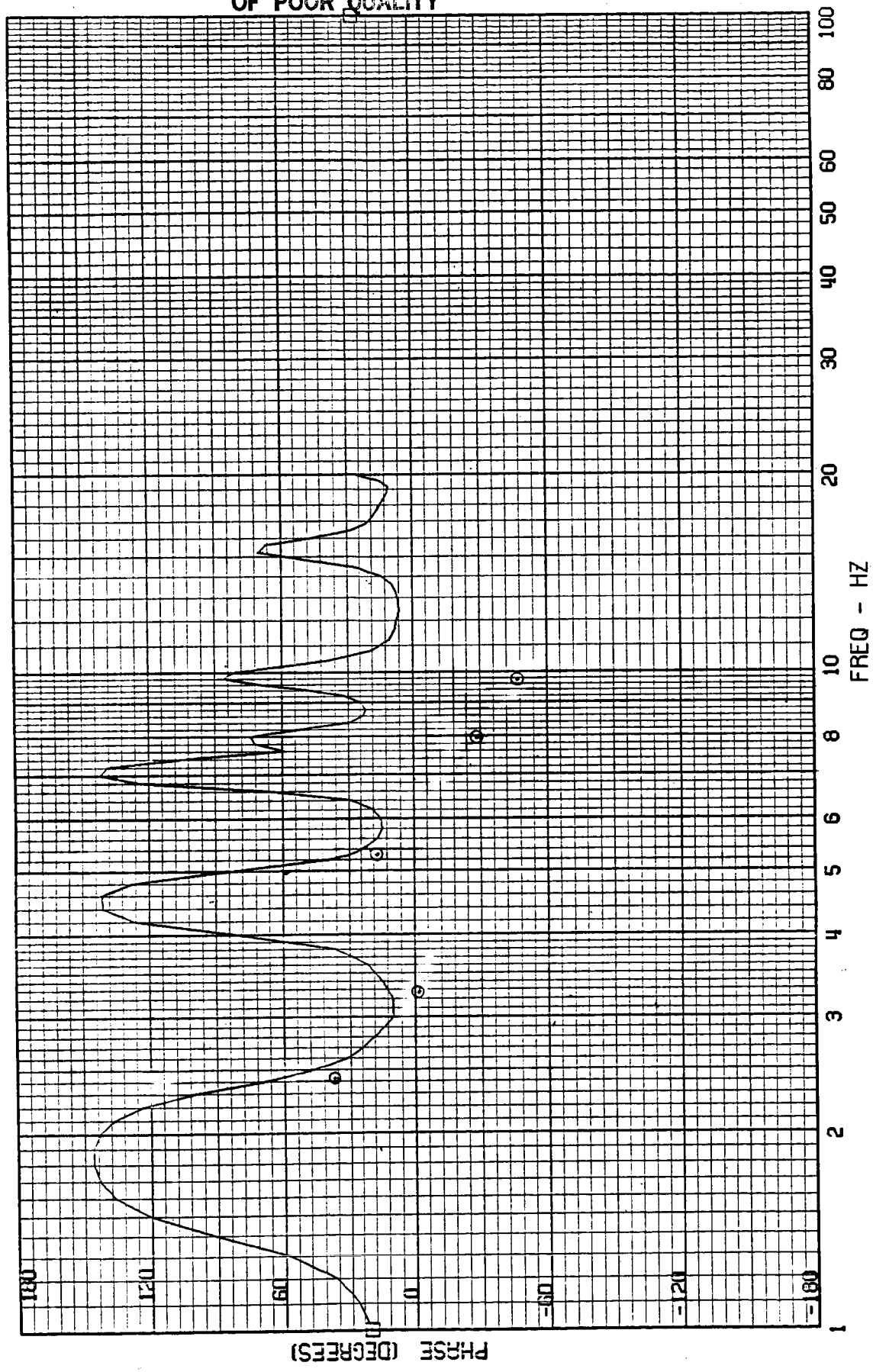

TEST POINT 1 - MACH=.70 - 400 KEAS - CASE 1
A-4004 - COCKPIT ACCEL

FRAME 2
5 /4 /82

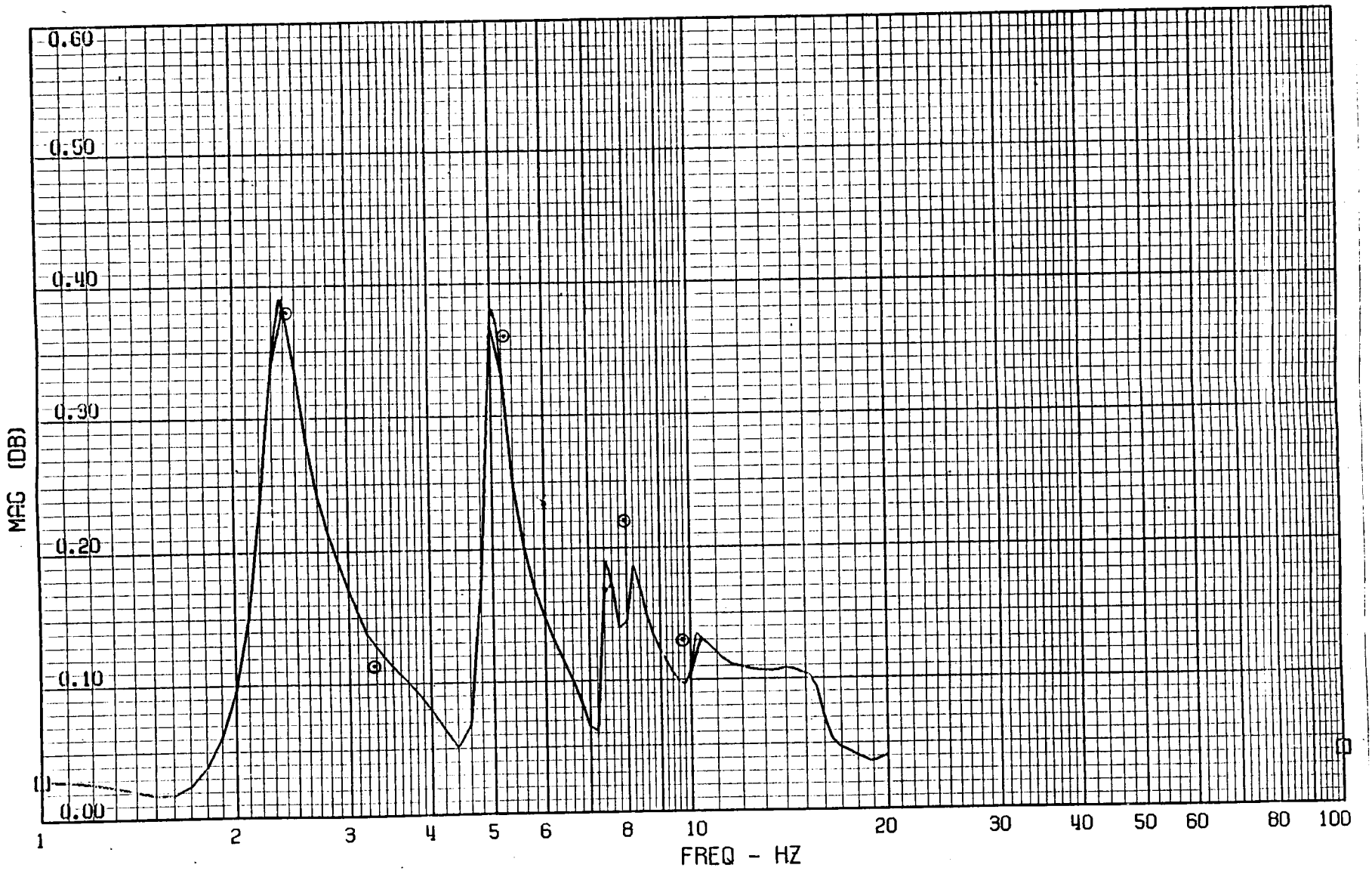

ORIGINAL PAGE IS
OF POOR QUALITY

FRAME 2
5 /4 /82

TEST POINT 1 - MACH=.70 - 400 KEAS - CASE 1
A-4004 - COCKPIT ACCEL

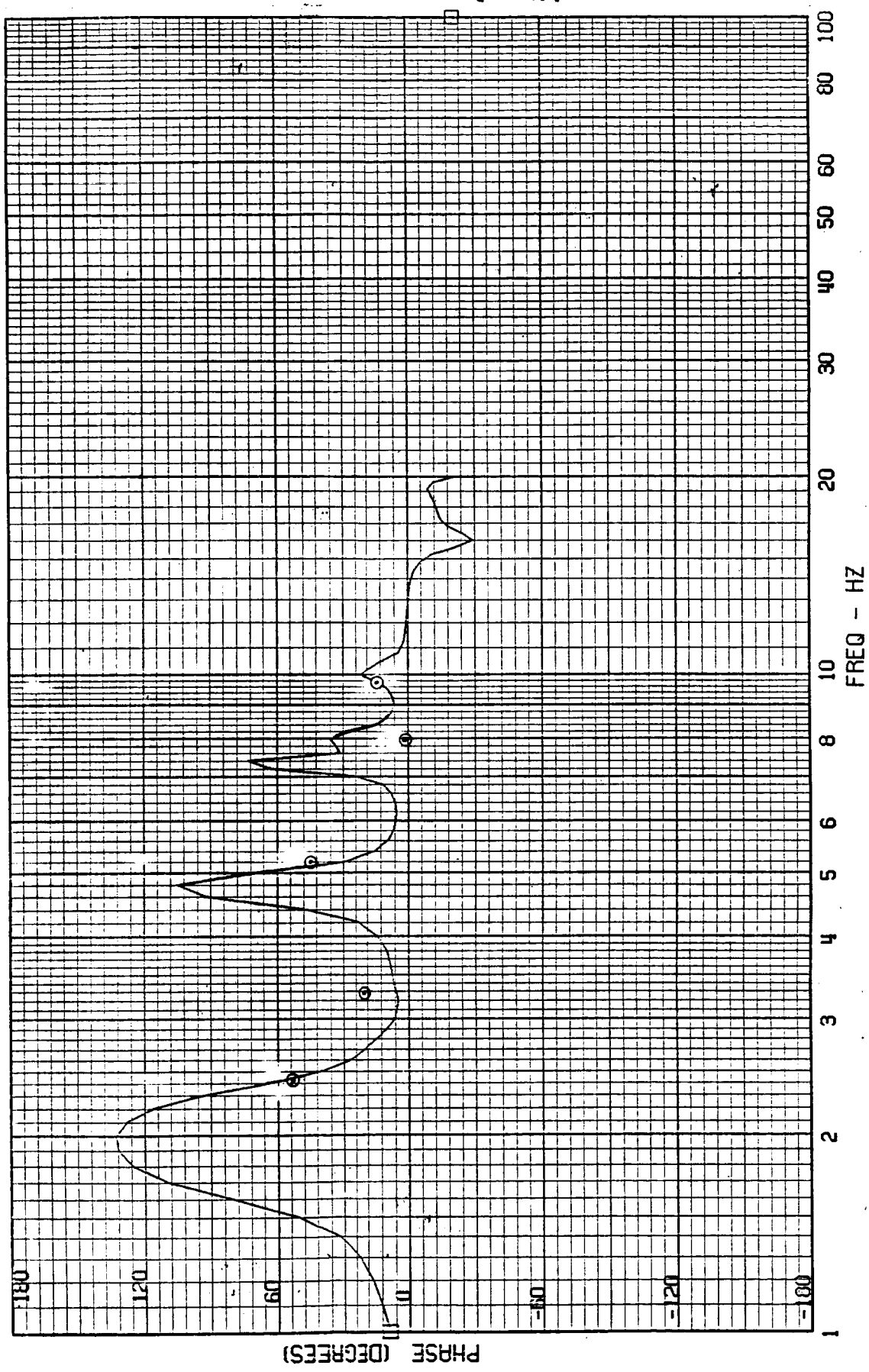

TEST POINT 1 - MACH=.70 - 400 KEAS - CASE 1
A-4028 - FORWARD MISSION BAY ACCEL

FRAME 3
5 /4 /82

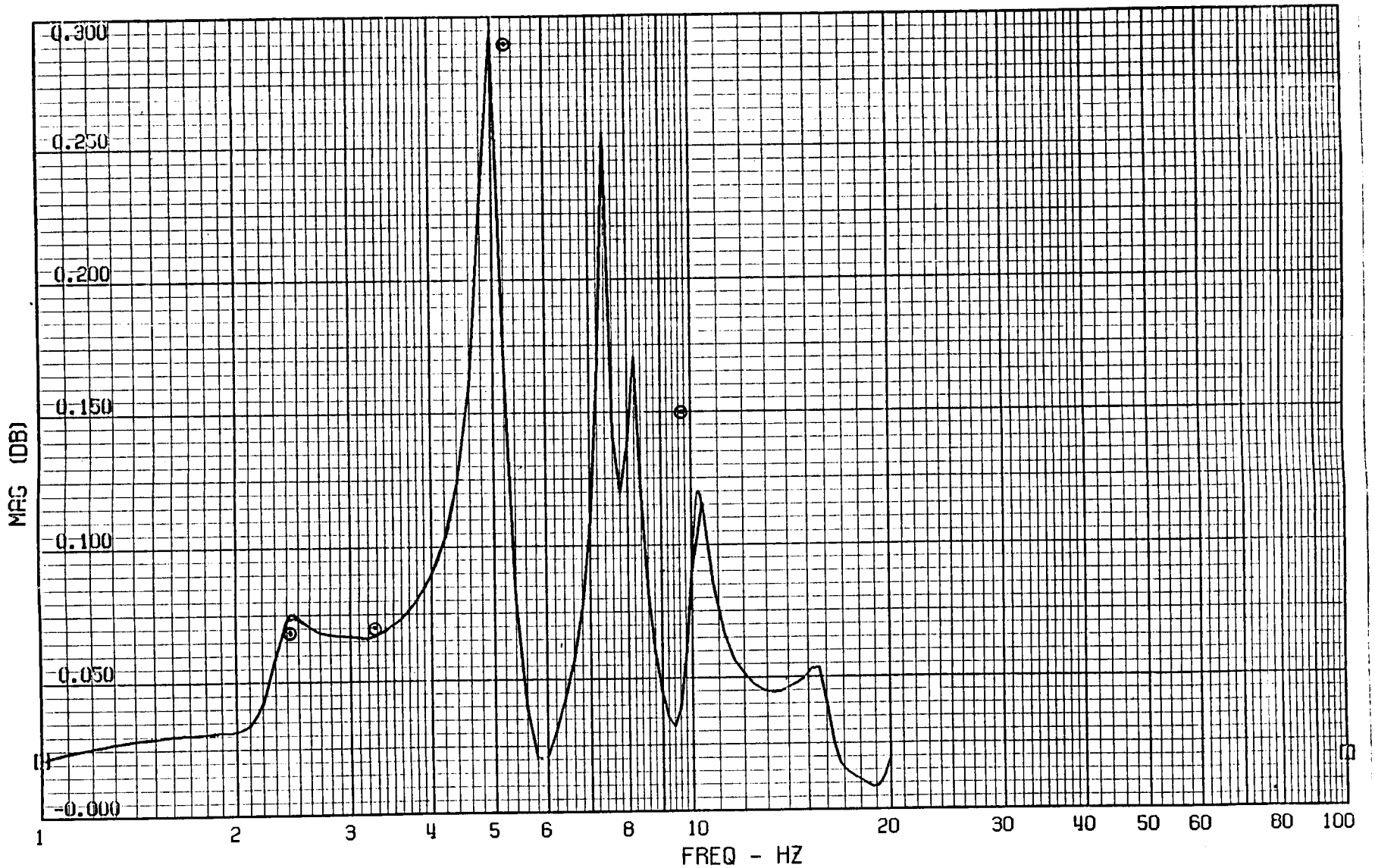

FRAME 3
5 /4 /82

TEST POINT 1 - MACH=.70 - 400 KEAS - CASE 1
A-4020 - FORWARD MISSION BAY ACCEL

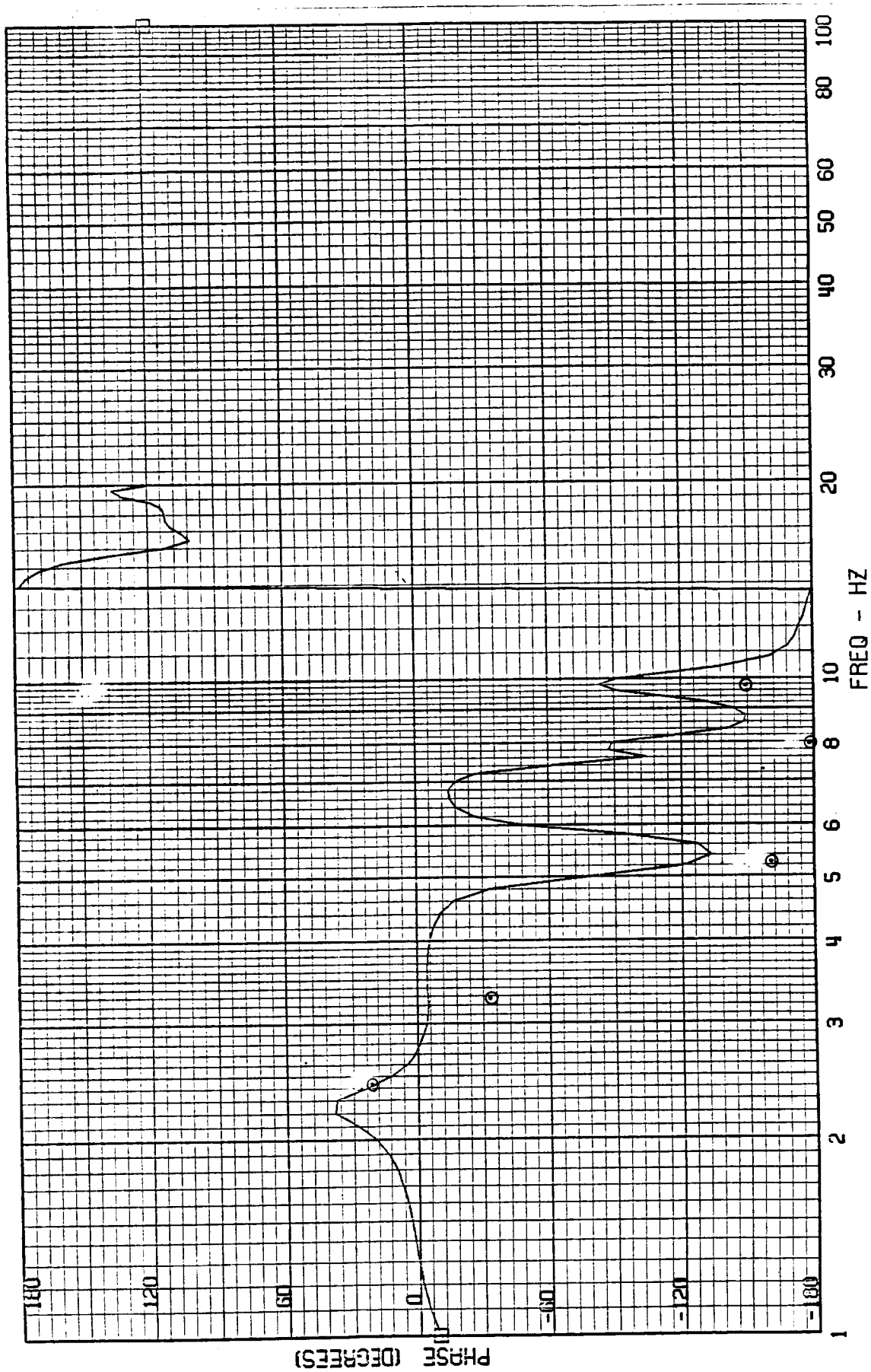

TEST POINT 1 - MACH=.70 - 400 KEAS - CASE 1
A-4029 - AFT MISSION BAY ACCEL

FRAME 4
5 /4 /82

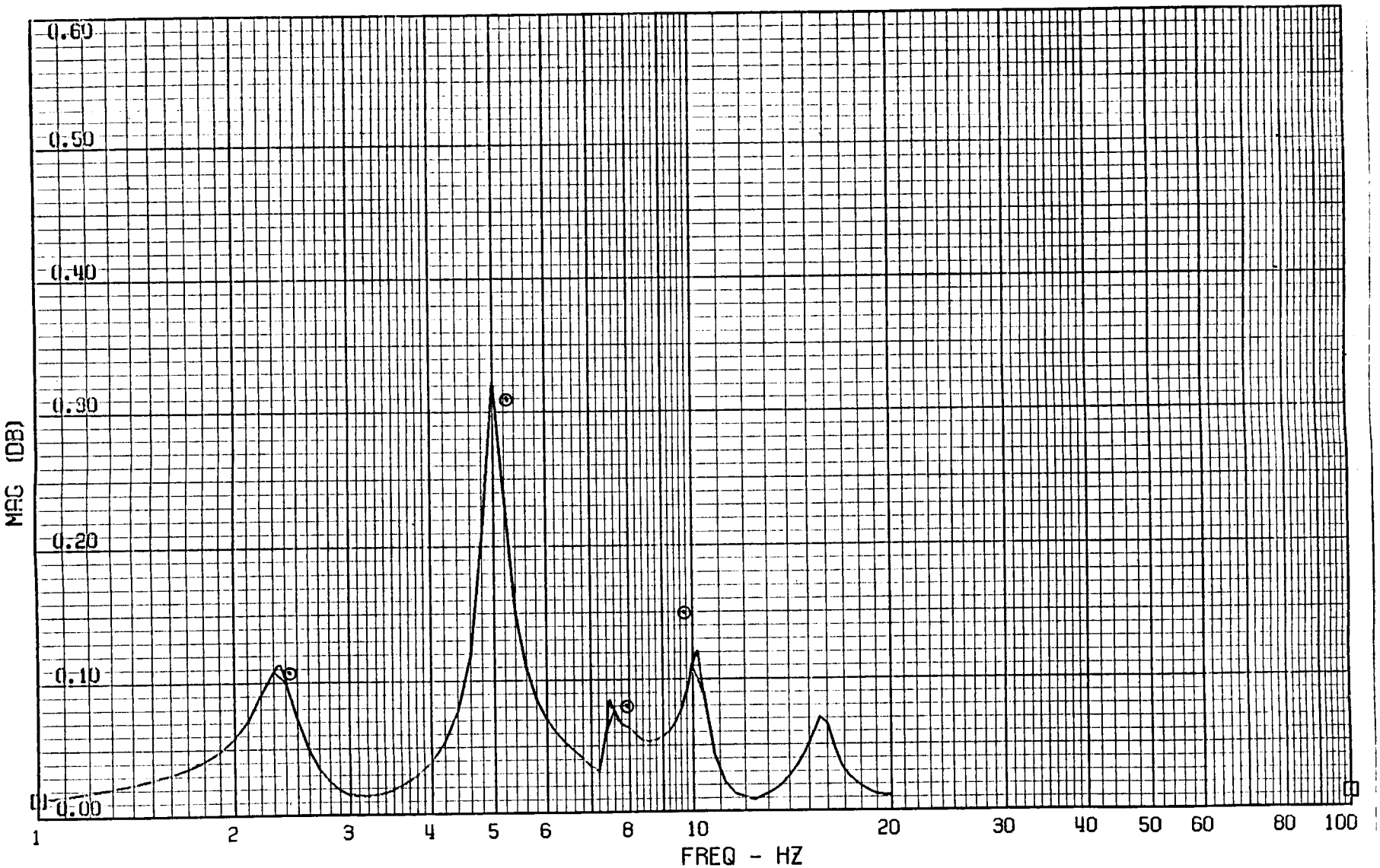

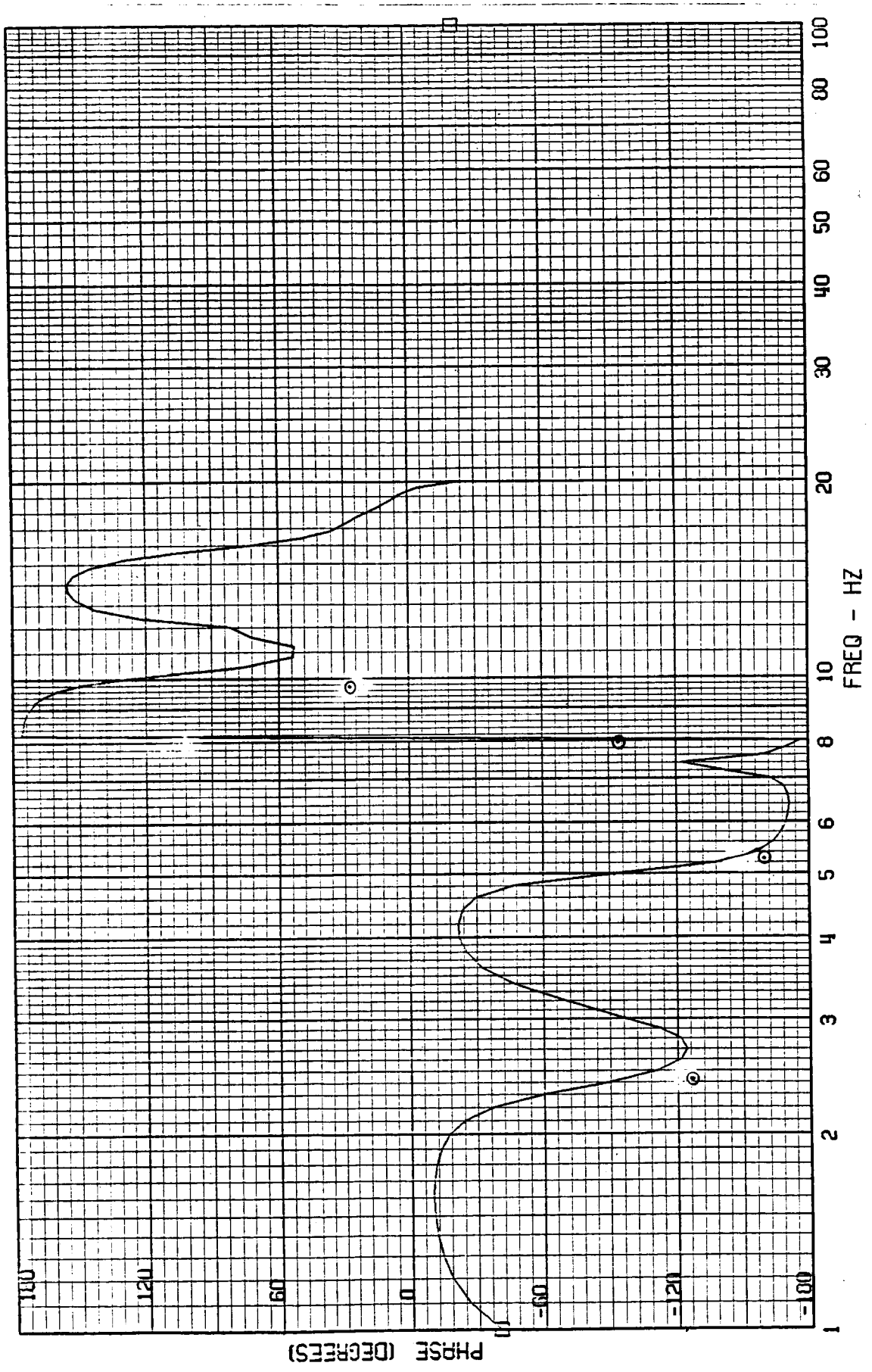

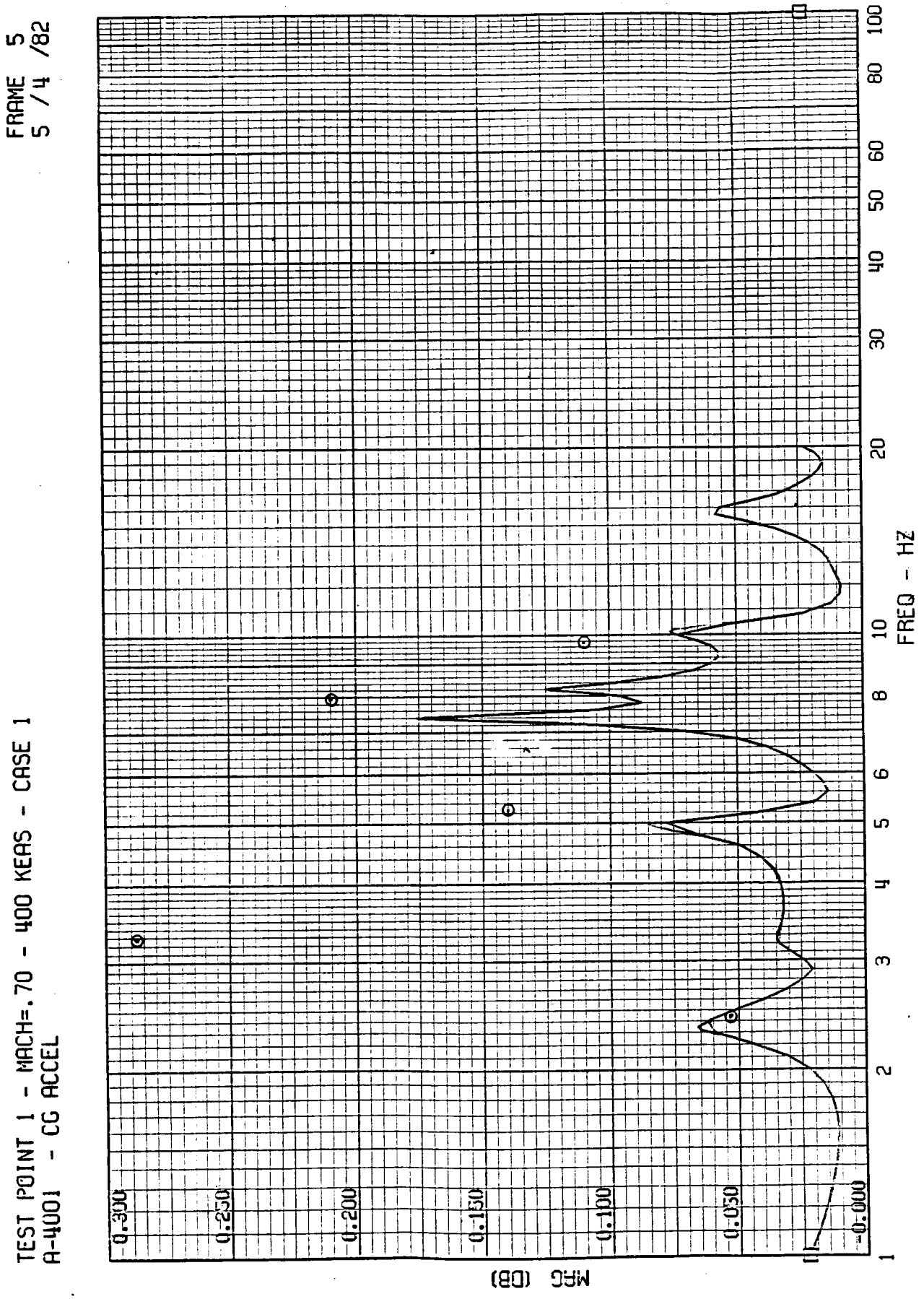
TEST POINT 1 - MACH=.70 - 400 KEAS - CASE 1
A-4001 - CG ACCEL
FRAME 5
5 /4 /82
MAG (DB)
0.300
0.250
0.200
0.150
0.100
0.050
0.000
1
2
3
4
5
6
8
10
20
30
40
50
60
80
100
FREQ - HZ

FRAME 5
5 /4 /82

TEST POINT 1 - MACH=.70 - 400 KEAS - CASE 1
A-4001 - CG ACCEL

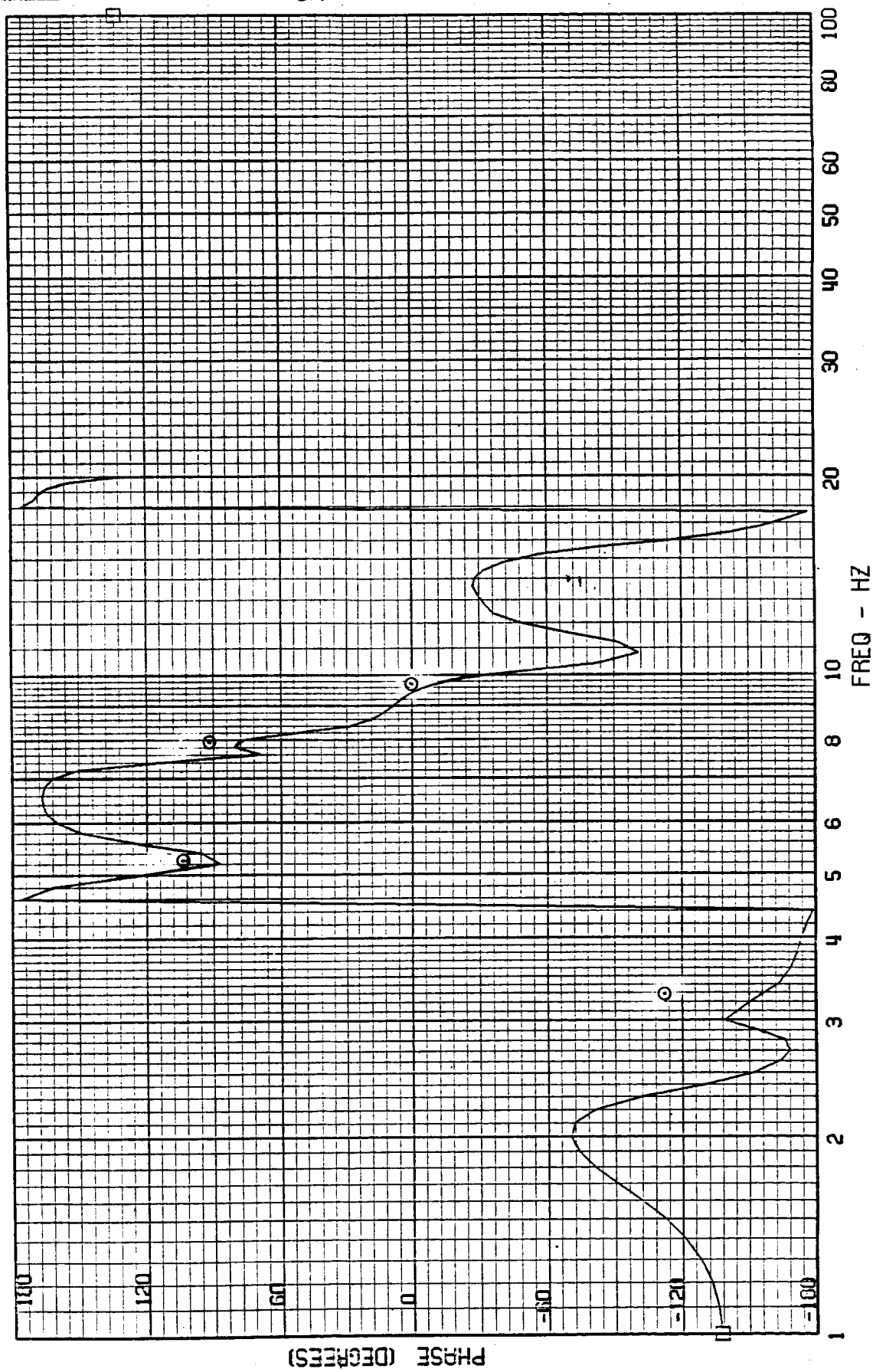

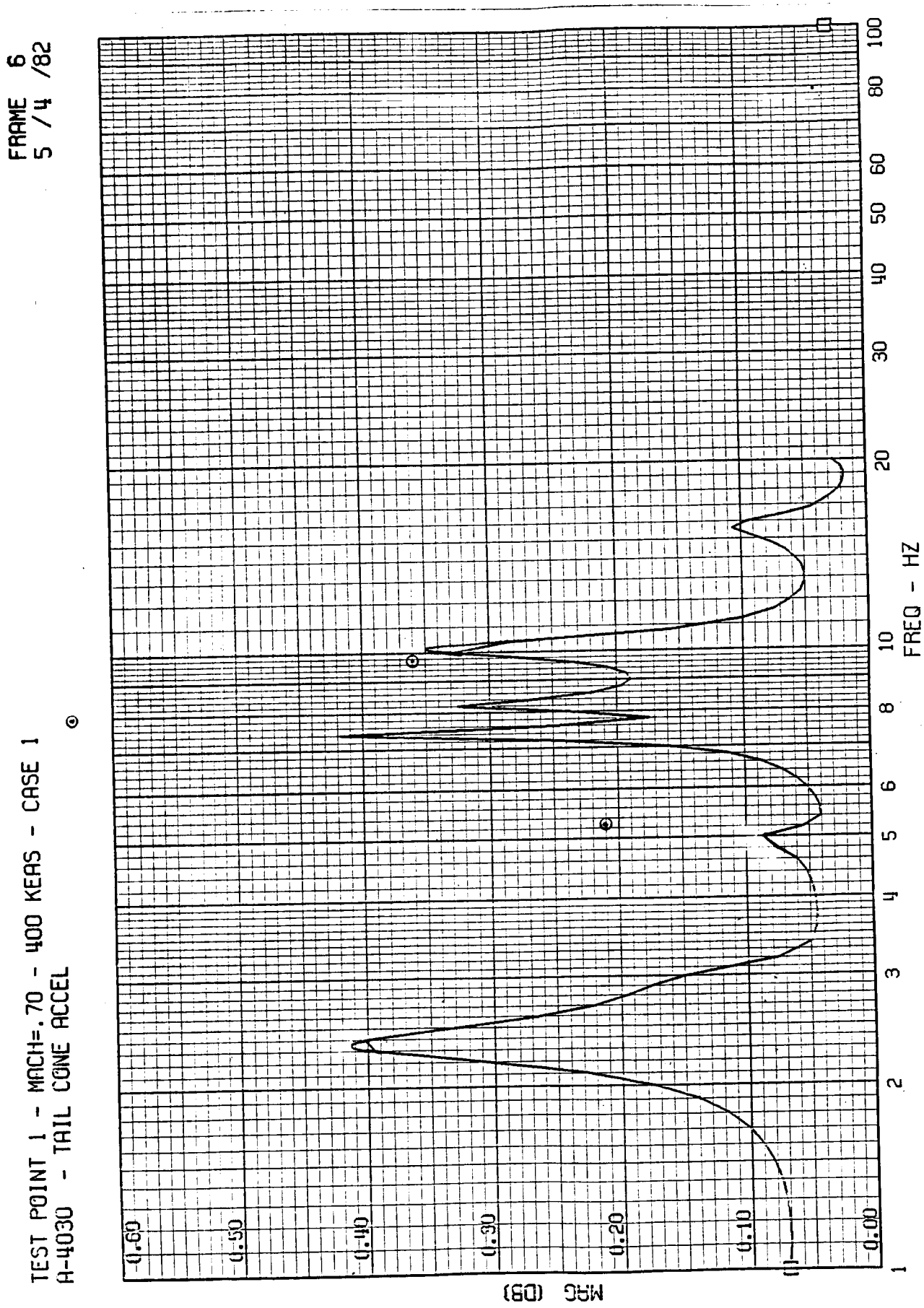
FRAME 6
5 /4 /82
TEST POINT 1 - MACH=.70 - 400 KEAS - CASE 1
A-4030 - TAIL CONE ACCEL
MAG (DB)
0.60
0.50
0.40
0.30
0.20
0.10
0.00
1
2
3
4
5
6
8
10
20
30
40
50
60
80
100
FREQ - HZ

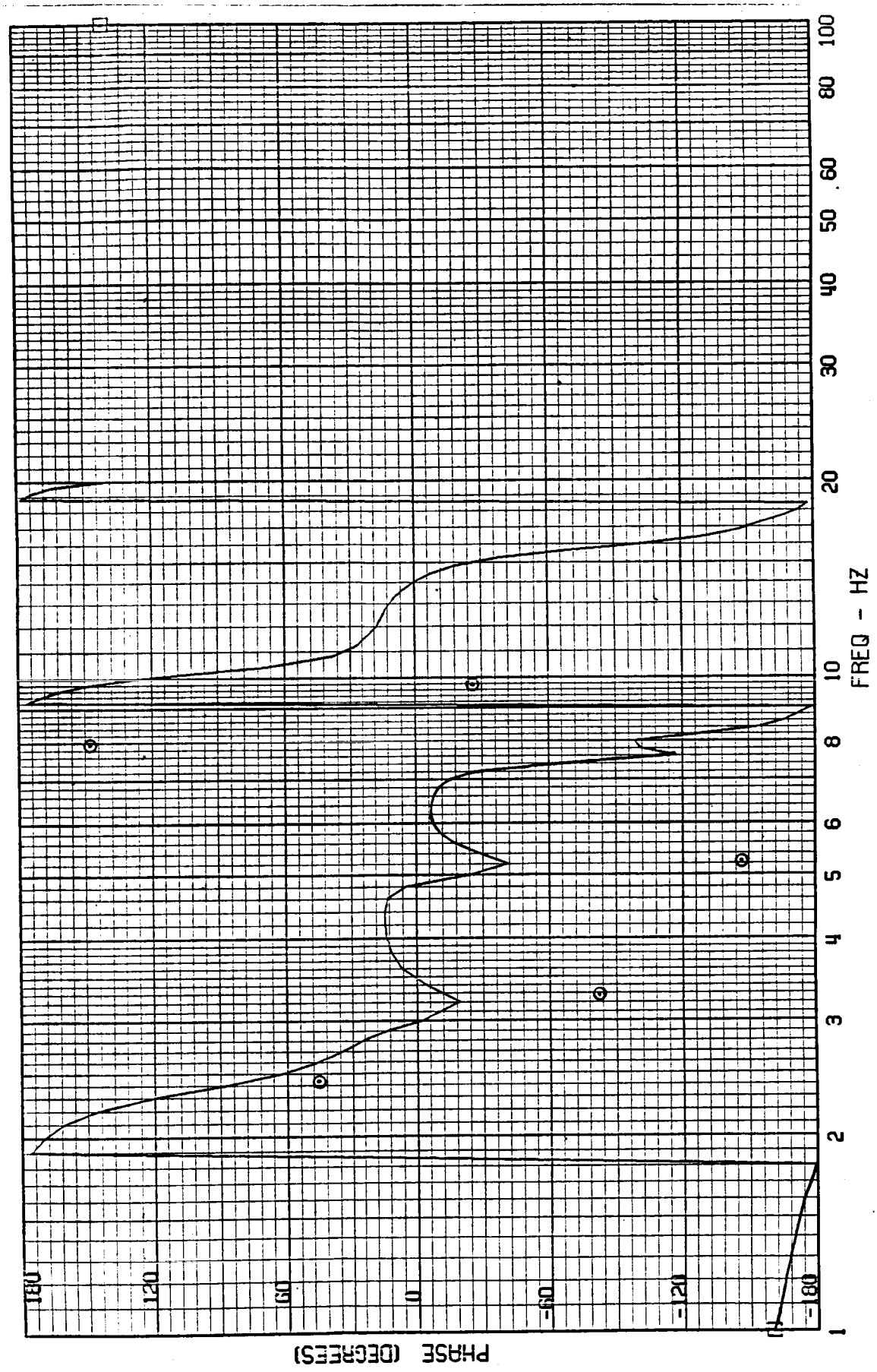

FRAME 7
5 /4 /82
TEST POINT 1 - MACH=.70 - 400 KEAS - CASE 1
A-4033 - OUTER WING ACCEL
MAG (DB)
0.60
0.50
0.40
0.30
0.20
0.10
0.00
1
2
3
4
5
6
8
10
20
30
40
50
60
80
100
FREQ - HZ

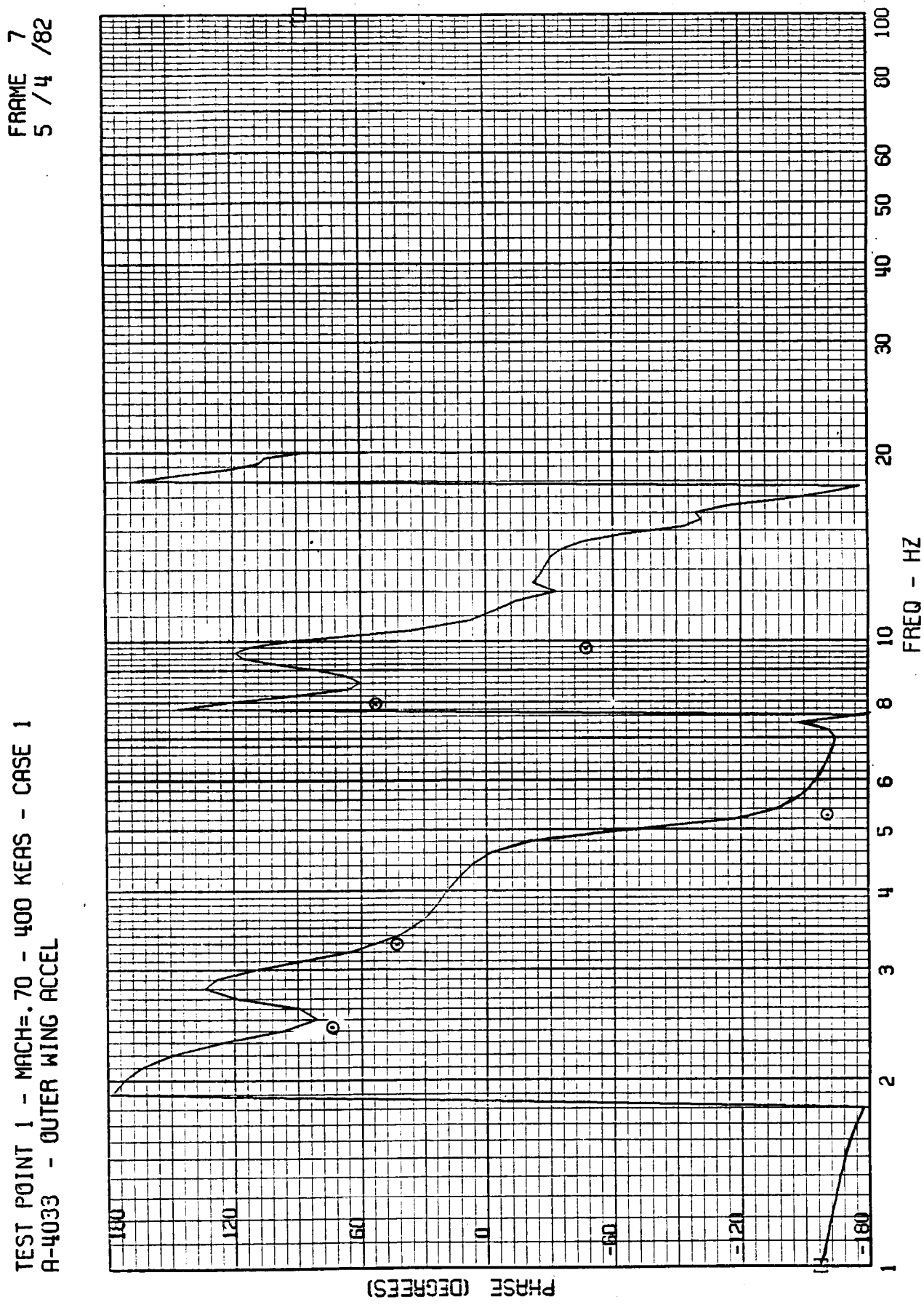

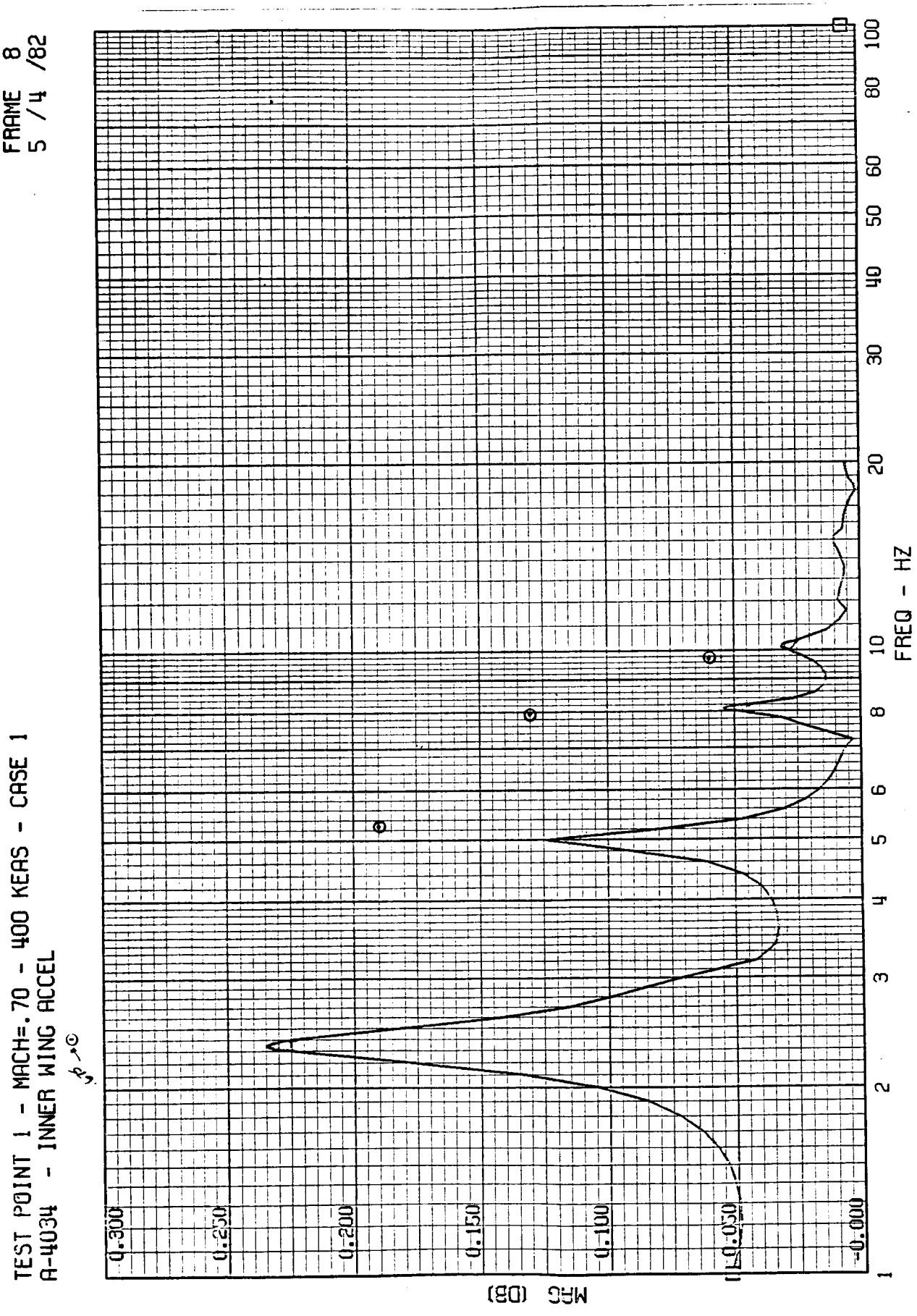
FRAME 8
5 /4 /82
TEST POINT 1 - MACH=.70 - 400 KEAS - CASE 1
A-4034 - INNER WING ACCEL
MAG (DB)
0.300
0.250
0.200
0.150
0.100
0.050
-0.000
1
2
3
4
5
6
8
10
20
30
40
50
60
80
100
FREQ - HZ

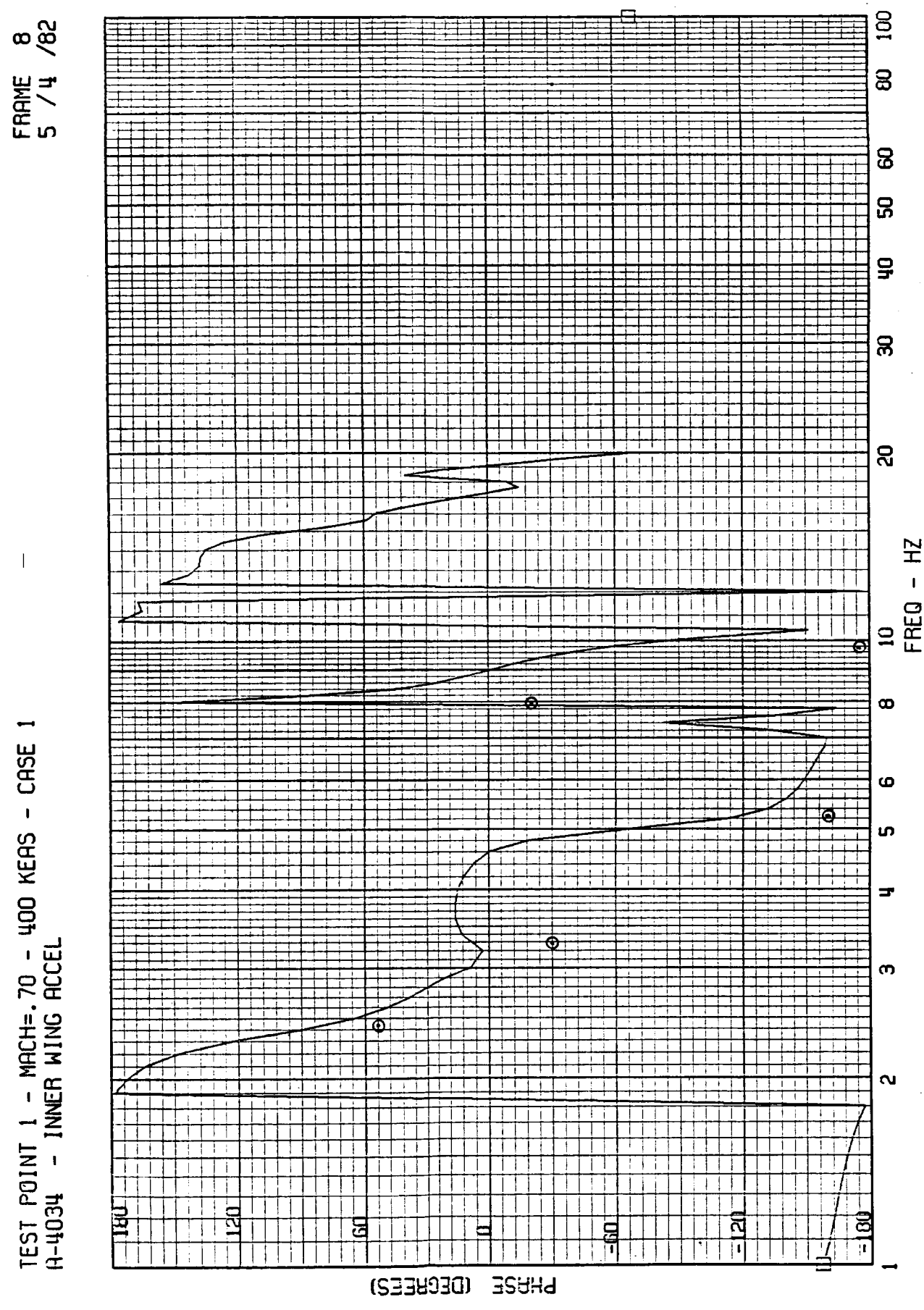

TEST POINT 1 - MACH=.70 - 400 KEAS - CASE 1
RWCLACC - NACELLE ACCEL

FRAME 9
5 /4 /82

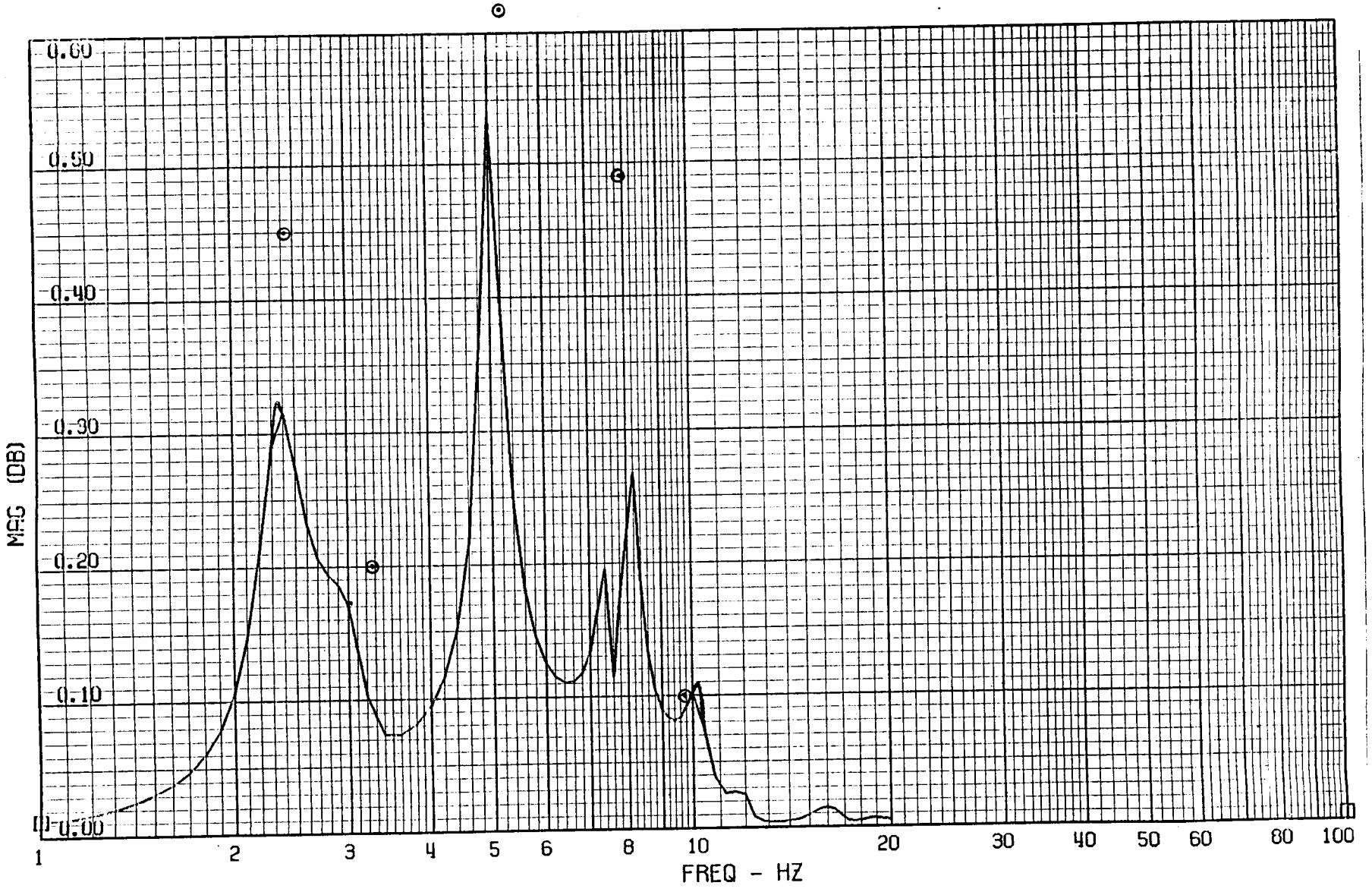

TEST POINT 1 - MACH=.70 - 400 KEAS - CASE 1
RWCLACC - NACELLE ACCEL

FRAME 9
5 /4 /82

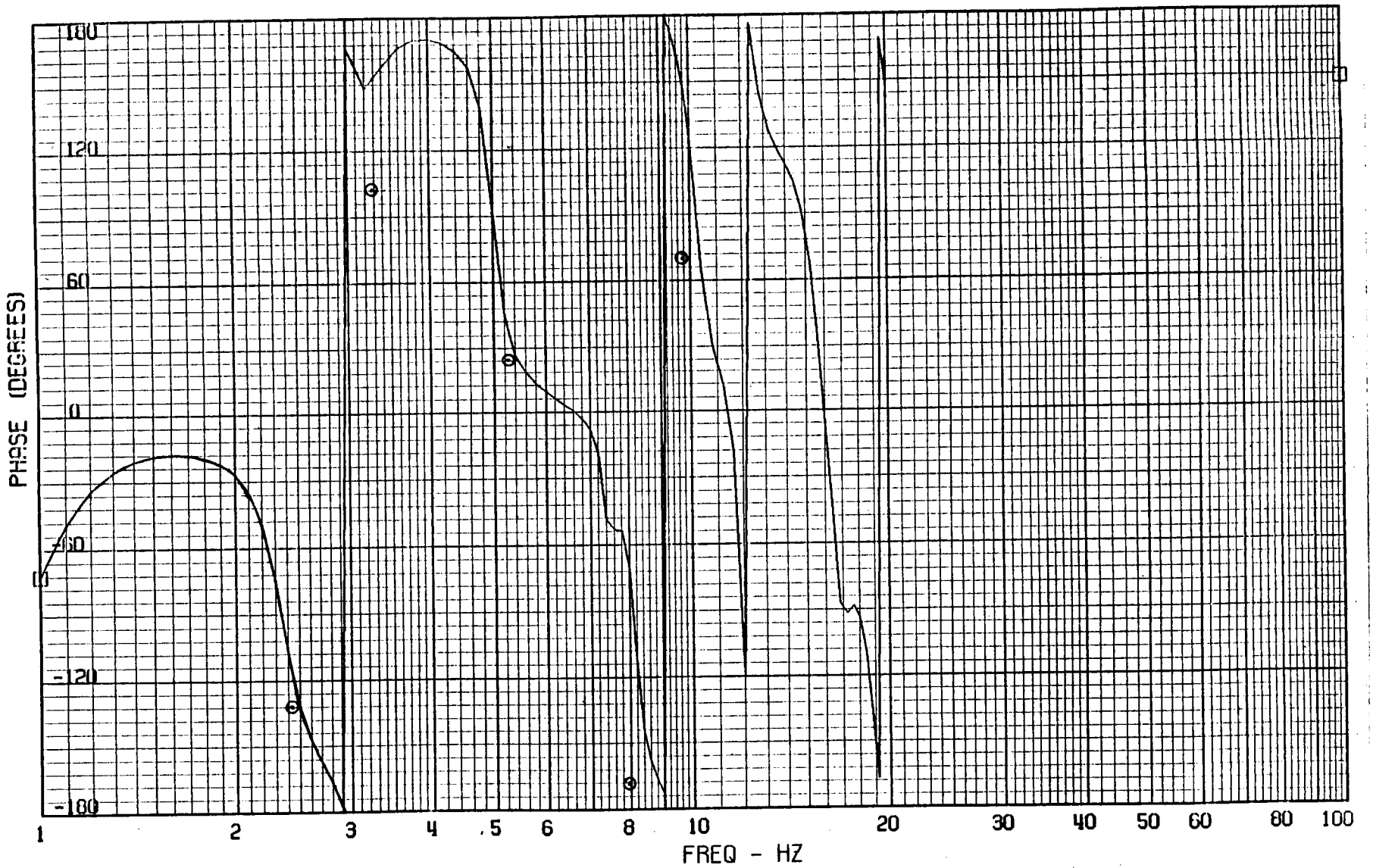

TEST POINT 1 - MACH=.70 - 400 KEAS - CASE 1
RRUDACC - RUDDER ACCEL

FRAME 10
5 /4 /82

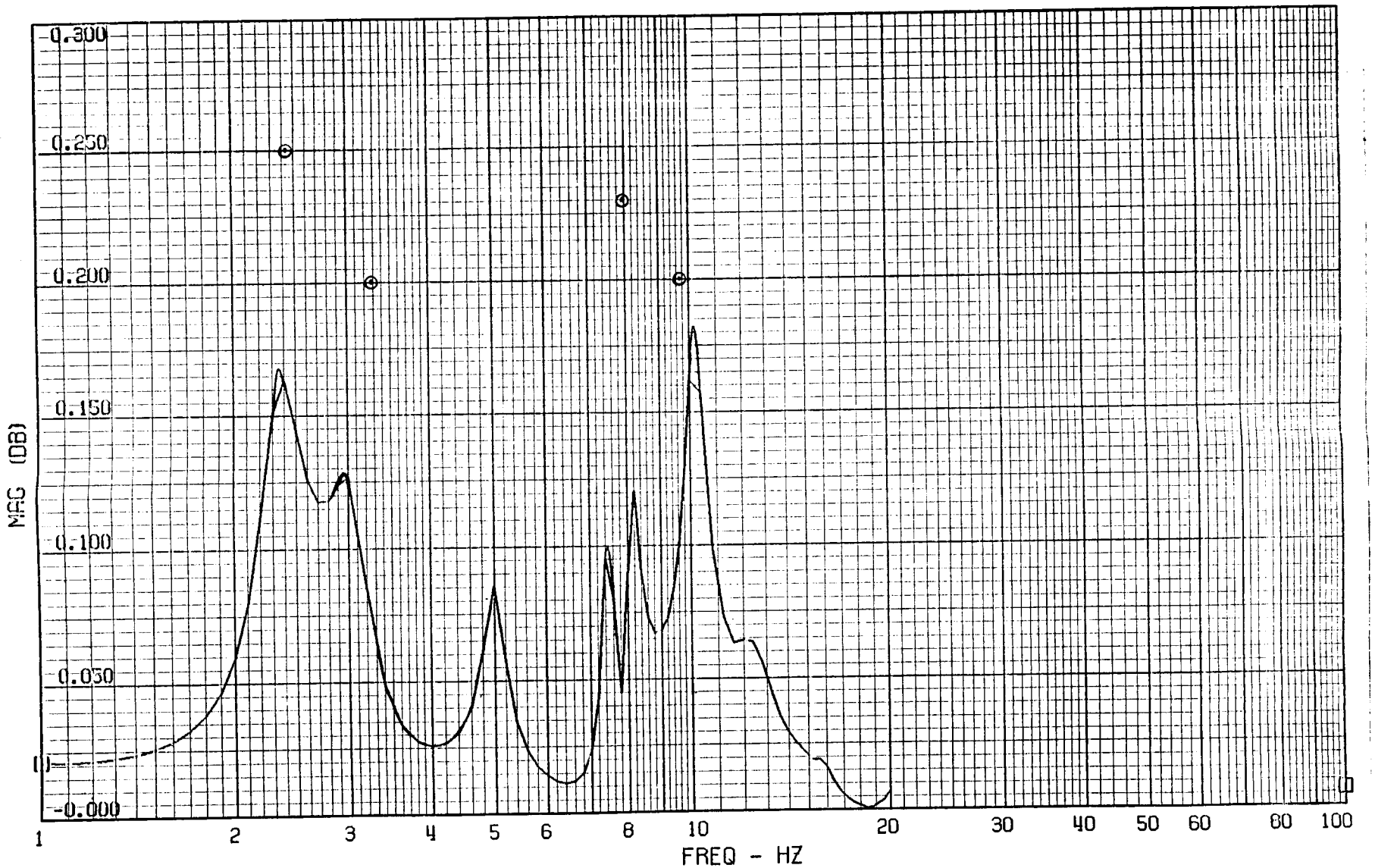

140

TEST POINT 1 - MACH=.70 - 400 KEAS - CASE 1
RRUDACC - RUDDER ACCEL

FRAME 10
5 /4 /82

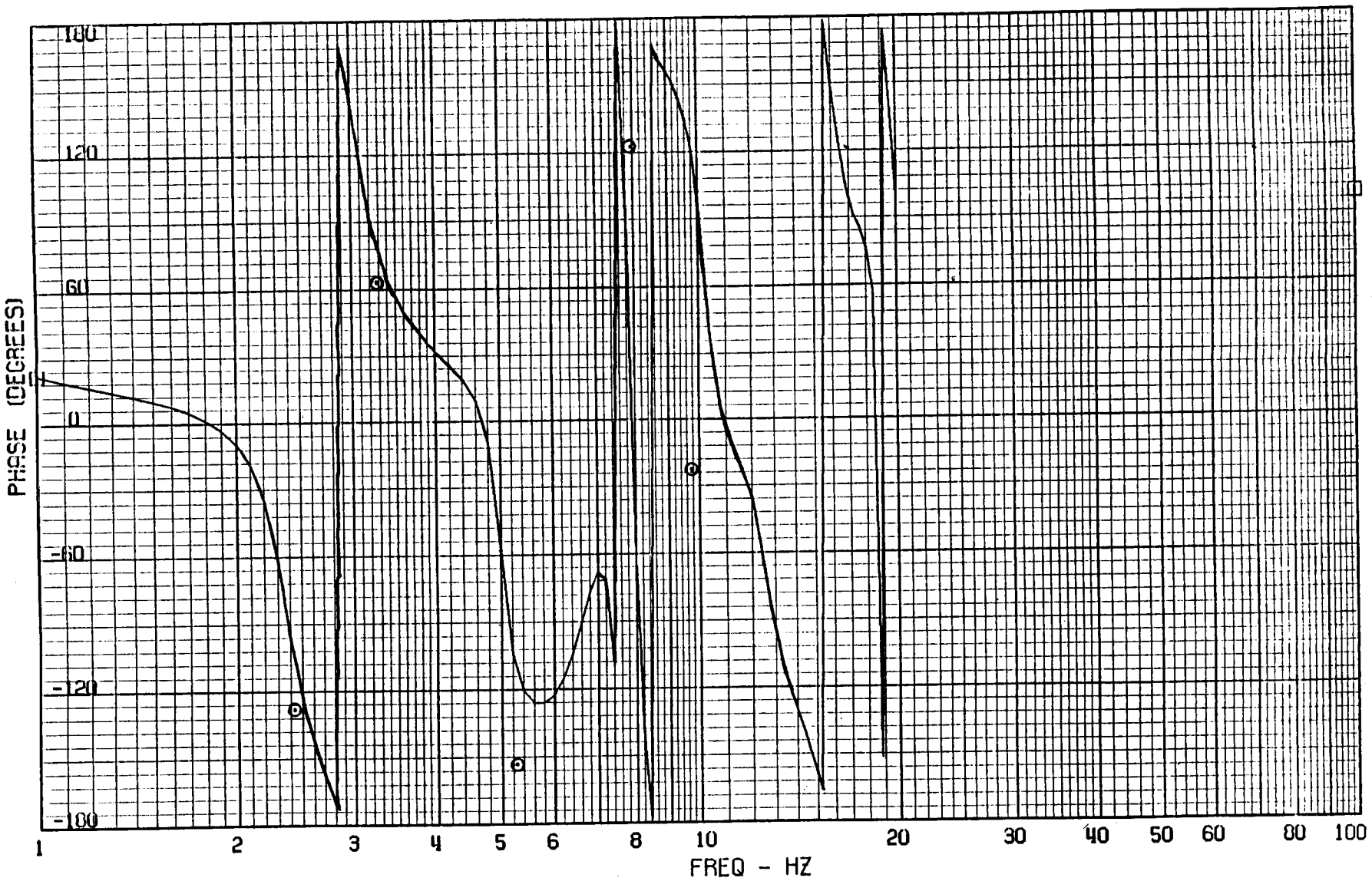

ORIGINAL PAGE IS
OF POOR QUALITY

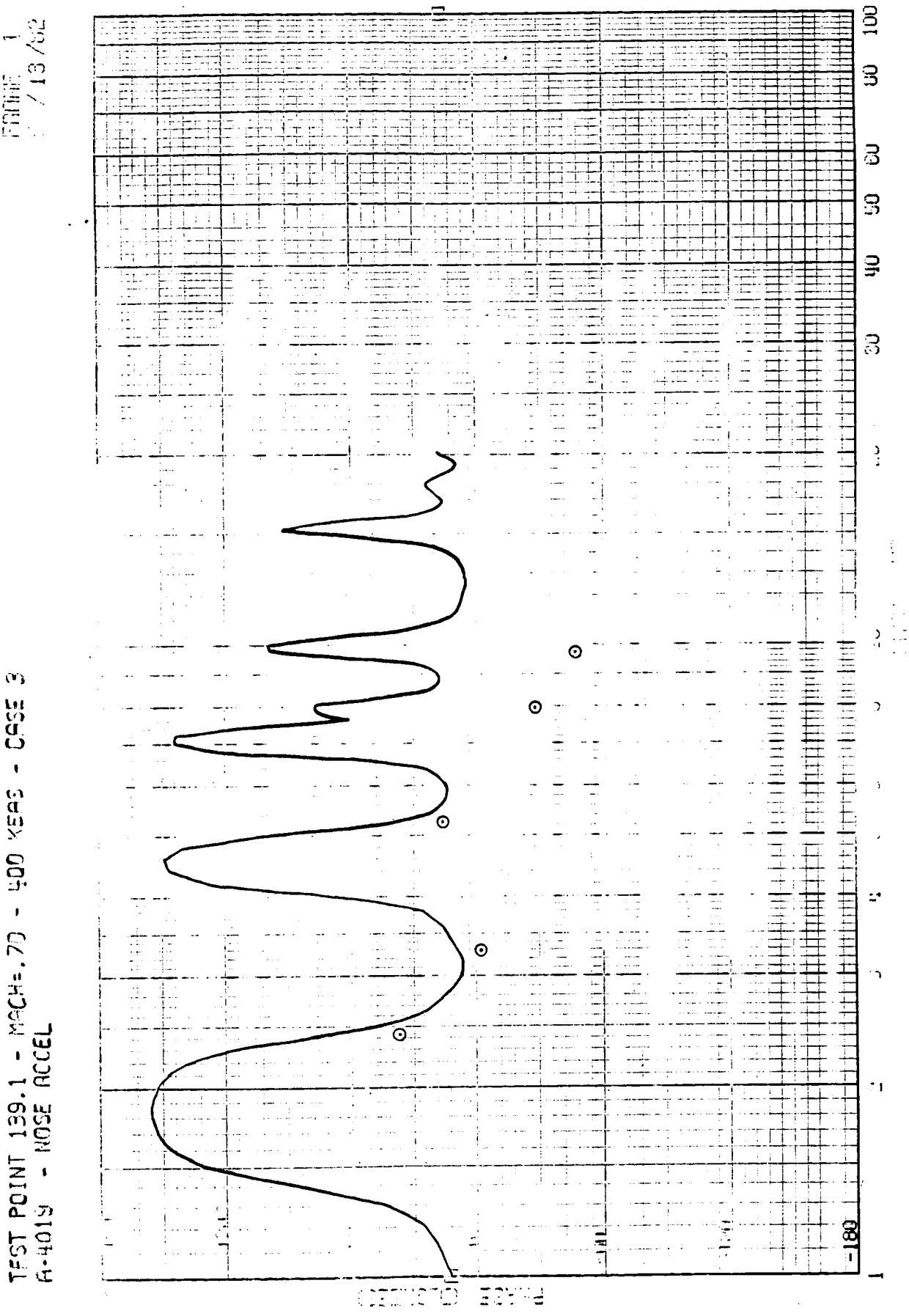

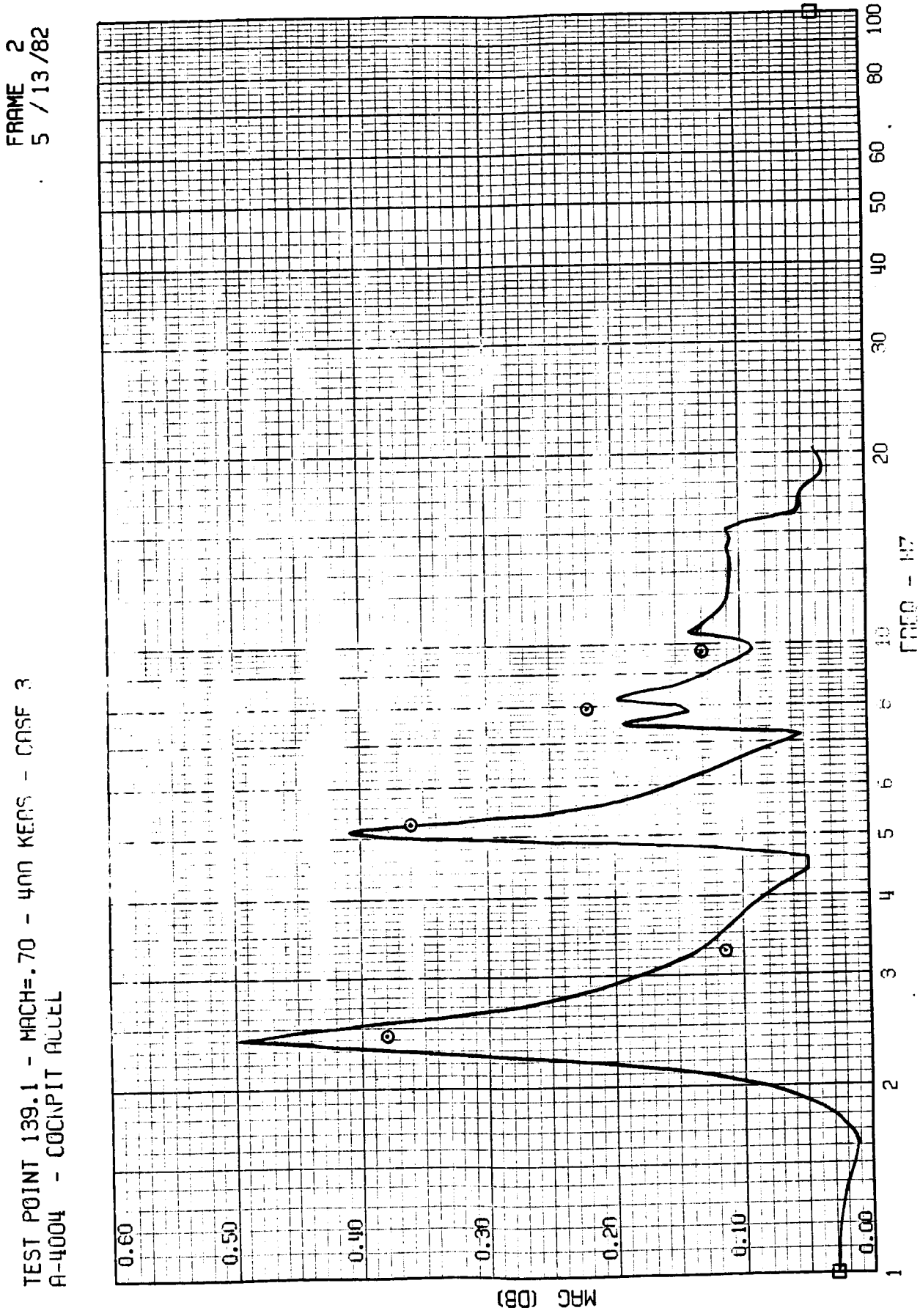

FRAME 2
5 /13 /82

TEST POINT 139.1 - [illegible] - 300 KEAS - CASE 3
A-4004 - COCKPIT ACCEL

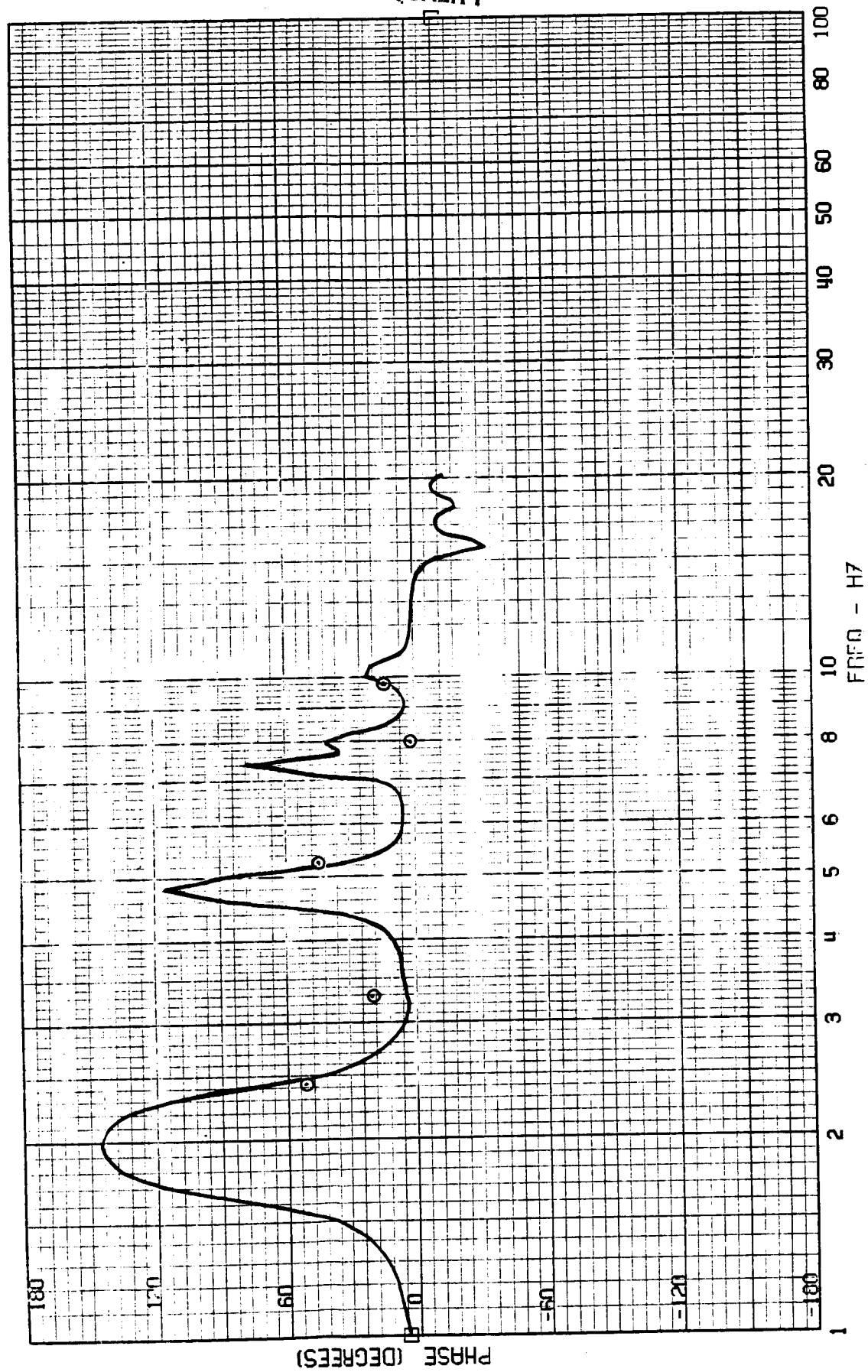

TEST POINT 139.1 - MACH=.70 - 400 KEAS - CASE 3
A-4028 - FORWARD MISSION BAY ACCEL

FRAME 3
5 /13 /82

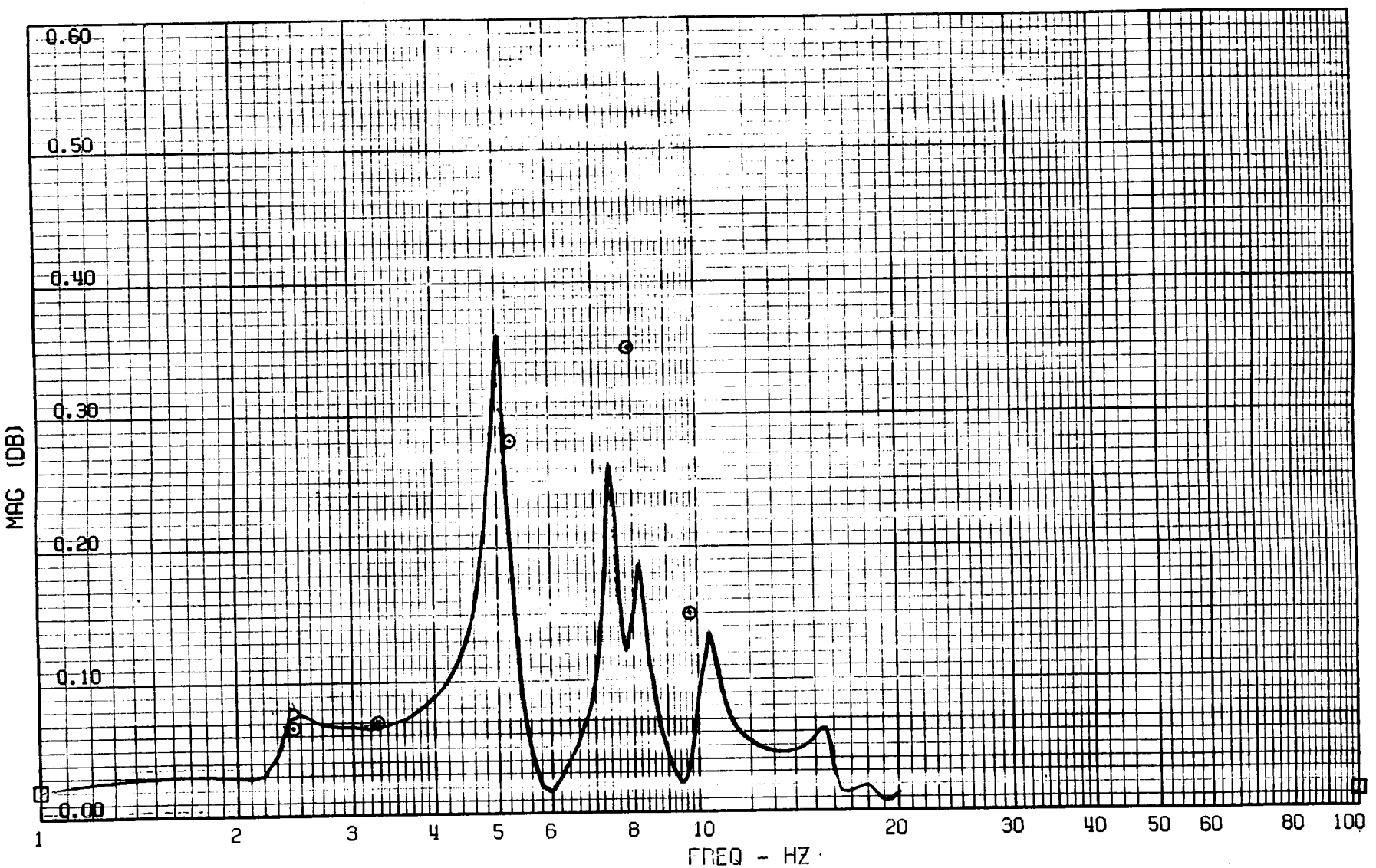

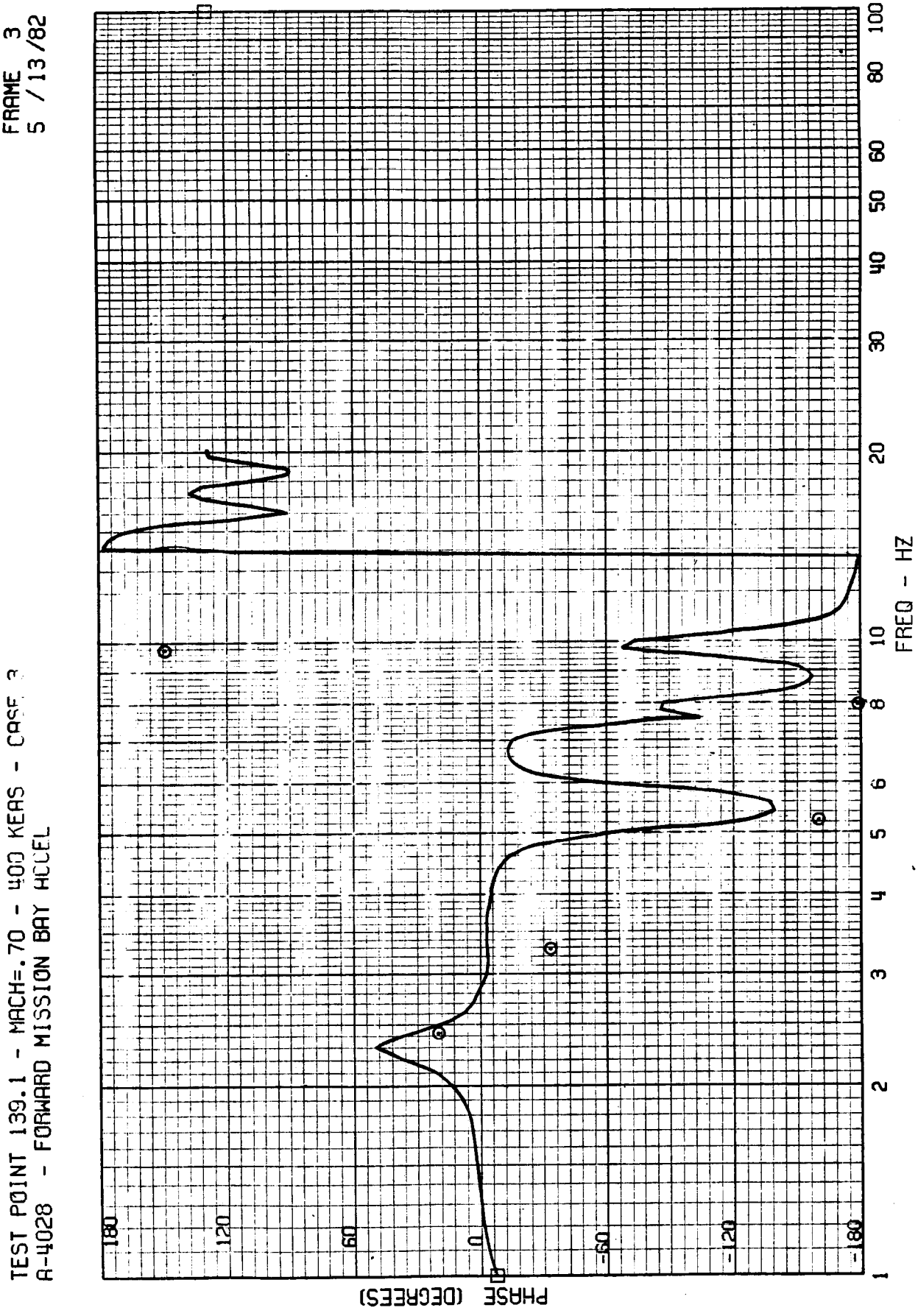

TEST POINT 139.1 - MACH=.70 - 400 KEAS - CASE 3
A-4029 - AFT MISSION BAY ACCEL

FRAME 4
5 / 13 /82

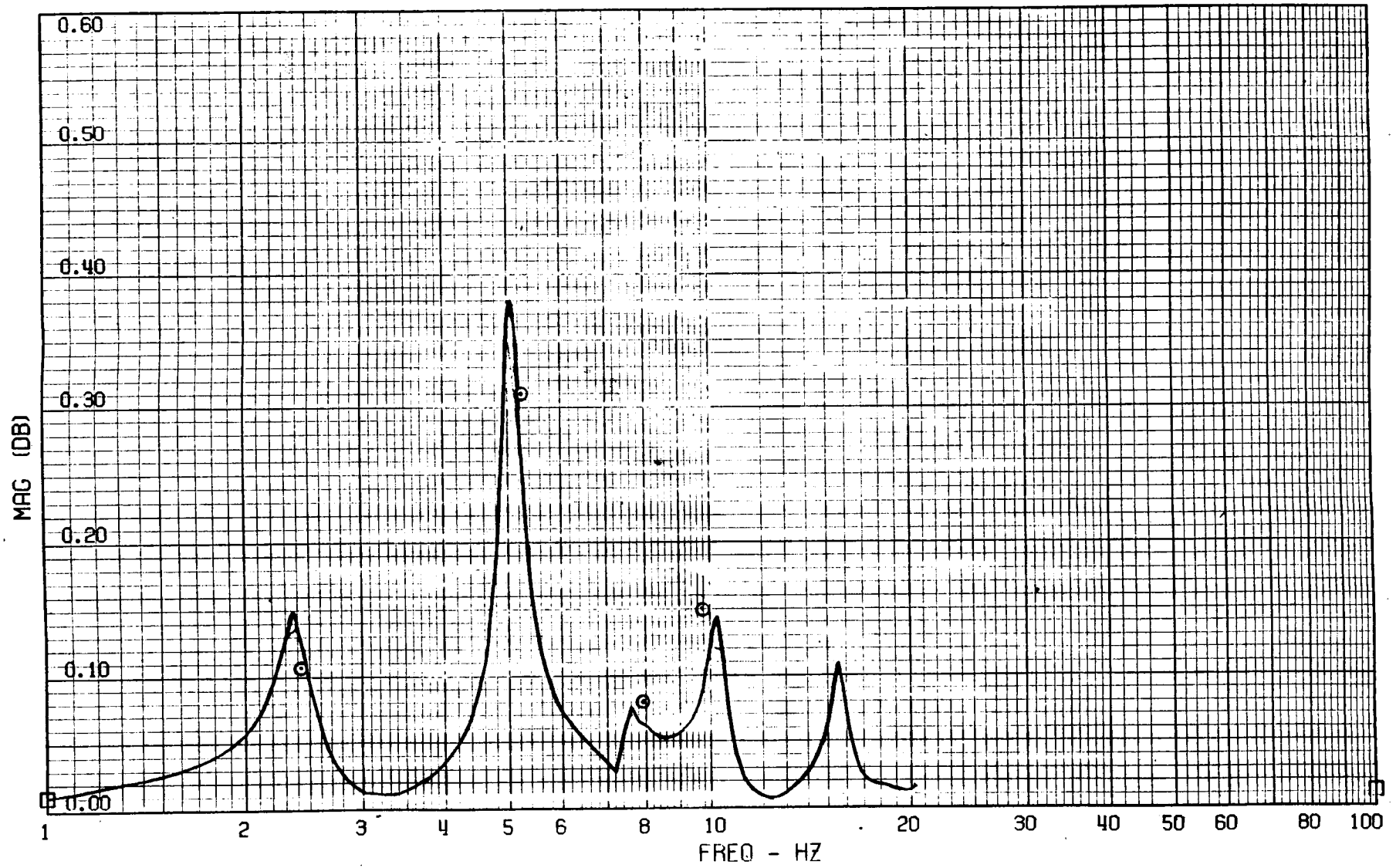

148

FRAME 4
5 /13 /82

TEST POINT 139.1 - MACH=.70 - 400 KEAS - CASE 3
A-4029 - AFT MISSION BAY ACCEL

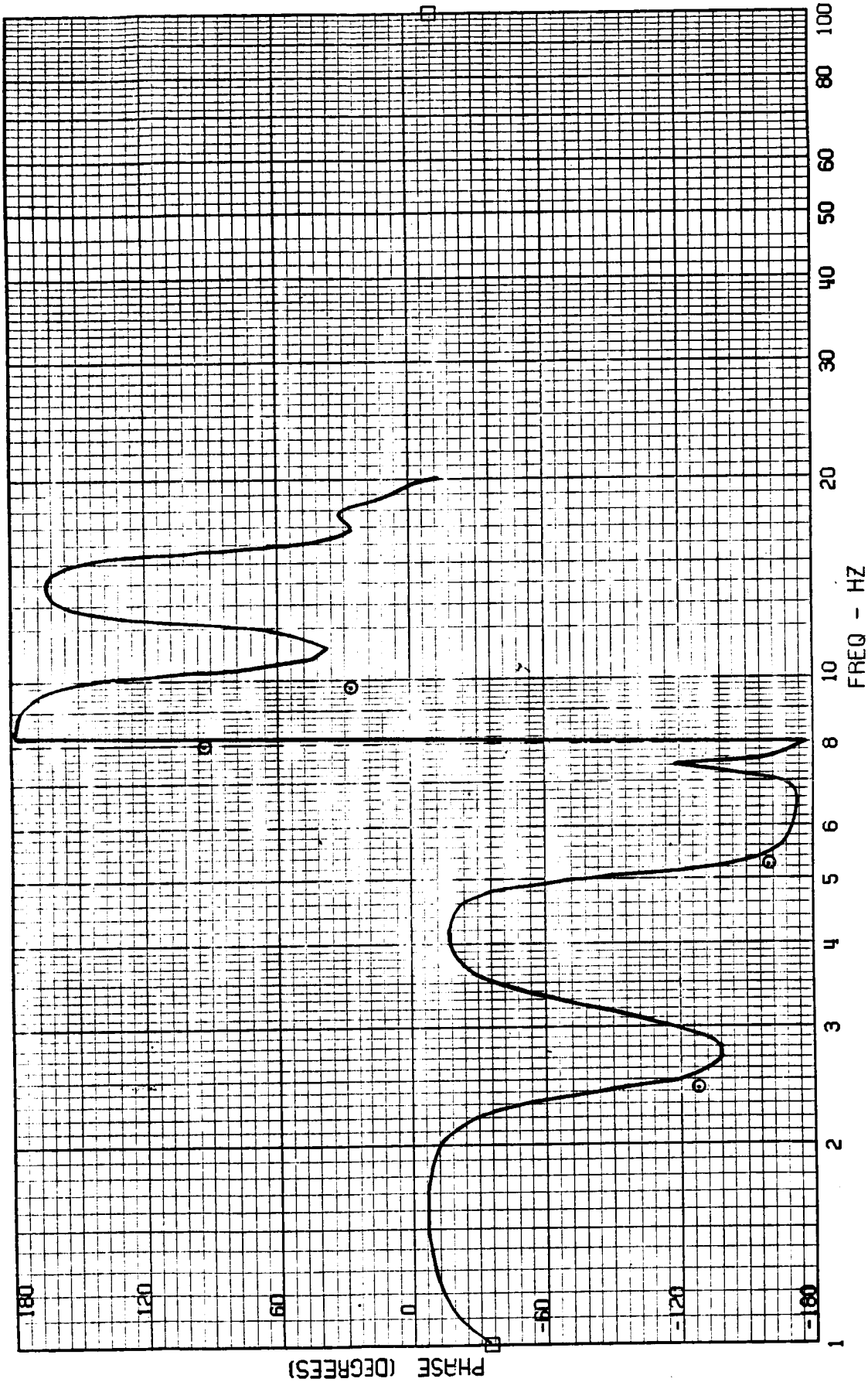

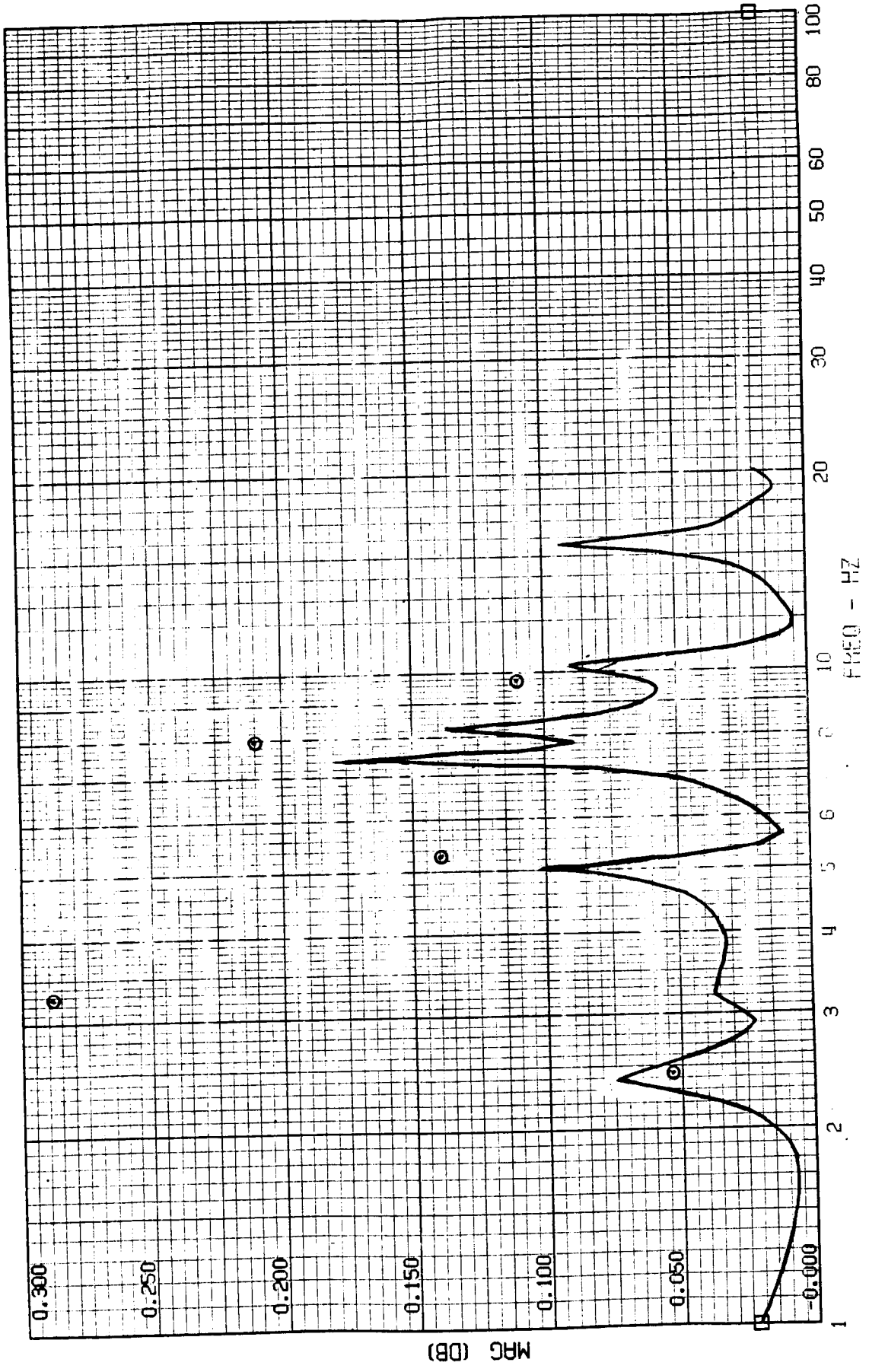
FRAME 5
5 / 13 /82
TEST POINT 139.1 - MACH=.70 - 400 KEAS - CASE 3
A-4001 - CG ACCEL
MAG (DB)
0.300
0.250
0.200
0.150
0.100
0.050
-0.000
1
2
3
4
5
6
10
20
30
40
50
60
80
100
FREQ - HZ

TEST POINT 139.1 - MACH=.70 - 400 KEAS - CASE 3
A-4001 - CG ACCEL

FRAME 5
5 / 13 / 82

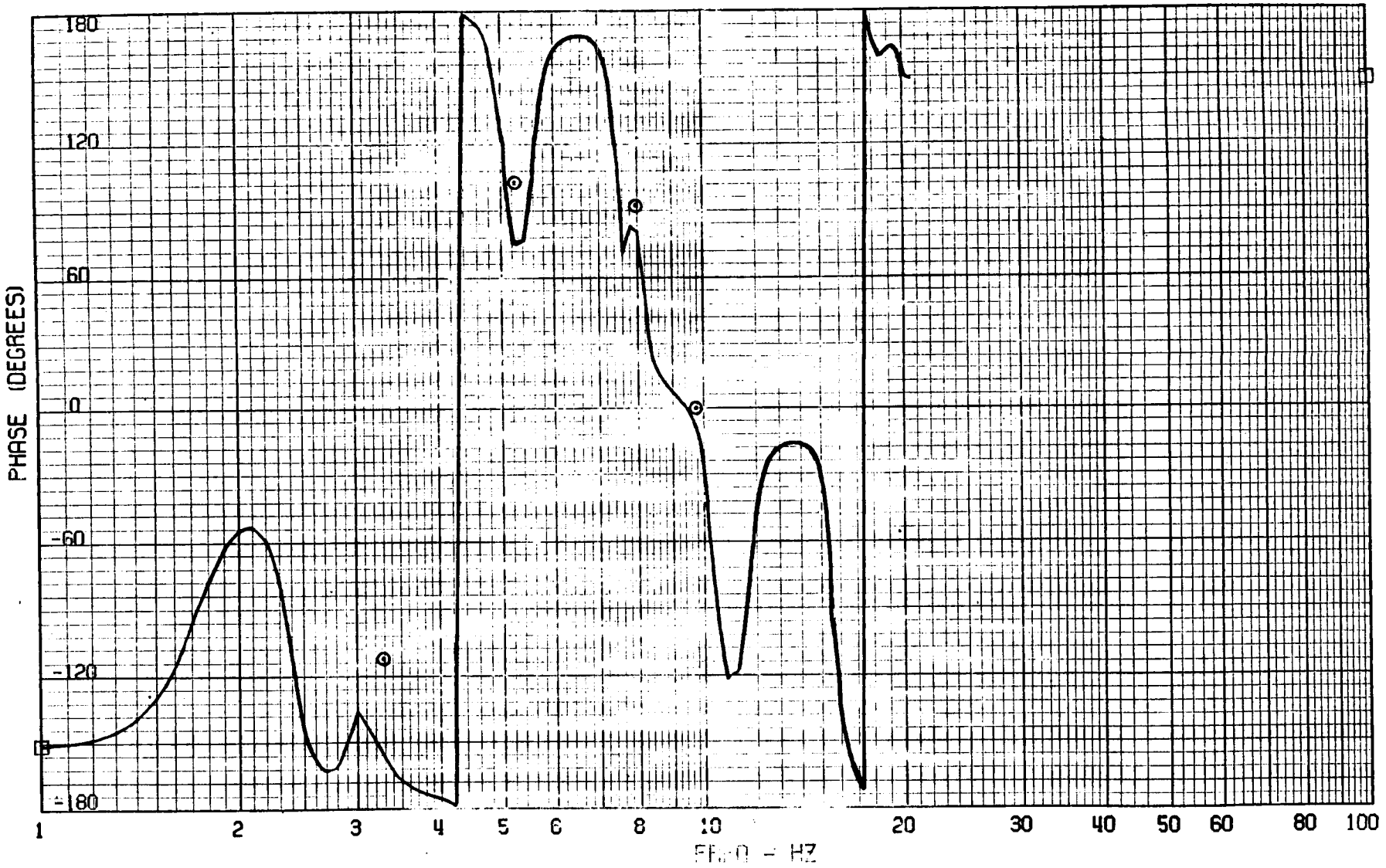

151

TEST POINT 139.1 - MACH=.70 - 400 KEAS - CASE 3
A-4030 - TAIL CONE ACCEL

FRAME 6
5 /13 /82

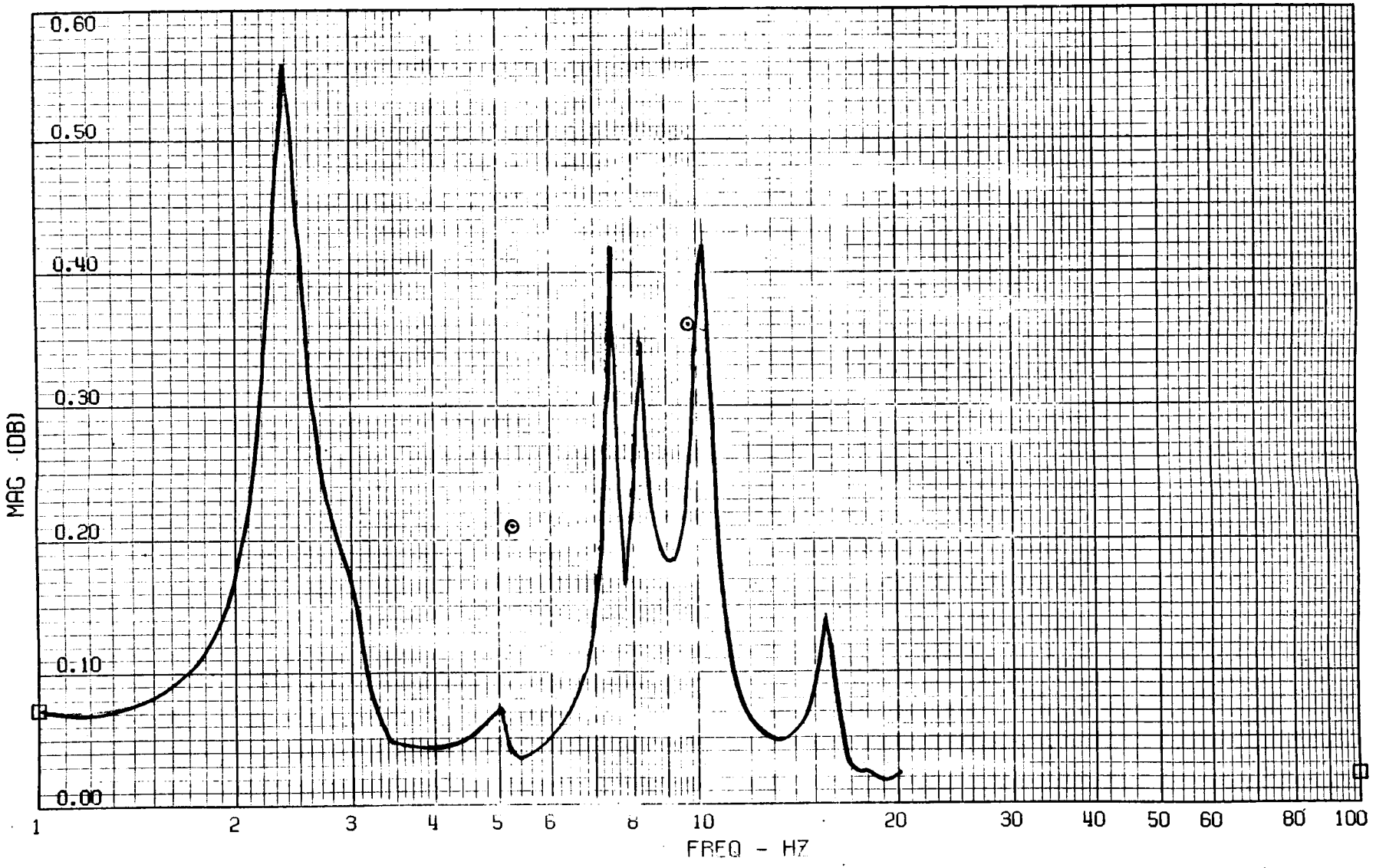

SF 3043

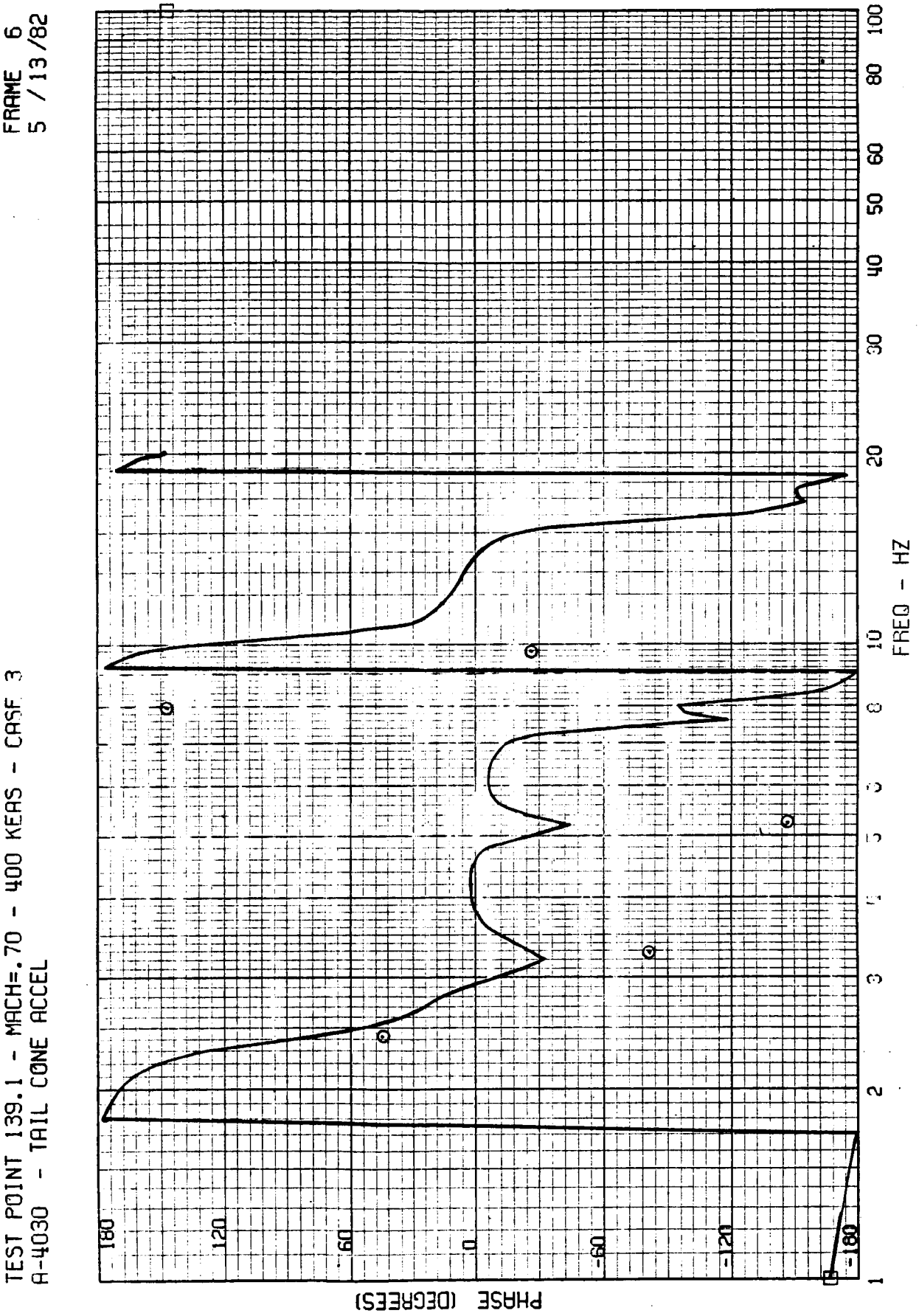

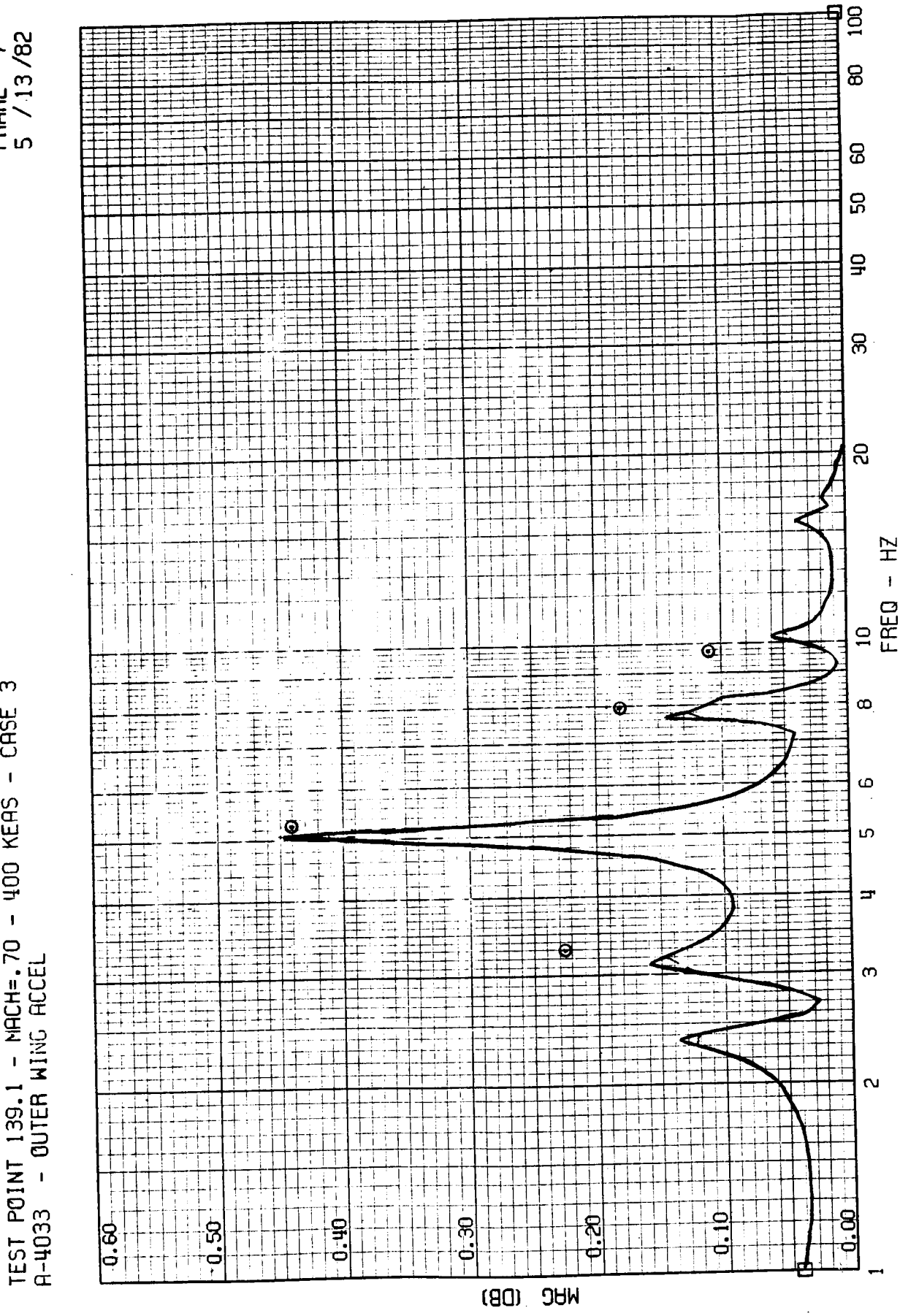
TEST POINT 139.1 - MACH=.70 - 400 KEAS - CASE 3
A-4033 - OUTER WING ACCEL
FRAME 7
5 /13 /82
MAG (DB)
0.60
0.50
0.40
0.30
0.20
0.10
0.00
FREQ - HZ
1
2
3
4
5
6
8
10
20
30
40
50
60
80
100

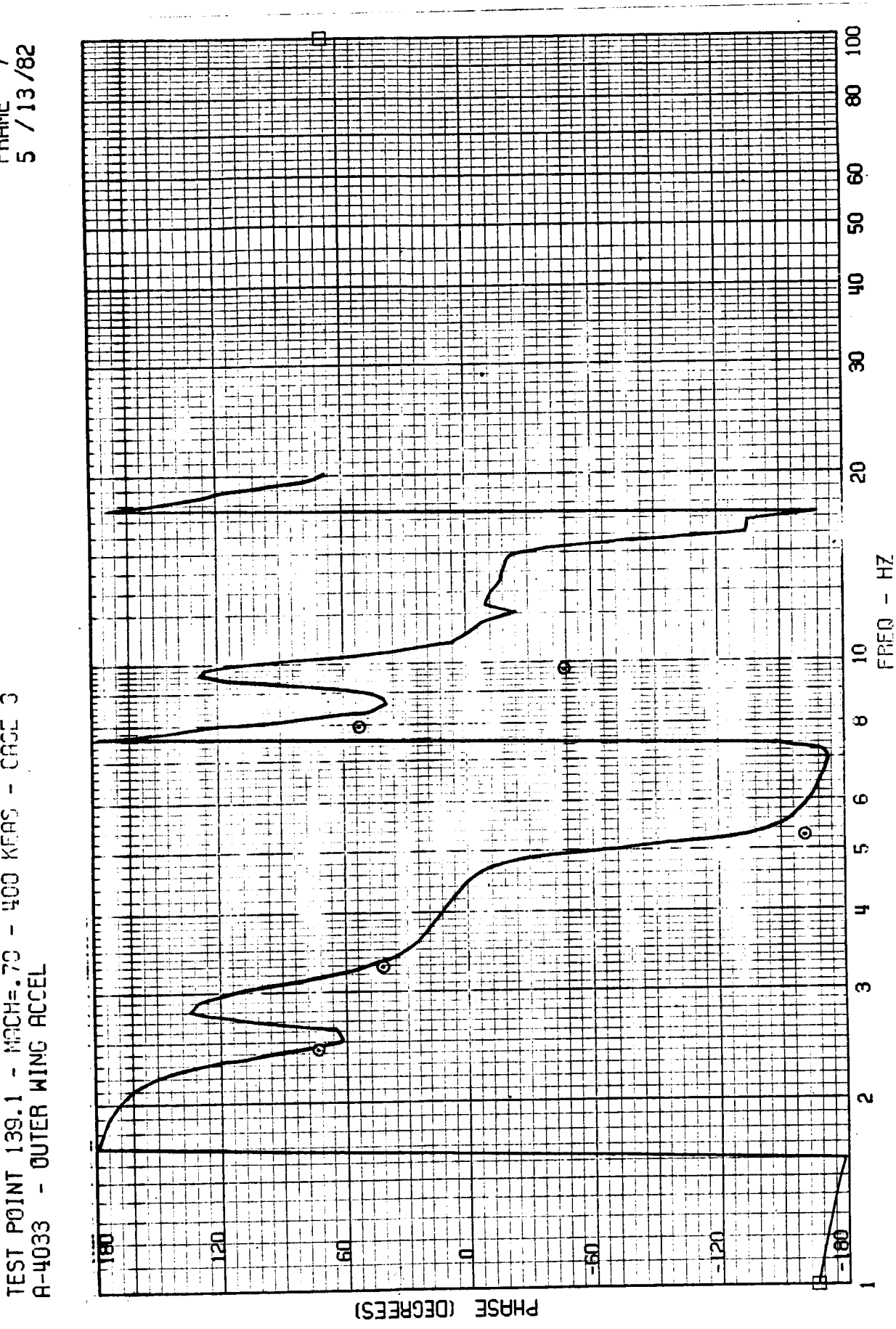

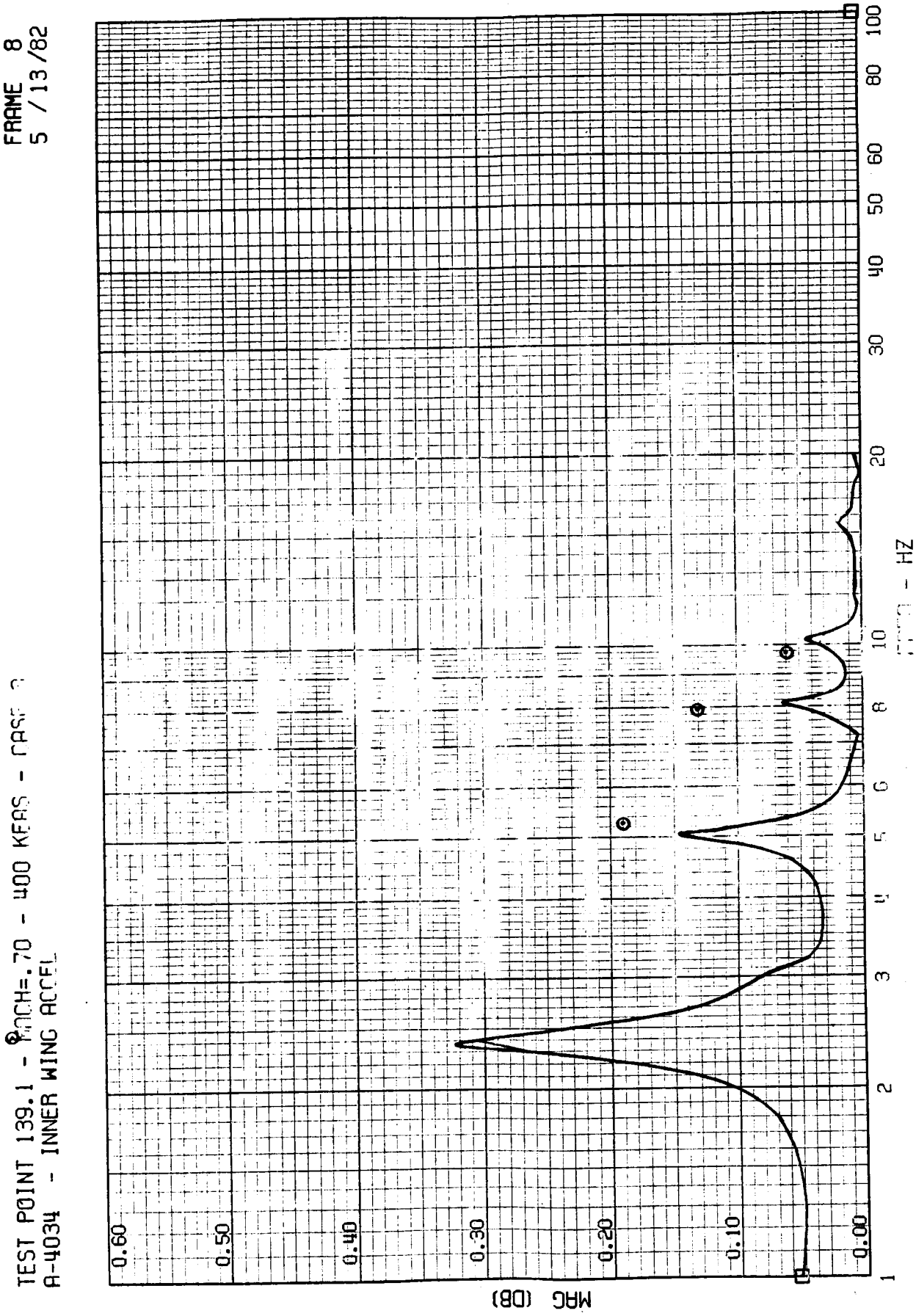
FRAME 8
5 / 13 /82
TEST POINT 139.1 - MACH=.70 - 400 KEAS - PASS 2
A-4034 - INNER WING ACCEL
MAG (DB)
0.60
0.50
0.40
0.30
0.20
0.10
0.00
1
2
3
4
5
6
8
10
20
30
40
50
60
80
100
HZ

FRAME 8
5 /13/82

TEST POINT 139.1 - MACH=.70 - 400 KEAS - CASE 3
A-4034 - INNER WING ACCEL

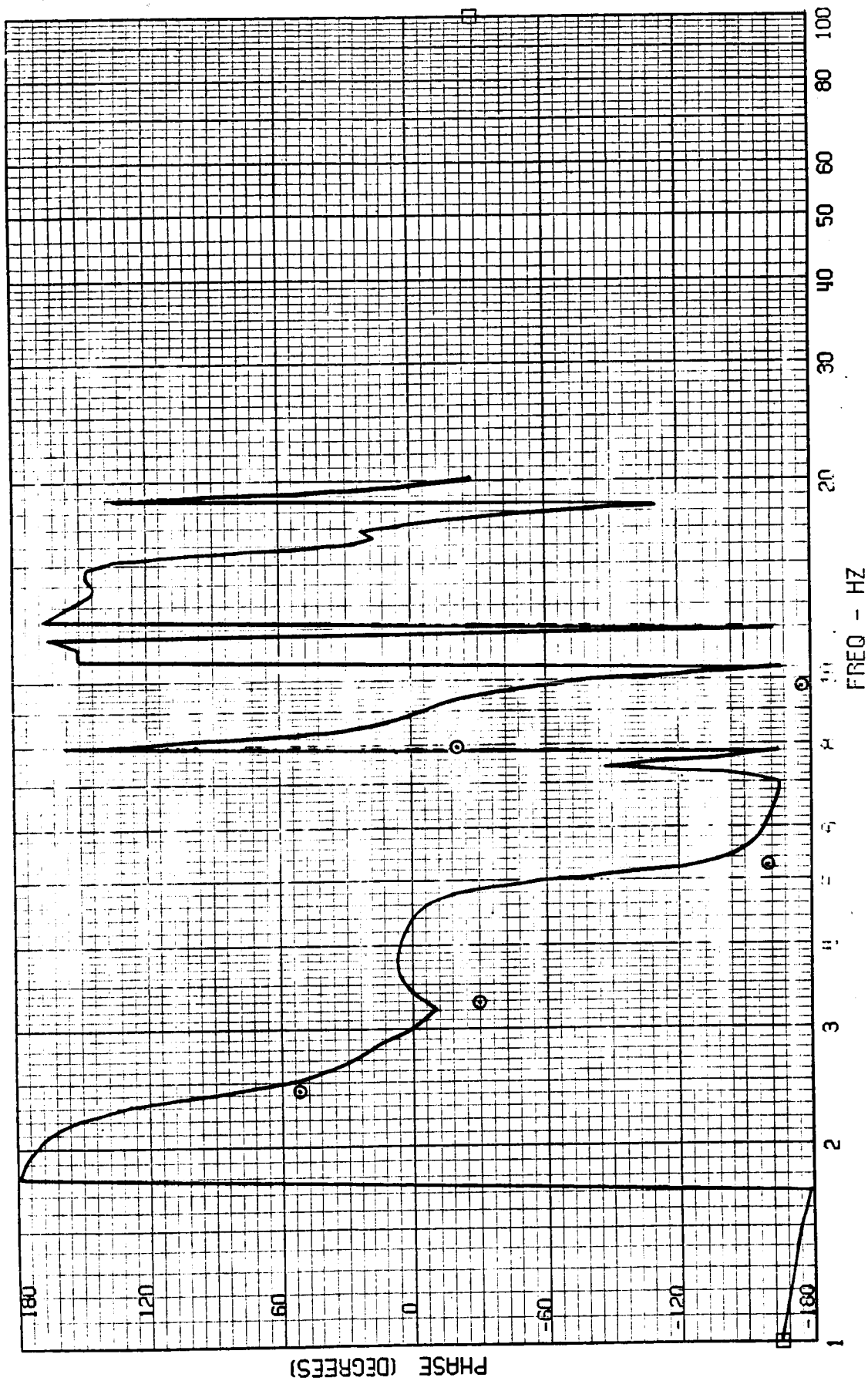

TEST POINT 139.1 - MACH=.70 - 400 KTAS - CASE 3
RWCLACC - NACELLE ACCEL

FRAME 9
5 /13/82

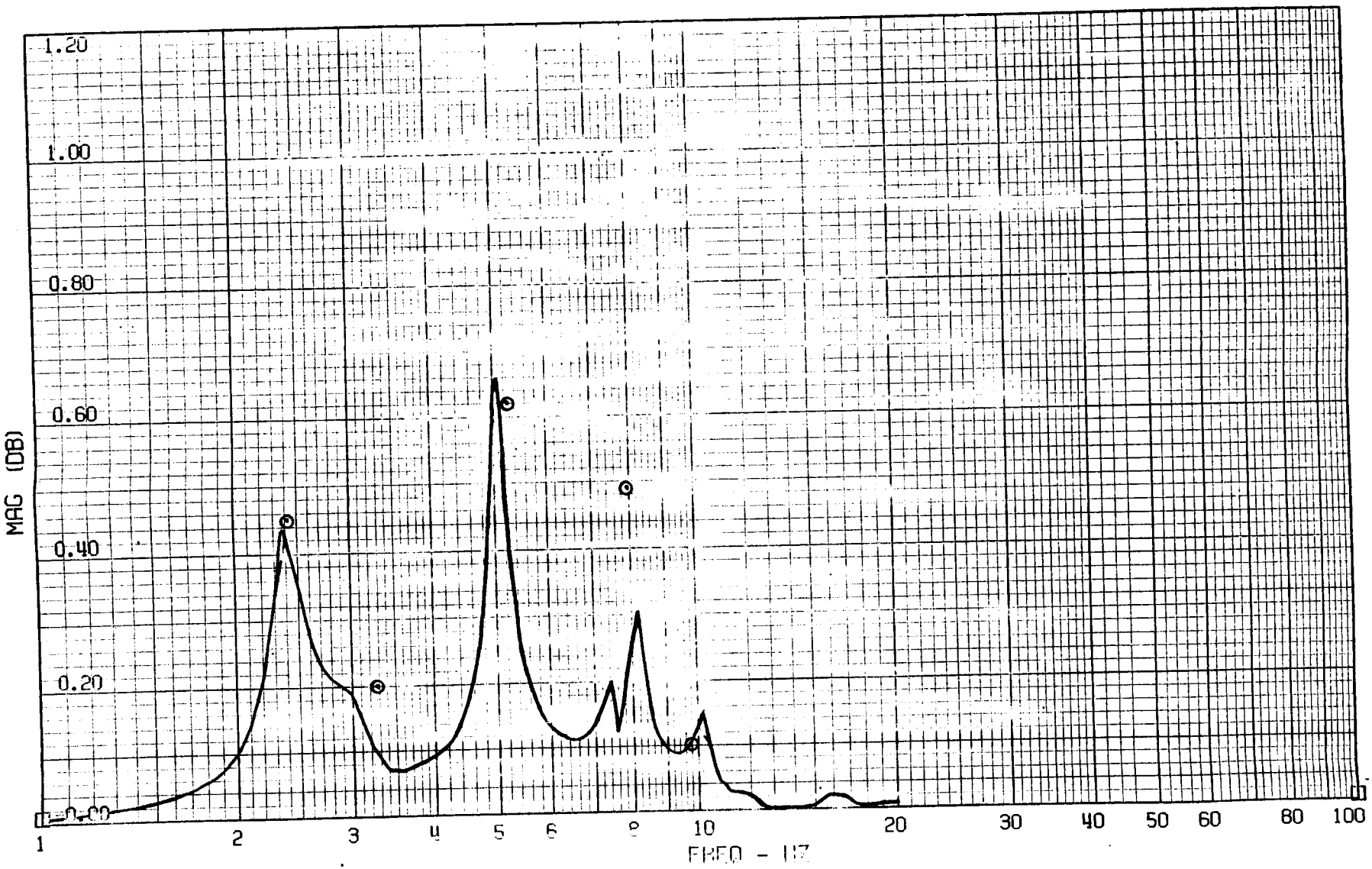

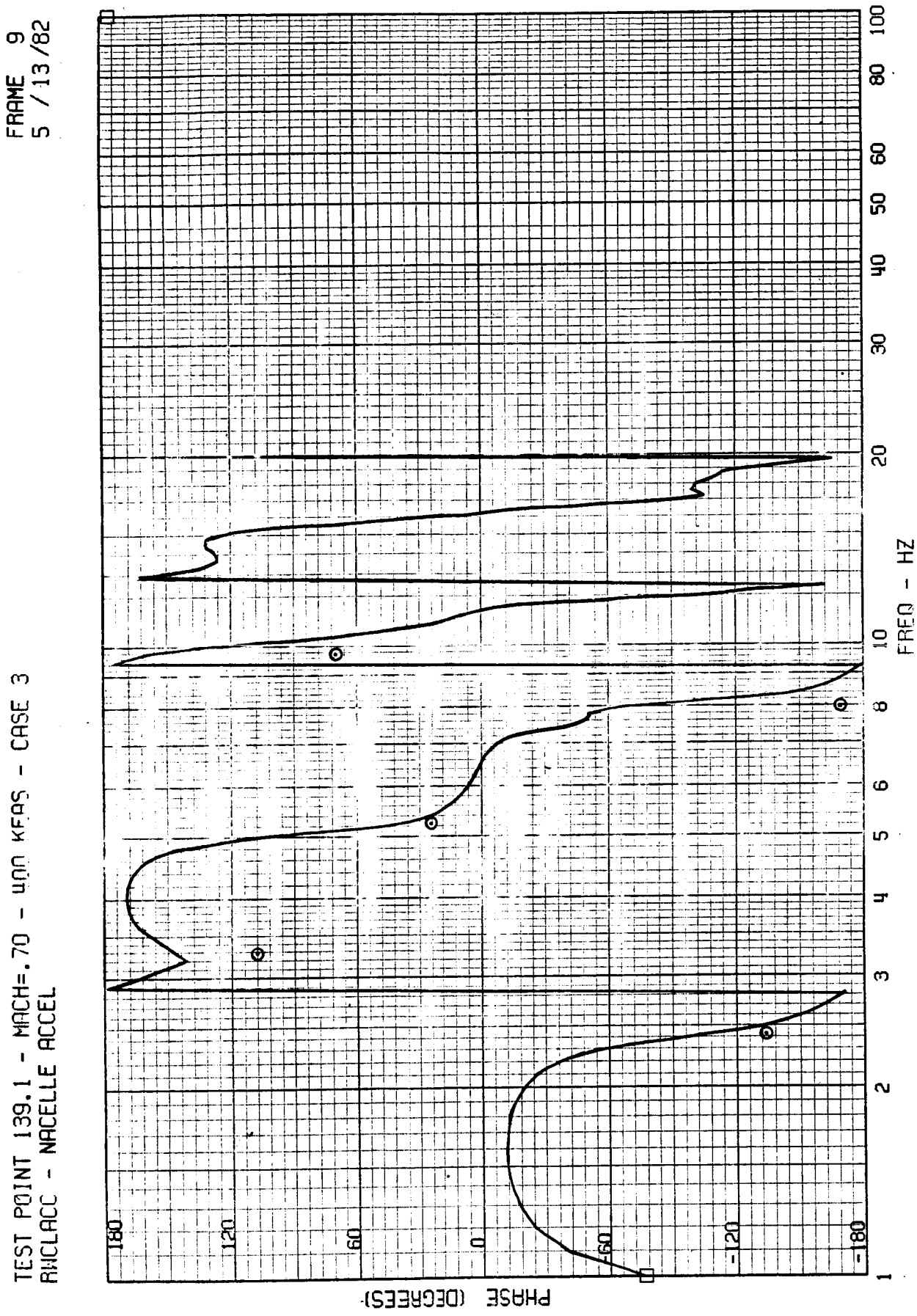

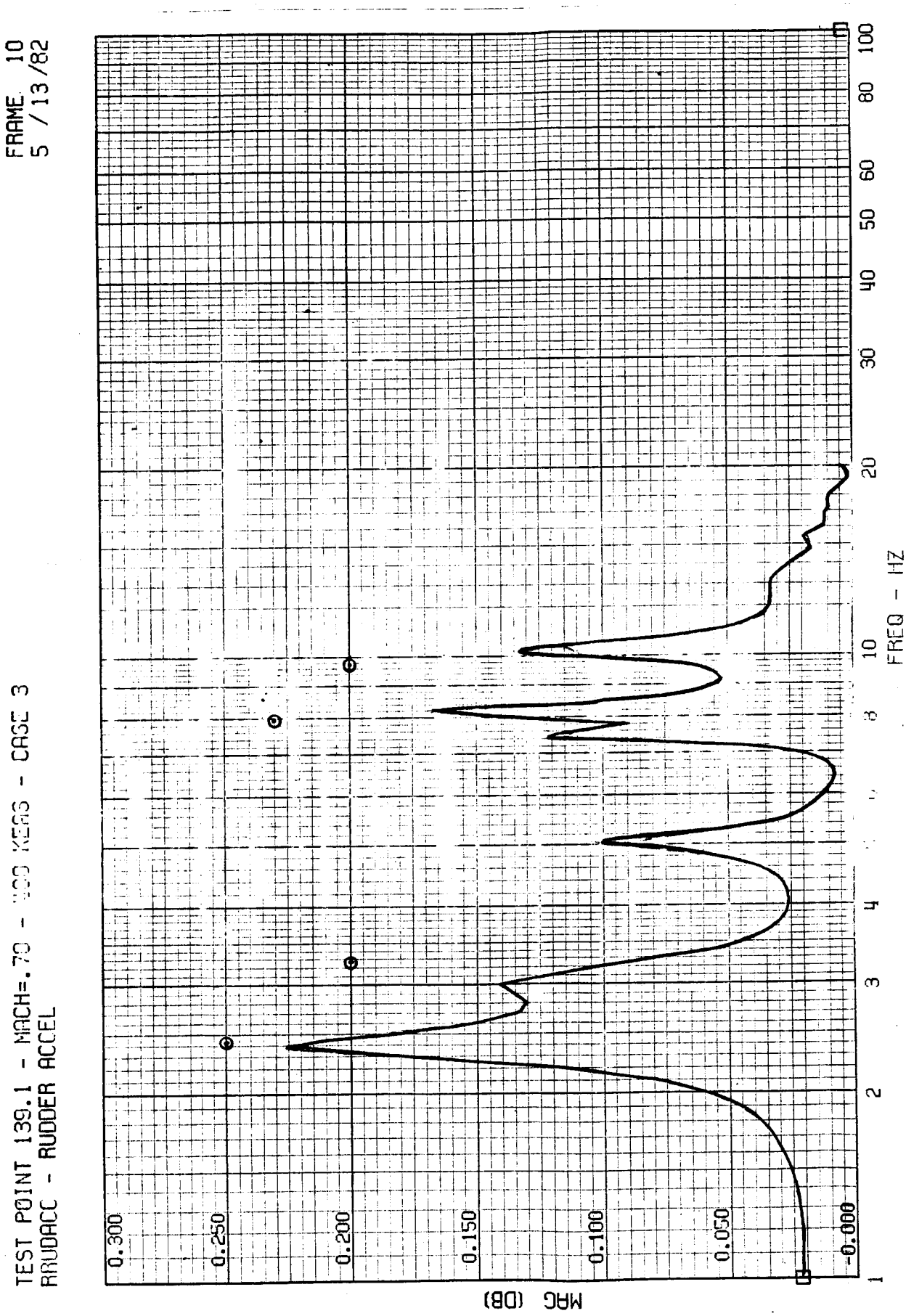
FRAME 10
5 /13 /82
TEST POINT 139.1 - MACH=.79 - [illegible] - CASE 3
RRUDACC - RUDDER ACCEL
MAG (DB)
0.300
0.250
0.200
0.150
0.100
0.050
-0.000
1
2
3
4
8
10
20
30
40
50
60
80
100
FREQ - HZ

FRAME 10
5 / 13 /82

TEST POINT 139.1 - MACH=.70 - 400 KEAS - CASE 3
RRUDACC - RUDDER ACCEL

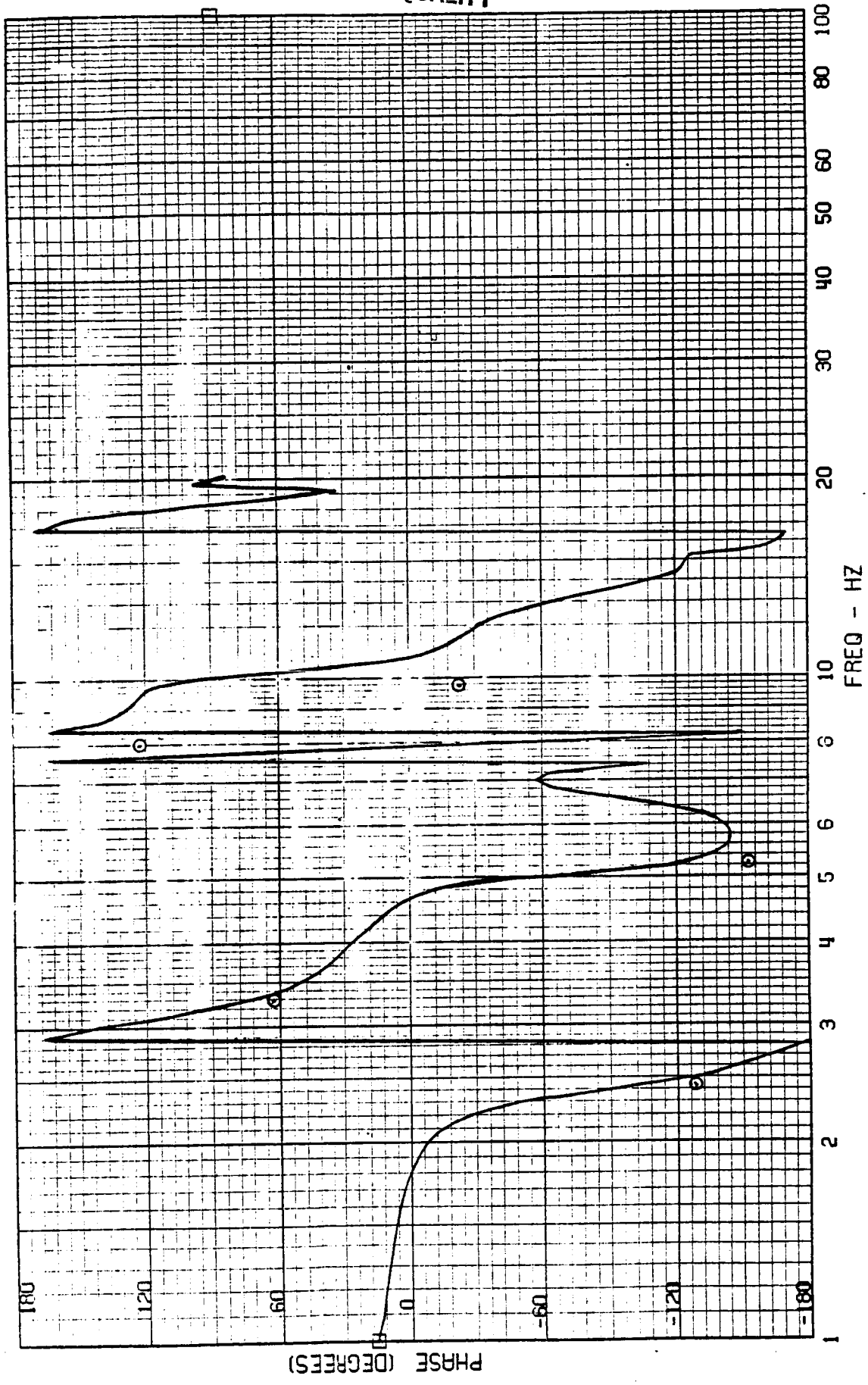

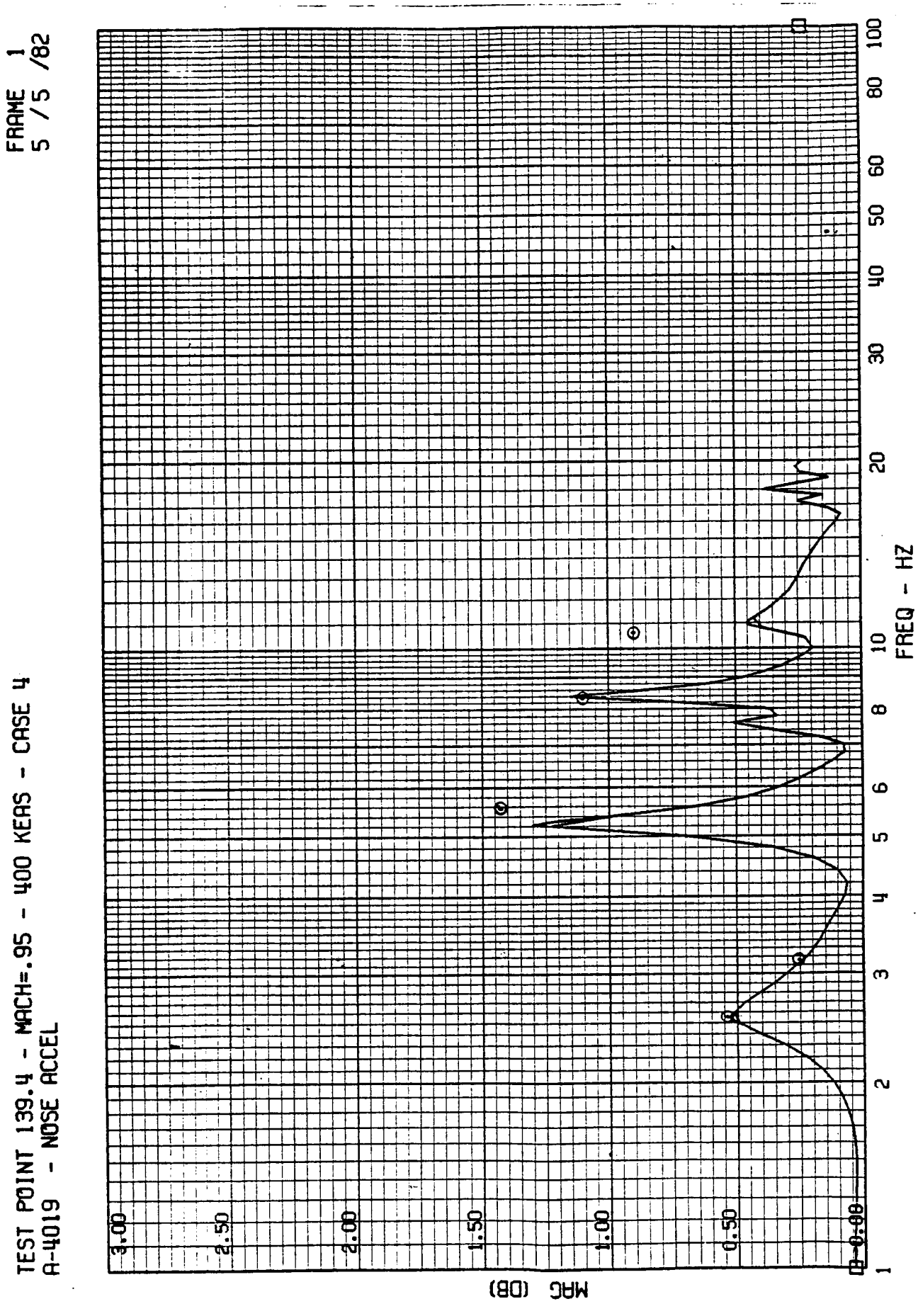
TEST POINT 139.4 - MACH=.95 - 400 KEAS - CASE 4
A-4019 - NOSE ACCEL
FRAME 1
5 /5 /82
MAG (DB)
3.00
2.50
2.00
1.50
1.00
0.50
0.00
FREQ - HZ
1
2
3
4
5
6
8
10
20
30
40
50
60
80
100

FRAME 1
5 /5 /82

TEST POINT 139.4 - MACH=.95 - 400 KEAS - CASE 4
A-4019 - NOSE ACCEL

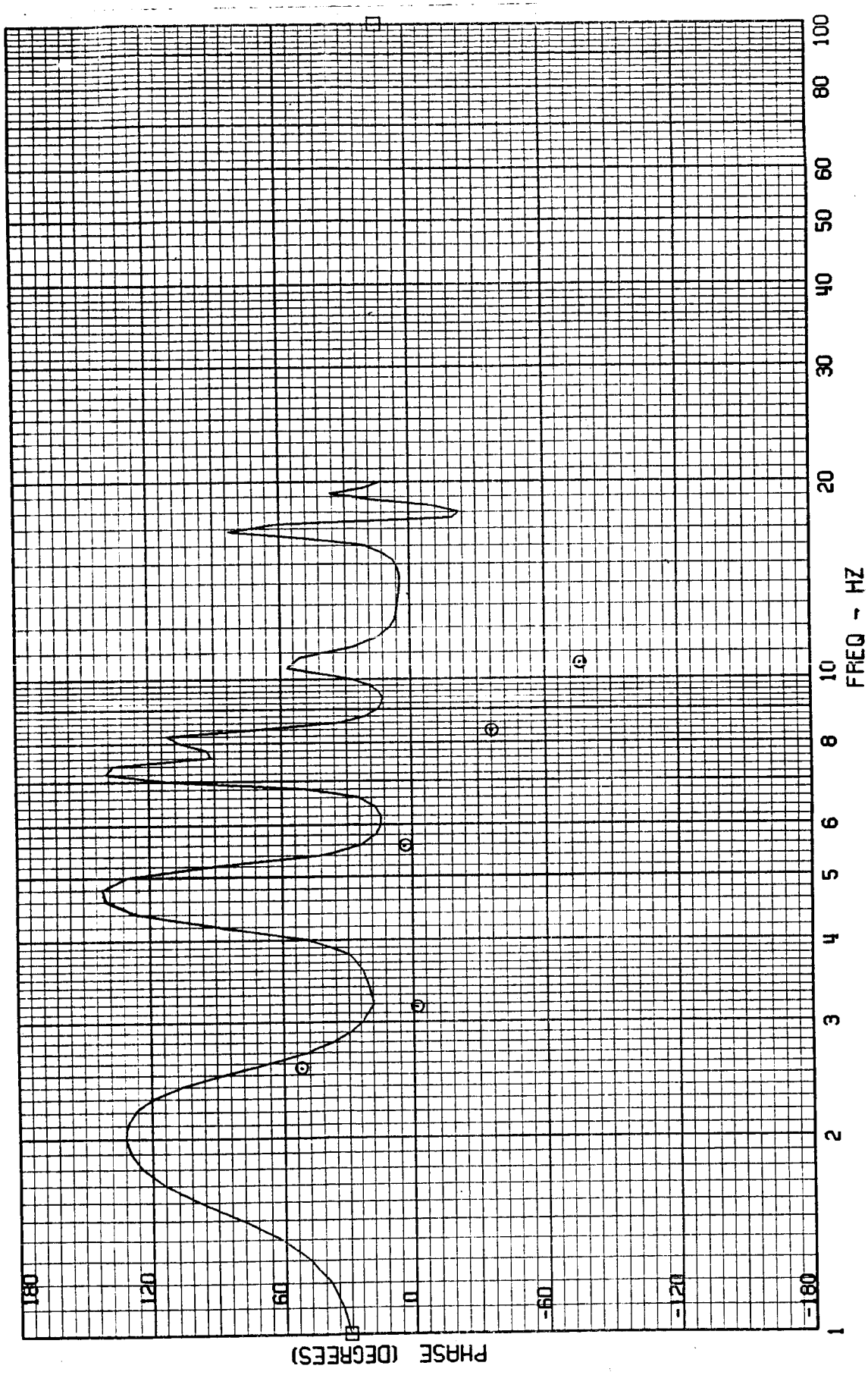

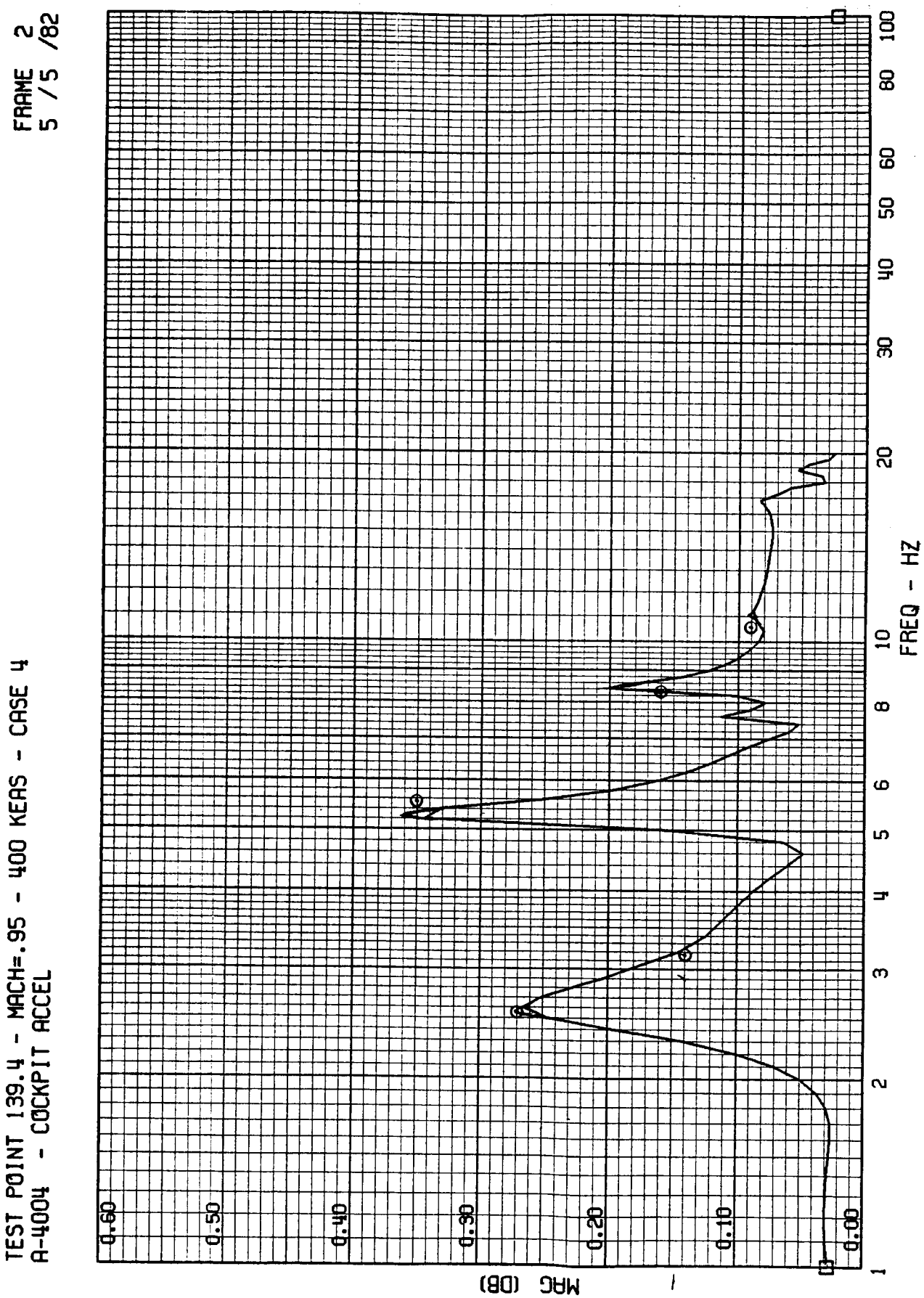
TEST POINT 139.4 - MACH=.95 - 400 KEAS - CASE 4
A-4004 - COCKPIT ACCEL
FRAME 2
5 /5 /82
MAG (DB)
0.60
0.50
0.40
0.30
0.20
0.10
0.00
1
2
3
4
5
6
8
10
20
30
40
50
60
80
100
FREQ - HZ

FRAME 2
5 /5 /82

TEST POINT 139.4 - MACH=.95 - 400 KEAS - CASE 4
A-4004 - COCKPIT ACCEL

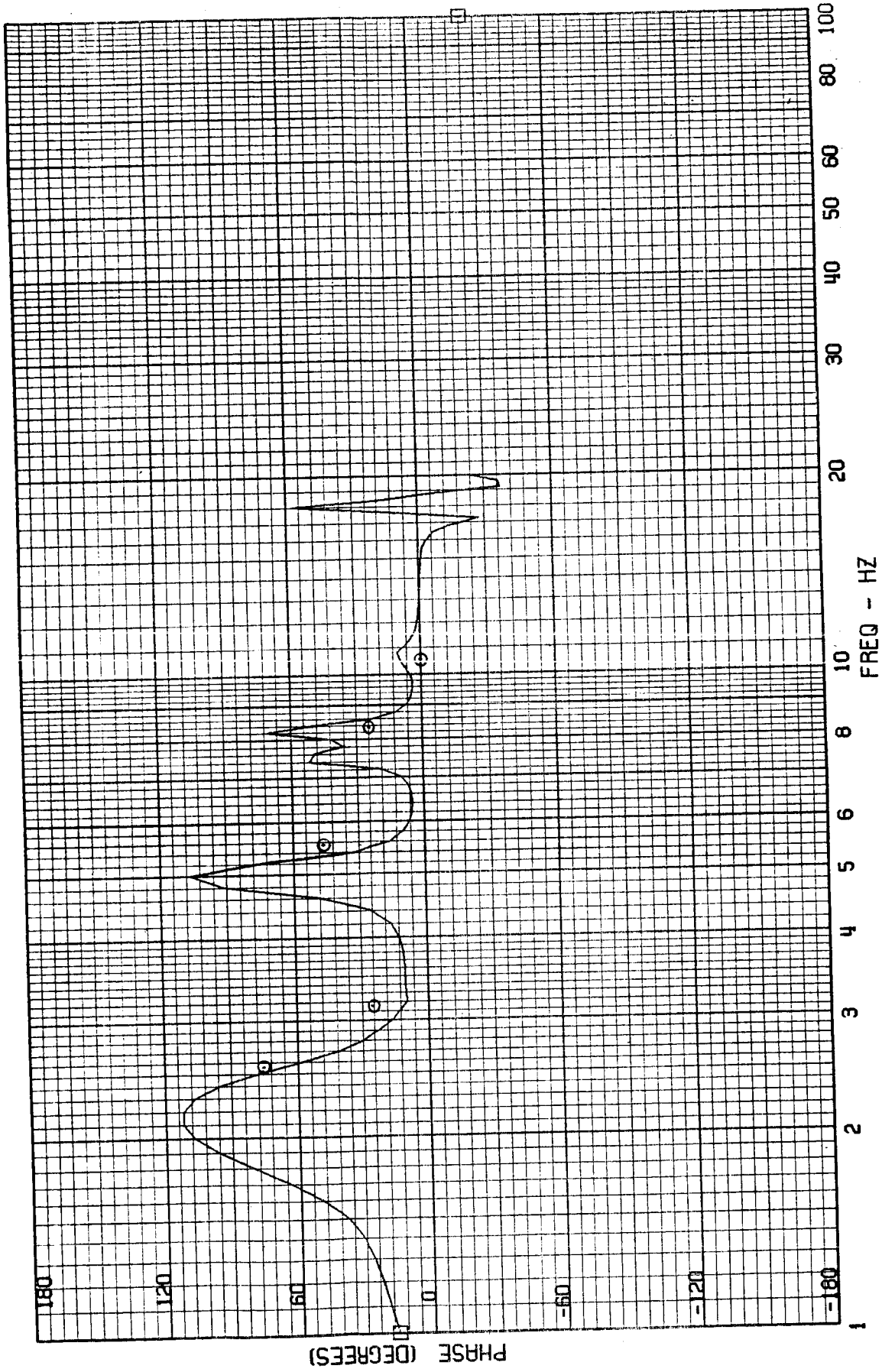

TEST POINT 139.4 - MACH=.95 - 400 KEAS - CASE 4
A-4028 - FORWARD MISSION BAY ACCEL

FRAME 3
5 /5 /82

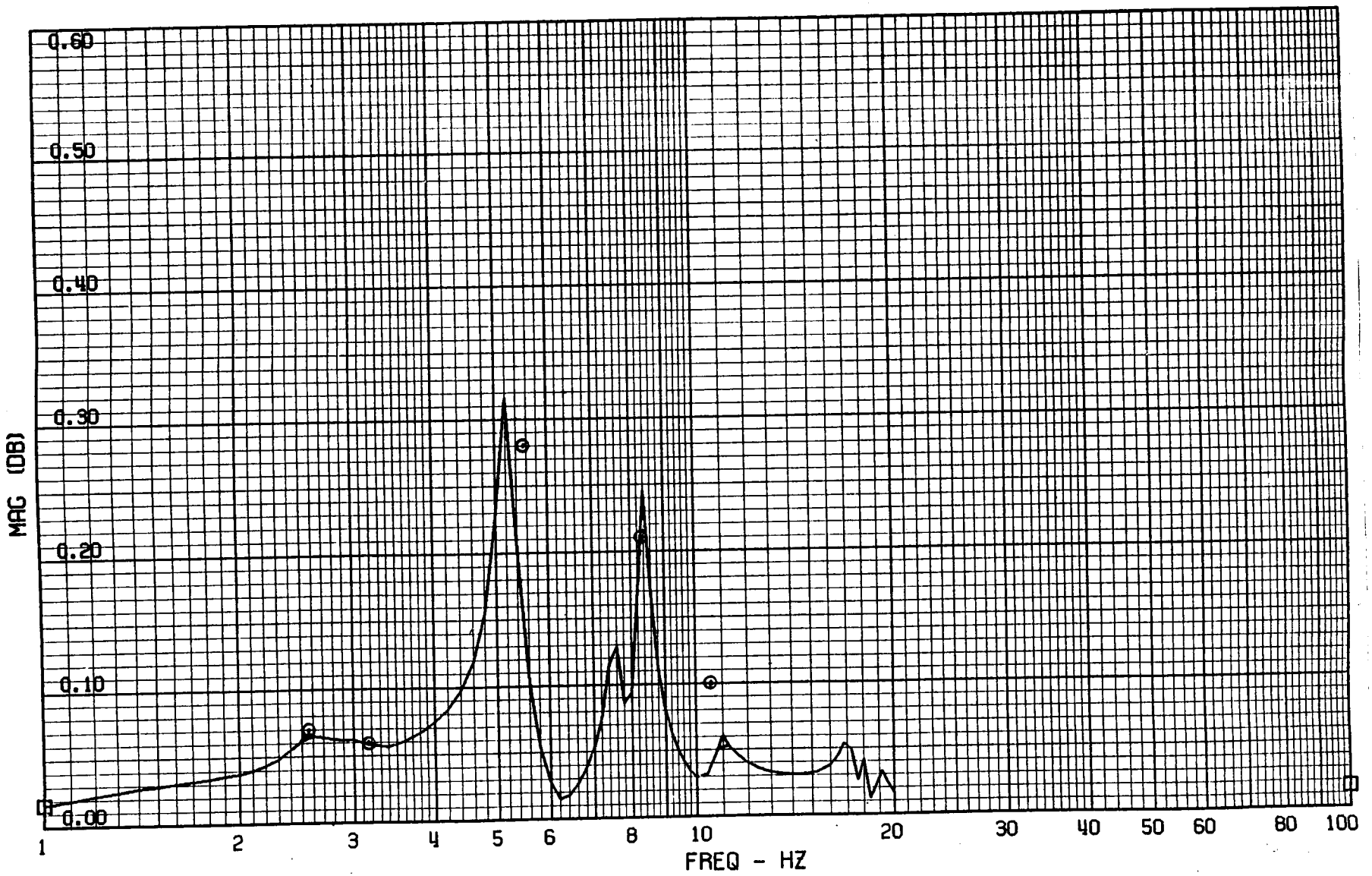

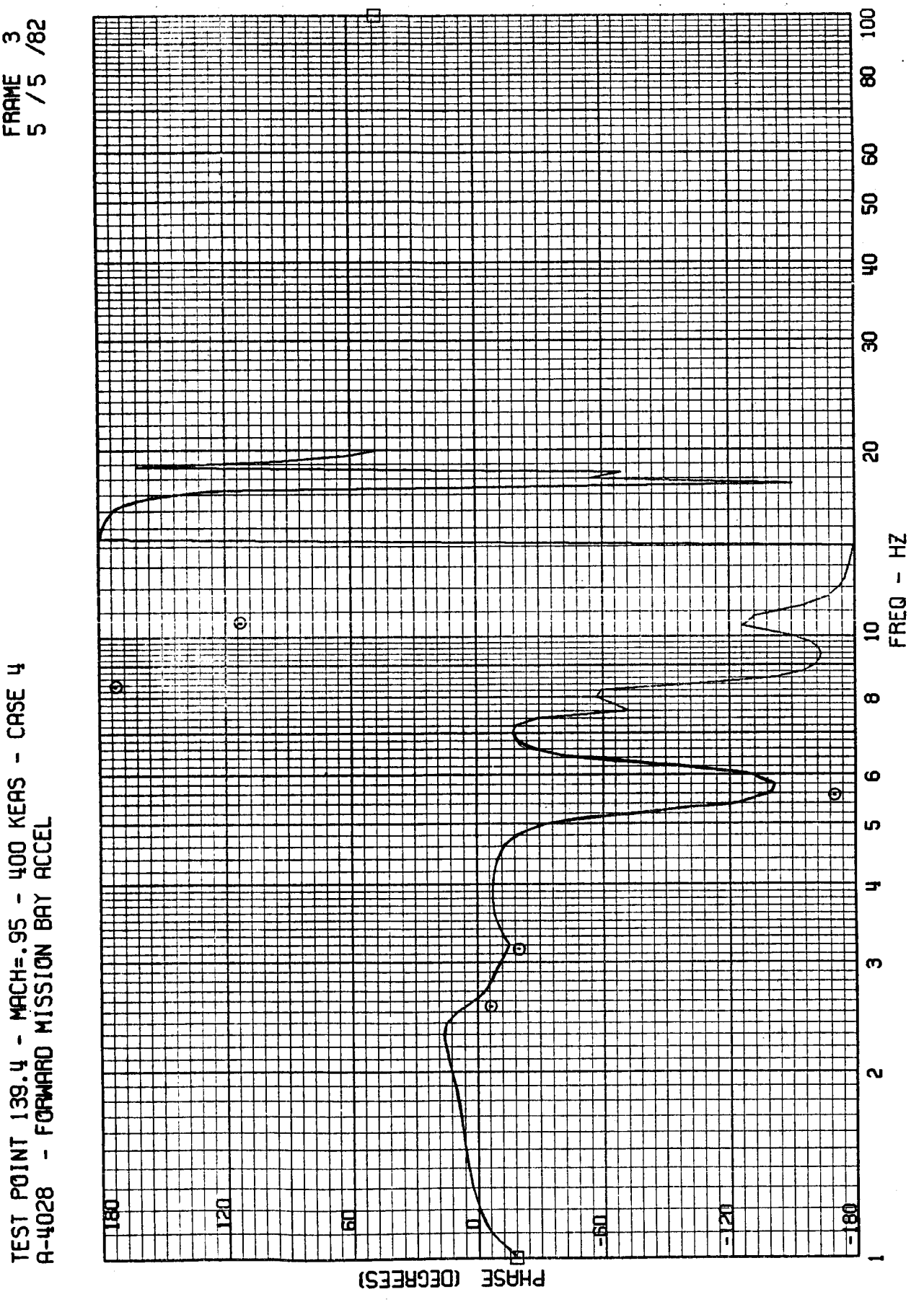

TEST POINT 139.4 - MACH=.95 - 400 KEAS - CASE 4
A-4029 - AFT MISSION BAY ACCEL

FRAME 4
5 /5 /82

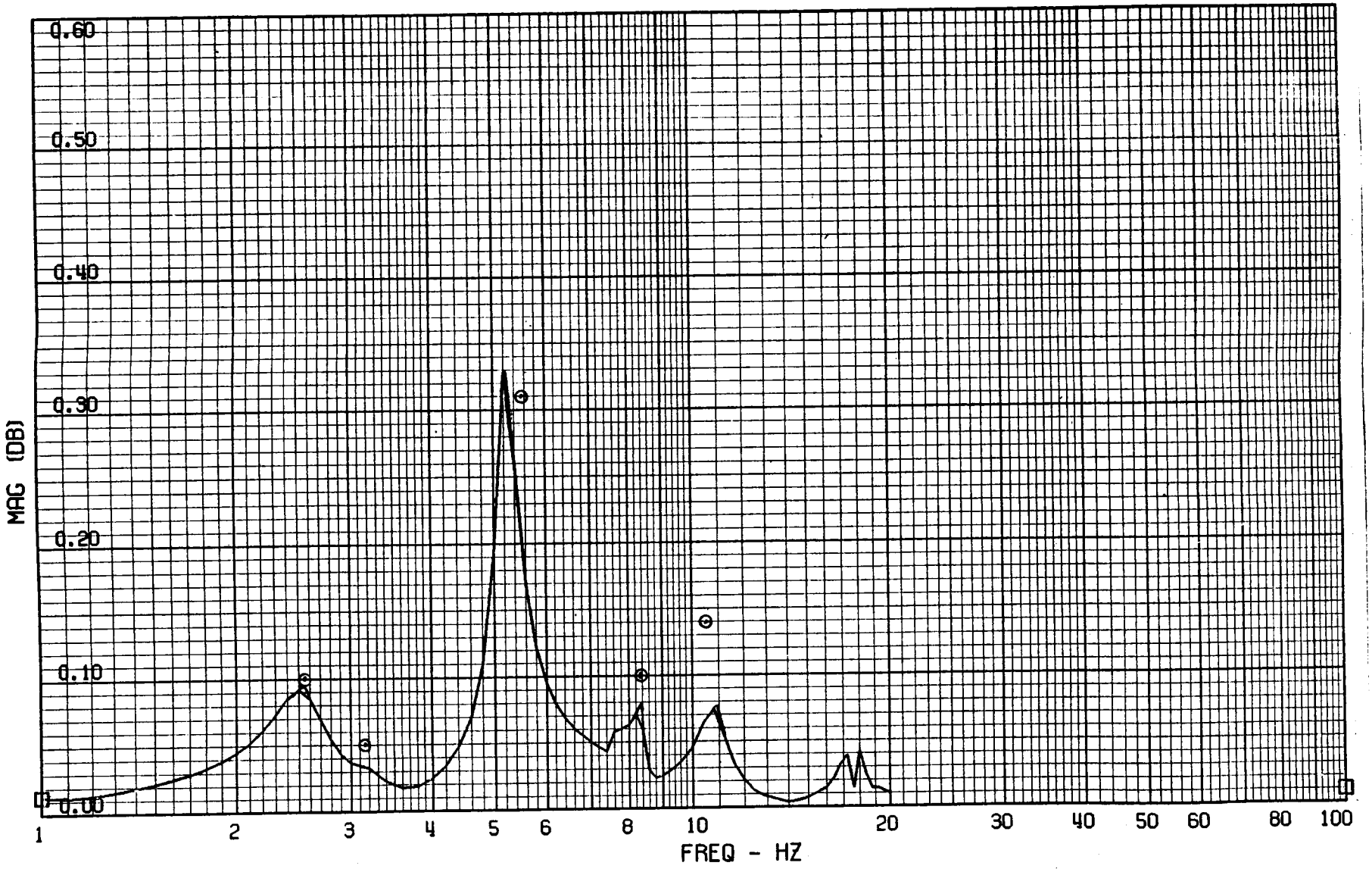

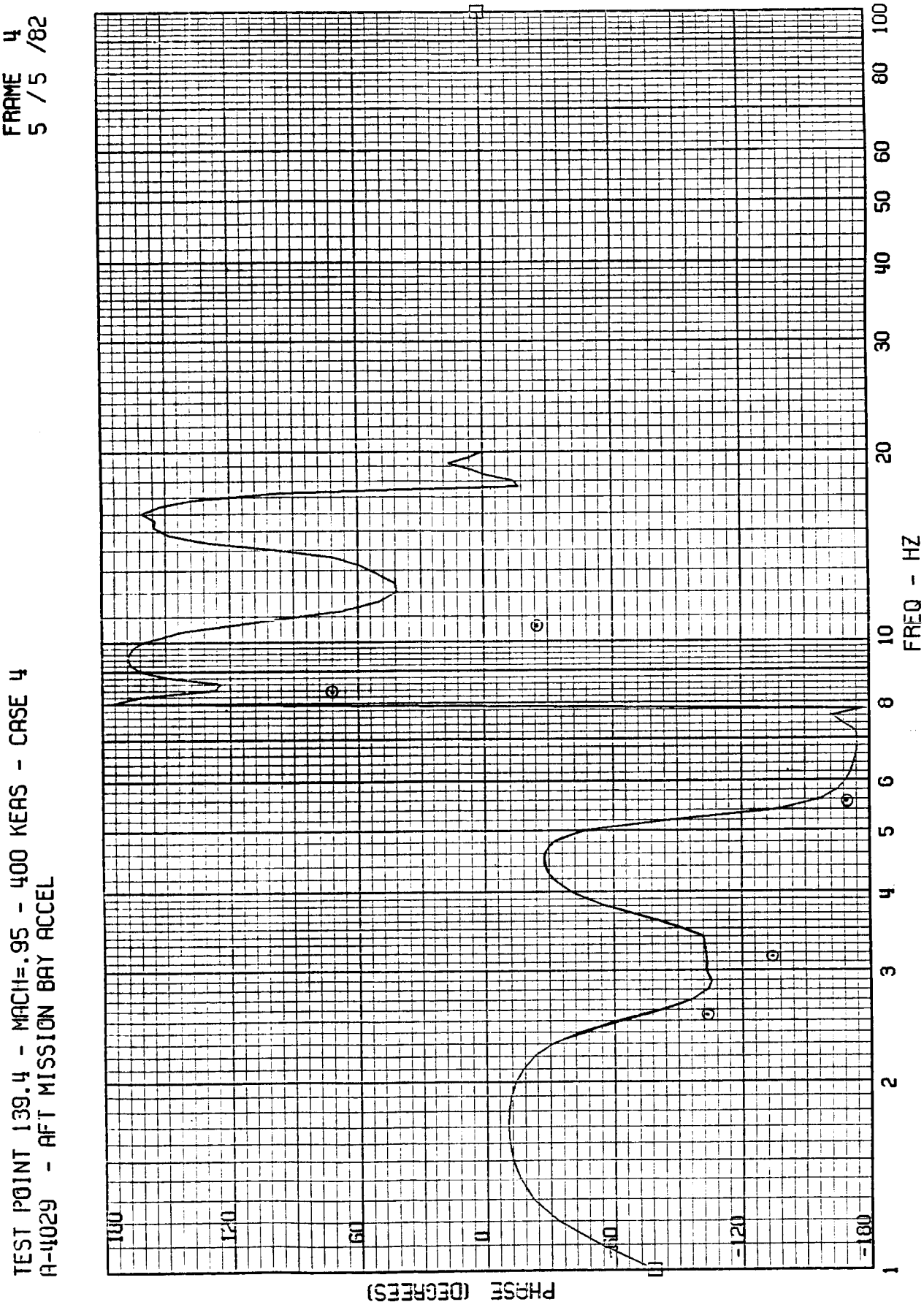
TEST POINT 139.4 - MACH=.95 - 400 KEAS - CASE 4
A-4029 - AFT MISSION BAY ACCEL
FRAME 4
5 /5 /82
PHASE (DEGREES)
180
120
60
0
-60
-120
-180
1
2
3
4
5
6
8
10
20
30
40
50
60
80
100
FREQ - HZ

TEST POINT 139.4 - MACH=.95 - 400 KEAS - CASE 4
A-4001 - CG ACCEL

FRAME 5
5 /5 /82

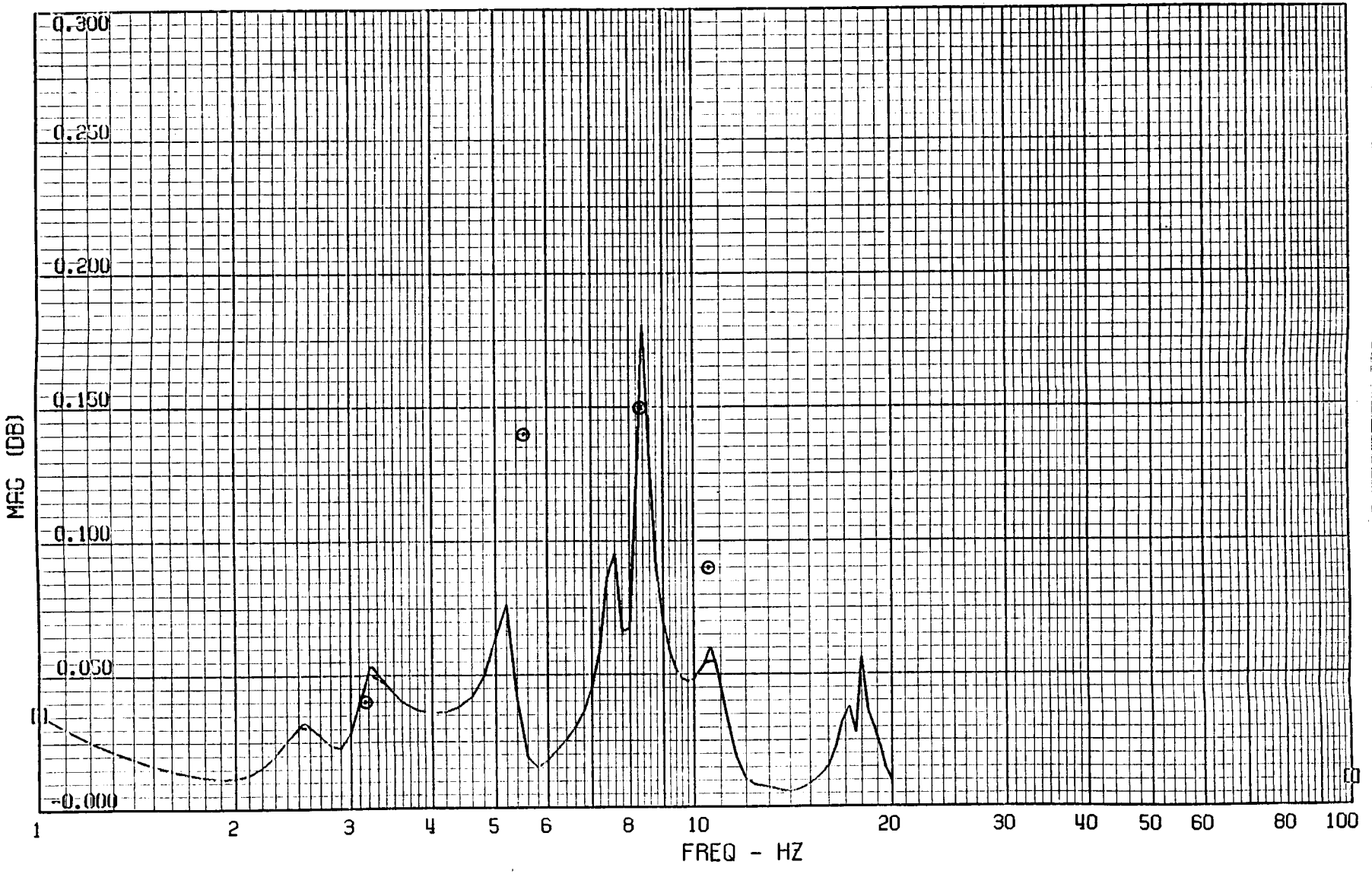

170

ORIGINAL PAGE IS
OF POOR QUALITY

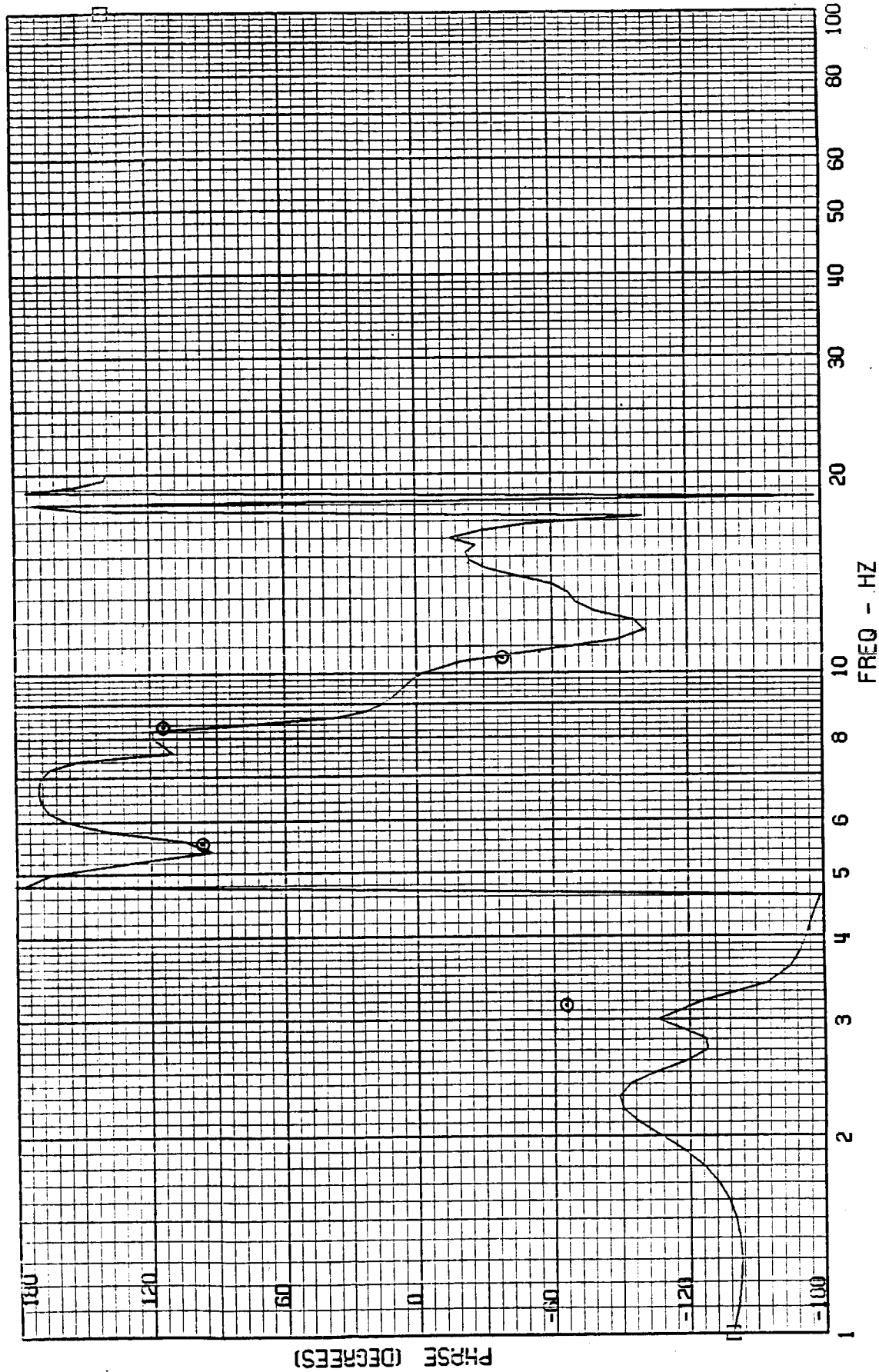

TEST POINT 139.4 - MACH=.95 - 400 KEAS - CASE 4
A-4030 - TAIL CONE ACCEL

FRAME 6
5 /5 /82

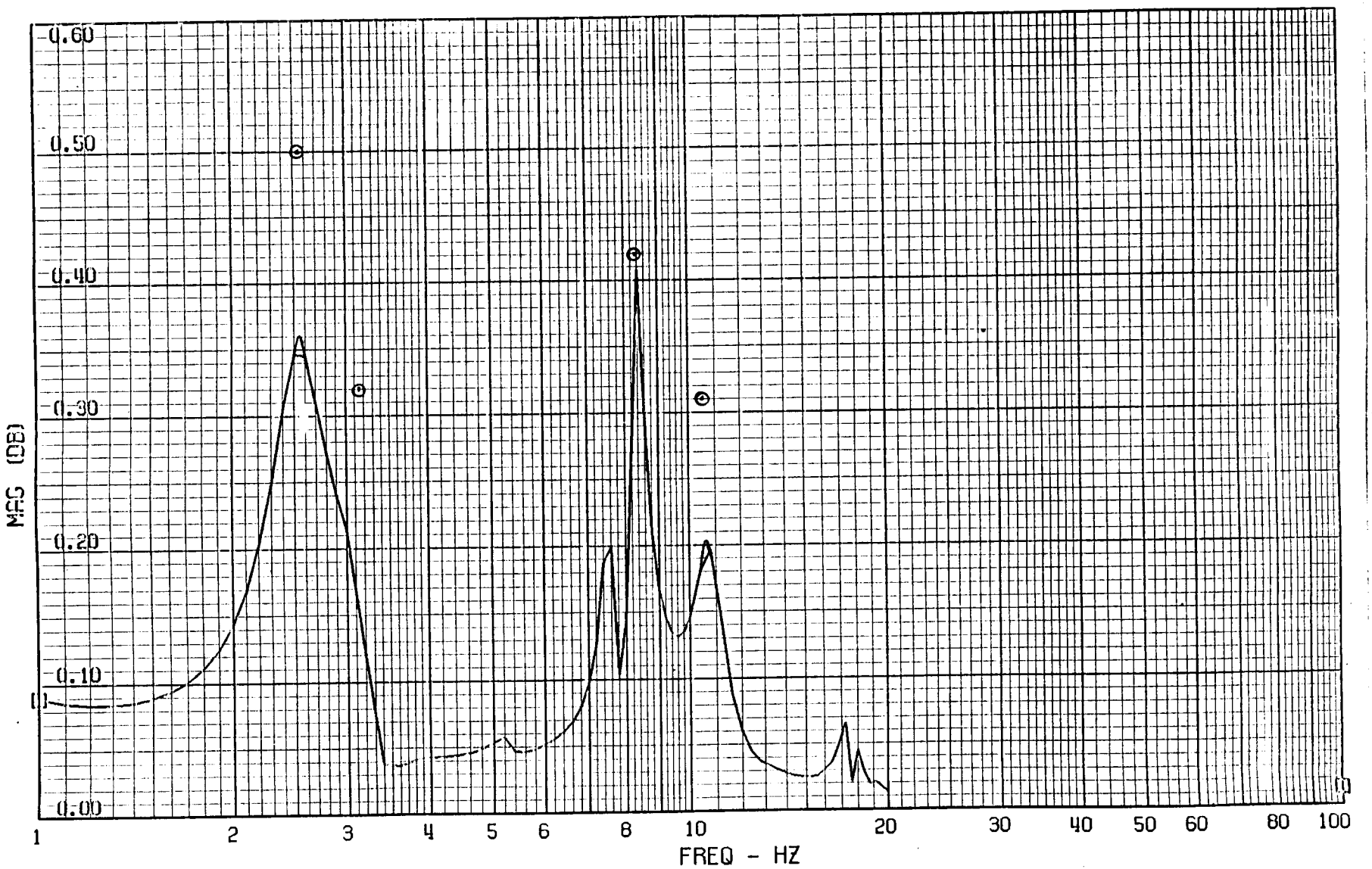

172

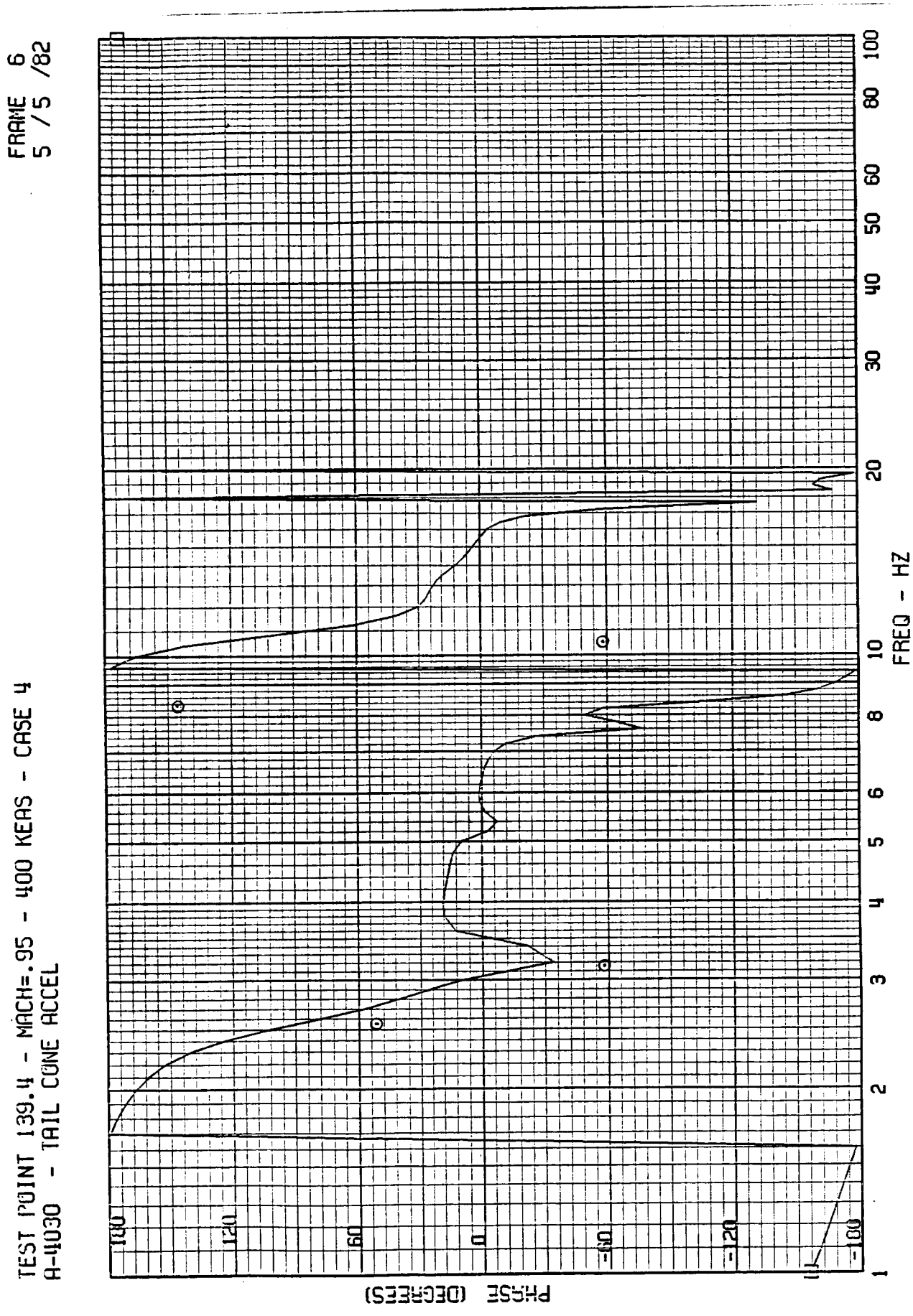
FRAME 6
5 /5 /82
TEST POINT 139.4 - MACH=.95 - 400 KEAS - CASE 4
A-4030 - TAIL CONE ACCEL
PHASE (DEGREES)
FREQ - HZ
180
120
60
0
-60
-120
-180
1
2
3
4
5
6
8
10
20
30
40
50
60
80
100

TEST POINT 139.4 - MACH=.95 - 400 KEAS - CASE 4
A-4033 - OUTER WING ACCEL

FRAME 7
5 /5 /82

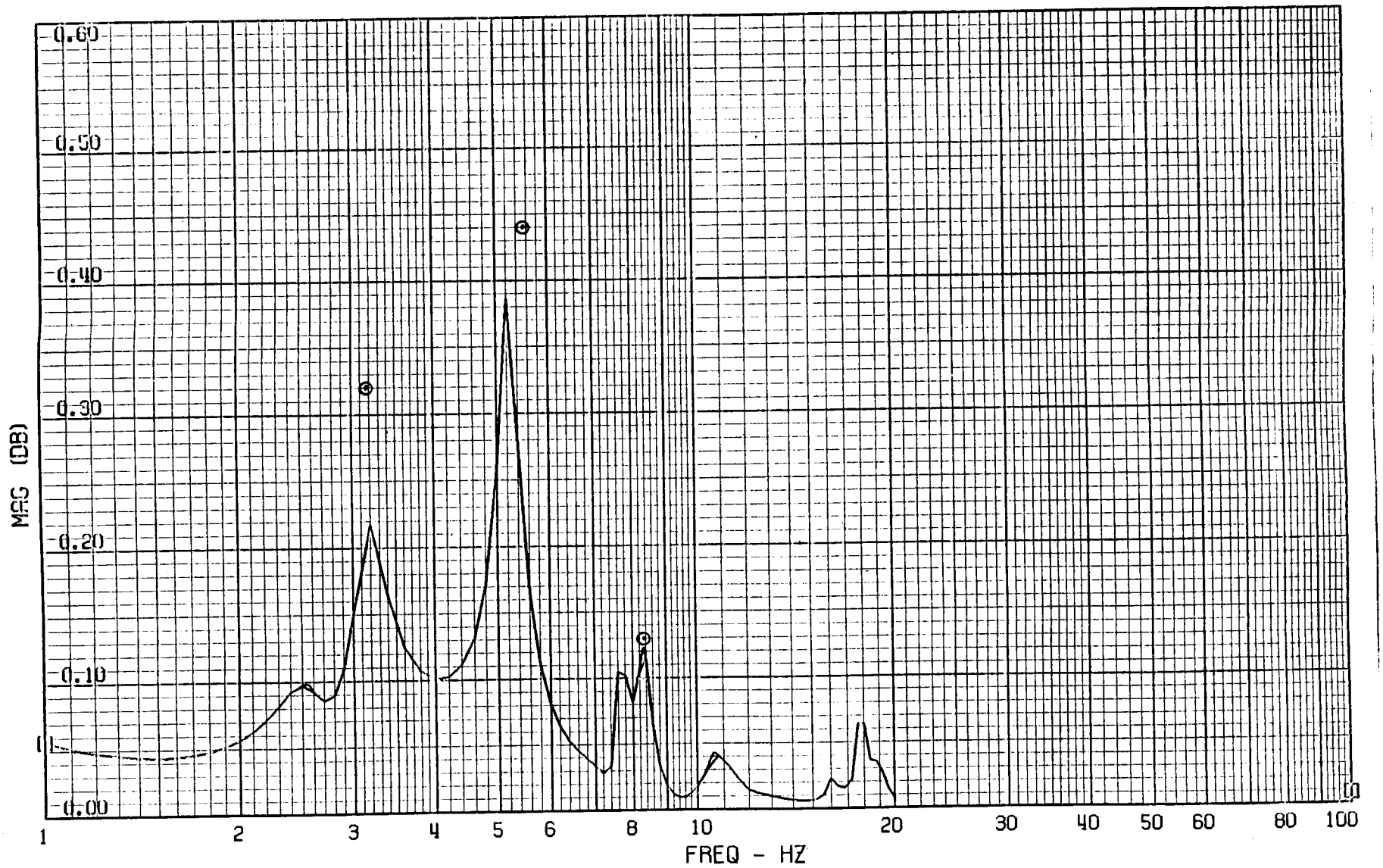

ORIGINAL PAGE IS
OF POOR QUALITY

FRAME 7
5/5/82

TEST POINT 139.4 - MACH=.95 - 400 KEAS - CASE 4
A-4033 - OUTER WING ACCEL

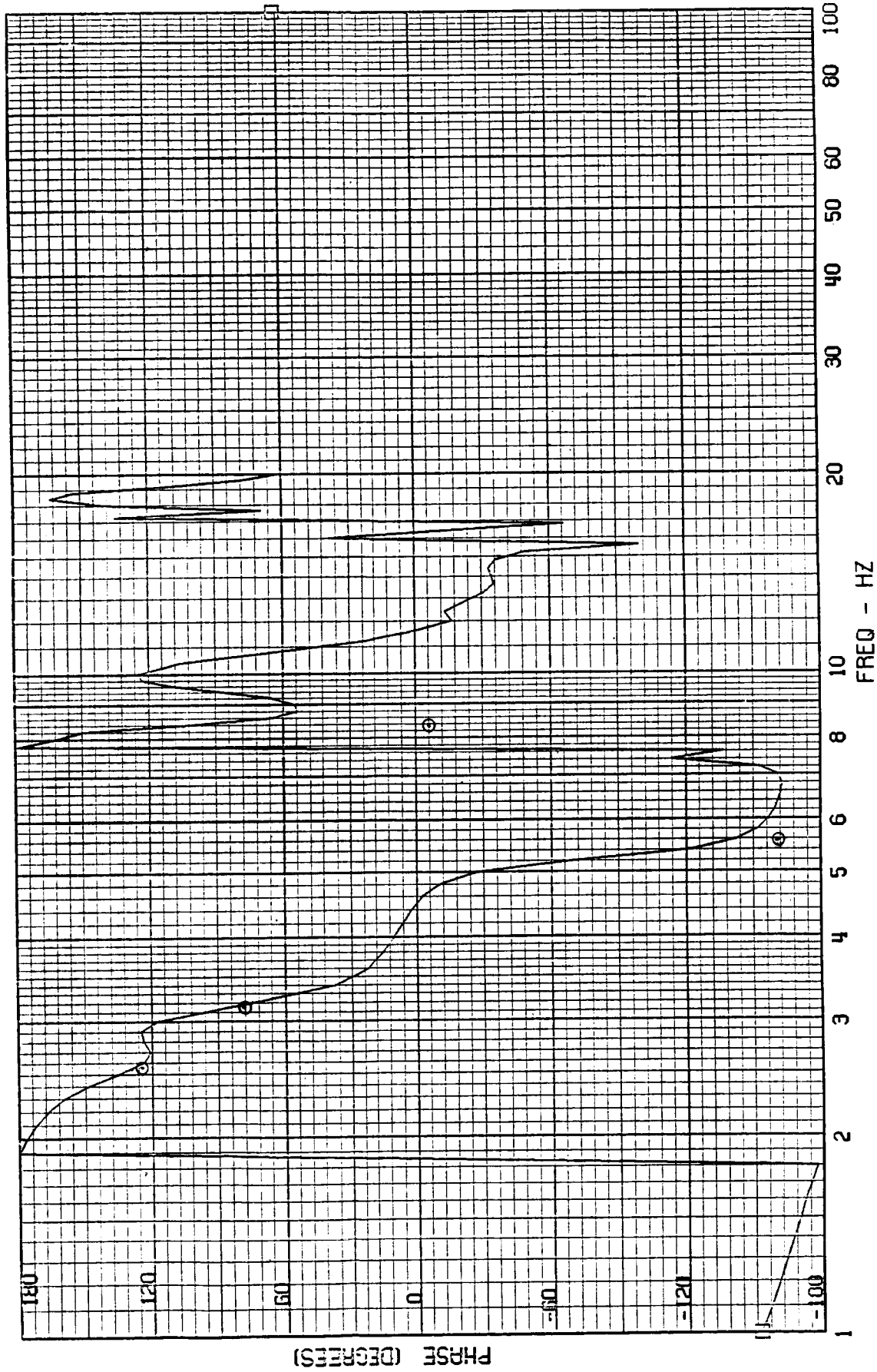

TEST POINT 139.4 - MACH=.95 - 400 KEAS - CASE 4
A-4034 - INNER WING ACCEL

FRAME 8
5 /5 /82

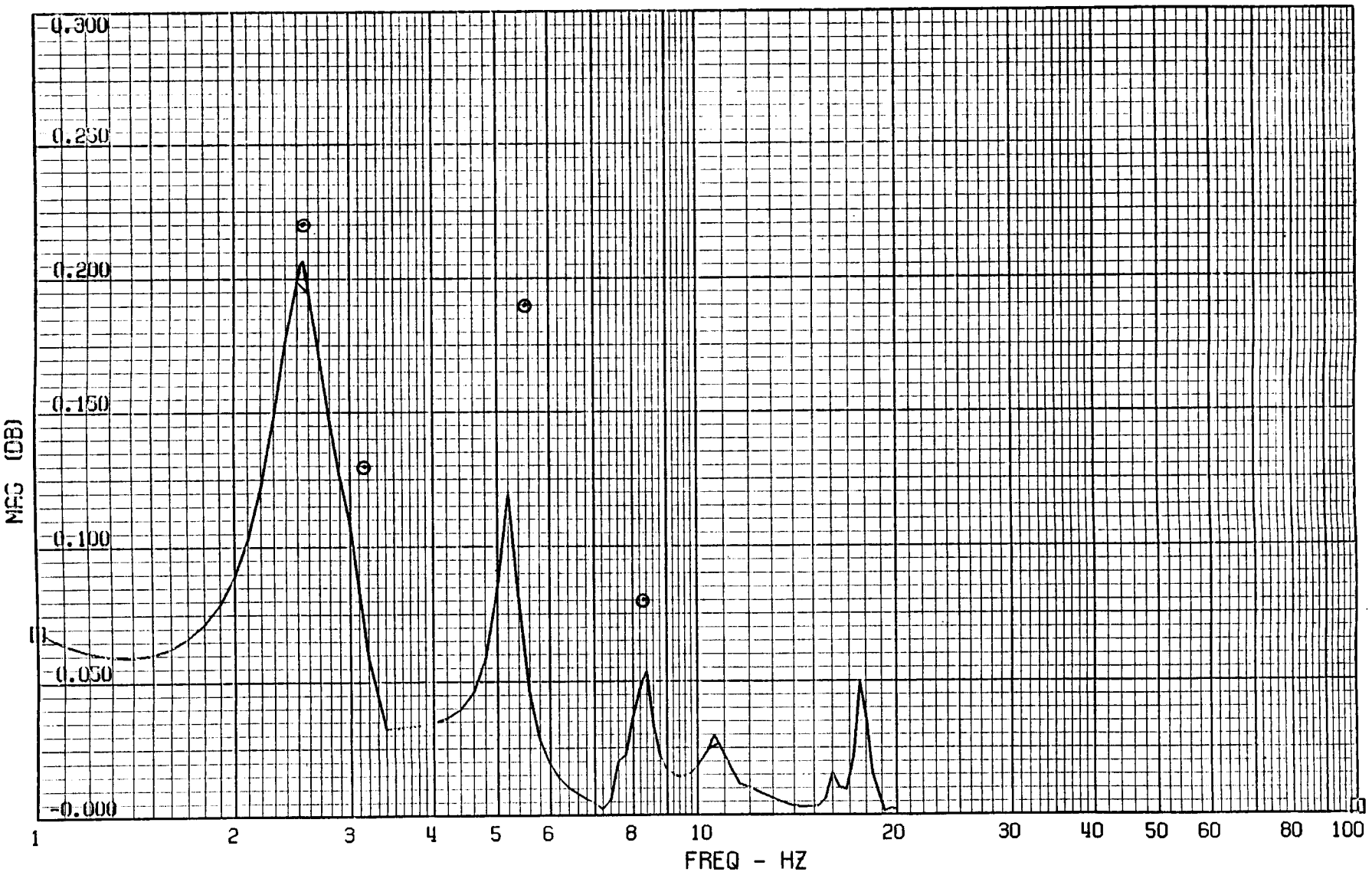

176

FRAME 8
5 /5 /82

TEST POINT 139.4 - MACH=.95 - 400 KEAS - CASE 4
A-4034 - INNER WING ACCEL

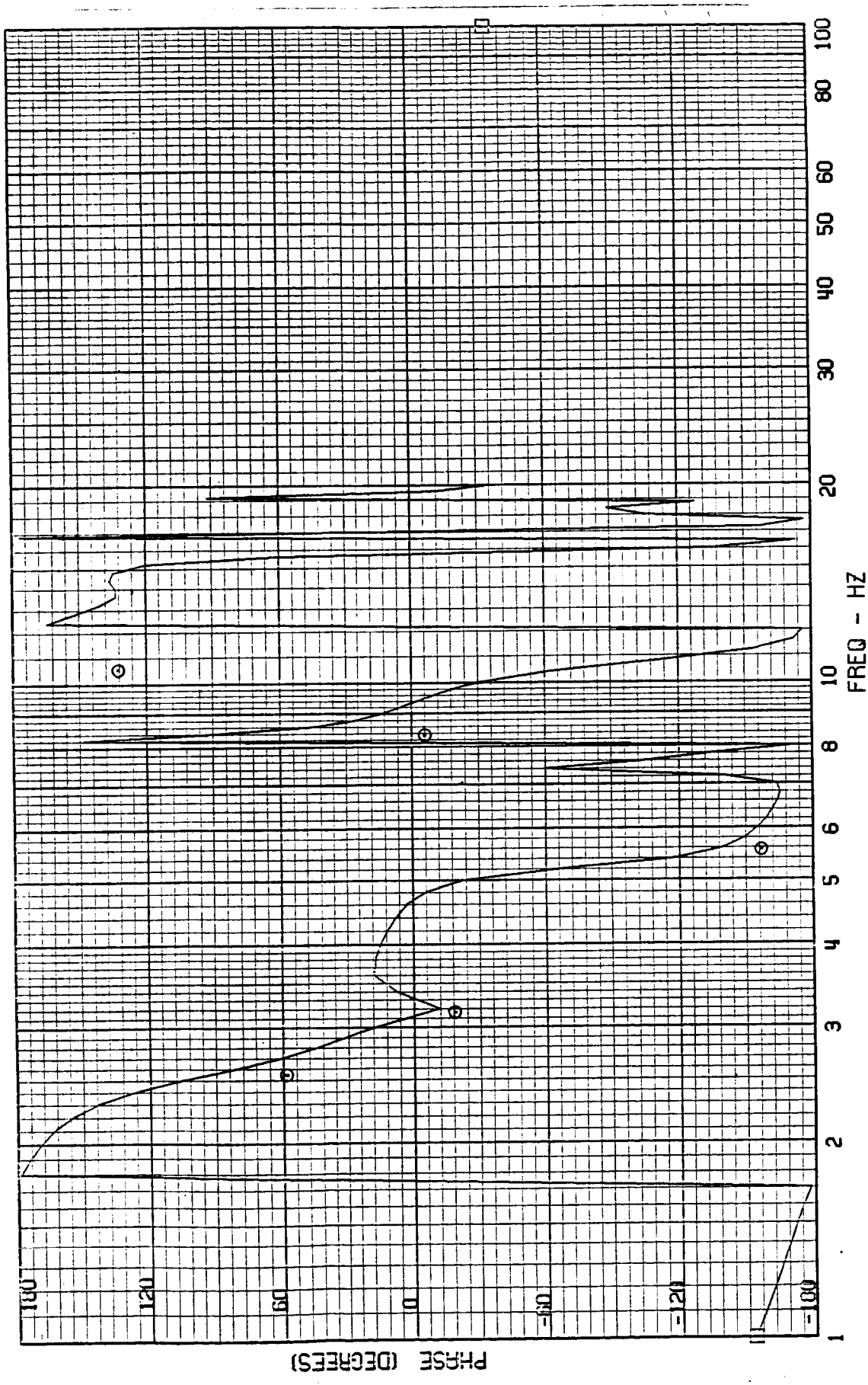

TEST POINT 139.4 - MACH=.95 - 400 KEAS - CASE 4
RWCLACC - NACELLE ACCEL ⊙

FRAME 9
5 /5 /82

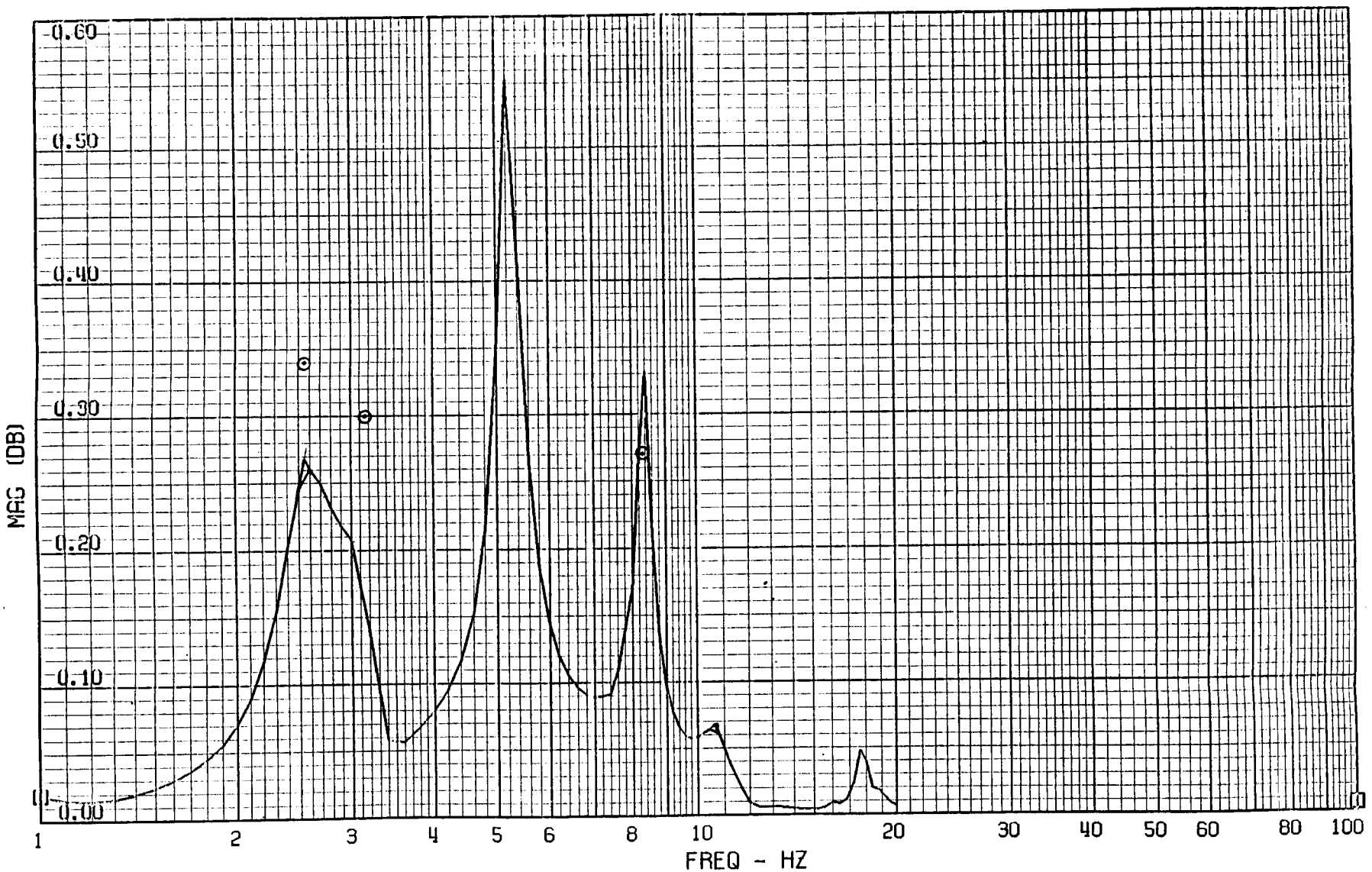

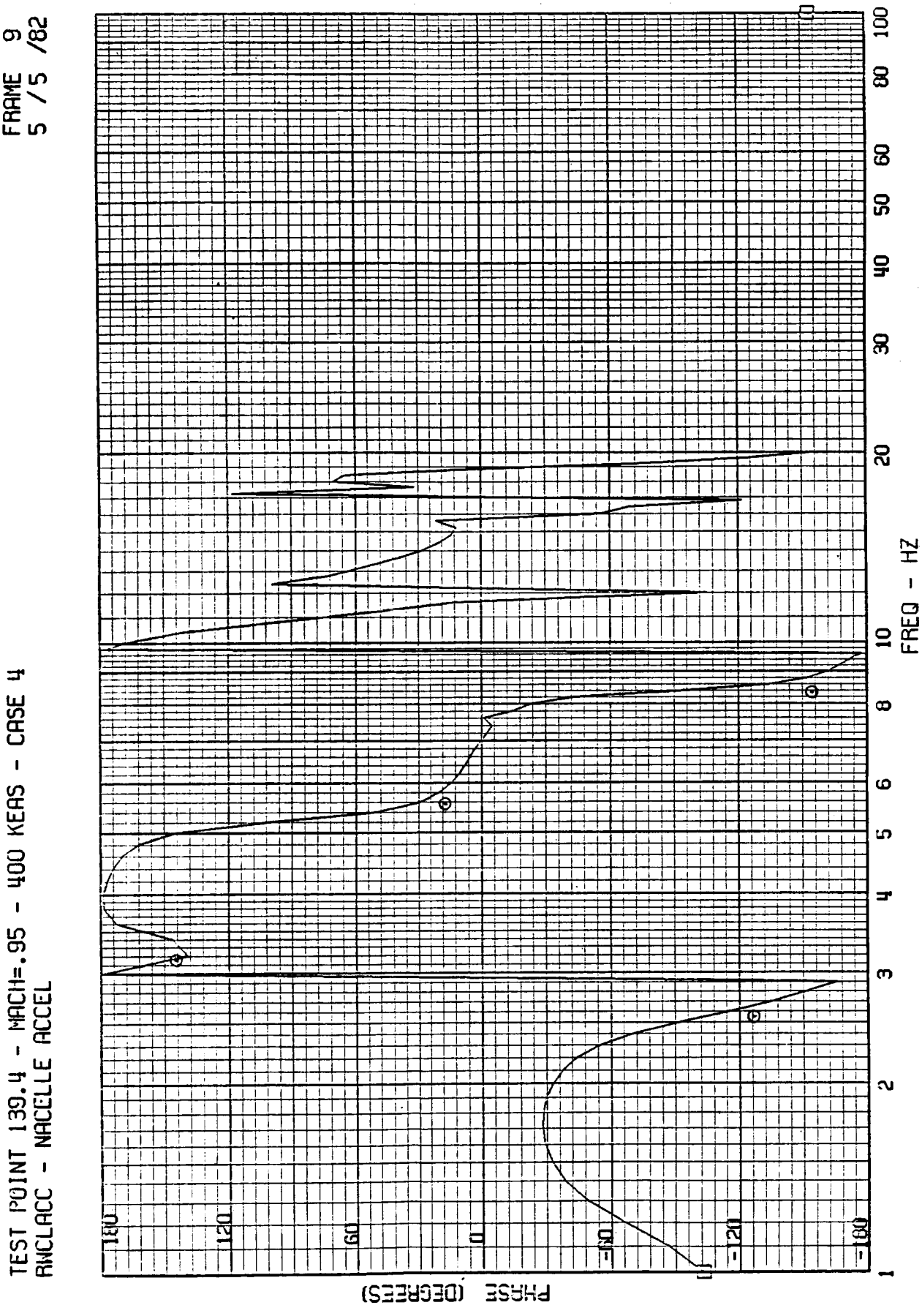

TEST POINT 139.4 - MACH=.95 - 400 KEAS - CASE 4
RRUDACC - RUDDER ACCEL

FRAME 10
5 /5 /82

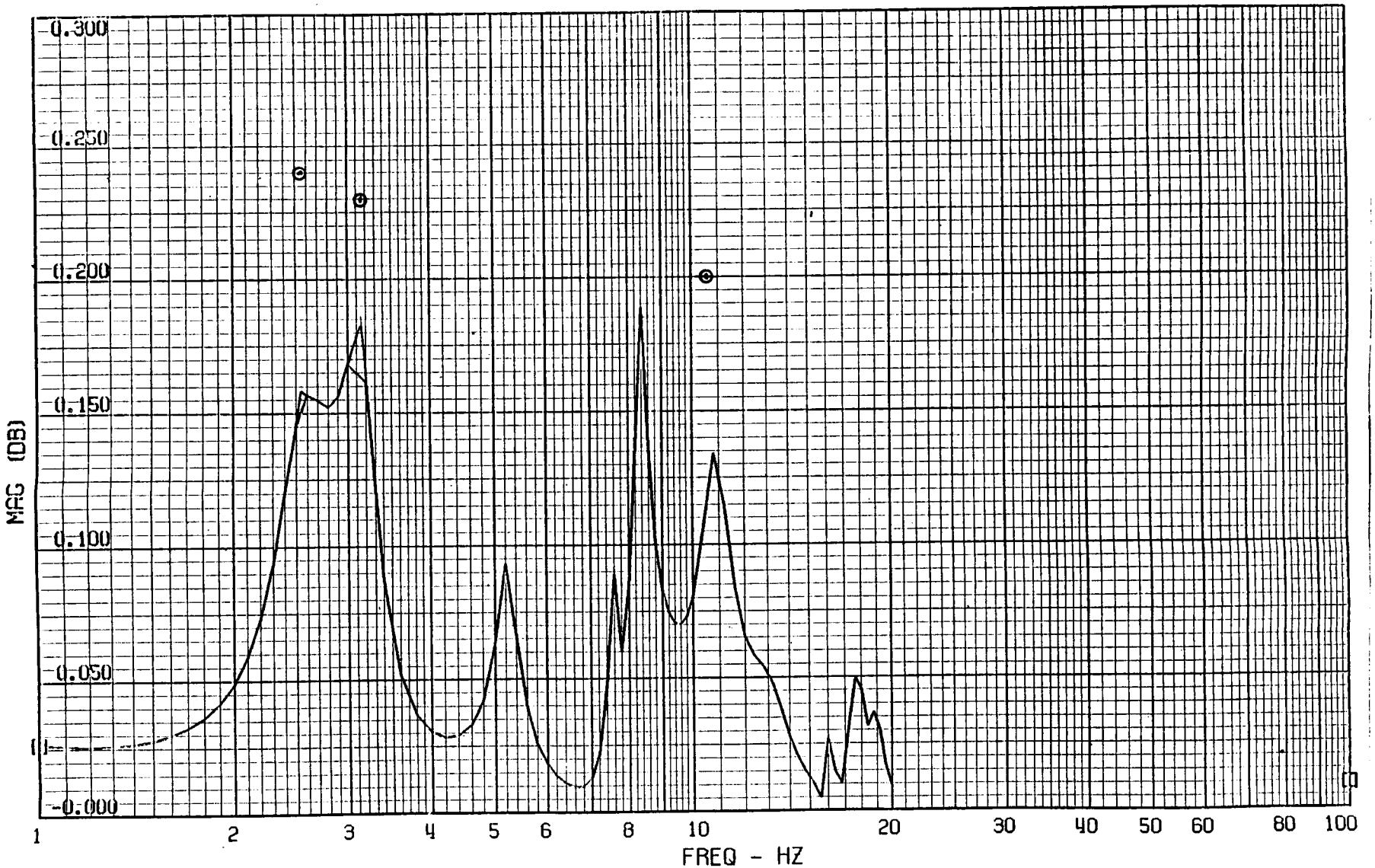

FRAME 10
5 /5 /82

TEST POINT 139.4 - MACH=.95 - 400 KEAS - CASE 4
RRUDACC - RUDDER ACCEL

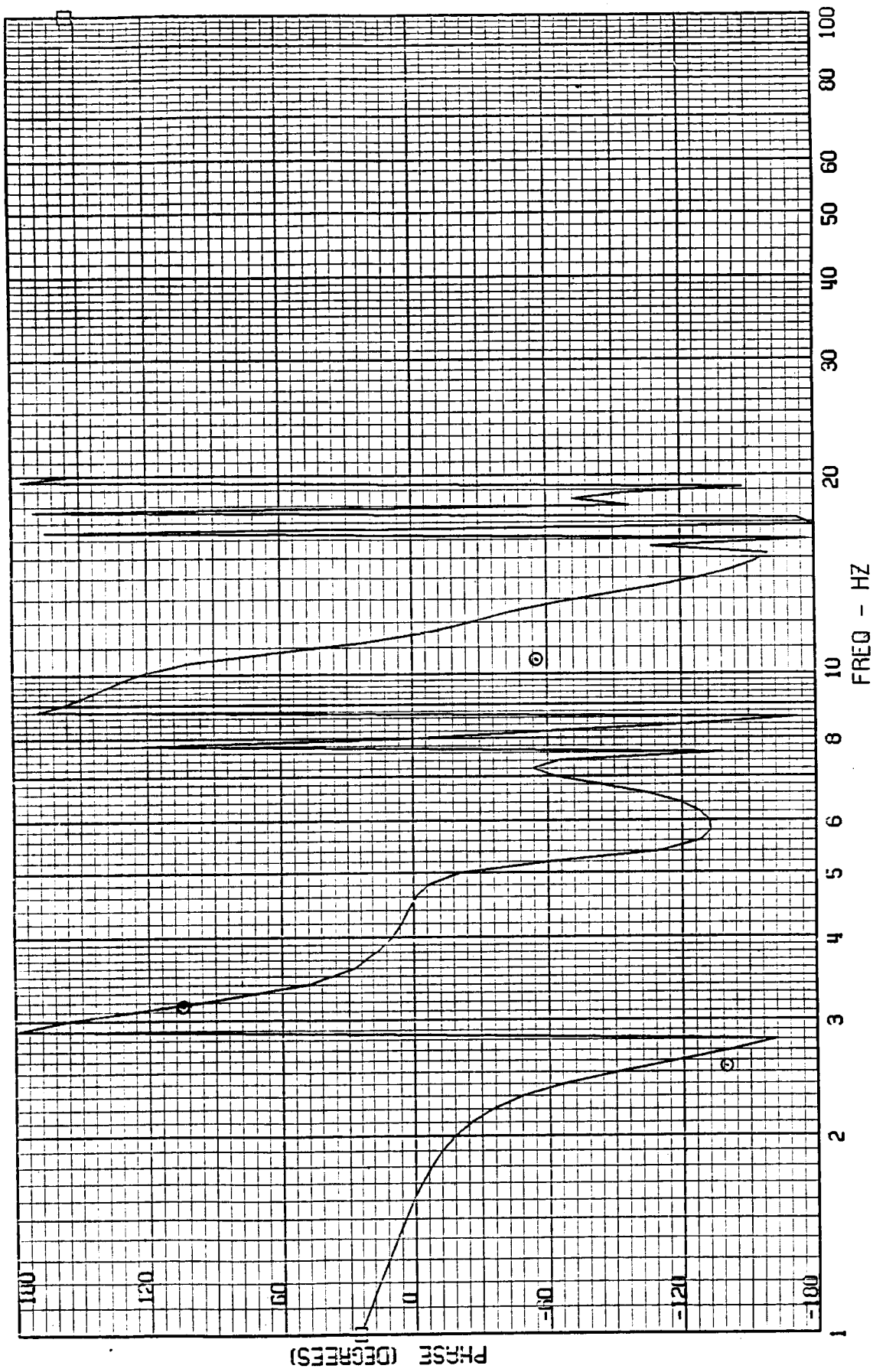

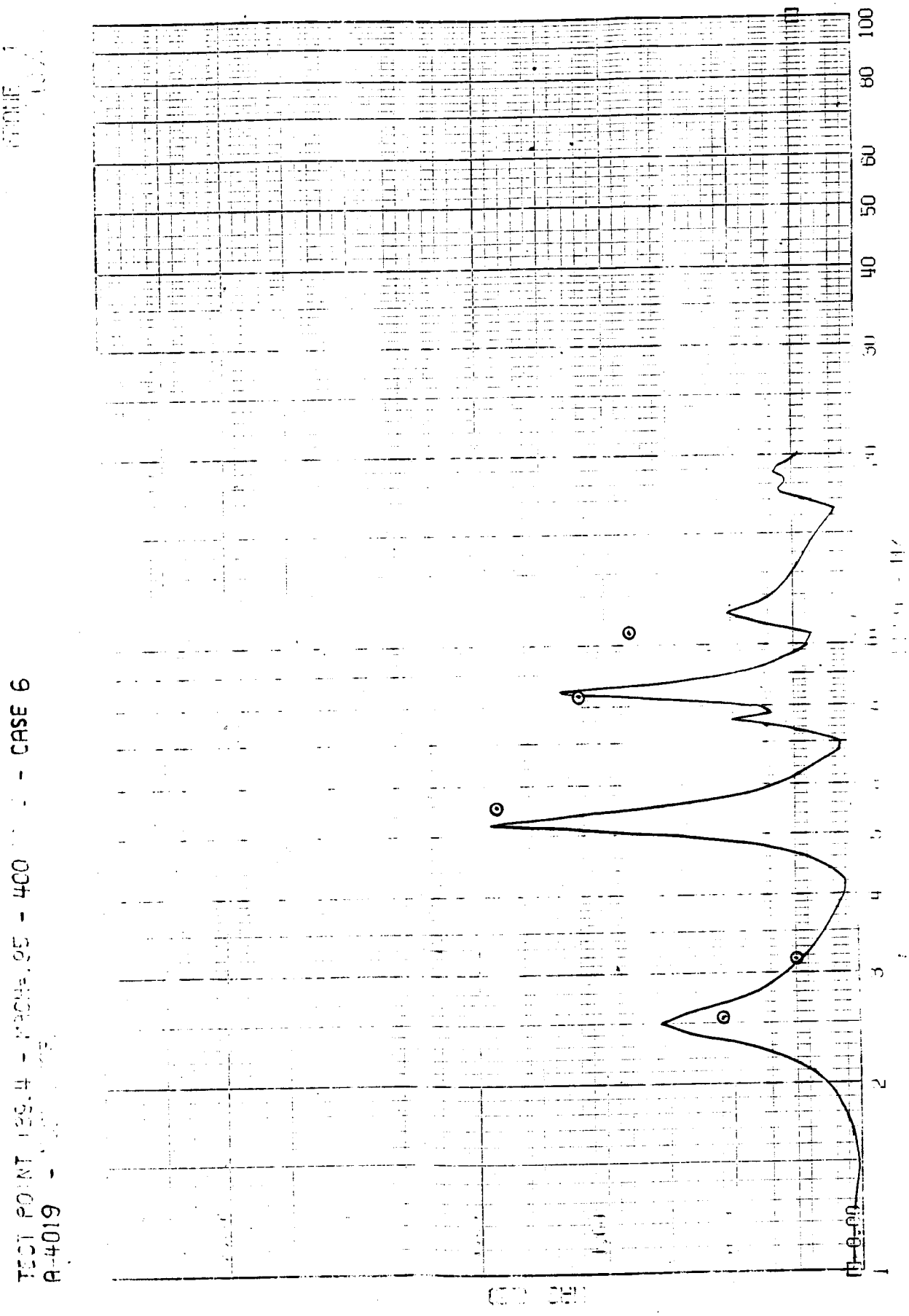

FRAME 1
5 / 13 /82

TEST POINT 139.4 - MACH=.95 - UNO KEAS - CASE 6
A-1019 - NOSE ACCEL

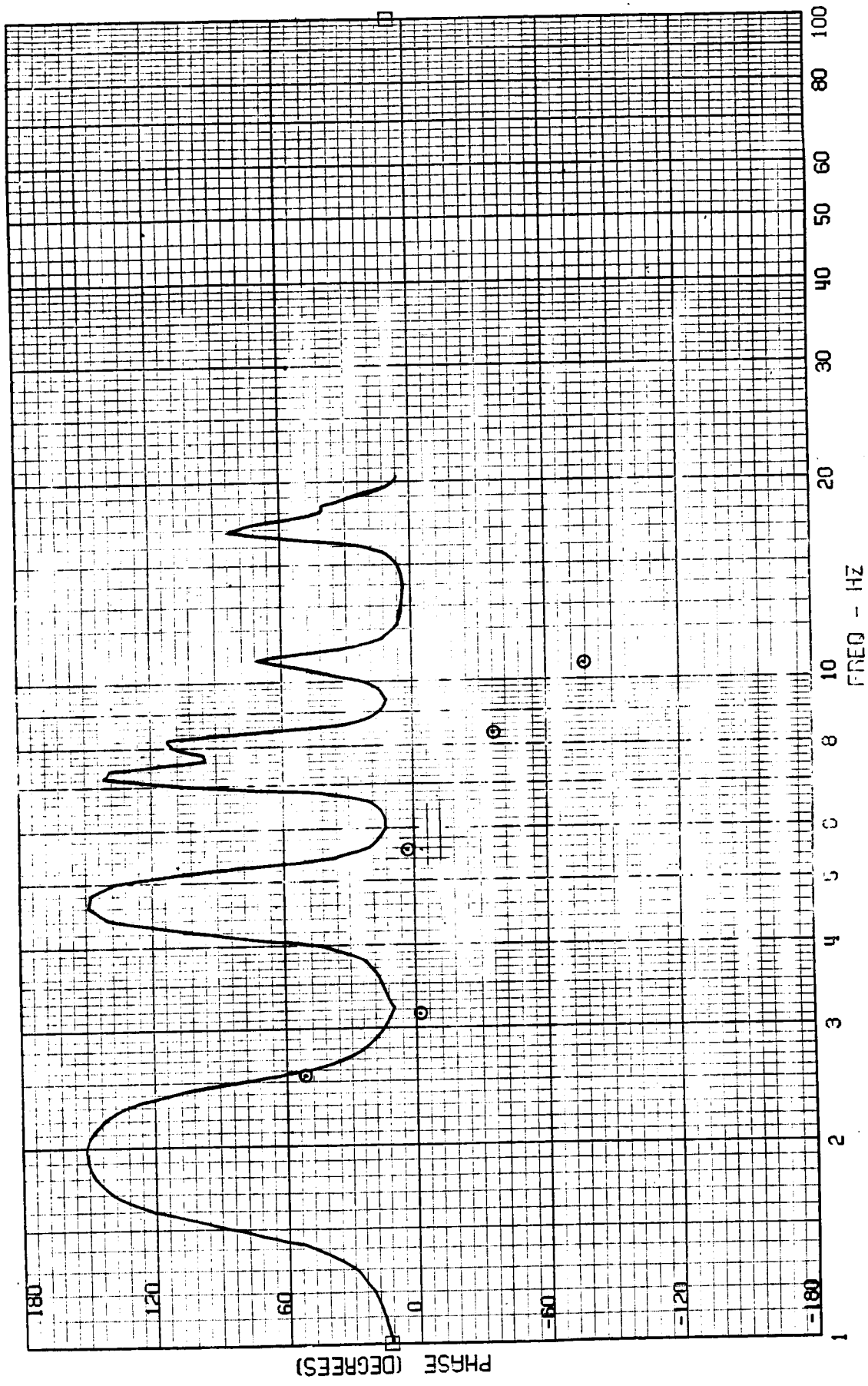

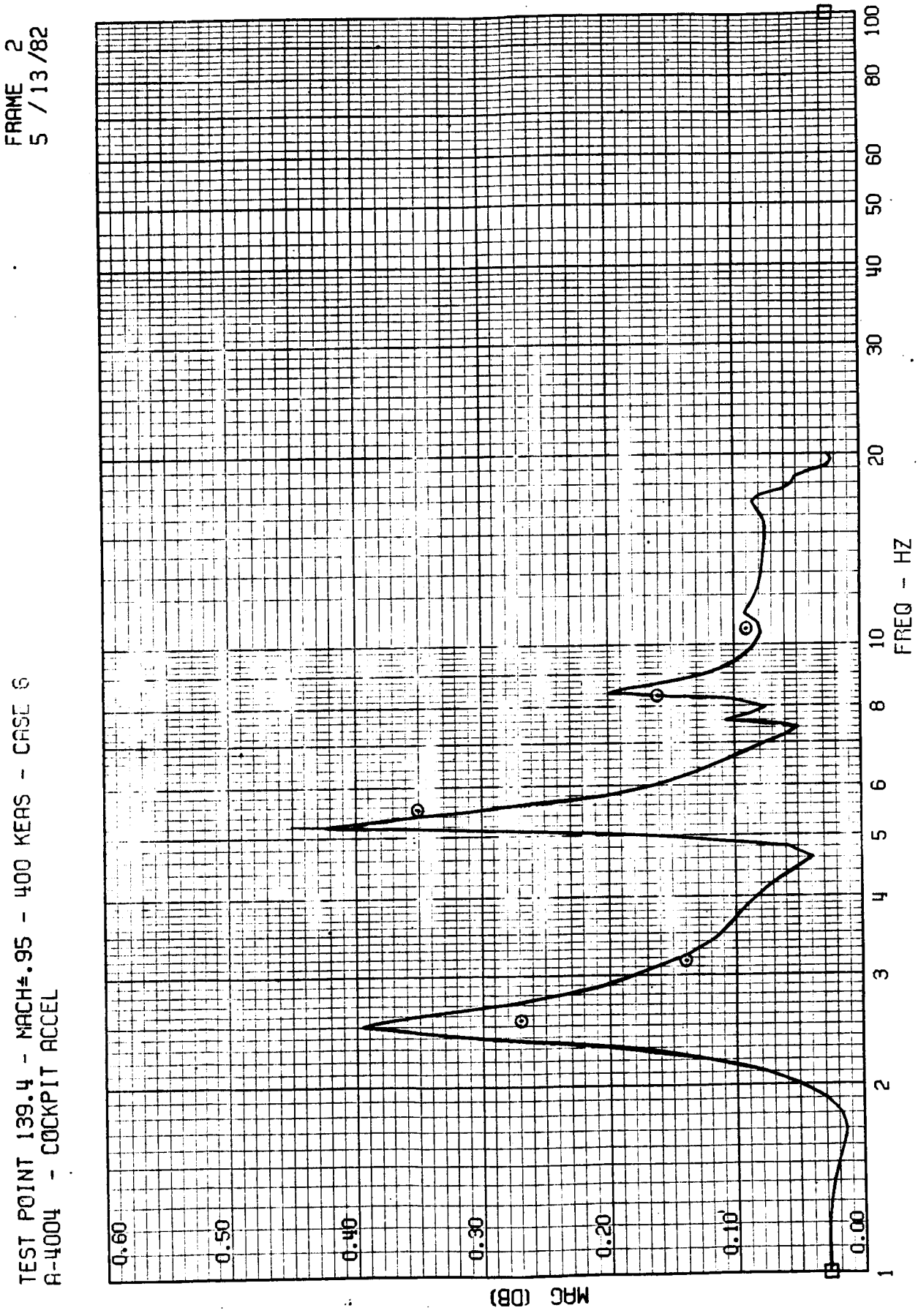

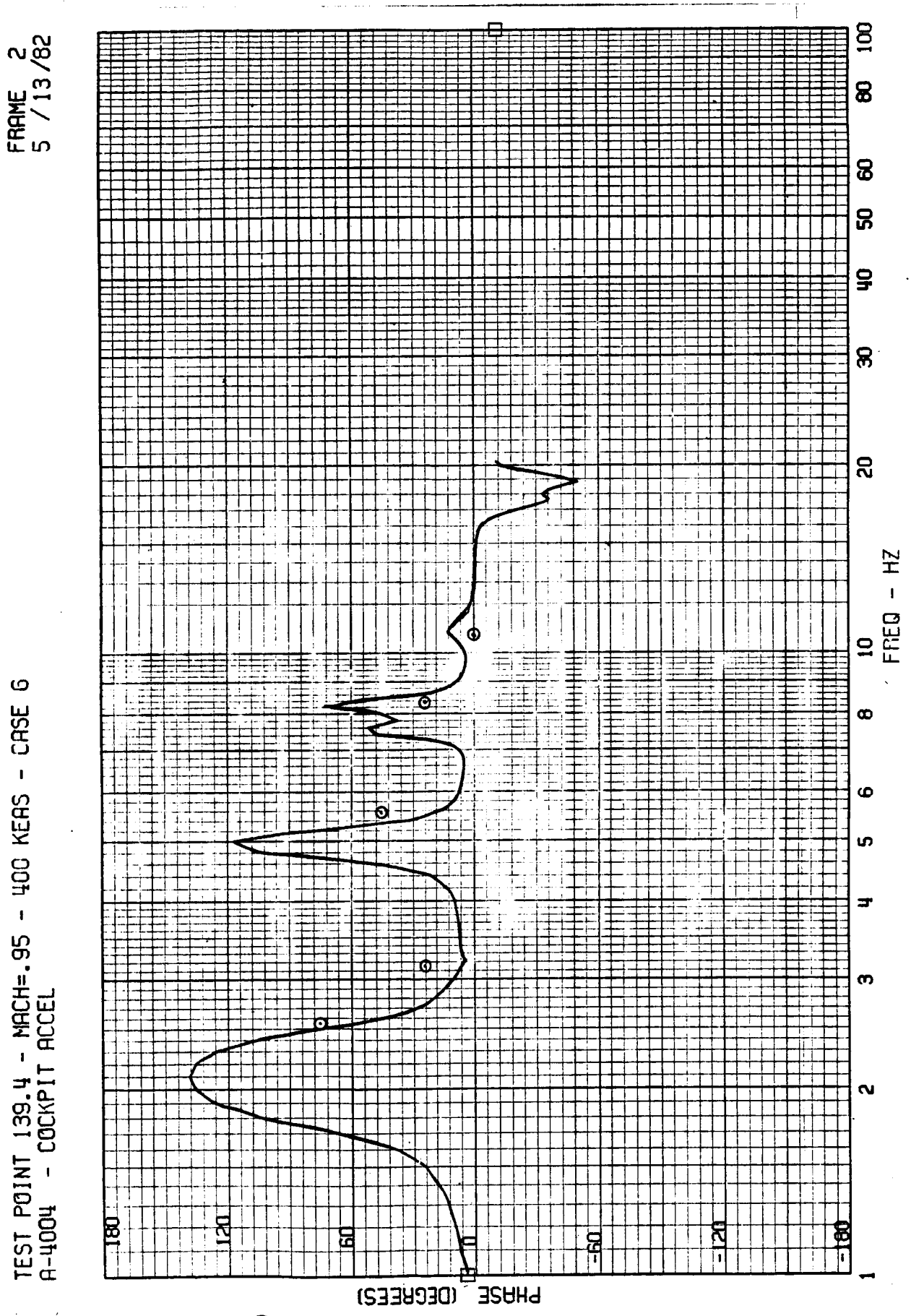

C-3

TEST POINT 139.4 - MACH=.95 - 400 KEAS - CASE 6
A-4028 - FORWARD MISSION BAY ACCEL

FRAME 3
5 /13 /82

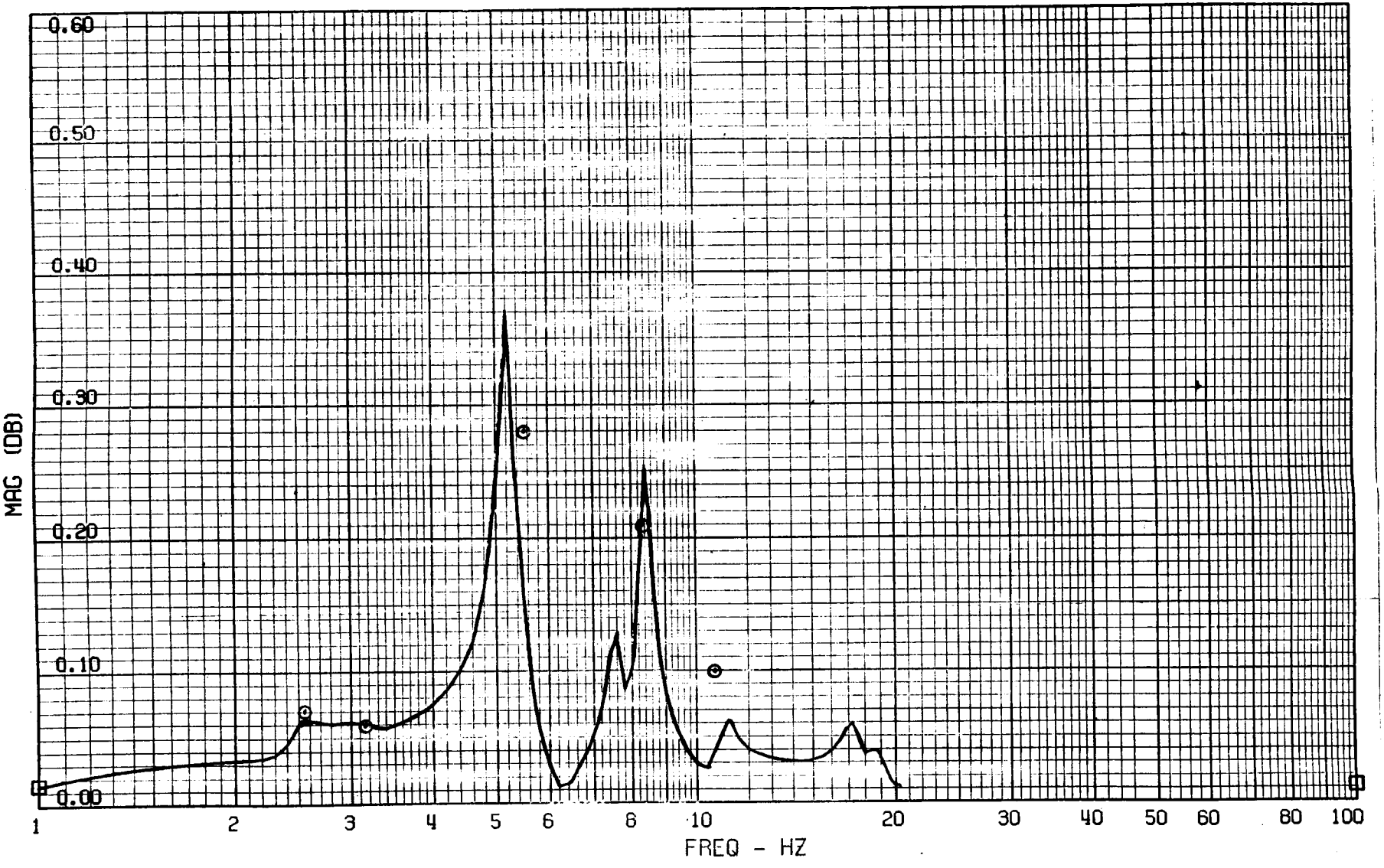

FRAME 3
5 /13 /82

TEST POINT 139.4 - MACH=.95 - 400 KEAS - CASE 6
A-4028 - FORWARD MISSION BAY ACCEL

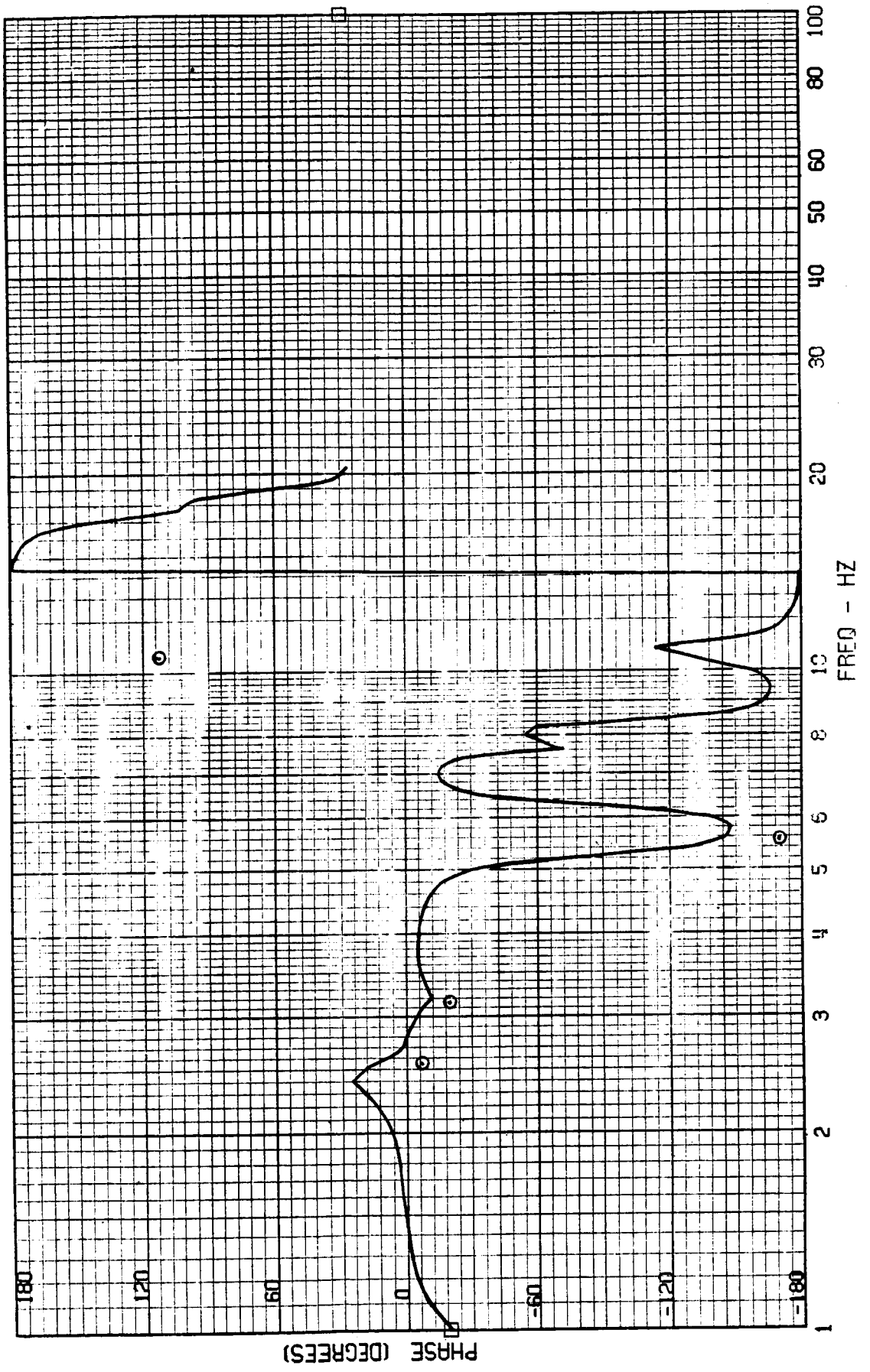

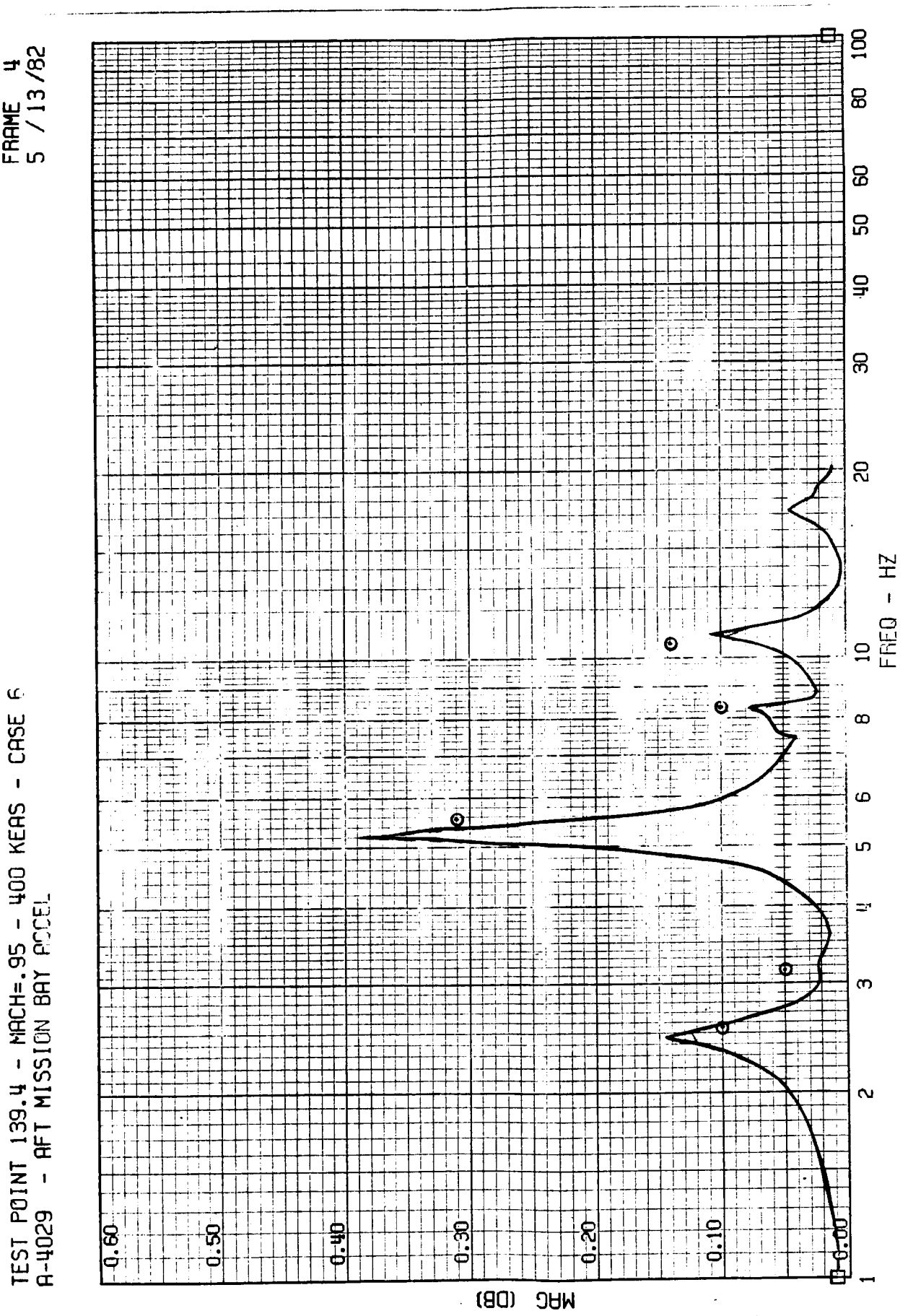
TEST POINT 139.4 - MACH=.95 - 400 KEAS - CASE 6
A-4029 - AFT MISSION BAY ACCEL
FRAME 4
5 / 13 /82
MAG (DB)
0.60
0.50
0.40
0.30
0.20
0.10
0.00
1
2
3
4
5
6
8
10
20
30
40
50
60
80
100
FREQ - HZ

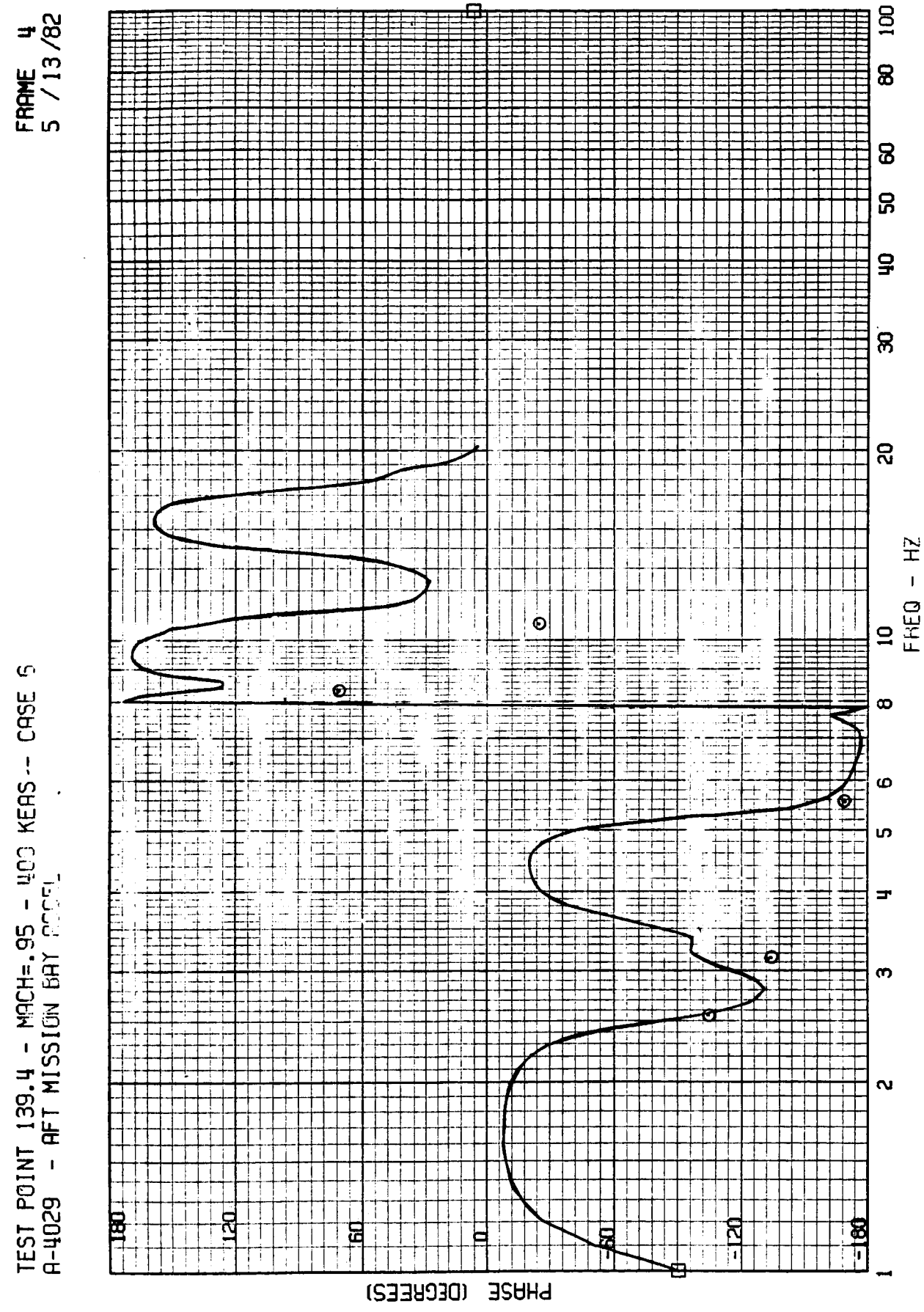

TEST POINT 139.4 - MACH=.95 - 400 KEAS - CASE 6
A-4001 - CG ACCEL

FRAME 5
5 /13 /82

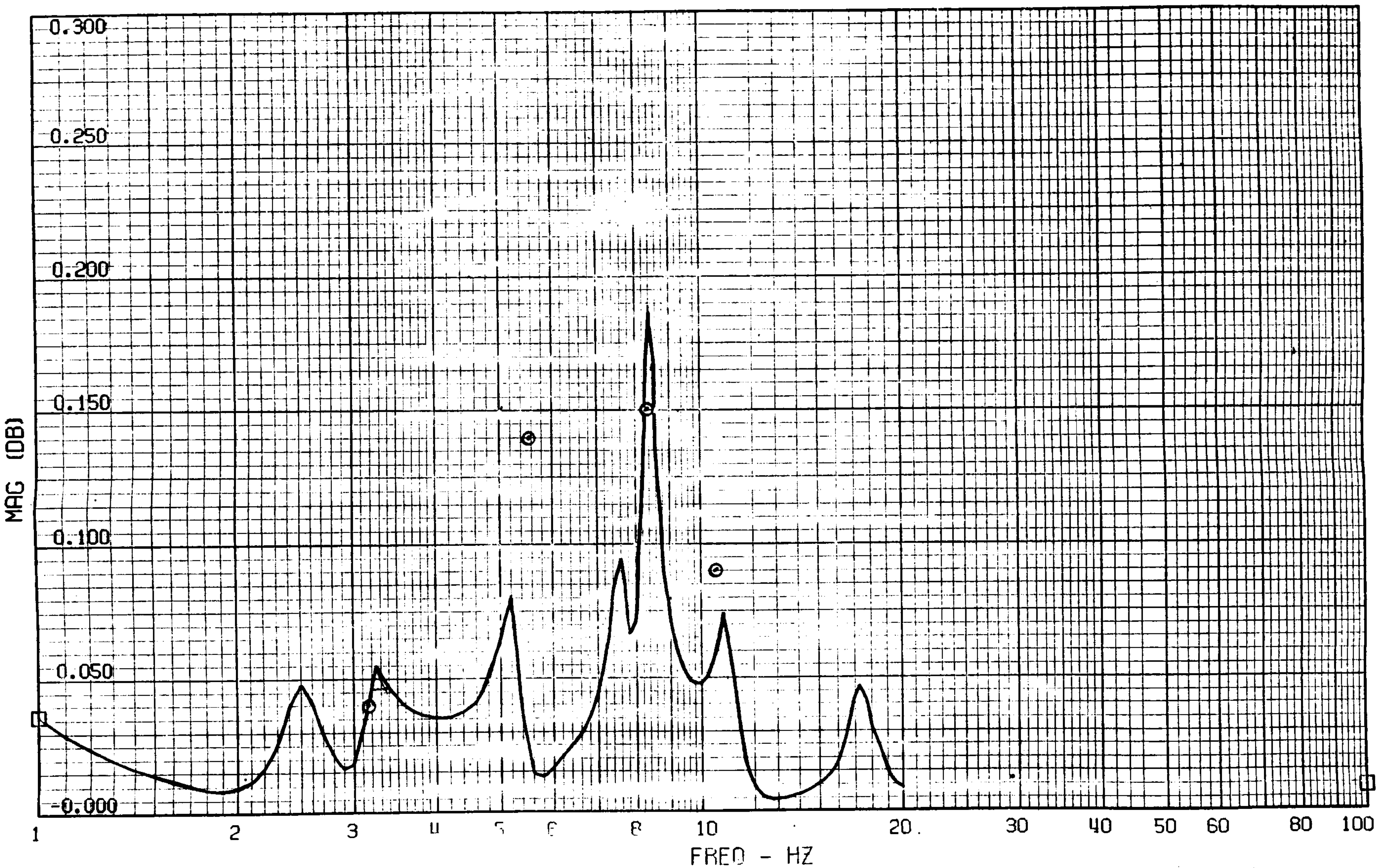

FRAME 5
5/13/82

TEST POINT 139.4 - MACH=.95 - 400 KEAS - CASE 6
A-4001 - CG ACCEL

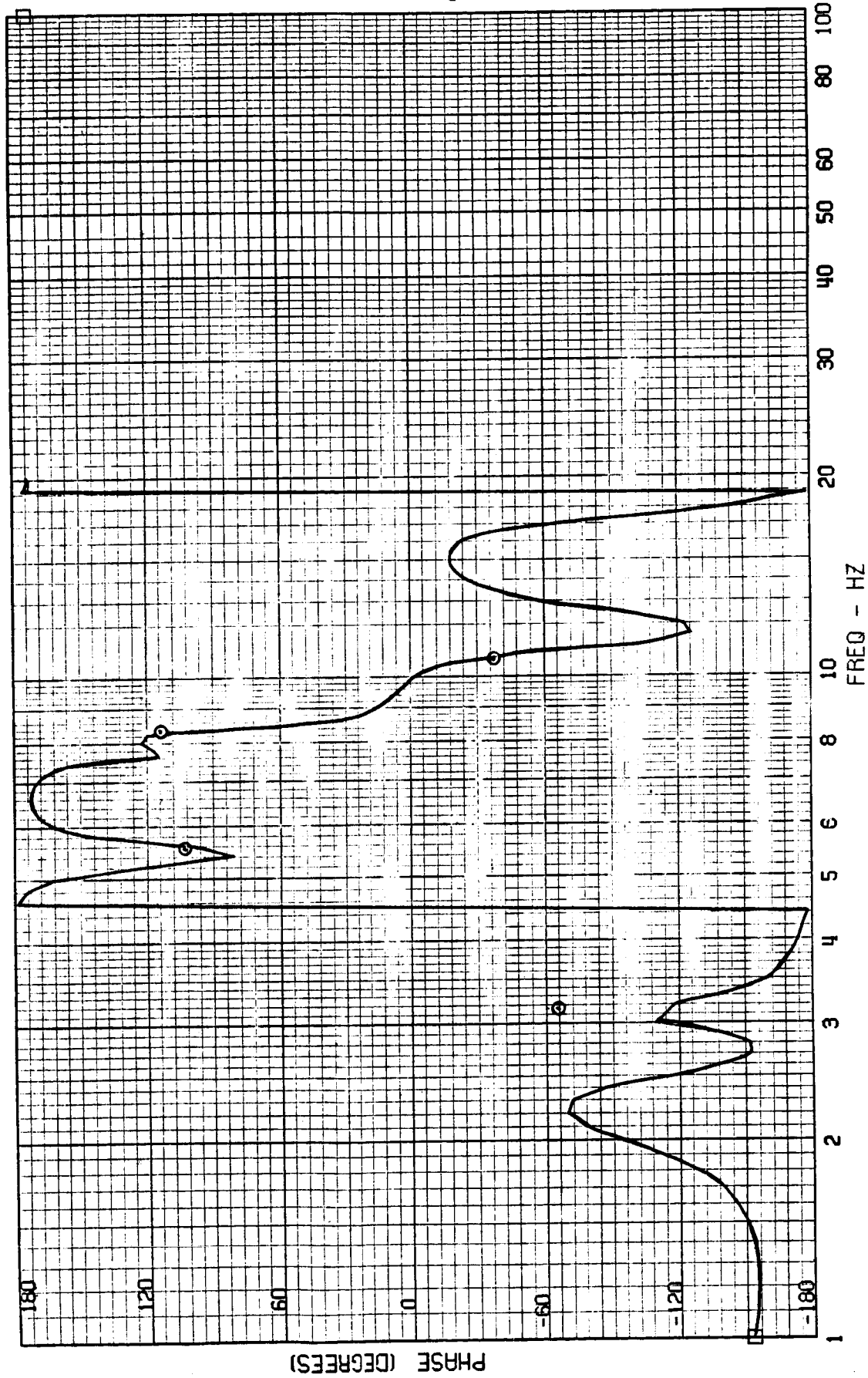

TEST POINT 139.4 - MACH=.95 - 400 KEAS - CASE 6
A-4030 - TAIL CONE ACCEL

FRAME 6
5 /13/82

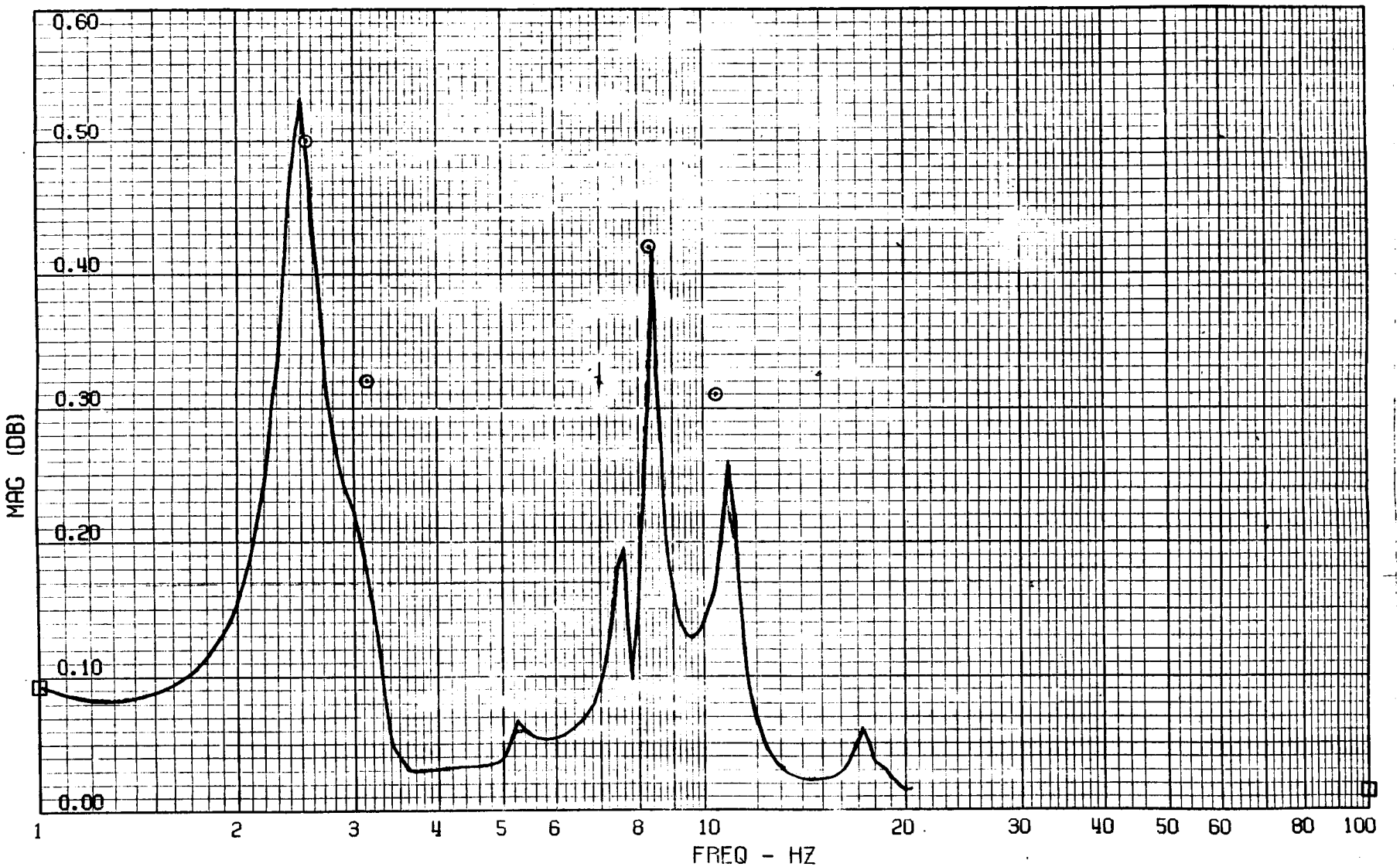

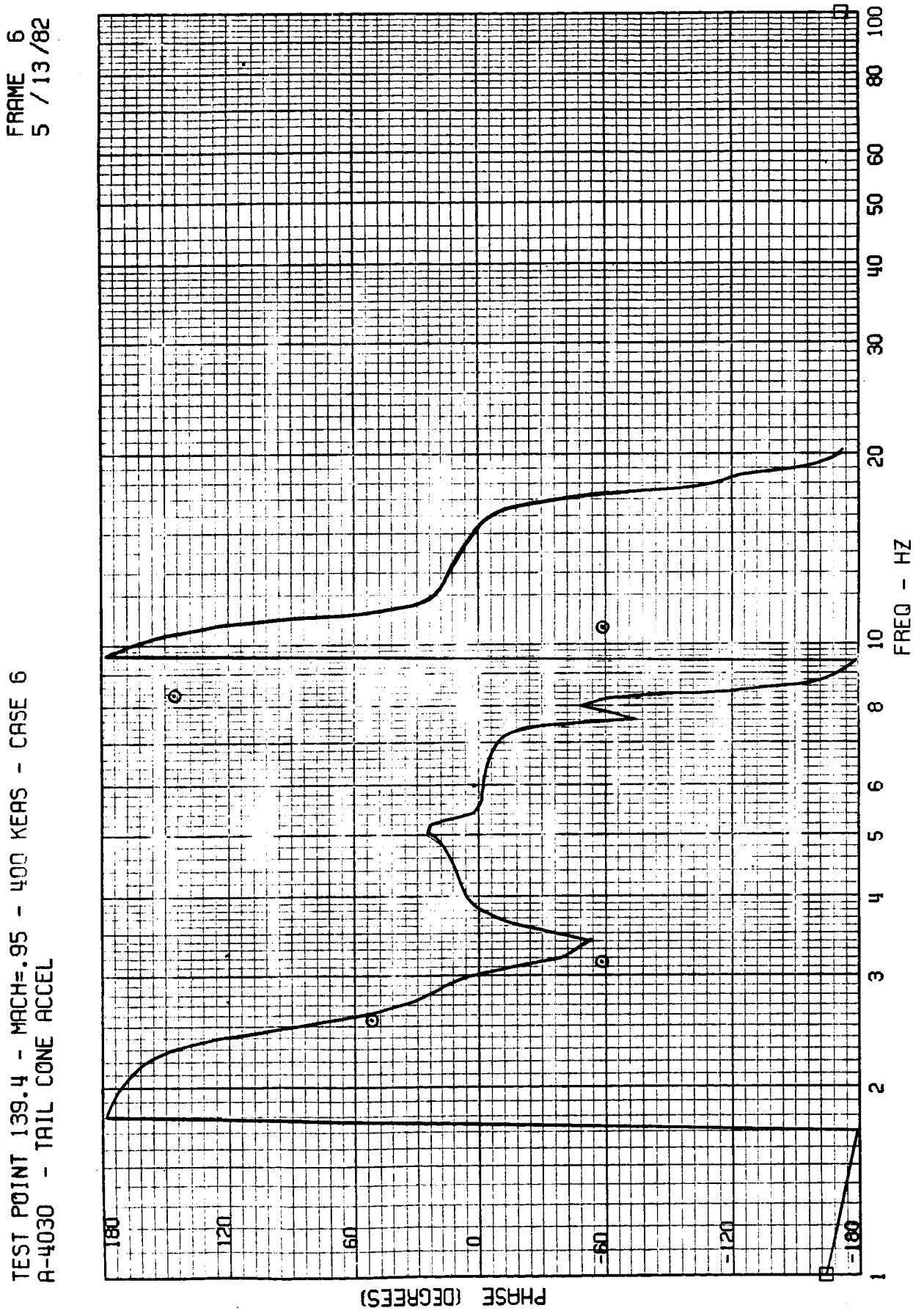
FRAME 6
5 / 13 /82
TEST POINT 139.4 - MACH=.95 - 400 KEAS - CASE 6
A-4030 - TAIL CONE ACCEL
PHASE (DEGREES)
180
120
60
0
-60
-120
-180
FREQ - HZ
1
2
3
4
5
6
8
10
20
30
40
50
60
80
100

TEST POINT 139.4 - MACH=.95 - 400 KEAS - CASE 6
A-4033 - OUTER WING ACCEL

FRAME 7
5 / 13 /82

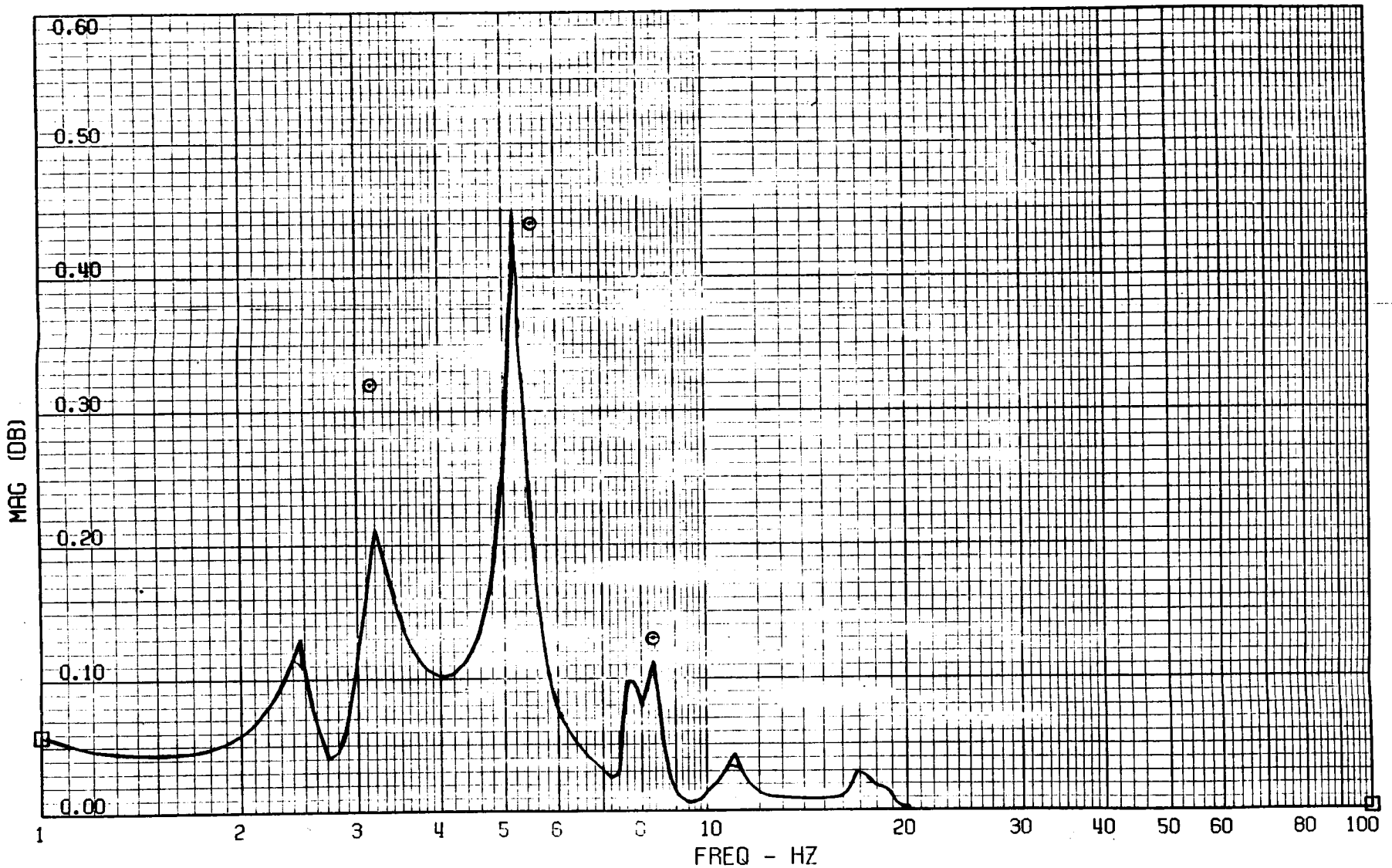

FRAME 7
5 /13 /82

TEST POINT 139.4 - MACH=.95 - 400 KEAS - CASE 6
A-4033 - OUTER WING ACCEL

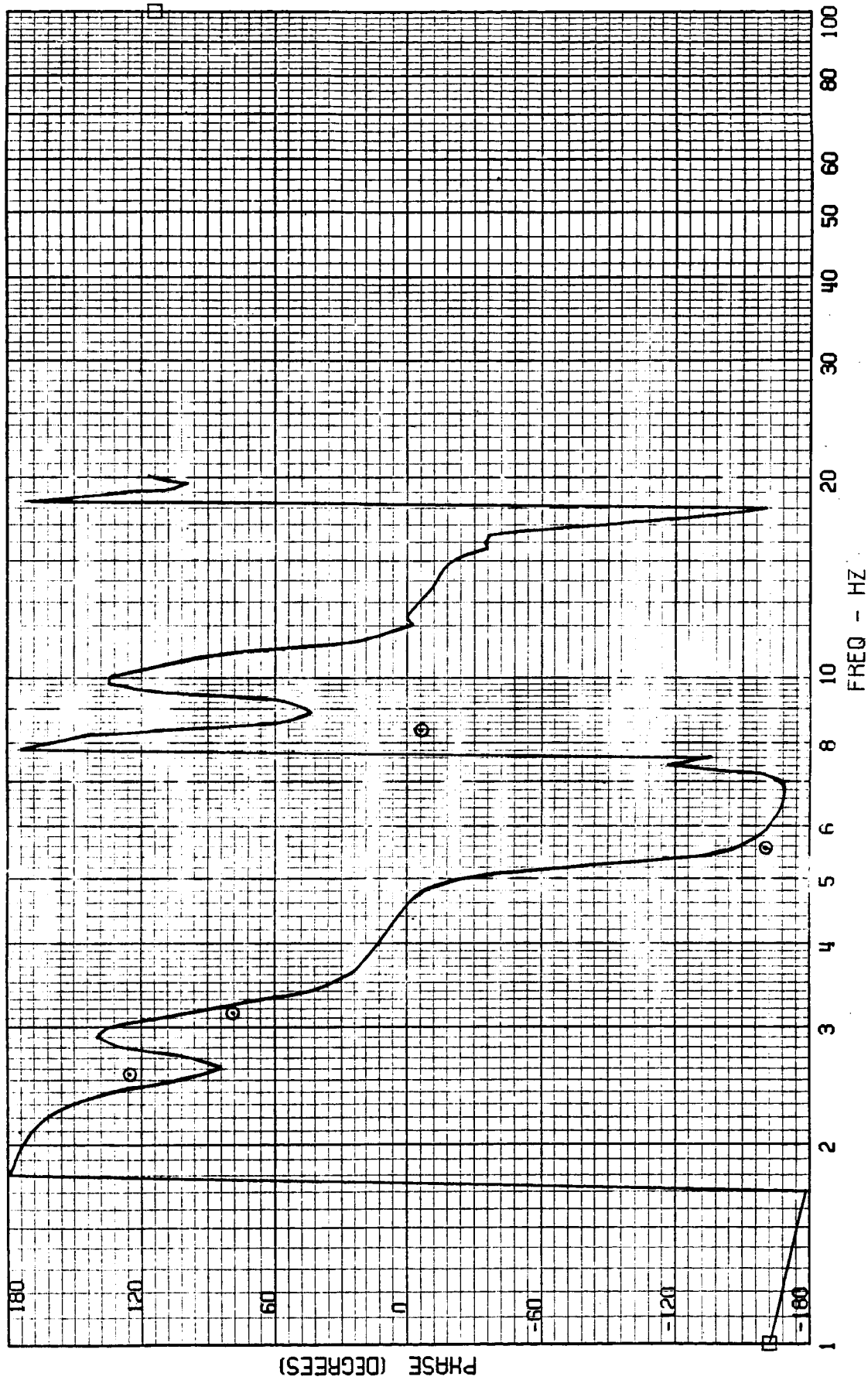

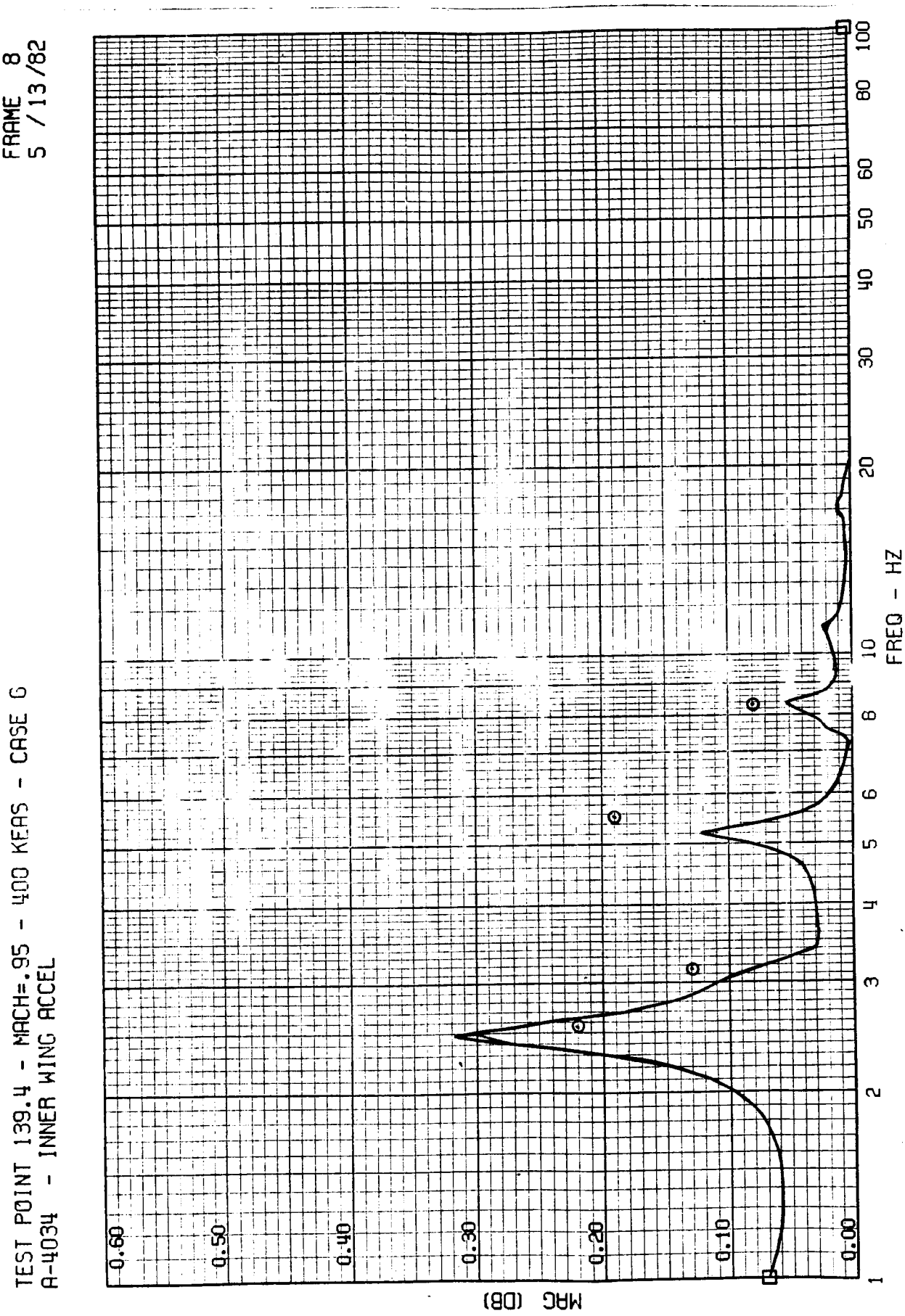
FRAME 8
5 /13 /82
TEST POINT 139.4 - MACH=.95 - 400 KEAS - CASE G
A-4034 - INNER WING ACCEL
MAG (DB)
0.60
0.50
0.40
0.30
0.20
0.10
0.00
FREQ - HZ
1
2
3
4
5
6
8
10
20
30
40
50
60
80
100

FRAME 8
5 /13/82

TEST POINT 139.4 - MACH=.95 - [illegible] KEAS - CASE 6
A-4034 - INNER WING ACCEL

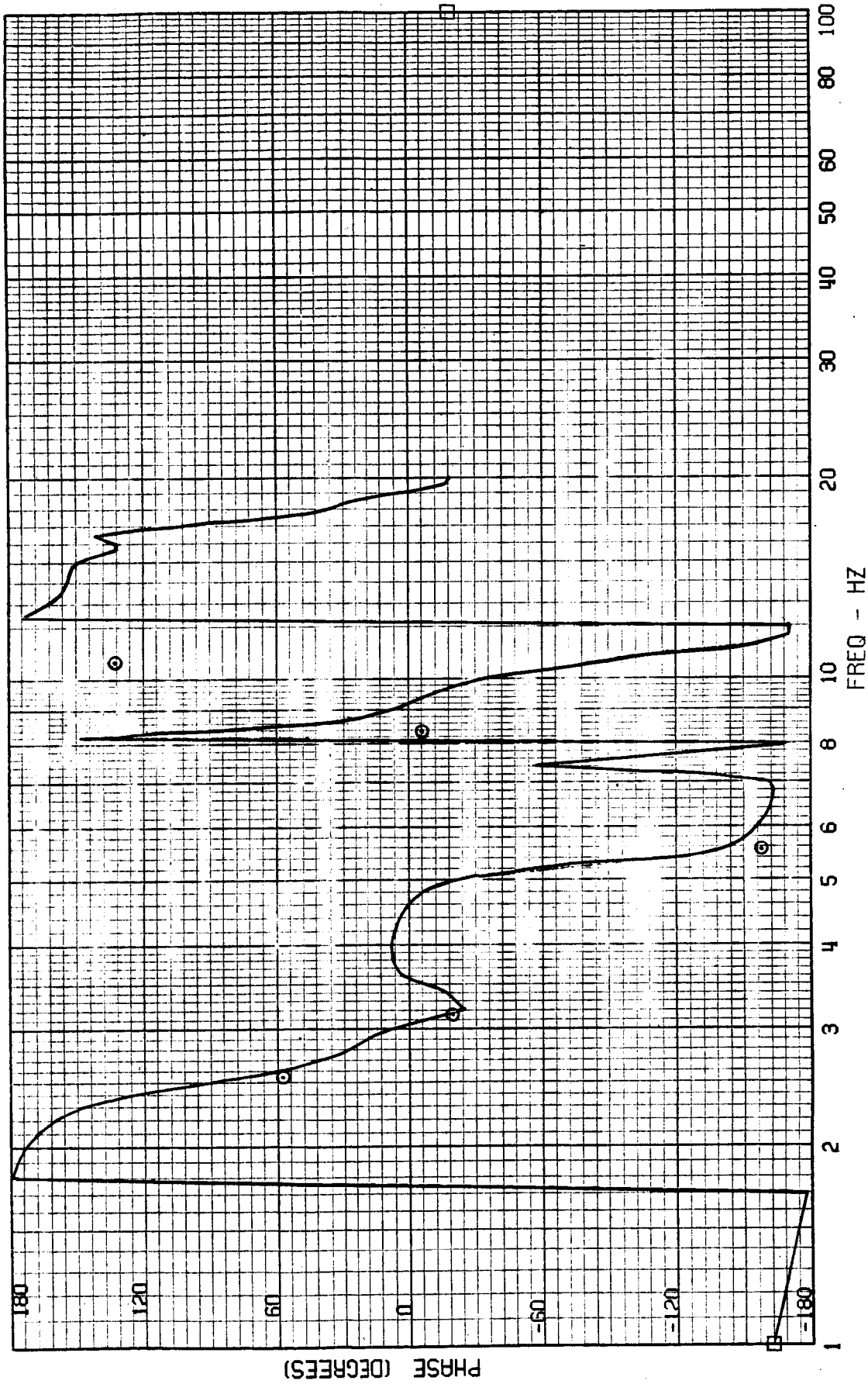

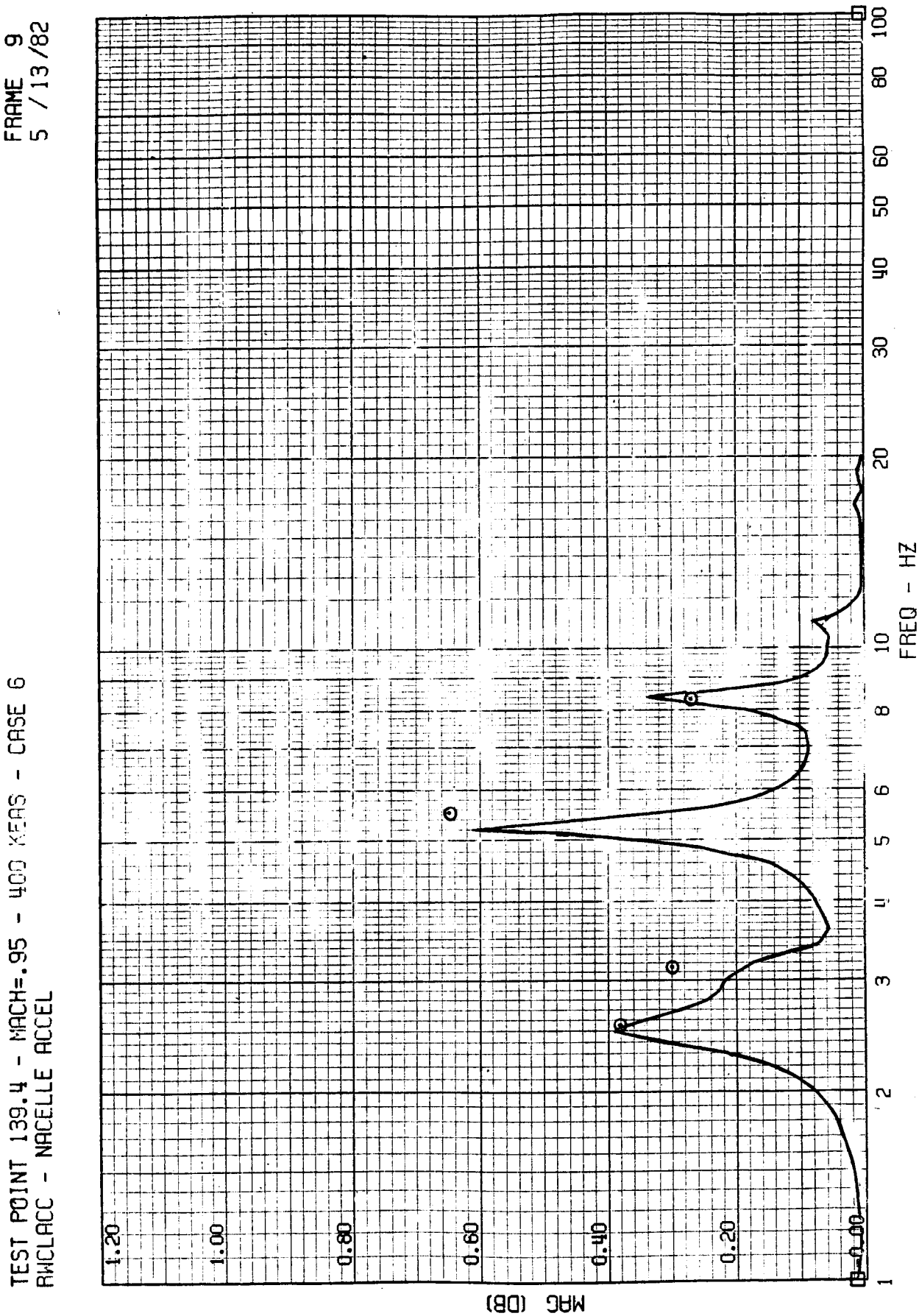
TEST POINT 139.4 - MACH=.95 - 400 KEAS - CASE 6
RWCLACC - NACELLE ACCEL
FRAME 9
5 /13 /82
MAG (DB)
1.20
1.00
0.80
0.60
0.40
0.20
0.00
1
2
3
4
5
6
8
10
20
30
40
50
60
80
100
FREQ - HZ

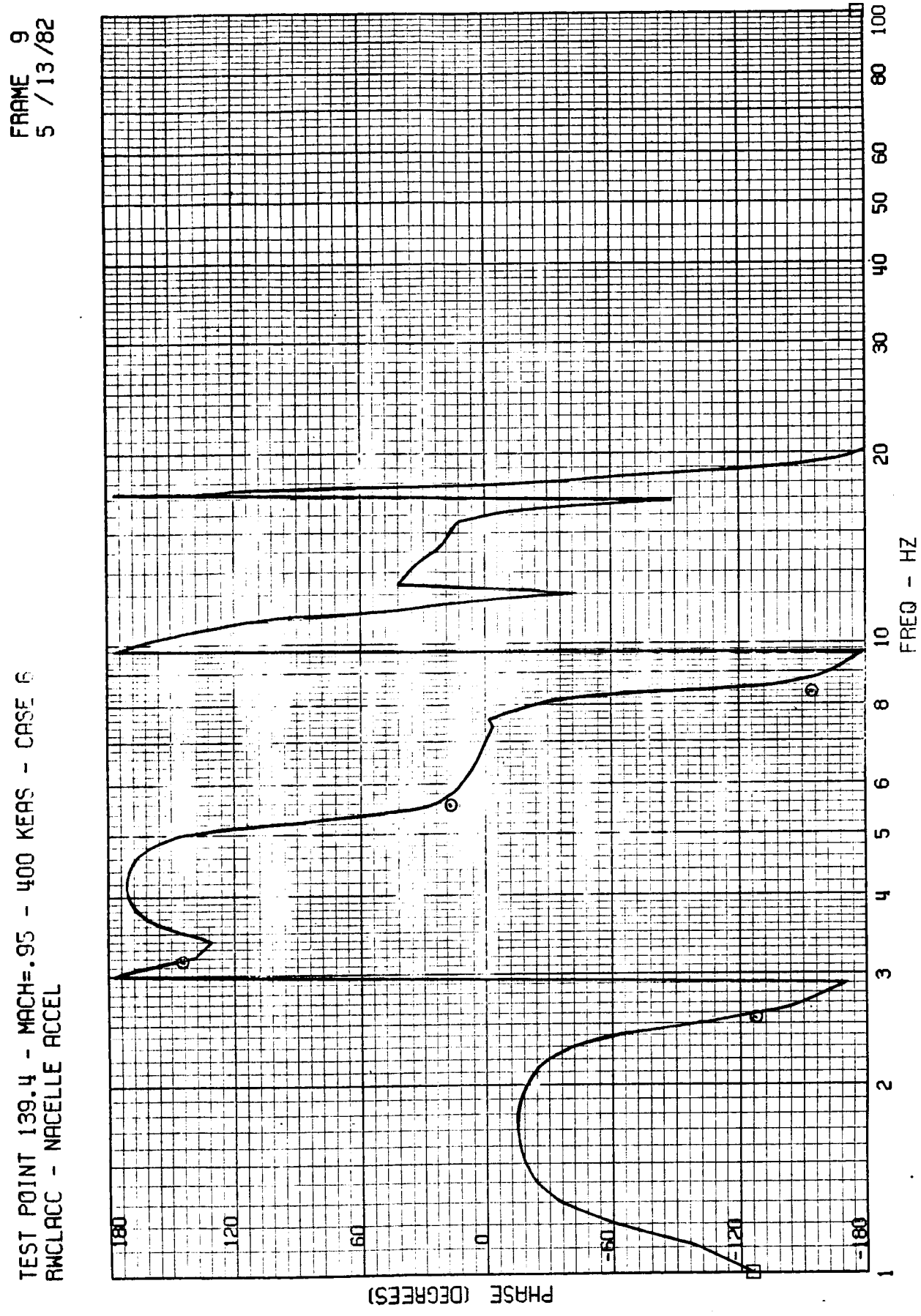

TEST POINT 139.4 - MACH=.95 - 400 KEAS - CASE 6
RRUDACC - RUDDER ACCEL

FRAME 10
5 /13 /82

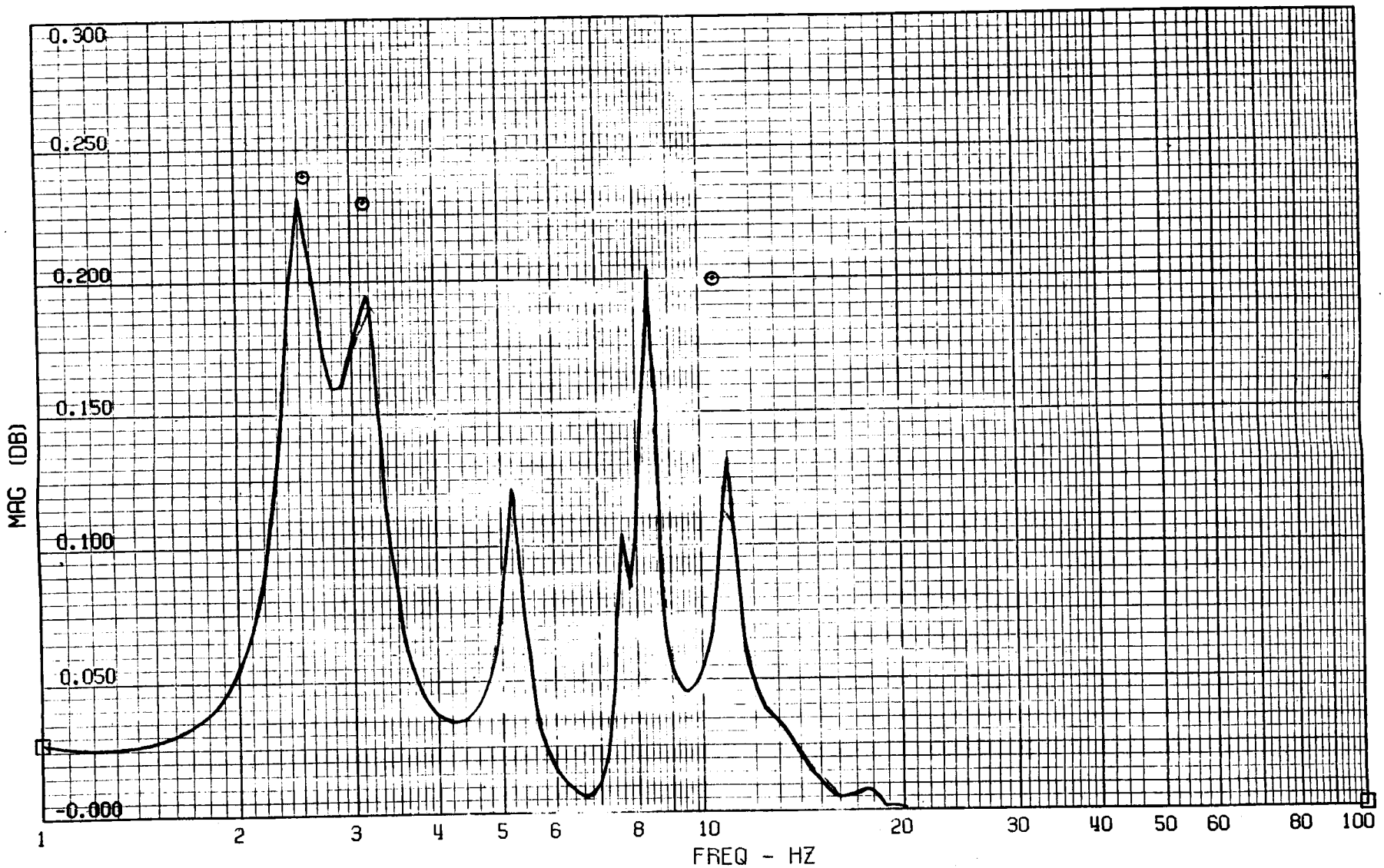

200

ORIGINAL PAGE IS
OF POOR QUALITY

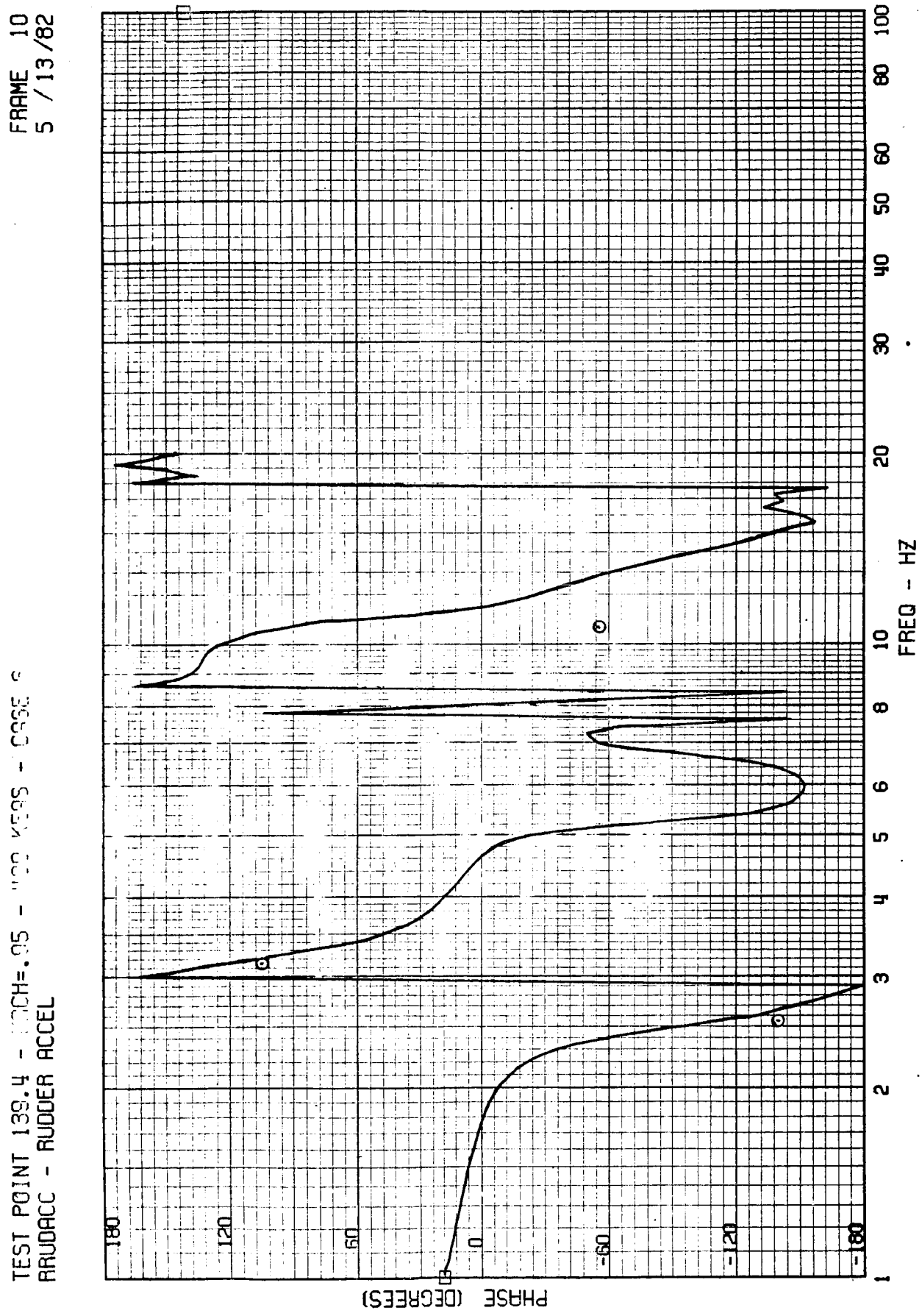

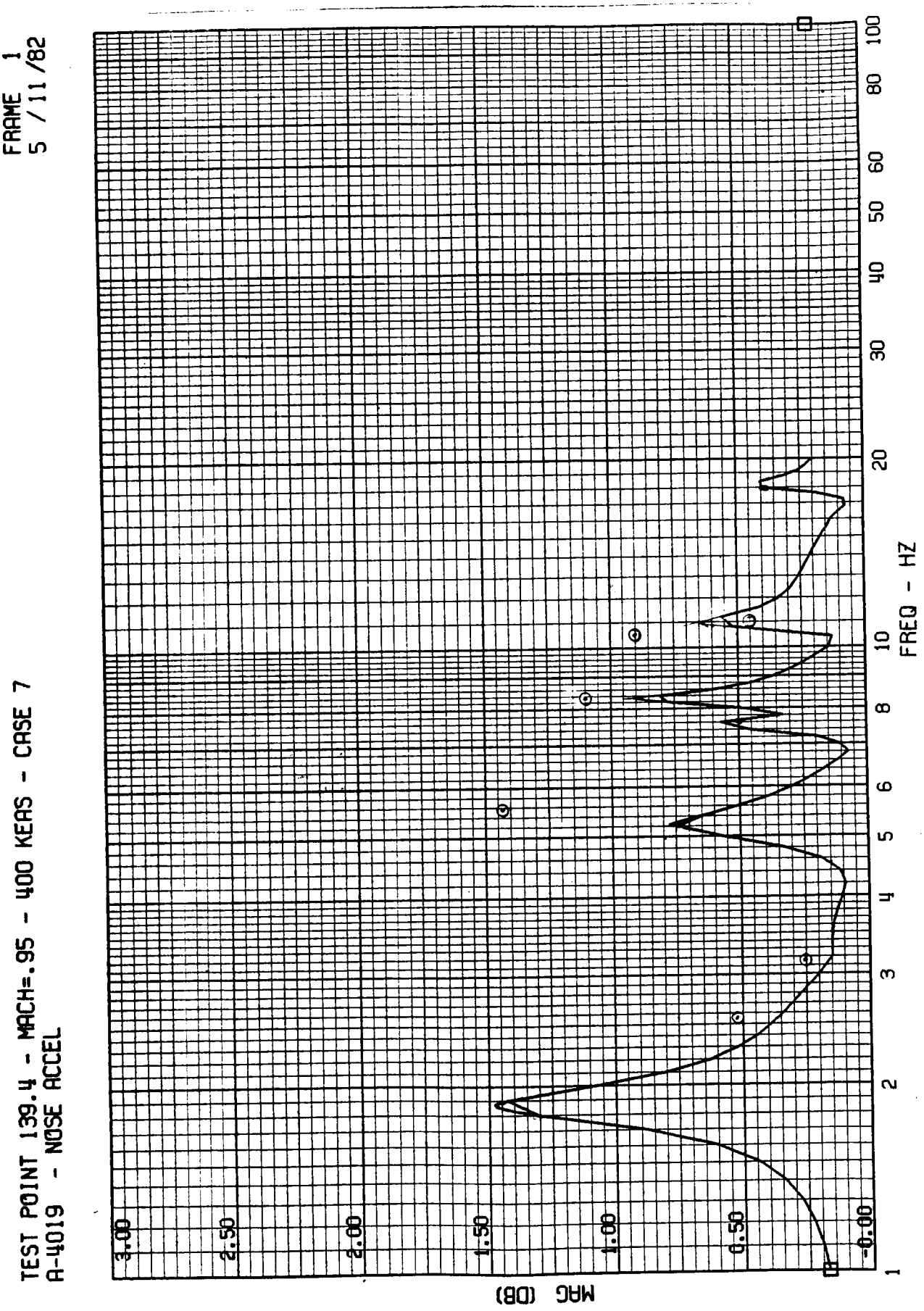
FRAME 1
5 / 11 /82
TEST POINT 139.4 - MACH=.95 - 400 KEAS - CASE 7
A-4019 - NOSE ACCEL
MAG (DB)
3.00
2.50
2.00
1.50
1.00
0.50
-0.00
1
2
3
4
5
6
8
10
20
30
40
50
60
80
100
FREQ - HZ

FRAME 1
5 /11 /82

TEST POINT 139.4 - MACH=.95 - 400 KEAS - CASE 7
A-4019 - NOSE ACCEL

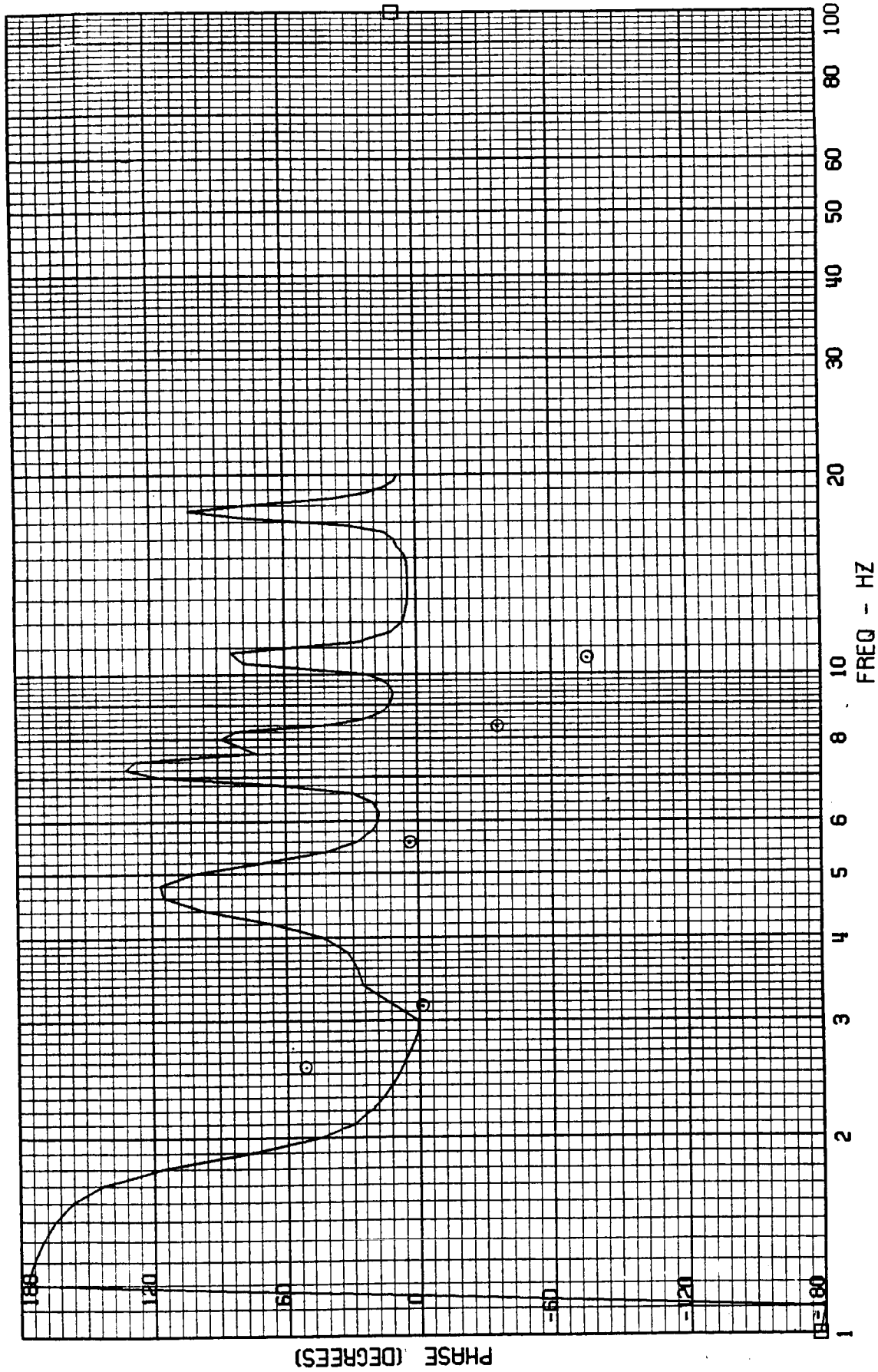

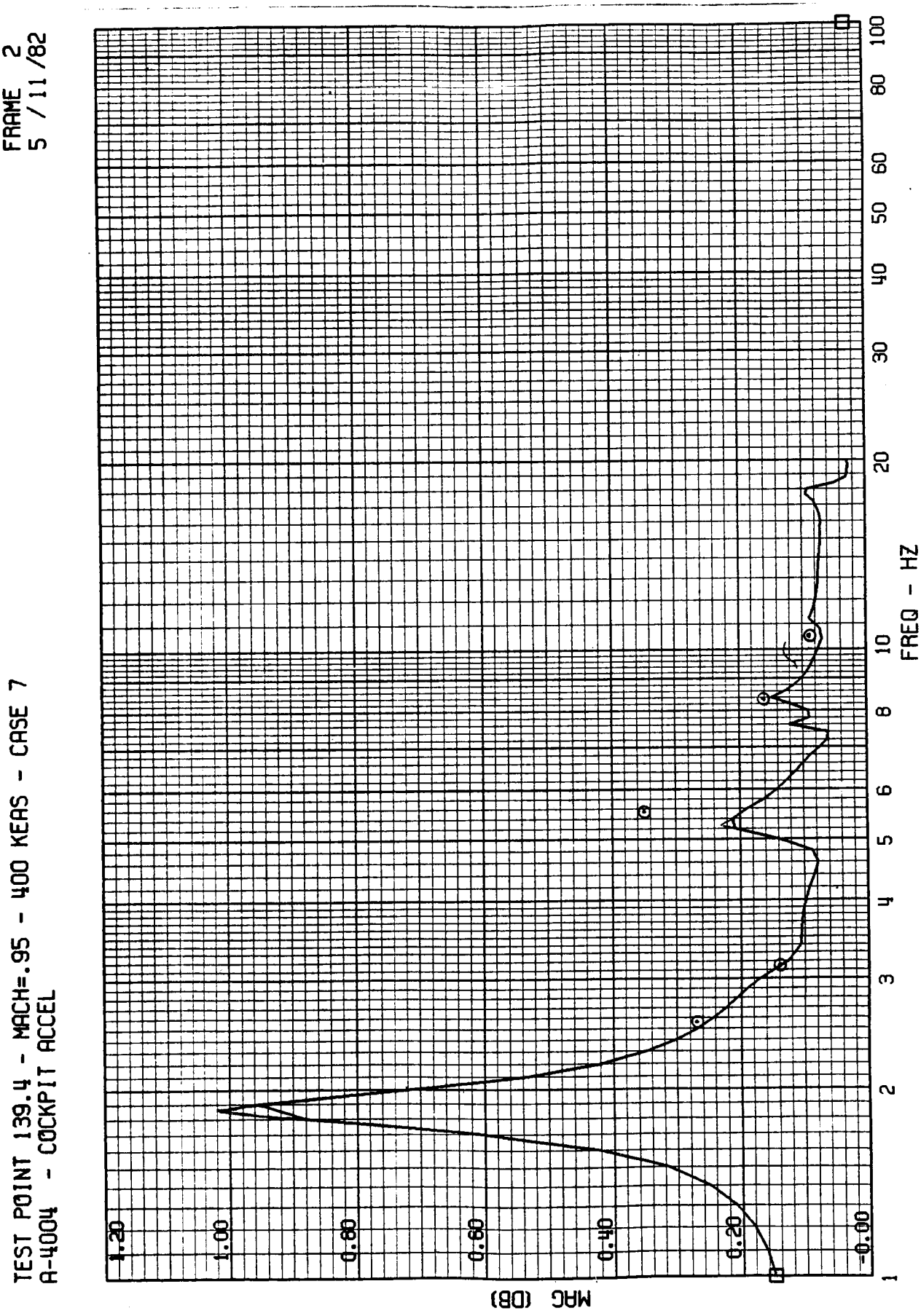
TEST POINT 139.4 - MACH=.95 - 400 KEAS - CASE 7
A-4004 - COCKPIT ACCEL
FRAME 2
5 /11 /82
MAG (DB)
1.20
1.00
0.80
0.60
0.40
0.20
-0.00
FREQ - HZ
1
2
3
4
5
6
8
10
20
30
40
50
60
80
100

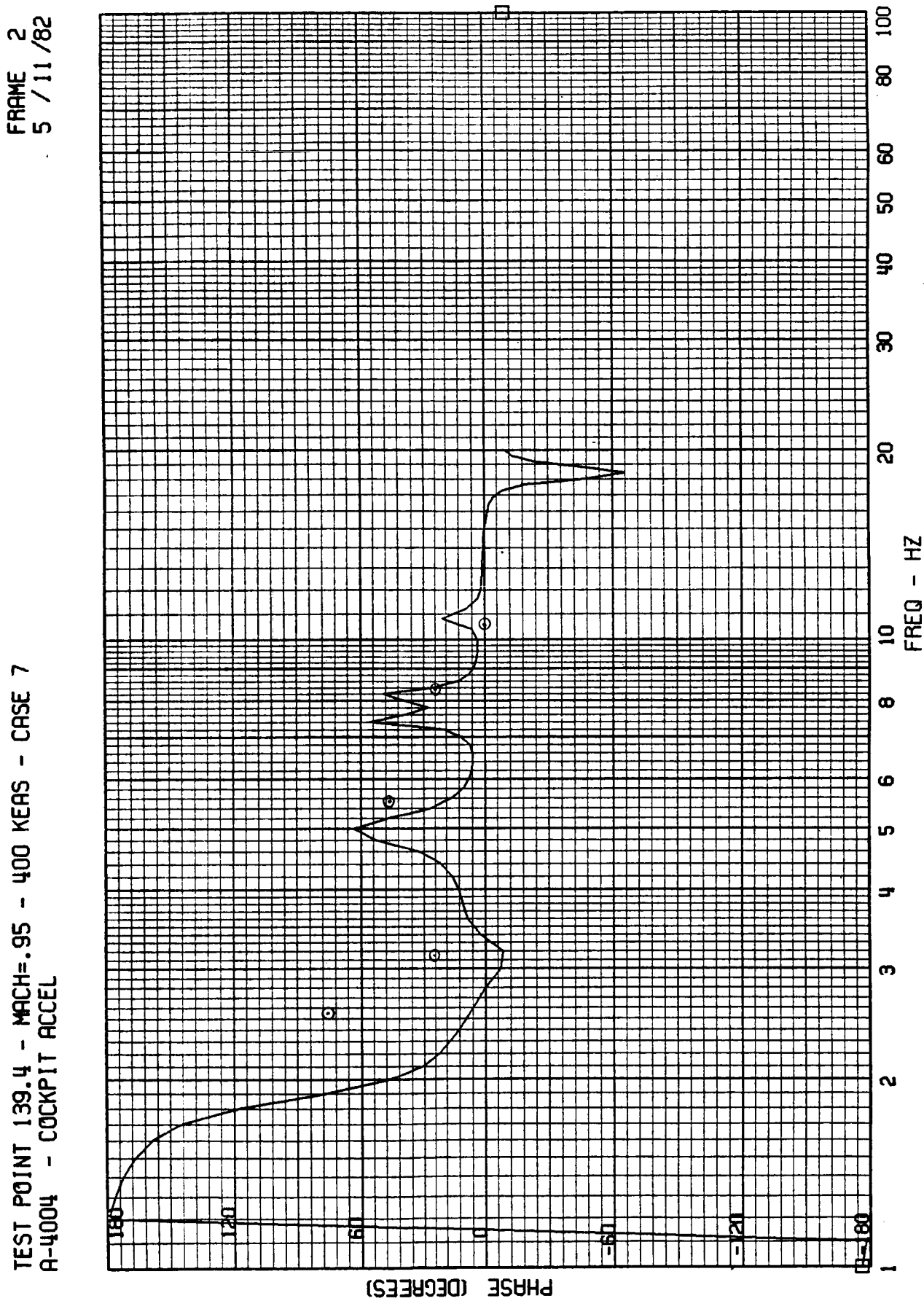

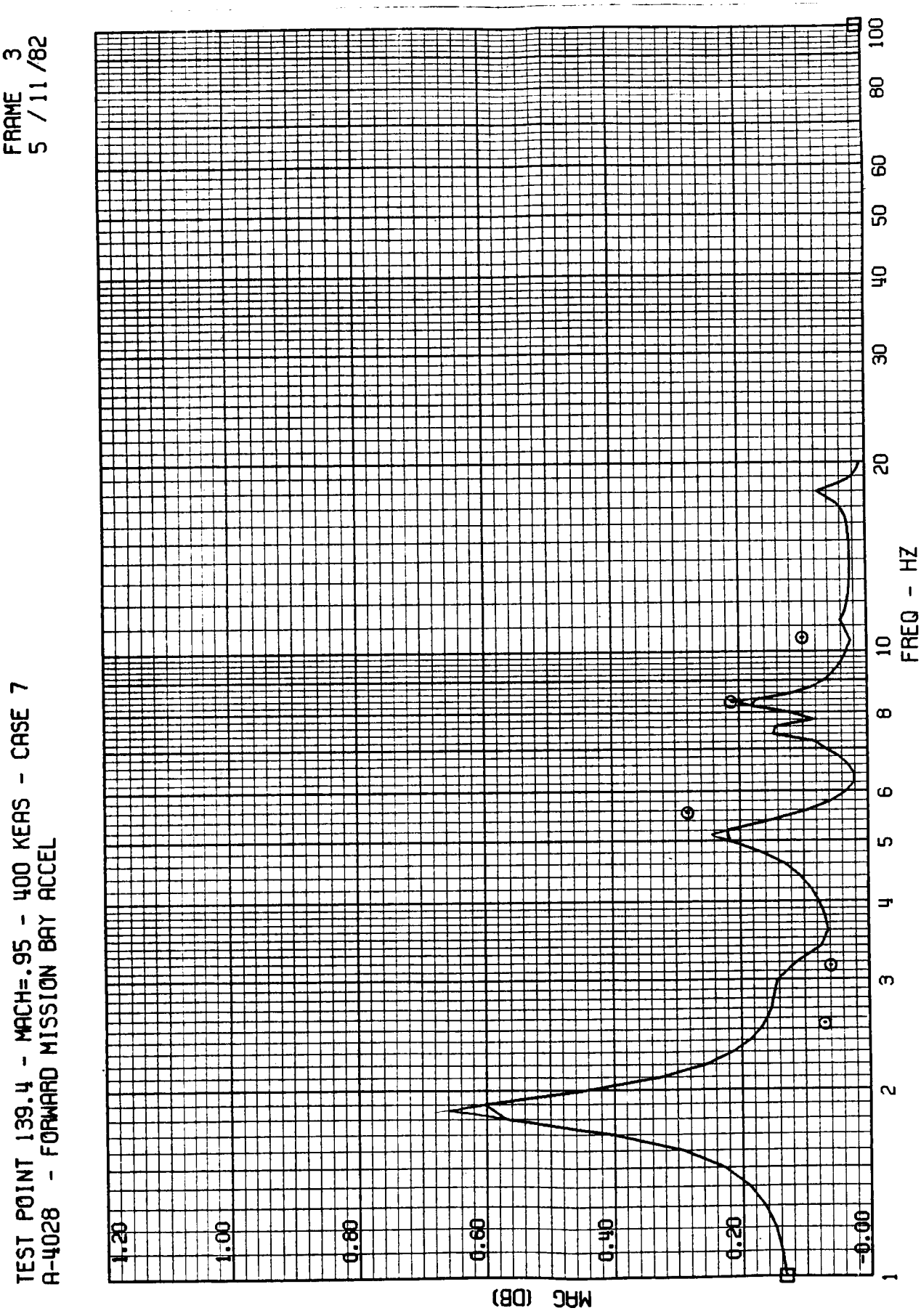
TEST POINT 139.4 - MACH=.95 - 400 KEAS - CASE 7
A-4028 - FORWARD MISSION BAY ACCEL
FRAME 3
5 /11 /82
MAG (DB)
1.20
1.00
0.80
0.60
0.40
0.20
-0.00
FREQ - HZ
1
2
3
4
5
6
8
10
20
30
40
50
60
80
100

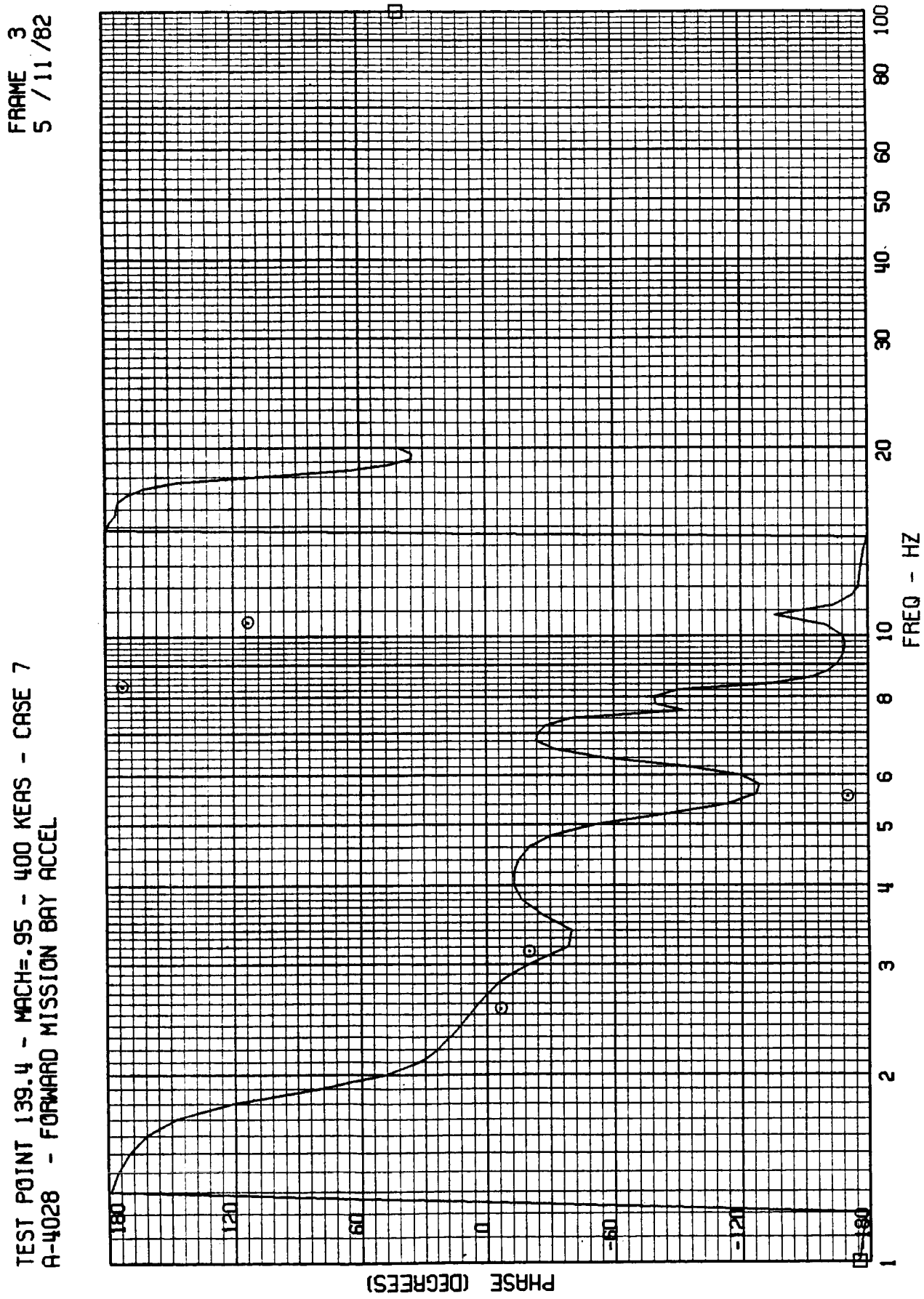
FRAME 3
5 / 11 /82
TEST POINT 139.4 - MACH=.95 - 400 KEAS - CASE 7
A-4028 - FORWARD MISSION BAY ACCEL
PHASE (DEGREES)
180
120
60
0
-60
-120
-180
1
2
3
4
5
6
8
10
20
30
40
50
60
80
100
FREQ - HZ

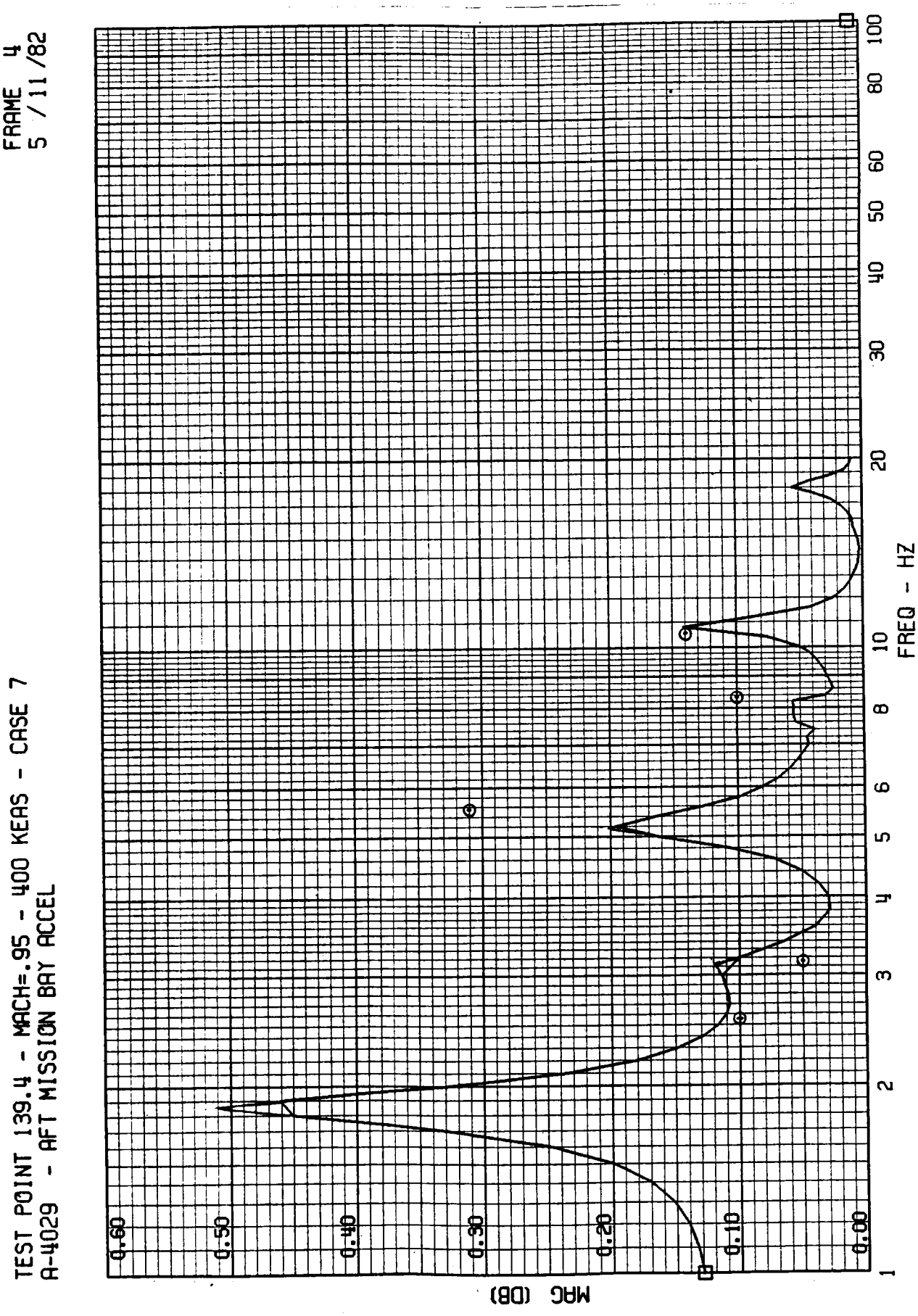
FRAME 4
5 /11 /82
TEST POINT 139.4 - MACH=.95 - 400 KEAS - CASE 7
A-4029 - AFT MISSION BAY ACCEL
MAG (DB)
0.60
0.50
0.40
0.30
0.20
0.10
0.00
FREQ - HZ
1
2
3
4
5
6
8
10
20
30
40
50
60
80
100

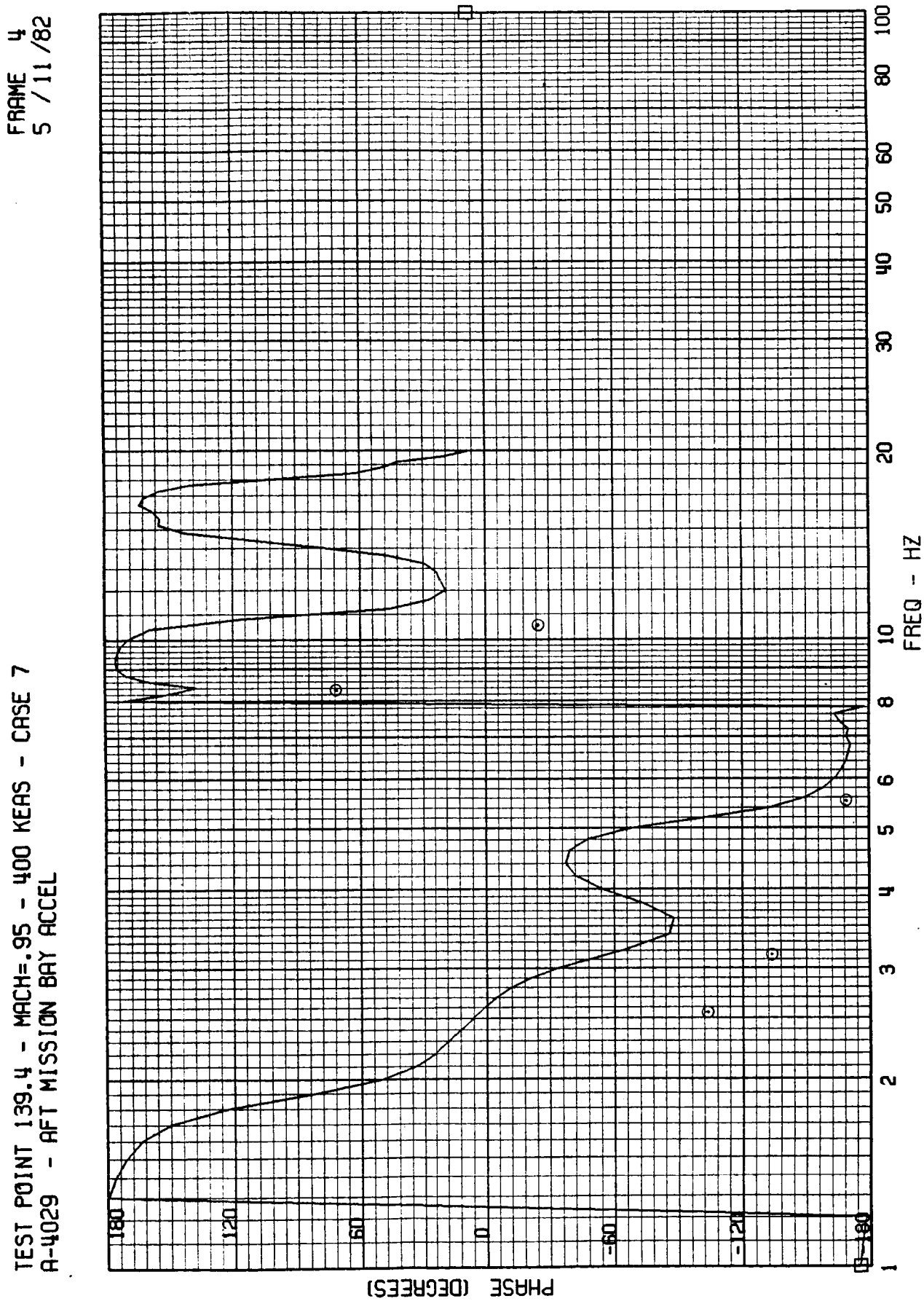

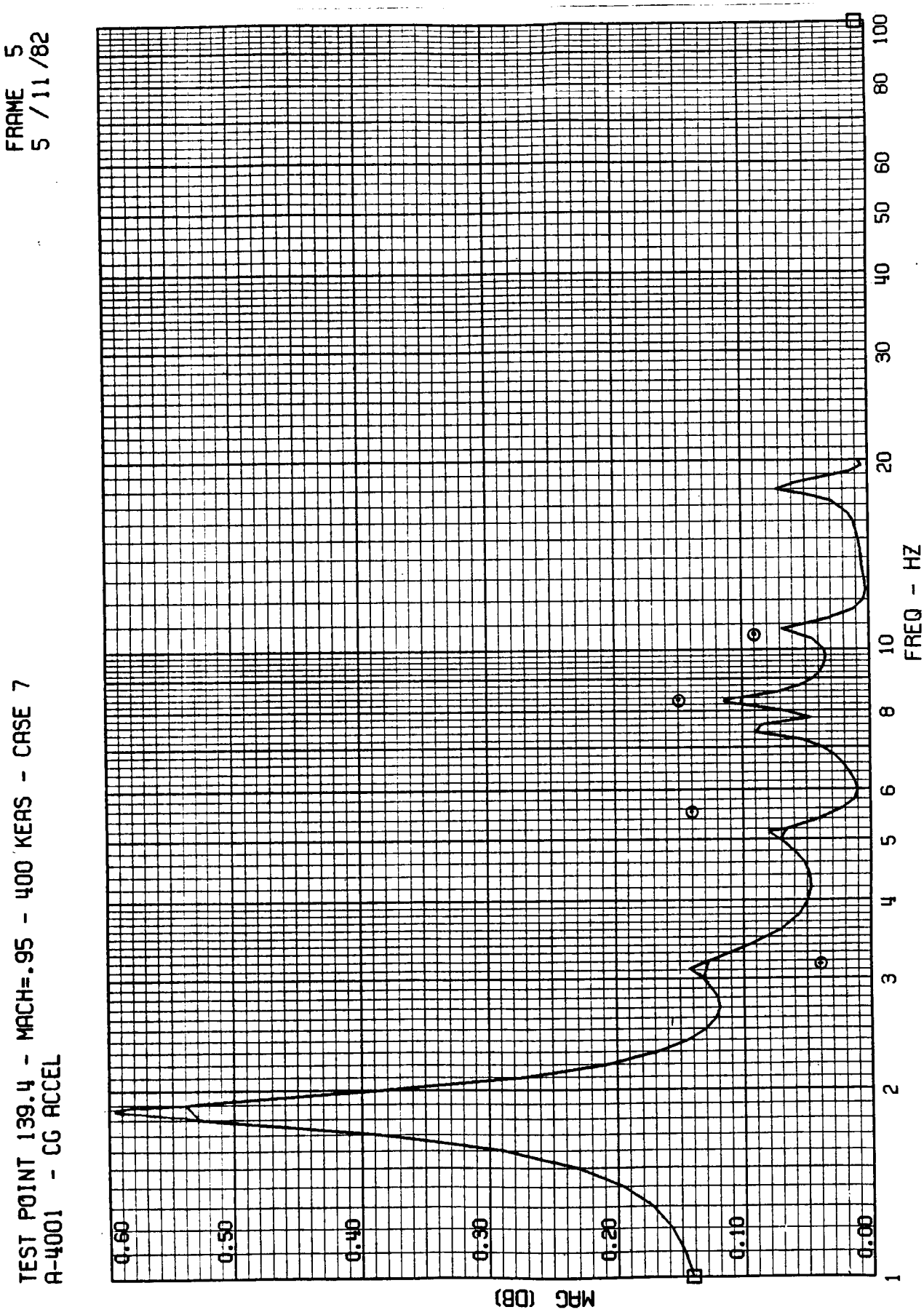
FRAME 5
5 /11 /82
TEST POINT 139.4 - MACH=.95 - 400 KEAS - CASE 7
A-4001 - CG ACCEL
MAG (DB)
0.60
0.50
0.40
0.30
0.20
0.10
0.00
FREQ - HZ
1
2
3
4
5
6
8
10
20
30
40
50
60
80
100

FRAME 5
5/11/82

TEST POINT 139.4 - MACH=.95 - 400 KEAS - CASE 7
A-4001 - CG ACCEL

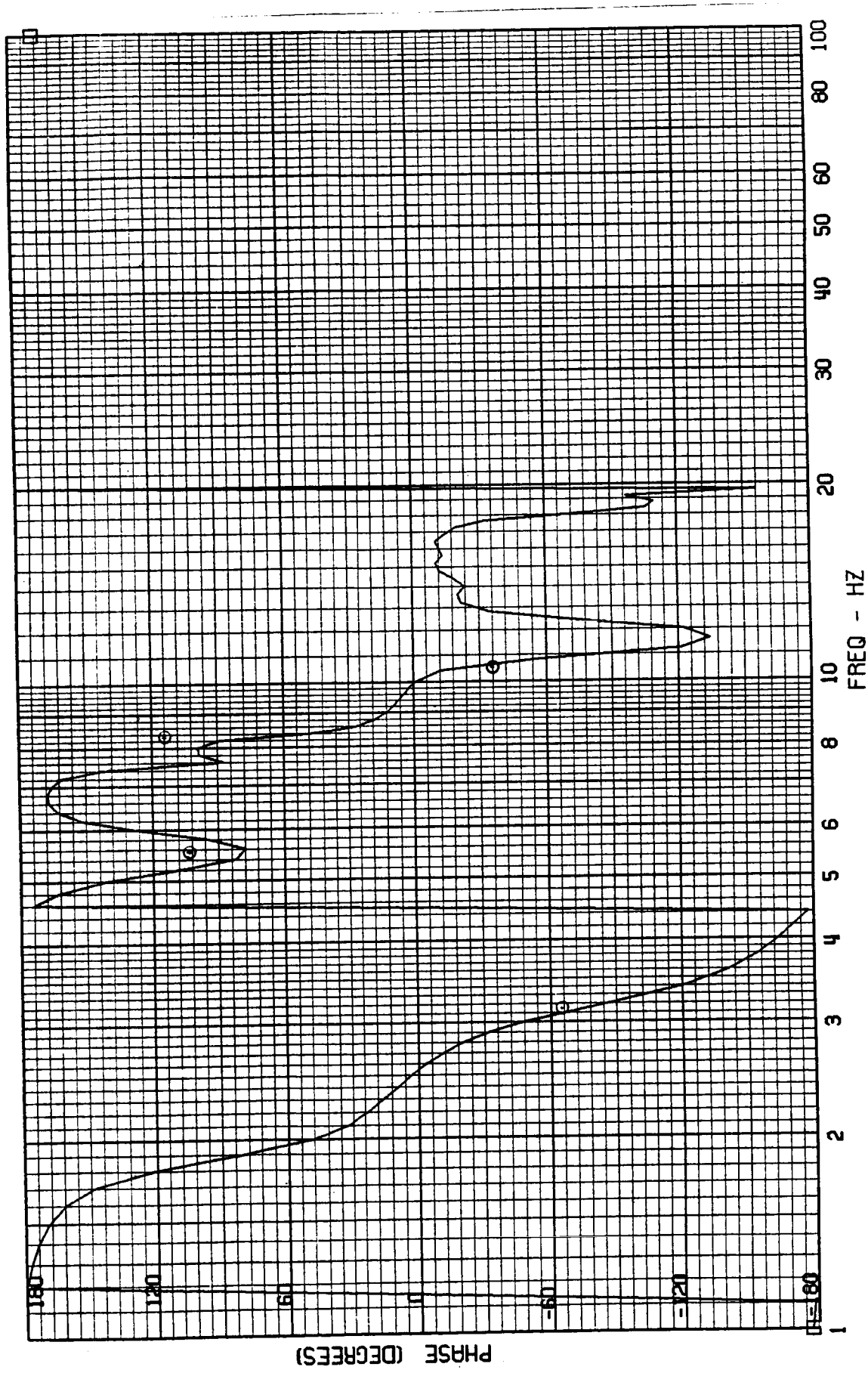

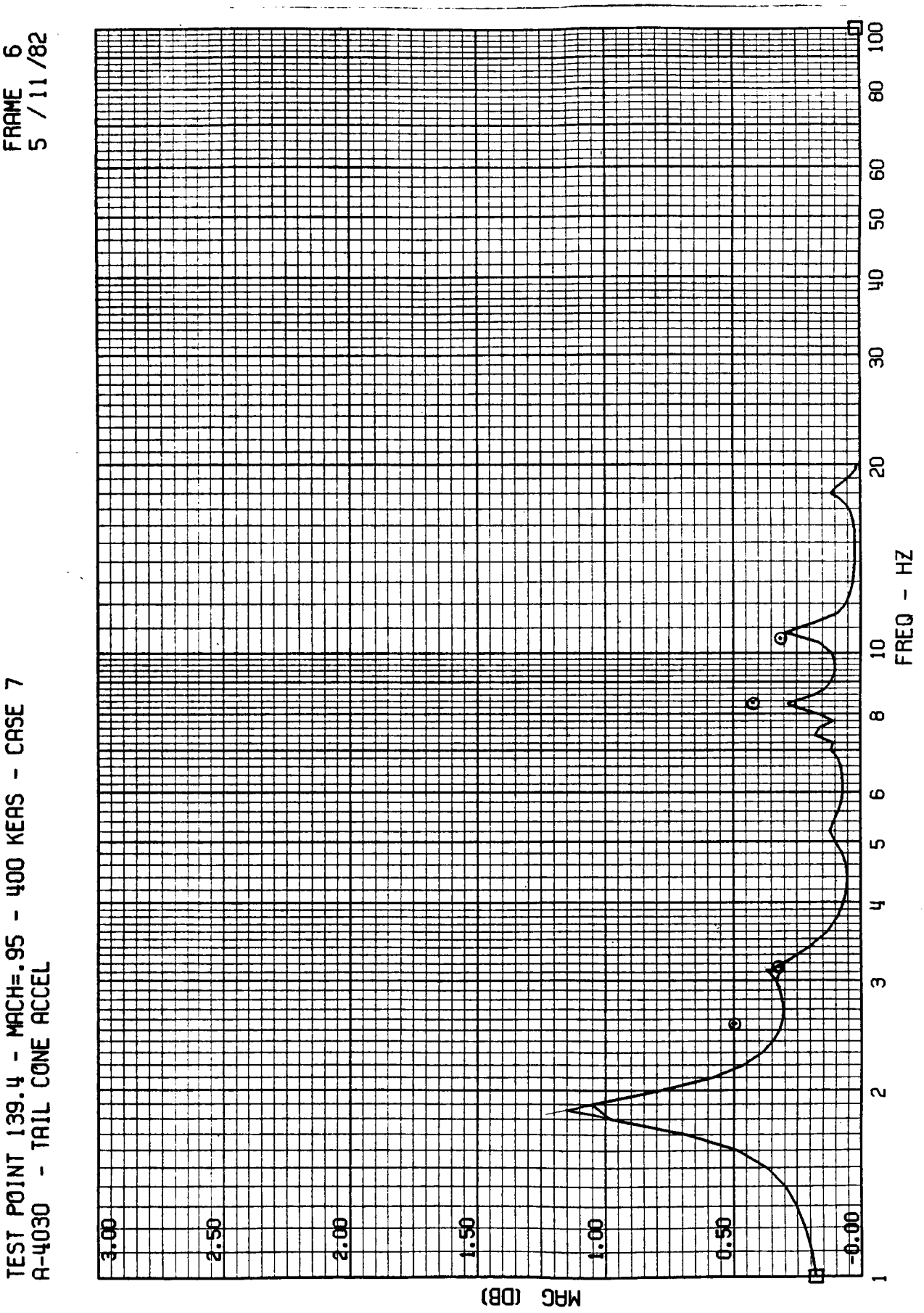
TEST POINT 139.4 - MACH=.95 - 400 KEAS - CASE 7
A-4030 - TAIL CONE ACCEL
FRAME 6
5 / 11 /82
MAG (DB)
3.00
2.50
2.00
1.50
1.00
0.50
-0.00
1
2
3
4
5
6
8
10
20
30
40
50
60
80
100
FREQ - HZ

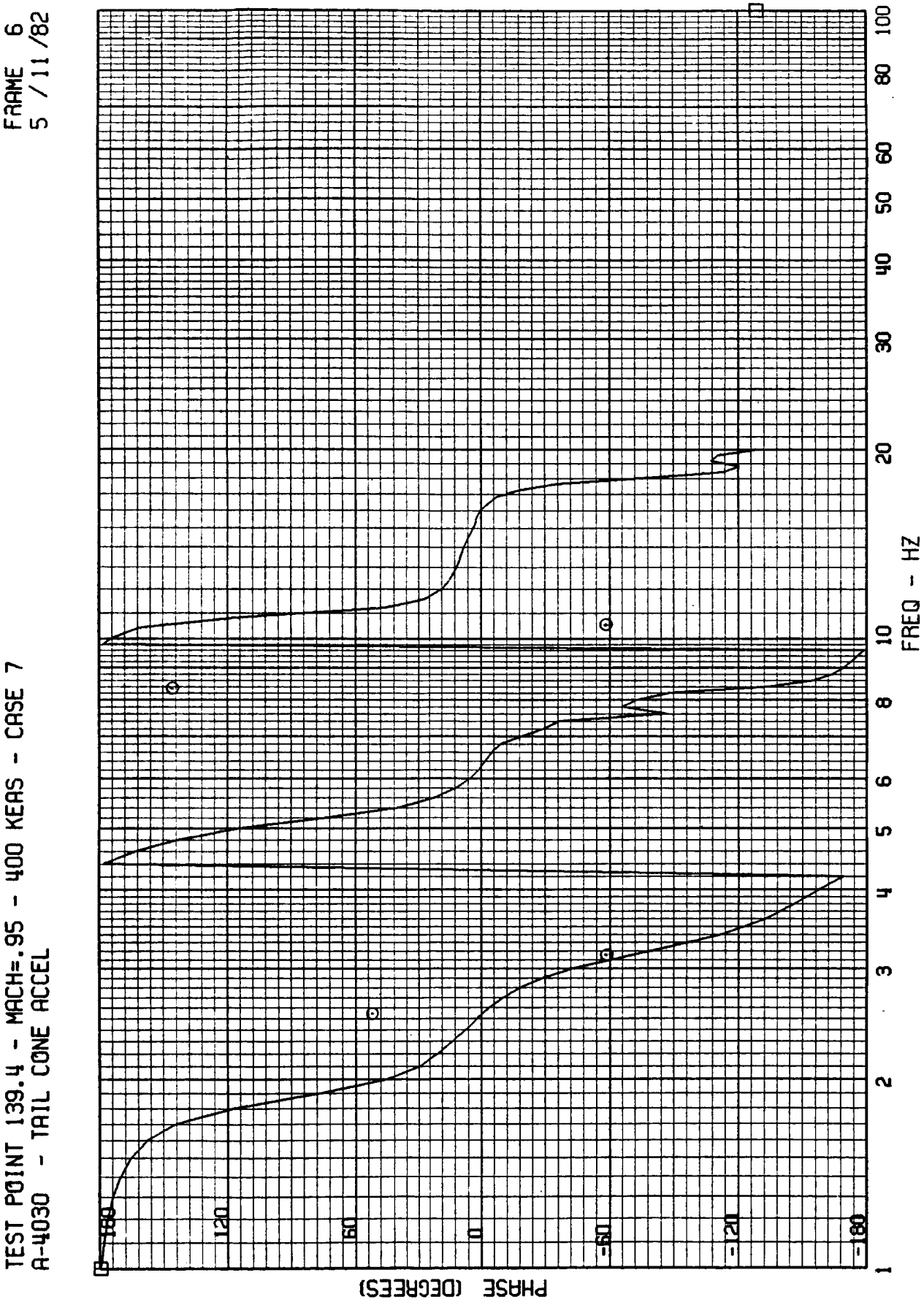

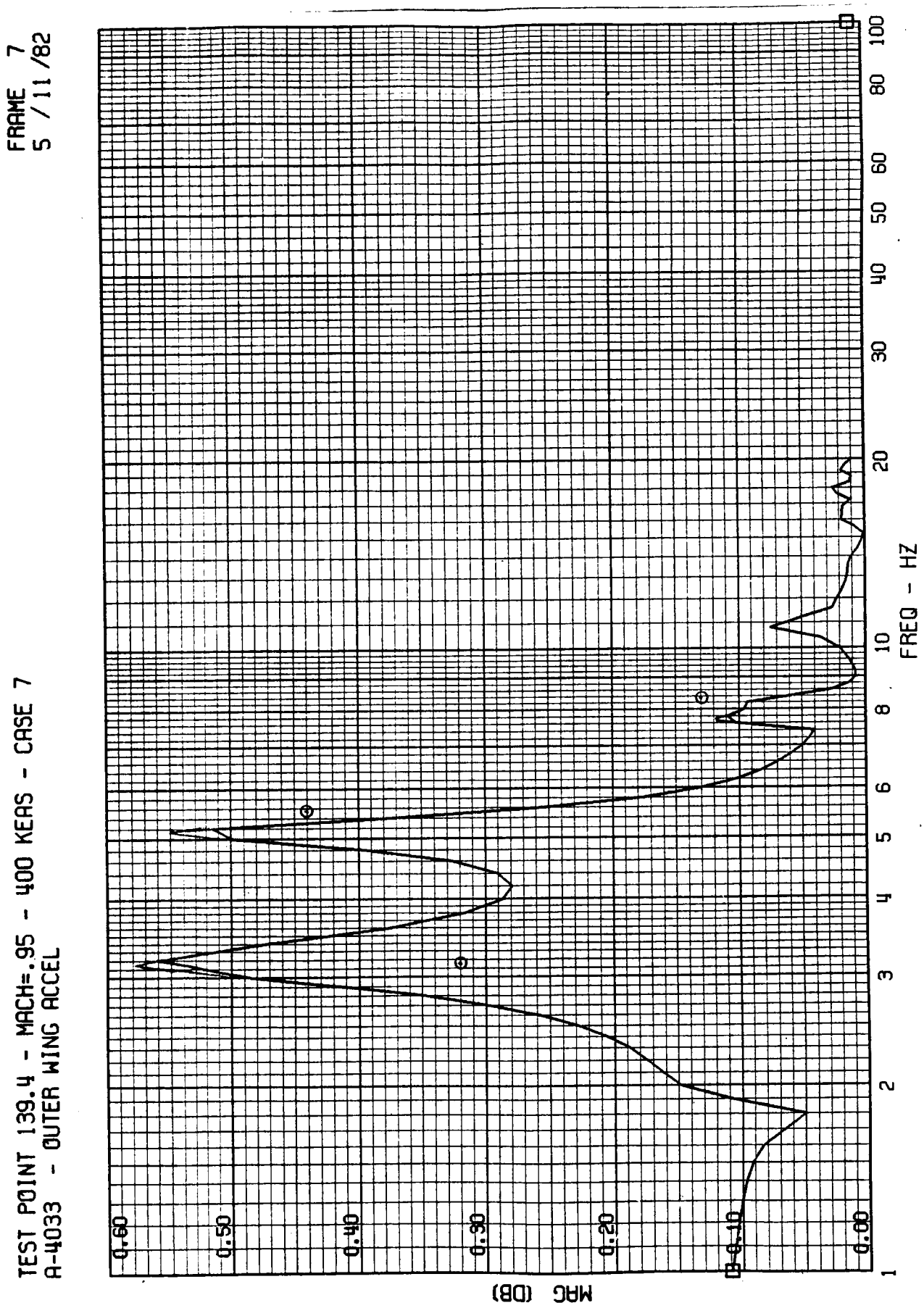
FRAME 7
5 /11 /82
TEST POINT 139.4 - MACH=.95 - 400 KEAS - CASE 7
A-4033 - OUTER WING ACCEL
MAG (DB)
0.60
0.50
0.40
0.30
0.20
0.10
0.00
FREQ - HZ
1
2
3
4
5
6
8
10
20
30
40
50
60
80
100

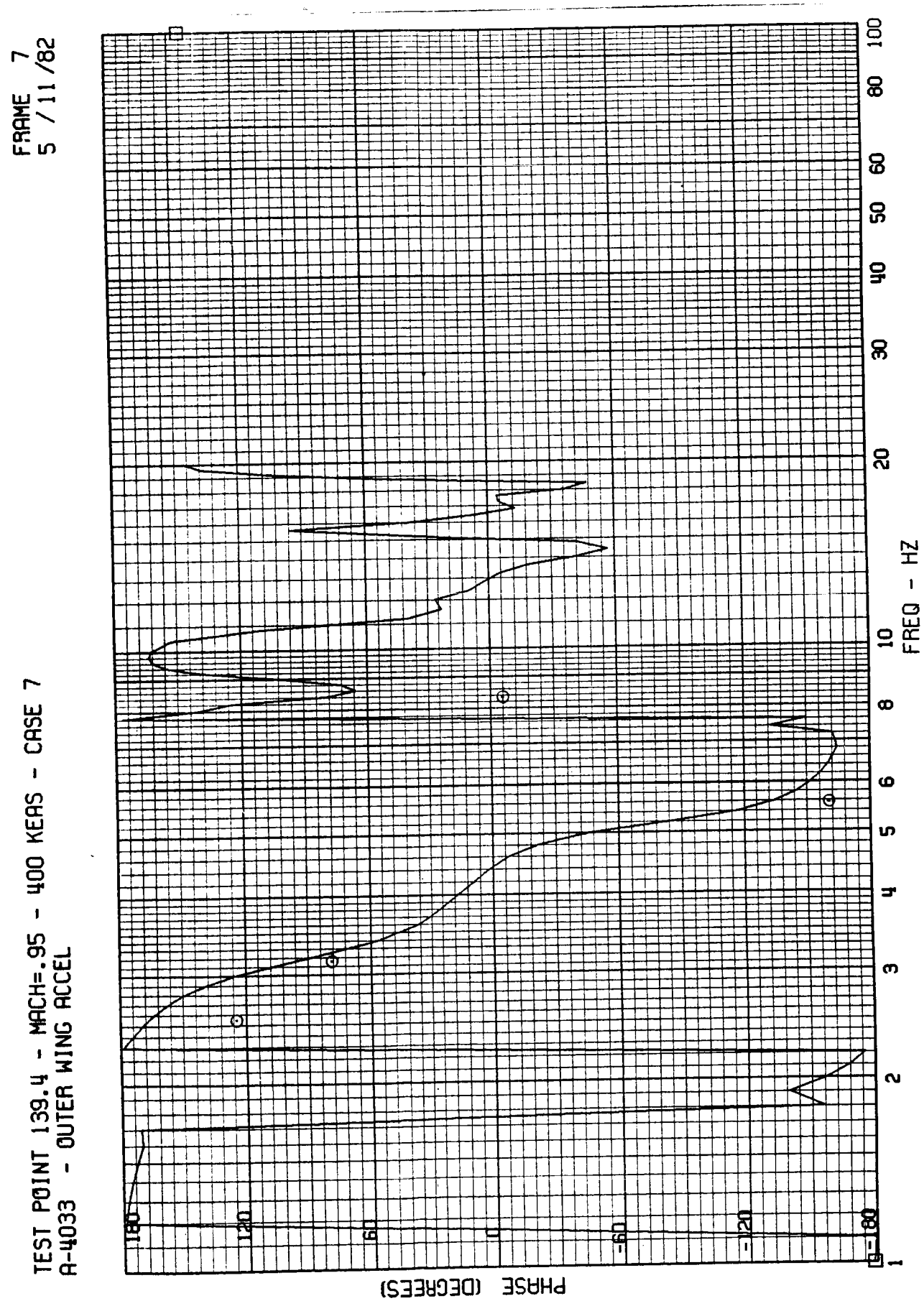
FRAME 7
5/11/82
TEST POINT 139.4 - MACH=.95 - 400 KEAS - CASE 7
A-4033 - OUTER WING ACCEL
PHASE (DEGREES)
180
120
60
0
-60
-120
-180
1
2
3
4
5
6
8
10
20
30
40
50
60
80
100
FREQ - HZ

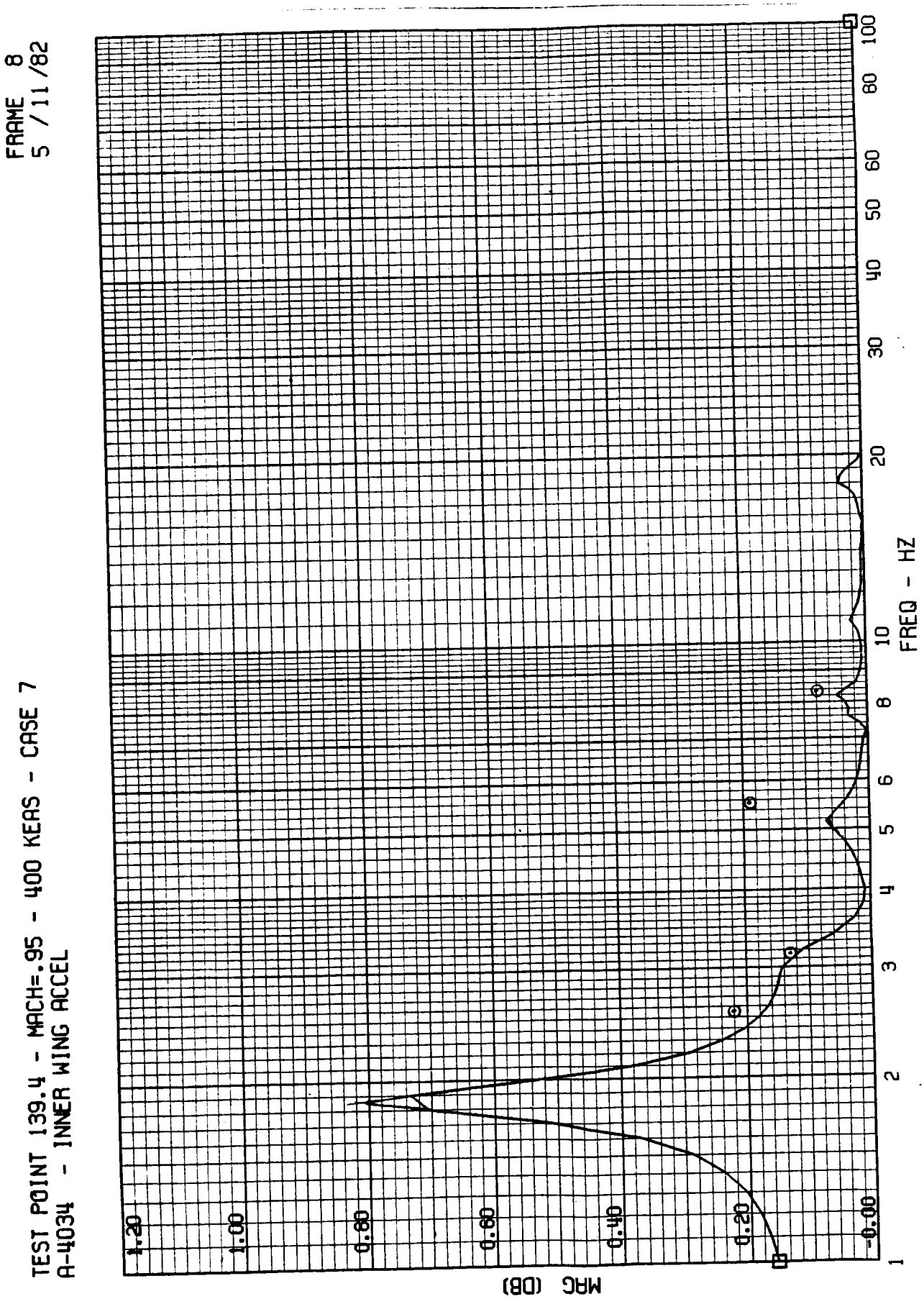
FRAME 8
5 /11 /82
TEST POINT 139.4 - MACH=.95 - 400 KEAS - CASE 7
A-4034 - INNER WING ACCEL
MAG (DB)
1.20
1.00
0.80
0.60
0.40
0.20
-0.00
FREQ - HZ
1
2
3
4
5
6
8
10
20
30
40
50
60
80
100

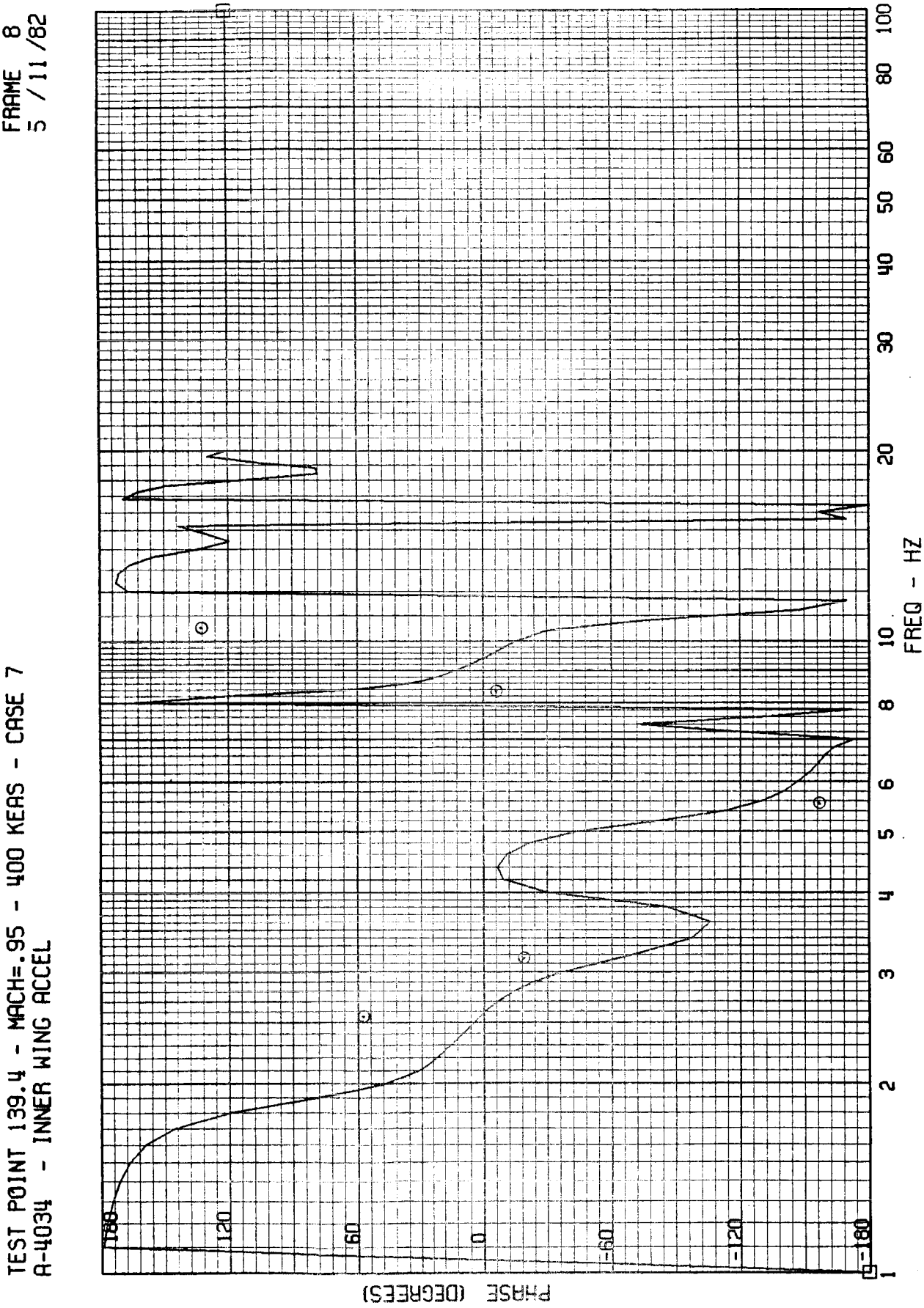

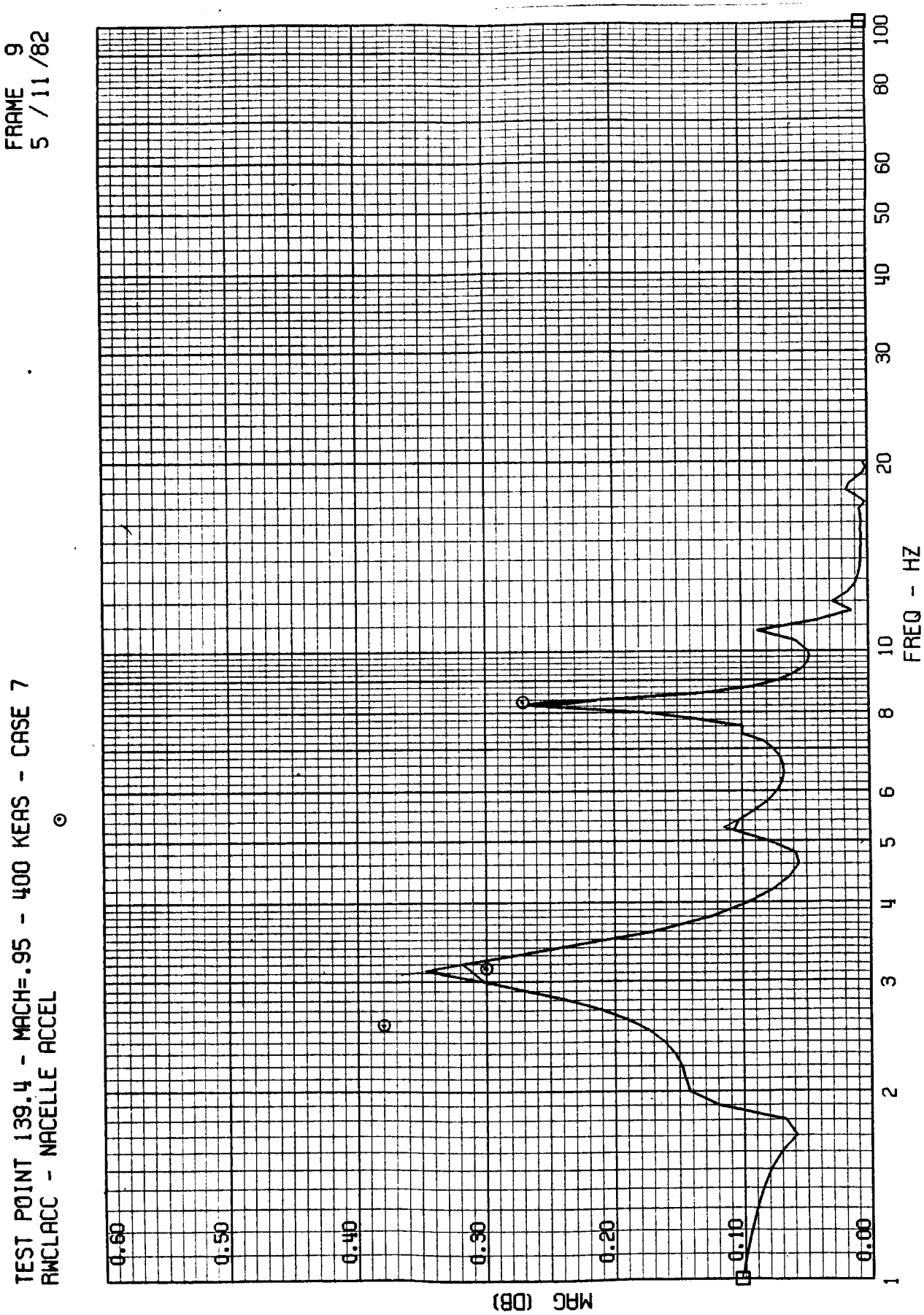
FRAME 9
5/11/82
TEST POINT 139.4 - MACH=.95 - 400 KEAS - CASE 7
RWCLACC - NACELLE ACCEL
MAG (DB)
0.60
0.50
0.40
0.30
0.20
0.10
0.00
1
2
3
4
5
6
8
10
20
30
40
50
60
80
100
FREQ - HZ

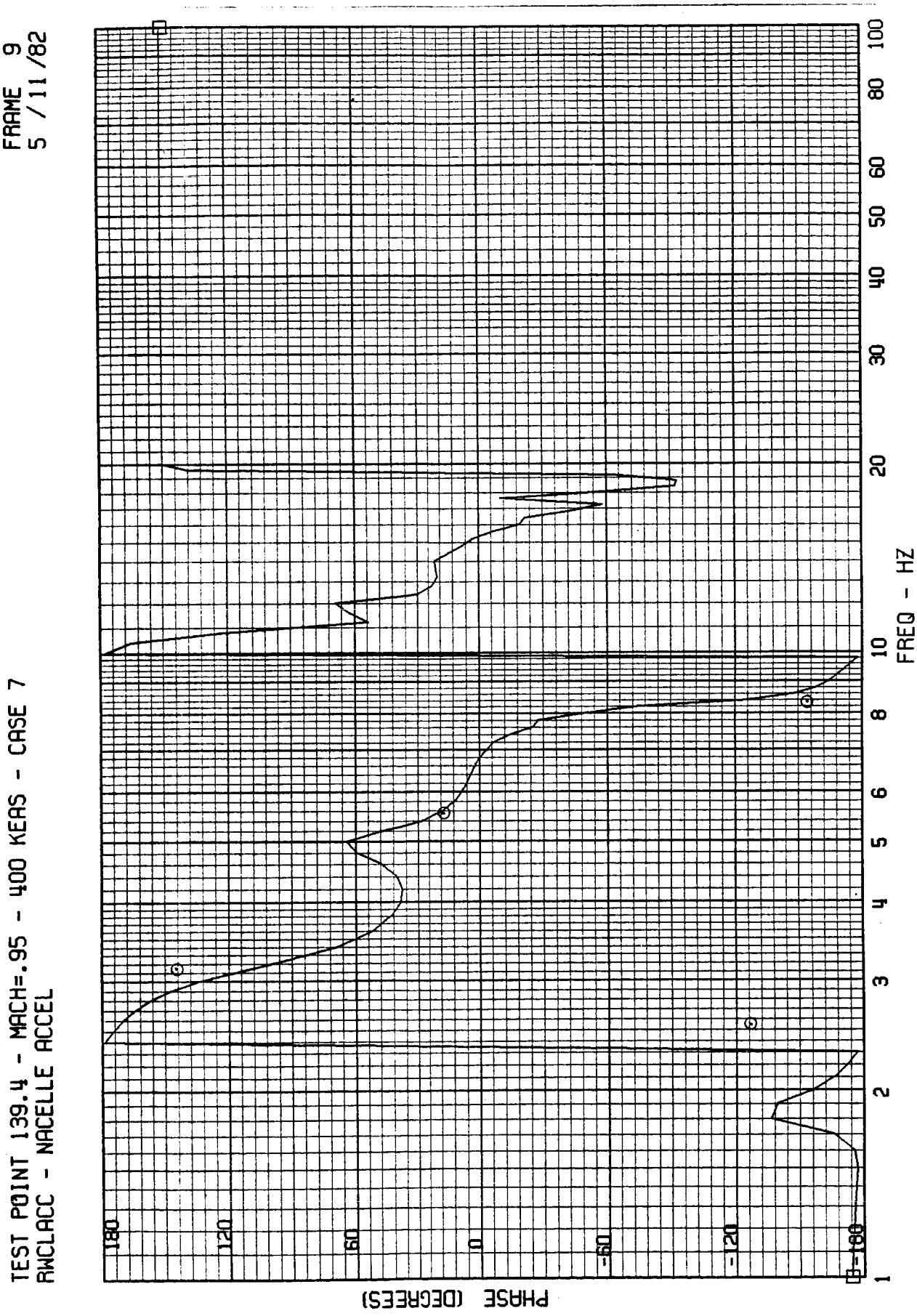

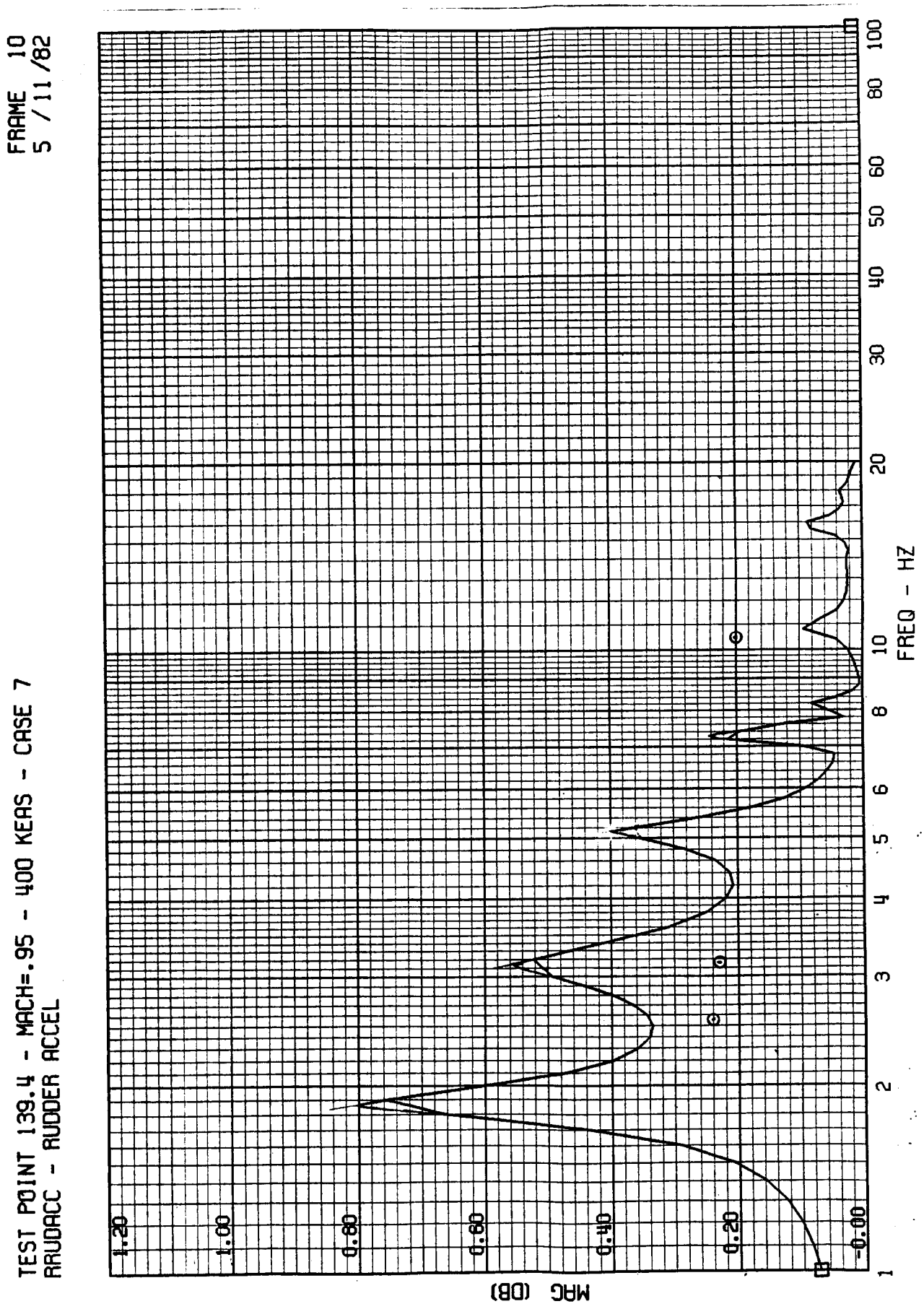
TEST POINT 139.4 - MACH=.95 - 400 KEAS - CASE 7
RRUDACC - RUDDER ACCEL
FRAME 10
5 / 11 /82
MAG (DB)
1.20
1.00
0.80
0.60
0.40
0.20
-0.00
1
2
3
4
5
6
8
10
20
30
40
50
60
80
100
FREQ - HZ

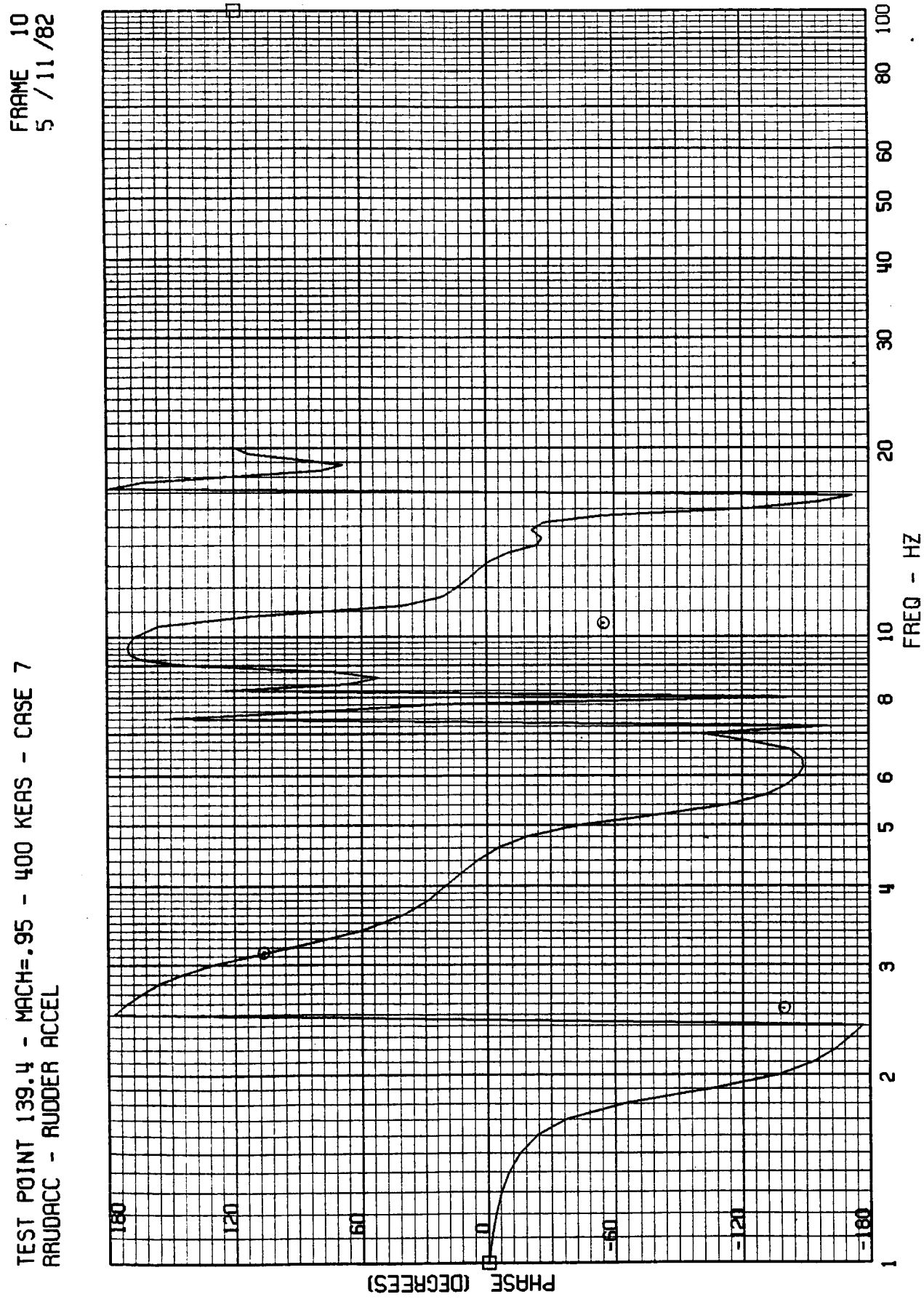
FRAME 10
5 / 11 /82
TEST POINT 139.4 - MACH=.95 - 400 KEAS - CASE 7
RRUDACC - RUDDER ACCEL
PHASE (DEGREES)
180
120
60
0
-60
-120
-180
FREQ - HZ
1
2
3
4
5
6
8
10
20
30
40
50
60
80
100

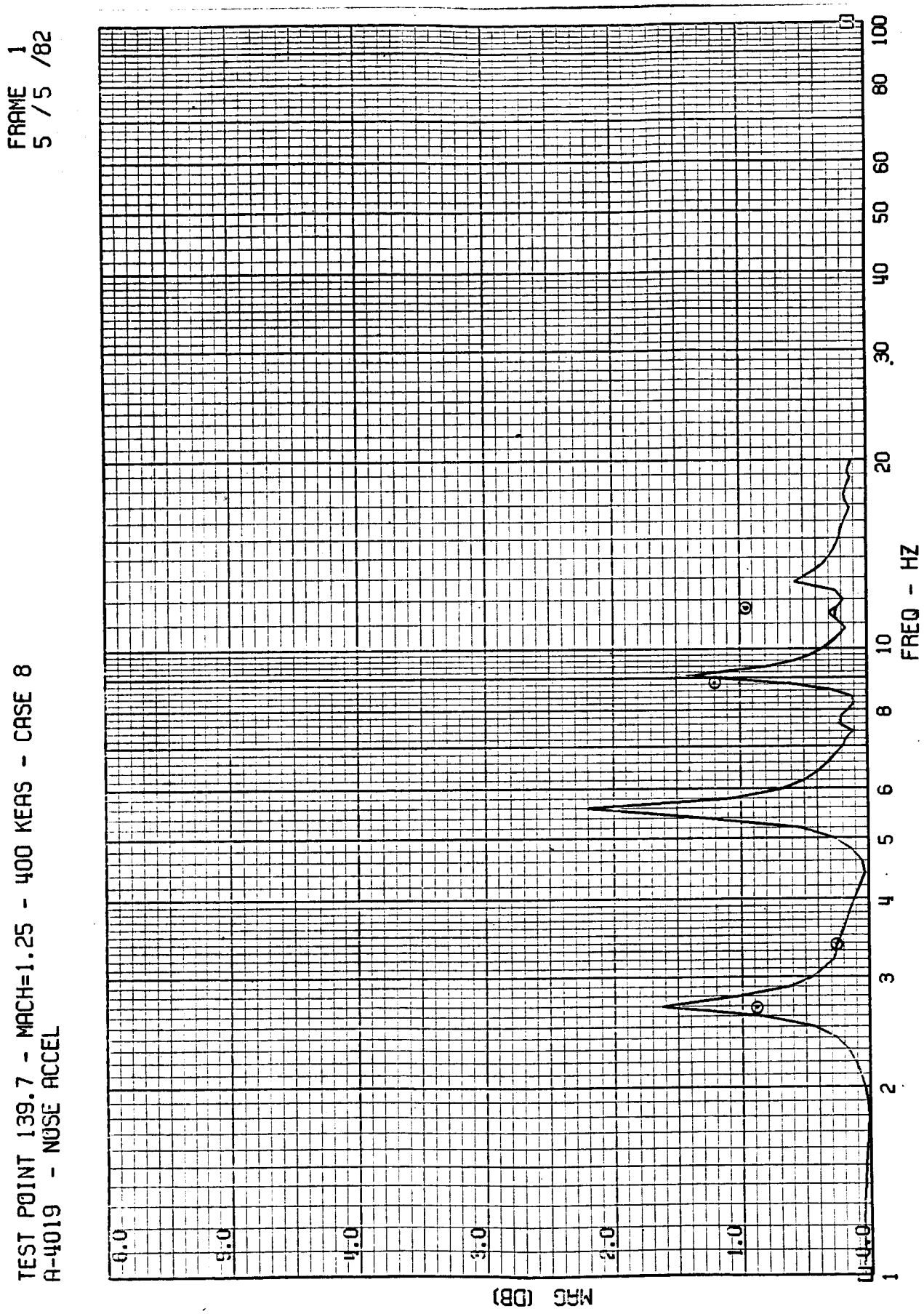
FRAME 1
5 /5 /82
TEST POINT 139.7 - MACH=1.25 - 400 KEAS - CASE 8
A-4019 - NOSE ACCEL
MAG (DB)
6.0
5.0
4.0
3.0
2.0
1.0
-0.0
1
2
3
4
5
6
8
10
20
30
40
50
60
80
100
FREQ - HZ

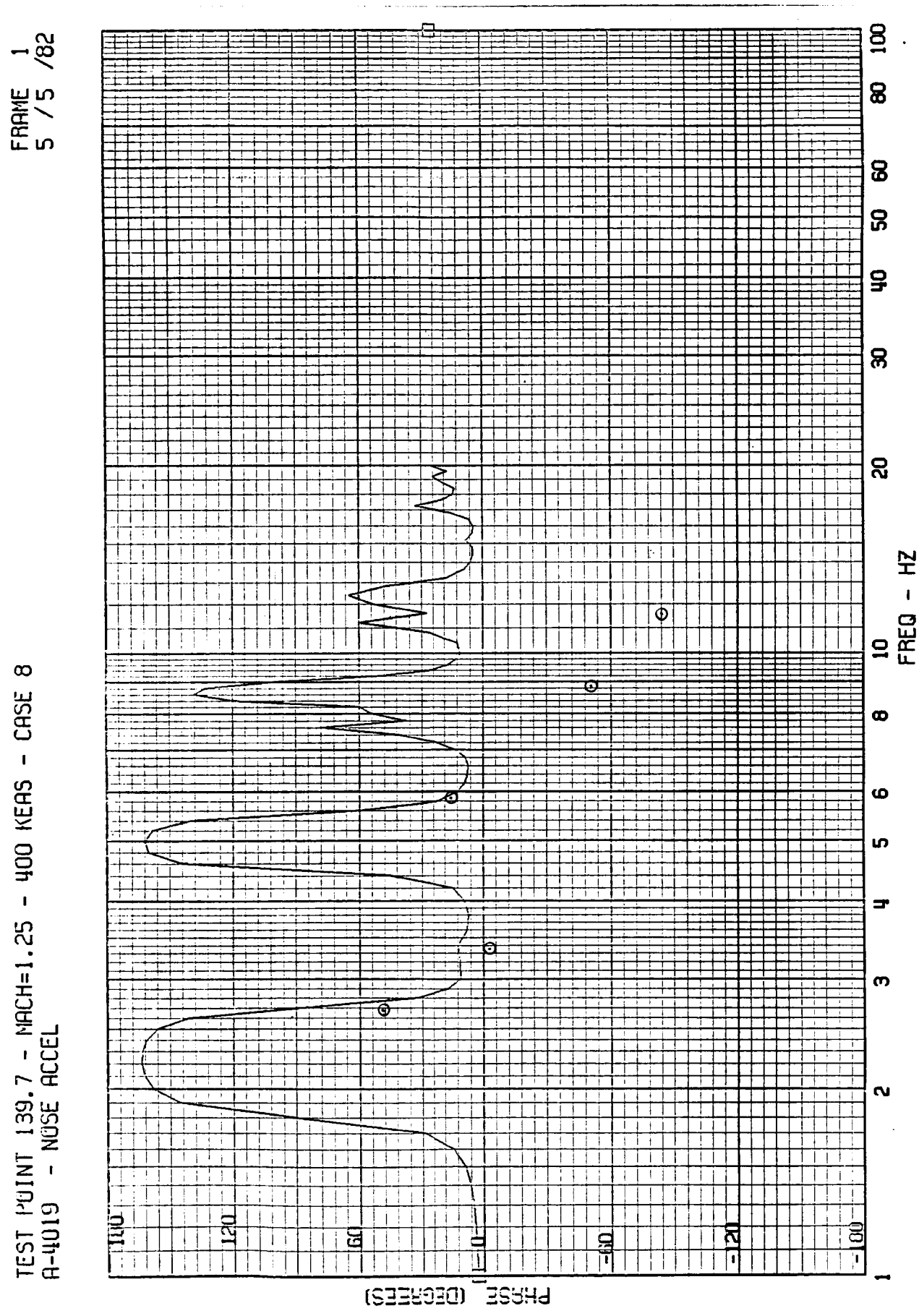
TEST POINT 139.7 - MACH=1.25 - 400 KEAS - CASE 8
A-4019 - NOSE ACCEL
FRAME 1
5 /5 /82
PHASE (DEGREES)
180
120
60
0
-60
-120
-180
1
2
3
4
5
6
8
10
20
30
40
50
60
80
100
FREQ - HZ

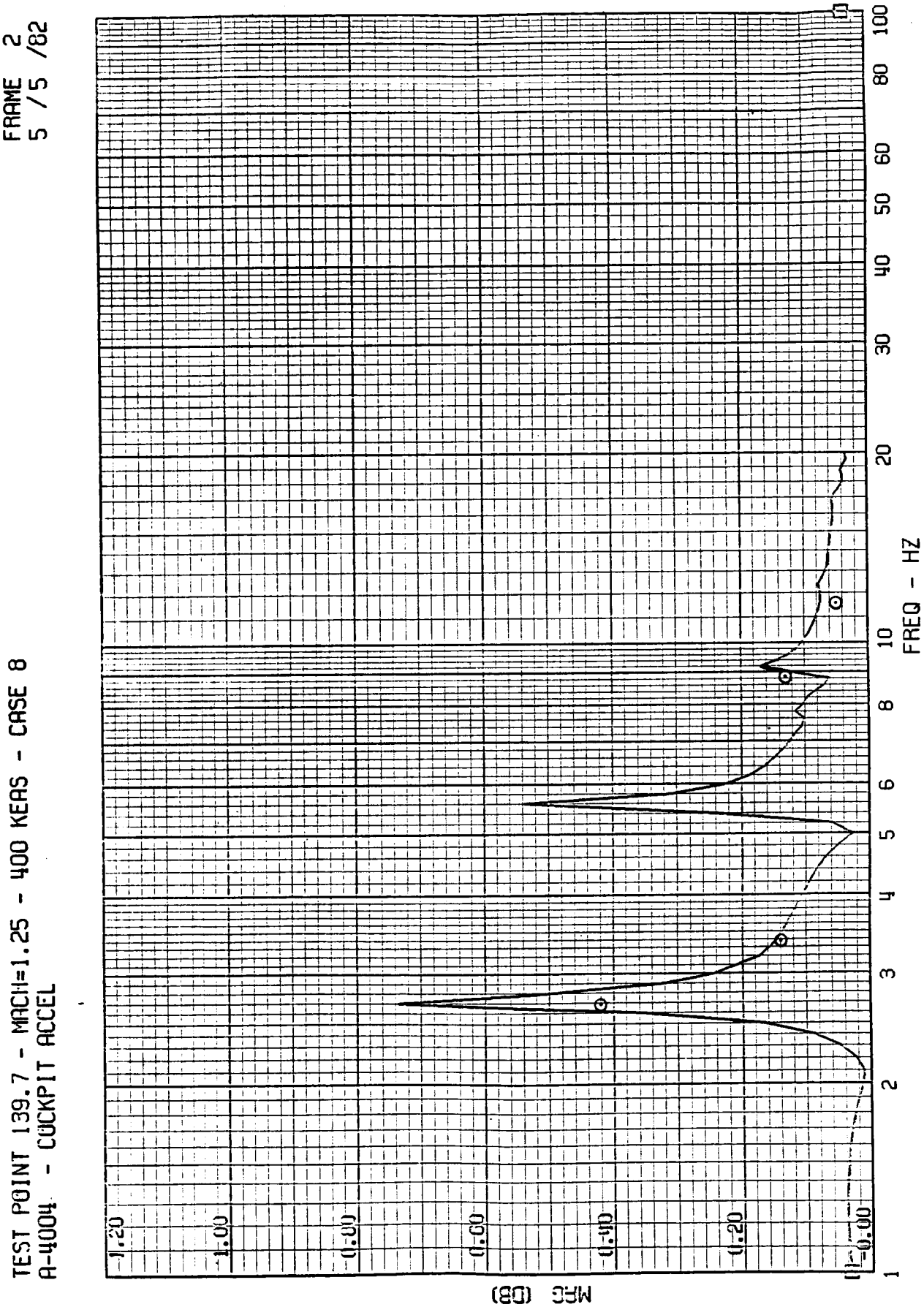
TEST POINT 139.7 - MACH=1.25 - 400 KEAS - CASE 8
A-4004 - COCKPIT ACCEL
FRAME 2
5 /5 /82
MAG (DB)
1.20
1.00
0.80
0.60
0.40
0.20
0.00
1
2
3
4
5
6
8
10
20
30
40
50
60
80
100
FREQ - HZ

FRAME 2
5/5/82

TEST POINT 139.7 - MACH=1.25 - 400 KEAS - CASE 8
A-4004 - COCKPIT ACCEL

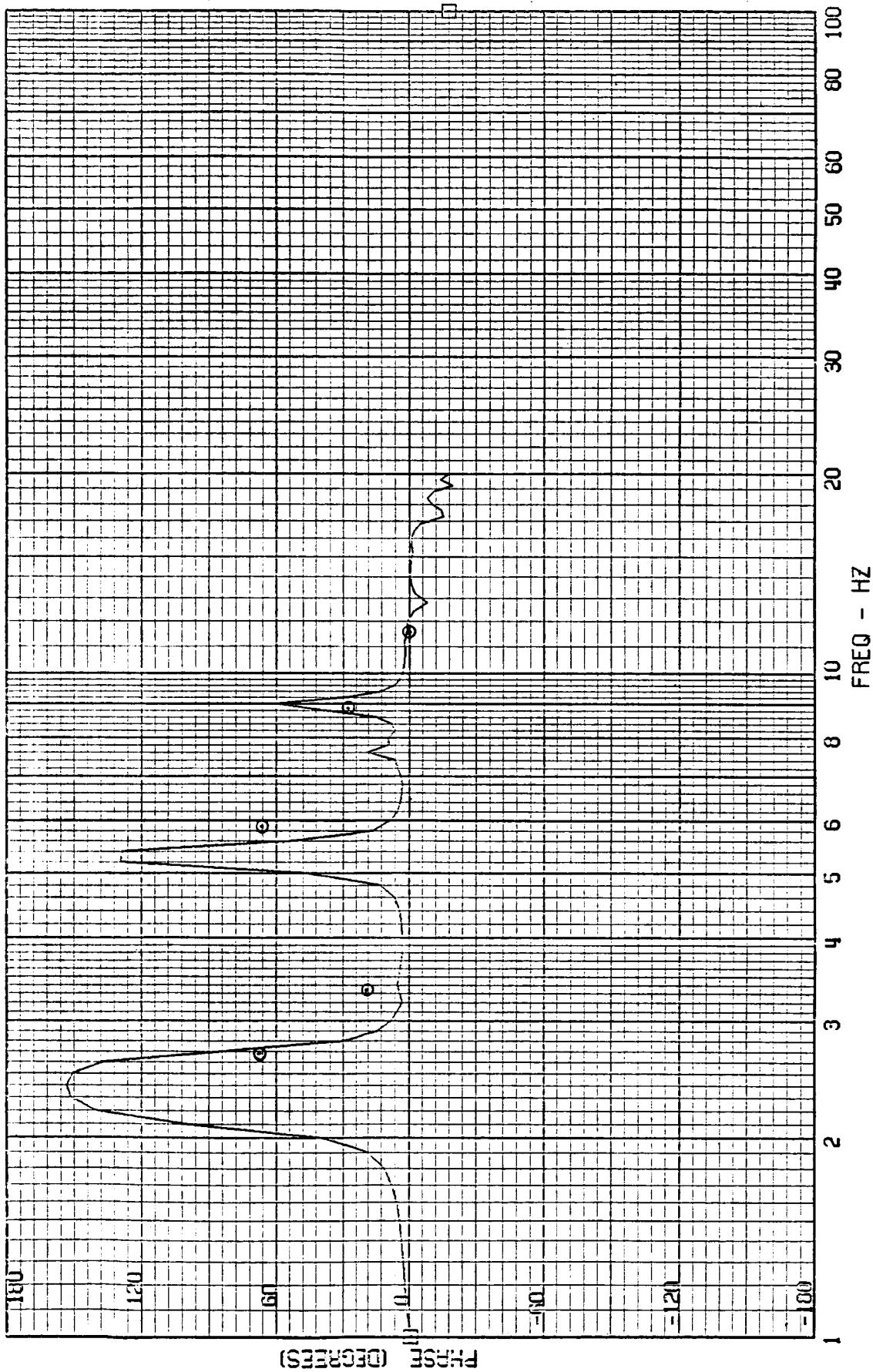

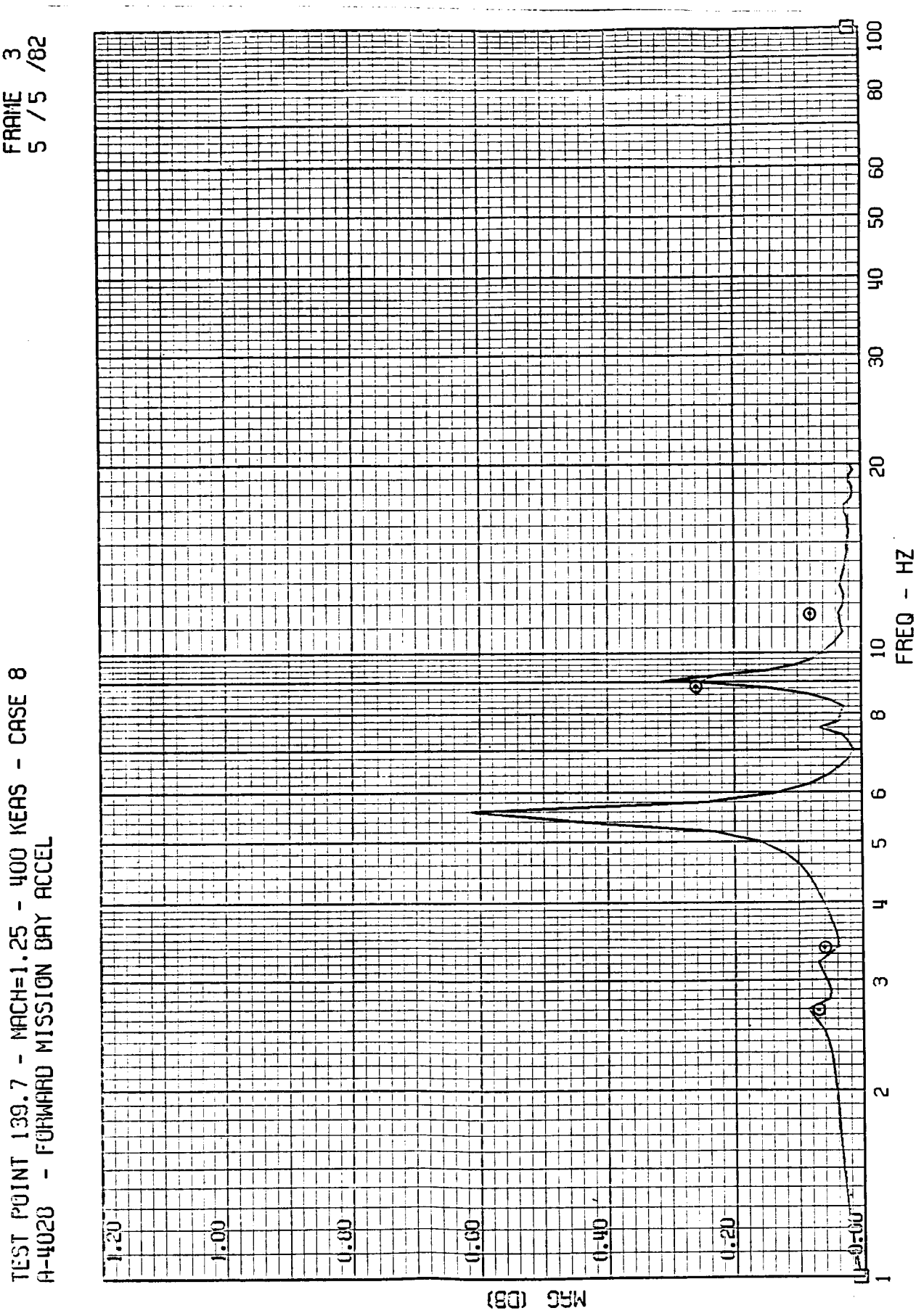
TEST POINT 139.7 - MACH=1.25 - 400 KEAS - CASE 8
A-4020 - FORWARD MISSION BAY ACCEL
FRAME 3
5 /5 /82
MAG (DB)
1.20
1.00
0.80
0.60
0.40
0.20
0.00
1
2
3
4
5
6
8
10
20
30
40
50
60
80
100
FREQ - HZ

ORIGINAL PAGE IS
OF POOR QUALITY

FRAME 3
5 /5 /82

TEST POINT 139.7 - MACH=1.25 - 400 KEAS - CASE 8
A-4020 - FORWARD MISSION BAY ACCEL

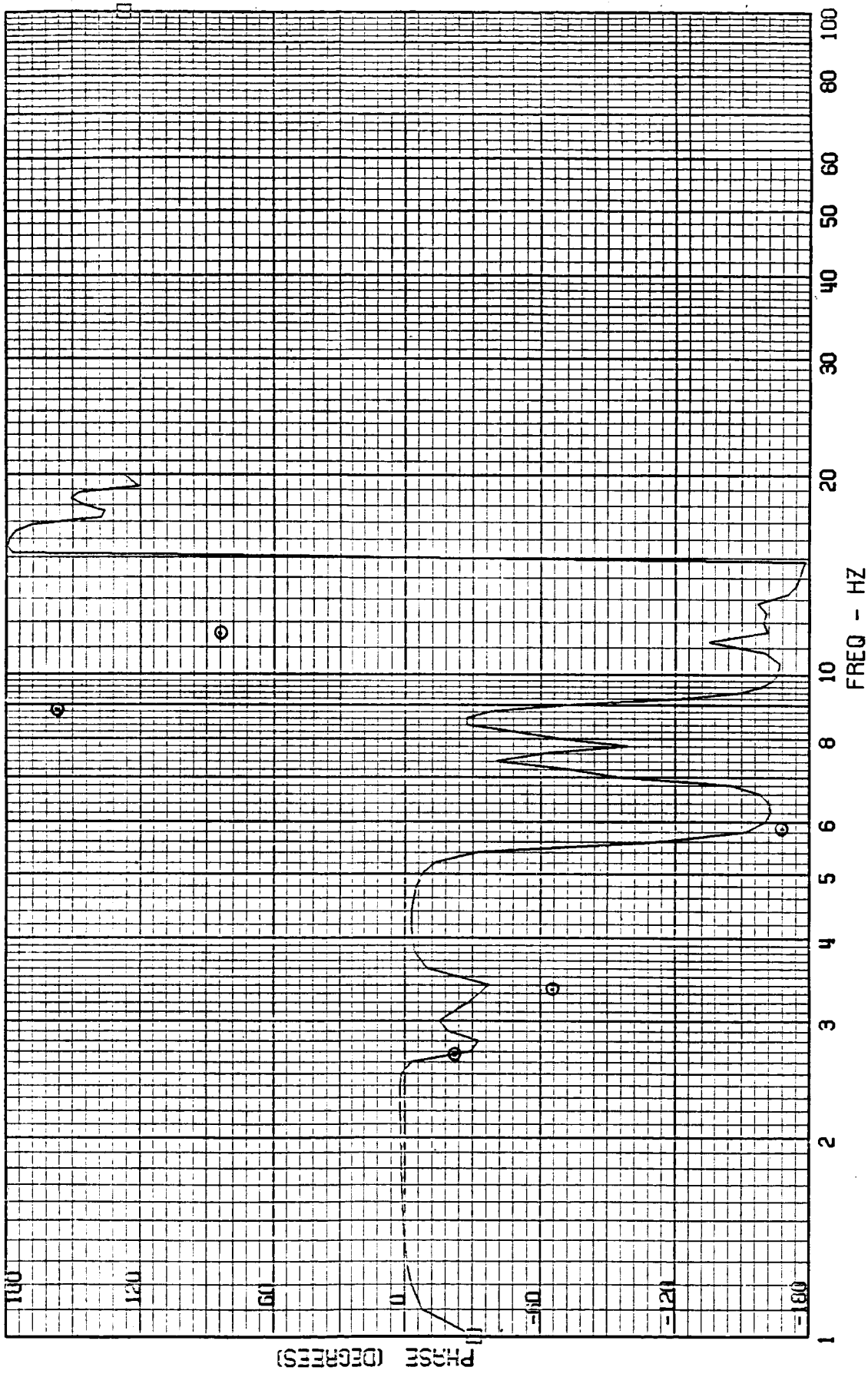

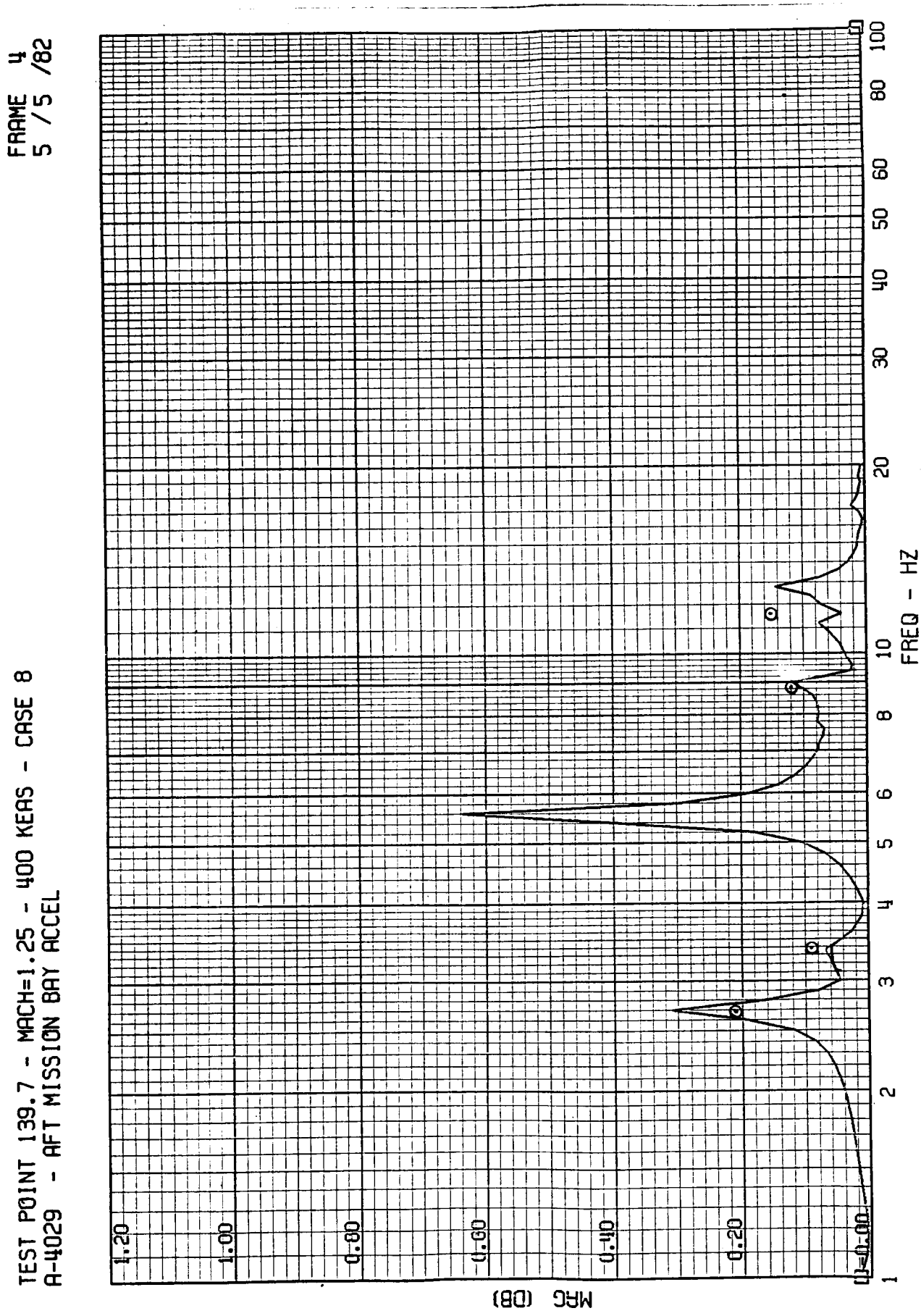
FRAME 4
5 /5 /82
TEST POINT 139.7 - MACH=1.25 - 400 KEAS - CASE 8
A-4029 - AFT MISSION BAY ACCEL
MAG (DB)
1.20
1.00
0.80
0.60
0.40
0.20
0=0.00
1
2
3
4
5
6
8
10
20
30
40
50
60
80
100
FREQ - HZ

FRAME 4
5 /5 /82

TEST POINT 139.7 - MACH=1.25 - 400 KEAS - CASE 8
A-4029 - AFT MISSION BAY ACCEL

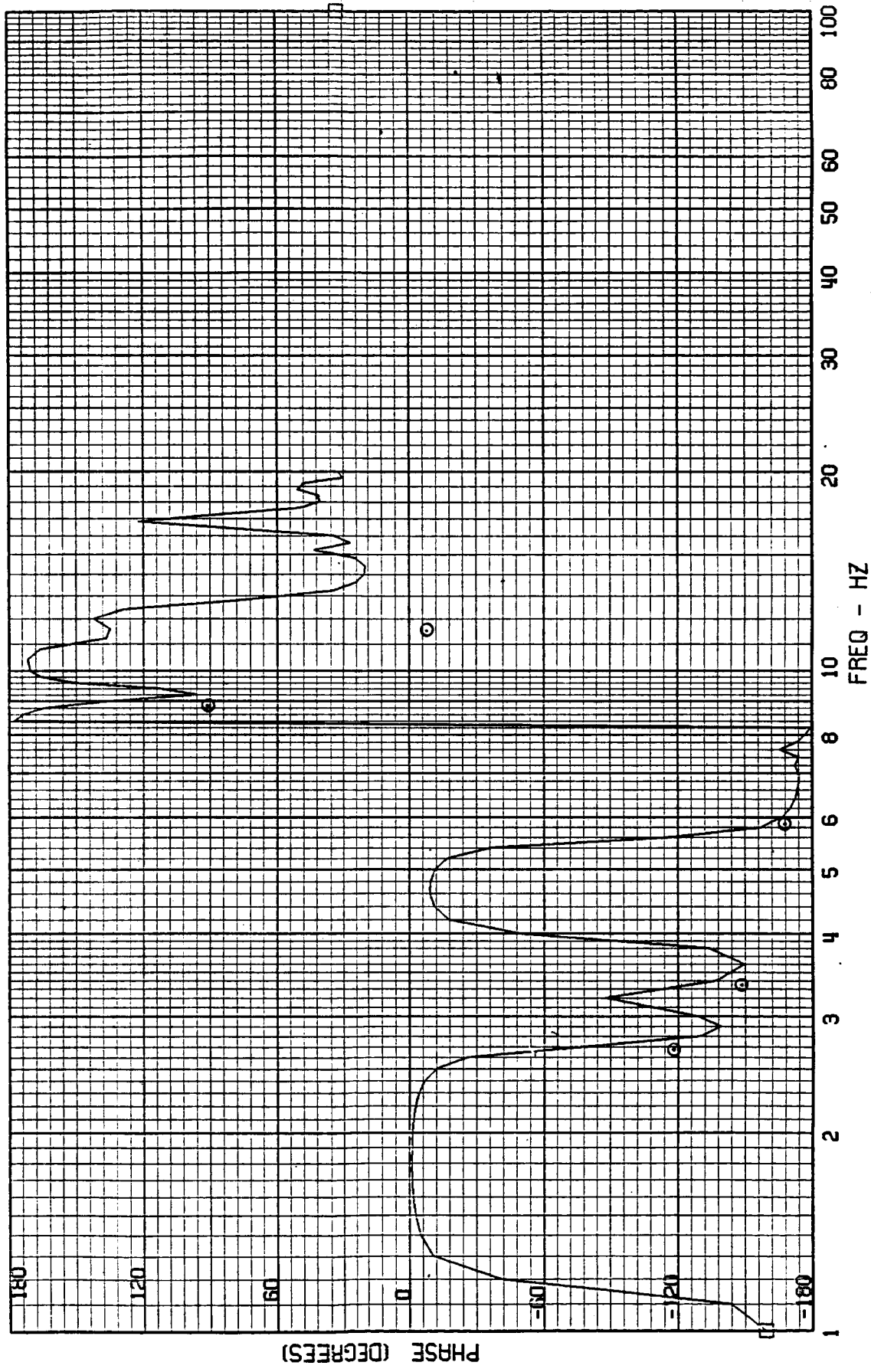

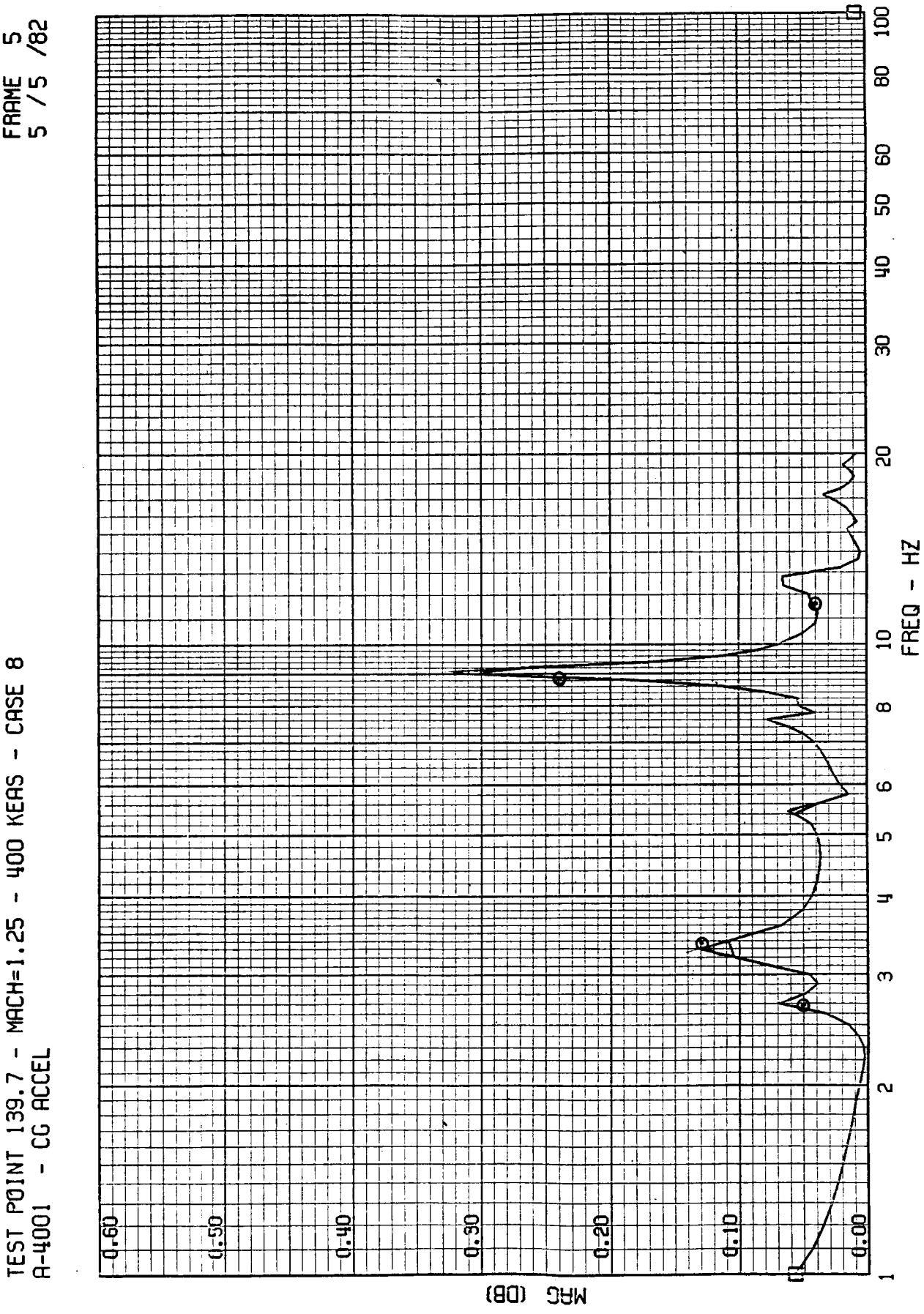
TEST POINT 139.7 - MACH=1.25 - 400 KEAS - CASE 8
A-4001 - CG ACCEL
FRAME 5
5 /5 /82
MAG (DB)
0.60
0.50
0.40
0.30
0.20
0.10
0.00
1
2
3
4
5
6
8
10
20
30
40
50
60
80
100
FREQ - HZ

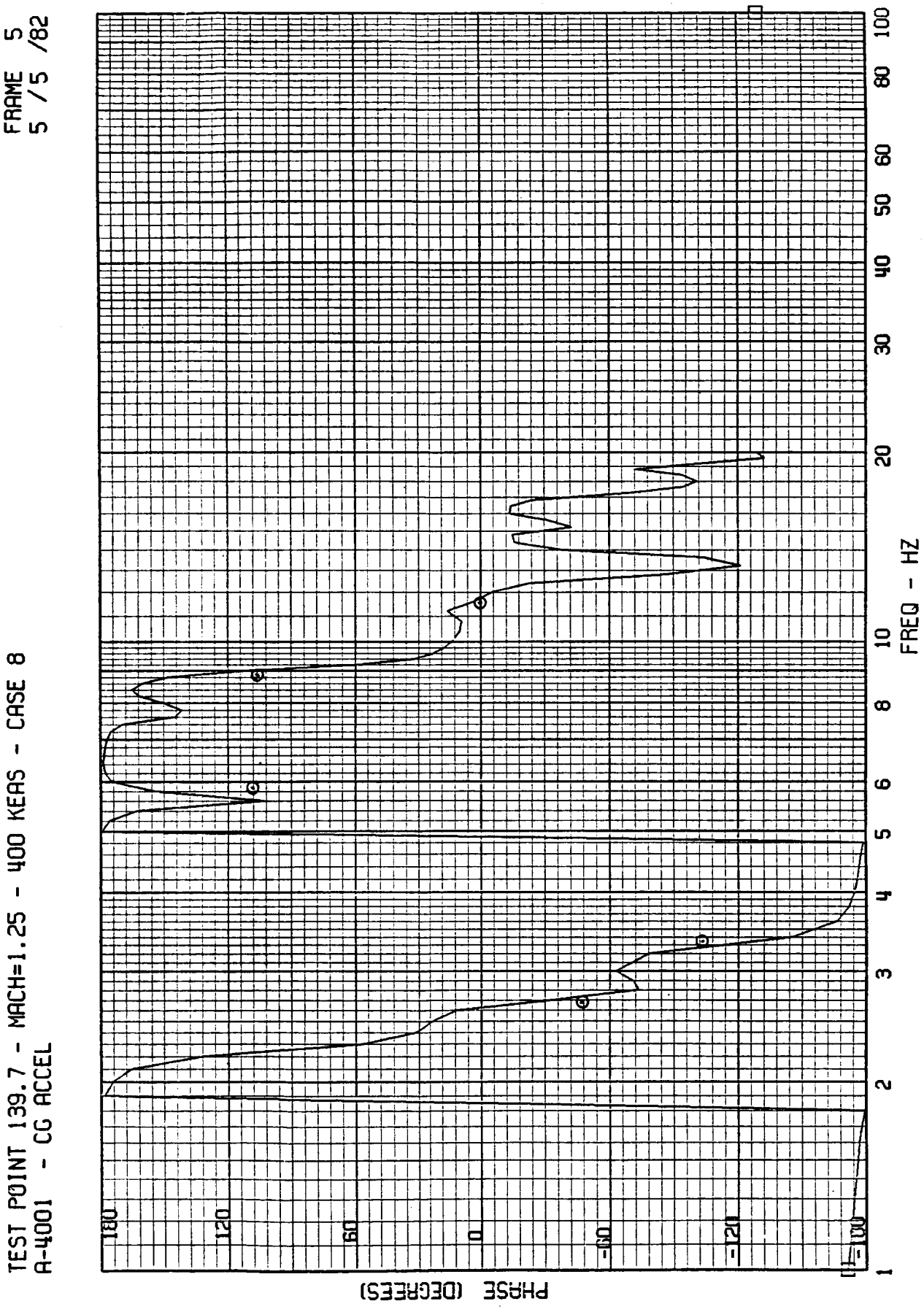
TEST POINT 139.7 - MACH=1.25 - 400 KEAS - CASE 8
A-4001 - CG ACCEL
FRAME 5
5 /5 /82
PHASE (DEGREES)
180
120
60
0
-60
-120
-180
1
2
3
4
5
6
8
10
20
30
40
50
60
80
100
FREQ - HZ

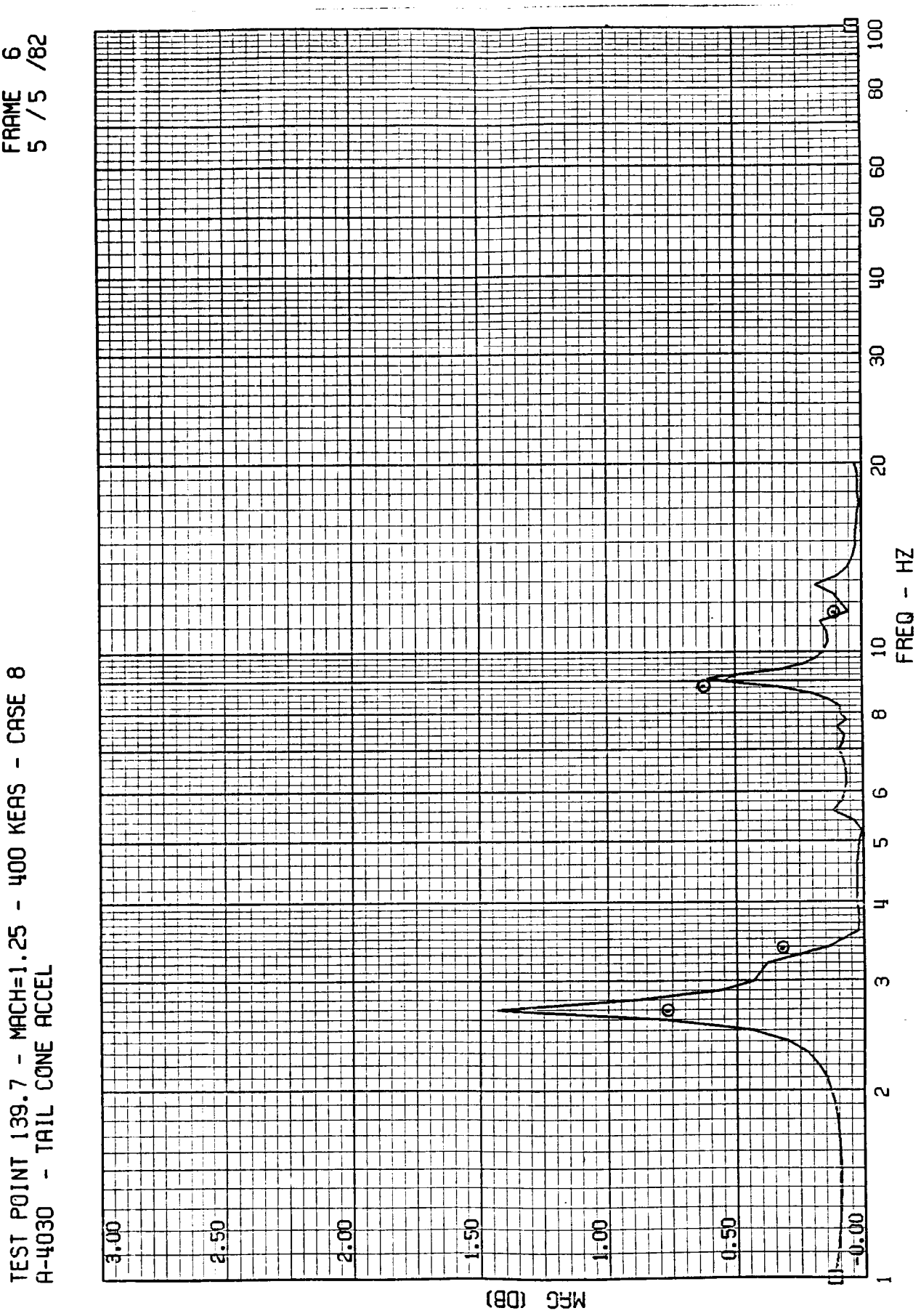
TEST POINT 139.7 - MACH=1.25 - 400 KEAS - CASE 8
A-4030 - TAIL CONE ACCEL
FRAME 6
5 /5 /82
MAG (DB)
3.00
2.50
2.00
1.50
1.00
0.50
-0.00
FREQ - HZ
1
2
3
4
5
6
8
10
20
30
40
50
60
80
100

ORIGINAL PAGE IS
OF POOR QUALITY

FRAME 6
5 /5 /82

TEST POINT 139.7 - MACH=1.25 - 400 KEAS - CASE 8
A-4030 - TAIL CONE ACCEL

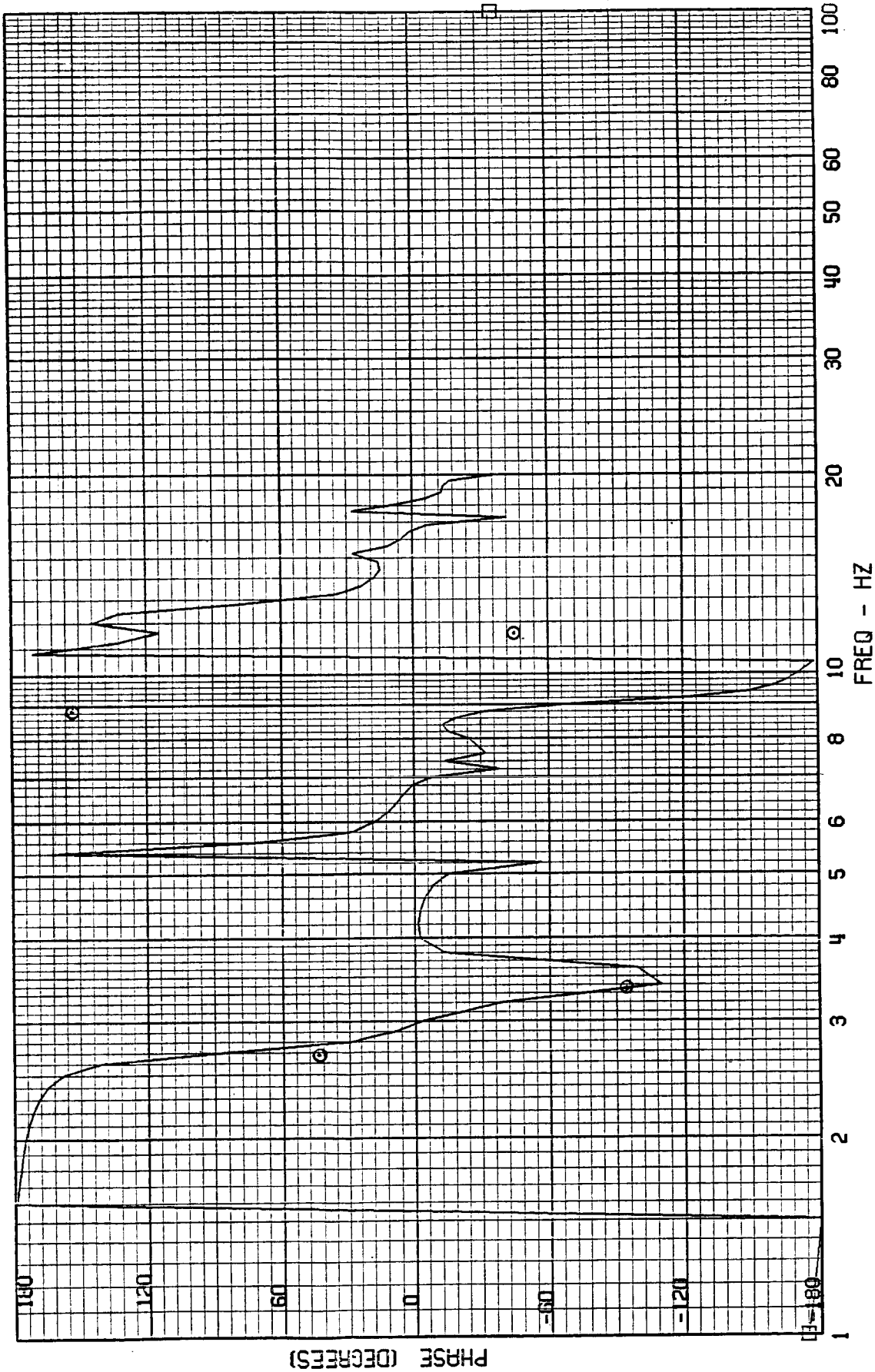

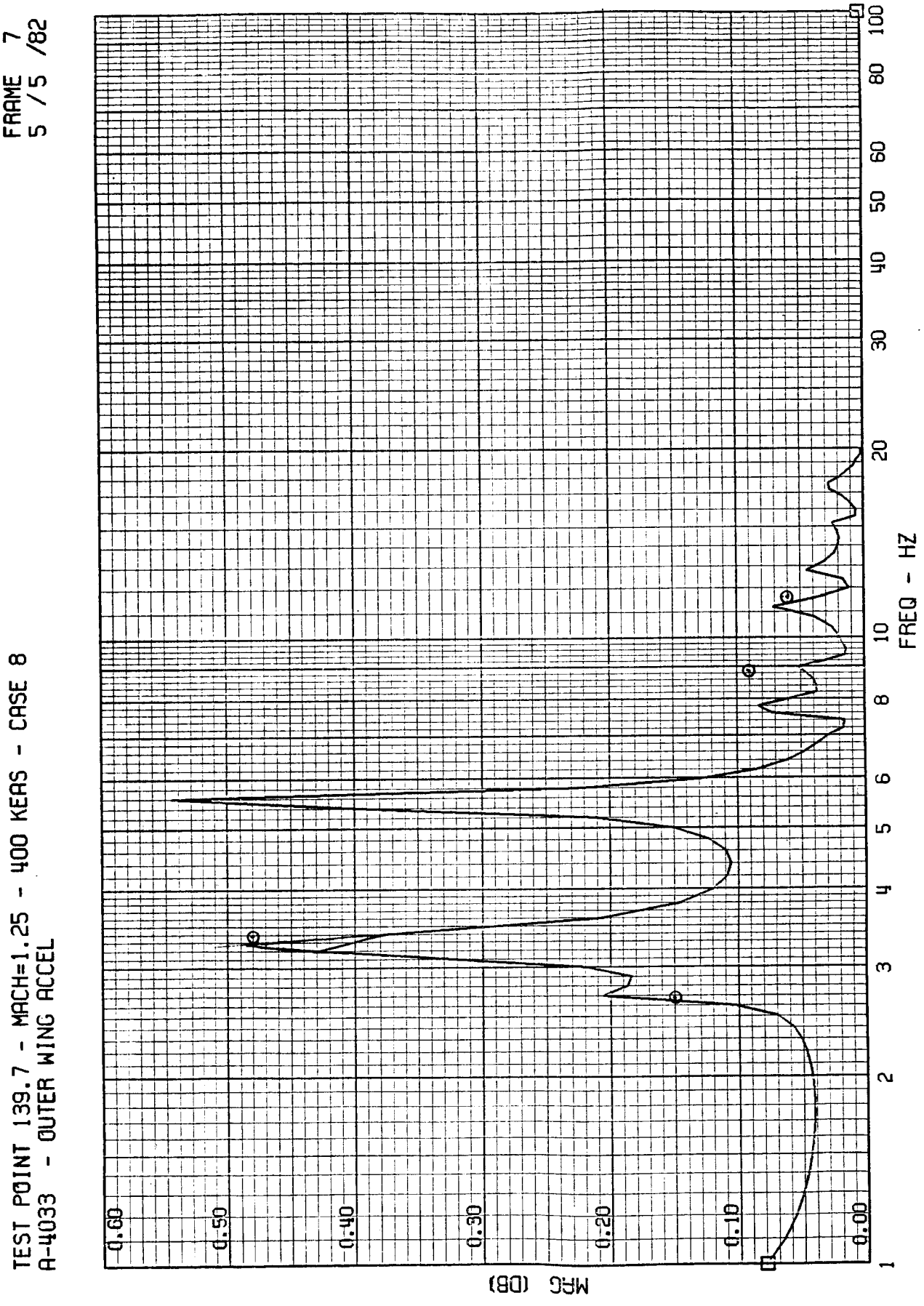
TEST POINT 139.7 - MACH=1.25 - 400 KEAS - CASE 8
A-4033 - OUTER WING ACCEL
FRAME 7
5 /5 /82
MAG (DB)
0.60
0.50
0.40
0.30
0.20
0.10
0.00
1
2
3
4
5
6
8
10
20
30
40
50
60
80
100
FREQ - HZ

ORIGINAL PAGE IS
OF POOR QUALITY

FRAME 7
5 /5 /82

TEST POINT 139.7 - MACH=1.25 - 400 KEAS - CASE 8
A-4033 - OUTER WING ACCEL

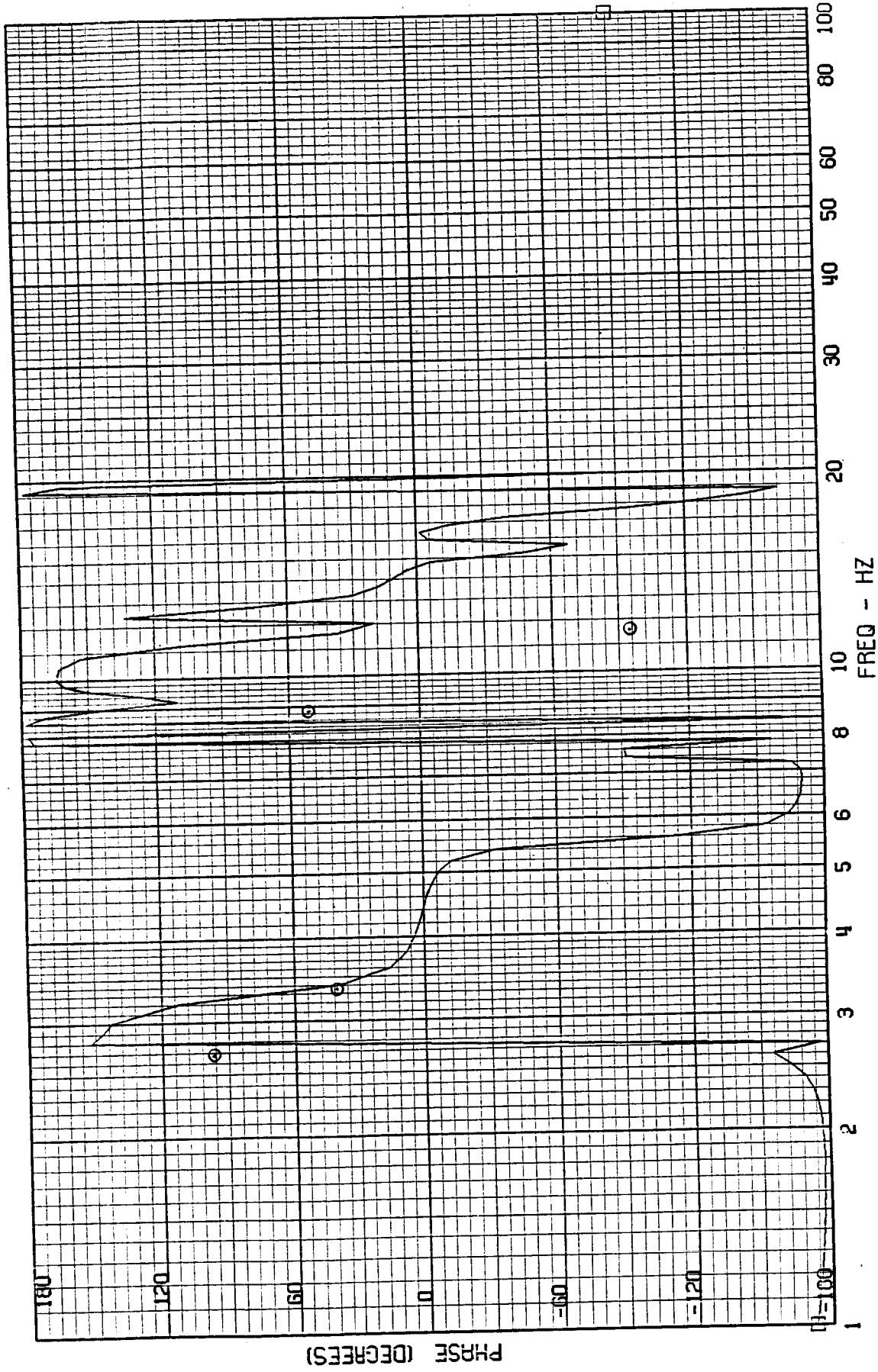

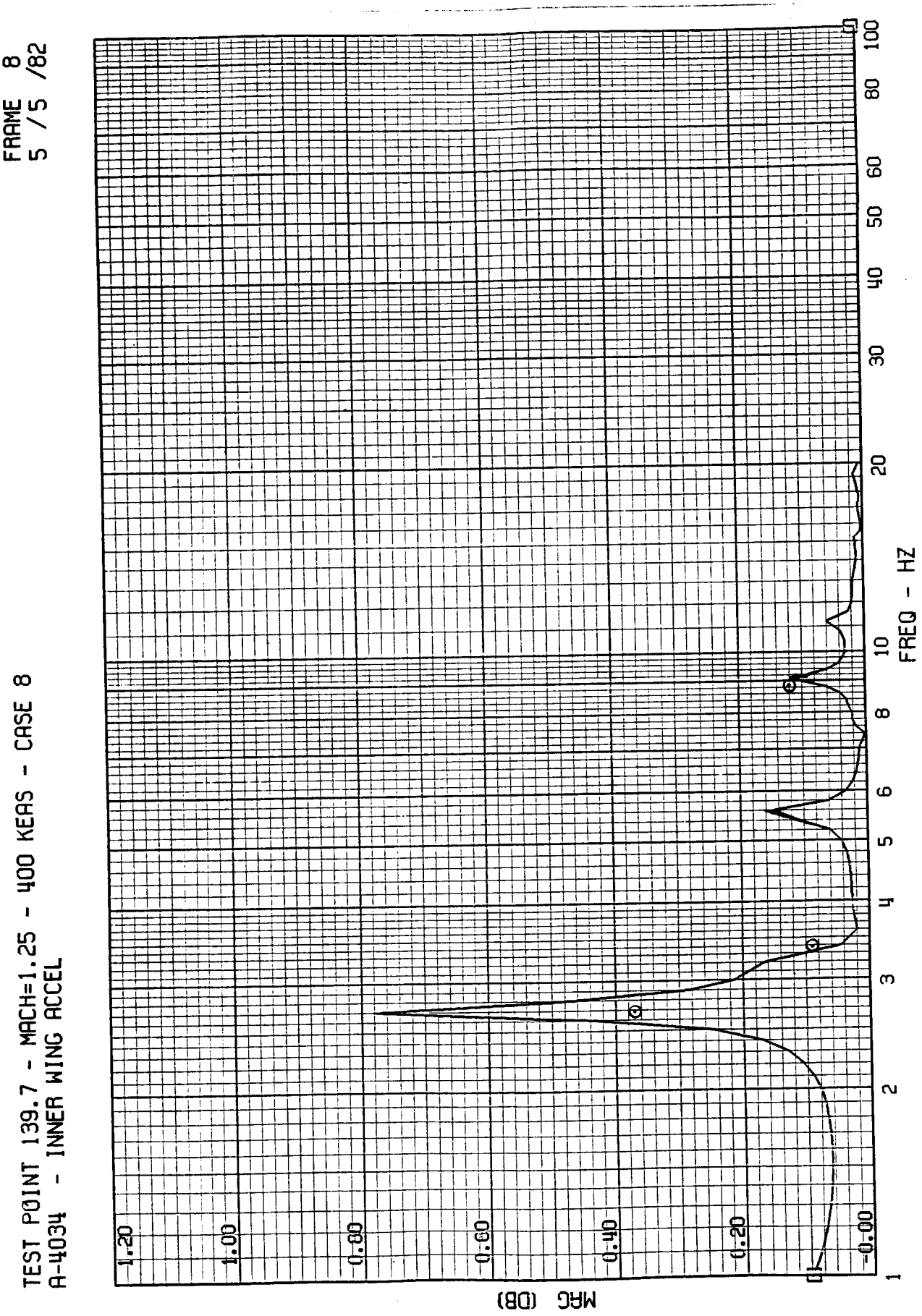
FRAME 8
5 /5 /82
TEST POINT 139.7 - MACH=1.25 - 400 KEAS - CASE 8
A-4034 - INNER WING ACCEL
MAG (DB)
1.20
1.00
0.80
0.60
0.40
0.20
-0.00
FREQ - HZ
1
2
3
4
5
6
8
10
20
30
40
50
60
80
100

ORIGINAL PAGE IS
OF POOR QUALITY

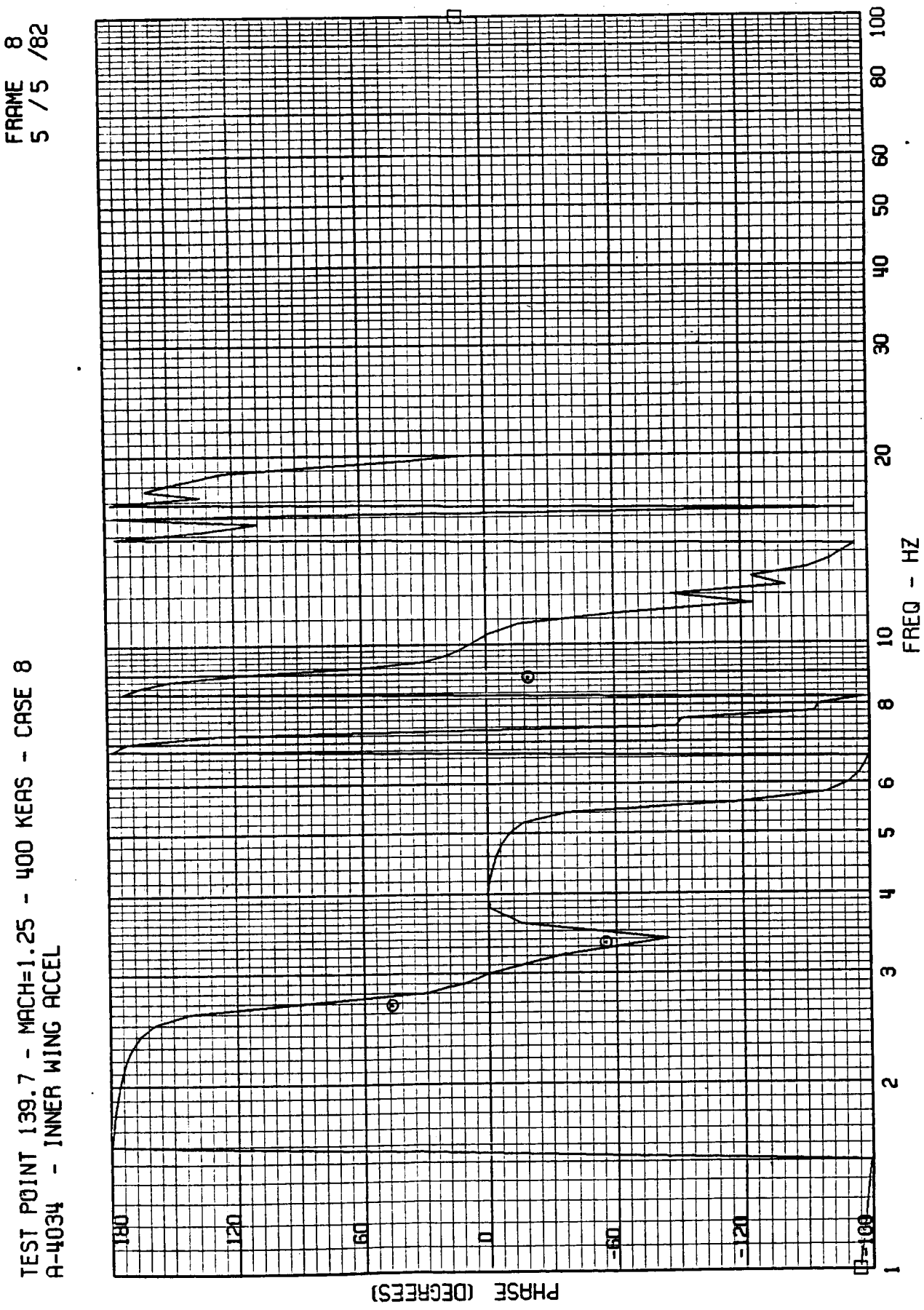

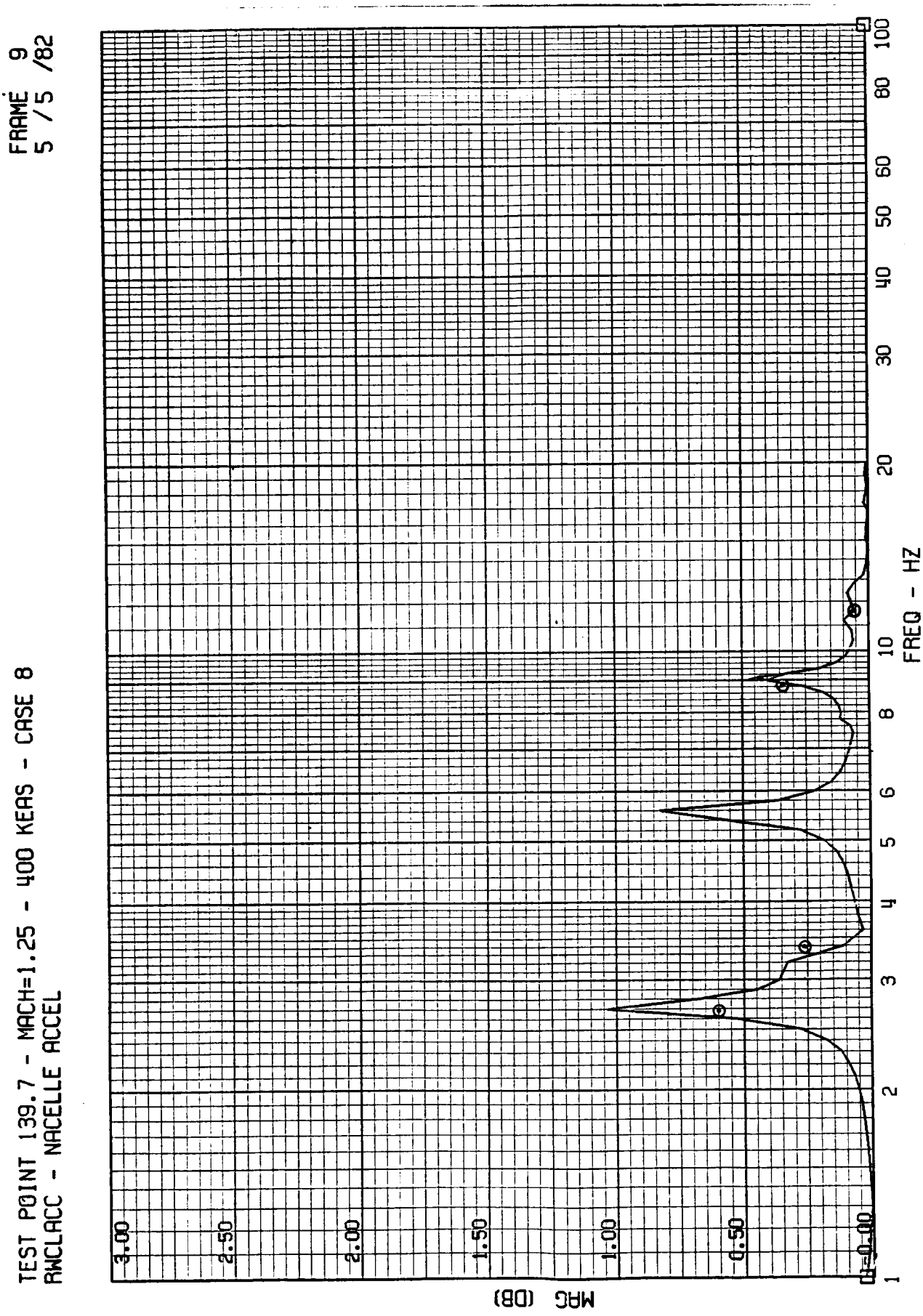
TEST POINT 139.7 - MACH=1.25 - 400 KEAS - CASE 8
RWCLACC - NACELLE ACCEL
FRAME 9
5 /5 /82
MAG (DB)
3.00
2.50
2.00
1.50
1.00
0.50
0.00
FREQ - HZ
1
2
3
4
5
6
8
10
20
30
40
50
60
80
100

FRAME 9
5 /5 /82

TEST POINT 139.7 - MACH=1.25 - 400 KEAS - CASE 8
RWCLACC - NACELLE ACCEL

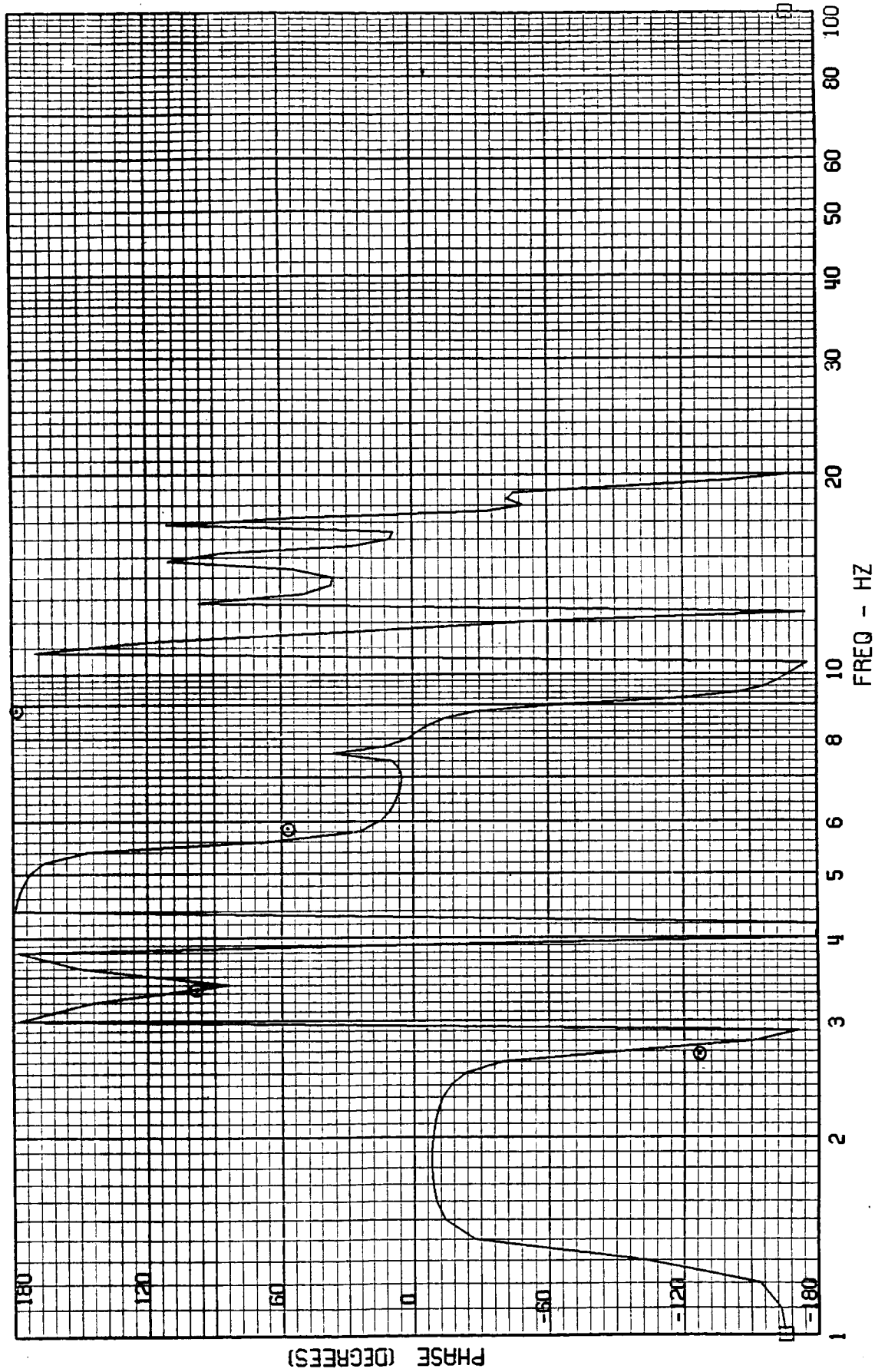

FRAME 10
5 /5 /82

TEST POINT 139.7 - MACH=1.25 - 400 KEAS - CASE 8
RAUDACC - RUDDER ACCEL

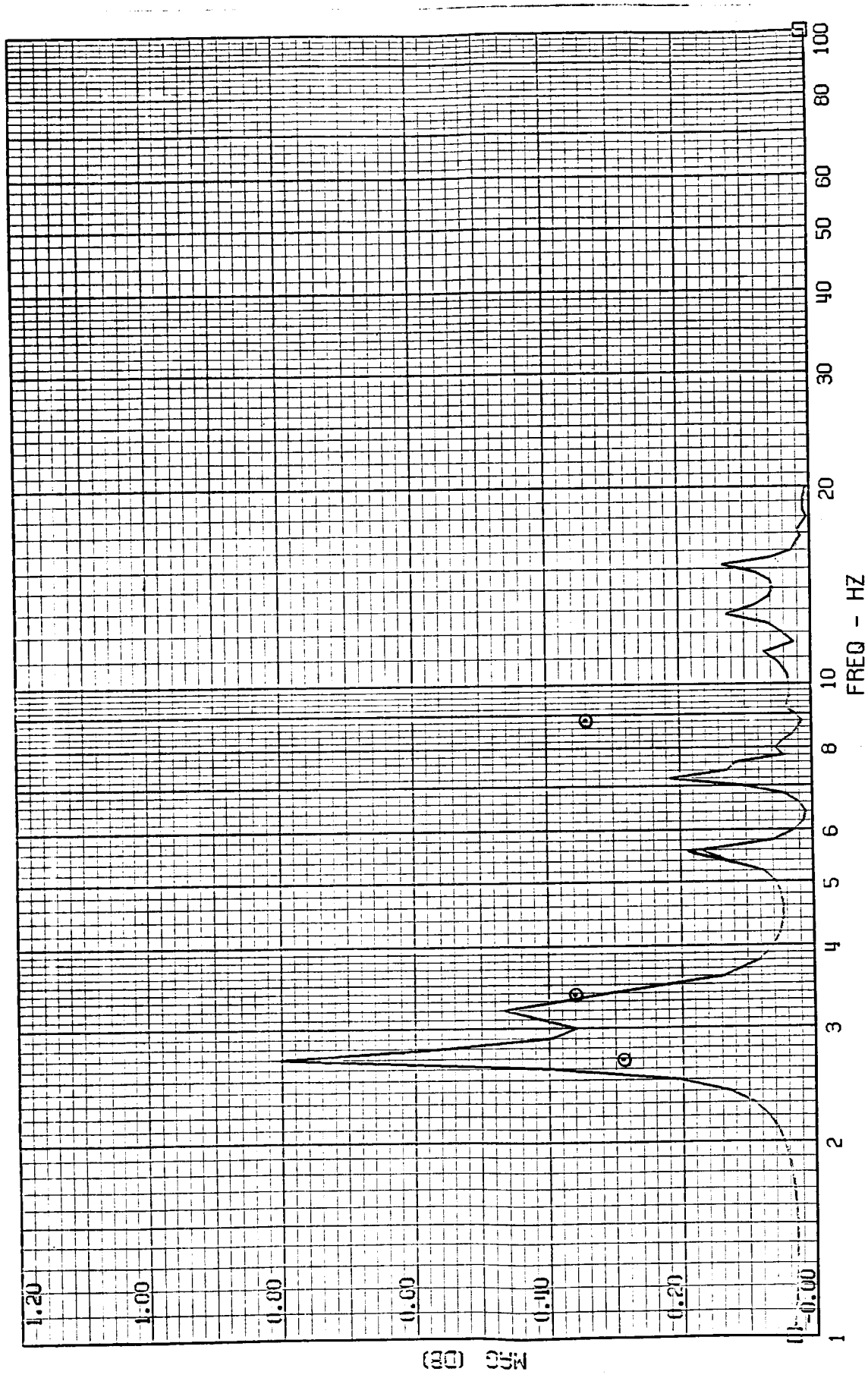

FRAME 10
5 /5 /82

TEST POINT 139.7 - MACH=1.25 - 400 KEAS - CASE 8
RRUDACC - RUDDER ACCEL

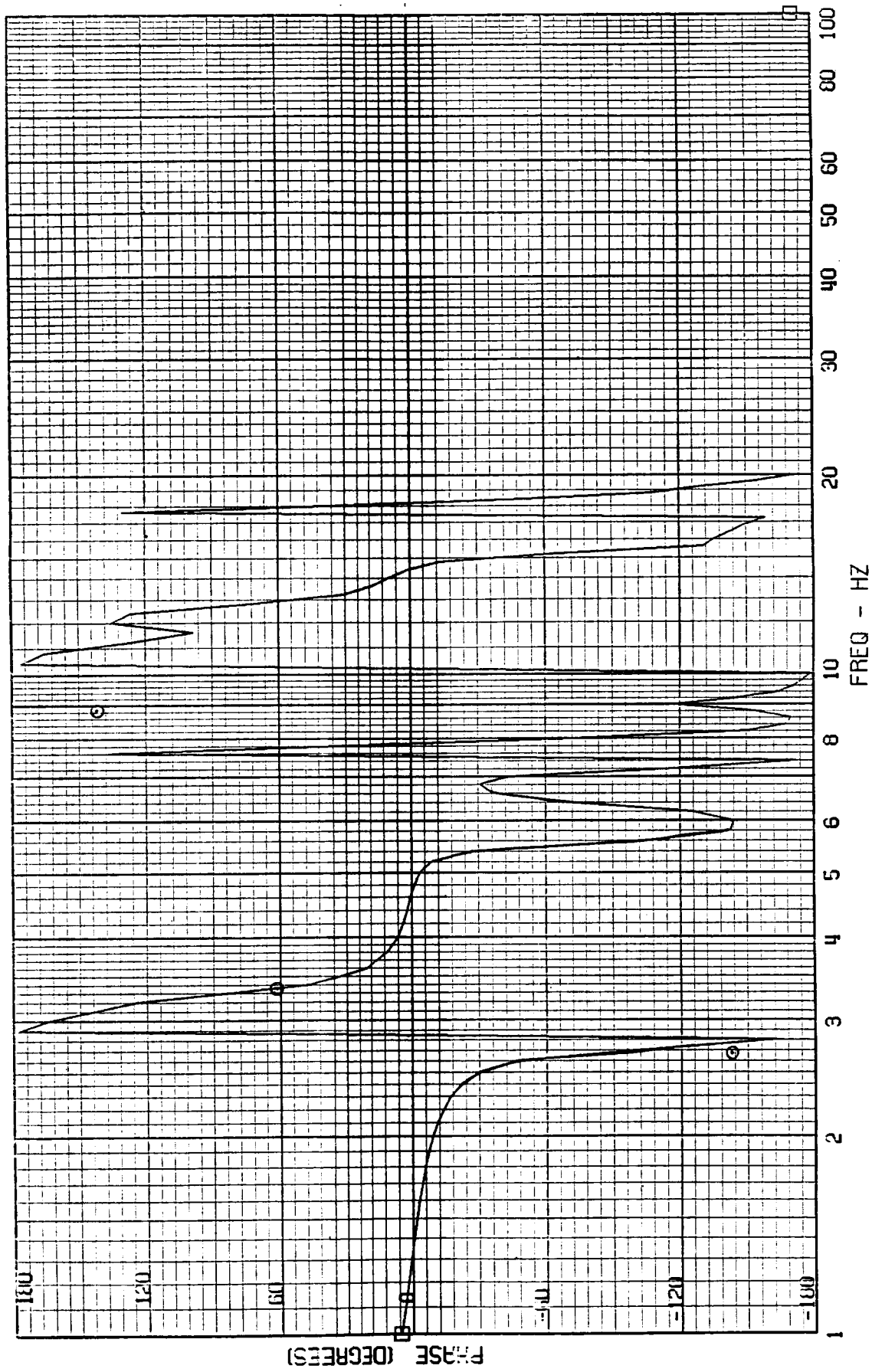

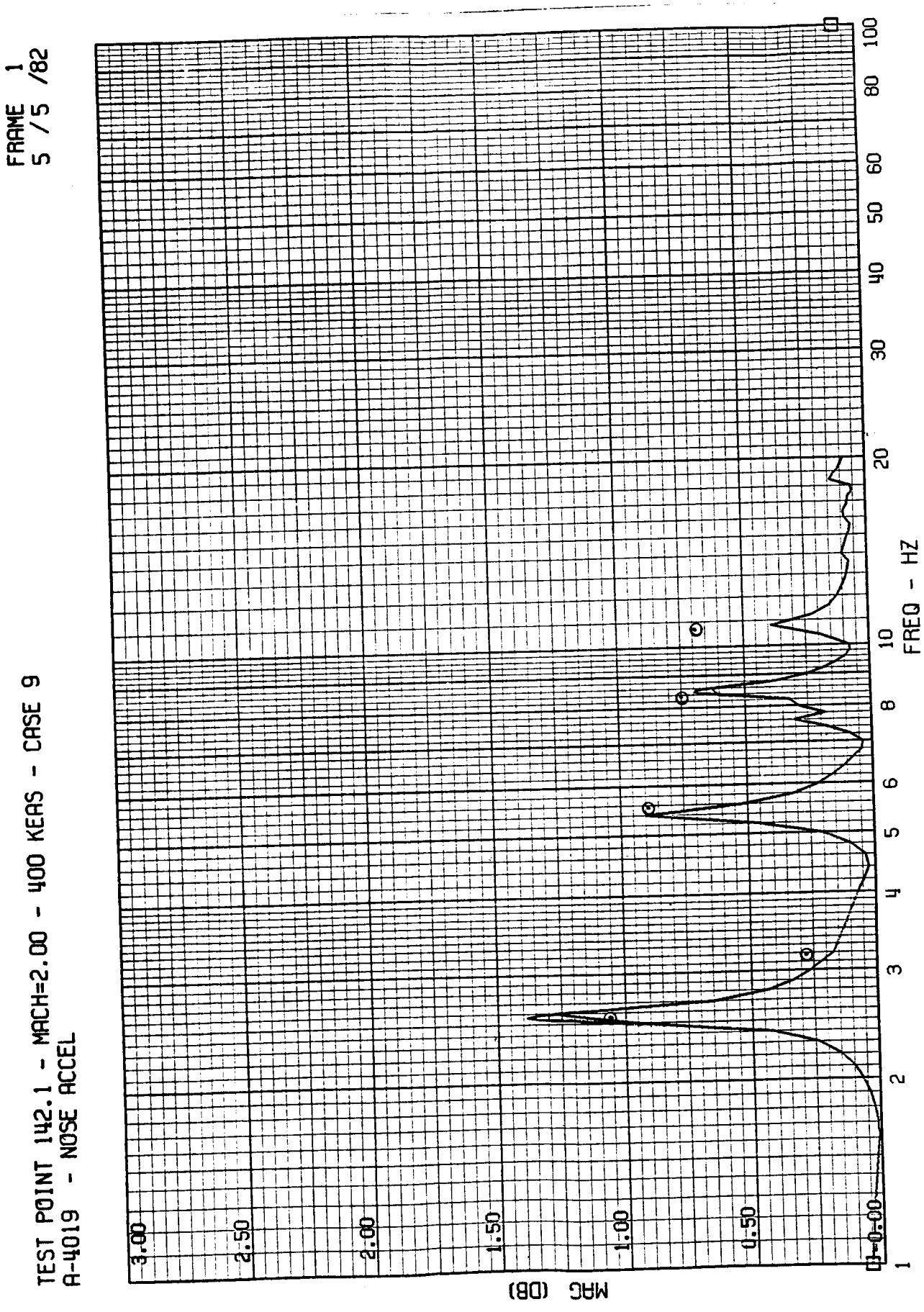
FRAME 1
5 /5 /82
TEST POINT 142.1 - MACH=2.00 - 400 KEAS - CASE 9
A-4019 - NOSE ACCEL
MAG (DB)
3.00
2.50
2.00
1.50
1.00
0.50
0.00
FREQ - HZ
1
2
3
4
5
6
8
10
20
30
40
50
60
80
100

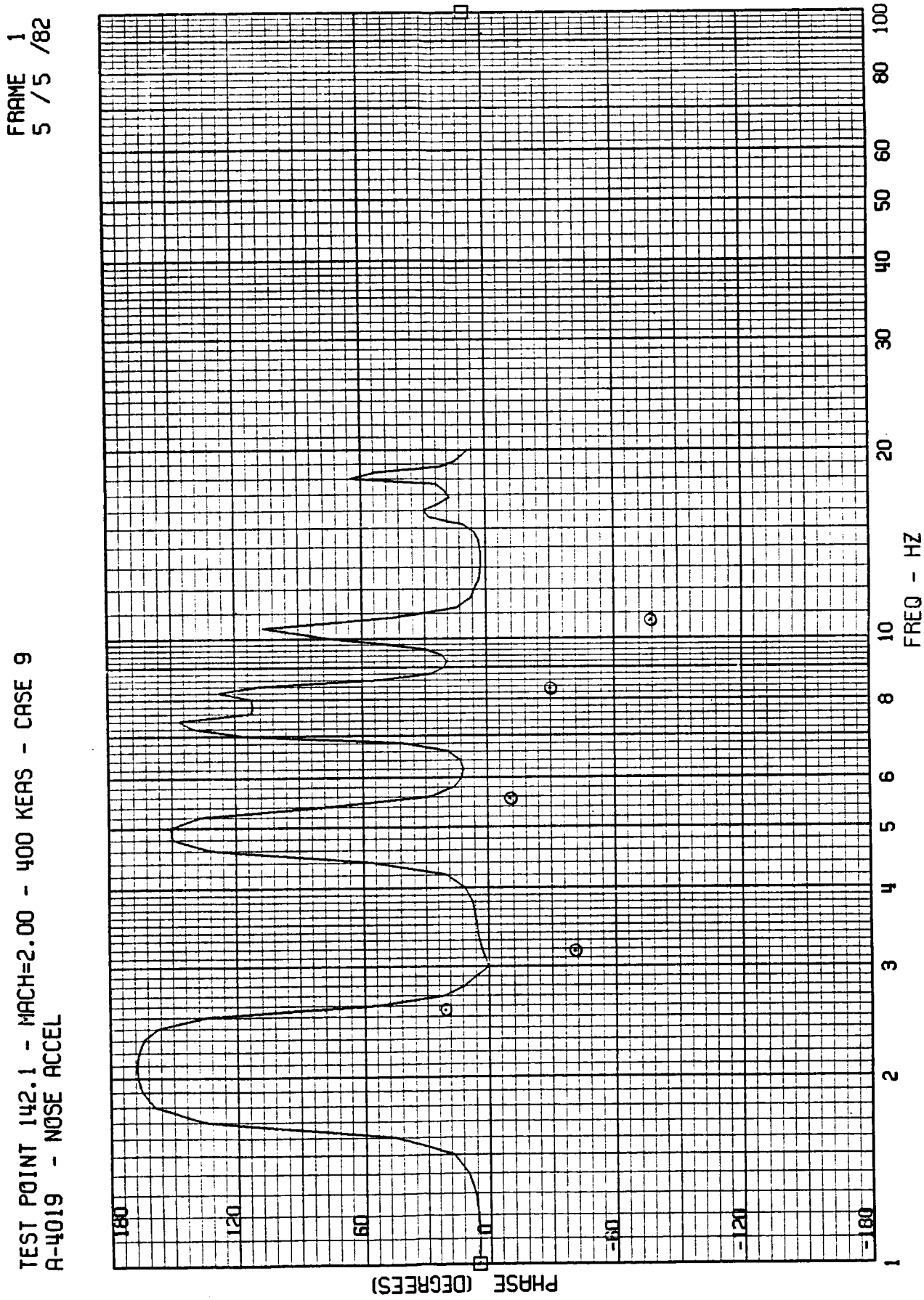

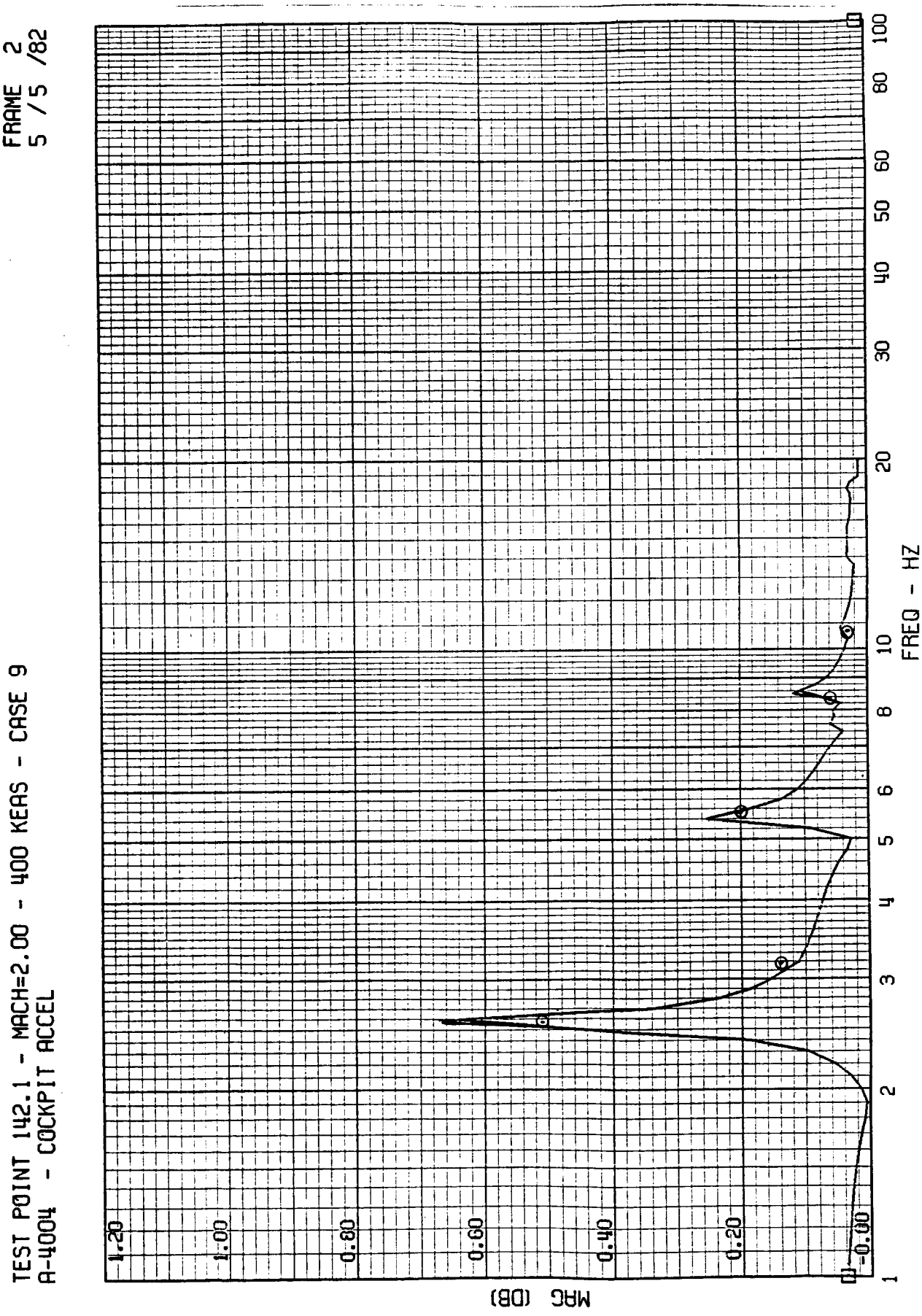
FRAME 2
5 /5 /82
TEST POINT 142.1 - MACH=2.00 - 400 KEAS - CASE 9
A-4004 - COCKPIT ACCEL
MAG (DB)
1.20
1.00
0.80
0.60
0.40
0.20
0.00
FREQ - HZ
1
2
3
4
5
6
8
10
20
30
40
50
60
80
100

ORIGINAL PAGE IS
OF POOR QUALITY

FRAME 2
5 /5 /82

TEST POINT 142.1 - MACH=2.00 - 400 KEAS - CASE 9
A-4004 - COCKPIT ACCEL

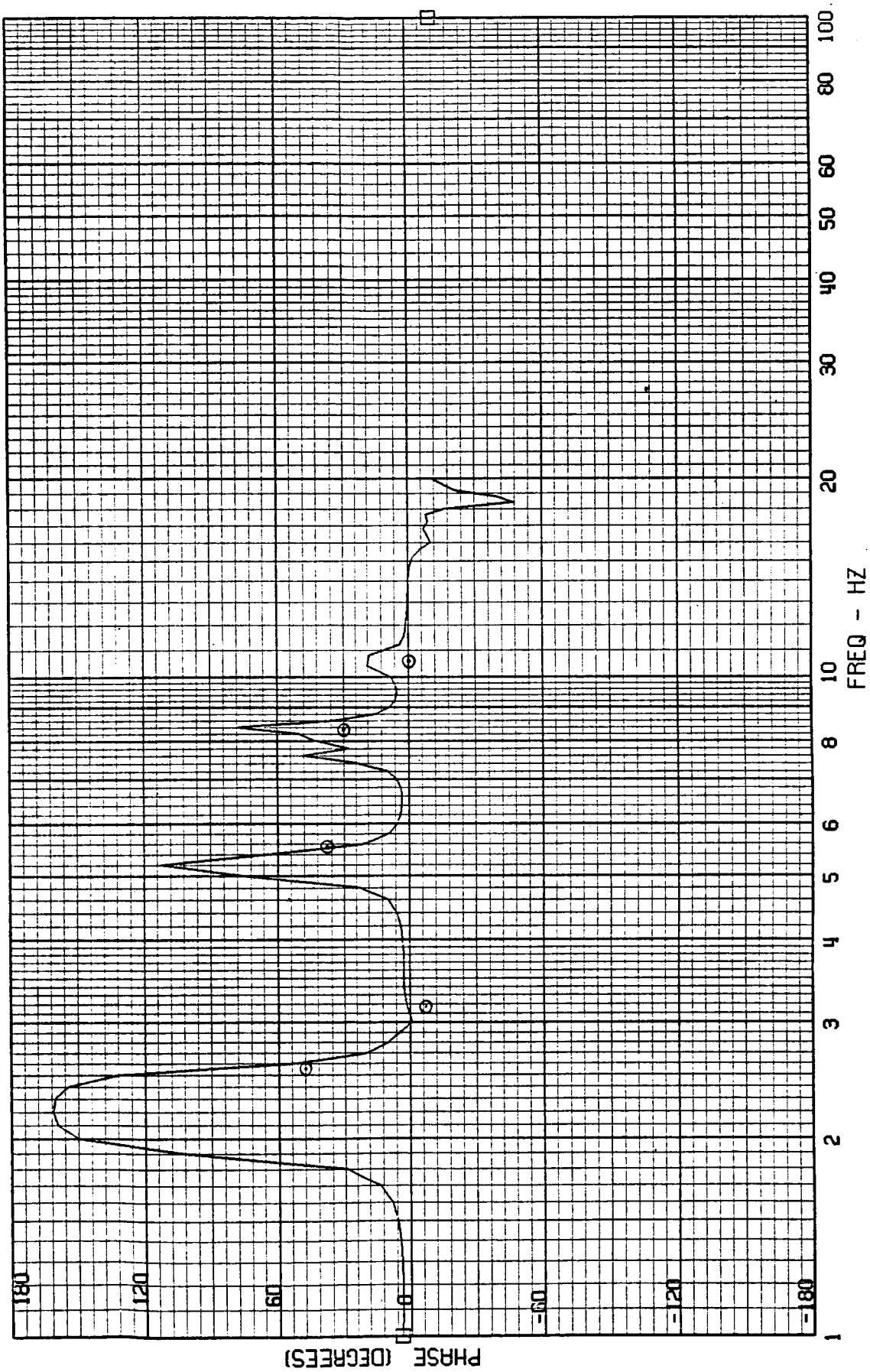

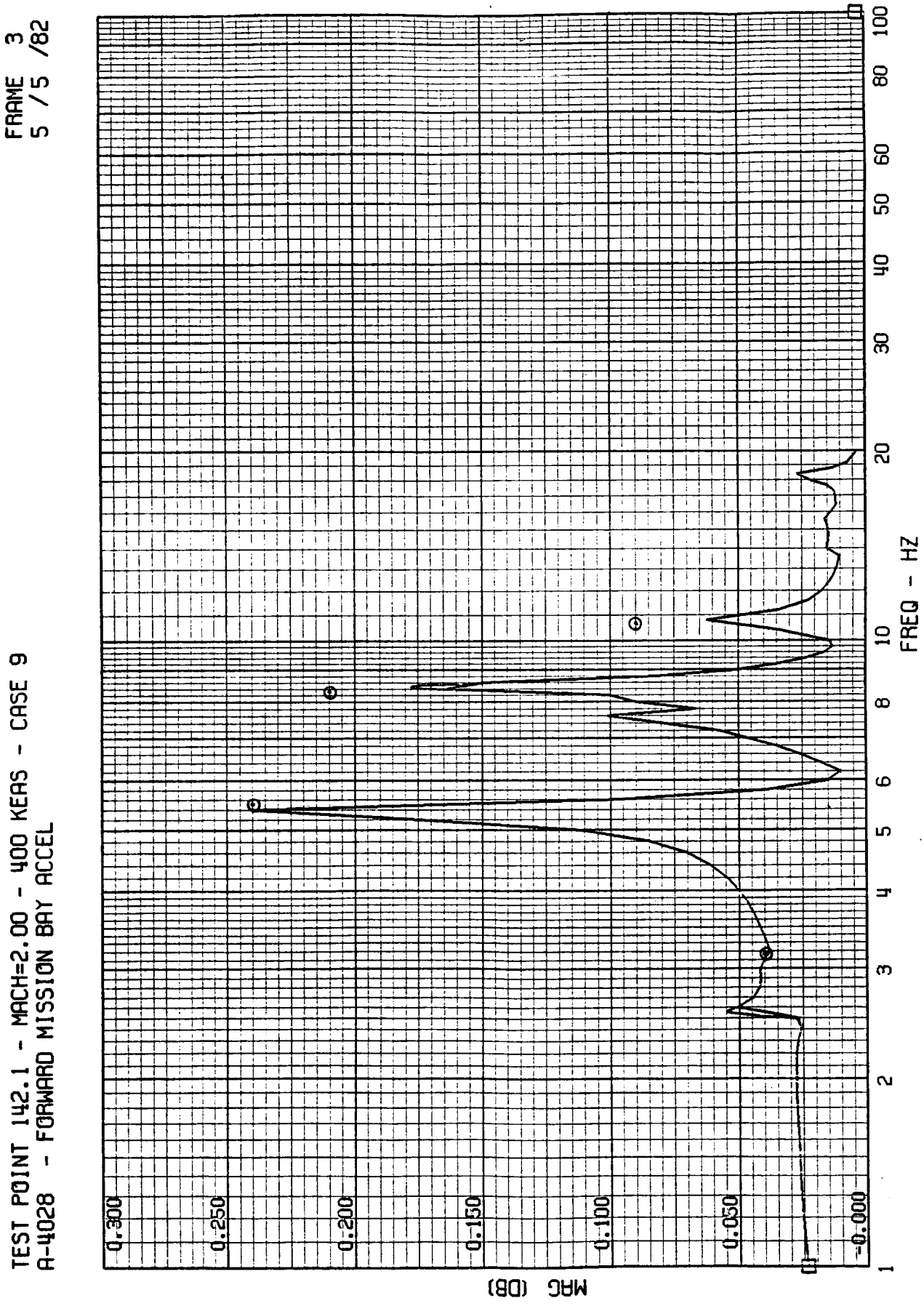
TEST POINT 142.1 - MACH=2.00 - 400 KEAS - CASE 9
A-4028 - FORWARD MISSION BAY ACCEL
FRAME 3
5 /5 /82
MAG (DB)
0.300
0.250
0.200
0.150
0.100
0.050
-0.000
FREQ - HZ
1
2
3
4
5
6
8
10
20
30
40
50
60
80
100

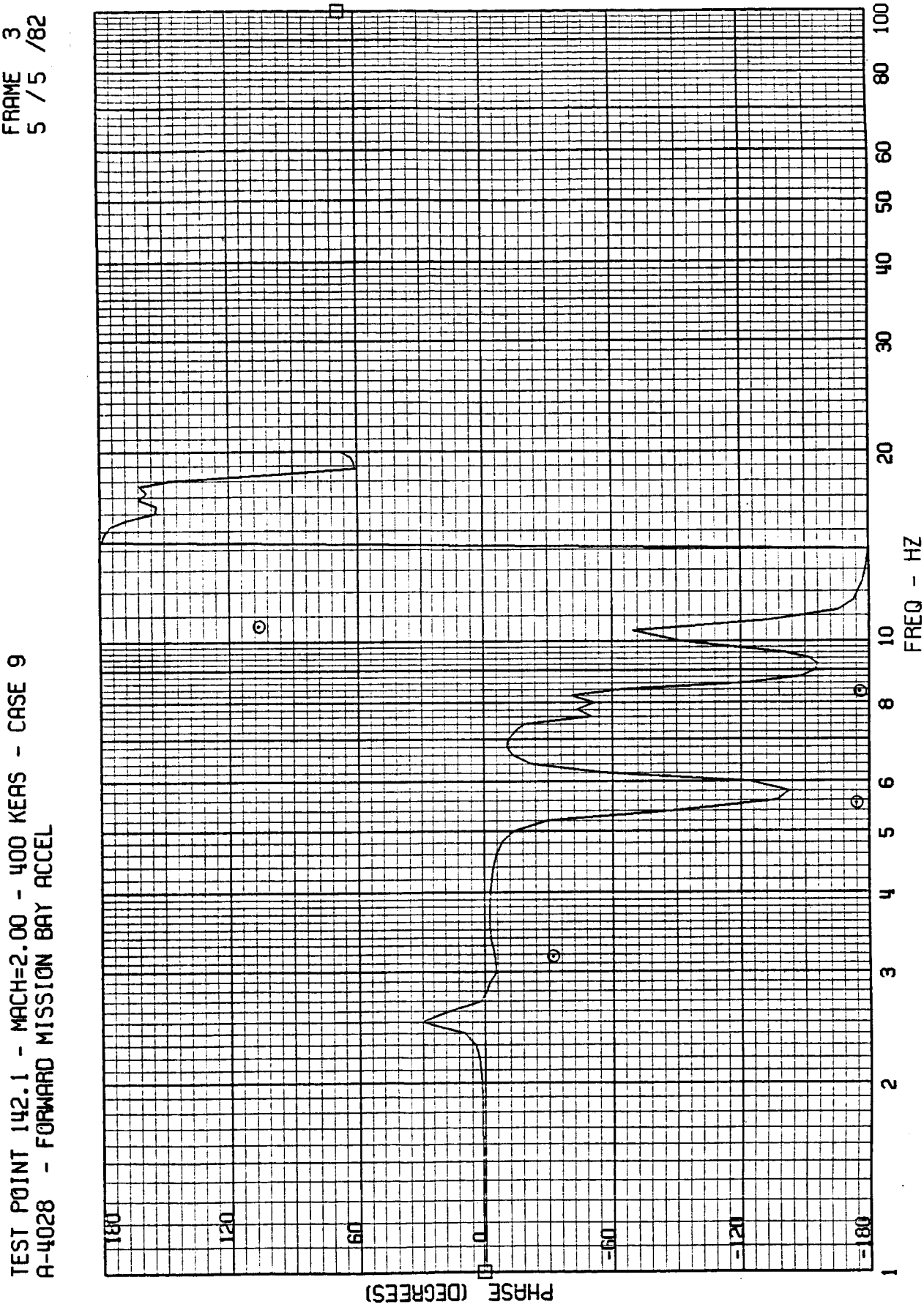
TEST POINT 142.1 - MACH=2.00 - 400 KEAS - CASE 9
A-4028 - FORWARD MISSION BAY ACCEL
FRAME 3
5 /5 /82
PHASE (DEGREES)
180
120
60
0
-60
-120
-180
1
2
3
4
5
6
8
10
20
30
40
50
60
80
100
FREQ - HZ

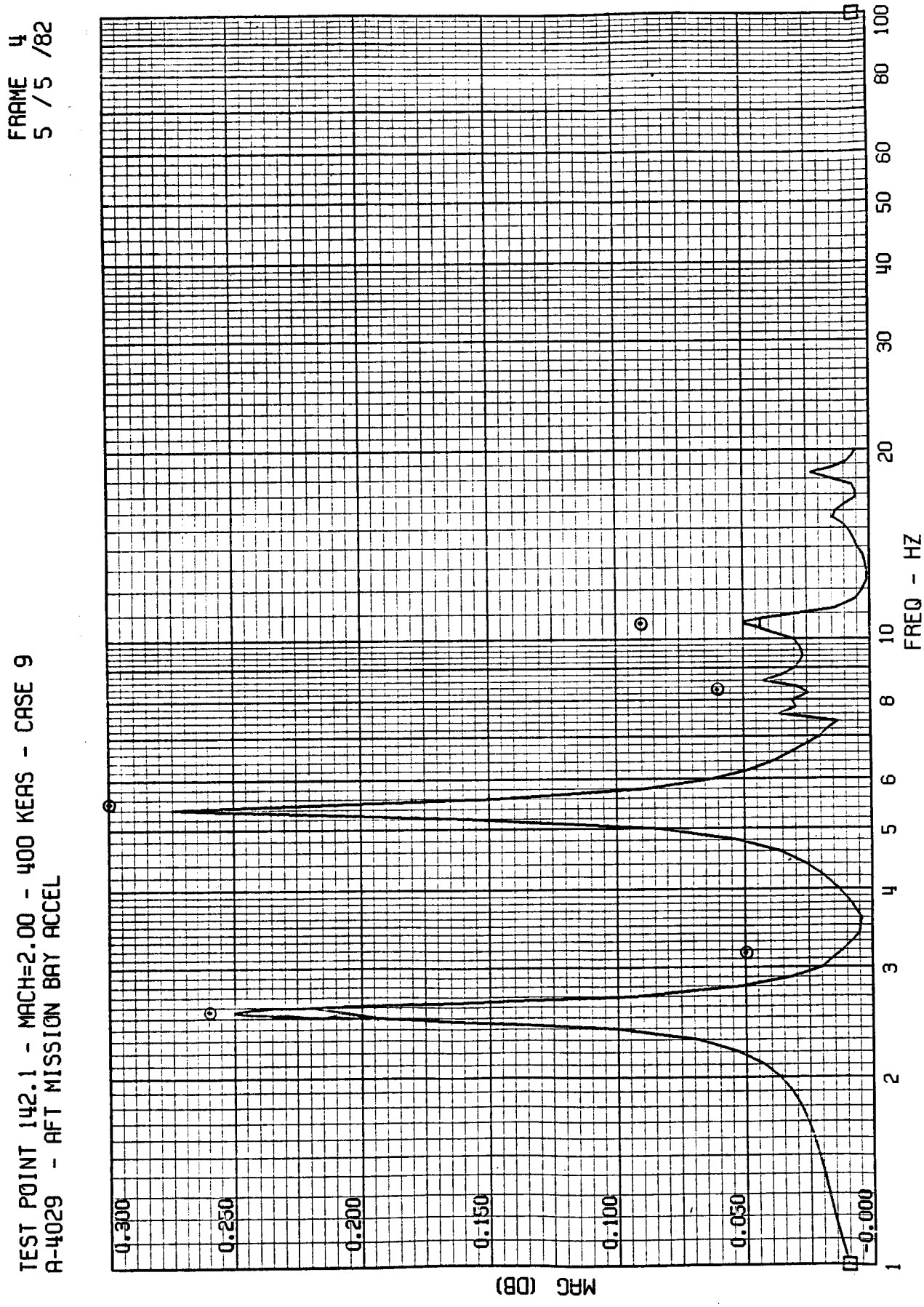
TEST POINT 142.1 - MACH=2.00 - 400 KEAS - CASE 9
A-4029 - AFT MISSION BAY ACCEL
FRAME 4
5 /5 /82
MAG (DB)
0.300
0.250
0.200
0.150
0.100
0.050
-0.000
1
2
3
4
5
6
8
10
20
30
40
50
60
80
100
FREQ - HZ

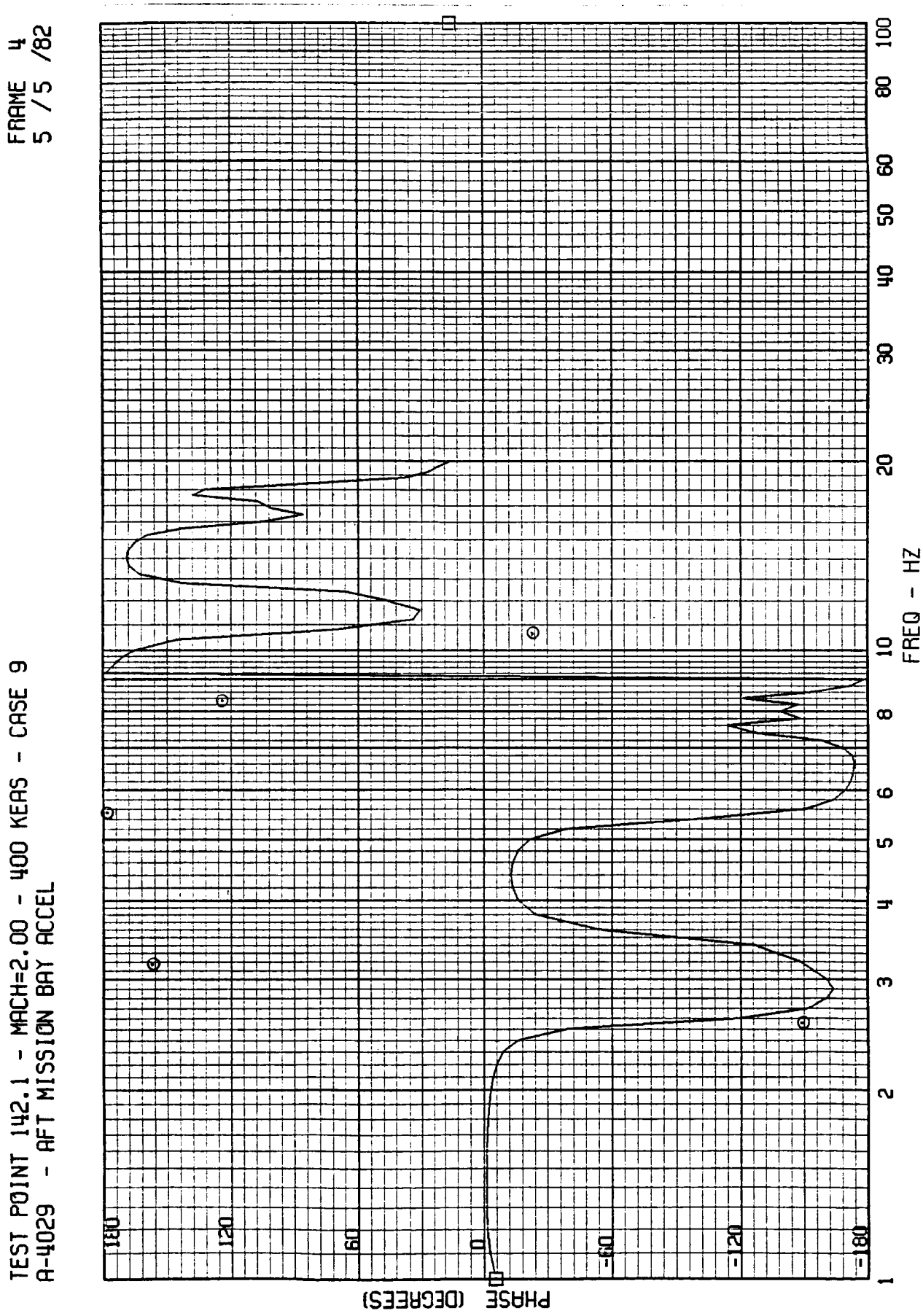
FRAME 4
5 /5 /82
TEST POINT 142.1 - MACH=2.00 - 400 KEAS - CASE 9
A-4029 - AFT MISSION BAY ACCEL
PHASE (DEGREES)
180
120
60
0
-60
-120
-180
1
2
3
4
5
6
8
10
20
30
40
50
60
80
100
FREQ - HZ

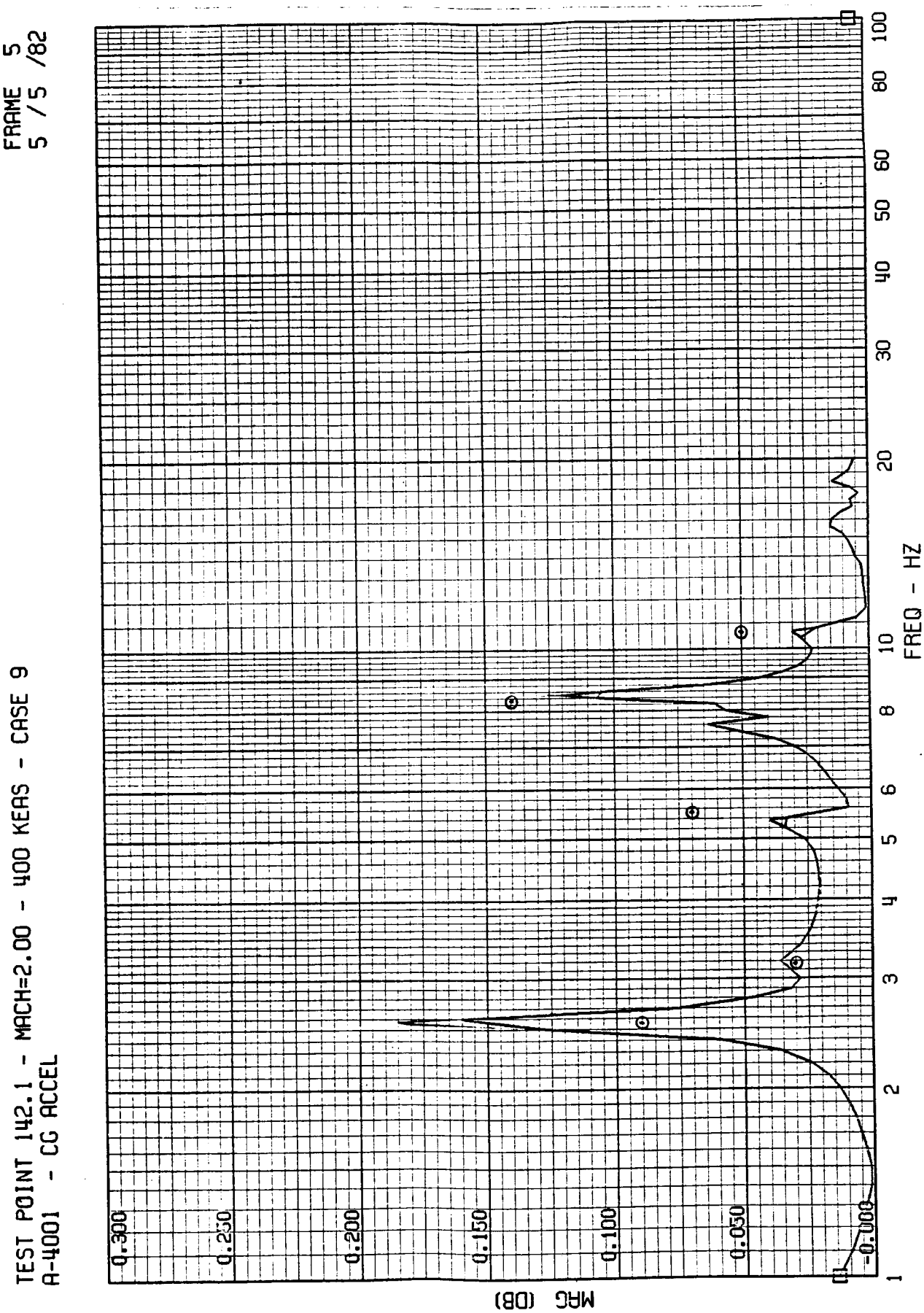
TEST POINT 142.1 - MACH=2.00 - 400 KEAS - CASE 9
A-4001 - CG ACCEL
FRAME 5
5 /5 /82
MAG (DB)
0.300
0.250
0.200
0.150
0.100
0.050
-0.000
1
2
3
4
5
6
8
10
20
30
40
50
60
80
100
FREQ - HZ

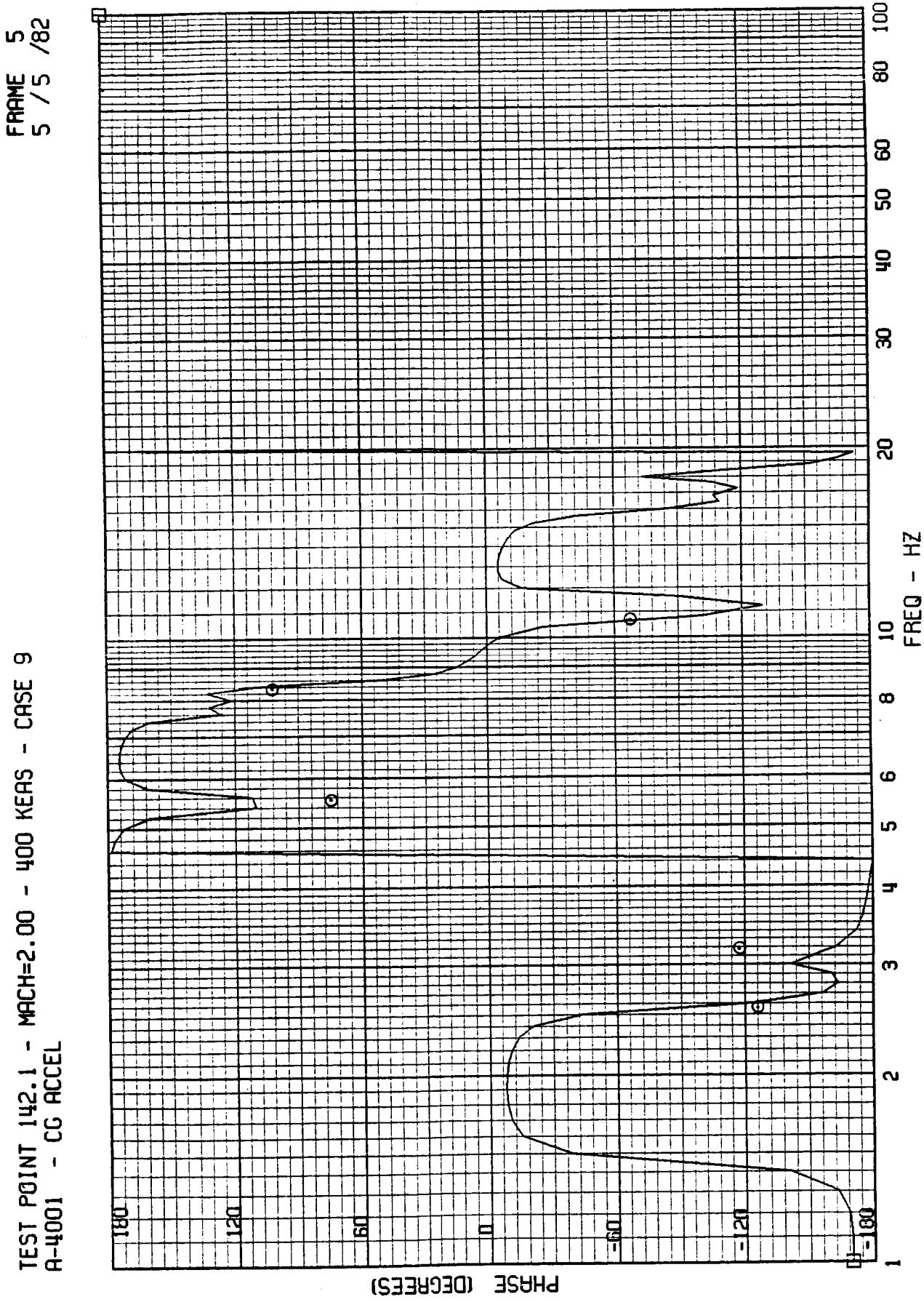
FRAME 5
5 /5 /82
TEST POINT 142.1 - MACH=2.00 - 400 KEAS - CASE 9
A-4001 - CG ACCEL
PHASE (DEGREES)
180
120
60
0
-60
-120
-180
1
2
3
4
5
6
8
10
20
30
40
50
60
80
100
FREQ - HZ

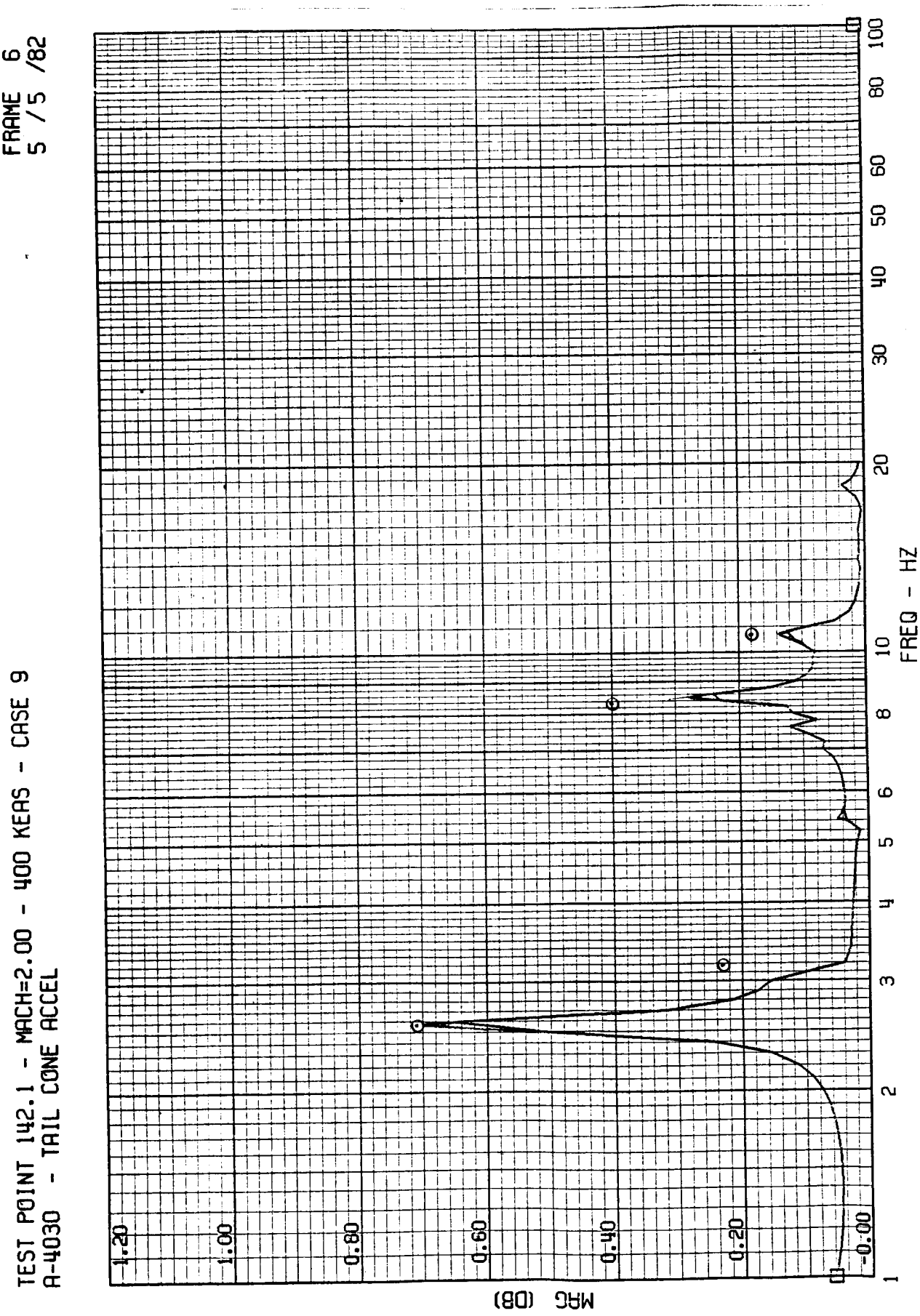
FRAME 6
5 /5 /82
TEST POINT 142.1 - MACH=2.00 - 400 KEAS - CASE 9
A-4030 - TAIL CONE ACCEL
MAG (DB)
1.20
1.00
0.80
0.60
0.40
0.20
-0.00
1
2
3
4
5
6
8
10
20
30
40
50
60
80
100
FREQ - HZ

FRAME 6
5 /5 /82

TEST POINT 142.1 - MACH=2.00 - 400 KEAS - CASE 9
A-4030 - TAIL CONE ACCEL

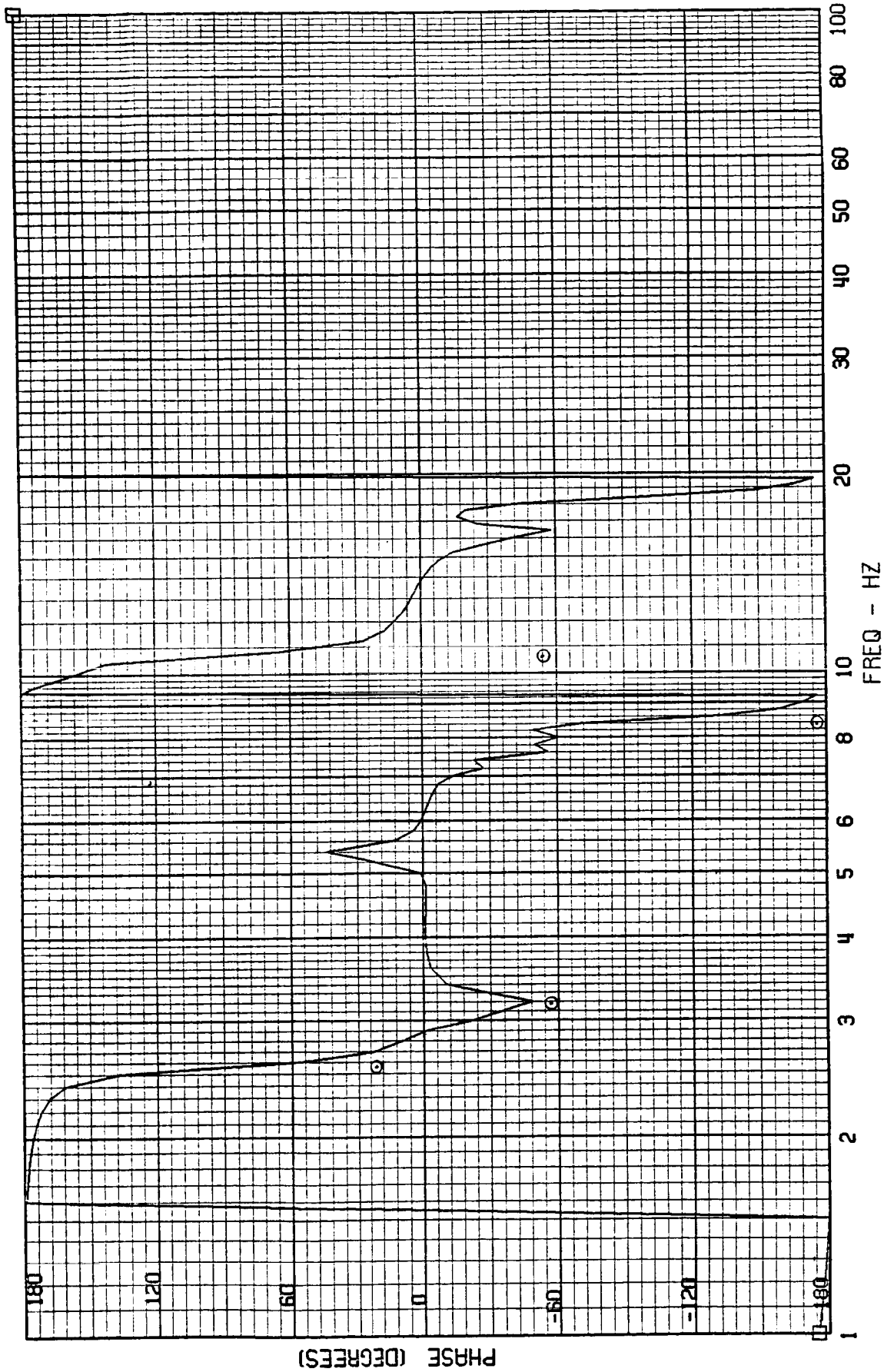

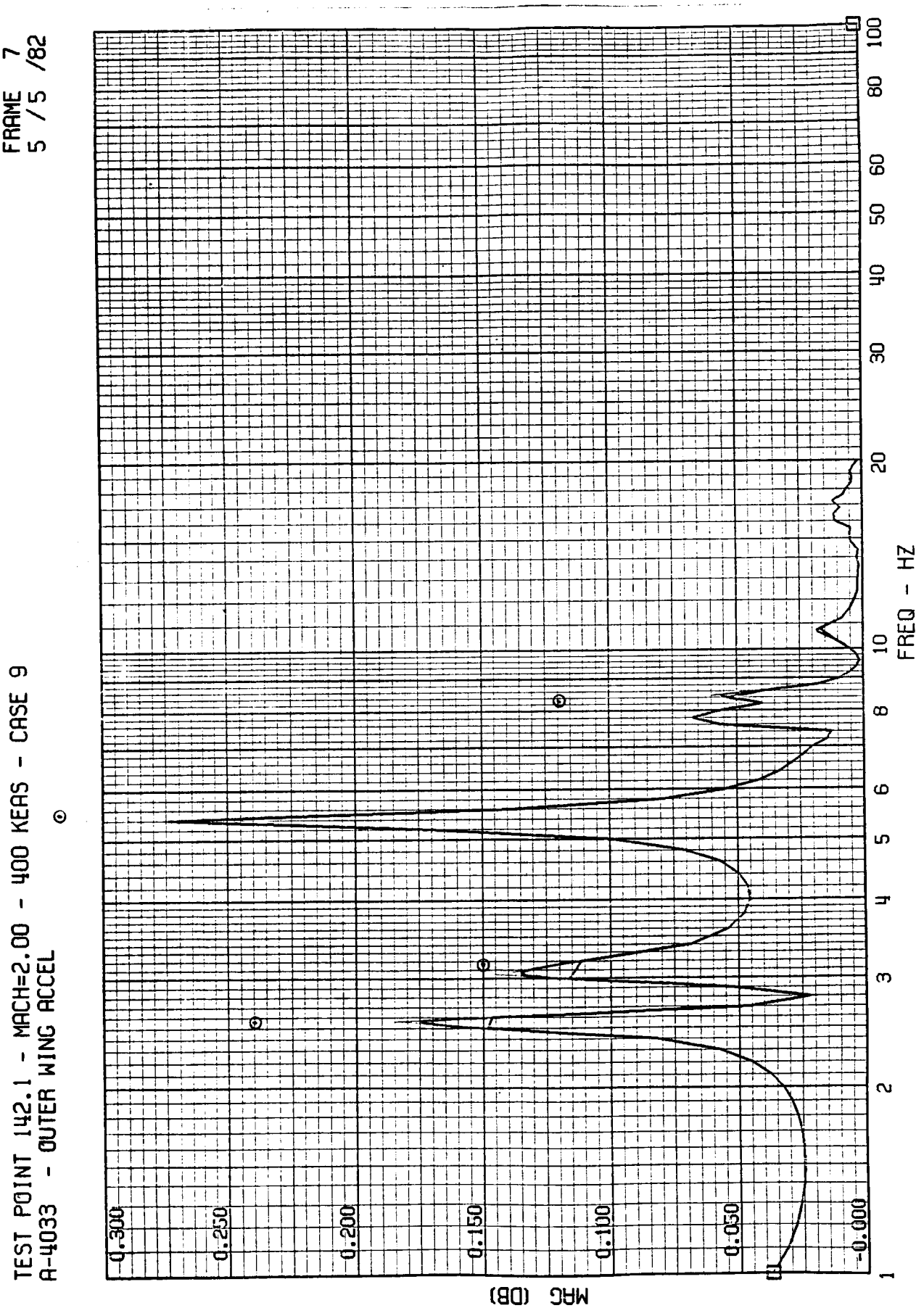
FRAME 7
5 /5 /82
TEST POINT 142.1 - MACH=2.00 - 400 KEAS - CASE 9
A-4033 - OUTER WING ACCEL
MAG (DB)
0.300
0.250
0.200
0.150
0.100
0.050
-0.000
1
2
3
4
5
6
8
10
20
30
40
50
60
80
100
FREQ - HZ

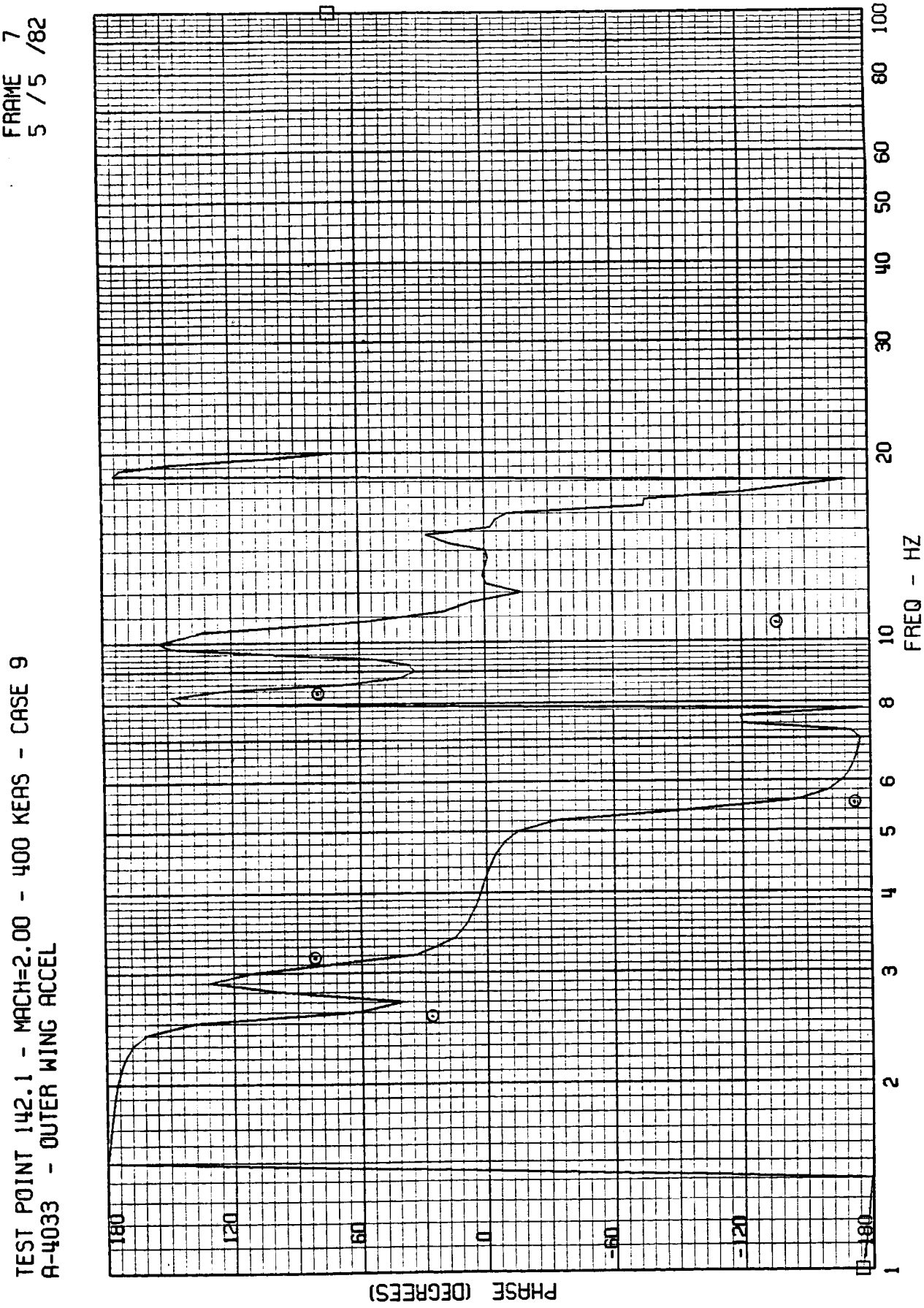
TEST POINT 142.1 - MACH=2.00 - 400 KEAS - CASE 9
A-4033 - OUTER WING ACCEL
FRAME 7
5 /5 /82
PHASE (DEGREES)
180
120
60
0
-60
-120
-180
1
2
3
4
5
6
8
10
20
30
40
50
60
80
100
FREQ - HZ

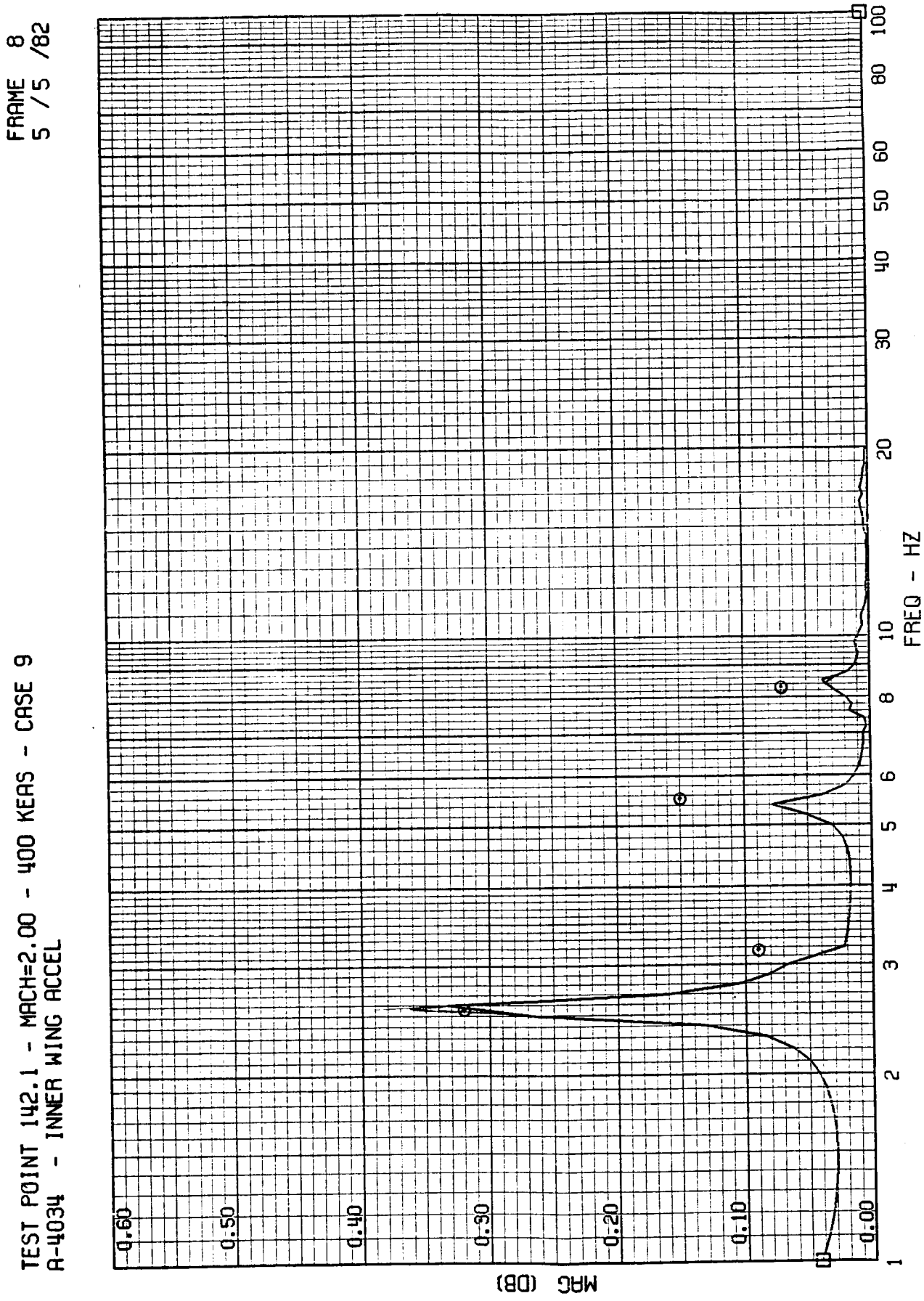
FRAME 8
5 /5 /82
TEST POINT 142.1 - MACH=2.00 - 400 KEAS - CASE 9
A-4034 - INNER WING ACCEL
MAG (DB)
0.60
0.50
0.40
0.30
0.20
0.10
0.00
FREQ - HZ
1
2
3
4
5
6
8
10
20
30
40
50
60
80
100

FRAME 8
5 /5 /82

TEST POINT 142.1 - MACH=2.00 - 400 KEAS - CASE 9
A-4034 - INNER WING ACCEL

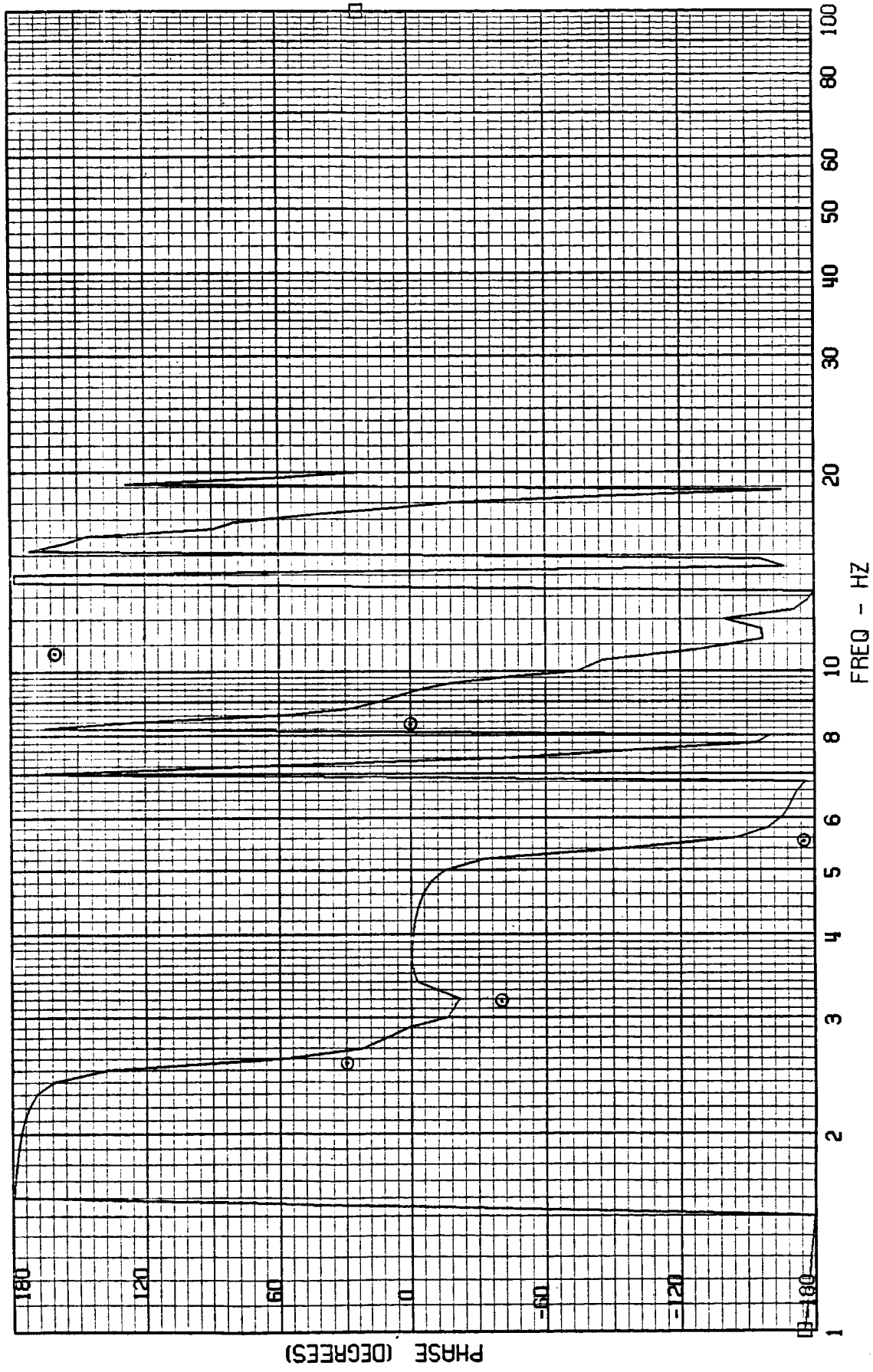

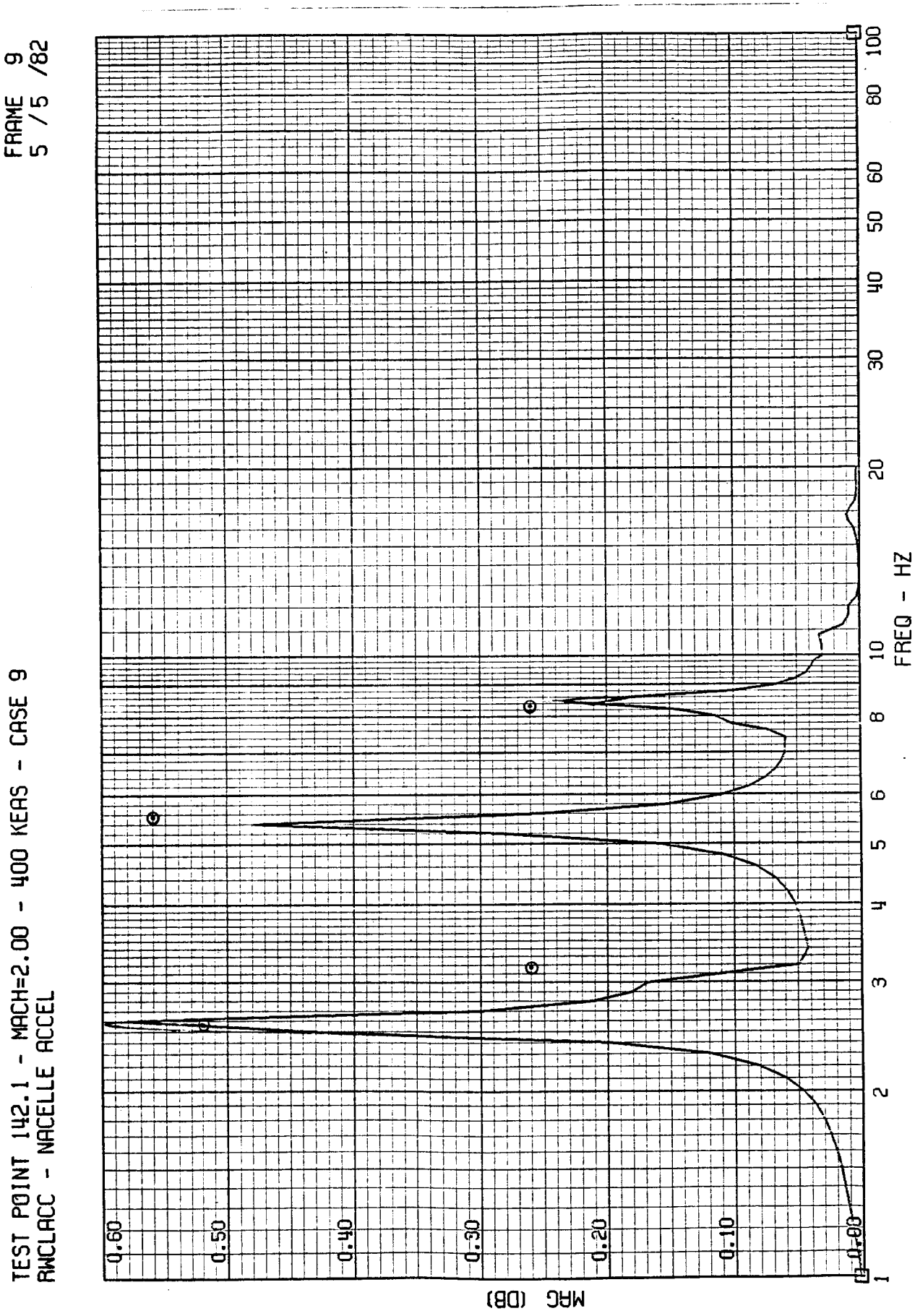
FRAME 9
5 /5 /82
TEST POINT 142.1 - MACH=2.00 - 400 KEAS - CASE 9
RWCLACC - NACELLE ACCEL
MAG (DB)
0.60
0.50
0.40
0.30
0.20
0.10
0.00
FREQ - HZ
1
2
3
4
5
6
8
10
20
30
40
50
60
80
100

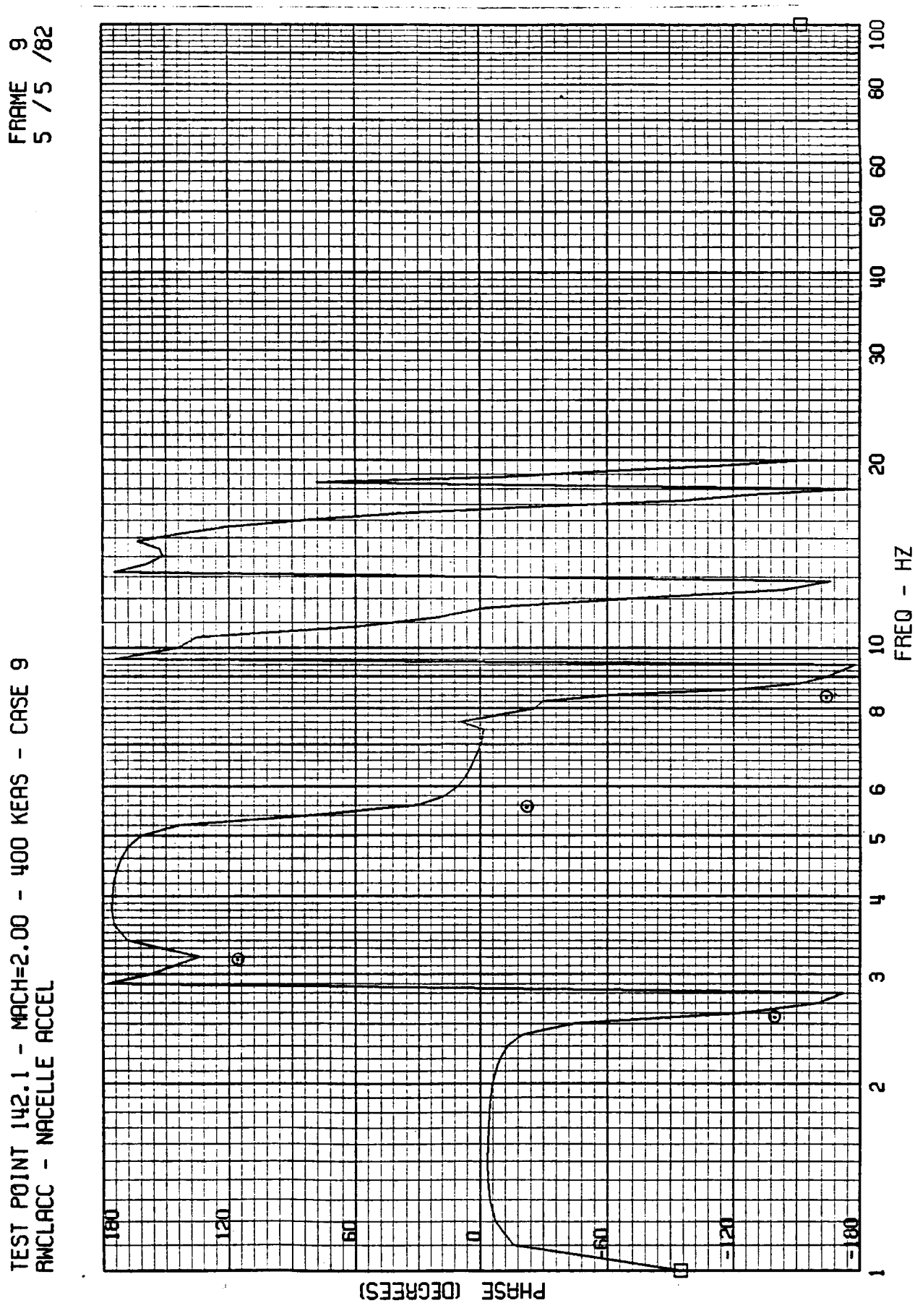
FRAME 9
5 /5 /82
TEST POINT 142.1 - MACH=2.00 - 400 KEAS - CASE 9
RWCLACC - NACELLE ACCEL
PHASE (DEGREES)
180
120
60
0
-60
-120
-180
1
2
3
4
5
6
8
10
20
30
40
50
60
80
100
FREQ - HZ

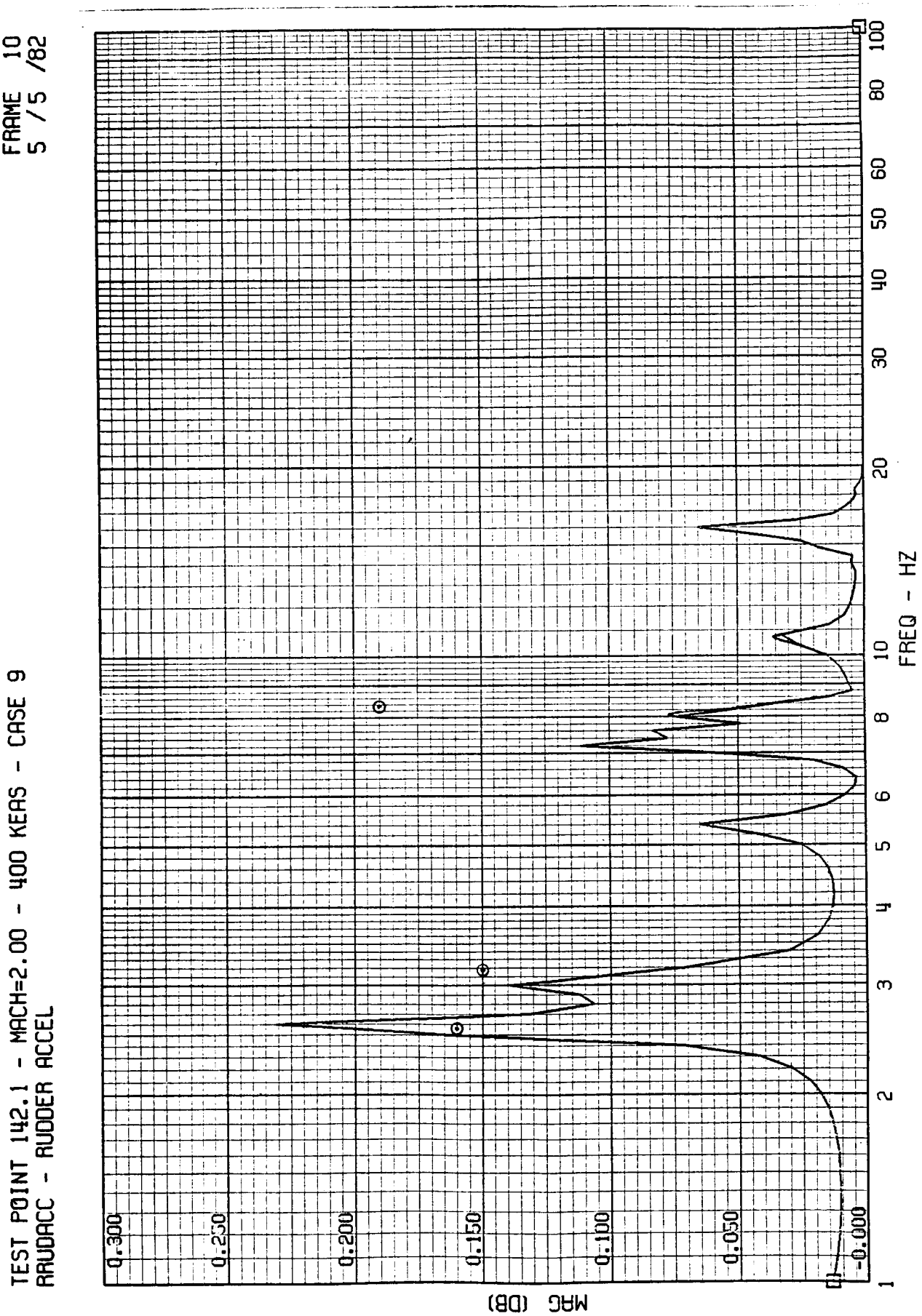
TEST POINT 142.1 - MACH=2.00 - 400 KEAS - CASE 9
RRUDACC - RUDDER ACCEL
FRAME 10
5 /5 /82
MAG (DB)
0.300
0.250
0.200
0.150
0.100
0.050
-0.000
FREQ - HZ
1
2
3
4
5
6
8
10
20
30
40
50
60
80
100

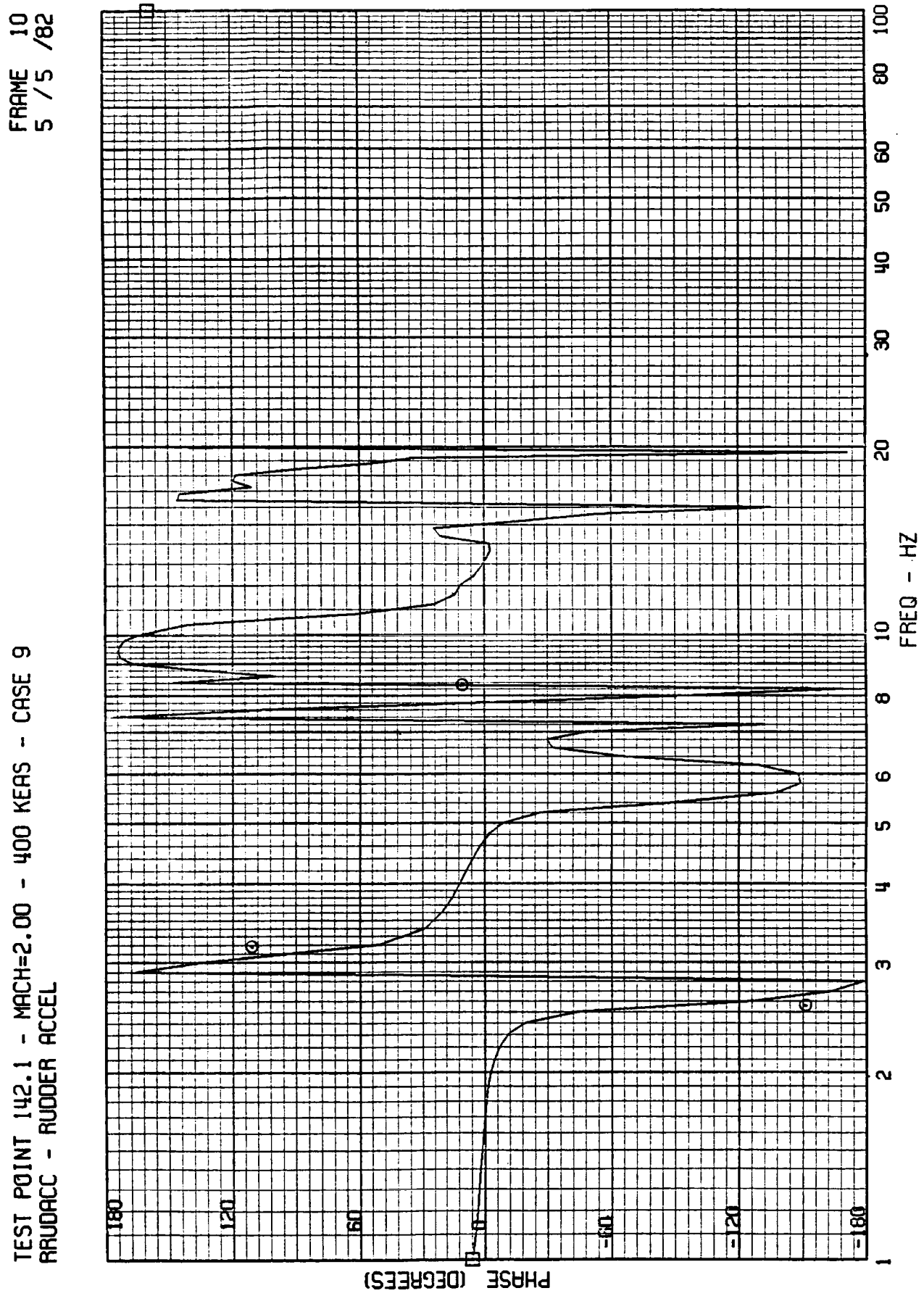
TEST POINT 142.1 - MACH=2.00 - 400 KEAS - CASE 9
RRUDACC - RUDDER ACCEL
FRAME 10
5 /5 /82
PHASE (DEGREES)
180
120
60
0
-60
-120
-180
1
2
3
4
5
6
8
10
20
30
40
50
60
80
100
FREQ - HZ

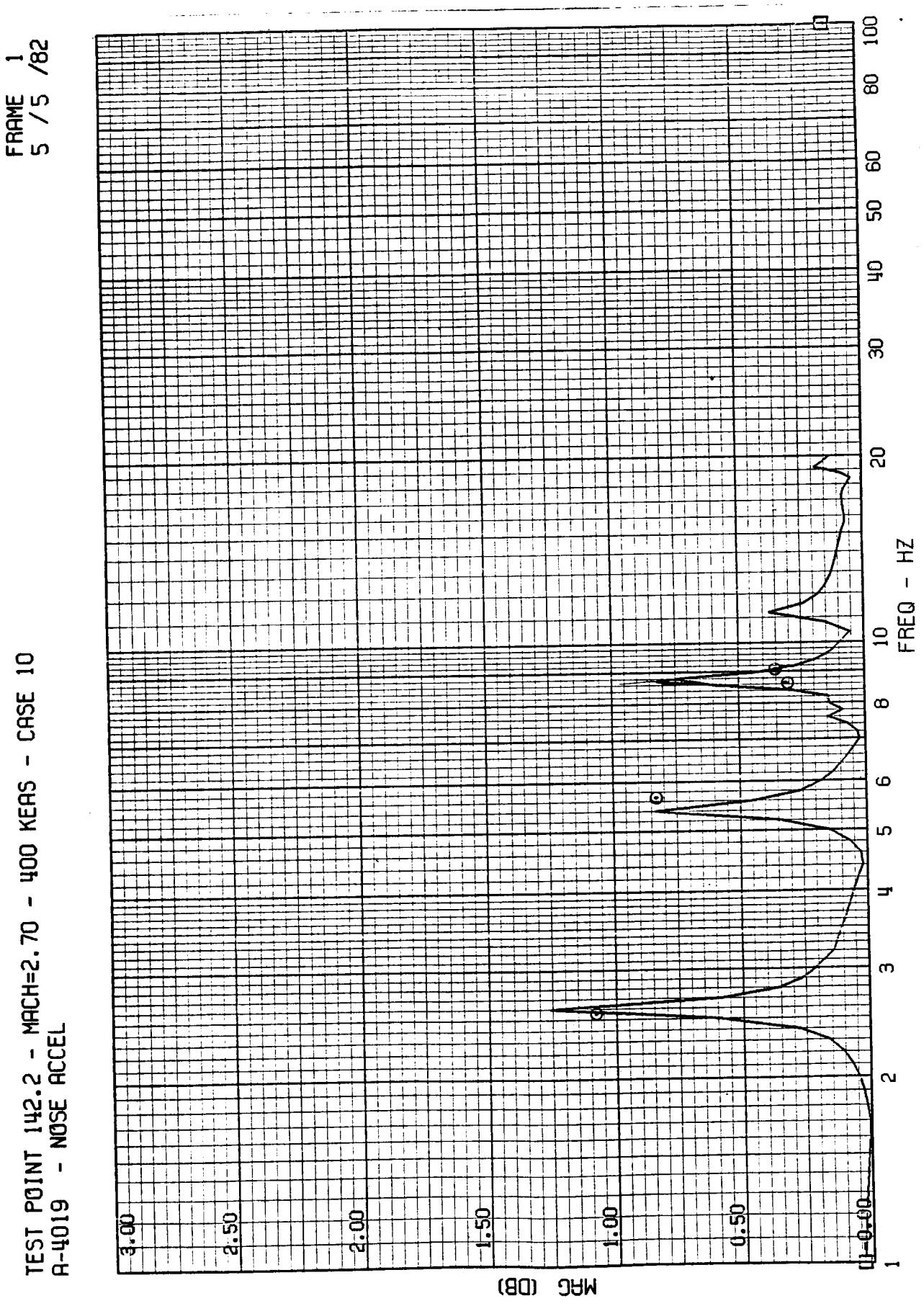
FRAME 1
5 /5 /82
TEST POINT 142.2 - MACH=2.70 - 400 KEAS - CASE 10
A-4019 - NOSE ACCEL
MAG (DB)
3.00
2.50
2.00
1.50
1.00
0.50
0.00
FREQ - HZ
1
2
3
4
5
6
8
10
20
30
40
50
60
80
100

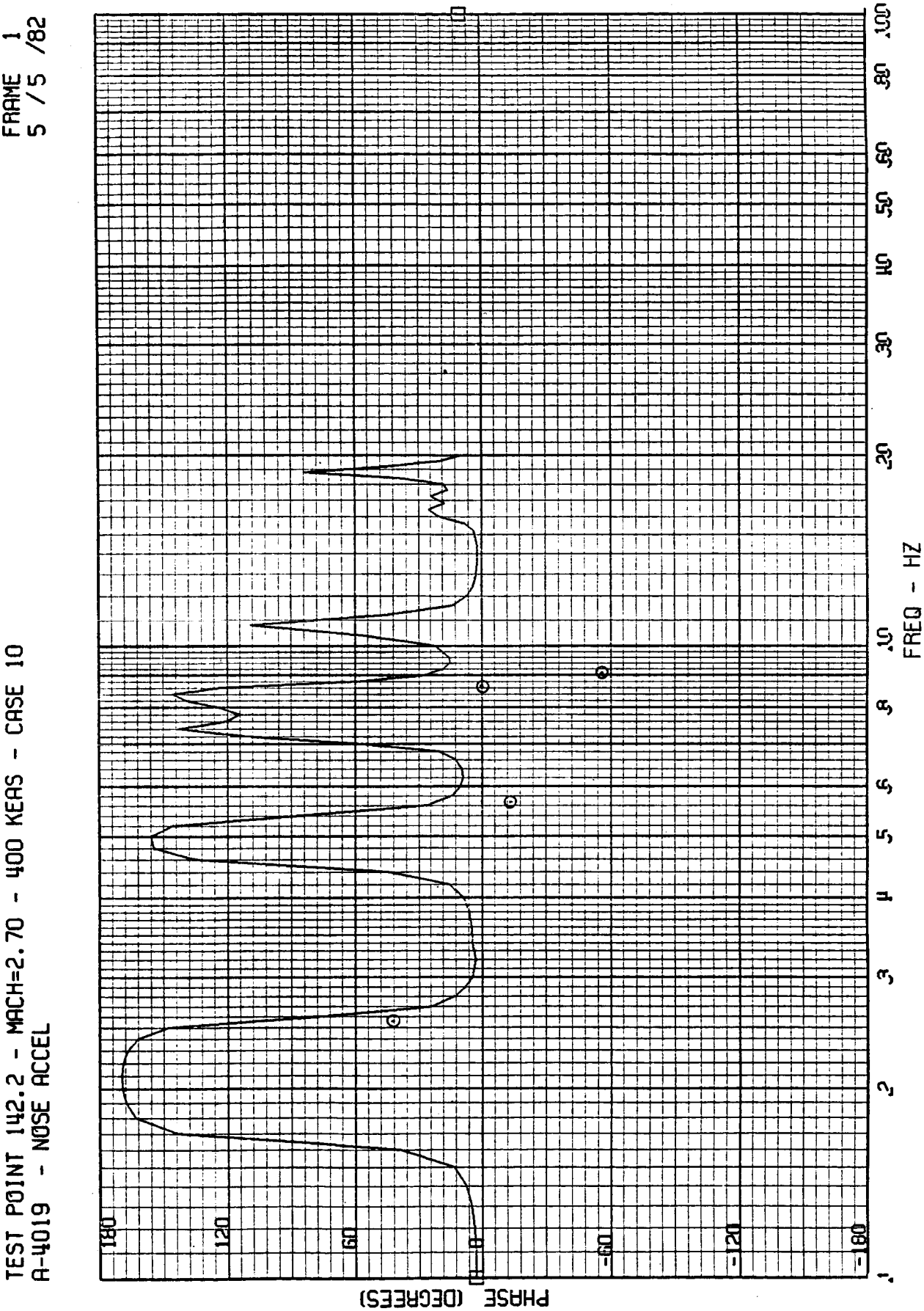

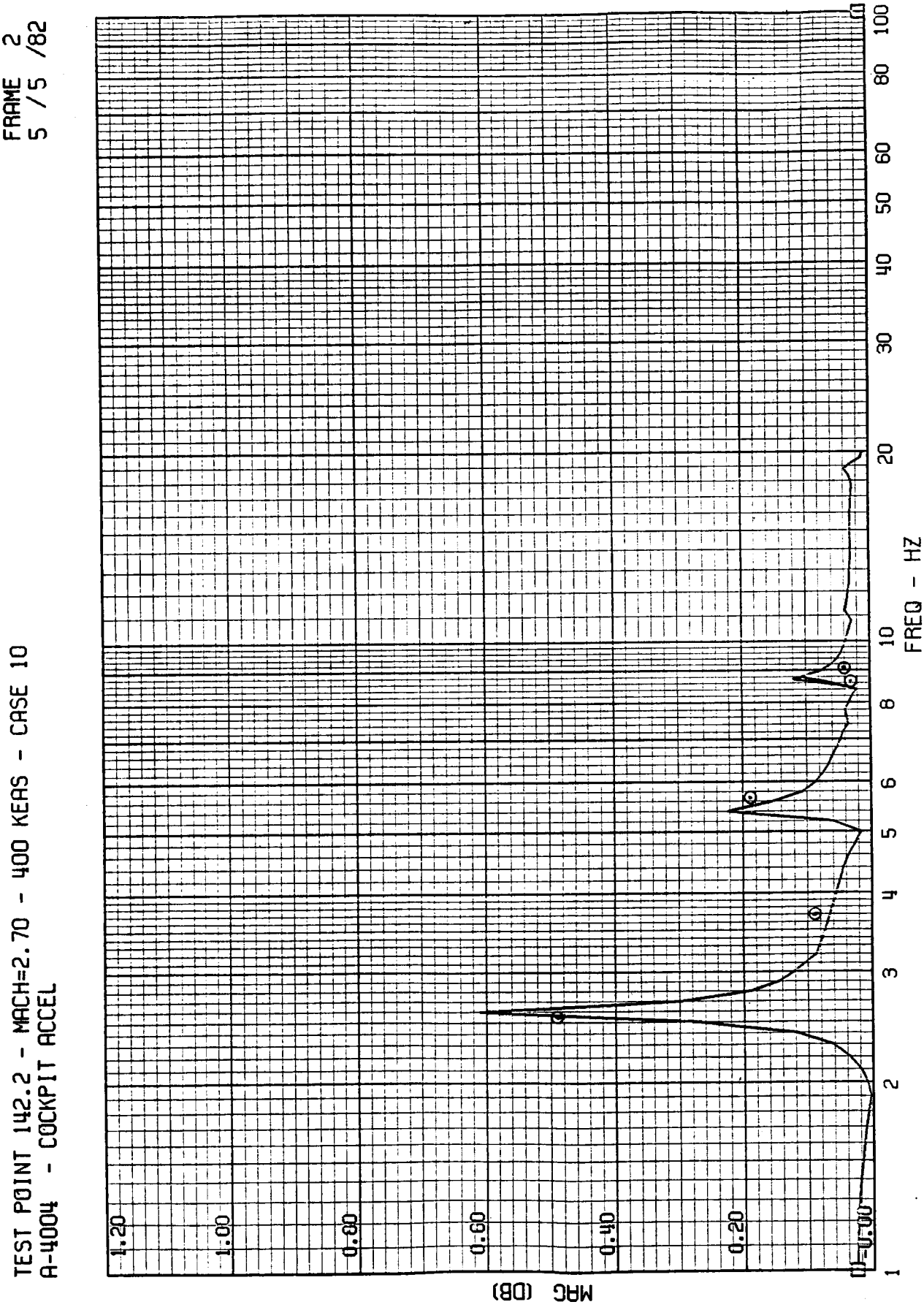
TEST POINT 142.2 - MACH=2.70 - 400 KEAS - CASE 10
A-4004 - COCKPIT ACCEL
FRAME 2
5 /5 /82
MAG (DB)
1.20
1.00
0.80
0.60
0.40
0.20
0.00
1
2
3
4
5
6
8
10
20
30
40
50
60
80
100
FREQ - HZ

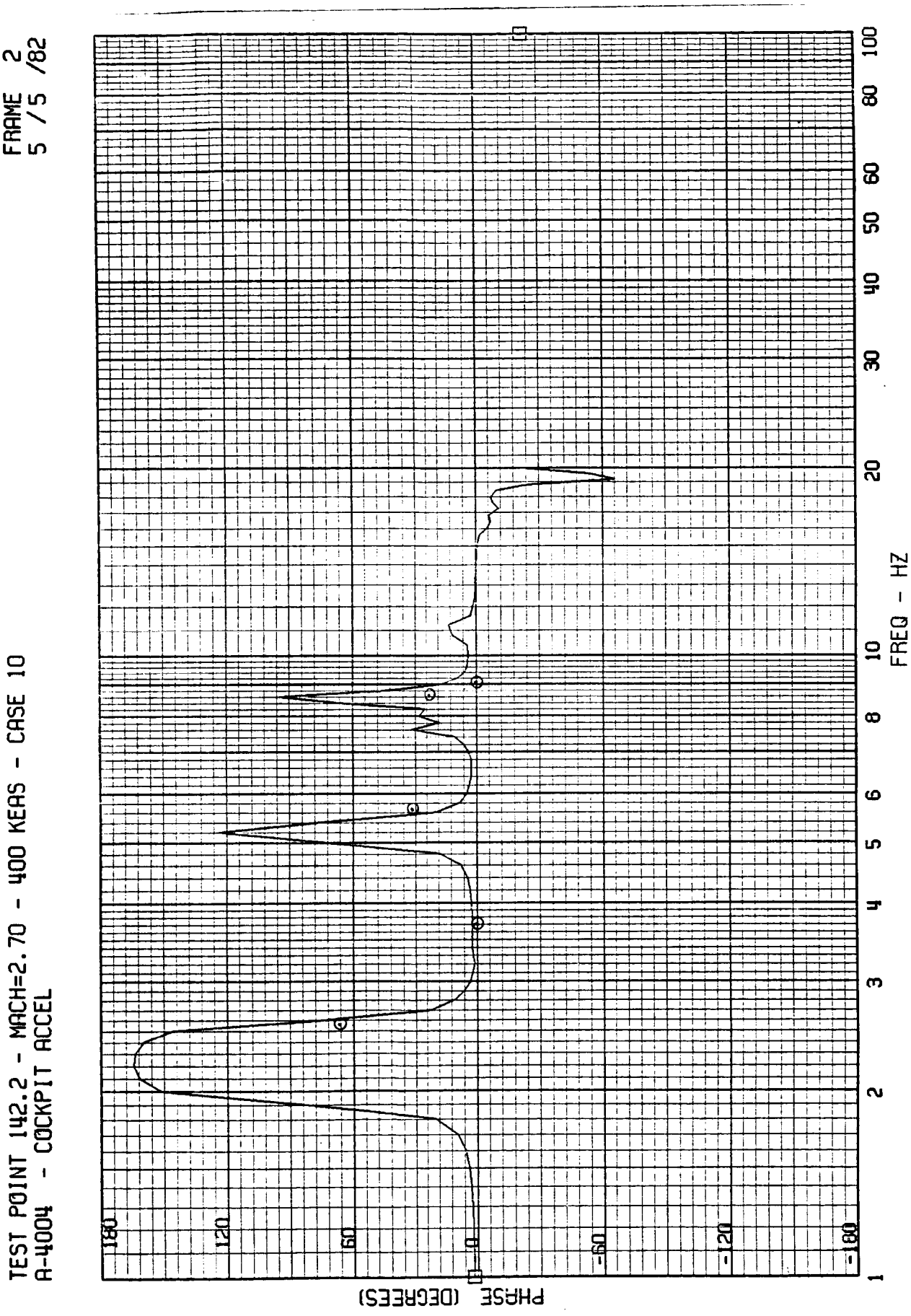
TEST POINT 142.2 - MACH=2.70 - 400 KEAS - CASE 10
A-4004 - COCKPIT ACCEL
FRAME 2
5 /5 /82
PHASE (DEGREES)
180
120
60
0
-60
-120
-180
1
2
3
4
5
6
8
10
20
30
40
50
60
80
100
FREQ - HZ

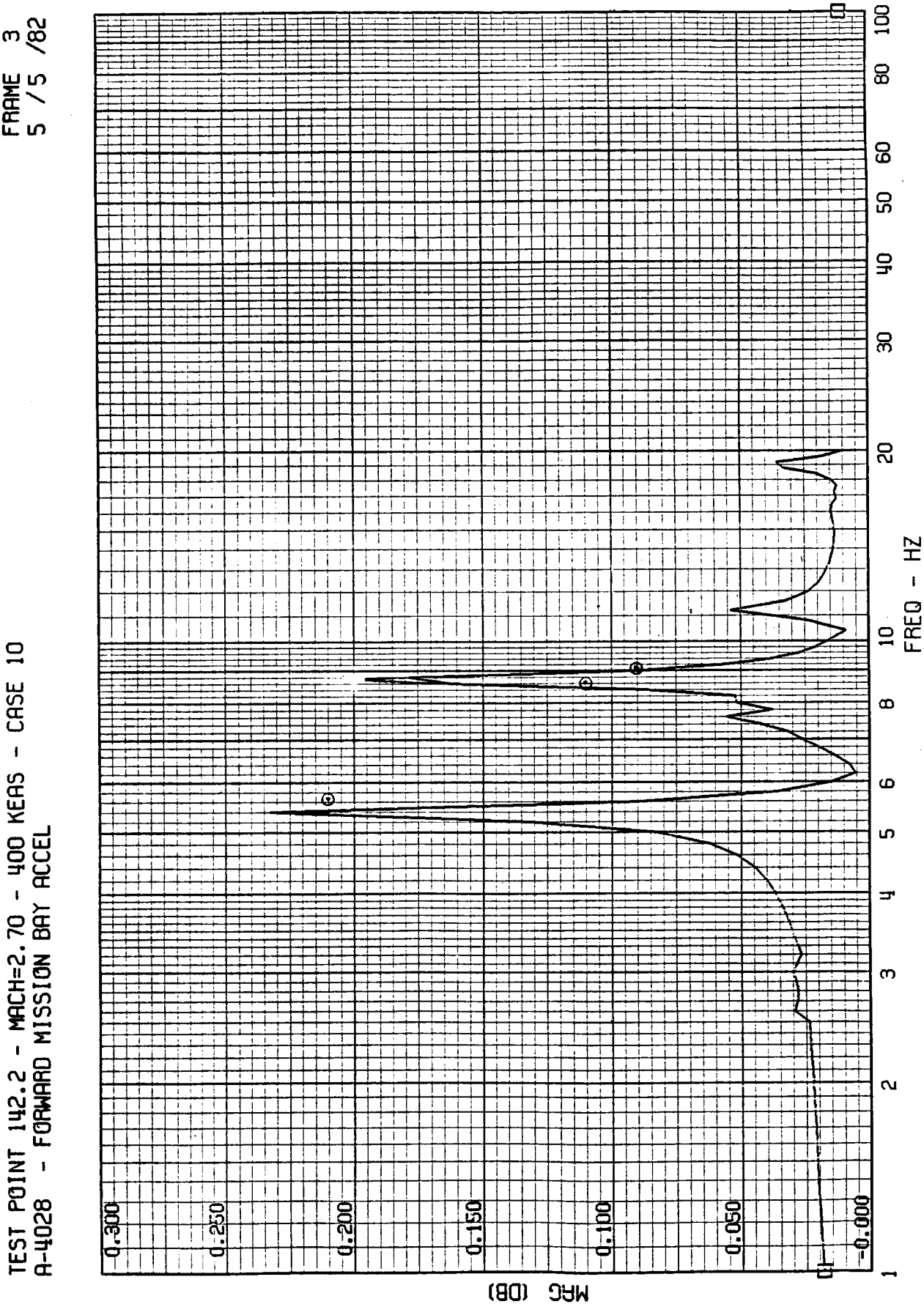
TEST POINT 142.2 - MACH=2.70 - 400 KEAS - CASE 10
A-4028 - FORWARD MISSION BAY ACCEL
FRAME 3
5 /5 /82
MAG (DB)
0.300
0.250
0.200
0.150
0.100
0.050
-0.000
1
2
3
4
5
6
8
10
20
30
40
50
60
80
100
FREQ - HZ

FRAME 3
5 /5 /82

TEST POINT 142.2 - MACH=2.70 - 400 KEAS - CASE 10
A-4028 - FORWARD MISSION BAY ACCEL

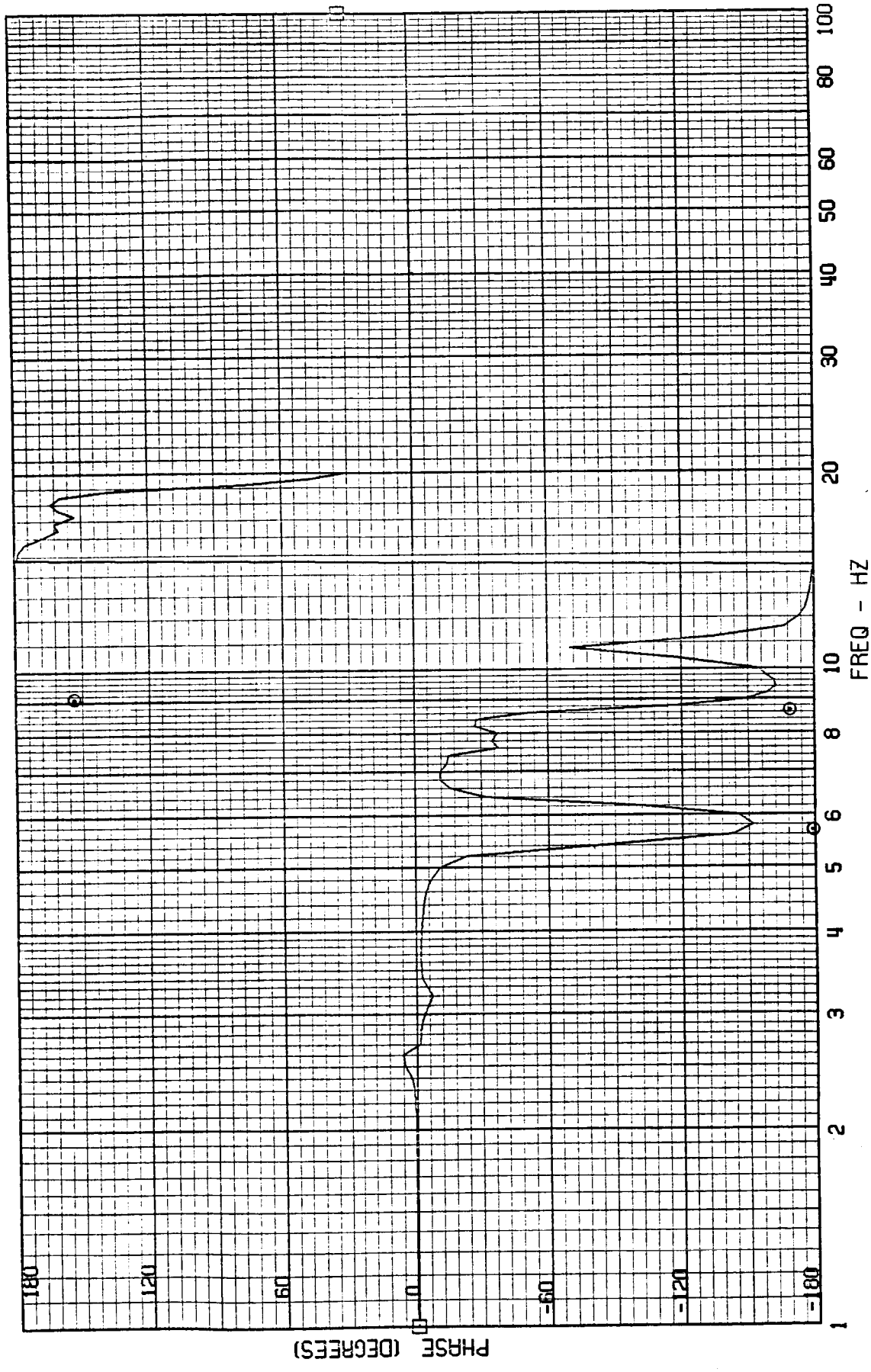

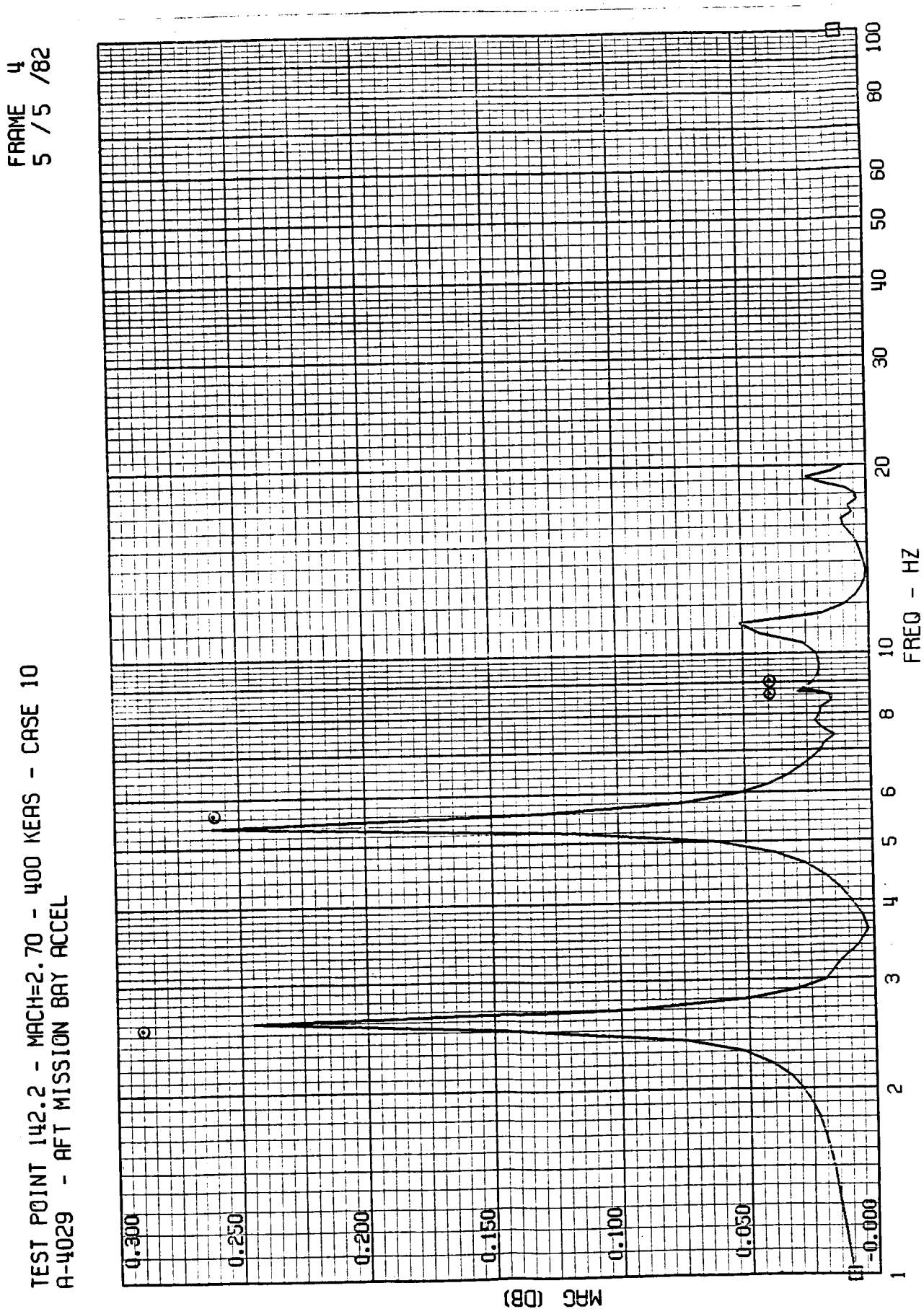
FRAME 4
5 /5 /82
TEST POINT 142.2 - MACH=2.70 - 400 KEAS - CASE 10
A-4029 - AFT MISSION BAY ACCEL
MAG (DB)
0.300
0.250
0.200
0.150
0.100
0.050
-0.000
1
2
3
4
5
6
8
10
20
30
40
50
60
80
100
FREQ - HZ

FRAME 4
5 /5 /82

TEST POINT 142.2 - MACH=2.70 - 400 KEAS - CASE 10
A-4029 - AFT MISSION BAY ACCEL

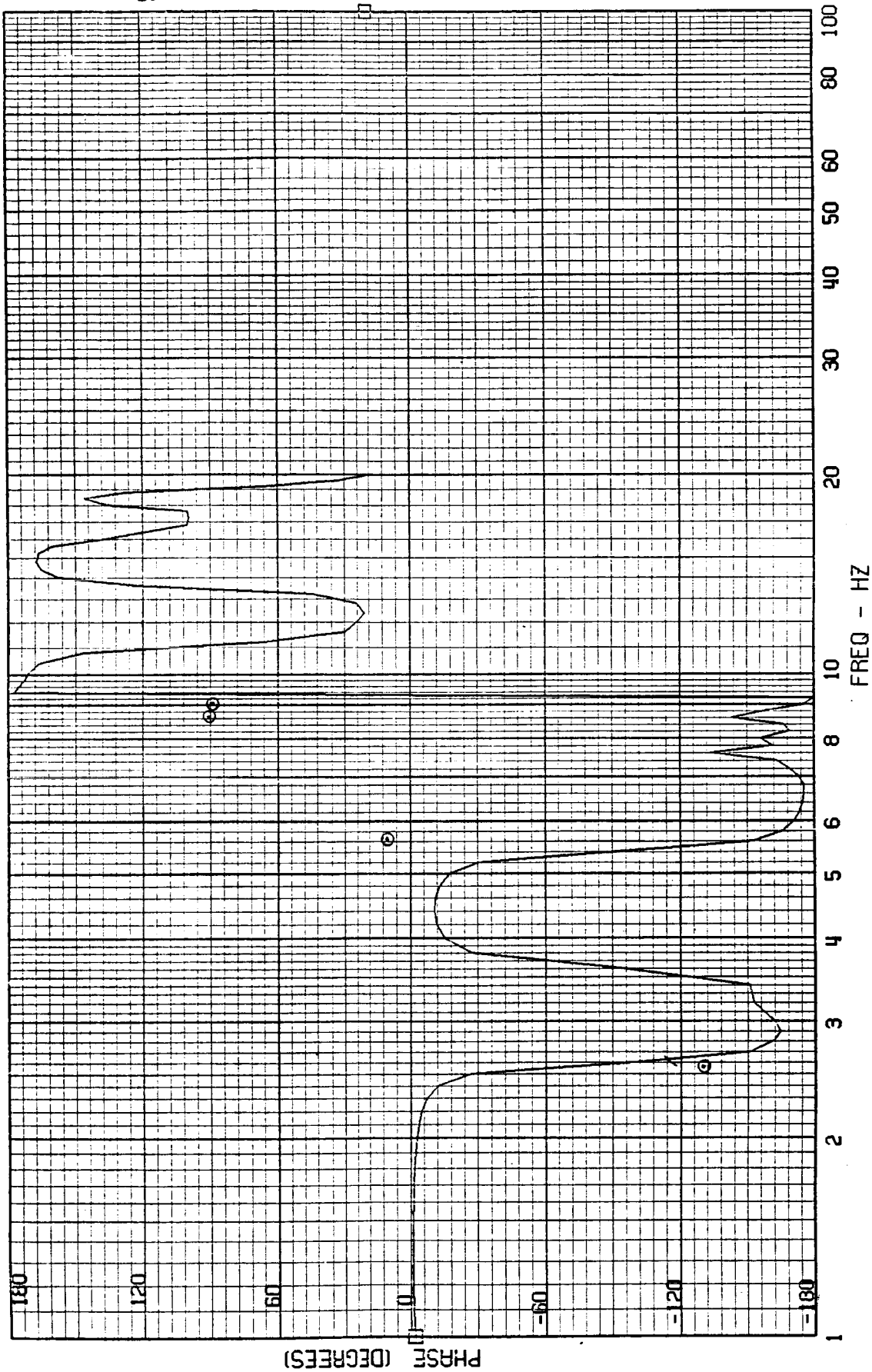

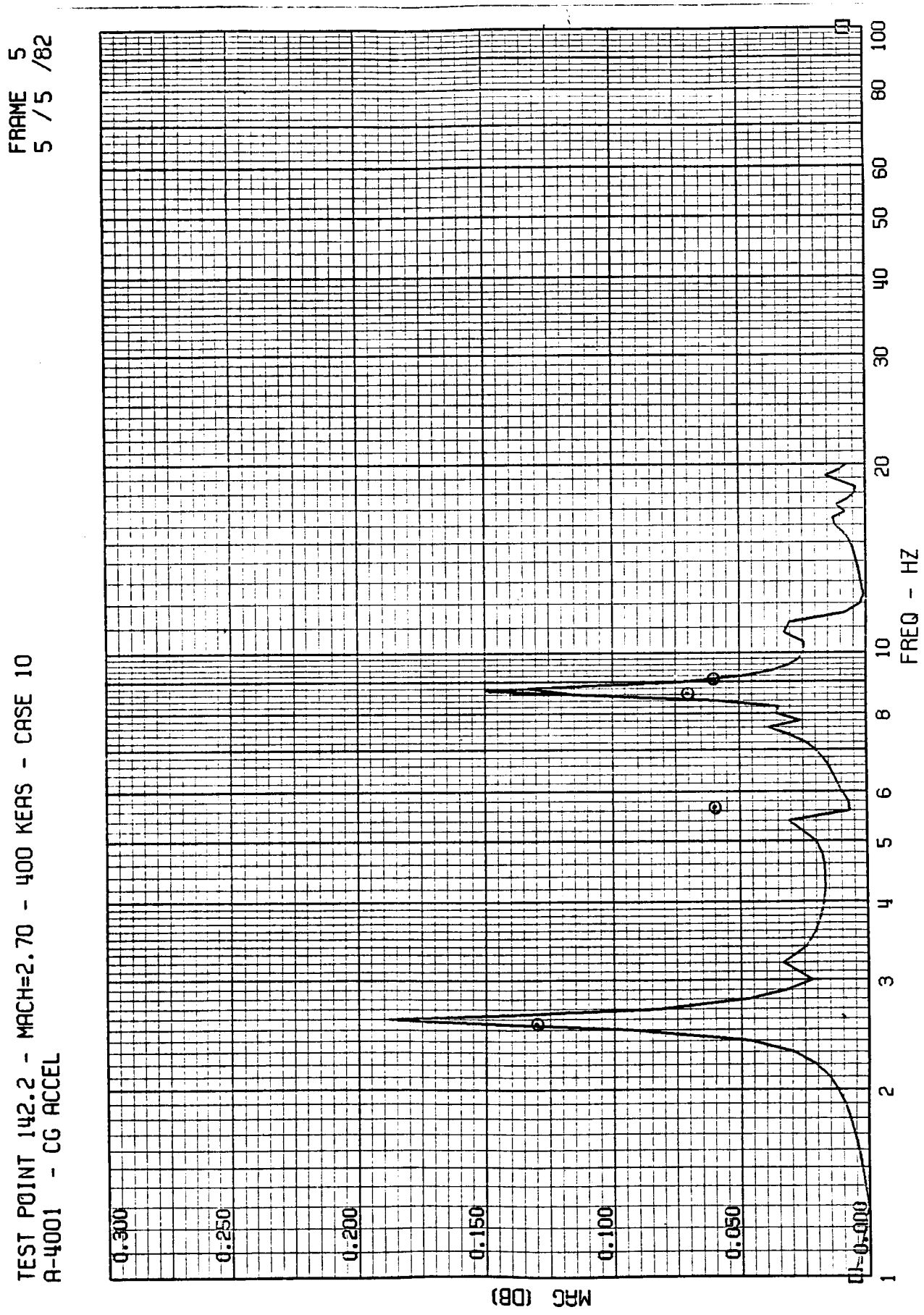
TEST POINT 142.2 - MACH=2.70 - 400 KEAS - CASE 10
A-4001 - CG ACCEL
FRAME 5
5 /5 /82
MAG (DB)
0.300
0.250
0.200
0.150
0.100
0.050
0.000
1
2
3
4
5
6
8
10
20
30
40
50
60
80
100
FREQ - HZ

FRAME 5
5 /5 /82

TEST POINT 142.2 - MACH=2.70 - 400 KEAS - CASE 10
A-4001 - CG ACCEL

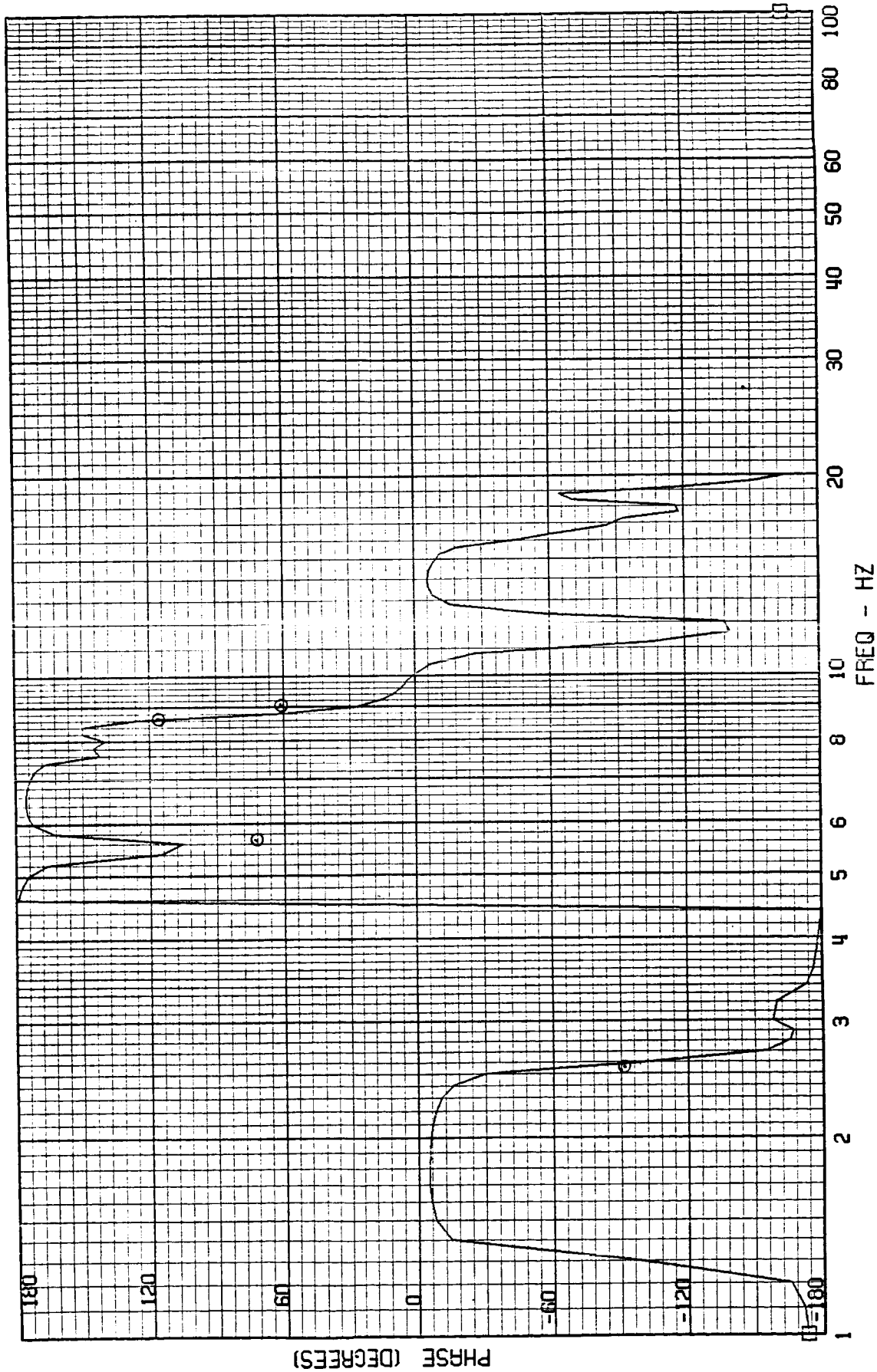

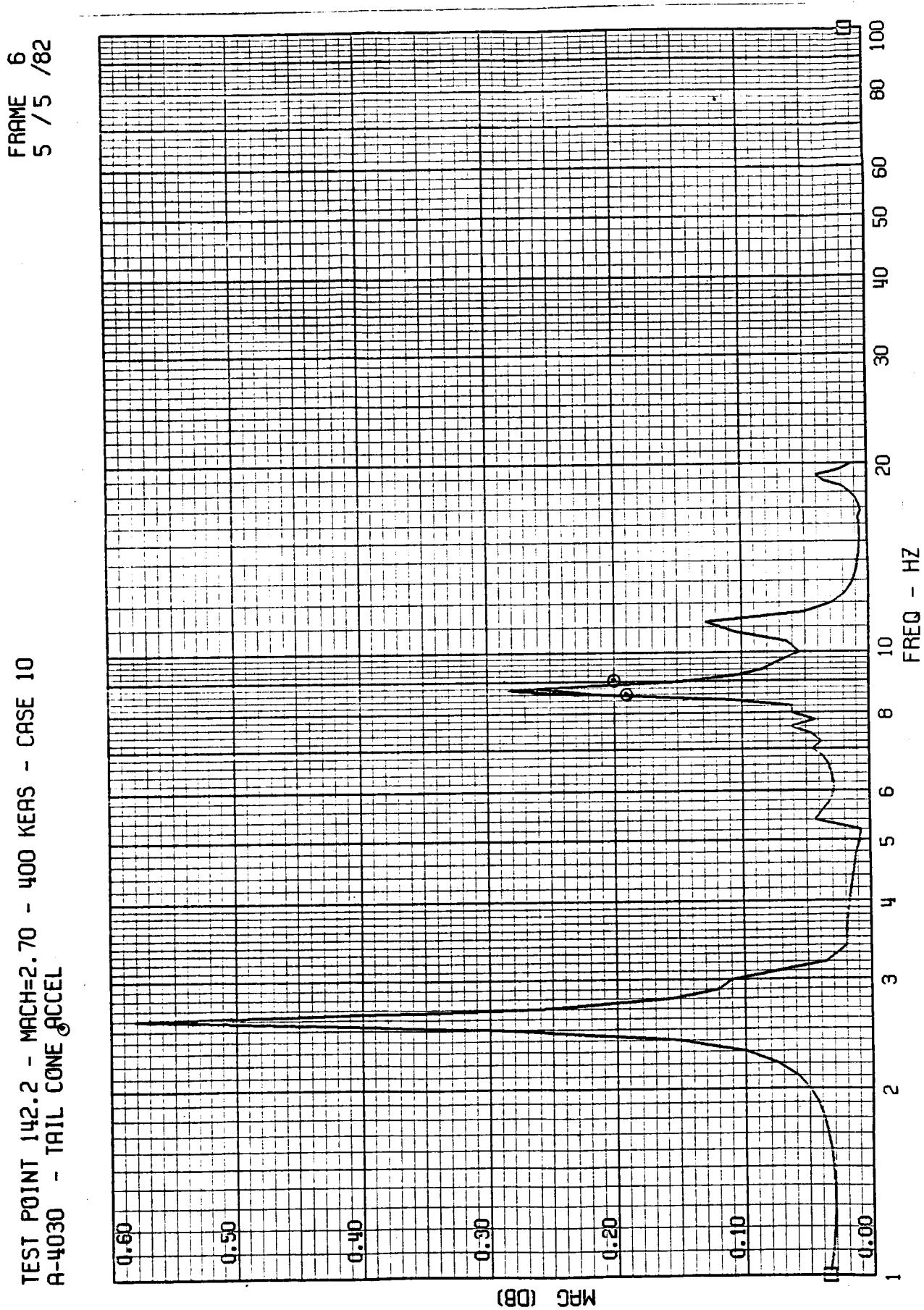
FRAME 6
5 /5 /82
TEST POINT 142.2 - MACH=2.70 - 400 KEAS - CASE 10
A-4030 - TAIL CONE @ACCEL
MAG (DB)
0.60
0.50
0.40
0.30
0.20
0.10
0.00
FREQ - HZ
1
2
3
4
5
6
8
10
20
30
40
50
60
80
100

FRAME 6
5 /5 /82

TEST POINT 142.2 - MACH=2.70 - 400 KEAS - CASE 10
A-4030 - TAIL CONE ACCEL

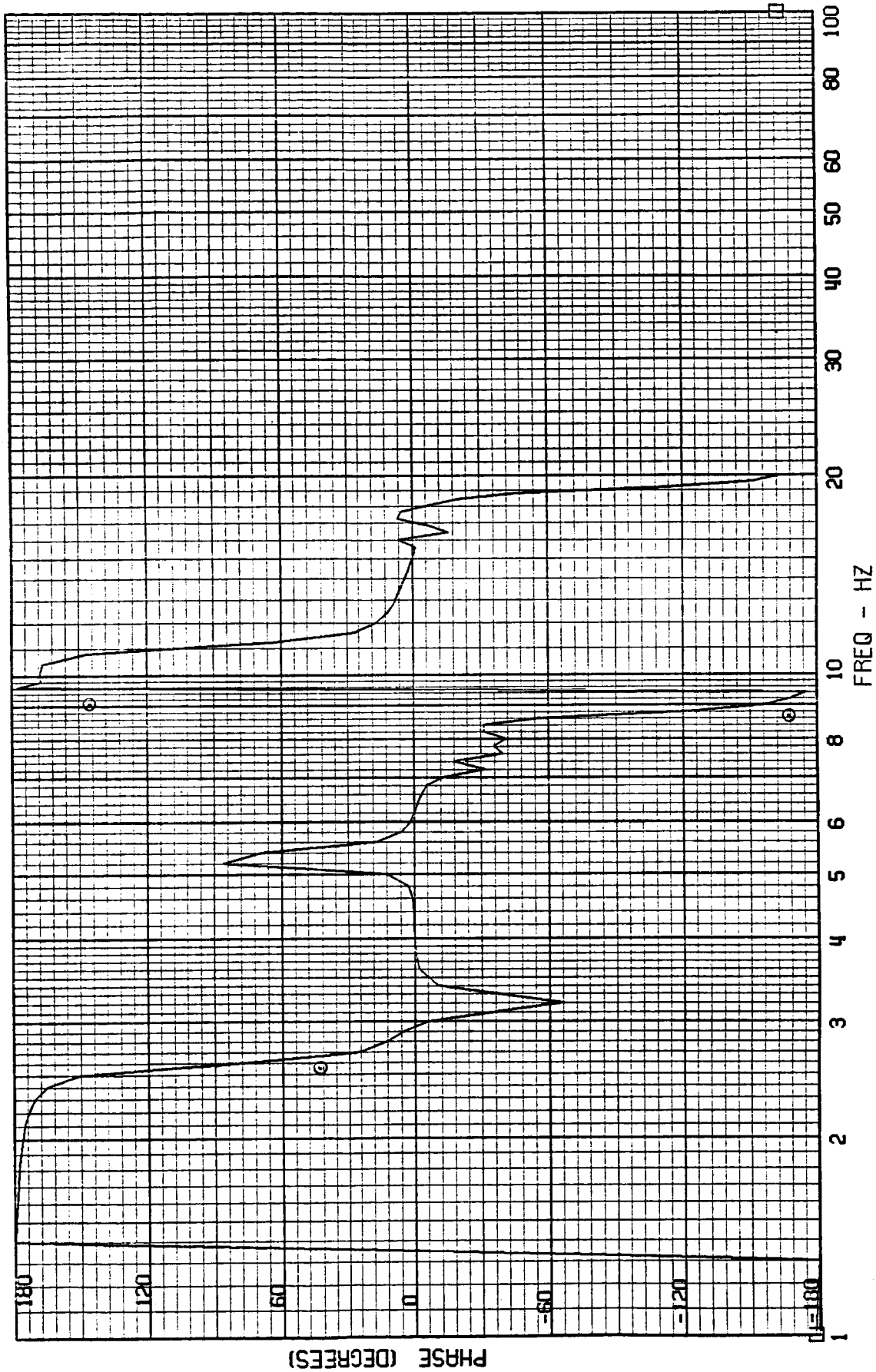

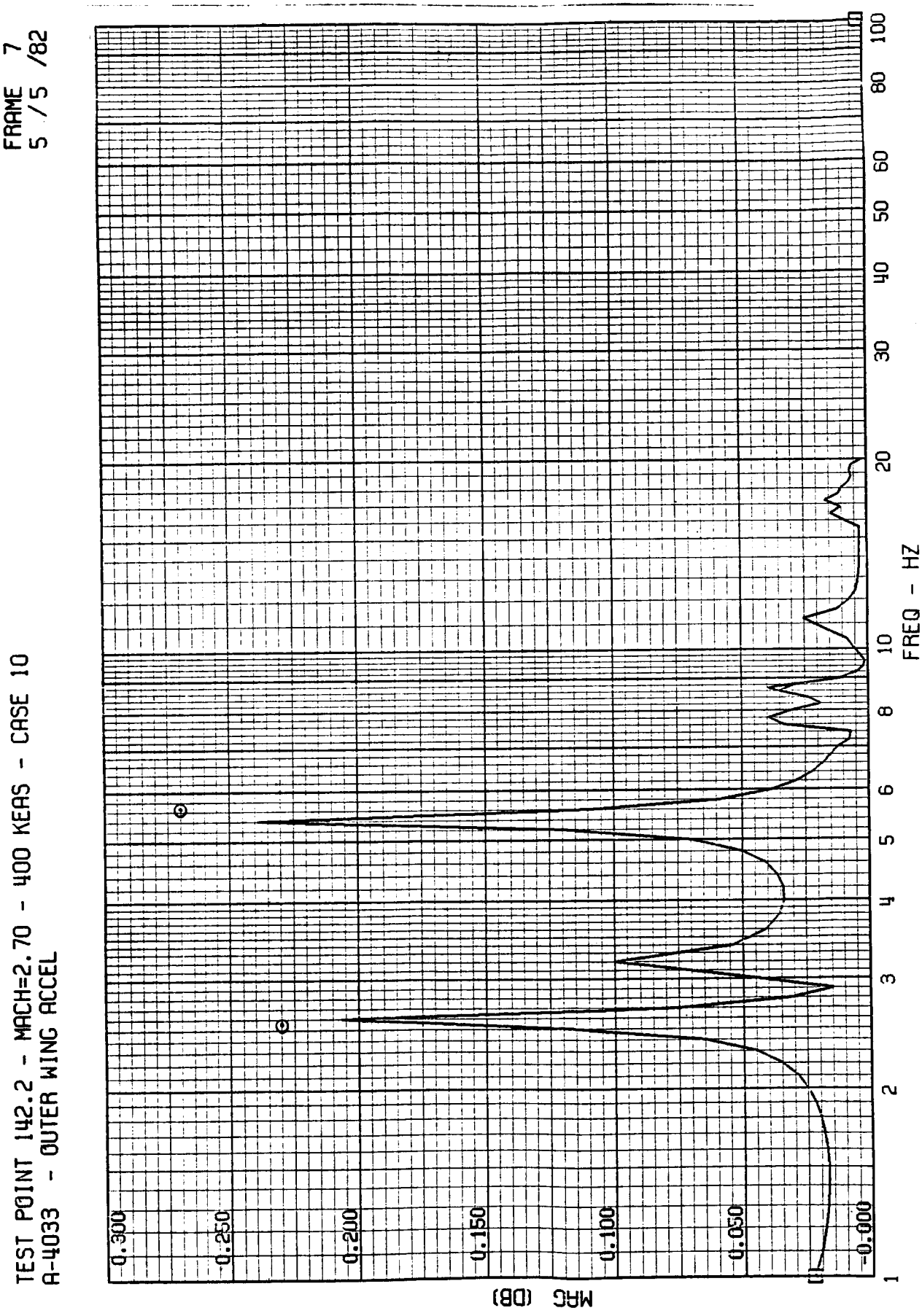
TEST POINT 142.2 - MACH=2.70 - 400 KEAS - CASE 10
A-4033 - OUTER WING ACCEL
FRAME 7
5 /5 /82
MAG (DB)
0.300
0.250
0.200
0.150
0.100
0.050
-0.000
FREQ - HZ
1
2
3
4
5
6
8
10
20
30
40
50
60
80
100

FRAME 7
5 /5 /82

TEST POINT 142.2 - MACH=2.70 - 400 KEAS - CASE 10
A-4033 - OUTER WING ACCEL

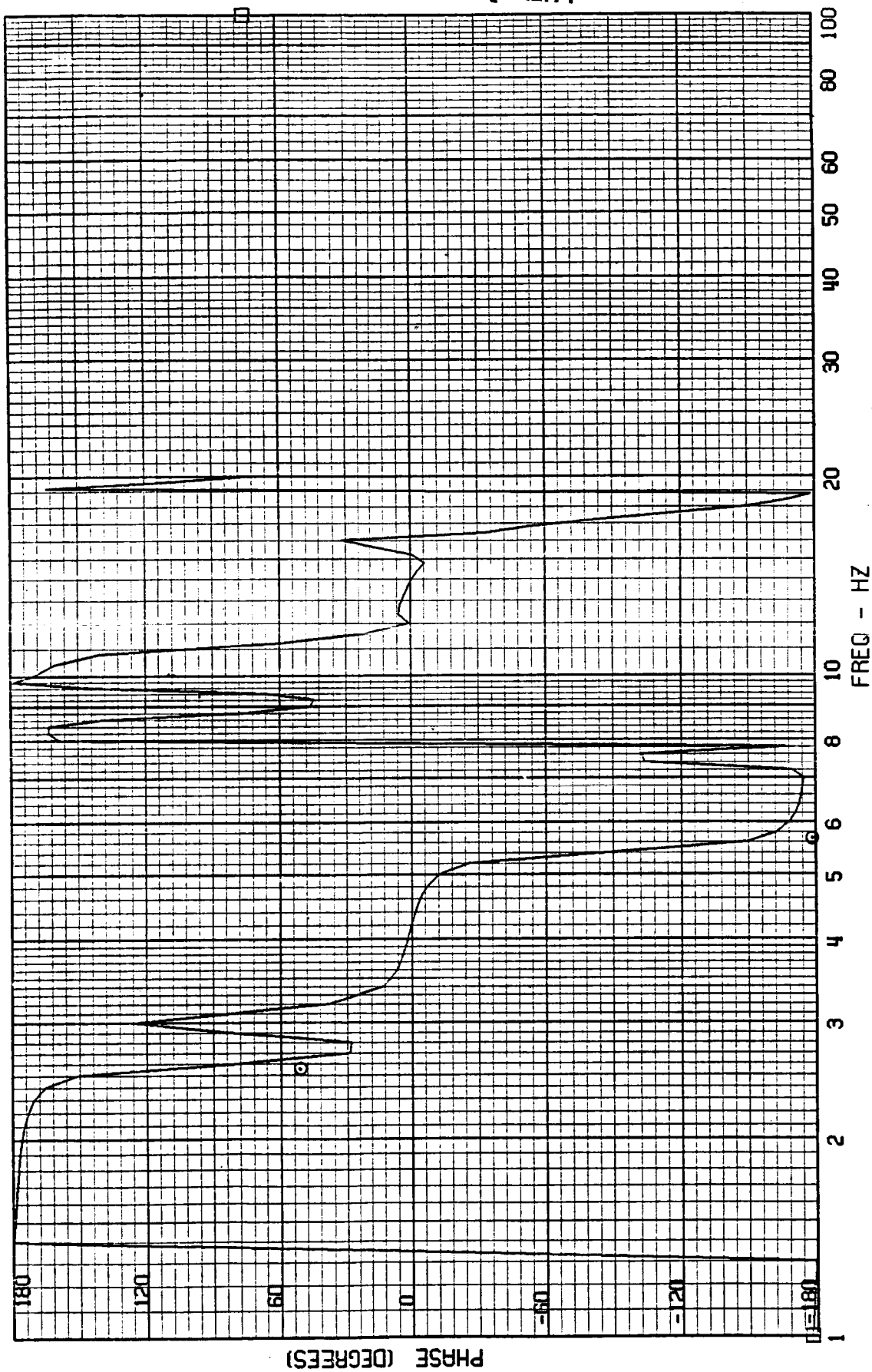

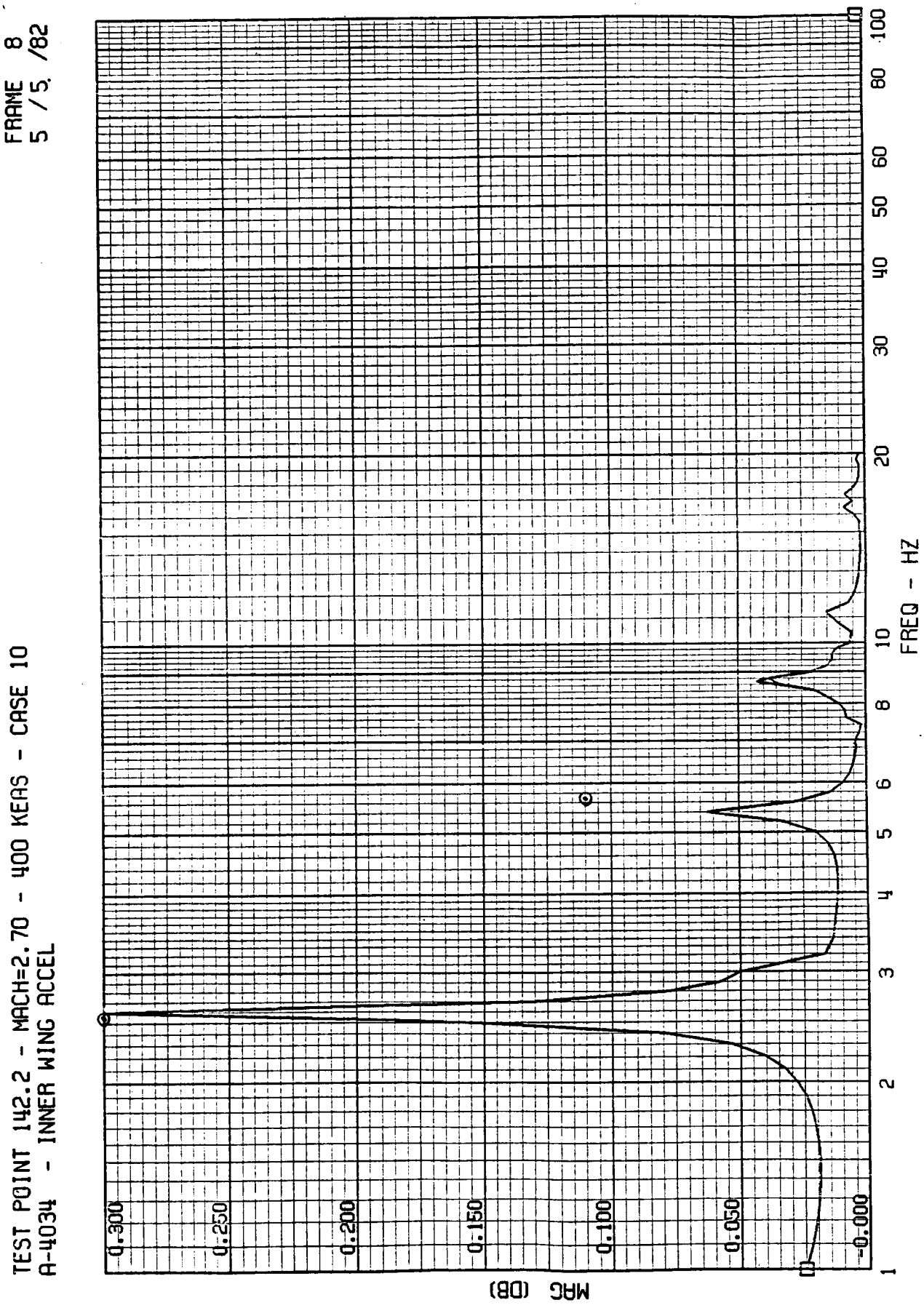
TEST POINT 142.2 - MACH=2.70 - 400 KEAS - CASE 10
A-4034 - INNER WING ACCEL
FRAME 8
5 /5 /82
MAG (DB)
0.300
0.250
0.200
0.150
0.100
0.050
-0.000
FREQ - HZ
1
2
3
4
5
6
8
10
20
30
40
50
60
80
100

FRAME 8
5 /5 /82

TEST POINT 142.2 - MACH=2.70 - 400 KEAS - CASE 10
A-4034 - INNER WING ACCEL

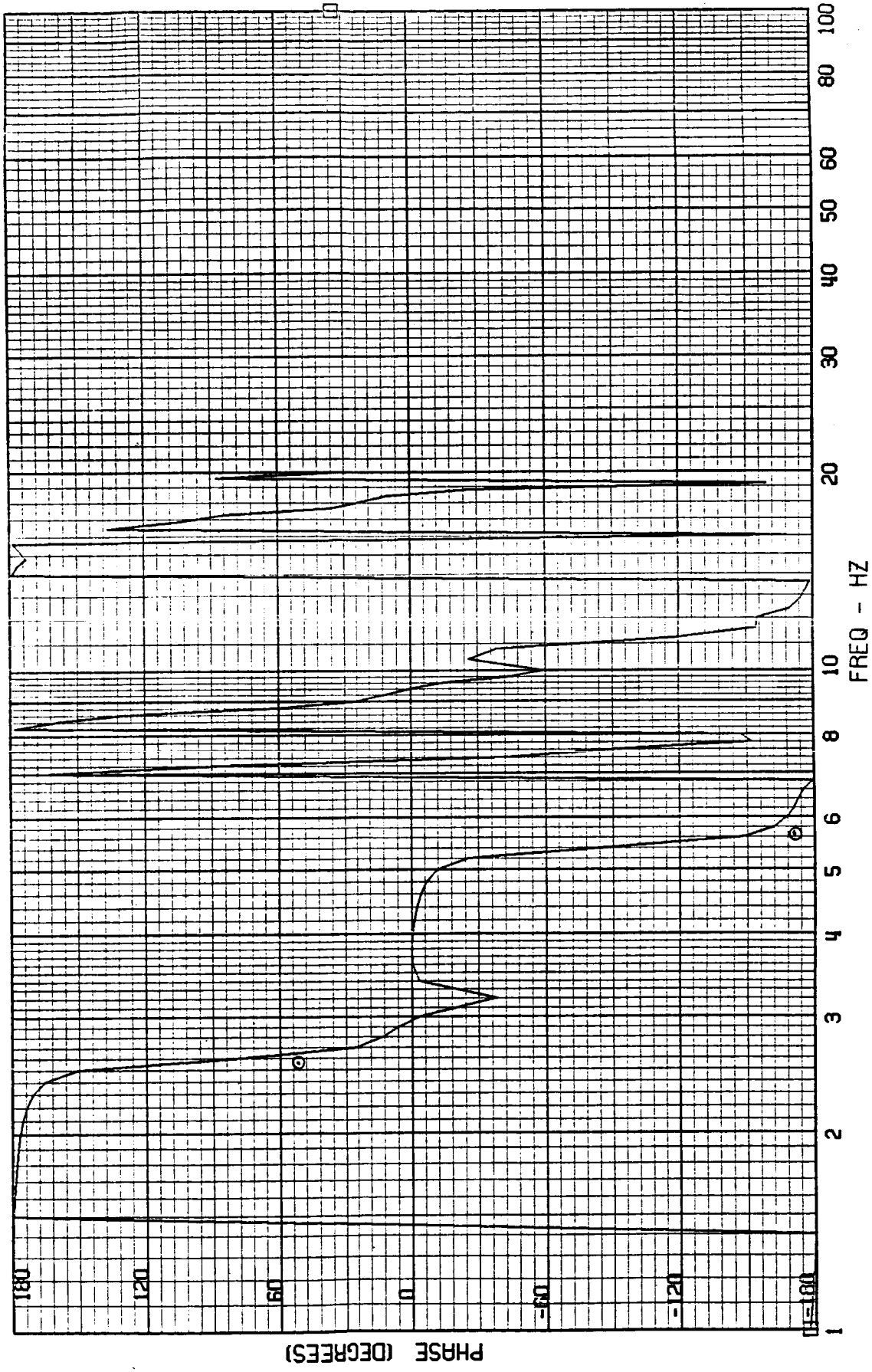

TEST POINT 142.2 - MACH=2.70 - 400 KEAS - CASE 10
RWCLACC - NACELLE ACCEL

FRAME 9
5 /5 /82

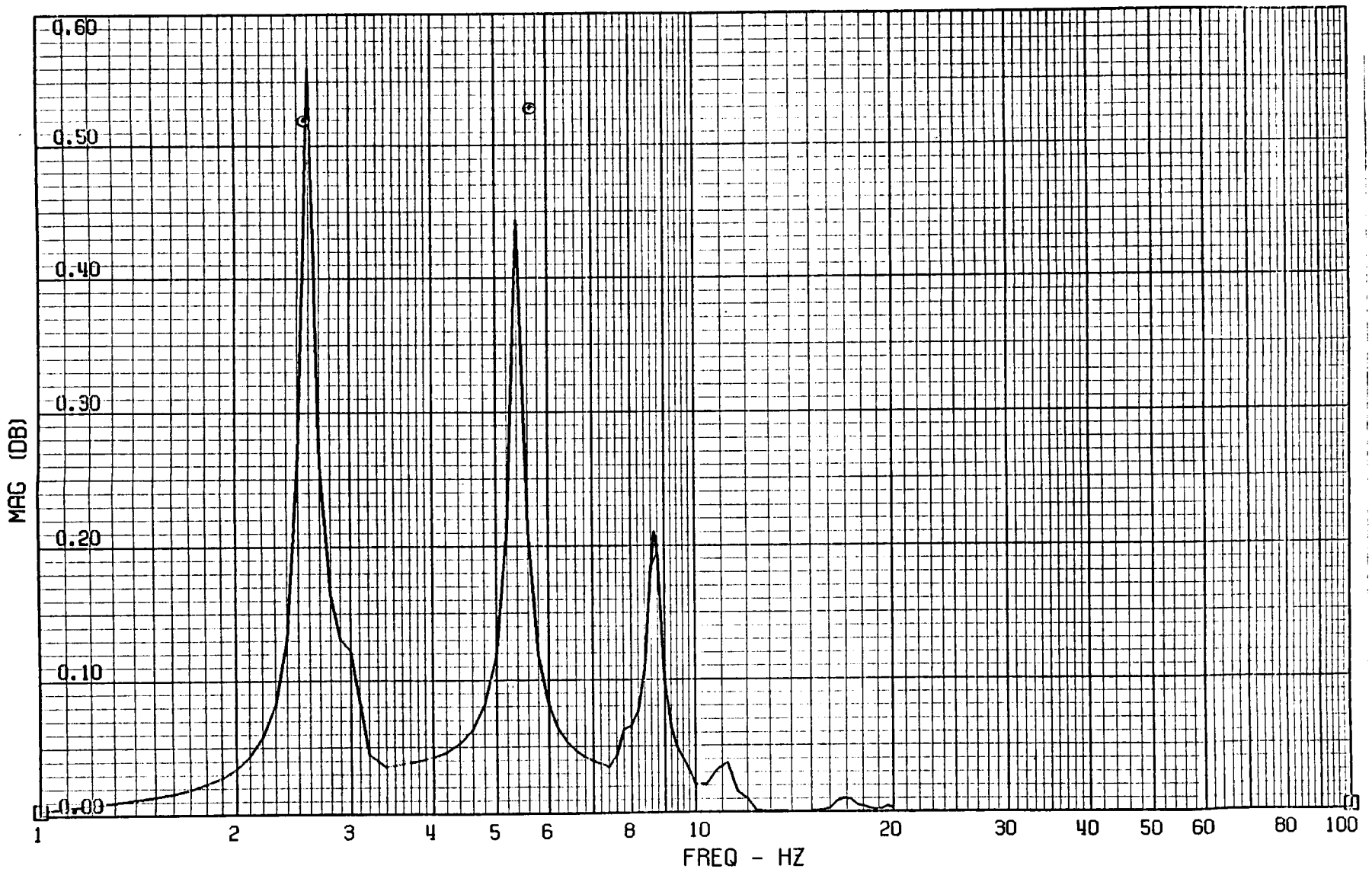

FRAME 9
5 /5 /82

TEST POINT 142.2 - MACH=2.70 - 400 KEAS - CASE 10
RWCLACC - NACELLE ACCEL

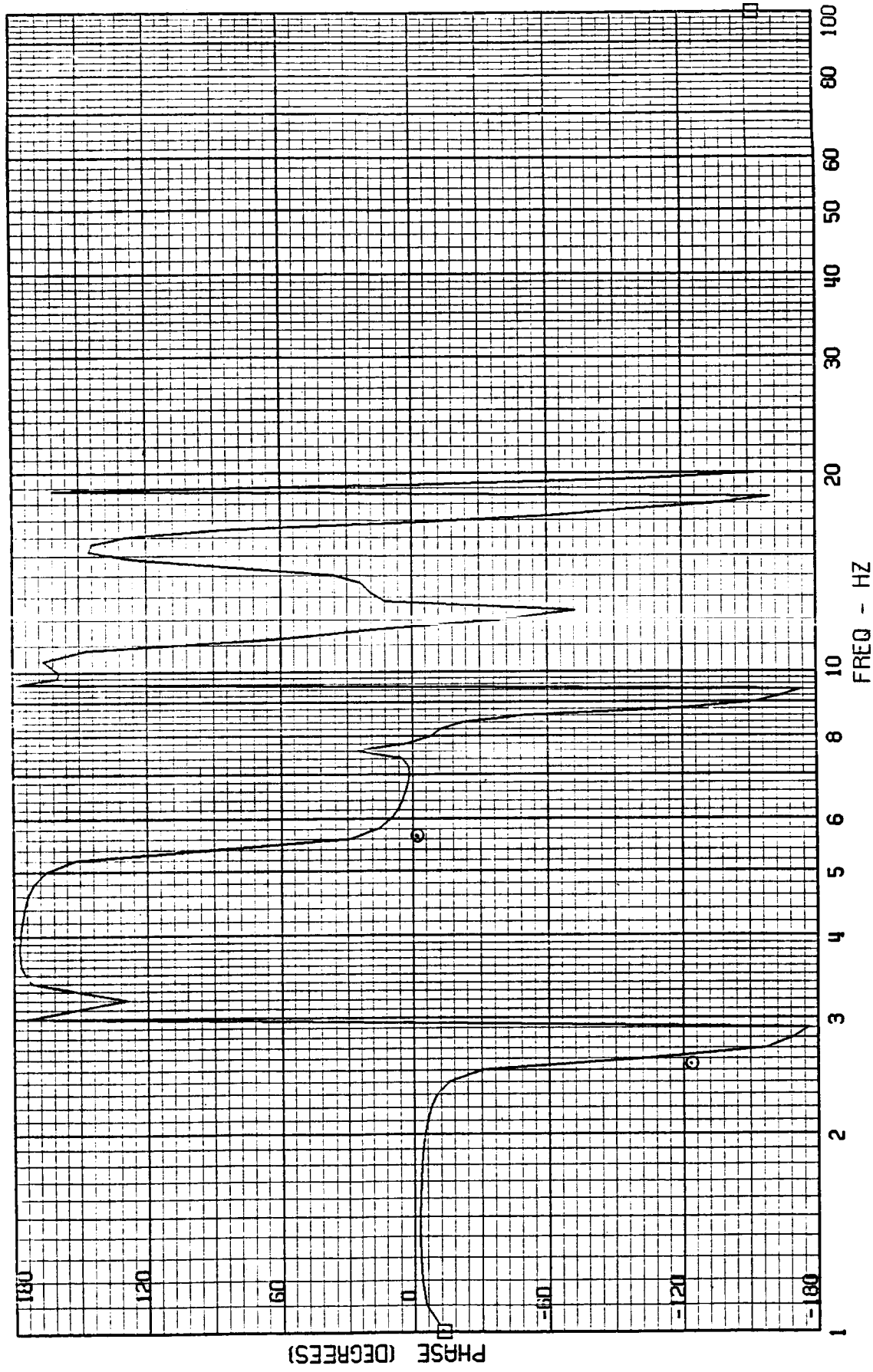

TEST POINT 142.2 - MACH=2.70 - 400 KEAS - CASE 10
RRUDACC - RUDDER ACCEL

FRAME 10
5 /5 /82

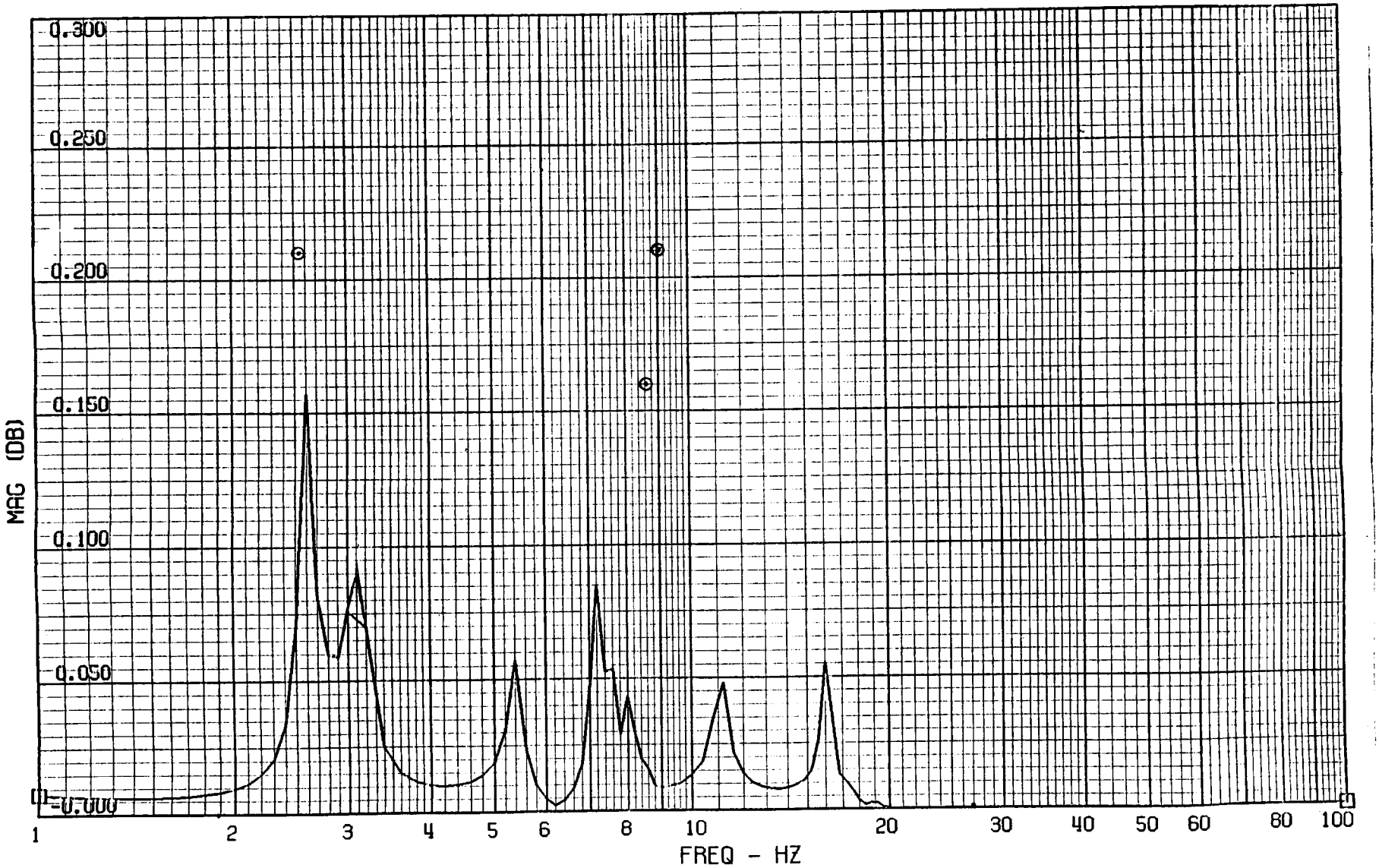

FRAME 10
5 /5 /82

TEST POINT 142.2 - MACH=2.70 - 400 KEAS - CASE 10
RRUDACC - RUDDER ACCEL

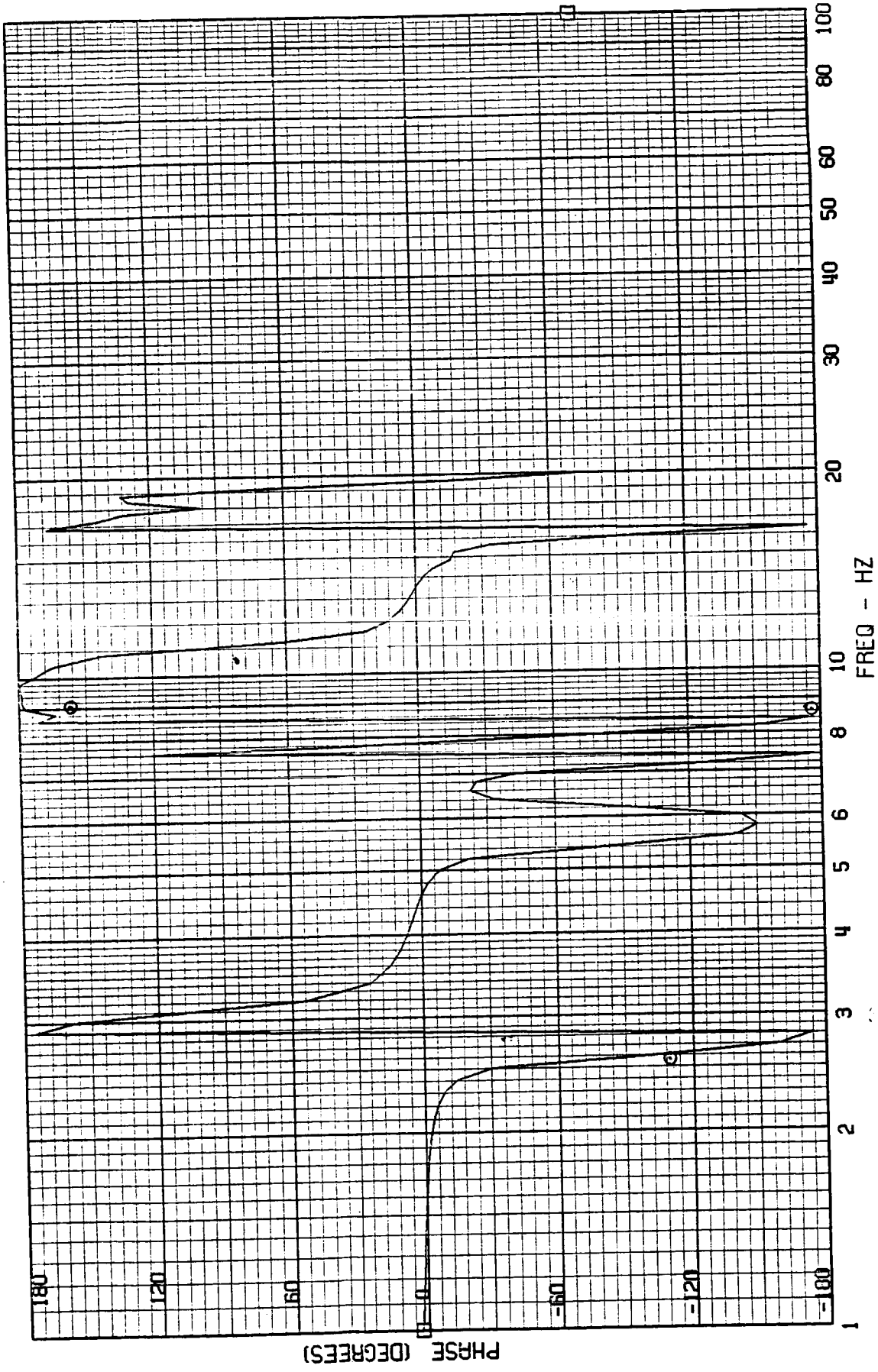

REFERENCES

1. Burris, P.M., and Bender, M.A., "Aircraft Load Alleviation and Mode Stabilization (LAMS)," AFFDL TR68-158, Air Force Flight Dynamics Lab., Wright-Patterson AFB, April, 1969.

2. Anon., "B-52 CCV Program Summary, Control System Synthesis, System Design and Aircraft Mod., Component and Aircraft Ground Tests, Control System Flight Validation, Fuel Mileage Improvement with Augmented Stability System," AFFDL TR74-92, Vols. I, II, III, IV, V, and VI, Air Force Flight Dynamics Lab, Wright-Patterson AFB, March 1975.

3. Wykes, John H., Nardi, Louis U., and Mori, Alva S., "XB-70 Structural Mode Control System Design and Performance Analyses," NASA CR-1557, July 1970.

4. Lock, Wilton P., Kordes, Eldon E., McKay, James M., and Wykes, John H., "Flight Investigation of a Structural Mode Control System for the XB-70 Aircraft," NASA TN D-7420, October 1973.

5. Edinger, Lester D., Schenk, Frederick L., and Curtis, Alan R., "Study of Load Alleviation and Mode Suppression (LAMS) on the YF-12A Airplane," NASA CR-2158, December 1972.

6. ECP YF12-75, "Canard for YF-12A," 10 September 1974. Lockheed internal document (unpublished).

7. ECP YF12-123, "Aeroelastic Response Analysis of the YF-12A Airplane with Canard/Shaker Vane for Comparison with Flight Test Data," 12 May 1980. Lockheed internal document (unpublished).

8. Terlizzi, Roy, "Functional Engineering Work Statement for YF-12A Shaker Vane Installation," SP-4217, 29 July 1974. Lockheed internal document (unpublished).

9. Thomas, A. G., "Development and Test Program For YF-12 Shaker Vane Electronics," SP-4511, 17 May 1976. Lockheed internal document (unpublished).

10. Wilson, Ronald J., Cazier, Jr., Frank W., and Larson, Richard R., "Results of Ground Vibration Tests on a YF12 Airplane," NASA Technical Memorandum X-2880, August 1973.

11. Kordes, E. E., Curtis, A. R., "Results of NASTRAN Modal Analyses and Ground Vibration Tests on the YF-12A Airplane," ASME 75-WA/Aero-8, 19 September 1975.

12. Albano, E., and Rodden, W. P., "A Doublet-Lattice Method for Calculating Lift Distributions on Oscillating Surfaces in Subsonic Flows," AIAA J., Vol. 7, No. 2, February 1969, pp. 279-285, and Vol. 7, No. 11, November 1969, p. 2192.

13. Rodden, W. P., Giesing, J. P., and Kálmán, T. P., "Refinement of the Nonplanar Aspects of the Subsonic Doublet-Lattice Lifting Surface Method," J. Aircraft, Vol. 9, No. 1, January 1972, pp. 69-73.

C-4

14. Giesing, J. P., Kálmán, T. P., and Rodden, W. P., "Subsonic Unsteady Aerodynamics for General Configurations; Part I, Vol. I - Direct Application of the Nonplanar Doublet Lattice Method," Air Force Flight Dynamics Laboratory Report No. AFFDL-TR-71-5, Part I, Vol. I, November 1971.

15. Giesing, J. P., Kálmán, T. P., and Rodden, W. P., "Subsonic Unsteady Aerodynamics for General Configurations; Part II, Vol. II - Computer Program N5KA," Air Force Flight Dynamics Laboratory Report No. AFFDL-TR-71-5, Part II, Vol. II, April 1972.

16. Giesing, J. P., Kálmán, T. P., and Rodden, W. P., "Subsonic Unsteady Aerodynamics for General Configurations; Part II, Vol. I - Application of the Doublet-Lattice Method and the Method of Images to Lifting-Surface/Body Interference," Air Force Flight Dynamics Laboratory Report No. AFFDL-TR-71-5, Part II, Vol. I, April 1972.

17. Giesing, J. P., Kálmán, T. P., and Rodden, W. P., "Subsonic Steady and Oscillatory Aerodynamics for Multiple Interfering Wings and Bodies," J. Aircraft, Vol. 9, No. 10, October 1972, pp. 693-702.

18. Mazelsky, B., and O'Connell, R. F., "Transient Aerodynamic Properties of Wings: Review and Suggested Electrical Representations for Analog Computers," Lockheed Aircraft Corp., Report No. LR11577, July 23, 1956.

19. Curtis, A. R., "Subsonic Kernel Function Program - Preliminary," SP 970, April 1, 1966, Lockheed-California Co., Burbank, Calif. Lockheed internal document (unpublished).

20. Watkins, C. E., Runyan, H. L., and Woolston, D. S., "On the Kernel Function of the Integral Equation Relating the Lift and Downwash Distributions of Oscillating Finite Wings in Subsonic Flow," NACA Report 1234, 1955.

21. Pines, S., Dugundji, J., and Neuringer, J., "Aerodynamic Flutter Derivatives for a Flexible Wing with Supersonic and Subsonic Edges," J. Aero. Sci., Vol. 22, No. 10, October 1955, pp. 693-700.

22. Moore, M. T., and Andrew, L. V., "Unsteady Aerodynamics for Advanced Configurations, Part IV - Application of the Supersonic Mach Box Method to Intersecting Planar Lifting Surfaces," Air Force Flight Dynamics Laboratory Report No. FDL-TDR-64-152, Part IV, February 1965.

23. Donato, V. W., and Huhn, C. R., Jr., "Supersonic Unsteady Aerodynamics for Wings with Trailing-edge Control Surfaces and Folded Tips," Air Force Flight Dynamics Laboratory Report No. AFFDL-TR-68-30, January 1968.

24. Hassig, H. J., Messina, A. F., Twomey, W. J., "Using a Partial Diaphragm When Applying the Supersonic Mach Box Method," AIAA Journal, February 1967.

25. Ashley, H., and Zartarian, G., "Piston Theory - A New Aerodynamic Tool for the Aeroelastician," J. Aero. Sci., Vol. 23, No. 12, December 1956, pp. 1109-1118.

26. Rodden, W. P., Farkas, E. F., Malcom, H. A., and Kliszewski, A. M., "Aerodynamic Influence Coefficients from Piston Theory: Analytical Development and Computational Procedure," Aerospace Corp., Report No. TDR-169(3230-11) TN-2, 15 August 1962.

27. Harder, R. L., and Desmarais, R. N., "Interpolation Using Surface Splines," J. of Aircraft, Vol. 9, No. 2, February 1972, pp. 189-191.

28. Hassig, H. J., "An Approximate True Damping Solution of the Flutter Equation by Determinant Iteration," J. Aircraft, Vol. 8, No. 11, November 1971.

29. "Flutter and Matrix Algebra System - FAMAS - Manual," LR 23657, April 20, 1970, Lockheed-California Co., Burbank, Calif. Lockheed internal document (unpublished).

1. Report No.	2. Government Accession No.	3. Recipient's Catalog No.
NASA CR-166623		

4. Title and Subtitle	5. Report Date
Flight and Analytical Investigations of a Structural Mode Excitation System on the YF-12A Airplane	April 1987
	6. Performing Organization Code
7. Author(s)	8. Performing Organization Report No.
E.A. Goforth, R.C. Murphy, J.A. Beranek, and R.A. Davis	H-1361
	10. Work Unit No.
9. Performing Organization Name and Address	RTOP 505-43-81
Lockheed-California Company Burbank, California 91520	11. Contract or Grant No.
	NASA E69204
	13. Type of Report and Period Covered
12. Sponsoring Agency Name and Address	Contractor Report - Final
National Aeronautics and Space Administration Washington, DC 20546	14. Sponsoring Agency Code

15. Supplementary Notes

NASA Technical Monitor: Glenn B. Gilyard, Ames Research Center, Dryden Flight Research Facility, Edwards, California 93523-5000

16. Abstract

A structural excitation system, using an oscillating canard vane to generate force, was mounted on the forebody of the YF-12A airplane. The canard vane was used to excite the airframe structural modes during flight in the subsonic, transonic, and supersonic regimes. Structural modal responses generated by the canard vane forces were measured at the flight test conditions by airframe-mounted accelerometers. Correlations of analytical and experimental aeroelastic results were made. Doublet lattice, steady state doublet lattice with uniform lag, Mach box, and piston theory all produced acceptable analytical aerodynamic results within the restrictions that apply to each. In general, the aerodynamic theory methods, carefully applied, were found to predict the dynamic behavior of the YF-12A aircraft adequately.

17. Key Words (Suggested by Author(s))	18. Distribution Statement
YF-12A; Excitation system; Modal response; Structural modes; Doublet lattice; Mach box; Piston theory	Unclassified — Unlimited Subject category 05

19. Security Classif. (of this report)	20. Security Classif. (of this page)	21. No. of Pages	22. Price*
Unclassified	Unclassified	294	A13

*For sale by the National Technical Information Service, Springfield, Virginia 22161.